



**UNIVERSITY OF NAIROBI**

***IN VITRO AND IN SILICO* PHARMACOLOGIC  
EVALUATION OF THE ANTIRETROVIRAL ACTIVITY OF  
*CROTON* SPECIES**

**BY**

**ERMIAS MERGIA TEREFE**

**U80/54741/2019**

**A Thesis Submitted for the Award of Doctor of Philosophy Degree in  
Molecular Pharmacology at the Department of Pharmacology and  
Pharmacognosy, University of Nairobi**

**2022**

# UNIVERSITY OF NAIROBI DECLARATION OF ORIGINALITY FORM

**Name of student:** Ermias Mergia Terefe

**Registration Number:** U80/54741/2019

**Faculty:** College of Health Sciences

**Department:** School of Pharmacy

**Section:** Pharmacology and Pharmacognosy

**Course Name:** Doctor of Philosophy in Molecular Pharmacology

**Title of work:** *In vitro* and *In silico* Pharmacologic Evaluation of the Antiretroviral activity of *Croton* species

## DECLARATION

1. I understand what plagiarism is, and I am aware of the university's policy in this regard.
2. I declare that this thesis is my original work and has not been submitted elsewhere for examination, the award of a degree or publication. Where other people's work or my own work has been used, this has properly been acknowledged and referenced in accordance with the University of Nairobi's requirements.
3. I have not sought or used the services of any professional agencies to produce this work.
4. I have not allowed and shall not allow anyone to copy my work with the intention of passing it off as his/her own work
5. I understand that any false claim with respect to this work shall result in disciplinary action in accordance with the university's anti-plagiarism policy.

Signature



Date

**June 04, 2022**

## DECLARATION

I declare that this thesis is my original work except where a reference is made. It has never been submitted elsewhere for examination, award of a degree, or publication. Where other people's work or my work has been used, this has properly been acknowledged and referenced in accordance with the University of Nairobi's requirements.



----- Date -- June 04, 2022-----

**Ermias Mergia Terefe**

U80/54741/2019

Department of Pharmacology, University of  
Nairobi.

This PhD research work has been submitted with our approval as university supervisors.



----- Date-- 09/06/2022-----

**Prof. Faith Apolot Okalebo**

Department of Pharmacology and Pharmacognosy, University of Nairobi



----- Date ----- 13/06/2022-----

**Prof. Solomon Derese**

Department of Chemistry, University of Nairobi



----- Date----- 13/06/2022-----

**Dr. Joseph Muriuki**

Centre for Virus Research, Kenya Medical Research Institute

## **DEDICATION**

I dedicate my dissertation work to my parents, wife and children. A special feeling of gratitude to my loving father, Eng. Mergia Terefe, whose words of encouragement and push for tenacity ring in my ears. My mother, Tirunesh Wakshuma, for all her continued prayers and support.

## **ACKNOWLEDGEMENTS**

First of all, I thank the Almighty God for his grace and all the strength he gave me during my Ph.D. project. I am grateful to my wife Blen Lemma Balcha and children (Dunamis, Juliana and Chris) for their patience during late hours of work and all moments of frustration and happiness during this journey.

My Special appreciation goes to my supervisors Prof. Faith A. Okalebo, Prof. Solomon Derese, and Dr. Joseph Muriuki, for graciously providing good supervision, critical review, and commitment to shaping the Ph.D. project and guiding me through the whole program. I am grateful for your patience as you guided, supported, and encouraged me through my research work.

I acknowledge United States International University- Africa (USIU-A) Internal grant no. 10-2854, University of Nairobi (UON), Kenya Medical Research Institute (KEMRI), and the Institute of Primate Research (IPR) for their support toward the successful completion of the research work. I am grateful to UON-ERC for awarding me with the ethical clearance to carry out the research.

I thank Dr. Kipruto A Sinei and Dr. Margaret Oluka, Department of Pharmacology and Pharmacognosy, University of Nairobi, for providing needful support during my work. I also wish to thank to the research team at the Royal Botanic Gardens, Kew (United Kingdom) for assisting me in the NMR and MS analysis of the pure compounds.

Thank you to all my colleagues in the School of Pharmacy and Health Sciences, United States International University, for your support in my Ph.D. journey. It is impossible to mention individually all the persons who helped me one way or another; however, I would like to record my gratitude for all their assistance, both professional and personal.

# ABSTRACT

## Introduction

The Human Immunodeficiency Virus (HIV) affects the body's defence mechanisms and leads to many opportunistic infections. Globally, more than half a million individuals lost their lives in 2020 due to this disease. Antiretroviral drugs have played a significant role in improving the quality of life of HIV-infected individuals. However, the side effects of these drugs, coupled with the virus's resistance to the various regimens, necessitate the search for potential new and effective antiretroviral medication.

## Objective

The objective of this study was to evaluate the cytotoxicity and anti-HIV activity of crude and solvent fractions of *Croton macrostachyus*, *Croton megalocarpus*, and *Croton dichogamus* and to isolate pure compounds with potential antiretroviral activity.

## Methods

Stem bark and leaves of *C. macrostachyus*, *C. megalocarpus*, and twigs of *C. dichogamus* are extracted using 1:1 v/v dichloromethane and methanol, followed by liquid-liquid partitioning using four different solvents. The crude and solvent fractions were tested for inhibition of laboratory-adapted HIV-1<sub>IIIB</sub> strain replication in the Human T-lymphocytic MT-4 cell line. In addition, using bioassay-guided fractionation, pure compounds with anti-HIV activity were isolated. Finally, the chemical structure of the new compounds was elucidated and mode of action predicted using in silico approach.

## Results

The highest anti-HIV activity was observed from the ethyl acetate fractions of the bark of *C. megalocarpus* ( $IC_{50} = 0.47 \pm 0.12 \mu\text{g/mL}$ ; selectivity index =346.3), the hexane fraction of the leaves of *C. macrostachyus* ( $IC_{50} = 0.02 \pm 0.01 \mu\text{g/mL}$ ; SI of 9752.7) and the methanol fraction of *C. dichogamus* ( $IC_{50} = 0.06 \pm 0.01 \mu\text{g/mL}$ ; SI of 318.5). In addition, nine compounds were isolated from the ethyl acetate fraction of the bark of *C. megalocarpus* (ermiasolide A, B and C, 4H- $\alpha$ ,7H- $\alpha$ ,10 $\alpha$ -eudesm-11-en-5 $\beta$ -ol, ermiasoid, lupeol, 11-acetoxy crotoascarin L, pinoresinol, and crotoascarin K), five compounds from the hexane fraction of the leaves of *C. macrostachyus* (2-methoxy benzyl benzoate, betulin, lupenone, lupeol acetate, lupeol) and four compounds from methanol fraction of the twigs of *C. dichogamus* (dihydroconiferyl acetate, crotoascarin  $\omega$ , (4-hydroxy-3-methoxyphenyl)-propyl benzoate,  $\beta$ -oplopanone). Among these compounds, six of them (ermiasolide A, ermiasolide B, ermiasolide C, ermiasoid, 11-acetoxy

crotoascarin L and crotoascarin ω) were previously undescribed new compounds with anti-HIV activity. The new compounds displayed the highest anti-HIV activity by inhibiting more than 70% of viral replication with an IC<sub>50</sub> value of less than 0.04 μg/mL. The *in vitro* assay showed that the bioactive compounds are more active in inhibiting more than 60 % of HIV-1 protease enzyme activity. In addition, molecular docking study showed that these compounds had strong binding with the HIV-1 PR at free binding energy of less than -7.00 kcal/mol and form hydrophobic and hydrogen bonding with several amino acids in the active site of the HIV protease enzyme and inhibit the binding of viral polypeptide to the catalytic domain of the enzyme.

### **Conclusion**

The isolated pure compounds have displayed potent inhibition of HIV-1 protease enzyme activity due to the strong binding of the compounds in the enzyme's active site and the formation of several hydrogen bonds with key residues.

**Keywords:** HIV, MT-4 cells, *Croton macrostachyus*, *Croton megalocarpus*, *Croton dichogamus*, Cytotoxicity, AntiHIV activity

## TABLE OF CONTENTS

DECLARATION .....	ii
DEDICATION .....	iii
ACKNOWLEDGEMENTS .....	iv
ABSTRACT .....	v
LIST OF TABLES .....	xi
LIST OF FIGURES .....	xiii
LIST OF SCHEMES .....	xv
LIST OF ACRONYMS AND ABBREVIATIONS .....	xvi
LIST OF APPENDICES .....	xvii
PUBLICATIONS .....	xxii
CHAPTER ONE .....	1
INTRODUCTION .....	1
1.1. Background Information .....	1
1.2. Statement of the problem .....	1
1.3. Objectives .....	2
1.3.1. General Objective .....	2
1.3.2. Specific Objectives .....	2
1.4. Justification and significance of the study .....	2
CHAPTER TWO .....	4
LITERATURE REVIEW .....	4
2.1. Literature review on HIV .....	4
2.1.1. History of HIV Pandemic .....	4
2.1.2. HIV Epidemiology .....	4
2.1.1. HIV-1 Structure and function .....	4
2.1.2. HIV Lifecycle .....	6



2.1.3. Pathogenesis and Natural History of HIV .....	8
2.2. Molecular biology of retroviral enzymes .....	10
2.2.1. Reverse transcriptase (RT) .....	10
2.2.2. HIV Integrase .....	11
2.2.3. HIV Protease.....	12
2.3. Antiretroviral drugs and resistance .....	14
2.3.1. Nucleoside and Nucleotide Reverse Transcriptase Inhibitors (NRTIs) .....	14
2.3.2. Non-Nucleoside Reverse Transcriptase Inhibitors (NNRTIs).....	16
2.3.3. Integrase Inhibitors .....	17
2.3.4. Protease and Maturation Inhibitors.....	18
2.3.5. Entry and Fusion Inhibitors .....	20
2.4. Discovery of New Antiretroviral Drugs.....	21
2.4.1. <i>In vitro</i> anti-HIV Assays.....	21
2.4.2. Computer-aided drug design and discovery ( <i>in silico</i> analysis).....	22
2.5. Medicinal Plants with anti-HIV activity .....	24
2.6. The <i>Croton</i> genus .....	26
2.6.1. Botanical information on <i>Croton</i> genus .....	26
2.6.2. Ethnomedicinal uses of <i>Croton</i> genus .....	28
2.6.3. The pharmacological activities of the genus <i>Croton</i> .....	32
2.6.4. <i>Croton macrostachyus</i> Hochst. ex Delile .....	34
2.6.5. <i>Croton megalocarpus</i> Hutch. ....	37
2.6.6. <i>Croton dichogamus</i> Pax.....	39
CHAPTER THREE .....	42
METHODOLOGY .....	42
3.1. Materials.....	42
3.2. Photochemical study of the medicinal plants .....	42
3.2.1. Collection of the plant specimen and ethical consideration .....	42

3.2.2. Preparation of Crude extract.....	43
3.2.3. Liquid-Liquid separation of the crude extracts.....	44
3.2.4. Chromatographic technique and isolation of pure compound.....	45
3.2.5. Structural elucidation of isolated compounds .....	47
3.3. <i>In vitro</i> assay for antiretroviral activity.....	48
3.3.1. Preparation of extracts and test compounds .....	48
3.3.2. Cell culture, maintenance, and viability test.....	48
3.3.3. Preparation of the virus and viral infectivity test .....	50
3.3.4. Cytotoxicity assay.....	52
3.3.5. Anti-HIV activity test .....	54
3.3.6. Statistical analysis.....	56
3.4. <i>In silico</i> antiretroviral activity .....	56
CHAPTER FOUR.....	58
RESULTS AND DISCUSSION .....	58
4.1. Yield for plant extraction .....	58
4.2. Cytotoxicity and antiretroviral activity of the crude extracts of <i>C. macrostachyus</i> , <i>C. megalocarpus</i> , and <i>C. dichogamus</i> .....	59
4.3. Evaluation of cytotoxicity and antiretroviral activity of solvent fractions of <i>C. macrostachyus</i> , <i>C. megalocarpus</i> , and <i>C. dichogamus</i> .....	60
4.3.1. Cytotoxicity and anti-HIV activity of solvent fractions of <i>C. megalocarpus</i> .....	60
4.3.2. Cytotoxicity and anti-HIV activity of solvent fractions of <i>C. macrostachyus</i> .....	64
4.3.3. Cytotoxicity and anti-HIV activity of solvent fractions of <i>C. dichogamus</i> .....	67
4.4. Isolation and characterization of compounds with a potential antiretroviral activity using bioassay-guided fractionation .....	70
4.4.1. <i>Croton megalocarpus</i> .....	70
4.4.2. <i>Croton macrostachyus</i> .....	95
4.4.2. <i>Croton dichogamus</i> .....	109

4.5. Investigation of the <i>in vitro</i> and <i>in silico</i> interaction of the isolated compounds against HIV enzymes .....	122
4.5.1. <i>In vitro</i> assays on the effect of pure compounds on retroviral enzymes .....	122
4.5.2. <i>In silico</i> anti-HIV activity of pure compounds .....	122
CHAPTER FIVE .....	131
CONCLUSION AND RECOMMENDATIONS .....	131
REFERENCES .....	133
APPENDICES .....	190

## LIST OF TABLES

Table 2.1-1: HIV Epidemiology in the world and Africa -----	5
Table 2.4-1: <i>In vitro</i> anti-HIV assays-----	22
Table 2.5-1: List of some plant species exhibiting anti-HIV activities-----	25
Table 2.6-1: Plants from the <i>Croton</i> genus that have displayed anti-HIV activity -----	27
Table 2.6-2: Ethnomedicinal uses of the <i>Croton</i> genus-----	28
Table 2.6-3: Phytochemicals isolated from <i>C. macrostachyus</i> -----	35
Table 2.6-4: Phytochemicals isolated from <i>C. megalocarpus</i> -----	38
Table 2.6-5: Phytochemicals isolated from <i>C. dichogamus</i> -----	39
Table 4.1-1: Yields of extracts obtained from <i>Croton</i> Species -----	58
Table 4.1-2: Weight of liquid/liquid partition of the crude extracts -----	58
Table 4.2-1: Cytotoxicity and anti-HIV activities of crude extracts of three <i>C.</i> species -----	59
Table 4.3-1: Cytotoxicity and anti-HIV activities of solvent fractions of <i>C. megalocarpus</i> --	60
Table 4.3-2: Cytotoxicity and anti-HIV-1 activities of solvent fractions of <i>C. macrostachyus</i> -----	65
Table 4.3-3: Cytotoxicity and anti-HIV-1 activities of solvent fractions of <i>C. dichogamus</i> --	68
Table 4.4-1: Compounds isolated from the stem bark of <i>C. megalocarpus</i> -----	70
Table 4.4-2: NMR data for 5 $\beta$ -Hydroxy-8 $\alpha$ -methoxy eudesm-7(11)-en-12,8-olide (ermiasolide A, E12) in CDCl <sub>3</sub> -----	73
Table 4.4-3: NMR data for 5 $\beta$ -Hydroxy-8 $\alpha$ -methoxy eudesm-7(11)-en-12,8-olide (ermiasolide A, E12) in DMSO -----	74
Table 4.4-4: NMR data for 5 $\beta$ ,8 $\alpha$ -dihydroxy eudesm-7(11)-en-12,8-olide (ermiasolide B, E22) in CDCl <sub>3</sub> -----	75
Table 4.4-5: NMR data for 5 $\beta$ ,8H- $\beta$ -hydroxy eudesm-7(11)-en-12,8-olide (ermiasolide C, E17) in CDCl <sub>3</sub> -----	77
Table 4.4-6: NMR data for 4H- $\alpha$ ,7H- $\alpha$ ,10 $\alpha$ -eudesm-11-en-5 $\beta$ -ol (E5) in CDCl <sub>3</sub> -----	78
Table 4.4-7: NMR data for Crotoascarin K (E23) in CDCl <sub>3</sub> -----	79
Table 4.4-8: NMR data for 11 $\beta$ -acetoxy crotoascarin L (E24)-----	81
Table 4.4-9: NMR data for 1 $\beta$ -Acetoxy-3 $\beta$ -chloro-5 $\alpha$ ,6 $\alpha$ -dihydroxycrotoascarin (Ermiasoid) (E37) -----	84
Table 4.4-10: NMR data for Pinoresinol (E2)-----	86
Table 4.4-11: NMR data for lupeol (E19) in CDCl <sub>3</sub> -----	87

Table 4.4-12: Cytotoxicity and anti-HIV-1 activities of pure compounds isolated from <i>C. megalocarpus</i> -----	88
Table 4.4-13: Compounds isolated from the stem bark of <i>C. macrostachyus</i> -----	95
Table 4.4-14: NMR data for 2-Methoxy benzyl benzoate (A5) in CDCl <sub>3</sub> -----	96
Table 4.4-15: NMR data for Lupenone (A4b) in CDCl <sub>3</sub> -----	98
Table 4.4-16: NMR data for Betulin (A19) in CDCl <sub>3</sub> -----	99
Table 4.4-17: NMR data for Lupeol acetate (A11) in CDCl <sub>3</sub> -----	102
Table 4.4-18: NMR data for Sitosterol (A16) in CDCl <sub>3</sub> -----	104
Table 4.4-19: NMR data for Stigmasterol (A15) in CDCl <sub>3</sub> -----	105
Table 4.4-20: Cytotoxicity and anti-HIV activities of pure compounds isolated from <i>C. macrostachyus</i> -----	107
Table 4.4-21: Compounds isolated from the twigs of <i>C. dichogamus</i> -----	109
Table 4.4-22: NMR data for dihydroconiferyl acetate (CD1a) in CDCl <sub>3</sub> -----	111
Table 4.4-23: NMR data for (4-Hydroxy-3-methoxyphenyl)-propyl benzoate (CD1b) in CDCl <sub>3</sub> -----	112
Table 4.4-24: NMR table for Crotoascararin $\omega$ (CD12a) -----	115
Table 4.4-25: NMR table for CD13: $\beta$ -Oplopanone (CD12b) -----	116
Table 4.4-26: Cytotoxicity and anti-HIV activities of pure compounds isolated from <i>C. dichogamus</i> -----	119
Table 4.5-1 HIV-1 Protease enzyme inhibition activity of compounds isolated from <i>C. megalocarpus</i> -----	122
Table 4.5-2: Molecular docking analysis of against HIV-1 RT in complex with Nevirapine (PDB ID: 1JLB) -----	123
Table 4.5-3: Molecular docking analysis of against HIV-1 PR in complex with Atazanavir (3EL9) -----	123
Table 4.5-4: Amino acids in the binding site of HIV-1 protease enzyme -----	124
Table 4.5-5: Ligand-protein interaction profile for compounds docked with HIV-1 PR (3EL9) -----	125

## LIST OF FIGURES

Figure 2.1-1: HIV structure -----	5
Figure 2.1-2: Structure and organization of the HIV-1 genome -----	6
Figure 2.1-3: Attachment and Fusion of HIV -----	7
Figure 2.1-4: Life cycle of HIV -----	8
Figure 2.1-5: Stages of HIV infection -----	9
Figure 2.2-1: The NRTIs and NtRTIs binding sites with HIV reverse transcriptase along with the NNRTIs binding site -----	11
Figure 2.2-2: Structural domains of integrase -----	12
Figure 2.2-3: Structure of the substrate and the binding subsites -----	13
Figure 2.2-4: Amino acid residue that forms binding sites of HIV-1 protease -----	14
Figure 2.3-1: Life cycle of HIV and the site of action of antiretroviral drugs -----	15
Figure 2.3-2: Chemical structures of nucleoside/tide reverse transcriptase inhibitors -----	15
Figure 2.3-3: Chemical structures of Non-Nucleoside Reverse Transcriptase Inhibitors -----	17
Figure 2.3-4: Molecular Target for Non-Nucleoside Reverse Transcriptase Inhibitors -----	17
Figure 2.3-5: Mechanism of action of integrase inhibitors -----	18
Figure 2.3-6: Chemical structures of integrase inhibitors -----	18
Figure 2.3-7: Chemical structures of protease inhibitors -----	19
Figure 2.3-8: Mechanism of action of protease inhibitors -----	19
Figure 3.3-1: MT-4 cell culture -----	49
Figure 3.3-2: Development of cytopathic effects in MT-4 cells -----	51
Figure 3.3-3: Conversion of MTT to Formazan by oxidoreductase enzymes -----	52
Figure 4.3-1: Cytotoxicity of solvent fractions of <i>C. megalocarpus</i> -----	62
Figure 4.3-2: Anti-HIV activity of solvent fractions of three <i>C. megalocarpus</i> -----	62
Figure 4.3-3: Cytotoxic effect for solvent fractions for <i>C. macrostachyus</i> -----	66
Figure 4.3-4: Anti-HIV activity of solvent fractions of <i>C. macrostachyus</i> -----	66
Figure 4.3-5: Cytotoxic effect of solvent fractions of <i>C. dichogamus</i> -----	68
Figure 4.3-6: Anti-HIV activity of solvent fractions of <i>C. dichogamus</i> -----	69
Figure 4.4-1: Pure compounds isolated from <i>C. megalocarpus</i> -----	71
Figure 4.4-2: Key COSY, HMBC and NOESY correlations observed for 1 $\beta$ -Acetoxy-3 $\beta$ - chloro-5 $\alpha$ ,6 $\alpha$ -dihydroxycrotocascarin (Ermiasoid) (E37) -----	85
Figure 4.4-3: Cytotoxicity of ermiasolides isolated from <i>C. megalocarpus</i> -----	89

Figure 4.4-4: Anti-HIV activity of ermiasolides from <i>C. megalocarpus</i> -----	90
Figure 4.4-5: Concentration-response curves analysis for the anti-HIV activity of pure compounds isolated from <i>C. megalocarpus</i> . -----	91
Figure 4.4-6: Eudesmane type sesquiterpenes isolated from <i>C. megalocarpus</i> -----	92
Figure 4.4-7: Crotofolane diterpenoids isolated from <i>C. megalocarpus</i> -----	94
Figure 4.4-8: Cytotoxicity and antiviral activity values of E37 -----	94
Figure 4.4-9: Pure compounds isolated from <i>C. macrostachyus</i> -----	95
Figure 4.4-10: Cytotoxicity of pure compounds isolated from <i>C. macrostachyus</i> -----	108
Figure 4.4-11: Anti-HIV activity of pure compounds isolated from <i>C. macrostachyus</i> -----	108
Figure 4.4-12: Concentration-response curve analysis for the anti-HIV activity of pure compounds isolated from <i>C. macrostachyus</i> -----	109
Figure 4.4-13: Pure compounds isolated from <i>C. dichogamus</i> -----	110
Figure 4.4-14: Key COSY, NOESY and HMBC correlations for compound CD12a-----	114
Figure 4.4-15 Cytotoxicity of Crotoascarin $\omega$ (CD12a) (1)-----	119
Figure 4.4-16 Anti-HIV activity effects of Crotoascarin $\omega$ (1)-----	120
Figure 4.4-17. Ligand-protein intereaction of Nevirapine and crotoascarin $\omega$ (CD12a) with HIV-1 RT (PDB ID: 1JLB)-----	121
Figure 4.4-18. Ligand-protein interactions of atazanavir and crotoascarin $\omega$ (CD12a) with HIV-1 PR (PDB ID: 3EL9)-----	121
Figure 4.5-1: 2D and 3D visualization of the interaction of 11 $\beta$ -Acetoxy crotoascarin L (E24) with HIV-1 PR (3EL9) -----	126
Figure 4.5-2: 2D and 3D visualization of the interaction of Ermiasoid (E37) with HIV-1 PR (3EL9)-----	128
Figure 4.5-3: 2D and 3D visualization of interactions of crotoascarin K (E23) with HIV-1 PR (3EL9)-----	129
Figure 4.5-4: 2D and 3D visualization of the interaction of pinoresinol (E2) with HIV-1 PR (3EL9)-----	129
Figure 4.5-5: 2D and 3D visualization of the interactions of ermiasolide A (E12) with HIV-1 PR (3EL9)-----	130

## **LIST OF SCHEMES**

Scheme 3.2-1: Flow chart of liquid-liquid extraction of plant extracts-----45



## LIST OF ACRONYMS AND ABBREVIATIONS

ABC	Abacavir
ADMET	Absorption, Distribution, Metabolism, Excretion, and Toxicity
AIDS	Acquired Immune Deficiency Virus
ARV	Antiretroviral Drugs
AZT	Zidovudine
CDC	Center for Disease Control
COSY	Correlation Spectroscopy
DEPT	Distortionless Enhancement by Polarization Transfer
DMSO	Dimethyl sulfoxide
EACC	European Collection of Authenticated Cell Cultures
EBV	Epstein-Barr virus
EFV	Efavirenz
ELISA	Enzyme Linked Immunosorbent Assay
HMBC	Heteronuclear Multi Bond Correlation Spectroscopy
HRMS	High Resolution Mass Spectrometry
HSQC	Heteronuclear Single Quantum Coherence Spectroscopy
MTT	3-(4,5-dimethylthiazol-2-yl)-2,5-diphenyltetrazolium bromide
NACC	National AIDS Control Council
NVP	Nevirapine
PBS	Phosphate buffer saline
PMTCT	Prevention of Mother to child transmission
PrEP	Pre-exposure prophylaxis
TAM	Thymidine analogue mutations
TDF	Tenofovir
VMMC	Voluntary medical male circumcision

## LIST OF APPENDICES

Appendix 1	Mass Spectrum of 5 $\beta$ -hydroxy-8 $\alpha$ -methoxy eudesm-7(11)-en-12, 8-olide (ermiasolide A) (E12)-----	190
Appendix 2	<sup>1</sup> H NMR Spectra for 5 $\beta$ -hydroxy-8 $\alpha$ -methoxy eudesm-7(11)-en-12,8-olide (ermiasolide A) (E12)-----	191
Appendix 3	<sup>13</sup> C NMR Spectra for 5 $\beta$ -hydroxy-8 $\alpha$ -methoxy eudesm-7(11)-en-12, 8-olide (ermiasolide A) (E12)-----	192
Appendix 4	DEPT Spectrum for 5 $\beta$ -hydroxy-8 $\alpha$ -methoxy eudesm-7(11)-en-12, 8-olide (ermiasolide A) (E12)-----	193
Appendix 5	HSQCDEPT Spectra for 5 $\beta$ -hydroxy-8 $\alpha$ -methoxy eudesm-7(11)-en-12,8-olide (ermiasolide A) (E12)-----	194
Appendix 6	HMBC Spectrum for 5 $\beta$ -hydroxy-8 $\alpha$ -methoxy eudesm-7(11)-en-12, 8-olide (ermiasolide A) (E12)-----	195
Appendix 7	COSY Spectrum for 5 $\beta$ -hydroxy-8 $\alpha$ -methoxy eudesm-7(11)-en-12,8-olide (ermiasolide A) (E12)-----	196
Appendix 8	NOSEY Spectrum for 5 $\beta$ -hydroxy-8 $\alpha$ -methoxy eudesm-7(11)-en-12,8-olide (ermiasolide A) (E12)-----	197
Appendix 9	Mass Spectrum of 5 $\beta$ ,8 $\alpha$ -dihydroxy eudesm-7(11)-en-12,8-olide (ermiasolide B) (E22)-----	198
Appendix 10	<sup>1</sup> H NMR spectra of 5 $\beta$ ,8 $\alpha$ -dihydroxy eudesm-7(11)-en-12,8-olide (ermiasolide B) (E22)-----	199
Appendix 11	<sup>13</sup> C NMR spectra of 5 $\beta$ ,8 $\alpha$ -dihydroxy eudesm-7(11)-en-12,8-olide (ermiasolide B) (E22)-----	200
Appendix 12	DEPT spectrum of 5 $\beta$ ,8 $\alpha$ -dihydroxy eudesm-7(11)-en-12,8-olide (ermiasolide B) (E22)-----	201
Appendix 13	HSQCDEPT spectrum of 5 $\beta$ , 8 $\alpha$ -dihydroxy eudesm-7(11)-en-12,8-olide (ermiasolide B) (E22)-----	202
Appendix 14	HMBC spectrum of 5 $\beta$ ,8 $\alpha$ -dihydroxy eudesm-7(11)-en-12,8-olide (ermiasolide B) (E22)-----	203
Appendix 15	COSY spectrum of 5 $\beta$ , 8 $\alpha$ -dihydroxy eudesm-7(11)-en-12,8-olide (ermiasolide B) (E22)-----	204

Appendix 16	NOESY spectrum of 5 $\beta$ , 8 $\alpha$ -dihydroxy eudesm-7(11)-en-12,8-olide (ermiasolide B) (E22)-----	205
Appendix 17	Mass spectrum of 5 $\beta$ ,8H- $\beta$ -hydroxy eudesm-7(11)-en-12, 8-olide (ermiasolide C) (E17)-----	206
Appendix 18	<sup>1</sup> H NMR spectra of 5 $\beta$ ,8H- $\beta$ -hydroxy eudesm-7(11)-en-12, 8-olide (ermiasolide C) (E17)-----	207
Appendix 19	<sup>13</sup> C NMR spectra of 5 $\beta$ ,8H- $\beta$ -hydroxy eudesm-7(11)-en-12, 8-olide (ermiasolide C) (E17)-----	208
Appendix 20	DEPT spectrum of 5 $\beta$ ,8H- $\beta$ -hydroxy eudesm-7(11)-en-12, 8-olide (ermiasolide C) (E17)-----	209
Appendix 21	HSQCDEPT spectrum of 5 $\beta$ ,8H- $\beta$ -hydroxy eudesm-7(11)-en-12, 8-olide (ermiasolide C) (E17)-----	210
Appendix 22	HMBC spectrum of 5 $\beta$ ,8H- $\beta$ -hydroxy eudesm-7(11)-en-12, 8-olide (ermiasolide C) (E17)-----	211
Appendix 23	COSY spectrum of 5 $\beta$ ,8H- $\beta$ -hydroxy eudesm-7(11)-en-12, 8-olide (ermiasolide C) (E17)-----	212
Appendix 24	NOESY spectrum of 5 $\beta$ ,8H- $\beta$ -hydroxy eudesm-7(11)-en-12, 8-olide (ermiasolide C) (E17)-----	213
Appendix 25	Mass spectrum of 4H- $\alpha$ ,7H- $\alpha$ ,10 $\alpha$ -eudesm-11-en-5 $\beta$ -ol (E5) -----	214
Appendix 26	<sup>1</sup> H NMR spectrum of 4H- $\alpha$ ,7H- $\alpha$ ,10 $\alpha$ -eudesm-11-en-5 $\beta$ -ol (E5)-----	215
Appendix 27	<sup>13</sup> C NMR spectrum of 4H- $\alpha$ ,7H- $\alpha$ ,10 $\alpha$ -eudesm-11-en-5 $\beta$ -ol (E5)-----	216
Appendix 28	DEPT spectrum of 4H- $\alpha$ ,7H- $\alpha$ ,10 $\alpha$ -eudesm-11-en-5 $\beta$ -ol (E5)-----	217
Appendix 29	HSQCDEPT spectrum of 4H- $\alpha$ ,7H- $\alpha$ ,10 $\alpha$ -eudesm-11-en-5 $\beta$ -ol (E5)-----	218
Appendix 30	HMBC spectrum of 4H- $\alpha$ ,7H- $\alpha$ ,10 $\alpha$ -eudesm-11-en-5 $\beta$ -ol (E5)-----	219
Appendix 31	COSY spectrum of 4H- $\alpha$ ,7H- $\alpha$ ,10 $\alpha$ -eudesm-11-en-5 $\beta$ -ol (E5) -----	220
Appendix 32	NOSEY spectrum of 4H- $\alpha$ ,7H- $\alpha$ ,10 $\alpha$ -eudesm-11-en-5 $\beta$ -ol (E5) -----	221
Appendix 33	Mass spectrum of Crotoascarin K (E23) -----	222
Appendix 34	<sup>1</sup> H NMR spectrum of Crotoascarin K (E23)-----	223
Appendix 35	<sup>13</sup> C NMR spectrum of Crotoascarin K (E23) -----	224
Appendix 36	DEPT spectrum of Crotoascarin K (E23) -----	225
Appendix 37	HSQCDEPT spectrum of Crotoascarin K (E23) -----	226
Appendix 38	HMBC spectrum of Crotoascarin K (E23)-----	227
Appendix 39	COSY spectrum of Crotoascarin K (E23)-----	228

Appendix 40 NOESY spectrum of Crotoascarin K (E23)-----	229
Appendix 41 Mass spectrum of 11-acetoxy crotoascarin L (E24)-----	230
Appendix 42 <sup>1</sup> H NMR spectrum of 11-acetoxy crotoascarin L (E24) -----	231
Appendix 43 <sup>13</sup> C NMR spectrum of 11-acetoxy crotoascarin L (E24)-----	232
Appendix 44 DEPT spectrum of 11-acetoxy crotoascarin L (E24)-----	233
Appendix 45 HSQCDEPT spectrum of 11-acetoxy crotoascarin L (E24)-----	234
Appendix 46 HMBC spectrum of 11-acetoxy crotoascarin L (E24) -----	235
Appendix 47 COSY spectrum of 11-acetoxy crotoascarin L (E24) -----	236
Appendix 48 NOESY spectrum of 11-acetoxy crotoascarin L (E24) -----	237
Appendix 49 Mass spectrum of 1 $\beta$ -acetoxy-3 $\beta$ -chloro-5 $\alpha$ ,6 $\alpha$ -dihydroxycrotoascarin L (Ermiasoid) (E37) -----	238
Appendix 50 <sup>1</sup> H NMR spectrum of 1 $\beta$ -acetoxy-3 $\beta$ -chloro-5 $\alpha$ ,6 $\alpha$ -dihydroxycrotoascarin L (Ermiasoid) (E37) -----	239
Appendix 51 <sup>13</sup> C NMR spectrum in DMSO of 1 $\beta$ -acetoxy-3 $\beta$ -chloro-5 $\alpha$ ,6 $\alpha$ - dihydroxycrotoascarin L (Ermiasoid) (E37) -----	240
Appendix 52 <sup>13</sup> C NMR spectrum of 1 $\beta$ -acetoxy-3 $\beta$ -chloro-5 $\alpha$ ,6 $\alpha$ -dihydroxycrotoascarin L (Ermiasoid) (E37) -----	241
Appendix 53 DEPT spectrum of 1 $\beta$ -acetoxy-3 $\beta$ -chloro-5 $\alpha$ ,6 $\alpha$ -dihydroxycrotoascarin L (Ermiasoid) (E37) -----	242
Appendix 54 HSQCDEPT spectrum of 1 $\beta$ -acetoxy-3 $\beta$ -chloro-5 $\alpha$ ,6 $\alpha$ -dihydroxycrotoascarin L (Ermiasoid) (E37) -----	243
Appendix 55 HMBC spectrum of 1 $\beta$ -acetoxy-3 $\beta$ -chloro-5 $\alpha$ ,6 $\alpha$ -dihydroxycrotoascarin L (Ermiasoid) (E37) -----	244
Appendix 56 COSY spectrum of 1 $\beta$ -acetoxy-3 $\beta$ -chloro-5 $\alpha$ ,6 $\alpha$ -dihydroxycrotoascarin L (Ermiasoid) (E37) -----	245
Appendix 57 NOESY spectrum of 1 $\beta$ -acetoxy-3 $\beta$ -chloro-5 $\alpha$ ,6 $\alpha$ -dihydroxycrotoascarin L (Ermiasoid) (E37) -----	246
Appendix 58 <sup>1</sup> H NMR spectra of Pinoresinol (E2)-----	247
Appendix 59 HSQC spectrum of Pinoresinol (E2) -----	248
Appendix 60 HMBC spectrum of Pinoresinol (E2) -----	249
Appendix 61 COSY spectrum of Pinoresinol (E2) -----	250
Appendix 62 <sup>1</sup> H NMR spectra of 3 $\beta$ -Hydroxylup-20(29)-ene (lupeol) (E19)-----	251
Appendix 63 <sup>13</sup> C NMR spectra of 3 $\beta$ -Hydroxylup-20(29)-ene (lupeol) (E19)-----	252

Appendix 64 $^1\text{H}$ NMR spectra of 2-Methoxy benzyl benzoate (A5)-----	253
Appendix 65 $^{13}\text{C}$ NMR spectra of 2-Methoxy benzyl benzoate (A5) -----	254
Appendix 66 DEPT spectrum of 2-Methoxy benzyl benzoate (A5) -----	255
Appendix 67 HSQCDEPT spectrum of 2-Methoxy benzyl benzoate (A5)-----	256
Appendix 68 HMBC spectrum of 2-Methoxy benzyl benzoate (A5)-----	257
Appendix 69 COSY spectrum of 2-Methoxy benzyl benzoate (A5)-----	258
Appendix 70 $^1\text{H}$ NMR spectrum of Lupenone (A4b) -----	259
Appendix 71 $^{13}\text{C}$ NMR spectrum of Lupenone (A4b) -----	260
Appendix 72 DEPT spectrum of Lupenone (A4b) -----	261
Appendix 73 HSQCDEPT spectrum of Lupenone (A4b) -----	262
Appendix 74 HMBC spectrum of Lupenone (A4b)-----	263
Appendix 75 COSY spectrum of Lupenone (A4b)-----	264
Appendix 76 NOESY spectrum of Lupenone (A4b)-----	265
Appendix 77 $^1\text{H}$ NMR spectrum of Betulin (A19) -----	266
Appendix 78 $^{13}\text{C}$ NMR spectrum of Betulin (A19) -----	267
Appendix 79 DEPT spectrum of Betulin (A19) -----	268
Appendix 80 HSQCDEPT spectrum of Betulin (A19) -----	269
Appendix 81 HMBC spectrum of Betulin (A19) -----	270
Appendix 82 COSY spectrum of Betulin (A19)-----	271
Appendix 83 NOSEY spectrum of Betulin (A19)-----	272
Appendix 84 $^1\text{H}$ NMR spectrum of Lupeol acetate (A11) -----	273
Appendix 85 $^{13}\text{C}$ NMR spectrum of Lupeol acetate (A11) -----	274
Appendix 86 DEPT spectrum of Lupeol acetate (A11)-----	275
Appendix 87 HSQCDEPT spectrum of Lupeol acetate (A11)-----	276
Appendix 88 HMBC spectrum of Lupeol acetate (A11) -----	277
Appendix 89 COSY spectrum of Lupeol acetate (A11) -----	278
Appendix 90 NOSEY spectrum of Lupeol acetate (A11) -----	279
Appendix 91 $^1\text{H}$ NMR spectrum of Lupeol (A7) -----	280
Appendix 92 $^{13}\text{C}$ NMR spectrum of Lupeol (A7) -----	281
Appendix 93 DEPT spectrum of Lupeol (A7)-----	282
Appendix 94 HSQCDEPT spectrum of Lupeol (A7) -----	283
Appendix 95 HMBC spectrum of Lupeol (A7) -----	284
Appendix 96 COSY spectrum of Lupeol (A7)-----	285

Appendix 97	NOESY spectrum of Lupeol (A7)	286
Appendix 98	<sup>1</sup> H NMR Spectra for Sitosterol (A15) and Stigmasterol (A16)	287
Appendix 99	<sup>1</sup> H NMR Spectra for CD1 (mixture of Dihydroconiferyl acetate (CD1a) and (4-Hydroxy-3-methoxyphenyl)-propyl benzoate (CD1b))	288
Appendix 100	<sup>13</sup> C NMR Spectra for CD1 (mixture of Dihydroconiferyl acetate (CD1a) and (4-Hydroxy-3-methoxyphenyl)-propyl benzoate (CD1b))	289
Appendix 101	DEPT Spectra for CD1 (mixture of Dihydroconiferyl acetate (CD1a) and (4-Hydroxy-3-methoxyphenyl)-propyl benzoate (CD1b))	290
Appendix 102	HSQCDEPT Spectra for CD1 (mixture of Dihydroconiferyl acetate (CD1a) and (4-Hydroxy-3-methoxyphenyl)-propyl benzoate (CD1b))	291
Appendix 103	HMBC Spectra for CD1 (mixture of Dihydroconiferyl acetate (CD1a) and (4-Hydroxy-3-methoxyphenyl)-propyl benzoate (CD1b))	292
Appendix 104	COSY Spectra for CD1 (mixture of Dihydroconiferyl acetate (CD1a) and (4-Hydroxy-3-methoxyphenyl)-propyl benzoate (CD1b))	293
Appendix 105	NOESY Spectra for CD1 (mixture of Dihydroconiferyl acetate (CD1a) and (4-Hydroxy-3-methoxyphenyl)-propyl benzoate (CD1b))	294
Appendix 106	<sup>1</sup> H NMR Spectra for crotonoscarin ω (CD12a)	295
Appendix 107	<sup>13</sup> C NMR Spectra for crotonoscarin ω (CD12a)	296
Appendix 108	DEPT Spectra for crotonoscarin ω (CD12a)	297
Appendix 109	HSQCDEPT Spectra for crotonoscarin ω (CD12a)	298
Appendix 110	COSY Spectra for crotonoscarin ω (CD12a)	299
Appendix 111	NOESY Spectra for crotonoscarin ω (CD12a)	300
Appendix 112	<sup>1</sup> H NMR Spectra for β-Oplopanone (CD12b)	301
Appendix 113	<sup>13</sup> C NMR Spectra for β-Oplopanone (CD12b)	302
Appendix 114	DEPT Spectra for β-Oplopanone (CD12b)	303
Appendix 115	HSQCDEPT Spectra for β-Oplopanone (CD12b)	304
Appendix 116	HMBC Spectra for β-Oplopanone (CD12b)	305
Appendix 117	COSY Spectra for β-Oplopanone (CD12b)	306
Appendix 118	NOESY Spectra for β-Oplopanone (CD12b)	307
Appendix 119	<sup>1</sup> H NMR CD6a and CD6b (Sitosterol and stigmasterol)	308

## PUBLICATIONS

1. **Terefe, E. M.**, Okalebo, F. A., Derese, S., Muriuki, J., Rotich, W., Mas-Claret, E., Sadgrove, N., Padilla-González, G. F., Prescott, T. A. K., Siddique, H., & Langat, M. K. (2022). Constituents of *Croton megalocarpus* with Potential Anti-HIV Activity. *Journal of Natural Products*. <https://pubmed.ncbi.nlm.nih.gov/35709365/>
2. **Terefe, E. M.**, Okalebo, F. A., Derese, S., Langat, M. K., Mas-Claret, E., Aljarba, N. H., Alkahtani, S., Batiha, G. E.-S., Ghosh, A., El-Masry, E. A., & Muriuki, J. (2022). In vitro anti-HIV and cytotoxic effects of pure compounds isolated from *Croton macrostachyus* Hochst. Ex Delile. *BMC Complementary Medicine and Therapies* 2022 22:1, 22(1), 1–10. <https://pubmed.ncbi.nlm.nih.gov/35705943/>
3. **Terefe E. M.**, Okalebo F. A., Derese S., Muriuki J., Amuhaya E. K., Munyendo L. W., Janapati Y., Obila J., Mosweta J. (2022). Cytotoxicity and antiretroviral activity of the leaf and stem bark extracts of *Croton macrostachyus*. *Pharmaceutical Journal of Kenya*, 26(1), 2022. <https://psk.or.ke/journals/article-98>
4. **Terefe, E. M.**, Okalebo, F. A., Derese, S., Batiha, G. E.-S., Youssef, A., Alorabi, M., & Muriuki, J. (2022). Cytotoxicity and anti-HIV activities of extracts of the twigs of *Croton dichogamus* Pax. *BMC Complementary Medicine and Therapies* 2022 22:1, 22(1), 1–8. <https://pubmed.ncbi.nlm.nih.gov/35216601/>
5. **Terefe, E. M.**; Okalebo, F. A.; Derese, S.; Muriuki, J.; Batiha, G. E.-S. In Vitro Cytotoxicity and Anti-HIV Activity of Crude Extracts of *Croton Macrostachyus*, *Croton Megalocarpus* and *Croton Dichogamus*. *J. Exp. Pharmacol.* **2021**, 13, 971–979. <https://pubmed.ncbi.nlm.nih.gov/35221732/>

# CHAPTER ONE

## INTRODUCTION

### 1.1. Background Information

Since the outbreak of the human immunodeficiency virus (HIV) pandemic, globally, more than 75.7 million people have been infected with HIV, resulting in more than 33 million death due to Acquired Immunodeficiency Syndrome (AIDS)-related diseases (UNAIDS, 2020). Currently, 38 million people live with the virus, out of which 54% (20.7 million) live in Southern and East African regions. In 2019, over 1.7 million people were infected by the virus (UNAIDS, 2020). In that year, the global death caused by the epidemic had reached more than half a million, with more than 300,000 of these deaths occurring in Southern and East Africa. Globally, among the 38 million people living with HIV, more than 10 million people did not have access to antiretroviral treatment as of the end of June 2020. Thus, more than 25% (5 million) of Southern and East African people do not have access to the treatment (UNAIDS, 2020).

Substantial advances have been made in antiretroviral therapy (ART) after the discovery of zidovudine in 1987 (McLeod & Hammer, 1992; Sperling, 1998a). At that time, zidovudine was prescribed as monotherapy for only patients with advanced, symptomatic disease as a five times daily dose. In mid-1996, it was discovered that antiretroviral drugs are far more effective when three or more are taken simultaneously (Sperling, 1998b). This combination therapy (comprising at least three ARV agents) has shown a significant decline in viral replication and improvement in patients' quality of life (Erik, 2010).

Although ART has contributed significantly to reducing death due to HIV, toxicities of the drugs, problems with adherence related to lifelong therapy, and drug resistance are challenging problems for the success of HIV care and treatment (Montessori *et al.*, 2004). In this study, we explored the anti-HIV activity of three plants from the genus *Croton*.

### 1.2. Statement of the problem

HIV/AIDS has a detrimental economic, psychosocial, and health-related impact on countries, households, and individuals around the world. As the number of people infected with HIV rises, medical treatment costs rise, and national resources shift to the HIV/AIDS program (World Health Organization, 2016). Furthermore, HIV-infected individuals are susceptible to a variety of opportunistic infections (OI), which can reduce their productivity and shorten their



lives and also co-administration of other drugs to treat OI's might result in drug interactions that can impair ARV therapy or induce serious side effects (Narayan *et al.*, 2013).

The development of drug resistance has also posed a great challenge for treating clients, since many cases where patients are not responding even to second-line regimens. Moreover, this problem continues to be a danger to the worldwide struggle to end the epidemic by 2030 (UNAIDS, 2016). Hence, there is a need to discover novel drugs with antiretroviral activity. One of the systematic approaches to tackle these challenges is to discover new drugs by identifying bioactive antiretroviral compounds from natural products. *Croton* species have gained attention by providing different bioactive phytochemicals used to treat bacterial and viral infections (Saslis-Lagoudakis *et al.*, 2012). This study evaluated the antiretroviral activity of *C. macrostachyus*, *C. megalocarpus*, and *C. dichogamus* using *in vitro* and *in silico* approaches.

### **1.3. Objectives**

#### **1.3.1. General Objective**

The main objective of this research was to evaluate the *in vitro* and *in silico* antiretroviral activity of *C. macrostachyus*, *C. megalocarpus*, and *C. dichogamus* against HIV.

#### **1.3.2. Specific Objectives**

The specific objectives of the research were to:

1. Evaluate the cytotoxicity and antiretroviral activity of crude extracts from *C. macrostachyus*, *C. megalocarpus*, and *C. dichogamus*
2. Evaluate the cytotoxicity and antiretroviral activity of solvent fractions of *C. macrostachyus*, *C. megalocarpus*, and *C. dichogamus*
3. Isolate pure compounds with a potential antiretroviral activity using bioassay-guided fractionation
4. Demonstrate the interaction of isolated pure compounds with HIV enzymes by using *in vitro* assays and *in silico* molecular docking approaches

### **1.4. Justification and significance of the study**

There is a need to identify local alternatives, less expensive and less toxic drugs for the treatment of HIV. As herbs are the primary source of drugs, the search for new antiretroviral compounds can start from herbal medicines used by traditional healers as a remedy for HIV and related opportunistic infections. The plants included in this study, *C. macrostachyus*, *C.*

*megalocarpus*, and *C. dichogamus*, are used by herbal practitioners in Africa. These plants have promising antibacterial, antifungal, antiviral and anticancer effects (Singh, 2018; Obey *et al.*, 2016a; Al-Asmari *et al.*, 2015).

Different parts of *C. macrostachyus*, *C. megalocarpus*, and *C. dichogamus* are used as herbal medicine by HIV patients for the treatment of pneumonia (Kamau *et al.*, 2016), respiratory problems (Muthee *et al.*, 2011; Njoroge *et al.*, 2006), diabetes (Keter & Mutiso, 2012), wounds (Kamau *et al.*, 2016), and as a purgative (Degu *et al.*, 2016).

The *Croton* genus has gained the attention of many researchers for its potential source of bioactive compounds against HIV. Ravanelli *et al.*, (2016) have shown that alkaloids isolated from *C. echinocarpus* leaves have significant *In vitro* anti-HIV activity by inhibiting the HIV-1 reverse transcriptase enzyme. Tietjen *et al.*, (2016b) reported that *C. megalobotrys* is widely used in Botswana to treat HIV, diarrhea, loss of appetite, and stomach problems.

Considering the wide medicinal use of these plants by HIV-positive patients, this research evaluated the effect of the crude and solvent fractions in inhibiting viral replication. It also investigated the anti-HIV activity of the isolated pure compounds in an *in vitro* and *in silico* experiments. The findings of this study could lead to the development of new antiviral agents that are less toxic and more efficacious.

## CHAPTER TWO

### LITERATURE REVIEW

#### 2.1. Literature review on HIV

##### 2.1.1. History of HIV Pandemic

In 1981, the first case of HIV/AIDS was identified (CDC, 1981). It was discovered two years later that HIV was the cause of the syndrome (Barré-Sinoussi *et al.*, 1983; Gallo *et al.*, 1983; Gottlieb *et al.*, 1981). HIV is the cause of the current epidemic (Heeney *et al.*, 2006; Heuverswyn *et al.*, 2006). HIV comprises four genetically distinct groups, namely M, N, O, and P (Sharp & Paul, 2011). Group M is further classified into nine subtypes/clades (A to D, F to H, J, and K) and is responsible for nearly all human infections worldwide (Sharp & Paul, 2011). In terms of antiretroviral medication, multiple studies demonstrate that patients infected with distinct clades of group M virus had similar responses to antiretroviral therapy. However, the diversity of the virus is a central problem in the design of an HIV vaccine (Walker & Burton, 2008).

##### 2.1.2. HIV Epidemiology

Sexual intercourse is the main route for the transmission of HIV. Other transmission routes include blood transfusion, vertical transmission from mother to child, and percutaneous exposure (Capriotti, 2018; Fettig *et al.*, 2014; Fox & Fidler, 2010; Gelmon *et al.*, 2009; CDC, 2006). Due to ongoing transmission and new HIV infection, as shown in **Table 2.1-1**, in 2019, approximately 0.7 million people died, with 1.7 million new HIV infections (UNAIDS, 2020).

##### 2.1.1. HIV-1 Structure and function

The human immune deficiency virus belongs to the family of retroviridae, the subfamily Lentivirinae and the genus Lentiviridae. It uses RNA as genetic material (Sharp & Paul, 2011). Viruses are simple in Structure and cannot replicate (Mcgilvray & Willis, 2004) by themselves and thus require the components of other cells for replication (require host cells to replicate). As shown in **Figure 2.1-1**, HIV has a spherical shape consisting of two single-stranded ribonucleic acids (RNAs) and three enzymes enclosed by an envelope (Sundquist & Kräusslich, 2012; Buchschacher, 2003).

Table 2.1-1: HIV Epidemiology in the world and Africa (UNAIDS, 2020)

Key Indicators	Global data (millions)	Eastern & Southern Africa (millions)	Western & Central Africa (millions)	Middle East & Northern Africa
Adult and children Living with HIV	38.0 [31.6– 44.5]	20.7 [18.4–23.0]	4.9 [3.9– 6.2]	240,000 [170,000–400,000]
Adult and children newly infected with HIV	1.7 [1.2– 2.2]	0.73 [0.58–0.94]	0.24[0.15–0.39]	20,000 [11,000– 38,000]
Adult and child deaths due to AIDS	0.69 [0.5– 0.97]	0.3 [0.23– 0.39]	0.14 [0.1–0.21]	8000 [4900–14, 000]

The HIV-1 genome comprises 9 genes that code for 15 viral proteins (Frankel & Young, 1998). The structural genes include *gag* (group-specific antigen), *pol* (polymerase), and *env* (envelope) (**Figure 2.1-2**). Accessory genes include *vif*, *vpr*, *vpu*, and *nef*. They generally modulate host responses to the virus; two regulatory genes, *tat*, and *rev* regulate the replication cycle (Strebel, 2013; Strauss & Strauss, 2008).

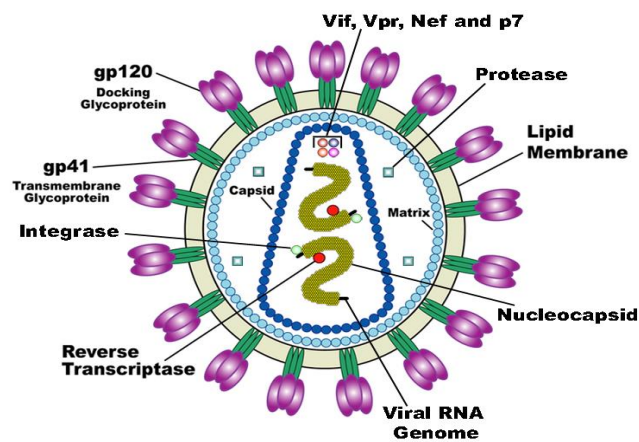
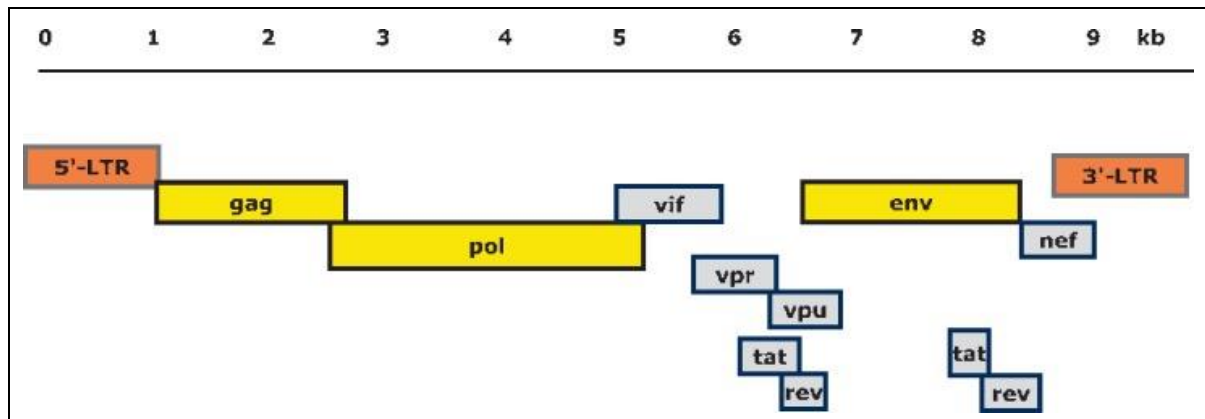


Figure 2.1-1: HIV structure (Altmann, 2010)

The polymerase gene (*pol*) encodes Pr160GagPol. Pr160GagPol is cleaved into protease (PR), reverse transcriptase (RT), and integrase (IN) by the viral protease (Freed, 2001). The *gag* gene produces four structural proteins: p24 (viral capsid), p6 and p7 (nucleocapsid proteins), and p17 (viral matrix) (Adamson & Freed, 2007; Freed, 1998).



**Figure 2.1-2: Structure and organization of the HIV-1 genome**

(Rainer Seitz, 2016).

The *env* gene encodes gp160 polyprotein precursor. Sundquist & Kräusslich, (2012) and Buchschacher, (2003), found that the glycoproteins gp 120 and gp 41 are made from gp 160. The gp120 protrudes from the envelope's surface, making it easier to adhere to CD4. In addition, the viral lipid envelope surrounds an internal protein layer called the matrix (p17), which is derived from the *gag* polyprotein (p55) following proteolytic processing and is anchored to the internal surface of the virus envelope (Aloia *et al.*, 1993; Checkley *et al.*, 2011). As a result, targeting viral proteins and enzymes is the primary strategy adopted to develop ARVs currently used to treat HIV-1 infection.

## 2.1.2. HIV Lifecycle

### 2.1.4.1. Attachment and Fusion

CD4 T lymphocytes and macrophages are primary targets of HIV infection (Douek *et al.*, 2002). **Figure 2.1-3** shows that a conformational change on gp120 aids in binding the coreceptors, CCR5 or CXCR4 (Engelman & Cherepanov, 2012). This binding induces a conformational change on gp41 resulting in membrane fusion where the virus is internalized by endocytosis (Miyachi *et al.*, 2009). Then, viral components are released to the cytosol of the host cell (Chan *et al.*, 1997; Esté & Telenti, 2007).

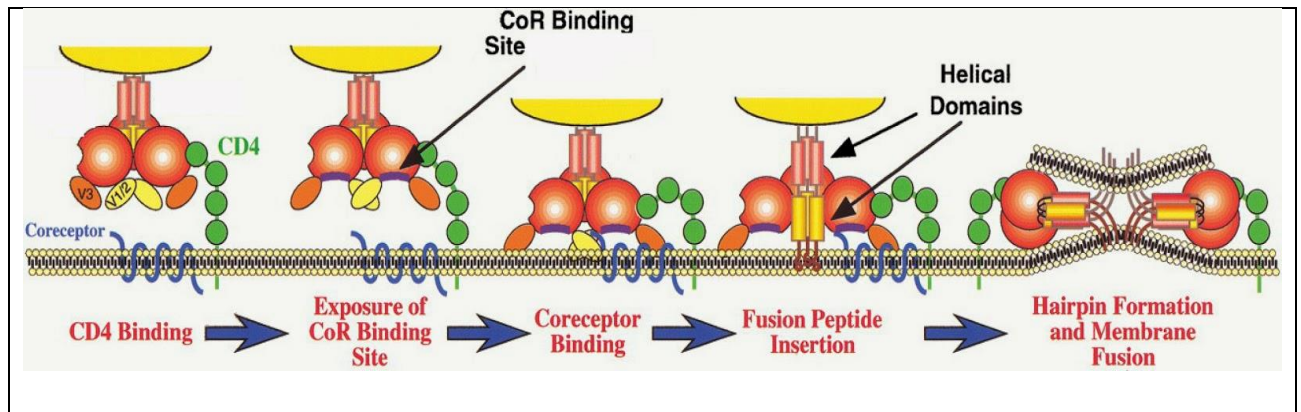


Figure 2.1-3: Attachment and Fusion of HIV

#### 2.1.4.2. Uncoating and Reverse Transcription

Inside the cytoplasm, HIV releases its RNA and enzymes (RT, IN, and PR) through a process termed uncoating (Miyauchi *et al.*, 2009; Fassati & Goff, 2001). Then, the RT enzyme performs the reverse transcription of viral RNA through its three domains/subunits in three consecutive steps, including the conversion of ssRNA to ssDNA (by reverse transcriptase domain), conversion of ssDNA to dsDNA (by polymerase domain), and final degradation of the prior RNA template (by RNase H domain) (Cimarelli & Darlix, 2014). The RT enzyme's lack of endonuclease activity has contributed to a high rate of mutation and is responsible for primary resistance to ARVs (Schinazi *et al.*, 2013; Menéndez-Arias, 2009).

#### 2.1.4.3. Integration

As shown in **Figure 2.1-4**, integration takes place once the reverse transcription process is completed, and a preintegration complex (including the integrase, proteins, cellular proteins, and viral dsDNA) is formed in the cytosol and translocated to the nucleus with the aid of host proteins such as transportin-SR2 (Miller *et al.*, 1997). Then, dsDNA is integrated into the host chromosomal site with active transcription by the enzyme integrase (Wang *et al.*, 2007).

#### 2.1.4.4. Transcription and replication

The host cell molecular machinery performs the transcription and replication of proviral DNA, DNA-dependent RNA polymerase II (pol II) (**Figure 2.1-4**). First, host pol II and viral transcription activator (tat) is involved in the transcription process (Carine, Sophie & Alessandro, 2013). Then, post-translational modifications are performed once the viral RNA is made (Karn & Stoltzfus, 2012). Finally, the enzyme protease cleaves gag and Gag-pol polyproteins, which facilitates the assembly and formation of mature infectious virions (Kohl *et al.*, 1988).

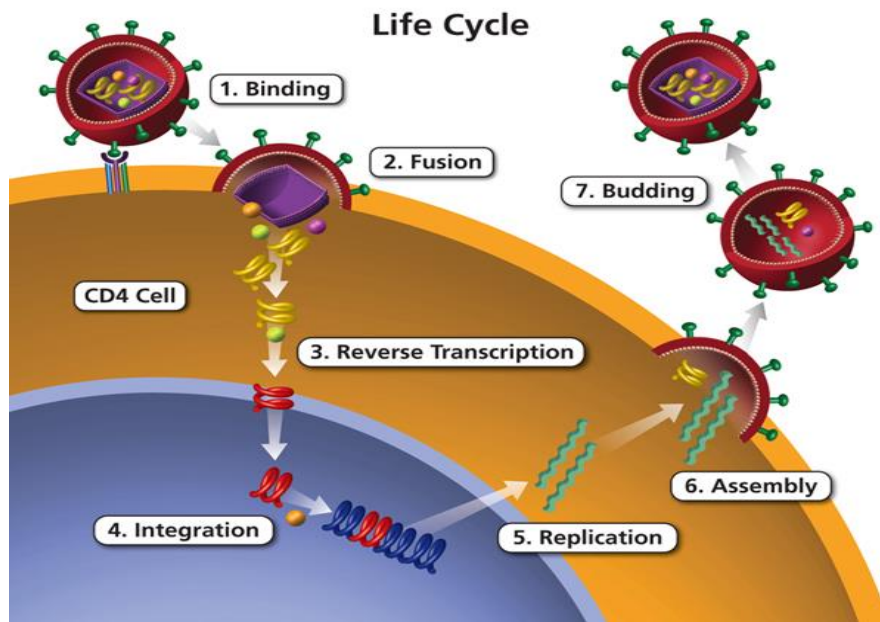


Figure 2.1-4: Life cycle of HIV  
(AIDS info.nih.gov, 2018)

### 2.1.3. Pathogenesis and Natural History of HIV

Indirect and direct mechanisms of injury underlie the pathogenesis of HIV infection. Indirect injury is associated with immune suppression leading to opportunistic infections. HIV affects all elements of the immune system. CD4 depletion occurs through syncytium formation, apoptosis, and autoimmunity (Hazenberg *et al.*, 2003; Scheller & Jassoy, 2001).

The depletion of CD4 occurs due to the elimination of HIV-infected cells by virus-specific immune responses, loss of plasma membrane integrity because of viral budding, and interference with cellular RNA processing (Brenchley *et al.*, 2004; Grossman *et al.*, 2002). Furthermore, HIV indirectly causes a decrease in CD4 cell count by inducing cytomorphological changes (cytopathic effects), such as syncytium & plaque formation, cell transformation or lysis, apoptosis, and autoimmunity. Thus, not only does the virus destroy and disrupt the immune system, but it can also manipulate the immune system to its replicative advantage.

A decline in immune status parallels the decline in CD4 number and function, which limits the immune responses to intracellular infections and malignancy, resulting in the occurrence of different opportunistic infections (Bowen *et al.*, 2016; Capriotti, 2018; Gray & Cohn, 2013; Ismail & Lee, 2011; Miceli *et al.*, 2011; Tan *et al.*, 2012). HIV also causes direct injury to different body parts by attacking target cells. For example, it causes encephalopathy and peripheral neuropathy (Evans *et al.*, 2011); it causes HIV-associated nephropathy (Wyatt

& Klotman, 2009). In addition, HIV causes cardiomyopathy (Barbaro, 2005), hypogonadism (Ashby *et al.*, 2014; Rochira & Guaraldi, 2014), dysmotility, and malabsorption (Nemechek *et al.*, 2000).

HIV infection follows the following stages of progression: primary HIV infection, asymptomatic stage/clinical latent stage, and AIDS. **Figure 2.1-5** shows that the initial stage following HIV infection is called primary HIV infection. Patients develop nonspecific ‘flu-like symptoms during this stage, which can not be used to directly diagnose HIV infection because the symptoms are nonspecific. These symptoms include fever, fatigue, pharyngitis, lymphadenopathy, and rash (Maartens *et al.*, 2014; Winslow & Kerdel, 2015).

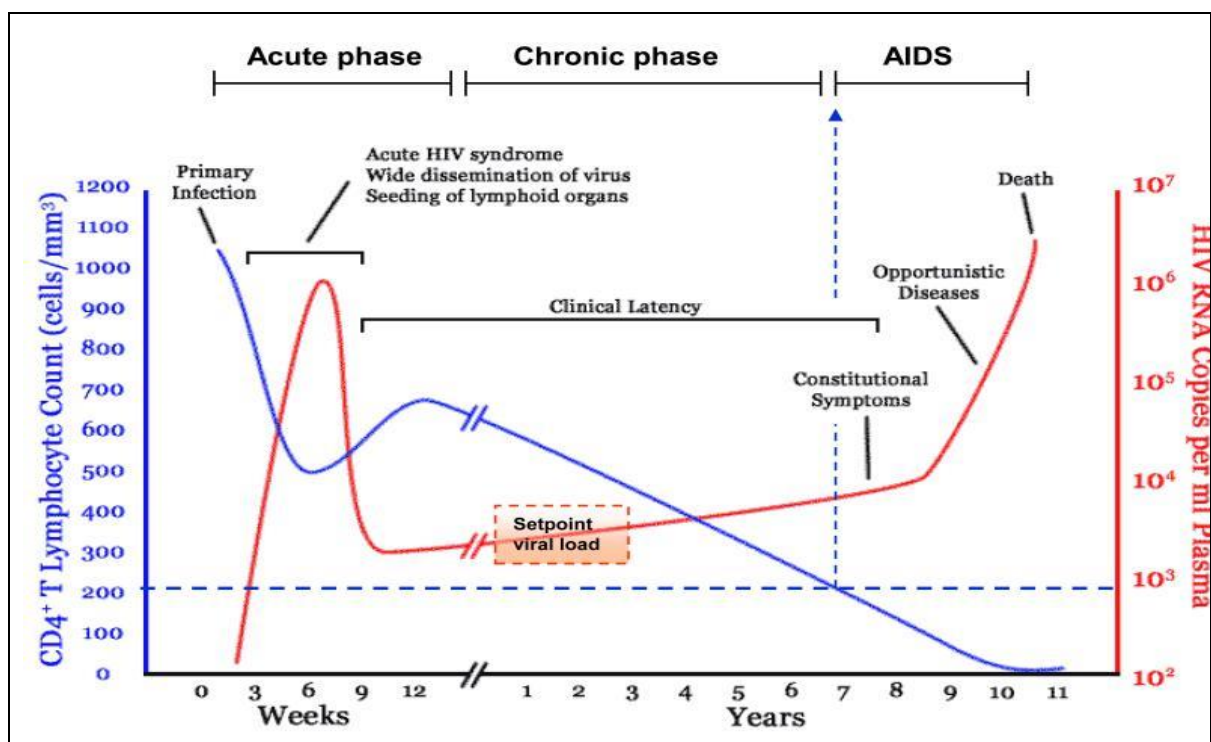


Figure 2.1-5: Stages of HIV infection (An & Winkler, 2010)

During primary infection, the patient could test negative for HIV-specific antibodies despite the presence of infection (Overbaugh & Morris, 2012). Thus, antibody testing should be repeated after 3 months. This stage is called the window period and is characterized by a very high viral load signifying extreme infectivity despite false-negative antibody results (Daar *et al.*, 2008; Rangsin *et al.*, 2004). Clinical management of patients during this time includes symptomatic treatment, counseling for risk reduction, and repeat antibody testing. Patients are most likely to transmit HIV during the early stage of infection (Herbert *et al.*, 2014). The second stage is termed the asymptomatic stage/latent infection. The infected individual may not show symptoms that could last up to 10 years until it presents with constitutional symptoms



defining AIDS. Then, the individual's immune system declines while the replication of the virus continues. Finally, after 8-10 years, various opportunistic infections manifest as AIDS (Melhuish & Lewthwaite, 2018; Sabin & Lundgren, 2013).

## **2.2. Molecular biology of retroviral enzymes**

### **2.2.1. Reverse transcriptase (RT)**

Reverse transcriptase is encoded by a gene called *pol*, which is found on the *gag* gene in all retroviruses (Götte *et al.*, 1999). The viral protease cleaves a Gag-Pol polyprotein to generate HIV reverse transcriptase (Hughes, 2014). Reverse transcriptase in the form of a heterodimer consists of two subunits: p66 and p51. The p66 subunit is 560 amino acids long, while p51 comprises the first 440 amino acids of p66 (di Marzo Veronese *et al.*, 1986; Lightfoote *et al.*, 1986; Seniya *et al.*, 2015).

RNase H and Polymerase are the two domains that make up the p66 subunit. Depending on the nucleic acid substrate, the active sites of RNase H and polymerase consist of 17 to 18 base pairs apart along with the nucleic acid (Jacobo-Molina *et al.*, 1993; Sarafianos *et al.*, 2001). The polymerization is proceeded by three aspartic acid residues (Asp-110, Asp-185, and Asp-186) that help in the position of two divalent metal ions ( $Mg^{+2}$ ) (Götte *et al.*, 1999; Hughes, 2014). In addition, the active site of RNase H contains four amino acid residues (Asp-443, Glu-478, Asp-498, and Asp-549) that help to place two  $Mg^{+2}$  ions in a way that they do not form close contact with the RNA strand, that's why RNase H is unable to break the nucleotide (Gao *et al.*, 1998; Ghosh *et al.*, 1996; Powell *et al.*, 1997).

The NNRTI pocket is composed of hydrophobic and hydrophilic residues. The hydrophobic residues are (Tyr-181, Tyr-188, Phe-227, Trp-229, Tyr-232, and Tyr-318 of p66) while the hydrophilic residues are (Lys-101, Lys-103, Ser-105, Asp-192, Glu-224 and His-235 of p66 and Glu-138 of p51) (Sluis-Cremer *et al.*, 2004). Thus, the solvent-accessible entrance is formed by Leu-100, Lys-101, Lys-103, Val-179, Tyr-181, and Glu-138 (**Figure 2.2-1**).

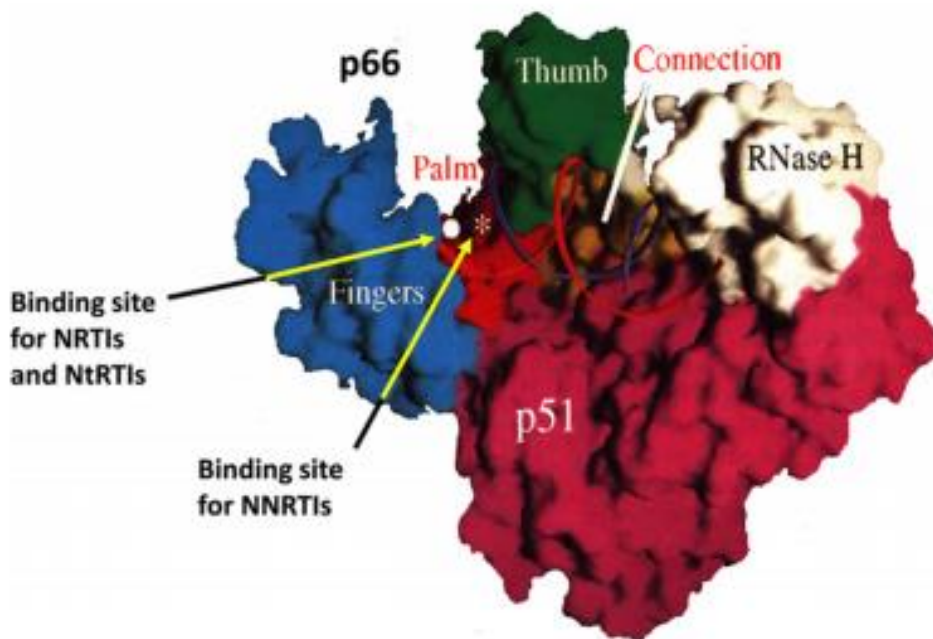


Figure 2.2-1: The NRTIs and NtRTIs binding sites with HIV reverse transcriptase along with the NNRTIs binding site (Jacobo-Molina *et al.*, 1993)

### 2.2.2. HIV Integrase

HIV integrase is a polynucleotide transferase protein with a molecular weight of 32 kDa. As depicted in **Figure 2.2-2**, integrase is made up of 3 structural and functional domains: a zinc-binding domain (N-terminal), a catalytic domain (core), and a DNA-binding domain (C-terminal). The N-terminal (residues 1–50) contains a zinc-binding HHCC motif that promotes the production of tetramers, which are the enzyme's active form (Hajimahdi & Zarghi, 2016; Zheng *et al.*, 1996). The C-terminal domain (CTD) binds to DNA in a nonspecific manner consisting of amino acids from 213 to 288. The catalytic domain (residues 50 to 212) has a highly conserved catalytic triad of DDE motif, which coordinates divalent metal ions ( $Mn^{+2}$  or  $Mg^{+2}$ ) and contains residues Asp-64, Asp-116, and Glu-152 (Kulkosky *et al.*, 1992).

For activity, integrase, like most nucleotide transferase enzymes, needs two divalent metal ions bound in the active site (Quashie *et al.*, 2012). Mutagenesis of these residues has been observed to fully eliminate all catalytic activity (Gerton *et al.*, 1998). The phosphodiester cleavage and bond formation processes catalyzed during the integration sequence require these divalent metal ions. According to some research, these metal cofactors are divalent magnesium ions (Ding *et al.*, 1995; Hsiou *et al.*, 1996). The catalytic domain includes the enzyme active

site, although the zinc-binding and DNA binding domains are required for full functional activity (Engelman *et al.*, 1993)

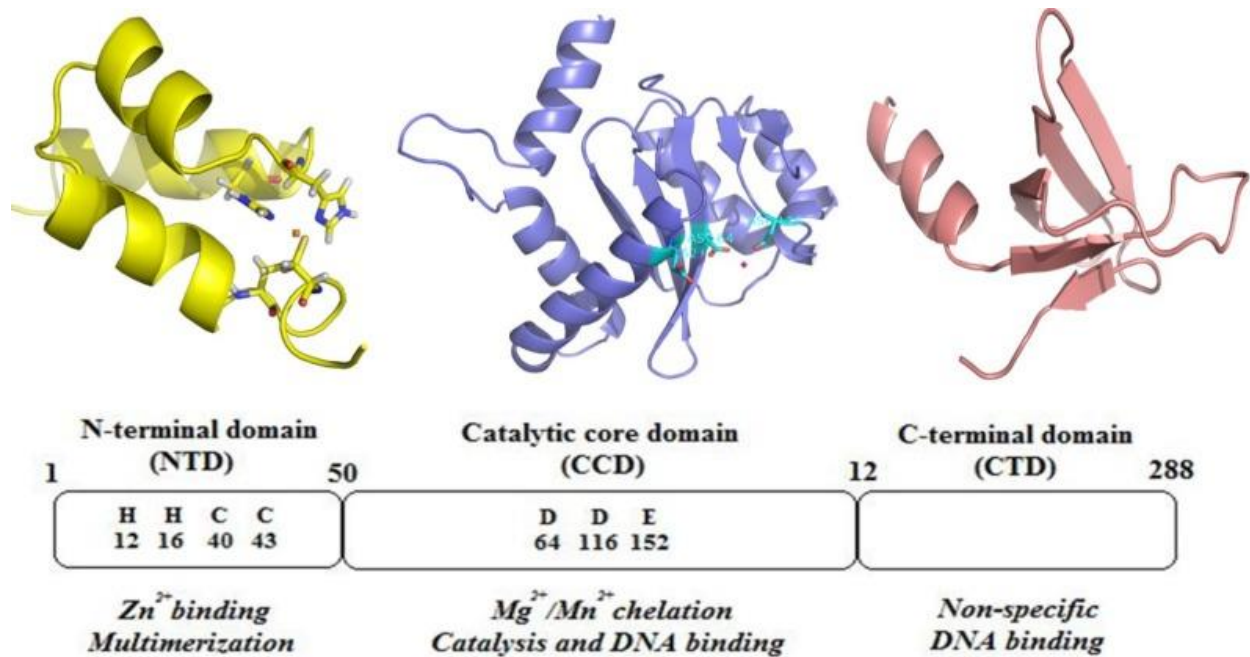


Figure 2.2-2: Structural domains of integrase IN (Hajimahdi & Zarghi, 2016)

### 2.2.3. HIV Protease

The HIV protease enzyme is a symmetrical dimer of two identical protein units, each consisting of 99 amino acids. Each subunit of the homodimer protein contains a catalytic aspartic acid Asp-25. Thus, the amino acid sequence of HIV protease is PQITLWQRPLVTIKIGGQLKEALLDTGADDTVLEEMSLPGRWPKMIGGIGGFIKVR QYDQILIEICGHKAIGTVLVGPTPVNIIGRNLLTQIGCTLNF (Ishima *et al.*, 2001). The amino acids Asp-25, Thr-26, and Gly-27 are located on the floor of the active site and provide a flap to act as the ceiling (Coop, 2019). During virion maturation and retrovirus multiplication, the enzyme cleaves various peptide bonds in viral polypeptides, including gag, gag-pol, and polyproteins, but, crucially, it cleaves bonds between proline and an aromatic residue (phenylalanine or tyrosine) (**Figure 2.2-3**). As the viral infectivity depends on protease enzyme activity, it is a potential target for anti-AIDS drugs research (Lv *et al.*, 2015).

The confirmation of the flexible region, which can be open, semi-open, or closed, helps the substrate enter the active site (Hornak *et al.*, 2006). In addition, the intermolecular bonding between the two subunits helps to stabilize the subunits. Most of the protease interface is made up of the four anti-parallel beta-strands (Sluis-Cremer & Tachedjian, 2002). As shown in

**Figure 2.2-3**, the active site has eight binding subsites (S1, S2, S3, S4, S4', S3', S2', and S1') that bind to the P1, P2, P3, P4, P4', P3', P2', and P1' residues of an octa-peptide substrate. The Phe-Pro or Tyr-Pro sequences are recognized by HIV-1 protease as retrovirus-specific cleavage sites (Andersson *et al.*, 2003).

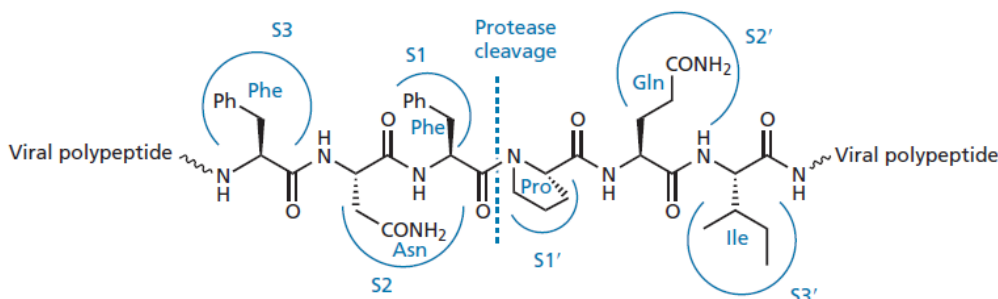


**Figure 2.2-3: Structure of the substrate and the binding subsites (Coop, 2019).**

The S1 subsite is relatively large and hydrophobic and contains Ile-50, Ile-84, Val-82, Thr-80, and Pro-81 (Figure 2.2-5). The S2 subsites are relatively small and hydrophobic compared with the S4 and S3 subsites and are predicted to accommodate smaller hydrophobic P2 residues (Bhatarai & Garg, 2008). The S2 subsite contains residues like Asp-29, Asp-30, Ala-28, Ile-47, Gly-48, and Ile-50. The S3 subsite is usually large and, similar to S4, is partly exposed to solvent at the enzyme's surface. The S3 subsites of HIV-1 contain residues like Arg-8, Gly-48, Leu-23, Val-82, Thr 80, and Pro-81 (Thr-80' and Pro-81' are part of S3 and S1 subsites). The S4 subsite is close to the protein surface and is more hydrophobic (**Figure 2.2-4**). The residues at subsite S4 are Asp-30, Met-46, Ile-47, Gly- 48, and Gln-58 (Babine & Bender, 1997; Bhatarai & Garg, 2008).

The aspartic acids Asp-25 and Asp-25' on the floor of the active site are involved in the catalytic mechanism (Coop, 2019). Most of the inhibitors are designed to imitate the substrate transition state of HIV protease. The inhibitor's OH group forms hydrogen bonds with the COOH group of Asp-25 and Asp-25' in the protease active site residues. Therefore, the residues of HIV protease that interact with the inhibitors, such as Gly-27, Asp-29, Asp-30, and Gly-48, are highly conserved. The mutations that accumulate the drug resistance affect the structure of HIV protease, resulting in treatment failure (Lv *et al.*, 2015).

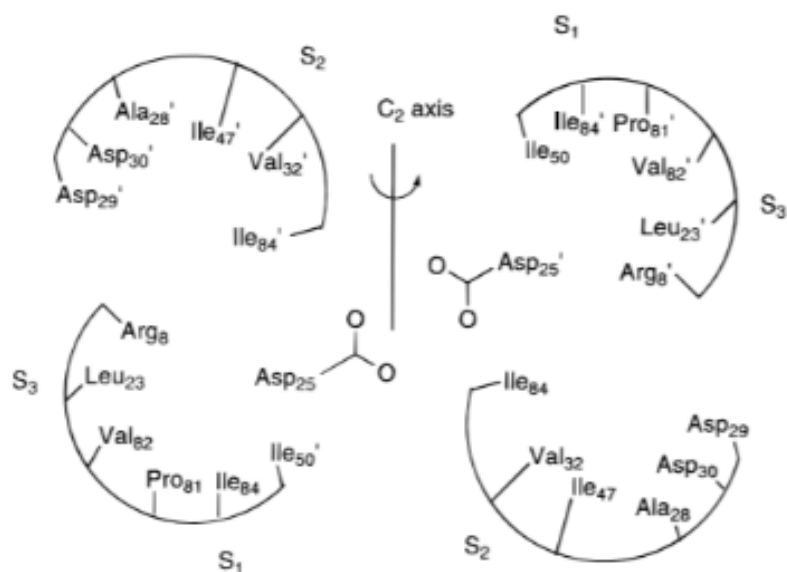


Figure 2.2-4: Amino acid residue that forms binding sites of HIV-1 protease

### 2.3. Antiretroviral drugs and resistance

Antiretroviral drugs can be classified as nucleoside/nucleotide reverse transcriptase inhibitors (NRTIs), non-nucleoside reverse transcriptase inhibitors (NNRTIs), protease inhibitors (PIs), integrase strand transfer inhibitors (INSTIs), and entry inhibitors. As depicted in **Figure 2.3-1**, antiretroviral drugs target the different stages of viral replication.

#### 2.3.1. Nucleoside and Nucleotide Reverse Transcriptase Inhibitors (NRTIs)

Nucleoside/nucleotide reverse transcriptase inhibitors (NRTIs) include zidovudine (AZT/ZDV), lamivudine (3TC), tenofovir (TDF) and abacavir (ABC) (Erik, 2010). The chemical structure of these drugs is depicted in **Figure 2.3-2** (Kakuda, 2000). All NRTIs are prodrugs that will be converted to active triphosphorylated forms by cellular enzymes (Kakuda, 2000), except TDF, which requires only two phosphorylation steps (Chapman *et al.*, 2003). Bioactivation of NRTIs is carried out by several cellular enzymes (cytoplasmic or mitochondrial kinases and phosphotransferases), which sequentially transform the parent drug to monophosphate diphosphate, and finally, active triphosphate forms (Arts & Hazuda, 2012; Erik, 2010; Othumpangat & Noti, 2018). The pharmacologically active moiety for all NRTIs is an intracellular 5'-triphosphate metabolite. Active NRTI triphosphate competitively binds to the reverse transcriptase enzyme (DNA polymerase  $\gamma$ ) active site and terminates the DNA chain elongation step (Arts & Hazuda, 2012; Cihlar & Ray, 2010; Kakuda, 2000).

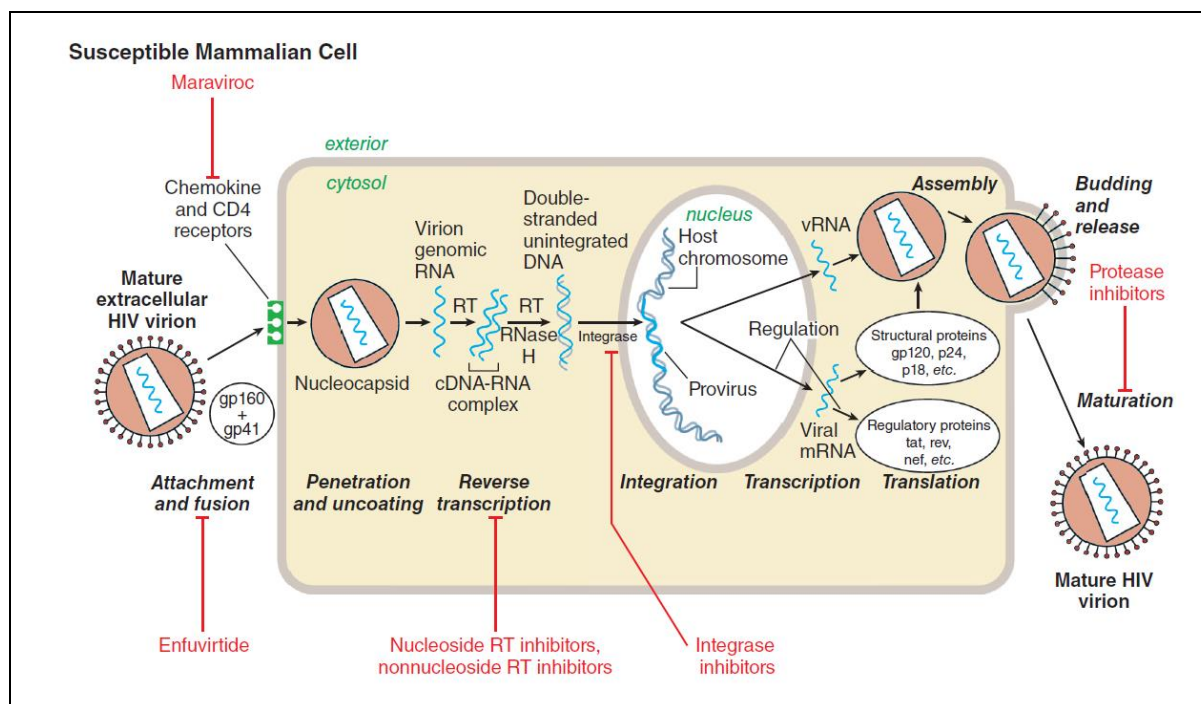


Figure 2.3-1: Life cycle of HIV and the site of action of antiretroviral drugs (Brunton *et al.*, 2017)

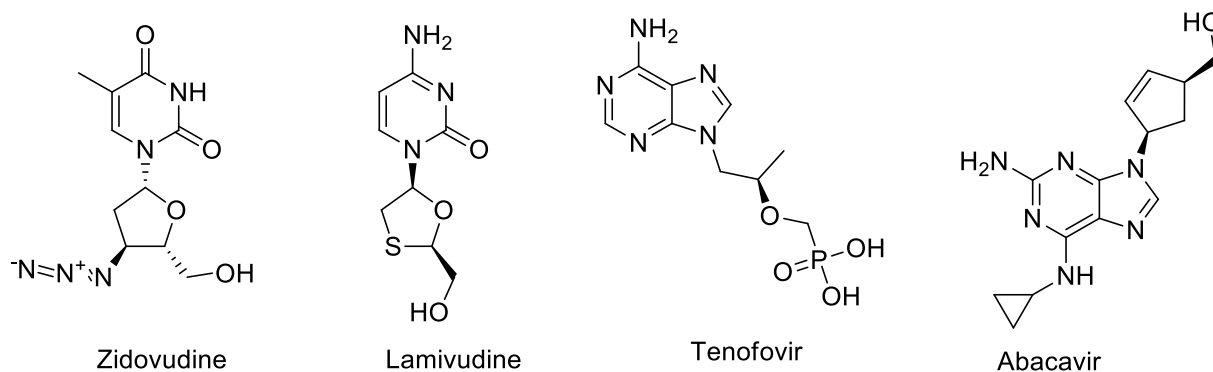


Figure 2.3-2: Chemical structures of nucleoside/tide reverse transcriptase inhibitors

The toxicities of NRTIs could be related to the binding of some drugs to mitochondrial DNA polymerase  $\gamma$ , which could lead to the inhibition of mitochondrial DNA synthesis and hence mitochondrial toxicity (Lee *et al.*, 2003). Those with low affinity for DNA polymerase  $\gamma$ , such as 3TC, FTC, and TDF, do not cause mitochondrial toxicity, such as peripheral neuropathy, pancreatitis, lipoatrophy, hepatic steatosis, and myopathy (Arts & Hazuda, 2012; Erik, 2004). Stavudine (d4T) and didanosine (ddI) are strongly associated with metabolic toxicity and long-term complications. Hence, countries have withdrawn both drugs from their national ARV medication list (World Health Organization, 2013). The other toxicities of

NRTIs include anemia, neutropenia, thrombocytopenia, lactic acidosis, and peripheral neuropathy (Foster & Lyall, 2008; Moyle, 2000; Russell *et al.*, 2008). The lack of endonuclease activity contributes to a mutation during reverse transcription. As a result, HIV cannot correct incorporated nucleotides, which causes the translation of amino acids from the changed nucleotide sequence, resulting in the formation of proteins with different shapes and structures. Thymidine analogue mutations (TAMs) decrease susceptibility to ZDV, d4T, ABC, and TDF (Marcelin *et al.*, 2004). Mutations selected by regimens lacking thymidine analogue (non-TAMs) include M184V alone, M184V + K65R, or L74V+ K65R, which causes intermediate resistance to TDF, ABC, 3TC, and FTC and increased susceptibility to ZDV (Inzaule *et al.*, 2016; Miller, 2004). The M184V mutation is selected by lamivudine, and it reduces viral fitness (Gallant, 2006).

### **2.3.2. Non-Nucleoside Reverse Transcriptase Inhibitors (NNRTIs)**

The non-nucleoside reverse transcriptase inhibitors (NNRTIs) include nevirapine (NVP), efavirenz (EFV), etravirine, rilpivirine, and delavirdine (Arts & Hazuda, 2012). **Figure 2.3-3** shows the chemical structure of these drugs. They are non-competitive inhibitors of reverse transcriptase enzymes (Sluis-Cremer & Tachedjian, 2008), which bind to the hydrophobic pocket in the p66 subunit and cause conformational change in the enzyme (**Figure 2.3-4**) (Béthune, 2010).

One of the common toxicities of NNRTIs is rash, which starts to manifest in the first month of treatment. Severe rash and hepatotoxicity leading to treatment discontinuation are frequently noted with NVP. CNS toxicities are common even after the first dose of EFV (Béthune, 2010; Waters *et al.*, 2007).

Amino acid substitution type of mutations at the binding site of NNRTIs lead to resistance. A single point mutation (K103N) has been reported for NVP (Bachelier *et al.*, 2000; Torti *et al.*, 2001). Cross-resistance among NNRTIs is a major clinical concern, as both NVP and EFV are cornerstones of first-line regimens. This has driven the development of second-generation NNRTIs (etravirine) with an improved resistance profile, with the aim of offering treatment-experienced patients the chance to benefit from the convenient dosing and good tolerance profile of NNRTIs (Béthune, 2010; Minuto & Haubrich, 2008)

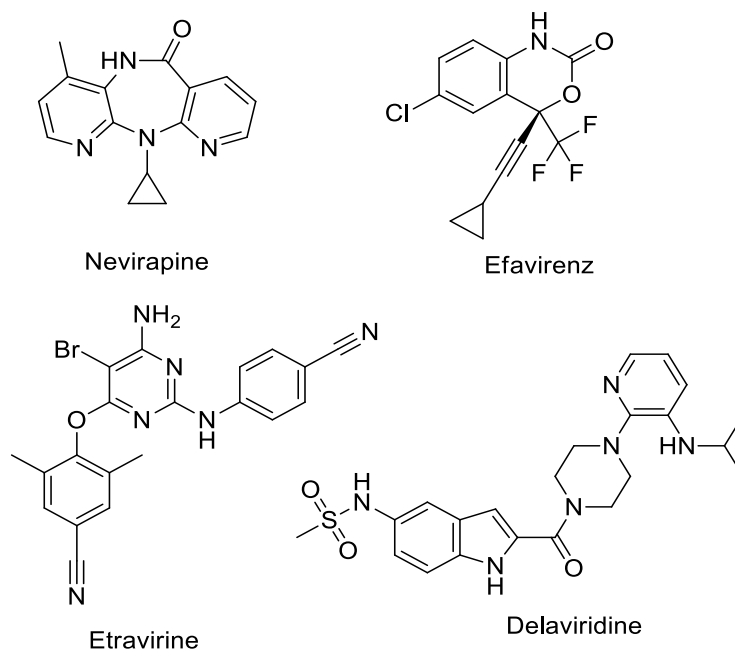


Figure 2.3-3: Chemical structures of Non-Nucleoside Reverse Transcriptase Inhibitors

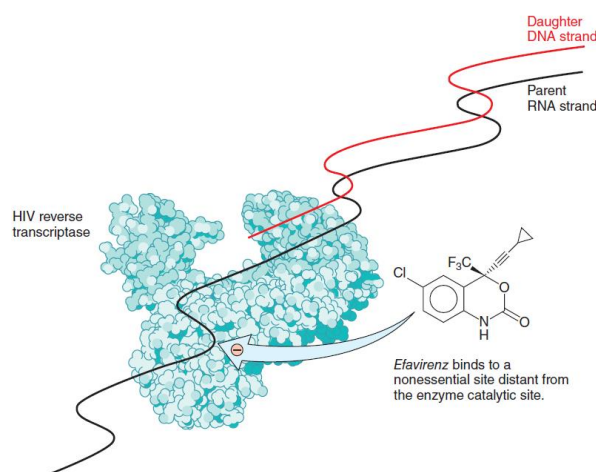


Figure 2.3-4: Molecular Target for Non-Nucleoside Reverse Transcriptase Inhibitors (Brunton *et al.*, 2017)

### 2.3.3. Integrase Inhibitors

Integrase inhibitors are also called integrase strand transfer inhibitors (INSTIs), as they target strand transfer reactions (Arts & Hazuda, 2012; McColl & Chen, 2010) and prevent the integration of dsDNA to the host chromosome (**Figure 2.3-5**). The integrase inhibitors available in clinical use include dolutegravir (DLV) and raltegravir (RAL) (McColl & Chen, 2010). **Figure 2.3-6** depicts their chemical Structure.



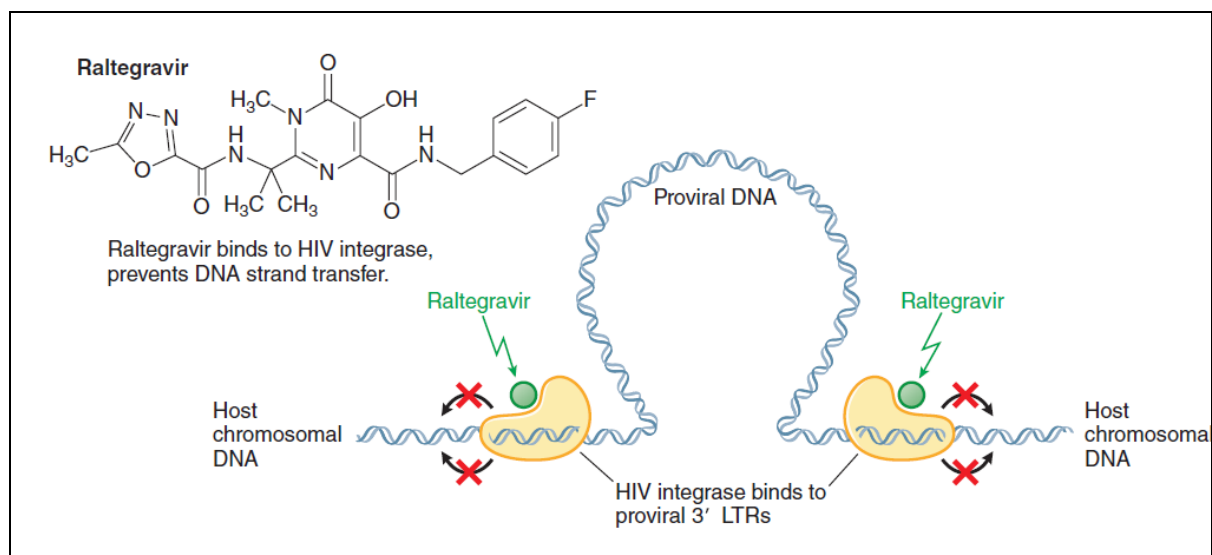


Figure 2.3-5: Mechanism of action of integrase inhibitors (Brunton *et al.*, 2017)

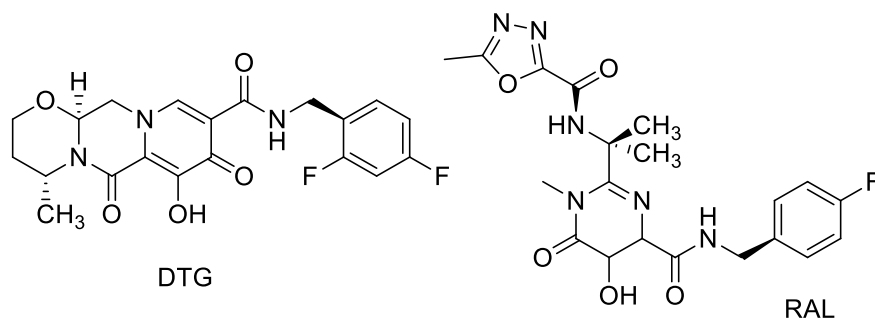


Figure 2.3-6: Chemical structures of integrase inhibitors

Common toxicities of integrase inhibitors include allergic reactions, headache, nausea, diarrhea, hyperglycemia, liver problems, trouble sleeping, tiredness, and changes in body fat (Lepik *et al.*, 2018). Mutations that cause the drug resistance to InSTIs are selected in the integrase-binding site near the amino acid residues essential for the proper functioning of  $Mg^{2+}$  cofactors (Arts & Hazuda, 2012; Hare *et al.*, 2010; Hazuda *et al.*, 2000). Primary signature mutations in residues Y143, N155, or Q148 of the integrase gene have been identified to cause development of drug resistance against integrase inhibitors (Fransen *et al.*, 2009; McColl & Chen, 2010).

#### 2.3.4. Protease and Maturation Inhibitors

Protease inhibitors include lopinavir (LPV/r), atazanavir (ATV/r), darunavir, ritonavir (r), nelfinavir (NFV), indinavir, saquinavir-SGC, saquinavir-HGC, amprenavir, and fosamprenavir (Arts & Hazuda, 2012; Wensing *et al.*, 2010). **Figure 2.3-7** shows the chemical

structures of LPV and ATV. Protease inhibitors were designed using a computational molecular docking approach, where their Structure was driven by viral peptides, which are substrates of protease (Leung *et al.*, 2000; Wlodawer & Vondrasek, 1998). Protease inhibitors (PI) inhibit the formation of mature infectious virions (**Figure 2.3-8**). Except for nelfinavir, which failed to show increased bioavailability, “boosting” with ritonavir increases plasma concentrations (Hull & Montaner, 2011; Wensing *et al.*, 2010). Boosting indinavir resulted in high peak plasma levels, which caused nephrotoxicity, and as a result, it is not commonly utilized (Leth *et al.*, 2004; Voigt *et al.*, 2002).

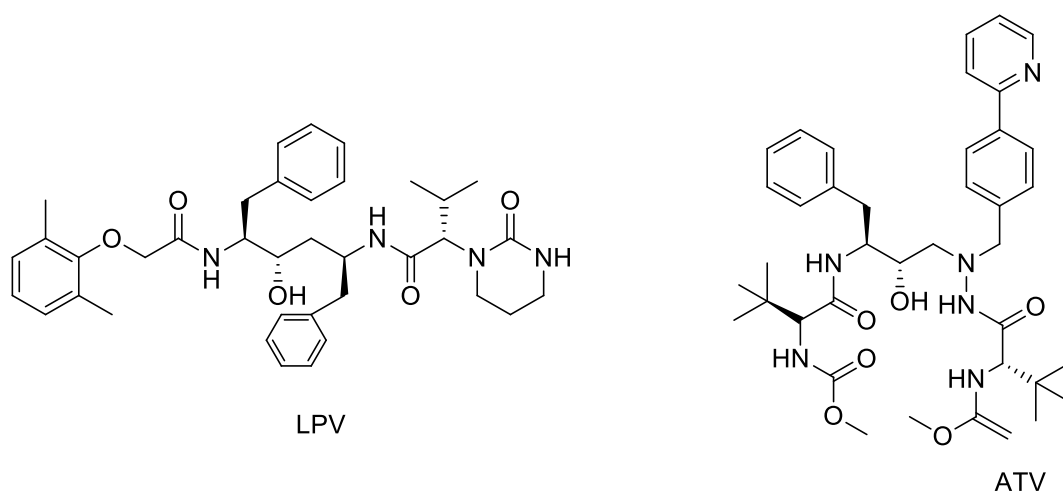


Figure 2.3-7: Chemical structures of protease inhibitors

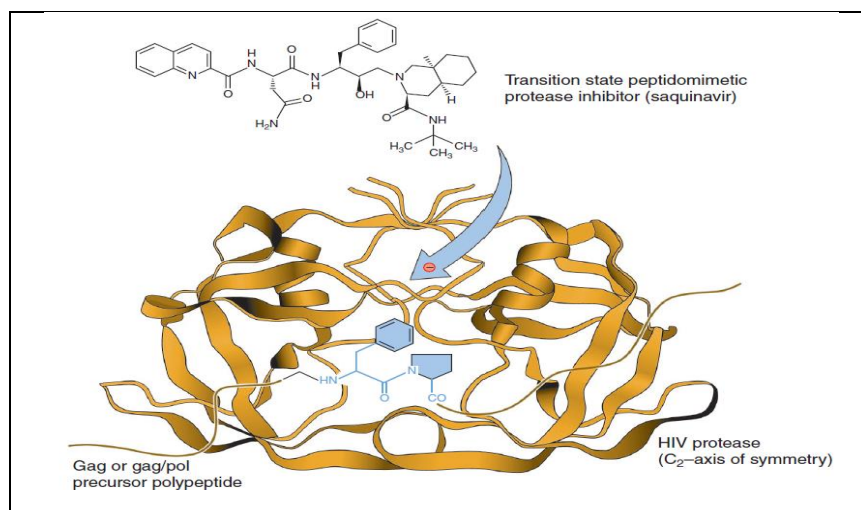


Figure 2.3-8: Mechanism of action of protease inhibitors

The toxicities of protease inhibitors include gastrointestinal intolerance, hepatitis, insulin resistance/diabetes, lipodystrophy, lipid abnormalities, bleeding, and electrocardiographic changes. The most common side effect of PIs is gastrointestinal

intolerance. Nausea and vomiting can be treatment-limiting (Boesecke & Cooper, 2008). These side effects were observed with all protease inhibitors but were most significant with complete dosing of ritonavir (600 mg twice daily), which is no longer used. All PIs can cause liver inflammation, although RTV has been more frequently associated with severe liver toxicity. Elevated liver enzymes can occur at any time during PI treatment (Herman & Easterbrook, 2001). Most protease inhibitors, except unboosted atazanavir, are associated with significant lipid abnormalities, such as hypertriglyceridemia and hypercholesterolemia. Lipodystrophy is a long-term complication of PI therapy, including metabolic (hyperglycemia and hyperlipidemia) and morphologic abnormalities (fat atrophy and fat deposition) (Busti *et al.*, 2004). Changes in body fat distribution have been reported in as many as 80% of patients receiving PIs (Reust, 2011).

Due to the modest size of the viral protease (11 kDa), resistance to protease inhibitors was thought to be unusual when they were first discovered (Arts & Hazuda, 2012). However, the protease gene is highly plastic, and resistance to all approved PIs has been documented, with polymorphisms found in 49 of the 99 codons that make up the protease gene and more than 20 alterations linked to drug resistance (Arts & Hazuda, 2012; Wensing *et al.*, 2010). Furthermore, resistance to PIs occurs in stages, with a mutation in the substrate-binding cleft being the most common alteration (Miller, 2001). The enzyme's overall size increases as a result of a resistance-inducing mutation in the binding site. As a result, it decreases the inhibitor's capacity to bind, lowering the drug's susceptibility (Wensing *et al.*, 2010). Protease inhibitors drug resistance can also be caused by mutations in the gag protein, a protease substrate (Clavel & Hance, 2004; Dam *et al.*, 2009; Gupta *et al.*, 2012).

### **2.3.5. Entry and Fusion Inhibitors**

HIV-1 infection is a multi-step process involving interactions between viral envelope proteins and cell surface receptors and coreceptors. To promote fusion, HR1 and HR2 domains of gp-41 must interact with each other. The presence of a heterologous protein that can imitate these domains disrupts these viral protein domains' interactions and prevents fusion. Entry inhibitors inhibit the attachment of virus particles to receptors on target cells (Esté & Telenti, 2007). Drugs in this class are divided into fusion inhibitors and CCR5 antagonists. Fusion inhibitors prevent the viral and CD4 membranes from fusing (Tilton & Doms, 2010). In 2003, the first entrance inhibitor, enfuvirtide (T-20), a synthetic peptide corresponding to the two domains, was approved (Arts & Hazuda, 2012; Kilby *et al.*, 1998; Lalezari *et al.*, 2003; Tilton

& Doms, 2010). Enfuvirtide is a synthetic peptide that has a sequence that is identical to a portion of gp41's HR2 domain and competes with HR1 for binding (Arts & Hazuda, 2012; Kilby *et al.*, 1998). However, its use has been restricted due to formulation difficulties and the development of drug resistance (Tilton & Doms, 2010; Wei *et al.*, 2002).

The CCR5 antagonists bind to the receptor's transmembrane helices (Dragic *et al.*, 2000), causing a conformational shift in the receptor that inhibits HIV-1 envelope recognition (Tilton & Doms, 2010). Vicriviroc, aplaviroc, and maraviroc are three CCR5 receptor antagonists demonstrated to inhibit HIV-1 in humans. However, since 2007, the FDA has only approved Maraviroc (MVC) as the only one (Arts & Hazuda, 2012; Tilton & Doms, 2010). Maraviroc binds to CCR5's hydrophobic transmembrane cavity, causing the chemokine receptor's shape to alter and prevent it from binding to gp120 (Arts & Hazuda, 2012; Dragic *et al.*, 2000; Tilton & Doms, 2010). Because MVC targets a host cell protein, the development of drug resistance to it differs from that of other antiretrovirals. Tropism and switching are two possible resistance mechanisms. For example, most people with HIV-1 infection possess viruses that only use CCR5 as a coreceptor for infection in the early stages (Lobritz *et al.*, 2010). However, as the infection proceeds, dual tropic viruses that employ the CXCR4 coreceptor begin to arise (Schuitemaker *et al.*, 1992).

The CCR5 inhibitors can cause outgrowth of CXCR4 viruses and treatment failure in patients with a mixed population of circulating viruses, CCR5-tropic and CXCR4-tropic viruses (Lobritz *et al.*, 2010). As a result, genotypic or phenotypic tropism testing is required before using CCR5 inhibitors and only individuals who have no CXCR4 tropic viruses are eligible for treatment with these medications (Kagan *et al.*, 2012).

## **2.4. Discovery of New Antiretroviral Drugs**

### **2.4.1. *In vitro* anti-HIV Assays**

Natural products or isolated chemicals can be tested in human T-cell lines, including Jurkat, CEM-SS, MT4, H9, and PBMCs, for anti-HIV and cytotoxic activities using 3-(4,5-dimethylthiazol-2-yl)-2,5-diphenyltetrazolium bromide (MTT) or sodium 3-[1-(phenylamino)-carbonyl]-3,4-tetrazolium bis(4-methoxy-6-nitro)benzene-sulfonic acid hydrate (XTT) assays (Bahuguna *et al.*, 2017; Szucs *et al.*, 1988). The several assays that could be used to evaluate drug candidates' anti-HIV activity are listed in **Table 2.4-1**. The 50 percent cytotoxic concentration (CC<sub>50</sub>), 50 percent effective concentration (IC<sub>50</sub>), and selectivity index (SI), which is the ratio of CC<sub>50</sub>/EC<sub>50</sub>, can all be used to express the outcome. As a result, SI

represents the test material's antiviral activity as well as its ultimate toxicity. A high SI value suggests that the test substance is not harmful and has high antiviral activity. The *in vitro* therapeutic index of drugs being investigated for further preclinical development investigations can be estimated using MTT or XTT (Pauwels *et al.*, 1988).

Table 2.4-1: *In vitro* anti-HIV assays

Target	Assays
HIV-1 Replication	MTT
	XTT
gp120/CD4 interaction	gp120 ELISA
Reverse Transcriptase Enzyme	Radio-active method
	Non-radioactive ELISA
	RNase H activity
Integrase Enzyme	Radio-active method
	Non-radioactive ELISA
Protease	Fluorometric method
	HPLC-based method
	Pepsin assay (indirect method)

The effect of natural products or isolated compounds on reverse transcriptase enzymes can be evaluated by using tritium-labeled substrate & poly(rA). p(dT)12-18 as template primer or by using nonradioactive ELISA and/or by ribonuclease H activity (Ahn *et al.*, 2004; Li *et al.*, 2008; Świderek *et al.*, 2012). The effect on integrase enzyme can be evaluated with recombinant HIV-Integrase by using radiolabeled oligonucleotide substrate (Lee-Huang *et al.*, 1995; Pommier & Neamati, 1999) or by using a non-radioactive ELISA kit (Ng *et al.*, 2002; Nutan *et al.*, 2013). Activity against protease enzymes can be assayed using 2 direct methods (fluorometric or HPLC method) or an indirect method using pepsin enzyme as a substitute for HIV protease (Yust *et al.*, 2004).

#### 2.4.2. Computer-aided drug design and discovery (*in silico* analysis)

Computer-aided drug design and discovery (CADD) (*in silico*) research can speed up drug development by minimizing the need for costly laboratory work and clinical trials (Prieto-Martínez *et al.*, 2019). For example, CADD is being used to find hits (active drug candidates), select leads (most likely candidates for further evaluation), and optimize leads that transform biologically active compounds into appropriate drugs by improving their pharmacokinetic properties (Gurung *et al.*, 2021). Furthermore, computational methods aid in determining a compound's drug-likeness (Ghose *et al.*, 1999; Lipinski *et al.*, 2001; Veber *et al.*, 2002).

Many biological processes, such as signal transmission, cell control, and molecular recognition, rely on macromolecular assemblies such as enzyme-substrate, drug-protein, drug-nucleic acid, protein-nucleic acid, and protein-protein interactions (Gurung *et al.*, 2021; Prieto-Martínez *et al.*, 2019). To understand the interaction mechanisms and devise therapeutic interventions, molecular docking is essential for determining the binding mode and affinity between constituent molecules in molecular recognition (Lv *et al.*, 2015). Molecular docking is a computer-assisted method for determining the kind, strength, and direction of drug and receptor/target interactions (Kitchen *et al.*, 2004). Molecular docking studies can be performed using software such as GOLD from CCDC and GLIDE from Schrodinger, MOE, and Auto Dock Vina from Scripps Research Institute. The more negative the values, the better the binding free energy between the enzyme and the ligands (Granchi *et al.*, 2015; Kumar *et al.*, 2014; Seal *et al.*, 2011).

Molecular docking can be used for three different purposes: first, for hit identification, where docking combined with a scoring function can be used to quickly screen large databases of potential drugs *in silico* to identify molecules that are likely to bind to the protein target of interest; second, for lead optimization, where docking can be used to predict where and in which relative orientation a ligand binds to a protein; and third, for lead optimization, where docking can be used to predict where and in which relative orientation Third, protein-ligand docking may be used to forecast contaminants that enzymes can degrade, which can then be used to build more potent and selective analogs; and finally, bioremediation, where protein-ligand docking can also be used to predict pollutants that enzymes can degrade.

We used the Molecular Operating Environment (MOE) 2015 docking tool in this research. This tool was chosen from among a variety of accessible resources for docking because of its user-friendly graphical interface. It provides a clear graphical representation of the data by displaying the locations and interactions of ligand and receptor-binding residues. The S-score is a numerical metric used in MOE to prioritize receptor–ligand-binding affinities for all possible binding geometries. The MOE is used in a variety of fields, including structure-based design, fragment-based design, pharmacophore discovery, medicinal chemistry applications, biologics applications, protein and antibody modeling, molecular modeling and simulations, cheminformatics, and QSAR, and the development and deployment of methods. The software calculates the S score by identifying salt bridges, hydrogen bonds, hydrophobic interactions, sulfur-LP, cation-, and solvent exposure. Based on the S score, inhibitor-receptor protein interactions are predicted (Clark & Labute, 2007).

## 2.5. Medicinal Plants with anti-HIV activity

It is estimated that there are more than 350,000 plant species in the world (Christenhusz & Byng, 2016). One-third of these species are found in Africa (Chingwaru *et al.*, 2015). As explained in Section 1.1, 54% (20.7 million) of HIV-positive people live in Southern and East African regions, where more than 25% of them do not have access to antiretroviral therapy. As the HIV epidemic still affects many people's lives, there is a high demand for safe, effective, and affordable medicines for use in the treatment of HIV. In addition, with the emergence of drug-resistant HIV variants, there is a greater need to search for effective inhibitors of HIV. The lack of access to care and treatment still pushes the African community to rely on medicinal plants to treat various diseases, including opportunistic infections secondary to HIV. Despite the issue of access, many people are culturally inclined to visit traditional healers who use medicinal plants, as the use of different parts of plants for treating illness is part of African traditional medicine practice (Mahomoodally, 2013). Therefore, screening natural products offers a chance to find compounds that can inhibit the replication of HIV (Narayan *et al.*, 2013).

Patients use various plants to treat HIV or opportunistic infections (Bessong & Obi, 2006; Cos *et al.*, 2002). **Table 2.5-1** summarizes medicinal plants exhibiting anti-HIV activities. *In vitro* activity testing of several medicinal plants have shown that natural products exert their anti-HIV activity by different modes of action. Some of these plants include *Hypoxis hemerocallidea* and *Sutherlandia frutescens* (Maroyi, 2014), *Plectranthus barbatus*, *Siphonochilus natalensis* (Chingwaru *et al.*, 2015; Maroyi, 2014), *Erythrina abyssinica* (Mohammed *et al.*, 2012), *Cassia fistula* (Xu *et al.*, 1996), *Bulbine alooides* (Klos *et al.*, 2009) and *Dodonaea angustifolia* (Asres *et al.*, 2001).

Burack *et al.*, (1996) reported the anti-HIV activity of *Artemisia annua*, with an IC<sub>50</sub> of 2.0 µg/ml. In a related study, Gerenc̄er *et al.*, (2006) demonstrated the antiviral and protective effects of *Cassia abbreviata* from the cytopathic effect of HIV. *Cassia abbreviata* displayed an IC<sub>50</sub> of 102.8 µg/mL. Asres & Bucar, (2005) reported that punicalagin, an ellagitannin isolated from the acetone fraction of *Combretum molle*, inhibits the replication of HIV with a selectivity index (SI) of 16. Justiprocumin B, an active compound isolated from *Justicia gendarussa*, has shown potent activity against HIV with IC<sub>50</sub> values in the range of 15–21 nM (Jiratchariyakul *et al.*, 2001).

Table 2.5-1: List of some plant species exhibiting anti-HIV activities

Ser. No.	Plant	Plant Part	Phytochemicals with Anti-HIV activity and their action	Reference
1.	<i>Allanblackia stuhlmannii</i> (Engl.)	Whole plant	Benzophenone; <i>In vitro</i> anti HIV activity	(Fuller <i>et al.</i> , 1999)
2.	<i>Annona squamosa</i> L.	Fruit	Diterpenoids; IC <sub>50</sub> = 0.8 µg/ml; SI > 5; Inhibits HIV-1 replication in H9 lymphocyte cells	(Wu <i>et al.</i> , 1996)
3.	<i>Aristolochia manshuriensis</i> Kom.	Stem	Oxoperezinone; Inhibit HIV-1 replication; IC <sub>50</sub> = 17.5 µg/mL; SI= 1.43	(Wu <i>et al.</i> , 2003)
4.	<i>Avicennia marina</i> var. <i>rumphiana</i> (Hallier f.)	Seed	Iridoid glycoside; IC <sub>50</sub> = 0.1 µg/ml; Restricts HIV-1 replication on the early stage of HIV infection.	(Behbahani, 2014)
5.	<i>Calophyllum lanigerum</i> Miq.	Whole plant	Calanolide; <i>In vitro</i> anti-HIV activity	(Galinis <i>et al.</i> , 1996)
6.	<i>Cassine crocea</i> (Thunb.) C.Presl	Leaf	Glycoside; Potent <i>In vitro</i> anti-HIV activity.	(Prinsloo <i>et al.</i> , 2010)
7.	<i>Castanospermum austral</i> A. Cunn. & C. Fraser	Leaf	Alkaloid; <i>In vitro</i> anti-HIV activity	(Taylor <i>et al.</i> , 2016)
8.	<i>Celastrus hindsii</i> Benth.	Stem bark	Triterpene; anti-HIV replication activity in H9 lymphocyte cells; IC <sub>50</sub> =0.8 µg/ml.	(Kuo & Kuo, 1997)
9.	<i>Detarium microcarpum</i> Guill. & Perr	Root	Flavonoids; <i>In vitro</i> anti-HIV activity	(Mahmood <i>et al.</i> , 1993)
10.	<i>Drymaria diandra</i> Blume	Stem bark	Alkaloid; Anti-HIV effects in H9 lymphocytes; IC <sub>50</sub> =0.699 µg/mL; SI of 20.6.	(Hsieh <i>et al.</i> , 2004)
11.	<i>Euphorbia erythradenia</i> Boiss.	Aerial part	Triterpene; <i>In vitro</i> anti-HIV activity	(Ayatollahi <i>et al.</i> , 2016)
12.	<i>Euphorbia neriifolia</i> L.	Stem bark	Diterpenoids; <i>In vitro</i> anti-HIV activity; IC <sub>50</sub> = 3.58; SI = 8.6	(Zhao <i>et al.</i> , 2014)



Ser. No.	Plant	Plant Part	Phytochemicals with Anti-HIV activity and their action	Reference
13.	<i>Homalanthus nutans</i> (G. Forst.) Guill.	Stem bark	Prostratin; <i>In vitro</i> anti-HIV activity	(Cox, 1993)
14.	<i>Ipomoea cairica</i> (L.) Sweet	Whole plant	Lignans; <i>In vitro</i> anti-HIV activity	(Schröder <i>et al.</i> , 1990)
15.	<i>Maytenus macrocarpa</i> (Ruiz & Pav.) Briq.	Stem bark	Triterpenes; anti-HIV activity in C8166 cells infected with HIV-1 <sub>MN</sub> IC <sub>50</sub> = 1 µg/mL; SI= 35	(Piacente <i>et al.</i> , 2006)
16.	<i>Mimusops elengi</i> L.	Bark	Saponin; <i>In vitro</i> anti-HIV activity	(Hayashi <i>et al.</i> , 1995)
17.	<i>Panax ginseng</i> C.A. Mey.	Root	Saponin; Inhibit HIV-1 replication; IC <sub>50</sub> =13.4 µg/mL	(Zhang <i>et al.</i> , 2002)
18.	<i>Panax zingiberensis</i> C.Y. Wu & K.M. Feng	Rhizome	Zingibroside; Anti-HIV-1 activity IC <sub>50</sub> = 91.3 µM; CC <sub>50</sub> = 46.2 µM)	(Hasegawa <i>et al.</i> , 1994)
19.	<i>Rheum tanguticum</i> Maxim. ex Balf.	Leaf	Glycosides; Moderate anti-HIV activity	(Piacente <i>et al.</i> , 1996)
20.	<i>Tripterygium wilfordii</i> Hook. f.	Roots	Diterpene; anti-HIV replication activity in H9 lymphocyte cells; IC <sub>50</sub> = 1 µg/ml	(Ke <i>et al.</i> , 1992)
21.	<i>Toddalia asiatica</i> (L.) Lam.	Root	Alkaloid; <i>In vitro</i> anti-HIV activity	(Rashid <i>et al.</i> , 1995)
22.	<i>Trigonostemon thyrsoideus</i> Stapf	Stem	Diterpenoid; Inhibit HIV-1 induced cytopathic effects; IC <sub>50</sub> = 2.19 µg/mL; TI >90.	(Zhang <i>et al.</i> , 2010)
23.	<i>Tripterygium wilfordii</i> Hook. f.	Roots	Sesquiterpene pyridine Alkaloids; potent anti-HIV activity; IC <sub>50</sub> = <0.10 µg/mL; TI >1000	(Duan <i>et al.</i> , 2000)

## 2.6. The *Croton* genus

### 2.6.1. Botanical information on *Croton* genus

Members of the Euphorbiaceae family are found mainly in tropical Africa (Radcliffe-Smith, 2001). The family Euphorbiaceae is notable because they produce a milky sap (rich in secondary metabolites, mainly alkaloids and terpenoids) and comprises over 300 genera, of

8,000-9000 species (Wurdack & Davis, 2009). The family members have a diverse distribution, are subclassified into five subfamilies; including Acalyphoideae, Crotonoideae, Euphorbioideae, Oldfieldioideae, and Phyllanthoideae (Govaerts *et al.*, 2000; Palgrave, 2002). Members of the Euphorbiaceae family have displayed anti-HIV activity in several experimental studies (**Table 2.6-1**). This study evaluates the antiretroviral efficacy of three African *Croton* species: *C. macrostachyus*, *C. megalocarpus*, and *C. dichogamus*.

The name “*Croton*” is a Greek word referring to thick, smooth seeds, a common feature of most *Croton* species. The genus *Croton* belongs to the *Crotonoideae* subfamily. The genus consists of 1300 trees, shrubs or small trees, with variously stellate hairy or lepidote scales distributed worldwide in the tropics and subtropics (Wurdack & Davis, 2009; Caruzo *et al.*, 2011 and Berry *et al.*, 2005). *Croton* species are widely distributed in warm tropical regions like tropical America, India, and Africa. In addition, a wide diversity of *Croton* plants is reported in Madagascar, West Indies, and southern Brazil. The leaves of *Croton* plants are alternate, sometimes opposite, rarely whorled, simple, and usually have two glands at the top of the petiole. Contact with some of these plant leaves can cause dermatitis. Their fruits occur as three-lobed capsules, while seeds of others are reported to be tumor promoters (Palgrave, 2002 and Mabberley, 2008).

Table 2.6-1: Plants from the *Croton* genus that have displayed anti-HIV activity

Ser. No.	Plant	Plant Part	Reference
1.	<i>Croton billbergianus</i> Müll. Arg.	Trunk	(Matsuse <i>et al.</i> , 1998)
2.	<i>Croton gratissimus</i> Burch.	Leaf	(Ali <i>et al.</i> , 2002)
3.	<i>Croton tiglium</i> L.	Seed	(El-Mekkawy <i>et al.</i> , 2000)
4.	<i>Croton zambesicus</i> Müll. Arg.	Seed	(Ali <i>et al.</i> , 2002; Hussein <i>et al.</i> , 1999)
5.	<i>Croton tiglium</i>	Seed	(El-Mekkawy <i>et al.</i> , 1998, 2000)
6.	<i>Croton megalobotryus</i>	Bark	(Tietjen <i>et al.</i> , 2016)

## 2.6.2. Ethnomedicinal uses of *Croton* genus

The common ethnomedicinal uses of the different *Croton* species are summarized in **Table 2.6-2**.

Table 2.6-2: Ethnomedicinal uses of the *Croton* genus

Scientific Name (Other names, region)	Reported use	References
<i>Croton alienus</i> (Kenya)	Antimicrobial activities	(Ndunda <i>et al.</i> , 2013)
	Antileishmanial activities	
	Antiplasmodial activities	
<i>Croton arboreous</i> Millsp. (“Cascarillo”, Mexico)	Anti-inflammatory	(Aguilar-Guadarrama & Rios, 2004)
<i>Croton bonplandianum</i>	Antioxidant activity	(Keerthana <i>et al.</i> , 2013)
	Antimicrobial activity	(Jeeshna <i>et al.</i> , 2011) (Burgos <i>et al.</i> , 2015; Khanra <i>et al.</i> , 2016)
	Wound healing	(Divya <i>et al.</i> , 2011)
	Antidiabetic	(Qaisar <i>et al.</i> , 2014)
<i>Croton californicus</i> Müller Arg. (California, U.S.A.)	Pain reliever for rheumatism.	(Williams <i>et al.</i> , 2001, 2005)
<i>Croton cajucara</i> Benth. (“Sacaca”, Peru and Brazil)	Antioxidant activity- reduces hepatic oxidative stress	(Rodrigues <i>et al.</i> , 2012)
	Antimicrobial Activity	(Alviano <i>et al.</i> , 2005; Freires <i>et al.</i> , 2015)
	Antiprotozoal- Antileishmanial activity	(Lima <i>et al.</i> , 2015; Rosa <i>et al.</i> , 2003)
	Anti-ulcer activity	(Brito <i>et al.</i> , 1998; De Paula <i>et al.</i> , 2008)
	Antinociceptive activity	(Campos <i>et al.</i> , 2002; Rodrigues <i>et al.</i> , 2012; Rosa <i>et al.</i> , 2003)
	Antihyperlipidemic activity	(Bighetti <i>et al.</i> , 2004)
<i>Croton celtidifolius</i> Baill. (“Sangue-de- adave”, Brazil)	Anti-inflammatory and antioxidant	(Nardi <i>et al.</i> , 2003, 2007)
	Antinociceptive effect	(DalBó <i>et al.</i> , 2005, 2006; Nardi <i>et al.</i> , 2006)
	Antiplatelet activity	(Neiva <i>et al.</i> , 2008)
	Central nervous system activity, Neuroprotective activity	(Assis <i>et al.</i> , 2014; Moreira <i>et al.</i> , 2010)
	Anticancer activity	(Biscaro <i>et al.</i> , 2013)
	Cardioprotective activity	(Hort <i>et al.</i> , 2012)
<i>Croton draco</i> Cham. & Schlttdl (Mexico and Central America)	Cough, flu, diarrhea, and stomach ulcers, and wound healing, anti-septic	(Murillo <i>et al.</i> , 2001)

Scientific Name (Other names, region)	Reported use	References
<i>Croton eluteria</i> Bennett., Cascarilla”, Syn. <i>C. eluteria</i> (L.) Wright, West Indies, and Northern South America-Bahama Island)	Bronchitis, diarrhea, and dysentery Antipyretic and Antimalarial	(Vigor <i>et al.</i> , 2001)
<i>Croton echinocarpus</i> (Brazil)	Anti HIV activity	(Ravanelli <i>et al.</i> , 2016)
<i>Croton kongensis</i> Gagnep. (“Plao Ngeon” or “Plau Noi”; Thailand; China)	Dysmenorrhoea	(Thongtan <i>et al.</i> , 2003)
	Antimycobacterial activity	
<i>Croton lechleri</i> (one of the “sangre-de-drago” plants; Ecuador and Peru)	Wound healing, purgative and tonic	(Cai <i>et al.</i> , 1991, 1993)
	Anticancer and Antioxidant activity	(Alonso-Castro <i>et al.</i> , 2012; Lopes <i>et al.</i> , 2004; Montopoli <i>et al.</i> , 2012; Pieters <i>et al.</i> , 1993; Rossi <i>et al.</i> , 2003)
	Antisecretory/Antiulcer and Antidiarrheal activity	(Froldi <i>et al.</i> , 2009; Tamariz Ortiz <i>et al.</i> , 2013; Tradtrantip <i>et al.</i> , 2010)
	Immunomodulatory activity	(Risco <i>et al.</i> , 2003)
	Anti-inflammatory activity	(Perdue <i>et al.</i> , 1979)
<i>Croton macrostachys</i> Hochst. ex A. Rich ex Delile (Syn. <i>C. macrostachys</i> var. <i>mollissimus</i> Chiov.; (Madagascar, Somali, Sudan, Eritrea, Kenya, Angola Guinea, Liberia, Malawi, Zambia, and Zimbabwe)	Antidiabetic, purgative	(Obey <i>et al.</i> , 2016b; Salatino <i>et al.</i> , 2007)
	Antimicrobial activity	(Kalayou <i>et al.</i> , 2012; Tene <i>et al.</i> , 2009; Voukeng <i>et al.</i> , 2016)
	Antimalarial activity	(Bantie <i>et al.</i> , 2014)
	Ant mycobacterial activity	
	Antidiabetic	(Arika <i>et al.</i> , 2015)
	Anticancer activity	(Morris Kupchan <i>et al.</i> , 1969)
	Purgative and anti-inflammatory activity	(Mazzanti <i>et al.</i> , 1987)
<i>Croton malambo</i> Karsten (“Palomatias”, “Torco”; Venezuela and Colombia)	Antinociceptive and anti-inflammatory	(Suárez <i>et al.</i> , 2003)
	Antibacterial activity	(Suárez <i>et al.</i> , 2008)
	Antioxidant activity	(Colorado <i>et al.</i> , 2010)
<i>Croton megalobotrys</i> (Somalia, Kenya, Uganda, the Democratic Republic of the Congo, Rwanda, Burundi, Tanzania, Malawi, Zambia, and Mozambique.)	Antibacterial activity	(Selowa <i>et al.</i> , 2010)
	Anti-HIV Activity	(Tietjen <i>et al.</i> , 2016)
	Sexually transmitted illness	(Ndubani & Höjer, 1999; Tietjen <i>et al.</i> , 2018)
	Anti-plasmodial and Antioxidant	(Abosi & Majinda, 2015)
<i>Croton megalocarpus</i>	Antioxidant activity	(Kivevele <i>et al.</i> , 2011)
	Antibacterial activity	(Kariuki <i>et al.</i> , 2014)

Scientific Name (Other names, region)	Reported use	References
(Kenya Congo and Mozambique, Malawi and Zimbabwe)		
<i>Croton nepetaefolius</i> Baill., (“Marmeleirovermelho”. Brazil)	Antimicrobial and insecticidal activity	(Araújo <i>et al.</i> , 2006; Carneiro <i>et al.</i> , 2011; Gomes <i>et al.</i> , 2013; Morais <i>et al.</i> , 2006; Sá <i>et al.</i> , 2012)
	Antifungal activity	(Fontenelle <i>et al.</i> , 2008)
	Antispasmodic activity	(Magalhaes <i>et al.</i> , 2004)
	Antinociceptive activity	(Abdon <i>et al.</i> , 2002)
	Antioxidant activity	(Selene <i>et al.</i> , 2006)
	Cardiovascular – vasorelaxant activity	(Lahlou <i>et al.</i> , 1999)
	Antihypertensive activity	(Lahlou <i>et al.</i> , 2000)
<i>Croton oblongifolius</i> Roxb.,	Tonic, against flat worms, to treat dysmenorrhoea, as purgative, dyspepsia and dysentery. Chronic enlargement of the liver	(Ahmed <i>et al.</i> , 2002; Ngamrojanavanich <i>et al.</i> , 2003; Singh <i>et al.</i> , 1999; Sommit <i>et al.</i> , 2003)
<i>Croton palanostigma</i> Klotzsch (Peru)	Wound healing and intestinal inflammation.	(Miller <i>et al.</i> , 2012; Porrás-Reyes <i>et al.</i> , 1993)
	Anticancer activity	(Miller <i>et al.</i> , 2007; Sandoval <i>et al.</i> , 2002)
<i>Croton roxburghii</i> NP. (India)	Antidote in snake poisoning and for infertility, fever and wounds.	(Gupta <i>et al.</i> , 2004)
	Antibacterial and Antioxidant	(Mahbubur <i>et al.</i> , 2014; Panda, <i>et al.</i> , 2010; Rath <i>et al.</i> , 2011)
	Antifungal activity	(Sujogya <i>et al.</i> , 2010)
	Antimicrobial, anthelmintic, and antiviral activity	
<i>Croton sublyratus</i> Kurz (“Plau noi”; South-Eastern Asian Countries and Thailand)	Anti-helminthic and to treat dermatological problems	(Tansakul & De-Eknamkul, 1998; Vongchareonsathit & De-Eknamkul, 1998)s
	Antiulcer	(Kitazawa <i>et al.</i> , 1979)
<i>Croton schiedeanus</i> (“Almizclillo, Columbia)	Antihypertensive activity	(Guerrero <i>et al.</i> , 2001a, 2001b; Guerrero <i>et al.</i> , 2002; Guerrero <i>et al.</i> , 2004)
<i>Croton sylvaticus</i> (Syn. <i>C. verdickii</i> De Wild; <i>C. oxypetalus</i> Mull. Arg. and <i>C. stuhlmannii</i> Pax	Antimicrobial, anti-inflammatory, antioxidant, larvicidal	(Maroyi, 2017e)
	Antimicrobial activity	(Ndunda <i>et al.</i> , 2013)
	Antileishmanial activity	
	Antiplasmodial activity	

Scientific Name (Other names, region)	Reported use	References
(Ethiopia, Northern parts of Africa, South Africa, Angola)		
<i>Croton tiglium</i> L. (Asia)	Laxative	(Tsai <i>et al.</i> , 2004)
	Intestinal disorder	(Wang <i>et al.</i> , 2008)
	Antioxidant activity	(Saikia & Upadhyaya, 2011)
	Antidermatophyte activity	(Chien <i>et al.</i> , 2016)
	Anticancer activity	(Kupchan <i>et al.</i> , 1976)
	AntiHIV activity	(El-Mekkawy <i>et al.</i> , 2000)
<i>Croton tonkinensis</i> Gagnep. (“Kho sam Bac Bo”; Vietnam )	Stomach ache, abscesses, dyspepsia, impetigo, and gastric/duodenal ulcers.	(Giang <i>et al.</i> , 2003)
	Anti-tubercular activity	(Jang <i>et al.</i> , 2016)
	Anti-inflammatory activity	(Kuo <i>et al.</i> , 2013)
	Antibacterial activity	(Giang <i>et al.</i> , 2006)
<i>Croton urucurana</i>	Wound-healing and treating rheumatism	(Orlandi-Mattos <i>et al.</i> , 2002)
	Antiulcer activity	(Wolff Cordeiro <i>et al.</i> , 2012)
	Antibacterial activity	(Oliveira <i>et al.</i> , 2008; Peres <i>et al.</i> , 1997; Simionatto <i>et al.</i> , 2007)
	Antifungal activity	(Gurgel <i>et al.</i> , 2005)
	Antiinflammatory and antinociceptive activity	(Cordeiro <i>et al.</i> , 2016)
<i>Croton zehntneri</i> Pax. et Hoffm. “Canelade-cunhã”; Brazil)	Central nervous system effects- Antidepressant and anti-anxiety activity	(Bernardi <i>et al.</i> , 1991; Giorgi <i>et al.</i> , 1991; Lazarini <i>et al.</i> , 2000)
	Anthelmintic activity	(Camurça-Vasconcelos <i>et al.</i> , 2007)
	Adjuvant in antibiotic therapy	(Coutinho <i>et al.</i> , 2010)
	Wound healing	(Cavalcanti <i>et al.</i> , 2012; Malveira Cavalcanti <i>et al.</i> , 2012)
	Antifungal activity	(Fontenelle <i>et al.</i> , 2008)
	Antinociceptive activity	(Oliveira <i>et al.</i> , 2001)
	Antimicrobial activity	(Andrade <i>et al.</i> , 2015; Donati <i>et al.</i> , 2015)
	Antimalarial activity	(Mota <i>et al.</i> , 2012)
	Gastro protective activity, Hepatoprotective activity	(Andrelina <i>et al.</i> , 2013; Lima <i>et al.</i> , 2008)
<i>Croton zambesicus</i> (Syn. <i>C. amabilis</i> Muell.Arg.; Originally a Guineo-Congolese species but now Widespread in Tropical Africa)	Fever, dysentery and convulsions, anti-hypertensive, anti-microbial (urinary infections)	(Block <i>et al.</i> , 2002; Ngadjui <i>et al.</i> , 2002)
	Prevention of cardiovascular diseases	(Robert <i>et al.</i> , 2010)

Scientific Name (Other names, region)	Reported use	References
	Antimicrobial activity	(Abo <i>et al.</i> , 1999; Okokon & Nwafor, 2010b)
	Antiplasmodial activity	(Okokon & Nwafor, 2009a)
	Antiproliferative, antioxidant, and antibacterial activities	(Yagi <i>et al.</i> , 2016)
	Antiulcer and anticonvulsant activity	(Okokon & Nwafor, 2009b)
	Anti-inflammatory, analgesic, and antipyretic activities	(Okokon & Nwafor, 2010)
	Nephroprotective effect	(Okokon <i>et al.</i> , 2011)

### 2.6.3. The pharmacological activities of the genus *Croton*

The antibacterial effect of *Croton lechleri* against gram-positive *Staphylococcus aureus* was reported by Chen *et al.*, (1994), who isolated 2,4,6-trimethoxyphenol, 1,3,5-trimethoxybenzene, crolechinic acid and korberins A and B from the blood-red sap of the plant. Alviano *et al.* (2005) reported the antimicrobial activity of linalool, a monoterpene isolated from *C. cajucara* against *S. aureus*, *Streptococcus mutans*, gram-negative anaerobic *Porphyromonas gingivalis* and *Candida albicans* (Alviano *et al.*, 2005). In another study, Gurgel *et al.*, (2005) demonstrated the antifungal activity of *C. urucurana* against *Tricophyton tonsurans*, *Epidermophyton floccosum*, *Tricophyton rubrum*, *Microsporum canis* and *Tricophyton mentagrophytes* (Gurgel *et al.*, 2005), which could be due to the tannin compounds, galocatechin and epigallocatechin (Gurgel *et al.*, 2005).

Different researchers have reported the antiviral activity of the proanthocyanidin tannin. Tannins have shown efficacy against herpes, influenza, and hepatitis viruses (Barnard *et al.*, 1993; Chen *et al.*, 1994; Jones, 2003; Orozco-Topete *et al.*, 1997; Ubillas *et al.*, 1994; Wyde *et al.*, 1993). Similarly, the works of Orozco-Topete *et al.*, (1997) have shown the anti-HIV activity of the same compound. In addition, the alkaloidal compound taspin, isolated from different *Croton* species, has been shown to inhibit the reverse transcriptase enzyme of HIV (Sethi, 1977). The phorbol esters 12-*O*-acetylphorbol-13-decanoate, 12-Odecadienylphorbol-13-(2-methylbutyrate and tetradecanoylphorbol-13-acetate (TPA) isolated from the seeds of *C. tiglium* have shown anti-HIV activity (El-Mekawy *et al.*, 1998, 2000). Furthermore, the derivative of phorbol esters, 12-*O*-acetylphorbol-13-decanoate, has shown potential anti-HIV activity as an inhibitor of HIV-1 proliferation (Masuda & Harada, 1993; Nakamura, 2004).

The aqueous extracts *C. cuneatus* (Pereira *et al.*, 1999), *C. malambo* (Suárez *et al.*, 2003), and *C. celtidifolius* (Nardi *et al.*, 2003) have antinociceptive and anti-inflammatory effects. The anti-inflammatory effects of volatile oils of *C. zehntneri* (Oliveira *et al.*, 2001), *C. cajucara* (Bighetti *et al.*, 1999), *C. nepetaefolius* (Abdon *et al.*, 2002), and *C. sonderianus* (Santos *et al.*, 2005) have been reported. In another study, Risco *et al.*, (2003) demonstrated that two phytochemicals, taspine or proanthocyanidins, isolated from *Croton* species possess anti-inflammatory effects. In an earlier study by Perdue *et al.*, (1979), the alkaloid taspine was reported to be a potential anti-inflammatory compound. The anti-inflammatory effect of taspine is attributed to the inhibition of sensory neuron activation (Miller *et al.*, 2001).

The following phytochemicals isolated from different *Croton* species possess anti-inflammatory efficacy: sesquiterpenes ( $5\alpha,10\beta$ -4(15)-eudesmen-1 $\beta$ ,6 $\beta$ - diol, spathulenol,  $5\alpha,10\beta$ -3-eudesmen-1 $\beta$ ,6 $\alpha$  diol and the diterpenoid junceic acid, cajucarinolide, and proanthocyanidins (Aguilar-Guadarrama & Rios, 2004; Carvalho *et al.*, 1996; DalBó *et al.*, 2005; Maciel *et al.*, 2000; Yoshitatsu *et al.*, 1992).

The antitumor effects of *C. lechleri* (Chen *et al.*, 1994) and *C. draco* (Gupta *et al.*, 1996) have been reported. Ethnobotanical and pharmacological efficacy of *C. lechleri* for the treatment of cancer has been reported by many investigators (Cai *et al.*, 1993; Graham *et al.*, 2000; Pieters *et al.*, 1993). Taspine, an alkaloid isolated from *C. lechleri*, has antiproliferative efficacy against the leukemia cell line (Montopoli *et al.*, 2012; Rossi *et al.*, 2003). In another study, the antitumor activity of *Croton palanostigma* was reported by Sandoval *et al.*, (2002). Trans-dehydrocrotonin, isolated from the bark of *C. cajucara*, has shown immunomodulatory and antitumor activity (Melo *et al.*, 2004) by inducing apoptosis and inhibiting cell differentiation (Maristella *et al.*, 2004; Maristella *et al.*, 2003).

Terpenoids isolated from *C. oblongifolius* have shown antitumor activity (Roengsumran *et al.*, 2001, 2002, 2004; Sommit *et al.*, 2003). In a related study, Kawai *et al.*, (2005) demonstrated that the acyclic diterpenoid plauntol, isolated from *C. sublyratus*, exhibits antitumor effects by inhibiting angiogenesis (Kawai *et al.*, 2005). Wound healing activity, antihemorrhagic activity, myorelaxant, antispasmodic and antihypertensive activities of the *Croton* genus have also been reported (Salatino *et al.*, 2007).



## **2.6.4. *Croton macrostachyus* Hochst. ex Delile**

### **2.6.4.1. Description of *Croton macrostachyus***

*C. macrostachyus* is a medium-sized tall tree or shrub that grows up to 30 meters (Edwards and Tadesse, 1995; Umberto, 2012). It is commonly known as a “broad-leaved *Croton*” or “rush foil”. It has various local/vernacular names, including “*bisana*” in Ethiopia, “*msinduzi, mutundu*” in Kenya (Dubale *et al.*, 2015; Lulekal *et al.*, 2013; Maroyi, 2017a; Teklehaymanot, 2009; Teklehaymanot *et al.*, 2007; Umberto, 2012). *C. macrostachyus* has a wide distribution in Africa, where in Kenya, it is widely found in the Karura Forest (Naturgucker., 2018).

### **2.6.4.2. Ethnomedicinal Uses of *Croton macrostachyus***

*C. macrostachyus* is used as a remedy for a variety of illnesses. The plant possesses various medicinal properties (Maroyi, 2017c) and treats constipation in Ethiopia, Cameroon, Rwanda, Kenya, Tanzania, Somalia, and Uganda. Usually, the decoction, macerated leaf, stem bark, or root is used (Ahmed *et al.*, 2013; Mazzanti *et al.*, 1987; Pascaline & Charles, 2011). In Kenya, the leaf and root decoction is used by many patients, including HIV-infected patients, as a cure for cough, back pain, bleeding, skin diseases, warts, pneumonia, and wounds (Jeruto *et al.*, 2008; Kareru *et al.*, 2007; Obey *et al.*, 2016b; Okello *et al.*, 2010; Pascaline *et al.*, 2010).

In Kenya, *C. macrostachyus* bark juice, leaf, and root decoction are used as remedy for backache, bleeding, cancer, colds, cough, diarrhea, dysmenorrhoea, east coast fever, malaria, measles, obesity, pneumonia, ringworm, skin diseases, typhoid, warts, and wounds (Agisho *et al.*, 2014; Bekele & Reddy, 2015; Mesfin *et al.*, 2009). The leaves of *C. macrostachyus* are used by farmers in Kenya as biological pest control when mixed with tobacco (*Nicotiana tabacum* L.) and boiled overnight (Edwards and Tadesse, 1995). In addition, roots of *Cucumis ficifolius* are often used in combination with *C. macrostachyus* bark as a remedy for abdominal and stomach pain (Teklay *et al.*, 2013). Similarly, *Allium sativum* is given with *C. macrostachyus* to treat malaria (Bekele & Reddy, 2015; Mesfin *et al.*, 2009).

### 2.6.4.3. Phytochemistry of *C. macrostachyus*

**Table 2.6-3** summarizes the compounds previously isolated from *C. macrostachyus*.

Table 2.6-3: Phytochemicals isolated from *C. macrostachyus*

Ser. No.	Name of compound	Part of the plant	Reference
1.	Sitosterol palmitate	Twigs	(Tala <i>et al.</i> , 2013a)
2.	Sitosterol	Stem bark and twigs	(Maroyi, 2017b; Tala <i>et al.</i> , 2013a)
3.	Stigmasterol	Stem bark and twigs	(Addae-Mensah <i>et al.</i> , 1992; Tala <i>et al.</i> , 2013)
4.	Betulin	Stem bark and twigs	(Addae-Mensah <i>et al.</i> , 1992; Maroyi, 2017b; Tala <i>et al.</i> , 2013; Tene <i>et al.</i> , 2009)
5.	Lupeol	Stem bark and twigs	(Addae-Mensah <i>et al.</i> , 1992; Tala <i>et al.</i> , 2013; Tene <i>et al.</i> , 2009)
6.	3 $\beta$ -Acetoxy taraxer-14-en-28-oic acid	Roots	(Kapingu <i>et al.</i> , 2000)
7.	Lupenone	Twigs	(Tala <i>et al.</i> , 2013a)
8.	Betulinic acid	Twigs	
9.	Zeroin	Twigs	
10.	28- <i>O</i> -Acetylbetulin	Twigs	
11.	Lupeol acetate	Twigs	
12.	Neoclerodan-5,10-en-19,6 $\beta$ ;20,12-diolide	Roots	(Kapingu <i>et al.</i> , 2000)
13.	(+) Hardwickiic acid	Stem bark and twigs	(Addae-Mensah <i>et al.</i> , 1989; Kapingu <i>et al.</i> , 2000)
14.	12-Oxo-hardwickiic acid	Stem bark and twigs	
15.	Crotomacrine	Fruits	(Tane <i>et al.</i> , 2004)
16.	Floridolide A	Stem bark	
17.	Trachyloban-19-oic acid	Roots	(Kapingu <i>et al.</i> , 2000)
18.	Trachyloban-18-oic acid	Roots	
19.	Crotomachlin	Stem bark and twigs	(Addae-Mensah <i>et al.</i> , 1989)
20.	Crotepoxide	fruits	(Ndunda, 2014) (Morris <i>et al.</i> , 1969)
21.	Lichexanthone	Twigs	(Tala <i>et al.</i> , 2013a)
22.	Methyl 2,4-dihydroxy-3,6-dimethylbenzoate	Twigs	
23.	Methyl gallate	Twigs	
24.	Benzoic acid	Twigs	

#### 2.6.4.4. Pharmacological effects of extracts of *C. macrostachyus*

Antibacterial effects of *C. macrostachyus* against *N. gonorrhoea* (Tefera *et al.*, 2012), *B. cereus*, *E. coli* and *P. aeruginosa* (Cyrus *et al.*, 2008) and *S. pyogenes* (Taye *et al.*, 2011) have been reported. In a related study, Obey *et al.*, (2016) reported that the ethyl acetate extract of stem bark of *C. macrostachyus* has good antibacterial activity against *E. coli*, *S. typhi*, *K. pneumoniae*, *E. aerogenes*, and *L. monocytogenes*. Taye *et al.*, (2011) demonstrated the antibacterial activity of methanol leaf extract against *S. pyogenes* with a minimum bacterial concentration (MBC) value of 7.81 mg/mL.

The antimycobacterial activity of *C. macrostachyus* in an *in vitro* experimental study was reported by Gemechu *et al.*, (2013). Semenya & Maroyi, (2013) also demonstrated the antimycobacterial activity of methanolic leaf extracts of *C. macrostachyus* with minimum inhibitory concentration (MIC) values ranging from 12.5 to 100 µg/mL. This study demonstrated that *C. macrostachyus* has potential as an herbal medicine in the treatment and management of tuberculosis, a leading cause of death in sub-Saharan Africa (Semenya & Maroyi, 2013).

Antimicrobial and antifungal effects of *C. macrostachyus* extracts have been reported by Desta, (1993) and Taniguchi & Kubo, (1993). The isolated diterpenoid 12-oxo-hardwickic acid has shown efficacy against *Candida albicans* (Tene *et al.*, 2009). Ngo Bum *et al.*, (2012) reported that decoctions of *C. macrostachyus* possess anticonvulsant effects (Lulekal *et al.*, 2008). The antimalarial efficacy of leaf and stem bark extracts of *C. macrostachyus* has been reported by Karunamoorthi & Ilango, (2010) and Owuor *et al.*, (2012). Bantie *et al.*, (2014) demonstrated a chemoprotective effect against malaria.

The anthelmintic efficacy of seed extracts of *C. macrostachyus* has been reported by Eguale *et al.*, (2007). Kamanyi *et al.*, (2009) demonstrated that extracts of stem bark of *C. macrostachyus* exhibited anti-inflammatory activity in experimental mouse models of inflammation (Kamanyi *et al.*, 2009). Similar findings were also reported by Nguielefack *et al.*, (2015).

Methanolic leaf extract of *C. macrostachyus* showed antioxidant activity with an IC<sub>50</sub> value of 0.11 mg/mL. The documented antioxidant activities of *C. macrostachyus* leaf extracts were probably due to flavonoids and phenols that have been isolated from fruits, leaves, and roots (Amuamuta *et al.*, 2015; Degu *et al.*, 2016; Eguale *et al.*, 2007). Flavonoids and phenolic compounds found in plants have antioxidant properties (Miguel *et al.*, 2014).

## **2.6.5. *Croton megalocarpus* Hutch.**

### **2.6.5.1. Description of *C. megalocarpus***

*C. megalocarpus* (family Euphorbiaceae) is a medium-sized tree or shrub that grows up to 35 meters tall (Thijssen, 1996). It is commonly planted as a shade tree (Maroyi, 2017e; Thijssen, 1996). The species name “*megalocarpus*” refers to the species’ relatively large fruits (Hyde, *et al.*, 2012; Hyde, 2013). *C. megalocarpus* is commonly known by various local/vernacular names including ‘*mbali*’ in East Africa, “*msuduzi*” in Kenya (Bussmann, 2006; Fratkin, 1996; Kipkore *et al.*, 2014; Kiringe, 2006), “*umunege*” in Rwanda, and “*umuraangara*” in Tanzania: (Ibrahim & Ibrahim, 1998; Johns *et al.*, 1994; Minja, 1994; Umberto 2012). *C. megalocarpus* is widely distributed in Africa (Maroyi, 2017e; Thijssen, 1996). It is considered one of the vital medicinal plants in Kenya (Njoroge *et al.*, 2010). It is found in Laikipia County and is traded in traditional herbal medicine (“*muthi*”) markets in Thika and Nairobi, Kenya (Njoroge, 2012).

### **2.6.5.2. Ethnomedicinal Uses of *C. megalocarpus***

*C. megalocarpus* is mainly used to treat respiratory problems (Muthee *et al.*, 2011; Grace *et al.*, 2006), fever (Ichikawa, 1987; Johns *et al.*, 1994; Nanyingi *et al.*, 2008), and wounds (Kamau *et al.*, 2016; Nanyingi *et al.*, 2008). In Kenya, *C. megalocarpus* is used in the treatment of constipation (Kipkore *et al.*, 2014) and as an herbal medicine for backache, chest problems (Bussmann, 2006; Kiringe, 2006), malaria (Bussmann, 2006; Cyrus *et al.*, 2008; Fratkin, 1996) and stomach ache (Bussmann, 2006; Fratkin, 1996; Kiringe, 2006).

The bark decoction is used for arthritis (Pascaline *et al.*, 2010), colds (Fratkin, 1996), cough, diarrhea (Gakuubi & Wanzala, 2012; Nanyingi *et al.*, 2008), fever (Ichikawa, 1987; Johns *et al.*, 1994; Nanyingi *et al.*, 2008), wounds (Kamau *et al.*, 2016; Nanyingi *et al.*, 2008), and vomiting induction (Kiringe, 2006). In addition, the leaf and root decoction of *C. megalocarpus* is used by HIV patients for the treatment of pneumonia (Kamau *et al.*, 2016), respiratory problems (Muthee *et al.*, 2011), wounds, and diabetes (Keter & Mutiso, 2012).

### 2.6.5.3. Phytochemistry of *C. megalocarpus*

**Table 2.6-4** summarizes the compounds previously isolated from *C. megalocarpus*.

Table 2.6-4: Phytochemicals isolated from *C. megalocarpus*

Ser. No	Compound name	Part of the plant	Reference
1.	Betulin	Stem bark	(Addae-Mensah <i>et al.</i> , 1992;
2.	3- $\beta$ -O-Acetoacetyl lupeol	Stem bark	Maroyi, 2017b; Tala <i>et al.</i> , 2013; Tene <i>et al.</i> , 2009)
3.	Aleuritic acid	Stem bark	(Aldhafer <i>et al.</i> , 2017; Langat <i>et al.</i> , 2012)
4.	Lupeol	Stem bark	(Barbosa <i>et al.</i> , 2003; Burns <i>et al.</i> , 2000; Stephane <i>et al.</i> , 2019)
5.	Chiromodine	Stem bark	(Addae-Mensah <i>et al.</i> , 1989; Markó
6.	Epoxychiromodine	Stem bark	<i>et al.</i> , 1999)
7.	Crotonolide E	Root	(Alqahtani, 2015; Liu <i>et al.</i> , 2014)
8.	Furocrotinsulolide A	Root	(Alqahtani, 2015; Graikou <i>et al.</i> , 2005)
9.	3 $\beta$ ,4 $\beta$ :15,16-diepoxy-13(16),14-ent-clerodadien-17,12S-olide	Root	(Alqahtani, 2015)
10.	3 $\beta$ ,4 $\beta$ :15,16-diepoxy-13(16),14-ent-clerodadiene	Root	(Alqahtani, 2015; Harinantenaina & Asakawa, 2007; Roengsumran <i>et al.</i> , 2001)
11.	<i>Trans</i> -annonene	Root	(Alqahtani, 2015; McCrindle <i>et al.</i> , 1976)
12.	Crotohalimaneic acid	Root	(Alqahtani, 2015; Ndunda B., 2014; Roengsumran <i>et al.</i> , 2004)
13.	7,13-abietadien-2-one	Root	(Alqahtani, 2015)
14.	7,13-abietadien-2-ol	Root	

### 2.6.5.4. Pharmacological effects of extracts of *C. megalocarpus*

The antibacterial efficacy of *C. megalocarpus* against *B. subtilis* and *S. aureus* has been documented by Matu & Van Staden, (2003). Kariuki *et al.*, (2014) demonstrated that aqueous extracts of *C. megalocarpus* have antibacterial activity against *P. aeruginosa*, *E. coli*, *K. pneumoniae* and *S. aureus*. The phytochemicals betulin, lupeol, lauric acid, and palmitoleic acid are responsible for the antibacterial activities of *C. megalocarpus* (Duric *et al.*, 2013; Ouattara *et al.*, 1997).

Lall *et al.*, (2006) demonstrated the antifungal activities of  $\beta$ -sitosterol, betulin, and lupeol against *Aspergillus flavus*, *Aspergillus niger*, *Cladosporium cladosporioides*, and *Phytophthora* spp. Similarly, Nisar *et al.*, (2013) reported the antifungal effects of betulin and lupeol against *Aspergillus flavus*, *Aspergillus niger*, *Candida albicans*, *Candida glabrata*, and

*Microsporium caris*. Matu & Van Staden, (2003) and other workers demonstrated the anti-inflammatory effect of *C. megalocarpus*, which is attributed to phytochemicals such as sitosterol (Nirmal *et al.*, 2012), betulin (Lin *et al.*, 2009), lupeol (Geetha & Varalakshmi, 1998), linoleic acid and linolenic acid (G. Zhao *et al.*, 2005), which have cyclooxygenase enzyme inhibition potential. Others have also reported the antinociceptive effects of linoleic acid, lupeol, and oleic acid (Lima *et al.*, 2013; Gichui, 2016; Mota *et al.*, 2015). Wambugu & Waweru, (2016) documented the wound healing activity of extracts of *C. megalocarpus*, where phytochemicals such as betulin, lupeol (Ebeling *et al.*, 2014), and linolenic acid (Lewinska *et al.*, 2015) are responsible for this activity.

## 2.6.6. *Croton dichogamus* Pax

### 2.6.6.1. Description of *C. dichogamus*

*C. dichogamus* Pax (Euphorbiaceae) grows as a shrub or tree in Ethiopia, Kenya, Madagascar, Mozambique, Tanzania, and Somalia (Govaerts, 1999). It grows up to 7.5 meters tall or more but is usually only 2 - 5 meters tall.

### 2.6.6.2. Ethnomedicinal uses of *C. dichogamus*

In East African countries, decoctions of leaves, roots, and whole plants are used to treat fever, chest ailments, stomach diseases, tuberculosis, impotence, and malaria (Jeruto *et al.*, 2008; Kokwaro, 1976). In Tanzania, the roots of *C. dichogamus* are milled and then mixed with porridge for the treatment of tuberculosis because the shrub is believed to be efficient in the management of respiratory ailments. The leaves are also used as a tonic, antimalarial and nutritional supplement. Patients inhale the smoke of burnt leaves to provide relief from fever (Hedberg *et al.*, 1983).

### 2.6.6.3. Phytochemistry of *C. dichogamus*

**Table 2.6-5** summarizes the compounds previously isolated from the stem bark of *C. dichogamus*.

Table 2.6-5: Phytochemicals isolated from *C. dichogamus*

Ser. No	Name of compound	Plant part	Reference
1.	Aleuritolic acid	Root	(Aldhafer <i>et al.</i> , 2017; Langat <i>et al.</i> , 2012)
2.	Crotonolide E	Root	(Alqahtani, 2015; Liu <i>et al.</i> , 2014)
3.	Furocrotinsulolide A	Root	(Alqahtani, 2015; Graikou <i>et al.</i> , 2005)

Ser. No	Name of compound	Plant part	Reference
4.	3 $\beta$ ,4 $\beta$ ,15,16-diepoxo-13(16),14-clerodadiene	Root	(Aldhafer <i>et al.</i> , 2017; Harinantenaina <i>et al.</i> , 2006)
5.	3 $\beta$ ,4 $\beta$ ,15,16-diepoxo-13(16),14- <i>ent</i> -clerodadiene-17,(12 <i>S</i> )-olide	Root	(Aldhafer <i>et al.</i> , 2017; Pudhom & Sommit, 2011)
6.	15,16-epoxy13(16),14- <i>ent</i> -clerodadien-3-one ( <i>trans</i> -cascarillone)	Root	(Aldhafer <i>et al.</i> , 2017)
7.	15,16-Epoxo-5,13(16),14- <i>ent</i> -halimatriene-3-ol	Root	
8.	15,16-epoxy4(18),13(16),14- <i>ent</i> -clerodatrien-3a-ol (gbaninol)	Root	
9.	15,16-epoxy-3 $\beta$ -hydroxy-5(10),13(16),14- <i>ent</i> -halimatriene-17,(12 <i>S</i> )-olide	Root	
10.	15,16-epoxy-3 $\alpha$ -hydroxy-4(18),13(16),14- <i>ent</i> -clerodatrien-17,(12 <i>S</i> )-olide (crotonolide F)	Root	
11.	Crotoxiide A	Leaves	(Jogia <i>et al.</i> , 1989)
12.	Crotoxiide B	Leaves	
13.	Crotohaumanoxiide	Root	(Aldhafer <i>et al.</i> , 2017; Li <i>et al.</i> , 2010; Tchissambou <i>et al.</i> , 1990)
14.	Crotodichogamoin A	Root	(Aldhafer <i>et al.</i> , 2017)
15.	Crotodichogamoin B	Root	
16.	Crothalimene A	Root	
17.	Crothalimene B	Root	
18.	Depressin	Root	(Aldhafer <i>et al.</i> , 2017; Li <i>et al.</i> , 2010)
19.	Cadalene	Root	(Aldhafer <i>et al.</i> , 2017)
20.	6 $\alpha$ -methoxy-patchoulan-4-ene (6a-methoxycyperene)	Root	(Aldhafer <i>et al.</i> , 2017; Barreto <i>et al.</i> , 2013)
21.	4-patchoulen-3-one (cyperotundone)	Root	(Aldhafer <i>et al.</i> , 2017)
22.	4-patchoulene (cyperene)	Root	
23.	1(6),7,9-cadinatriene-4 $\alpha$ ,5 $\beta$ -diol (4 $\alpha$ ,5 $\beta$ -corocalanediol)	Root	
24.	1,3,5-cadinatriene-(7 <i>R</i> ,10 <i>S</i> )-diol (10- <i>epi</i> -maninsigin D)	Root	

#### 2.6.6.4. Pharmacological effects of extracts of *C. dichogamus*

Magadula, (2012) demonstrated the antimycobacterial activity of an ethanolic root extract of *C. dichogamus* against *M. indicus pranii* and *M. madagascariense indicus*, giving a minimum inhibitory concentration (MIC) of 1.25 mg/ml (Magadula, 2012). Studies have shown that *C. dichogamus* has insecticidal activity against *Anopheles gambie* and is

extensively used to treat malaria in lake basins (Omara, 2020). In addition, the presence of a very high concentration of terpenoids in *C. dichogamus* has been linked to its antimicrobial properties (Magadula, 2012).

A recent study on the phytochemical constituents of most croton species pointed out that the presence of clerodane diterpenoids in these species results in higher anti-inflammatory activity than the standard drug used in the study (Somteds *et al.*, 2019). The high level of saponins in *C. dichogamus* crude stem extracts (Johns *et al.*, 1999) was confirmed to lower cholesterol levels in humans and animals by preventing endogenous and exogenous cholesterol absorption, thus lowering serum cholesterol (Thompson, 1993).



## CHAPTER THREE

### METHODOLOGY

#### 3.1. Materials

Commercial silica gel (100–200, 200–300, and 300–400 mesh; Qingdao, China) was used for column chromatography (CC). Sephadex LH-20 (Amersham Biosciences) was also used for CC. All solvents used for column chromatography were of analytical grade (Shanghai Chemical Reagents Co., Ltd.). Analytical TLC using precoated aluminum-backed plates (silica gel 60 F<sub>254</sub>, Merck) were used. Spots were detected on TLC under UV light at 254 or 365 nm, followed by spraying with 1% vanillin-sulfuric acid spray reagent and warming. Extraction and CC was performed at the research laboratory of United States International University, Kenya.

1D and 2D NMR spectra were recorded in CDCl<sub>3</sub> on a 400 MHz Bruker AVANCE NMR instrument at room temperature. Chemical shifts ( $\delta$ ) were expressed in ppm and were referenced against the solvent resonances at  $\delta_{\text{H}}$  7.26 and  $\delta_{\text{C}}$  77.23 ppm for <sup>1</sup>H and <sup>13</sup>C NMR for CDCl<sub>3</sub>. Structural assignments of the new compounds were made with additional information from 1H-1H COSY, HSQC, NOESY, and HMBC experiments. Mass spectra were recorded on a GC-MS Bruker MicroToF Mass Spectrometer by direct injection using a Bruker Bioapex-FTMS with electrospray ionization. The spectroscopic analysis was performed at the Jodrell Laboratory, Royal Botanic Gardens Kew (UK).

For the *in vitro* experiment, human T-lymphocyte MT-4 cells (ARP-120) and Human immunodeficiency virus type 1 (HIV-1<sub>III</sub>B) strain were obtained from the National Institute of Health (NIH) HIV Reagent Program. The *in vitro* cytotoxicity and anti HIV activity tests were carried out in the institute of primate research (IPR) and Kenya medical research institute (KEMRI), Kenya.

#### 3.2. Photochemical study of the medicinal plants

##### 3.2.1. Collection of the plant specimen and ethical consideration

The leaves and stem bark of *C. macrostachyus* and *C. megalocarpus* were collected from a USIU botanical garden in June 2020. The twigs of *C. dichogamus* were collected from Mwala Constituency, Machakos County, Kenya, in August 2020 (**Figure 3.2-1 to 3.2-3**). The collection of these medicinal plants was performed after obtaining the required ethical approval from the Kenyatta National Hospital-University of Nairobi Ethics and Research Committee

(KNH-UON ERC), approval number KNH/ERC/A/154 and research permit from the National commission for science, technology and innovation (NACOSTI), permit number NACOSTI/P/22/15579. Expert botanist and taxonomist performed taxonomic identification, and voucher specimen TEREFE E./044, TEREFE E./045 and TEREFE E./046 were deposited for *C. megalocarpus*, *C. macrostachyus*, and *C. dichogamus* respectively at the United States International University herbarium for future reference. After collection, the leaves were thoroughly washed and dried in the shade. Then, the dried leaves were pulverized using a mortar and pestle at the medicinal plants laboratory of United States International University Africa (USIU-A).

### 3.2.2. Preparation of Crude extract

The powdered plant materials were separately extracted with 1:1 CH<sub>2</sub>Cl<sub>2</sub>:CH<sub>3</sub>OH solvent using the cold maceration technique. Maceration was continued for 7 days with frequent agitation in an orbital shaker, and the extract was filtered. Extraction was repeated three times, and the filtrates of all portions were pooled. Finally, the extracts were concentrated using rotavapor at 30°C to obtain dry extracts. The extract was weighed and packed in a glass vial and stored in a desiccator over silica gel until use. The percentage yield was calculated using equation 1.

$$\text{Percentage yield} = \frac{\text{Mass (gm) of extract obtained}}{\text{Mass (gm) of dried plant}} \times 100 \dots \dots \text{Equation 1}$$

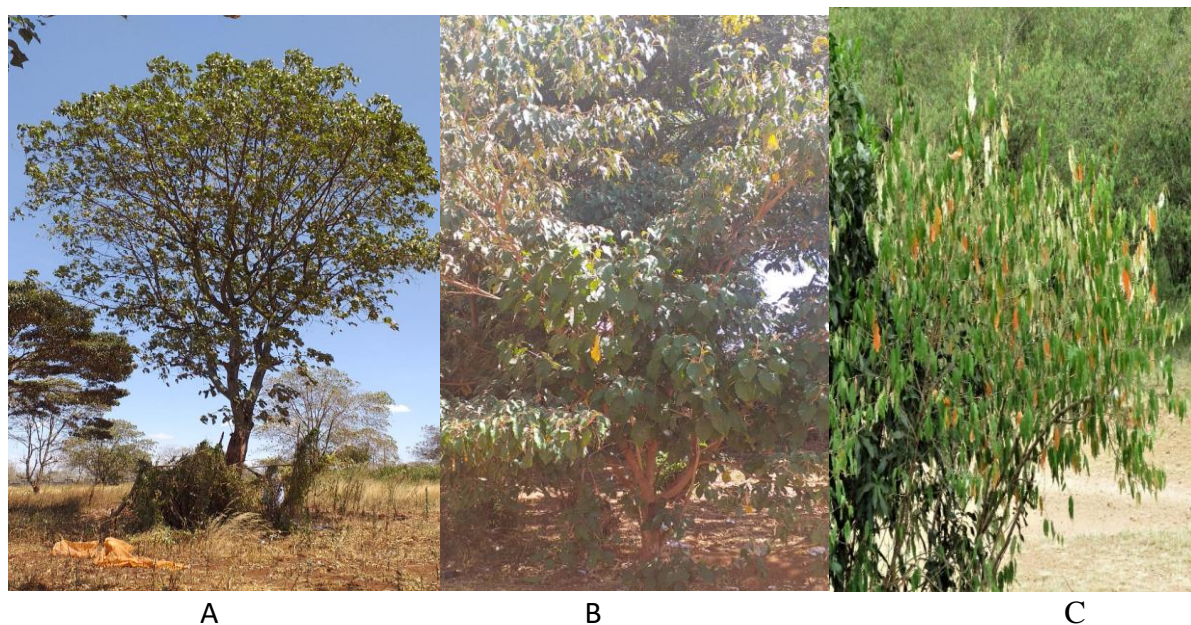


Figure 3.2-1: A, *C. macrostachyus*; B, *C. megalocarpus*; C, *C. dichogamus*



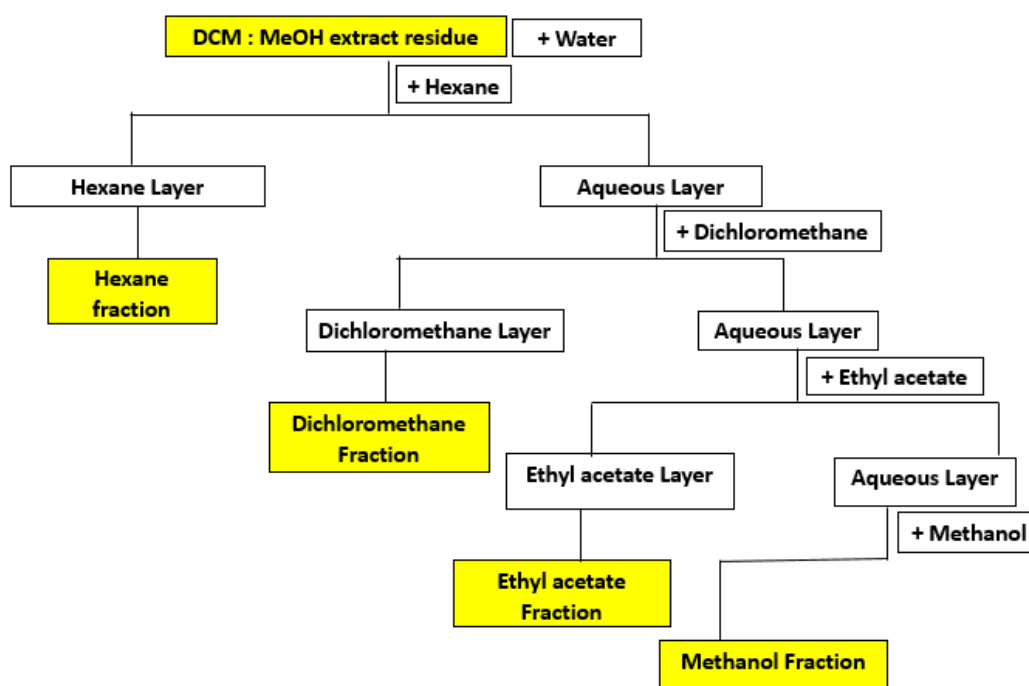
Figure 3.2-2: Collection of stem bark of *C. megalocarpus*



Figure 3.2-3: Crude and liquid-liquid extraction of the plant extracts

### 3.2.3. Liquid-Liquid separation of the crude extracts

The dried crude mass 1:1  $\text{CH}_2\text{Cl}_2:\text{CH}_3\text{OH}$  extracts of *C. megalocarpus*, *C. macrostachyus*, and *C. dichogamus* were separately dissolved in distilled water (200 mL) and successively partitioned using different solvents of increasing polarity (n-hexane, dichloromethane, ethyl acetate, and methanol) in separatory funnels, as shown schematically in **Scheme 3.2-1**. The different solvent fractions were concentrated under reduced pressure using a rotary evaporator, and the resulting product was dried in an oven at 30°C. The dried fractions were then transferred into separate vials and stored in a desiccator for further use.



Scheme 3.2-1: Flow chart of liquid-liquid extraction of plant extracts

#### 3.2.4. Chromatographic technique and isolation of pure compound

The different fractions of the three plants were subjected to column chromatography using 60-120 mesh silica gel and eluted successively with varying concentrations of ethyl acetate and n-hexane (E: H). Bioassay-guided fractionation was performed on the partitions showing the highest antiretroviral activity. Each fraction was then evaluated for antiretroviral activity, and the fraction with the highest activity was further subjected to open column chromatography on 200-400 mesh silica gel (**Figure 3.2-4 to 3.2-5**). Compound purity was determined using thin-layer chromatography (TLC) on precoated aluminium-backed plates (silica gel 60 F<sub>254</sub>, Merck), and compounds were visualized using UV radiation at 254 nm, followed by an anisaldehyde spray reagent (1 percent p-anisaldehyde:2 percent H<sub>2</sub>SO<sub>4</sub>: 97 percent cold MeOH) and heating. Final purifications were carried out in selected solvent systems using preparative thin layer chromatography (Merck 818133) and gravity column chromatography (Merck Art. 9385), which used a 2 cm diameter column packed with silica gel.



A

B

Figure 3.2-4: Column chromatography of the studied plant fractions

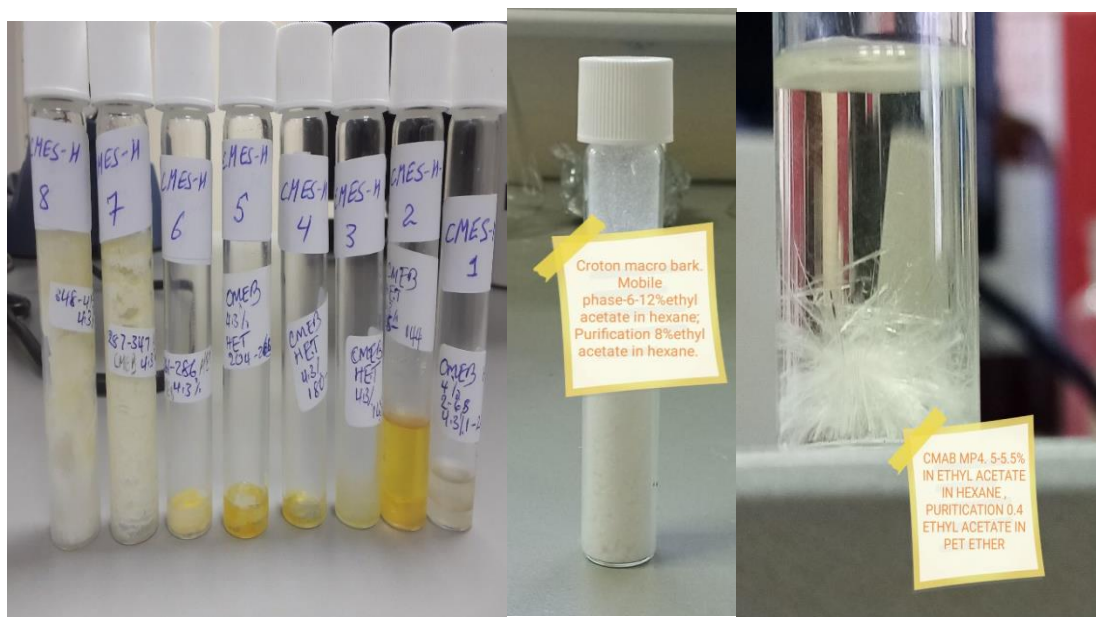


Figure 3.2-5: Examples of the isolated pure compounds

### 3.2.5. Structural elucidation of isolated compounds

The isolated pure compounds were characterized by nuclear magnetic resonance (NMR) and High-resolution mass spectrometry (HRMS) at the Jodrell Laboratory, Royal Botanic Gardens Kew (UK). A Perkin-Elmer Frontier/Spotlight 200 spectrometer was used to record FTIR spectra. In addition, 1D and 2D NMR spectra in CDCl<sub>3</sub> were collected at room temperature using 400 MHz Bruker AVANCE NMR equipment. Chemical shifts ( $\delta$ ) were measured in ppm and compared to the solvent resonances for <sup>1</sup>H and <sup>13</sup>C NMR for CDCl<sub>3</sub> at  $\delta_{\text{H}}$  7.26 and C 77.23 ppm.

The chemicals were analysed for HRMS using a Vanquish UHPLC system (Thermo Scientific, Waltham, MA, USA) linked to a 100 Hz photodiode array detector (PDA) and a Thermo Scientific Orbitrap Fusion Tribrid (Thermo Scientific) high-resolution tandem mass spectrometer. Chromatographic separation (5  $\mu$ L) was performed on a Luna C18 column (150 mm  $\times$  3 mm i.d., 3  $\mu$ m, Phenomenex, Torrance, CA, USA) using a mobile phase gradient of 0:90:10 to 90:0:10 (MeOH (A): water (C): acetonitrile + 1% formic acid (D)) over 60 min. Then, 90% A was held for 10 minutes and returned to initial conditions over 5 minutes at 30°C (flow rate: 400  $\mu$ L/min). UV detection done between 210 and 550 nm. Mass spectrometry detection was performed in positive and negative ionization modes using the full scan and data dependent MS<sup>2</sup> and MS<sup>3</sup> acquisition modes.

Total ion current (TIC) chromatograms were obtained over the range of 125–1800  $m/z$  using spray voltages of +3.5 kV and –2.5 kV for the positive and negative ionization modes, respectively. Four different scan events were recorded for each ionization mode as follows: 1) full scan; 2) MS<sup>2</sup> of the most intense ion in scan event 1; 3) MS<sup>3</sup> of the most intense ion in scan event 2; and 4) MS<sup>3</sup> of the second most intense ion in scan event 2. Additional parameters for the mass spectrometer included: full scan resolution, 60,000 FWHM; capillary temperature, 350°C; ion transfer tube temperature, 325°C; RF lens (%), 50; automatic gain control (AGC) target, 4.0e5 (Full scan) and 1.0e4 (MS<sup>n</sup>); intensity threshold, 1.0e4; CID collision energy, 35; activation Q, 0.25; and isolation window ( $m/z$ ), 4. Nitrogen was used as the drying, nebulizer, and fragmentation gas.

### **3.3. *In vitro* assay for antiretroviral activity**

#### **3.3.1. Preparation of extracts and test compounds**

Since most plant extracts and purified compounds are readily soluble in DMSO, (Cos *et al.*, 2009), the concentrated dried extracts were dissolved in 1% v/v dimethylsulfoxide (DMSO) and stored in 2 ml cryovials at 4°C until use. Each extract and pure compound were reconstituted to obtain a stock solution of 4 mg/ml. The stock solutions were filtered through a 0.22 µm membrane filter (Sigma, South Africa) and stored at 4°C until further use (Rege *et al.*, 2010).

#### **3.3.2. Cell culture, maintenance, and viability test**

Since the discovery of the Human Immunodeficiency Virus (HIV), much effort has been devoted to finding susceptible, highly permissive cell lines and developing reliable assays for detecting the multiplication of the virus. The first isolates of HIV were from mononuclear cells in the peripheral blood of patients with Acquired Immunodeficiency Syndrome (AIDS), and the first successful transmission of HIV to an established T-cell line, H9, was achieved by Popovic *et al.* (Popovic *et al.*, 1984; Szucs *et al.*, 1988). Other T-cell lines were found to be susceptible to HIV infection. Each of these cell lines had one thing in common: the presence of a CD4 epitope on the surface of the cell to which the envelope protein of HIV could bind (Szucs *et al.*, 1988).

Harada *et al.*, (1985) reported that a lymphocyte cell line, MT-4, was highly susceptible to HIV infection and typically grew in clusters. Without a virus, these cell aggregate to form into clusters after dissociation by pipetting within 2 to 3 hours. After superinfection with HIV, rapid induction and release of HIV antigens were observed, accompanied by a marked cytopathogenic effect (Harada and Yamamoto, 1985; Szucs *et al.*, 1988). Moreover, many scholars have used the MT-4 cell line to evaluate the anti-HIV activity of various compounds (Asres and Bucar, 2005; Weislow *et al.*, 1989).

In this study, human T-lymphocyte MT-4 cells (ARP-120) were obtained from the National Institute of Health (NIH) HIV Reagent Program, Division of AIDS, National Institute of Allergy and Infectious Diseases (NIAID), NIH; donated by Dr. Douglas Richman. Human T-lymphocytic MT-4 cells express CD4, CXCR4, and CCR5 and are used for cytotoxicity inhibition assays for antiviral drugs (Harada *et al.*, 1985; Larder *et al.*, 1989; Pauwels *et al.*, 1987). The vials containing frozen MT-4 cells were retrieved from the liquid nitrogen tank and rapidly thawed (Gao *et al.*, 2009).

In a tissue culture laminar flow hood, the exterior of the vials was decontaminated by spraying 70% ethanol. Then, the vial was opened and resuspended in 10 mL complete culture medium (CCM) containing RPMI-1640 with 2 mM L-glutamine supplemented with 10% fetal bovine serum (FBS), 10 mM HEPES buffer, 100 IU of penicillin/mL, 100 µg of streptomycin/mL, 1 ng of recombinant interleukin-2 (Invitrogen)/ml, and 2 µg of phytohemagglutinin/mL as described previously by Gao *et al.*, (2009). The CCM was sterilized with a 0.22 µm membrane filter before use. The cultures were incubated at 37°C in a humidified incubator with atmospheric conditions of 5% CO<sub>2</sub>. Every 3-5 days, the cultures were centrifuged, pelleted, and resuspended in 5-10 mL RPMI 1640 supplemented with 10% FBS. The culture flasks were routinely examined for changes using an inverted microscope (**Figure 3.3-1**), which determined the frequency of media changes. The cell count and viability were measured by the trypan blue dye exclusion technique (Miyoshi *et al.*, 1982).

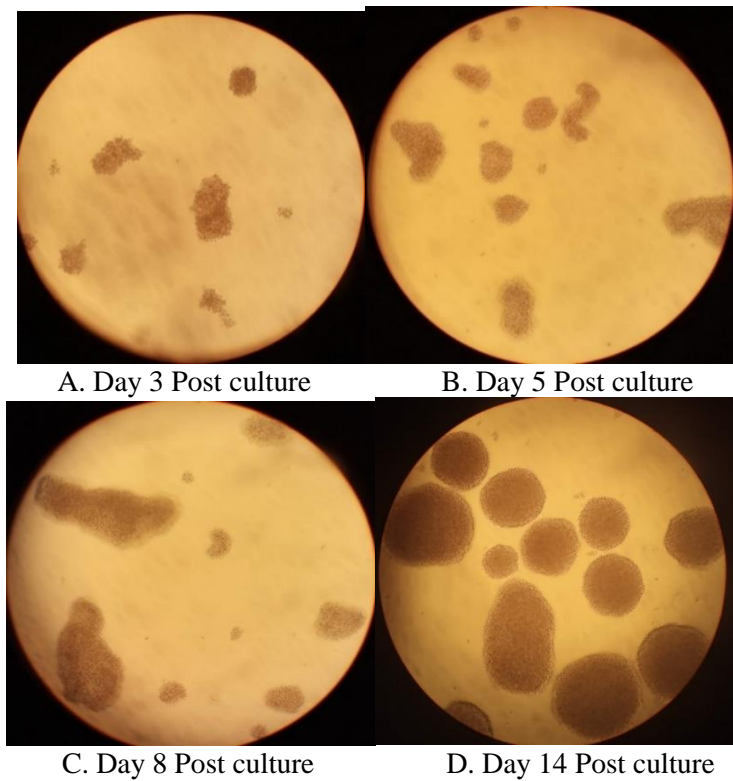


Figure 3.3-1: MT-4 cell culture

The dye exclusion test was used to determine the number of viable cells present in the cell suspension. This method is based on the principle that living cells possess intact cell membranes that exclude certain dyes, such as trypan blue, eosin, or propidium, whereas dead cells do not (Strober, 2015). Briefly, an aliquot of MT-4 cell suspension was centrifuged for 5 min at 1500 rpm, and the supernatant was discarded. The cell pellet was then resuspended in a 1 ml complete medium. Ten microliters of 0.4% trypan blue was mixed with 10 µL of MT-4



cell suspension and incubated for 3 minutes at room temperature. The percentage of cell viability was determined using a hemocytometer. The number of viable cells of a cell suspension, which was mixed with 0.2% Trypan Blue (Biowhittaker, Wakersville) (v/v 1:1), was determined. A drop of the mixture was applied to a hemocytometer. This mixture was spread across a grid by capillary action. Only the viable (translucent) cells that lay within or touched the left or top boundary were counted. The percentage cell viability was determined using equation (2). The number of viable cells per ml in the original sample was calculated using equation (3).

$$\% \text{ cell viability} = \frac{\text{Total viable cells (unstained)}}{\text{Total cells (Viable+dead)}} \times 100 \dots \dots \dots \text{Eq. 2}$$

$$\text{Number of viable cells per ml} = \text{Average No. of viable cells per square} \times \text{Dilution factor} \times 10^4 \dots \dots \dots \text{Eq. 3}$$

After the MT-4 cells were incubated over a 3-day period, they were then subcultured in RPMI, and stock cultures were stored at -70°C in a freezer until required. Cell maintenance was performed according to standard protocols Miyoshi *et al.*, (1982). All cell culture procedures were carried out in a Class III biological safety cabinet. The unit was swabbed/sterilized with 70% ethanol before and after each use.

### 3.3.3. Preparation of the virus and viral infectivity test

Human immunodeficiency virus type 1 (HIV-1<sub>IIIB</sub>) strain was obtained from the NIH HIV Reagent Program, Division of AIDS, NIAID, NIH. Dr. Robert Gallo donated human immunodeficiency virus-1 IIIB (ARP-398). HIV-1<sub>IIIB</sub> is highly capable of replicating in human T cell lines and appears to be well adapted for *in vitro* culture in T cells (Popovic *et al.*, 1984).

The frozen HIV-1<sub>IIIB</sub> vials were thawed by immersion in room temperature water, and the vial was swirled until viruses were thawed. Then, 400 µl of the virus was transferred to 75 cm<sup>2</sup> tissue culture flasks (T75) containing 10 mL of 1 x 10<sup>5</sup> pelleted MT4 cells/mL, vortexed, and incubated at 37°C for 1 hr for virus adsorption. After 1 hr, 20 ml of RPMI-1640 was added gently and mixed with vortexing. The cells were then pelleted by centrifuging at 1500 rpm for 5 min. The pelleted cells were then washed and resuspended in 30 ml RPMI 1640 with L-glutamine and 20% fetal bovine serum in a T75 flask, incubated at 37°C and monitored for the development of cytopathic effects (CPEs).

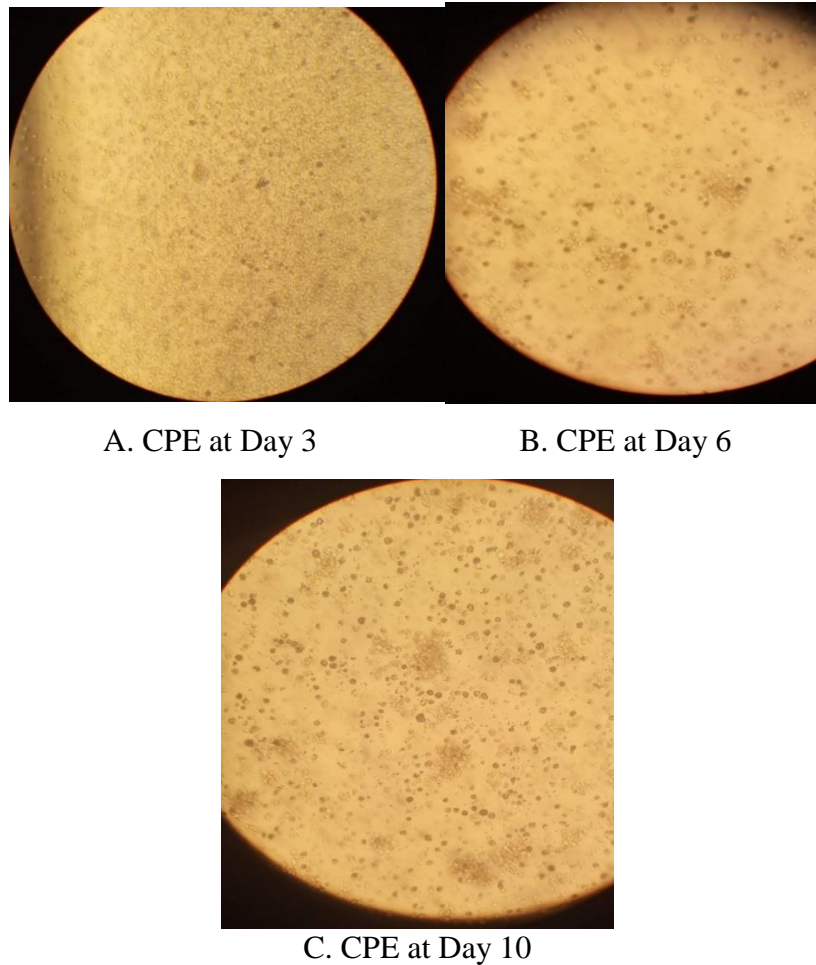


Figure 3.3-2: Development of cytopathic effects in MT-4 cells

MT-4 cells inoculated with HIV showed markedly different cell growth and viability patterns than mock-infected cells. The number of viable cells rapidly decreased at 24 hours post-infection, and by day 4, only 2-4% of the infected MT-4 cells were viable. In contrast, the mock-infected cells grew well, reaching a plateau between days 2 and 4. After 4 days, the viability of these cells began to decline appreciably. The infected cells displayed cytopathic effects (CPE), including became round, lost their surface characteristics, became refractile, and diminished in size. By day 3, many infected cells developed balloon-like, cytoplasmic swelling (**Figure 3.3-2**). The dose of the virus influenced the number of viable cells and the time course of appearance of these cytopathic effects. These observations agreed with previous reports of many scholars who used the MT-4 cell line to evaluate the anti-HIV activity of various compounds (Asres and Bucar, 2005; Harada and Yamamoto, 1985; Szucs *et al.*, 1988; Weislow *et al.*, 1989).

The virus infectivity test was performed to determine the infectious titer of the virus, which can cause cytopathic effects (CPE) in tissue culture over a reasonable period of 3 to 10

days while cells in culture remain viable (Gao *et al.*, 2009; Reed and Muench, 1938). In addition, this procedure was performed to quantify the amount of virus required to produce a cytopathic effect in 50% of cell culture replicates (TCID<sub>50</sub>) (Pauwels *et al.*, 1988). CPE induced by the virus was observed under a microscope after 3–4 days. The TCID<sub>50</sub> was then calculated as described by Reed & Muench, (1938) and Ramakrishnan, (2016). For the anti-HIV activity testing, 640 µL of HIV-1<sub>IIIIB</sub> virus at 1.26 X10<sup>8</sup> TCID<sub>50</sub>/ml was used to infect 1 x10<sup>8</sup> cell/ml. All procedures were carried out following biosafety guidelines defined in the BMBL, NIH-CDC HHS Publication No. (CDC) 21-1112 (CDC, 2009).

### 3.3.4. Cytotoxicity assay

#### 3.3.4.1. Cytotoxicity test using Human T-Lymphocyte MT-4 cells

A cytotoxicity test was conducted to evaluate the cytotoxicity of the plant extracts by measuring cell death caused by the plant extracts. The assay was conducted using an MTT colorimetric assay as described by Mosmann (1983) and Pauwels *et al.*, (1988). The MTT assay is based on the reduction of the yellow-colored tetrazolium salt MTT (3-(4,5-dimethylthiazol-2-yl)-2,5-diphenyltetrazolium bromide) by NAD(P)H-dependent cellular oxidoreductase enzymes (Berridge *et al.*, 2005) to an insoluble dark-blue colored formazan that can be measured spectrophotometrically (Mosmann, 1983) (**Figure 3.3-3**). Formazan production indicates the number of viable cells; therefore, an increase or decrease in cellular viability results in a change in the amount of formazan formed, which indicates the degree of cellular cytotoxicity (CC<sub>50</sub>) caused by the plant extract.

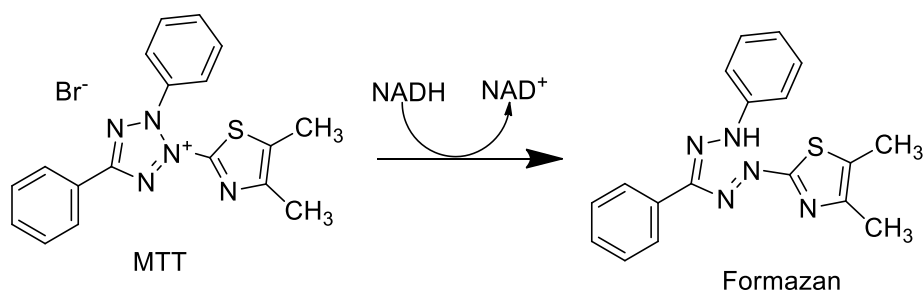


Figure 3.3-3: Conversion of MTT to Formazan by oxidoreductase enzymes

MTT (3-(4,5-dimethylthiazol-2-yl)-2,5-diphenyl tetrazolium bromide) was dissolved in PBS to obtain a final concentration of 5 mg/ml and filtered to sterilize and remove insoluble residue (ACTG Laboratory Technologist Committee, 2004; Szucs *et al.*, 1988). The assay was carried out in 96-well, flat-bottomed microtiter plates. To each well, 200 µL of MT-4 cells (1×10<sup>5</sup> cells) in growth media was added. The plates were preincubated for 24 h at 37°C to

allow stabilization. Then, 50 µL of the test compounds (at a concentration of 4 mg/ml) were added to the first column of the well. With a multichannel pipette, 50 µL was transferred (in triplicate) from the wells labeled 1 to wells labeled 2, and such transfers were continued (serial dilution), moving from left to right, changing tips prior to mixing contents of the next column of wells. Finally, 50 µL was discarded from the wells in column 12. Different concentrations (800 – 8.192×10<sup>5</sup> µg/mL) of test compounds were prepared through serial dilution. Each dilution was tested in triplicate. The negative control (NC) wells contained 50 µL of MT-4 cells in 0.5% DMSO (Weislow *et al.*, 1989). Positive control (zidovudine, tenofovir, abacavir and nevirapine) drugs were also added in triplicate.

A 96-well microtiter plate containing the test compounds and positive and negative controls was incubated at 37°C in a humidified atmosphere of 5% CO<sub>2</sub> for 5 days. After incubation, 20 µl of MTT reagent (5 mg/ml MTT in phosphate-buffered saline) was added to each test well and control well. The plate was further incubated at 37°C in a CO<sub>2</sub> incubator for 4 hours.

After 4 hours of incubation, 100 µl of DMSO was added to dissolve the dark-blue formazan crystals from surviving cells (Bahuguna *et al.*, 2017). After the formazan crystals were dissolved completely, the resulting optical density (OD) readings were measured relative to the controls on an ELISA plate reader at 570 nm at a reference wavelength of 620 nm (Szucs *et al.*, 1988). First, the percentage viability was determined using the formula in equation (4).

$$\% \text{ cell viability} = \frac{\text{Absorbance of treated cells}}{\text{Absorbance of negative control}} \times 100 \dots \dots \dots \text{Eq. 4}$$

The 50% cellular cytotoxicity concentration (CC<sub>50</sub>) was defined as the concentration of the test compound that reduced the absorbance of the negative control by 50%. A dose-response curve was plotted to enable the calculation of the concentrations that reduced the number of viable cells by 50% (CC<sub>50</sub>). The concentration that determined cell viability above 80% (CC<sub>20</sub>) was chosen as the maximum non-toxic concentration (MNTC). The maximum concentration that caused cytotoxic effects were calculated by using the formula in equation 5.

$$\% \text{ viability inhibition } (Emax_c) = \frac{\text{Abs.of -ve control} - \text{Abs.of treated wells}}{\text{Abs.of -ve control}} \times 100 \dots \dots \dots \text{Eq. 5}$$

### 3.3.4.2. FM-55-M1 cell viability assay

FM-55-M1 cell line is a tumor cell line from primary melanomas. FM-55-M1 cells (ECACC, UK) were maintained in a humidified incubator with 5% CO<sub>2</sub> at 37°C in RPMI-1640

media with L-glutamine supplemented with 10% fetal bovine serum and 1% penicillin/streptomycin. Cells were detached with trypsin, centrifuged at 200 RCF before resuspension in culture media, and seeded into transparent 96-well plates at 10,000 cells per well. Test compounds were serially diluted in DMSO before transferring into cell plates keeping DMSO at a constant concentration of 0.5% v/v. Cells were incubated with compounds for 72 hours before the addition of CellTiter 96 reagent (Promega, UK), and the absorbance was read at 490 nm in a Tecan Infinite M200 plate reader. Cell viability was determined relative to no compound controls.

### **3.3.5. Anti-HIV activity test**

#### **3.3.5.1. Inhibition of Cytopathic effect of HIV**

The effects of the test compounds in preventing cytopathic effects that occur as a result of HIV-1 replication were evaluated by MTT colorimetric assay. MT-4 cells suspended at  $1 \times 10^8$  cells/ml were infected with 640  $\mu\text{L}$  of HIV-1<sub>IIIB</sub> virus at  $1.26 \times 10^8$  TCID<sub>50</sub>/ml as described in section 3.3.4.1. After infection, 200  $\mu\text{L}$  HIV-infected MT-4 cells ( $1 \times 10^5$  cells/well) in growth media were added to each well. The plates were preincubated for 24 h at 37°C to allow stabilization. Then, 50  $\mu\text{L}$  of the test compounds (at a concentration of 4 mg/mL) were added to the first column of the well. With a multichannel pipette, 50  $\mu\text{L}$  was transferred (in triplicate) from the wells labeled 1 to wells labeled 2. Such transfers were continued (serial dilution), moving from left to right, changing tips prior to mixing contents of the next column of wells. Finally, 50  $\mu\text{L}$  was discarded from the wells in column 12. Different concentrations (800 to  $8.192 \times 10^5$   $\mu\text{g/mL}$ ) of test compounds were prepared through serial dilution. Each dilution was tested in triplicates. The microtiter plates were incubated at 37°C in a 5% CO<sub>2</sub> incubator for 5 days. Two negative controls, infected untreated cells, and uninfected untreated (mock) cells, and four positive controls (zidovudine, tenofovir, abacavir, and nevirapine) were also included. After 5 days of incubation, cell viability was determined by the MTT assay described in section 3.3.4.1 (Gustafson *et al.*, 2004; Pauwels *et al.*, 1988).

A dose-response curve was plotted to calculate the concentrations that reduced viral replication by 50% (IC<sub>50</sub>) (Gustafson *et al.*, 2004; Pauwels *et al.*, 1988; Weislow *et al.*, 1989). The effective inhibitory concentration at 50% (IC<sub>50</sub>) is defined as the concentration of the test compound that achieves 50% protection in infected cultures. The efficacy of the test compounds, was determined by calculating the viral inhibition rate (E<sub>maxAV</sub>) using equation 6, as previously described by (Betancur-Galvis *et al.*, 2002; Uğur *et al.*, 2017).

$$\text{Viral inhibition rate } (Emax_{AV}) = \frac{(OD_T)_{HIV} - (OD_C)_{HIV}}{(OD_C)_{mock} - (OD_C)_{HIV}} \times 100 \dots \text{Eq. 6}$$

Where,  $(OD_T)_{HIV}$  is the optical density measured at a given concentration of the test compound in HIV-infected cells;  $(OD_C)_{HIV}$  is the optical density measured for the negative control infected untreated cells;  $(OD_C)_{mock}$  is the optical density measured for the negative control uninfected untreated cells. The selectivity index (SI) of the test compounds was calculated using equation 7, as the ratio of 50% cytotoxic concentration (CC<sub>50</sub>) to 50% effective concentration (IC<sub>50</sub>). Thus, SI reflects both the antiviral activity and eventual toxicity of the test compounds. Thus, a high SI value indicates low toxicity of the test compound and high activity against the virus.

$$\text{Selectivity index (SI)} = \frac{\text{50\% cytotoxic concentration (CC50)}}{\text{50\% Inhibitory concentration (IC50)}} \dots \text{Eq. 7}$$

### 3.3.5.2. *In vitro* reverse transcriptase enzyme inhibition assay

The HIV-1 reverse transcriptase inhibition assay was conducted *in vitro* using the EnzChek® Reverse transcriptase assay kit (E-22064) provided by Molecular Probes (Eugene, Oregon, United States) following the manufacturer's instructions. Reverse transcriptase was purchased from Promega (Madison, Wisconsin, United States) (GoScript™ Reverse Transcriptase: catalogue number A5004), and enzyme dilution buffer was purchased from Thermo Fisher (Waltham, Massachusetts, United States) (catalogue number B19). Assays were performed in 96-well microtiter plate. GoScript™ RT was supplied at a concentration of 160 u/μL but was diluted to 53.3 u/μL in enzyme dilution buffer and frozen as 10 aliquots in volumes of 150 μL at -80°C. A preliminary run was conducted using titrants of RT to determine the ideal starting concentration, using a ladder approach with a starting concentration of 26.7 u/μL. A final enzyme concentration of 1.1 u/μL was used. Frozen stock solution was diluted to 3.4 u/μL in enzyme dilution buffer to obtain the aliquot concentration to give the final concentration of 1.1 u/μL after the reactants were combined. The assay was initiated by annealing the template and primer. A volume of 5 μL of the poly(A) ribonucleotide template was mixed with 5 μL of oligo d(t)<sub>16</sub> primer and allowed to anneal for an hour at room temperature. After annealing, a 10 μL volume of primer was diluted by adding 1.99 mL of polymerization buffer. This final solution was used as the reaction mixture. The reaction was commenced by combining 20 μL of the reaction mixture and 30 μL of the pure compound and thereafter adding 10 μL of the enzyme at 3.4 u/μL. The reaction was allowed to continue for 1 hour at 25°C and terminated with the addition of 30 μL of 15 mM EDTA. Then

180  $\mu\text{L}$  of PicoGreen® dsDNA quantitation reagent solution was added to the wells and 5 minutes were allowed to pass before reading the fluorescence intensity, using 480 nm as the excitation wavelength and 520 nm as the emission wavelength. The pure compounds were prepared by dissolving to a 20 mg/mL concentration in dimethyl sulfoxide and diluting in nuclease-free water. A starting concentration of 50  $\mu\text{g}/\text{mL}$  was used during initial testing, so the starting aliquot concentration was 100  $\mu\text{g}/\text{mL}$  to ensure a final concentration of 50  $\mu\text{g}/\text{mL}$ . A final concentration of 10  $\mu\text{g}/\text{mL}$  of the pure compounds was used for the *in vitro* enzyme assay. All compounds were assayed in triplicate.

#### **3.3.5.3. Protease enzyme inhibition assay**

The pure compounds were evaluated using an HIV-1 Protease Inhibitor Screening Kit (Fluorometric) (ab211106, Abcam, United Kingdom) at a concentration of 10  $\mu\text{g}/\text{mL}$  as previously described by Aldhafer *et al.*, (2017). Pepstatin (1 mM) and DMSO (1%, v/v) were used as a positive and negative control, respectively. Then, the HIV-1 protease fluorescent substrate was added, and fluorescence was measured (excitation/emission = 330/450 nm) in kinetic mode for 90 min at 37°C using a PerkinElmer EnSpire plate reader. The assay was performed according to the manufacturer's instructions (Ab211106 HIV-1 Protease Inhibitor Screening Kit (Fluorometric), 2020).

#### **3.3.6. Statistical analysis**

The  $\text{CC}_{50}$  and  $\text{IC}_{50}$  values were calculated with GraphPad Prism v9 using the equation for sigmoidal dose-response (variable slope). Statistical significance in the comparison between control drugs and extract cytotoxicity and antiviral activity parameters ( $\text{CC}_{50}$ ,  $\text{E}_{\text{maxC}}$ ,  $\text{IC}_{50}$ , and  $\text{E}_{\text{maxAV}}$ ) were determined by one-way ANOVA followed by Dunnett's post hoc tests. A difference was considered significant when  $p < 0.05$ .

#### **3.4. *In silico* antiretroviral activity**

For the computational study, Chem draw software version 19.1 was used for drawing the chemical structures, while MOE 2015 software was used for the molecular docking studies. To visualize the protein-ligand interactions, discovery Studio Visualizer 3.1 Studio (BIOVIA, 2017), LigPlot<sup>+</sup> (Laskowski & Swindells, 2011), and protein-ligand interaction profiler web-based tool (Adasme *et al.*, 2021) was used (Dassault Systèmes BIOVIA, 2018).

Molecular docking studies were performed on MOE2015 software package using the following files download from Protein Data Bank: HIV-1 RT in complex with known inhibitor Nevirapine (PDB ID: 1JLB), multidrug HIV-1 protease in complex with Atazanavir (3EL9),

wild-type HIV protease in complex with Darunavir (4LL3), and wild-type HIV-1 protease in complex with Lopinavir (6DJ1).

The proteins were prepared by first removing all water molecules, and in the case of proteases also the phosphate, formate and chloride ions present in the PDB file. Then, hydrogens were added, and the structures were protonated. For the ligands, they were energy minimized using force field MMFF94x on MOE2015.

To validate the docking protocol used, known inhibitors were removed from their corresponding binding pockets and redocked. The Root Mean Square Deviation (RMSD) value from the known co-crystallized conformation was  $< 3 \text{ \AA}$  in all cases. Compounds were then docked using MOE2015 with triangle matcher, scoring by London dG, 30 poses as placement method and rigid receptor, GBVI/WSA dG 5 poses as refinement method in all targets. The lowest scoring affinity pose in each ligand was used to study the ligand interactions.



## CHAPTER FOUR

### RESULTS AND DISCUSSION

This research investigated the cytotoxicity and anti-HIV activity of crude extracts, solvent fractions, and isolated pure compounds from three Kenyan *Croton* plants. Furthermore, the mode of action of pure compounds was predicted using computational methods. The results of this study are presented and discussed below.

#### 4.1. Yield for plant extraction

As shown in **Table 4.1-1.**, *C. megalocarpus* has a higher percentage yield than the other crude extracts. **Table 4.1-2** presents the yields after liquid-liquid extraction.

Table 4.1-1: Yields of extracts obtained from *Croton* Species

Plant species	Part extracted	Mass (gm) (1:1 DCM: MeOH)	Percentage yield (%w/w)
<i>C. macrostachyus</i>	Leaf	420 gm	12.6%
	Stem Bark	482 gm	9.5%
<i>C. megalocarpus</i>	Leaf	350 gm	17.5%
	Stem Bark	330 gm	6.5%
<i>C. dichogamus</i>	Twigs	450 gm	9.0%

Table 4.1-2: Weight of liquid/liquid partition of the crude extracts

Plant species	Part extracted	Weight of partitioned			
		Hexane fraction	DCM Fraction	Ethyl acetate	Methanol fraction
<i>C. macrostachyus</i>	Leaf	67 gm (30%)	104 gm (46.6%)	38 gm (17%)	14 gm (6.3%)
	Stem bark	50 gm (28.6%)	22 gm (12.6%)	28 gm (16%)	75 gm (42.9%)
<i>C. megalocarpus</i>	Leaf	60 gm (22.5%)	100 gm (37.5%)	22 gm (8.2%)	85 gm (31.8%)
	Stem bark	11 gm (0.08%)	80 gm (56.3%)	40 gm (28.2%)	11 gm (7.7%)
<i>C. dichogamus</i>	Twigs	34 gm (15.8%)	97 gm (45.1%)	4 gm (1.9%)	80 gm (37.2%)

#### 4.2. Cytotoxicity and antiretroviral activity of the crude extracts of *C. macrostachyus*, *C. megalocarpus*, and *C. dichogamus*

The cytotoxicity and anti-HIV-1 activity of the crude extracts (1:1 CH<sub>2</sub>Cl<sub>2</sub>:CH<sub>3</sub>OH) of the three plants are summarized in **Table 4.2-1**. The antiviral assay results indicated that, the crude leaf extracts of *C. megalocarpus* (ELC) and crude twig part extracts of *C. dichogamus* (CDC) extracts have the highest anti-HIV activity. The CDC displayed highest anti-HIV activity ( $E_{maxAV} = 73.7\%$ ) with wider selectivity index (SI) of 3116.0. The potency of CDC ( $IC_{50} = 0.001 \pm 0.00 \mu\text{g/mL}$ ), is similar to AZT and its efficacy is comparable to NVP and better than ABC. Though the crude bark extract of *C. megalocarpus* (EC) has the best efficacy ( $E_{maxAV} = 85.9\%$ ) of the extracts, it was the least potent with an  $IC_{50}$  value of  $3.73 \pm 1.20 \mu\text{g/mL}$  and also displayed narrow selectivity index (SI + 0.9) indicating its cytotoxicity (**Table 4.2-1**). All the tested extracts have shown cytotoxicity as compared to approved drugs with  $E_{maxC}$  greater than 36.8%. The crude (1:1 v/v DCM: Methanol) bark extract of *C. macrostachyus* (AC) was highly cytotoxic as compared to other extracts by inhibiting cell growth by 49.9 % with  $CC_{50}$  value of  $45.9 \pm 0.12 \mu\text{g/mL}$ . The crude leaf extract of *C. macrostachyus* (ALC) caused cytotoxicity at lowest  $CC_{50}$  value of  $0.008 \pm 0.00 \mu\text{g/mL}$ , comparable to AZT and NVP. Among the FDA approved antiretroviral drugs, Tenofovir was the least cytotoxic with a low  $E_{maxC}$  and high  $CC_{50}$ . NVP was cytotoxic of the approved drugs.

**Table 4.2-1: Cytotoxicity and anti-HIV activities of crude extracts of three *C. species***

Materials	Cytotoxicity			Antiviral activity		SI
	MNTC ( $\mu\text{g/mL}$ )	$CC_{50}$ ( $\mu\text{g/mL}$ )	$E_{maxC}$ (%)	$IC_{50}$ ( $\mu\text{g/mL}$ )	$E_{maxAV}$ (%)	
AZT	$0.38 \pm 0.19$	$0.53 \pm 0.29$	$36.28 \pm 0.83$	$0.002 \pm 0.00$	$83.5 \pm 0.57$	279.4
TDF	$4.92 \pm 0.71$	$6.73 \pm 0.24$	$13.17 \pm 0.43$	$0.04 \pm 0.01$	$80.55 \pm 0.46$	176.5
ABC	$0.18 \pm 0.03$	$0.26 \pm 0.00$	$17.83 \pm 0.57$	$0.05 \pm 0.031$	$58.67 \pm 0.43$	5.0
NVP	$0.57 \pm 0.0$	$0.82 \pm 0.0$	$39.13 \pm 0.65$	$0.24 \pm 0.09$	$72.53 \pm 0.47$	3.5
EC	$0.79 \pm 0.62$	$3.27 \pm 0.12$	$43.63 \pm 0.05$	$3.73 \pm 1.20$	$85.89 \pm 0.85$	0.9
ELC	$20.56 \pm 0.00$	$27.7 \pm 0.65$	$36.77 \pm 0.62$	$0.05 \pm 0.03$	$74.65 \pm 0.06$	571.3
AC	$8.33 \pm 0.43$	$45.9 \pm 0.12$	$49.96 \pm 0.21$	$1.56 \pm 0.39$	$74.36 \pm 0.74$	29.4
ALC	$0.006 \pm 0.00$	$0.008 \pm 0.00$	$37.42 \pm 0.44$	$0.05 \pm 0.01$	$73.80 \pm 0.89$	0.2
CDC	$3.35 \pm 0.62$	$4.70 \pm 0.26$	$42.37 \pm 0.71$	$0.001 \pm 0.00$	$73.74 \pm 0.48$	3116.0

Results are shown as means  $\pm$  S.E. M (n=3)

AZT, Zidovudine; TDF, Tenofovir; ABC, Abacavir; NVP, Nevirapine; EC, *C. megalocarpus* bark extract; ELC, *C. megalocarpus* leaf extract; AC, *C. macrostachyus* bark extract, ALC, *C. macrostachyus* leaf extract; CDC, *C. dichogamus* aerial part extract; MNTC, Maximum non-toxic concentration;  $CC_{50}$ , 50% cytotoxic concentration;  $E_{maxC}$ , Maximum cytotoxic effect %;  $IC_{50}$ , 50% antiviral effect concentrations;  $E_{maxAV}$ , maximum antiviral effect %; SI, selective index.

### 4.3. Evaluation of cytotoxicity and antiretroviral activity of solvent fractions of *C. macrostachyus*, *C. megalocarpus*, and *C. dichogamus*

#### 4.3.1. Cytotoxicity and anti-HIV activity of solvent fractions of *C. megalocarpus*

As depicted in **Table 4.3-1**, the hexane (EH) and ethyl acetate (EE) fractions of the bark showed the highest CC<sub>50</sub> values of 201.6 ± 0.95 and 162.4 ± 0.65 µg/mL, respectively. However, despite having a high CC<sub>50</sub> value, the EH fraction displayed the highest cytotoxic effect by inhibiting more than 79% cell viability. Similarly, the ethyl acetate fraction of the leaf (ELE) showed the highest cytotoxicity by inhibiting 80.3% of cell viability. In comparison, the methanol fraction of the leaves (ELM) and the ethyl acetate fraction of the bark (EE) showed minor cytotoxic effects than the other extracts tested. As depicted in **Figure 4.3-1**, the CC<sub>50</sub> of the EH, EE, and ELE fractions of *C. megalocarpus* was significantly (P <0.001) higher than that of the control drugs, which indicates that it requires higher concentrations of the fractions for cytotoxic effects to appear. In addition, despite having close or higher CC<sub>50</sub> values, which may indicate the safety of the tested substances, all the tested extracts had higher cytotoxic effects (E<sub>maxC</sub>) than the control drugs, indicating their possible high toxic effects with increasing concentration levels.

**Table 4.3-1: Cytotoxicity and anti-HIV activities of solvent fractions of *C. megalocarpus***

Materials	Cytotoxicity			Antiviral activity		SI
	MNTC (µg/mL)	CC <sub>50</sub> (µg/mL)	E <sub>maxC</sub> (%)	IC <sub>50</sub> (µg/mL)	E <sub>maxAV</sub> (%)	
AZT	0.38 ± 0.19	0.53 ± 0.29	36.28 ± 0.83	0.002 ± 0.00	83.5 ± 0.57	279.4
TDF	4.92 ± 0.71	6.73 ± 0.24	13.17 ± 0.43	0.04 ± 0.01	80.55 ± 0.46	176.5
ABC	0.18 ± 0.03	0.26 ± 0.00	17.83 ± 0.57	0.05 ± 0.031	58.67 ± 0.43	5.0
NVP	0.57 ± 0.0	0.82 ± 0.0	39.13 ± 0.65	0.24 ± 0.09	72.53 ± 0.47	3.5
EH	80.66 ± 0.55	201.6 ± 0.95	79.09 ± 0.91	0.26 ± 0.00	89.00 ± 0.01	780.5
ED	0.16 ± 0.05	5.07 ± 0.65	78.03 ± 0.98	0.04 ± 0.02	80.94 ± 0.29	139.4
EE	134.1 ± 0.05	162.4 ± 0.65	48.93 ± 0.05	0.47 ± 0.12	88.01 ± 0.00	346.3
EM	5.57 ± 0.69	25.2 ± 0.05	59.81 ± 0.25	0.46 ± 0.11	93.00 ± 0.00	55.2
ELH	3.48 ± 0.36	4.66 ± 0.41	31.49 ± 0.44	0.002 ± 0.00	72.93 ± 0.85	2972.0
ELD	0.81 ± 0.39	1.17 ± 0.151	36.64 ± 0.26	0.001 ± 0.00	82.87 ± 0.04	616.4
ELE	47.62 ± 0.25	148.3 ± 0.65	80.3 ± 0.71	12.71 ± 0.13	95.63 ± 0.38	11.7
ELM	0.18 ± 0.001	0.29 ± 0.09	30.02 ± 0.99	0.001 ± 0.00	93.40 ± 0.6	186.3

Results are shown as means ± S.E. M (n=3)

AZT, Zidovudine; TDF, Tenofovir; ABC, Abacavir; NVP, Nevirapine; EH, hexane fraction of *C. megalocarpus* bark extract; ED, dichloromethane fraction of *C. megalocarpus* bark extract; EE, ethylacetate fraction of *C. megalocarpus* bark extract; EM, methanol fraction of *C. megalocarpus* bark extract; ELH, hexane fraction of *C. megalocarpus* leaf extract; ELD, dichloromethane fraction of *C. megalocarpus* leaf extract; ELE, ethylacetate fraction of *C. megalocarpus* leaf extract; ELM, methanol fraction of *C. megalocarpus* leaf extract; MNTC, maximum nontoxic concentration; CC<sub>50</sub>, 50% cytotoxic concentration; E<sub>maxC</sub>, maximum cytotoxic effect %; IC<sub>50</sub>, 50% antiviral effect concentrations; E<sub>maxAV</sub>, maximum antiviral effect %; SI, selective index.

As shown in **Table 4.3-1**, all the tested solvent fractions showed inhibition of cytopathic effects at an  $IC_{50}$  value lower than the maximum non-toxic concentration (MNTC). Comparing the effect of the fractions in preventing CPE with the reference drugs, all the extracts showed similar efficacy to that of the control drugs. They showed non-significantly different  $E_{max_{AV}}$  values to that of the control drugs (**Figure 4.3-2**). The solvent fractions tested also showed  $IC_{50}$  values not significantly different from that of the control drugs, except for extract ELE, which displayed lower potency, as it showed a significantly higher  $IC_{50}$  value. The ethyl acetate (ELE) and methanol (ELM) fractions of the leaves prevented CPE by 95.63% and 93.4%, respectively. Similarly, the hexane fraction of the bark (EH) showed an  $E_{max_{AV}}$  value of 89.0 %. Despite their highest anti-HIV activity, these fractions displayed higher cytotoxicity. However, the bark's ethyl acetate (EE) fraction showed the highest anti-HIV activity ( $E_{max_{AV}} = 88.01\%$ ) at an  $IC_{50}$  value of  $0.47 \pm 0.12 \mu\text{g/mL}$  with a selectivity index of 346.3. This is comparable with the activity of AZT and TDF. Putting the cytotoxicity and anti-HIV activity all together, the EE fraction was found to be the safest and active fraction of *C. megalocarpus*.

#### **4.3.1.1. Discussion**

The cytotoxicity and anti-HIV activity of solvent fractions of *C. megalocarpus* was tested against laboratory-adapted strains of HIV (HIV-1<sub>III</sub>B) in human T-lymphocytic MT-4 cells to find possible anti-HIV drugs from natural sources. Medicinal properties of *C. megalocarpus* bark, leaves, and roots have been reported to treat or manage various human and animal diseases across the species' distributional area. Maroyi, (2017a) examined and documented 41 ethnomedicinal uses of *C. megalocarpus* in the literature, with Kenya accounting for 87.5 percent of the ethnomedicinal uses.

*C. megalocarpus* is used to cure a variety of ailments, including respiratory difficulties (Muthee *et al.*, 2011), fever (Ichikawa, 1987; Timothy Johns *et al.*, 1994; Nanyingi *et al.*, 2008), and wounds (Kamau *et al.*, 2016; Nanyingi *et al.*, 2008). For example, *C. megalocarpus* is used in Kenya to treat constipation (Kipkore *et al.*, 2014) as well as backache, chest difficulties (Bussmann, 2006; Kiringe, 2006), malaria (Bussmann, 2006; Cyrus *et al.*, 2008; Fratkin, 1996), and stomach ache (Bussmann, 2006; Fratkin, 1996; Kiringe, 2006). In addition, HIV-infected patients utilize *C. megalocarpus* leaf and root decoctions to treat pneumonia, respiratory difficulties, wounds, and diabetes (Keter & Mutiso, 2012). Four solvent fractions of *C. megalocarpus* leaf and stem bark were tested for their capacity to inhibit HIV-1

replication in this study. In addition, the MTT test was used to assess the toxicity of these extracts in human T-lymphocytic MT-4 cells.

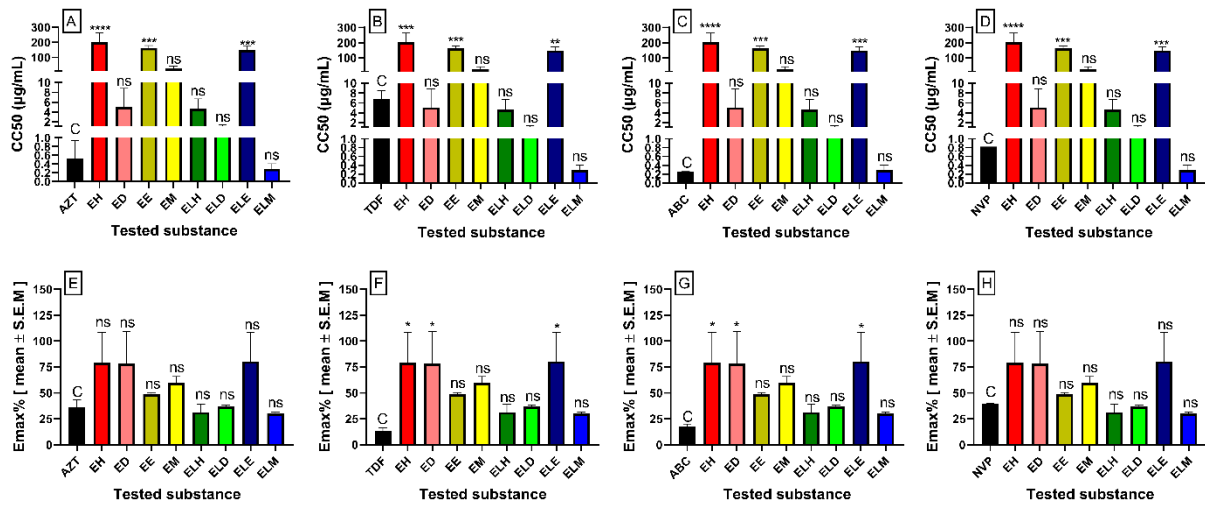


Figure 4.3-1: Cytotoxicity of solvent fractions of *C. megalocarpus*

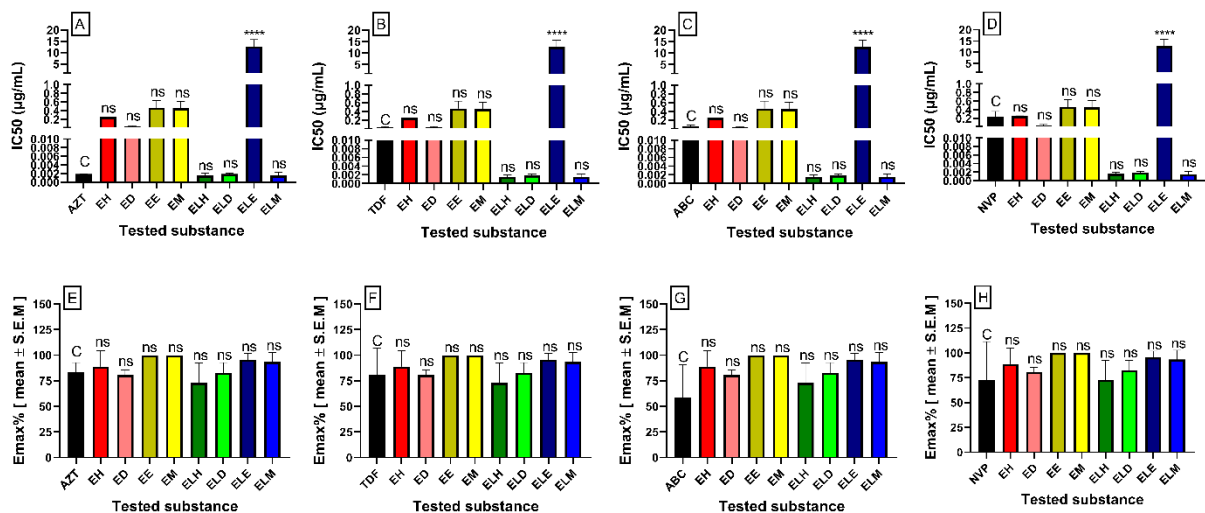


Figure 4.3-2: Anti-HIV activity of solvent fractions of three *C. megalocarpus*

The results are expressed as the mean of three independent experiments ± S.E.M. C, control; AC, *C. macrostachyus* bark extract; EH, Hexane fraction of *C. megalocarpus* bark extract; ED, Dichloromethane fraction of *C. megalocarpus* bark extract; EE, Ethylacetate fraction of *C. megalocarpus* bark extract; EM, methanol fraction of *C. megalocarpus* bark extract; ELH, Hexane fraction of *C. megalocarpus* leaf extract; ELD, Dichloromethane fraction of *C. megalocarpus* leaf extract; ELE, Ethylacetate fraction of *C. megalocarpus* leaf extract; ELM, methanol fraction of *C. megalocarpus* leaf extract; ns, not significant, \*Denotes p-value < 0.05, \*\* Denotes p-value < 0.01, \*\*\* Denotes p-value < 0.001.

The hexane (EH) and dichloromethane (ED) bark fractions had the most cytotoxicity, blocking 78-80 percent of the cell growth. The leaf's methanol fraction (ELM), on the other hand, showed the least cytotoxicity, inhibiting 30% of cell growth compared to the ethyl acetate fraction of the leaves (ELE), which inhibited cell viability by 80%. Cytotoxic chemicals

produce irreversible alterations in organelles and membrane transport systems and changes in cellular structures and activities.

The bark's ethyl acetate (EE) fractions had the highest efficacy in inhibiting the virus's cytopathic effect, followed by the leaves' ethyl acetate (ELE) and methanol fractions (ELM), which inhibited CPE by 95.63 percent and 93.4 percent, respectively. The bark fractions have shown to be less cytotoxic and more effective at reducing CPE than the leaf fractions. The EE and leaf dichloromethane (ELD) fractions had higher SI values of 346.3 and 616.4, respectively. Only extract ELE had lesser antiviral efficacy ( $E_{maxAV} = 72.93\%$ ) in this experiment while keeping a high selectivity index value ( $SI=2972$ ). The selectivity index represents the test drugs' antiviral efficacy as well as their eventual toxicity. A high SI value suggests that the test substance is not harmful and has high antiviral activity. With an  $IC_{50}$  value comparable to that of the control medicines ( $IC_{50}= 0.47$ ,  $SI=346.3$ ), the ethyl acetate fraction of the bark showed potential anti-HIV efficacy. Similarly, with SI values of 55.2 and 186.3, the methanol fractions of both the bark and leaf extracts respectively demonstrated excellent anti-HIV activity, preventing more than 80 percent of CPE in virus-infected cells. These findings corroborate those of a prior study on the same plant's pharmacologic effects. According to Matu & Van Staden, (2003), the methanol extract of *C. megalocarpus* has the strongest anti-inflammatory effect due to cyclooxygenase enzyme inhibition.

The terpenoids found in the solvent fractions may be responsible for the fractions' anti-HIV efficacy. Betulin, a triterpenoid isolated from the stem bark of *C. megalocarpus*, was shown to have antiviral effects in cell cultures infected with herpes simplex type I, influenza FPV/Rostock, and ECHO 6 viruses in a prior study (Pavlova *et al.*, 2003). Lupeol, a triterpenoid derived from the same plant, has shown anti-HSV action *In vitro* (M. K. Parvez *et al.*, 2019). Several terpenoids extracted from plants have been shown to have anti-HIV action in previous research. Celastrol-B, a triterpene isolated from *Calophyllum lanigerum*, had an  $EC_{50}$  of 0.8  $\mu\text{g/ml}$  and inhibited HIV replication in H9 lymphocyte cells (Y. H. Kuo & Kuo, 1997). In addition, Eurifoloids E and F, diterpenoids derived from *Euphorbia neriifolia*, were found to have considerable anti-HIV activity in a separate investigation, with  $EC_{50}$  values of 3.58 0.31 ( $SI = 8.6$ ) and 7.40 0.94  $\mu\text{M}$  ( $SI = 10.3$ ), respectively (Zhao *et al.*, 2014). Trigonothyrins A-C, highly functionalized daphnane diterpenoids isolated from the stems of *Trigonostemon thyrsoideum*, have shown to suppress HIV-1-induced cytopathic effects in another investigation, with an  $IC_{50}$  value of 2.19  $\mu\text{g/mL}$  and SI more than 90 (Zhang *et al.*, 2010).

#### 4.3.2. Cytotoxicity and anti-HIV activity of solvent fractions of *C. macrostachyus*

**Table 4.3-2** summarize the cytotoxicity and anti-HIV activity of four solvent fractions of *C. macrostachyus* leaf and stem bark. At  $CC_{50}$  values of  $0.25 \pm 0.07 \mu\text{g/mL}$  and  $0.58 \pm 0.05 \mu\text{g/mL}$ , respectively, the methanol (AM) and hexane (AH) fractions of *C. macrostachyus* bark were shown to be cytotoxic, decreasing cell growth ( $E_{\text{max}_C}$ ) by more than 49%. The ethyl acetate component of the bark (AE) was more cytotoxic, reducing cell viability by 63%. With an  $E_{\text{max}_C}$  value of 29.33 percent, the dichloromethane fraction (AD) exhibited reduced cytotoxicity. With a  $CC_{50}$  value of  $173.5 \mu\text{g/mL}$ , the hexane fraction of the leaves (ALH) demonstrated the most negligible cytotoxicity, followed by the ethyl acetate fraction of the leaves (ALE) with a  $CC_{50}$  value of  $165.9 \mu\text{g/mL}$ . Finally, the leaf's methanol fraction (ALM) had the maximum cytotoxicity, with a  $CC_{50}$  of  $6.28 \pm 0.51 \mu\text{g/mL}$  and a 54.47 percent inhibition of cell viability. The cytotoxic effect of the examined extracts and control medicines on the MT4 cell line was determined using the MTT assay and extracts AE, AM, and ALM were shown to have significantly higher cytotoxicity ( $P < 0.01$ ) than TDF and ABC (**Figure 4.3-3**). However, most of the extracts examined had a larger maximum cytotoxic effect ( $E_{\text{max}_C}$ ) than the control medicines, indicating that they could have more harmful effects at higher concentrations.

With an  $IC_{50}$  value of  $0.04 \pm 0.00 \mu\text{g/mL}$ , the dichloromethane fraction of the bark had better anti-HIV activity. Similarly, the ethyl acetate fraction of the bark (AE) reduced the cytopathic effect (CPE) by 86.53 percent with an  $IC_{50}$  value of  $3.69 \pm 0.11 \mu\text{g/mL}$ , which is substantially lower than the maximum non-toxic concentration ( $141.9 \pm 0.25 \mu\text{g/mL}$ ), yielding selectivity index of 46.6. The hexane fraction of the bark (AH) prevented 90.8 percent of cell death caused by CPE while being less potent ( $IC_{50} = 8.09 \pm 0.55 \mu\text{g/mL}$ ). The anti-HIV activity of the methanol fraction (AM) was lower ( $E_{\text{max}_{AV}} = 67.91\%$ ;  $SI = 0.5$ ). (**Table 4.3-2**).

With  $IC_{50}$  values of  $0.02 \pm 0.01 \mu\text{g/mL}$ , the hexane fraction of the leaves had the strongest anti-HIV activity, blocking 83 percent of the virus-induced cytopathic impact, yielding the highest selectivity index (SI) of 9752. The dichloromethane fraction of the leaf, on the other hand, had a reduced efficiency in suppressing viral reproduction, with an  $IC_{50}$  of  $5.37 \pm 0.13 \mu\text{g/mL}$  and a SI of 0.5. The antiviral activity of the tested fractions revealed that the control medications and the tested fractions had antiviral efficacy that was nearly identical, with  $E_{\text{max}_{AV}}$  values that were non-significantly different (**Figure 4.3-4**). Furthermore, with the exception of extracts AH and ALD, which revealed lesser potency as seen by the

significantly ( $P < 0.01$ ) greater  $IC_{50}$  value, most of the fractions had  $IC_{50}$  values that were not statistically different from those of the control medicines, showing comparable potency.

Table 4.3-2: Cytotoxicity and anti-HIV-1 activities of solvent fractions of *C. macrostachyus*

Materials	Cytotoxicity			Antiviral activity		SI
	MNTC ( $\mu\text{g/mL}$ )	$CC_{50}$ ( $\mu\text{g/mL}$ )	$E_{\text{maxC}}$ (%)	$IC_{50}$ ( $\mu\text{g/mL}$ )	$E_{\text{maxAV}}$ (%)	
<b>AZT</b>	$0.38 \pm 0.19$	$0.53 \pm 0.29$	$36.28 \pm 0.83$	$0.002 \pm 0.00$	$83.5 \pm 0.57$	279.4
<b>TDF</b>	$4.92 \pm 0.71$	$6.73 \pm 0.24$	$13.17 \pm 0.43$	$0.04 \pm 0.01$	$80.55 \pm 0.46$	176.5
<b>ABC</b>	$0.18 \pm 0.03$	$0.26 \pm 0.00$	$17.83 \pm 0.57$	$0.05 \pm 0.031$	$58.67 \pm 0.43$	5.0
<b>NVP</b>	$0.57 \pm 0.0$	$0.82 \pm 0.0$	$39.13 \pm 0.65$	$0.24 \pm 0.09$	$72.53 \pm 0.47$	3.5
<b>AH</b>	$0.18 \pm 0.09$	$0.25 \pm 0.07$	$49.11 \pm 0.16$	$8.09 \pm 0.55$	$90.8 \pm 0.88$	0.03
<b>AD</b>	$0.99 \pm 0.26$	$1.13 \pm 0.16$	$29.33 \pm 0.18$	$0.04 \pm 0.00$	$87.61 \pm 0.56$	26.2
<b>AE</b>	$141.9 \pm 0.25$	$171.8 \pm 0.1$	$63.05 \pm 0.32$	$3.69 \pm 0.11$	$86.53 \pm 0.71$	46.6
<b>AM</b>	$0.08 \pm 0.07$	$0.58 \pm 0.05$	$52.74 \pm 0.44$	$1.15 \pm 0.03$	$67.91 \pm 0.55$	0.5
<b>ALH</b>	$142.2 \pm 0.4$	$173.5 \pm 0.8$	$39.44 \pm 0.65$	$0.02 \pm 0.01$	$82.78 \pm 0.67$	9752.7
<b>ALD</b>	$1.328 \pm 0.66$	$2.47 \pm 1.37$	$29.64 \pm 0.54$	$5.37 \pm 0.13$	$76.45 \pm 0.14$	0.5
<b>ALE</b>	$100.9 \pm 0.51$	$165.9 \pm 0.65$	$42.89 \pm 0.84$	$0.05 \pm 0.03$	$83.81 \pm 0.01$	3186.7
<b>ALM</b>	$7.92 \pm 0.35$	$6.28 \pm 0.51$	$54.47 \pm 0.06$	$0.05 \pm 0.02$	$77.04 \pm 0.37$	138.6

Results are shown as mean  $\pm$  S.E. M (n=3)

AZT, zidovudine; TDF, tenofovir; ABC, abacavir; NVP, nevirapine; AH, hexane fraction of *C. macrostachyus* bark extract; AD, dichloromethane fraction of *C. macrostachyus* bark extract; AE, ethylacetate fraction of *C. macrostachyus* bark extract; AM, methanol fraction of *C. macrostachyus* bark extract; ALH, hexane fraction of *C. macrostachyus* leaf extract; ALD, dichloromethane fraction of *C. macrostachyus* leaf extract; ALE, ethylacetate fraction of *C. macrostachyus* leaf extract; ALM, methanol fraction of *C. macrostachyus* leaf extract; MNTC, maximum nontoxic concentration;  $CC_{50}$ , 50% cytotoxic concentration;  $E_{\text{maxC}}$ , maximum cytotoxic effect %;  $IC_{50}$ , 50% antiviral effect concentrations;  $E_{\text{maxAV}}$ , maximum antiviral effect %; SI, selective index.

#### 4.3.2.1. Discussion

Ethnobotanical and ethnopharmacological studies have confirmed the traditional usage of *C. macrostachyus* in treating various infectious disorders. HIV, hepatitis, amoebiasis, epilepsy, anthrax, jaundice, leprosy, malaria, cancer, ringworm, and skin illnesses are all treated with *C. macrostachyus* (Agisho *et al.*, 2014; Focho *et al.*, 2009; Tefera *et al.*, 2012). Leaf and root decoction of the leaves are used to treat cough, back pain, bleeding, skin problems, warts, pneumonia, and wounds (Kareru *et al.*, 2007; Obey *et al.*, 2016a; Okello *et al.*, 2010b; Pascaline *et al.*, 2010). In addition, *C. macrostachyus* has also been utilized in the past to treat viral infections. In Ethiopia, for example, a bark decoction of *C. macrostachyus* mixed with *Juniperus procera* leaves, *Eragrostis tef* (Zucc.) stems, and roots of *Cyphostemma cyphopetalum* is used as a rabies herbal treatment (Maroyi, 2017d). Based on this information, we tested the cytotoxicity and anti-HIV activity of solvent fractions of *C. macrostachyus* in human T-lymphocytic MT-4 cells against laboratory-adapted strains of HIV (HIV-1IIIB).



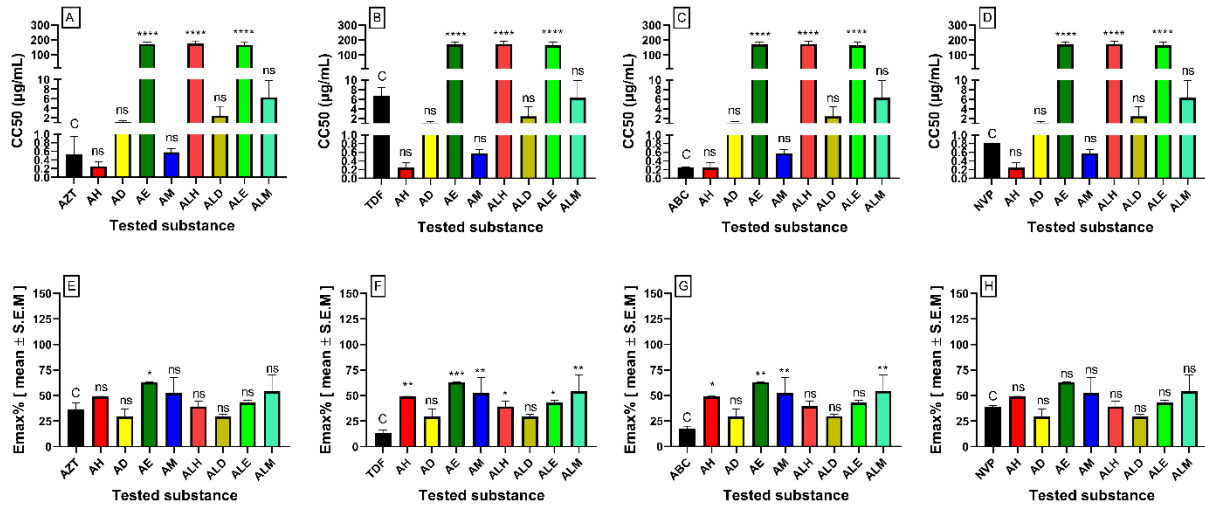


Figure 4.3-3: Cytotoxic effect for solvent fractions for *C. macrostachyus*

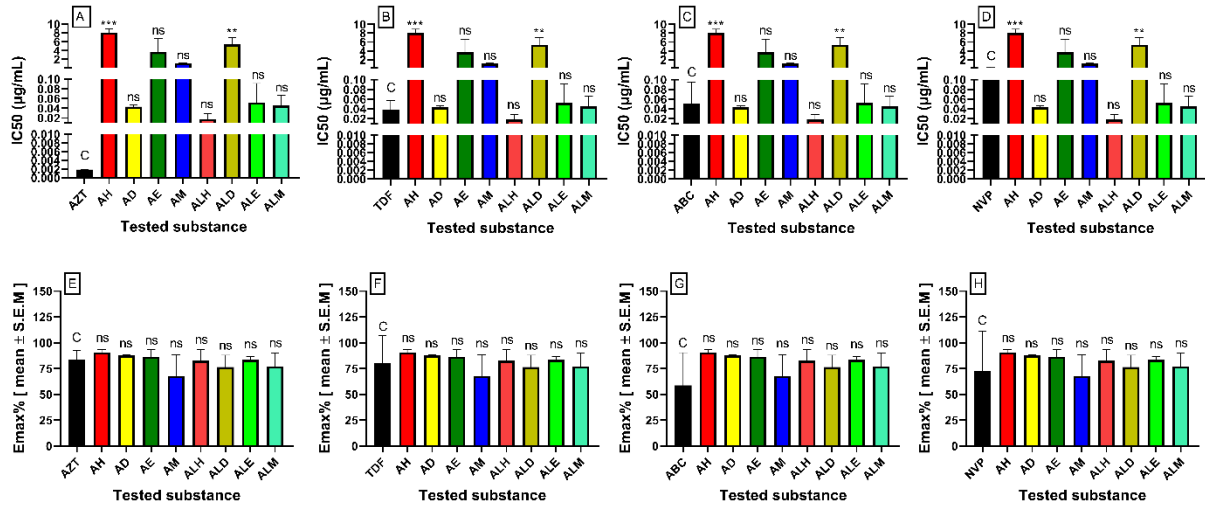


Figure 4.3-4: Anti-HIV activity of solvent fractions of *C. macrostachyus*

The results are expressed as the mean of three independent experiments  $\pm$  S.E.M. C, control; AH, hexane fraction of *C. macrostachyus* bark extract; AD, dichloromethane fraction of *C. macrostachyus* bark extract; AE, ethylacetate fraction of *C. macrostachyus* bark extract; AM, methanol fraction of *C. macrostachyus* bark extract; ALH, hexane fraction of *C. macrostachyus* leaf extract; ALD, dichloromethane fraction of *C. macrostachyus* leaf extract; ALE, ethylacetate fraction of *C. macrostachyus* leaf extract; ALM, methanol fraction of *C. macrostachyus* leaf extract; ns; not significant, \*Denotes p value < 0.05, \*\* Denotes p value < 0.01, \*\*\* Denotes p value < 0.001.

The CC<sub>50</sub> values of AE, ALH, and ALE were significantly higher than the control medicines, indicating that larger concentrations of these fractions are necessary for cytotoxic effects to manifest (**Figure 4.3-3**). ALH showed promise by suppressing 82.78 percent of the virus-induced cytopathic effect at a concentration substantially lower than the highest cytotoxic concentration (IC<sub>50</sub>= 0.02  $\pm$  0.01 µg/mL; MNTC=142.2  $\pm$  0.4 µg/mL; SI of 9752.7), demonstrating the fraction's efficacy and safety. Similarly, the leaves' ethyl acetate fraction

inhibited 83.81 percent CPE ( $IC_{50}=0.05 \pm 0.03 \mu\text{g/mL}$ ;  $MNTC=100.9 \pm 0.51 \mu\text{g/mL}$ ; SI of 3186.7). The selectivity index represents the test drugs' antiviral efficacy as well as their eventual toxicity. A high SI value suggests that the test substance is not harmful and has high antiviral activity.

Pentacyclic triterpenoids in the hexane and ethyl acetate leaf fractions could be responsible for the antiviral activity ( $E_{\text{max}_{AV}} > 80.8$  percent). Betulin, betulinic acid, lupeol, and lupeol-acetate were among the triterpenoids identified previously from *C. macrostachyus* (Addae-Mensah *et al.*, 1992; Maroyi, 2017b; Tala *et al.*, 2013; Tene *et al.*, 2009). Gutiérrez-Nicolás *et al.*, (2012), found that lupeol acetate reduces viral entrance into CD4 cells, while betulinic acid inhibits HIV-1 RT (Esposito *et al.*, 2013). The activity of the hexane and ethyl acetate fractions of the leaves of *C. macrostachyus* could be attributed to the phytochemical constituents.

#### 4.2.3. Cytotoxicity and anti-HIV activity of solvent fractions of *C. dichogamus*

**Table 4.3-3**, summarize the cytotoxicity and anti-HIV activity of solvent fractions of *C. dichogamus*. The  $CC_{50}$  value for the methanol fraction was  $19.58 \pm 0.79 \mu\text{g/mL}$ , indicating that cytotoxic effects require greater concentrations of the fraction. Furthermore, the dichloromethane fraction was linked to a considerably ( $P < 0.01$ ) higher maximum cytotoxic effect, inhibiting more than 60% of cell viability ( $E_{\text{max}_C}=66.22$  percent), implying that higher doses could lead to more deleterious effects (**Figure 4.3-5**).

The methanol fraction of *C. dichogamus* had high anti-HIV activity ( $E_{\text{max}_{AV}}=90.83$  percent), at a much lower concentration ( $IC_{50} = 0.06 \pm 0.01 \mu\text{g/mL}$ ) than the maximum non-toxic concentration ( $MNTC=15.4 \mu\text{g/mL}$ ), indicating the extract's safety (**Table 4.3-3**). The antiviral effect of the studied extracts was comparable to that of the control medicines, as shown in **Figure 4.3-6**. There was no significant difference in their viral-induced CPE inhibition,  $IC_{50}$  nor  $E_{\text{max}_{AV}}$  values.

Table 4.3-3: Cytotoxicity and anti-HIV-1 activities of solvent fractions of *C. dichogamus*

Materials	Cytotoxicity			Antiviral activity		SI
	MNTC (µg/mL)	CC <sub>50</sub> (µg/mL)	E <sub>max</sub> C (%)	IC <sub>50</sub> (µg/mL)	E <sub>max</sub> AV (%)	
AZT	0.38 ± 0.19	0.53 ± 0.29	36.28 ± 0.83	0.002 ± 0.00	83.5 ± 0.57	279.4
TDF	4.92 ± 0.71	6.73 ± 0.24	13.17 ± 0.43	0.04 ± 0.01	80.55 ± 0.46	176.5
ABC	0.18 ± 0.03	0.26 ± 0.00	17.83 ± 0.57	0.05 ± 0.031	58.67 ± 0.43	5.0
NVP	0.57 ± 0.0	0.82 ± 0.0	39.13 ± 0.65	0.24 ± 0.09	72.53 ± 0.47	3.5
CDD	49.7 ± 0.61	167 ± 0.18	66.22 ± 0.18	0.03 ± 0.02	81.3 ± 0.23	5491.61
CDE	0.84 ± 0.08	0.99 ± 0.2	42.38 ± 0.95	0.55 ± 0.27	77.89 ± 0.99	1.8
CDH	0.02 ± 0.01	0.04 ± 0.02	12.24 ± 0.37	0.03 ± 0.01	77.59 ± 3.52	0.9
CDM	15.4 ± 0.45	19.58 ± 0.79	42.2 ± 0.615	0.06 ± 0.01	90.83 ± 0.18	318.5

Results are shown as mean ± S.E. M (n=3)

AZT, zidovudine; TDF, tenofovir; ABC, abacavir; NVP, nevirapine; CDH, hexane fraction of *C. dichogamus* twig extract; CDD, dichloromethane fraction of *C. dichogamus* twig extract; CDE, ethylacetate fraction of *C. dichogamus* twig extract; CDM, methanol fraction of *C. dichogamus* twig extract; MNTC, maximum nontoxic concentration; CC<sub>50</sub>, 50% cytotoxic concentration; E<sub>max</sub>C, maximum cytotoxic effect %; IC<sub>50</sub>, 50% antiviral effect concentrations; E<sub>max</sub>AV, maximum antiviral effect %; SI, selective index.

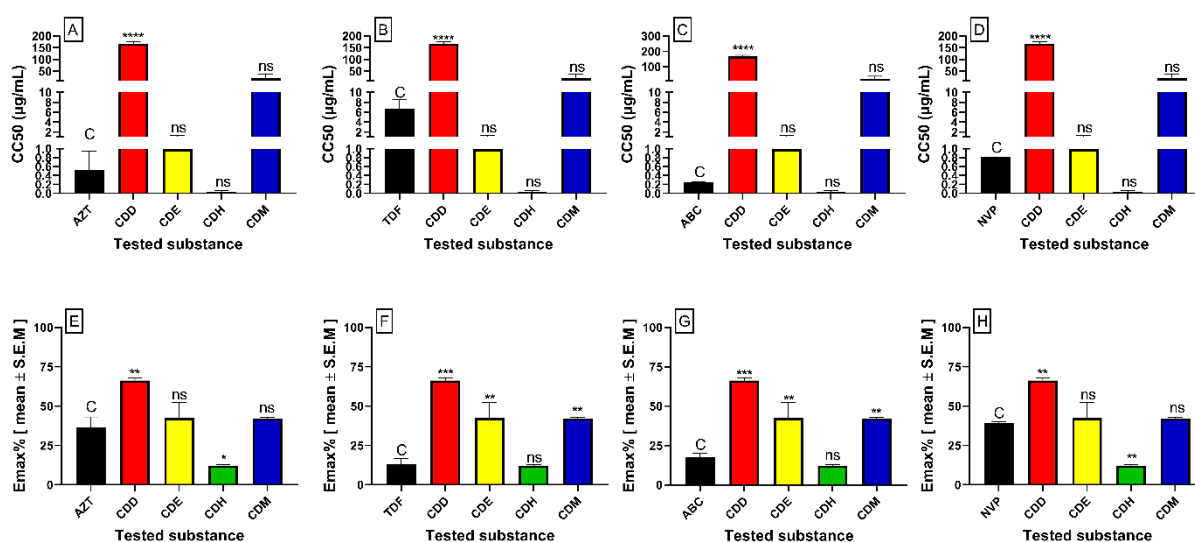


Figure 4.3-5: Cytotoxic effect of solvent fractions of *C. dichogamus*

The results are expressed as the mean of three independent experiments ± S.E.M. C, control; CDH, hexane fraction of *C. dichogamus* twig extract; CDD, dichloromethane fraction of *C. dichogamus* twig extract; CDE, ethylacetate fraction of *C. dichogamus* twig extract; CDM, methanol fraction of *C. dichogamus* twig extract; ns, not significant, \*Denotes p value < 0.05, \*\* Denotes p value < 0.01, \*\*\* Denotes p value < 0.001.

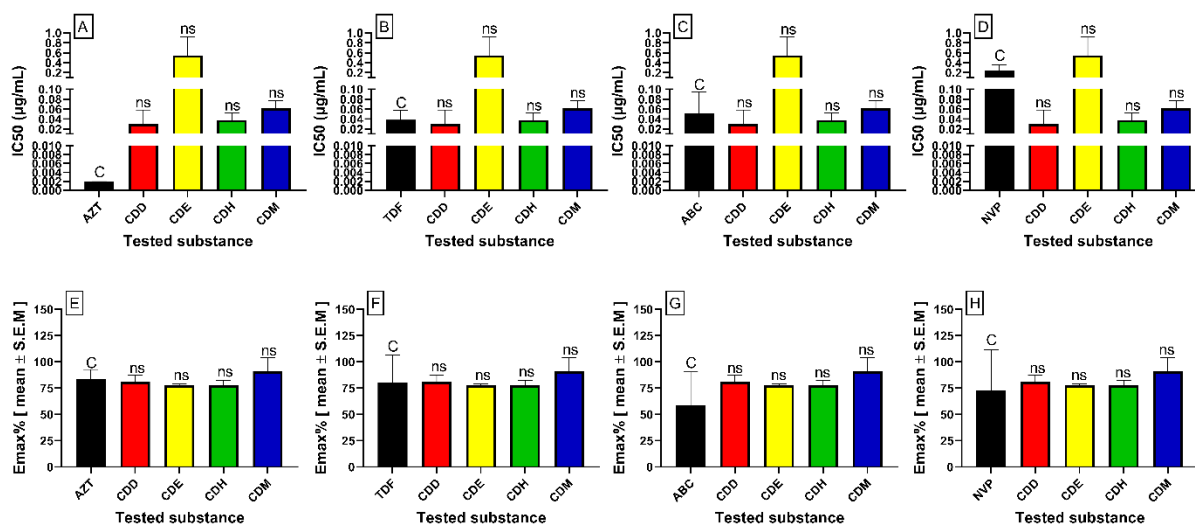


Figure 4.3-6: Anti-HIV activity of solvent fractions of *C. dichogamus*

The results are expressed as the mean of three independent experiments  $\pm$  S.E.M. C, control; CDH, hexane fraction of *C. dichogamus* twig extract; CDD, dichloromethane fraction of *C. dichogamus* twig extract; CDE, ethylacetate fraction of *C. dichogamus* twig extract; CDM, methanol fraction of *C. dichogamus* twig extract; ns, not significant, \*Denotes p value < 0.05, \*\* Denotes p value < 0.01, \*\*\* Denotes p value < 0.001.

#### 4.2.3.1. Discussion

According to our findings, the two solvent fractions (CDD and CDM) of *C. dichogamus* twig portions had CC<sub>50</sub> values greater than the control medicines, implying that larger fraction concentrations are necessary for cytotoxic effects. Furthermore, the methanol fraction was found to be less toxic (Emax<sub>C</sub> = 42.2%), whereas the dichloromethane fraction was found to be toxic, inhibiting cell viability by more than 60%.

Our findings on the plant's cytotoxicity are consistent with those of Aldhafer *et al.*, (2017), Shang *et al.*, (2013), and Pudhom & Sommit, (2011). For example, at a dose of 100 mM, Aldhafer *et al.*, (2017) found 10-epi-Maninsigin D, a diterpenoid isolated from the n-hexane fraction of the root of *C. dichogamus*, reduced the viability of Caco-2 human colon cancer cell lines by 43%. Using the MTT method, maninsigin D was cytotoxic to HL-60, A-549, SW-480, SMMC-7721, and MCF-7 human cell lines with IC<sub>50</sub> values > 40 mM (Shang *et al.*, 2013). In comparison to the other fractions, the methanol fraction had the best antiviral activity, inhibiting 90% of the virus's cytopathic effect on the cell line (IC<sub>50</sub>= 0.06 µg/mL). One or more terpenoids, saponins, or other bioactive chemicals may be responsible for the methanol extract's ability to block the virus's cytopathic effect.

#### 4.4. Isolation and characterization of compounds with a potential antiretroviral activity using bioassay-guided fractionation

##### 4.4.1. *Croton megalocarpus*

Based on the anti-HIV activity findings of the solvent fractions from *C. megalocarpus*, the ethyl acetate fraction from the stem bark of *C. megalocarpus* was subjected to column chromatography to yield nine pure bioactive compounds (**Table 4.4-1**). The chemical structure of these compounds is depicted in **Figure 4.4-1**. In this study we report the anti HIV activity of three new (previously undescribed) eudesmane type sesquiterpenes and two new crotofolane diterpenoids isolated from *C. megalocarpus*.

Table 4.4-1: Compounds isolated from the stem bark of *C. megalocarpus*

Ser No.	Name	Code
<b>Eudesmane type sesquiterpenes</b>		
1.	5 $\beta$ -hydroxy-8 $\alpha$ -methoxy eudesm-7(11)-en-12,8-olide (ermiasolide A)*	<b>E12</b>
2.	5 $\beta$ ,8 $\alpha$ -dihydroxy eudesm-7(11)-en-12,8-olide (ermiasolide B)*	<b>E22</b>
3.	5 $\beta$ ,8H- $\beta$ -hydroxy eudesm-7(11)-en-12,8-olide (ermiasolide C) *	<b>E17</b>
4.	4H- $\alpha$ ,7H- $\alpha$ ,10 $\alpha$ -eudesm-11-en-5 $\beta$ -ol	<b>E5</b>
<b>Crotofolane diterpenoids</b>		
5.	1 $\beta$ -acetoxy-3 $\beta$ -chloro-5 $\alpha$ ,6 $\alpha$ -dihydroxycrotocascarin L (Ermiasoid)*	<b>E37</b>
6.	11-acetoxy crotocascarin L*	<b>E24</b>
7.	Crotocascarin K	<b>E23</b>
<b>Other pure compounds</b>		
8.	3 $\beta$ -hydroxylup-20(29)-ene (lupeol)	<b>E19</b>
9.	Pinoresinol	<b>E2</b>

\*new or previously undescribed compounds

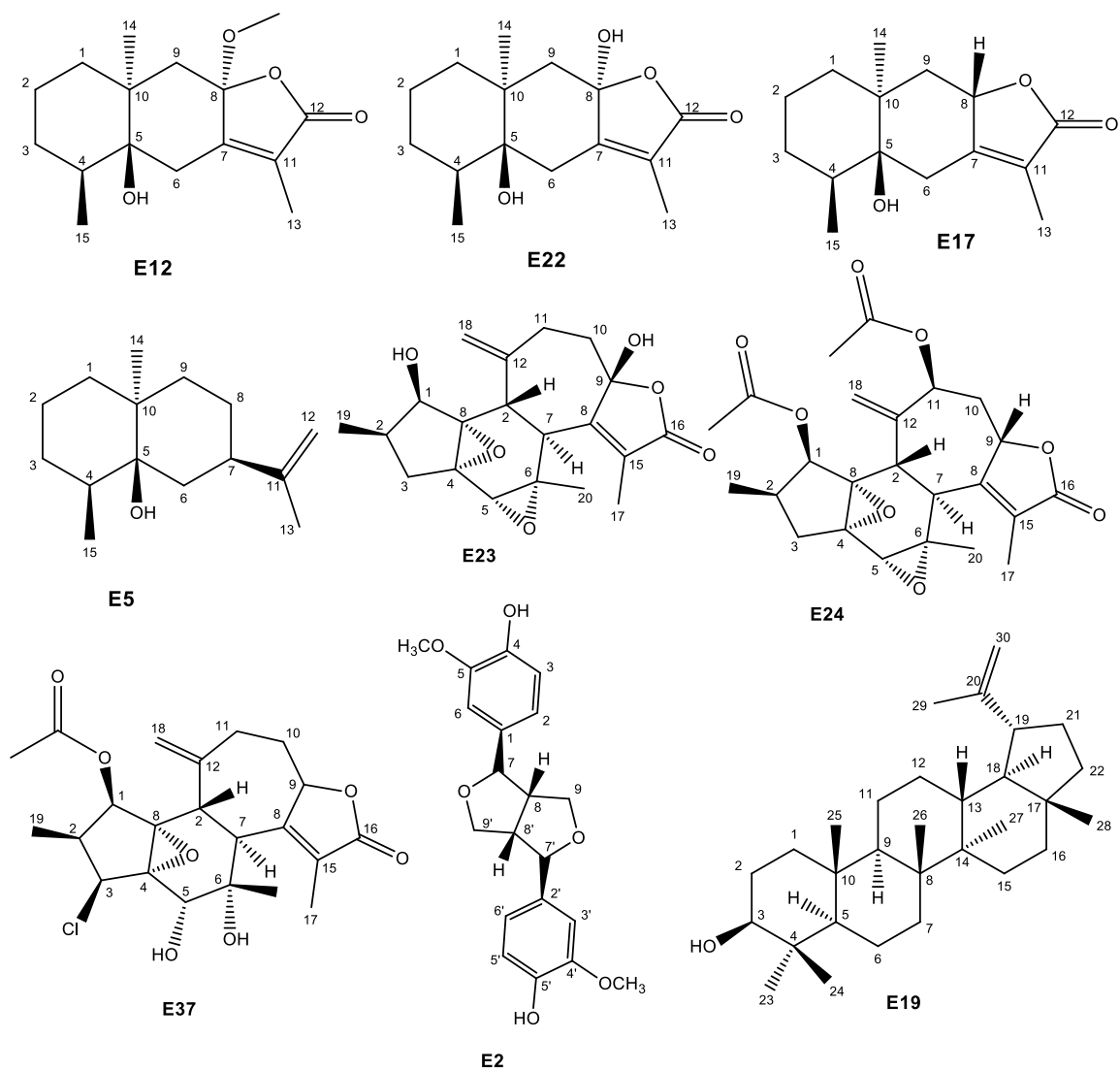
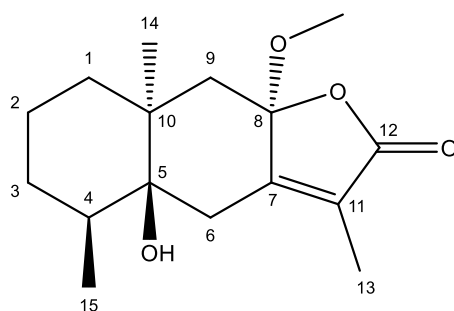


Figure 4.4-1: Pure compounds isolated from *C. megalocarpus*

#### 4.4.1.1. Chemistry of eudesmane type diterpenoids isolated from *C. megalocarpus*

##### 4.4.1.1.1. E12: 5 $\beta$ -Hydroxy-8 $\alpha$ -methoxy eudesm-7(11)-en-12,8-olide (Ermiasolide A)



**E12**

5 $\beta$ -Hydroxy-8 $\alpha$ -methoxy eudesm-7(11)-en-12,8-olide (compound **E12**) was isolated from the ethyl acetate soluble extract of the stem bark of *C. megalocarpus* as a brown oil. The HRMS spectrum (**Appendix 1**) showed a molecular ion peak at  $m/z$   $[M+H]^+$  281.1744 for  $C_{16}H_{22}O_4$  (calc.  $C_{16}H_{24}O_4 + H$ ,  $m/z$  281.1747). The  $^1H$  NMR spectrum (**Table 4.4-2 and 4.4-3**) of this compound showed four methyl proton resonances at  $\delta_H$  3.16 (s) for a methoxy group, 1.85 (d,  $J=1.3$ ), 1.24 (s), and 0.90 (d,  $J=6.7$ ) (**Appendix 2**). The  $^{13}C$ , DEPT, and HSQCDEPT NMR spectra (**Appendix 3-5**) supported 16 carbon resonances, including a carbonyl resonance at  $\delta_C$  172.0, two double bond resonances at 156.8 and 127.7, an anomeric methine carbon at 106.5, an oxygenated carbon resonance at 77.8, a methoxylated carbon at 50.4, and carbon resonances for 3 methyls, 5 methylenes, and 1 methine. The above information suggested that compound **E12** was a methoxylated sesquiterpenoid. The use of 2D NMR spectra, HMBC, and COSY (**Appendix 6-7**) suggested that an allylic carbon resonance at 1.85 was part of an  $\alpha,\beta$ -unsaturated carbonyl system with carbonyl carbon resonance at 172 and double bond carbon resonances at 156.8 and 127.7. A carbon resonance at 106.5 was assigned to an acetal group. It was observed in the HMBC spectrum to correlate with the methoxy group proton resonance and methylene proton resonances assignable to  $H_2-6$  and  $H_2-9$ . In addition,  $H_2-6$  proton resonances showed correlations in the HMBC spectrum with C-4, C-5, C-7, C-10, and C-11, whereas  $H_2-9$  showed correlations in the HMBC spectrum with C-1, C-5, C-7, C-8, and C-14. C-4 was observed to be a methine carbon resonance, which corresponded with a proton resonance at  $\delta_H$  1.96 (m) for H-4. The H-4 proton resonance was coupled with a methyl doublet proton at 0.90 (d,  $J=6.7$ ), attributable to H-15. In addition, H-4 was coupled to proton resonances for  $H_2-3$ , which were coupled to  $H_2-2$  in the COSY spectrum.  $H_2-2$  was also coupled

to H<sub>2</sub>-1 in the COSY spectrum. The above data suggested that compound E12 was a methoxylated sesquiterpenoid that was determined to be a eudesmane class.

The NOESY spectrum (**Appendix 8**) of compound **E12**, acquired using DMSO, showed that the methoxy groups H-4 and 3H-14 were on the same face of the molecule, whereas 5-OH and 3H-15 were on the other face of the molecule. The HRMS data  $[M+H]^+ = 280.1744$  supported the proposed structure; hence, **E12** was determined to be undescribed 5 $\beta$ -hydroxy-8 $\alpha$ -methoxy eudesm-7(11)-en-12,8-olide, trivially named **ermiasolide-A**.

Table 4.4-2: NMR data for 5 $\beta$ -Hydroxy-8 $\alpha$ -methoxy eudesm-7(11)-en-12,8-olide (ermiasolide A, E12) in CDCl<sub>3</sub>

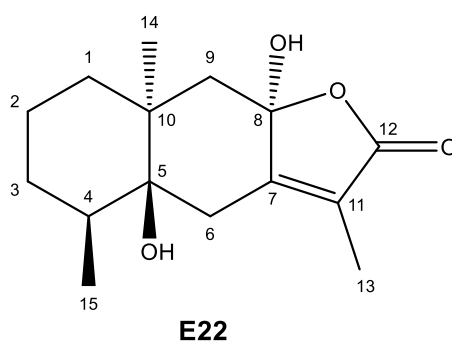
No.	<sup>13</sup> C NMR	<sup>1</sup> H NMR	HMBC (H→C)	COSY	NOESY
1 $\alpha$	34.3	1.52	2, 10	1 $\beta$ , 2 $\alpha$ , 2 $\beta$	1 $\beta$ , 2 $\alpha$ , 2 $\beta$
1 $\beta$		1.14	3	1 $\alpha$ , 2 $\alpha$ , 2 $\beta$	1 $\alpha$ , 2 $\alpha$ , 2 $\beta$
2 $\alpha$	20.0	1.67 m	x	1 $\alpha$ , 1 $\beta$ , 2 $\beta$	1 $\alpha$ , 1 $\beta$ , 2 $\beta$
2 $\beta$		1.59 m	x	1 $\alpha$ , 1 $\beta$ , 2 $\alpha$	1 $\alpha$ , 1 $\beta$ , 2 $\alpha$
3 $\alpha$	30.1	1.48 m	2	2 $\alpha$ , 2 $\beta$ , 3 $\beta$	2 $\alpha$ , 2 $\beta$ , 3 $\beta$
3 $\beta$		1.30 m	2	2 $\alpha$ , 2 $\beta$ , 3 $\alpha$	2 $\alpha$ , 2 $\beta$ , 3 $\alpha$
4	34.1	1.96 m	2, 5, 10	14, 3 $\alpha$ , 3 $\beta$	14
5	77.8	-	-	-	-
6 $\alpha$	32.0	2.71 d, 13.9	5, 7, 8, 10, 11	6 $\beta$	OCH <sub>3</sub>
6 $\beta$		2.27 dd, 1.4, 13.9	5, 7, 11	6 $\alpha$ , 13	14, 15, OCH <sub>3</sub>
7	156.8	-	-	-	-
8	106.5	-	-	-	-
9 $\alpha$	45.8	1.96 d, 13.7	7, 8, 10, 11	9 $\beta$	9 $\beta$ , 14, 15
9 $\beta$		1.82 d, 13.7	8, 7, 10	9 $\alpha$	9 $\alpha$
10	38.9	-	-	-	-
11	127.7	-	-	-	-
12	172.0	-	-	-	-
13	8.6	1.85 d, 1.3	7, 11, 12	6 $\beta$	OCH <sub>3</sub>
14	21.0	1.24 s	1, 5, 9, 10	-	4, 6 $\alpha$ , OCH <sub>3</sub>
15	15.3	0.90 d, 6.7	3,4,5	4	6 $\beta$
OCH <sub>3</sub>	50.4	3.16 s	8	-	6 $\alpha$ , 6 $\beta$ , 13, 14



Table 4.4-3: NMR data for 5 $\beta$ -Hydroxy-8 $\alpha$ -methoxy eudesm-7(11)-en-12,8-olide (ermiasolide A, E12) in DMSO

No.	<sup>13</sup> C NMR	<sup>1</sup> H NMR	HMBC (H→C)	COSY	NOESY
1 $\alpha$	33.4	1.60 m	2, 10	1 $\beta$ , 2 $\alpha$ , 2 $\beta$	1 $\beta$ , 2 $\alpha$ , 2 $\beta$
1 $\beta$		0.94 m	3	1 $\alpha$ , 2 $\alpha$ , 2 $\beta$	1 $\alpha$ , 2 $\alpha$ , 2 $\beta$
2 $\alpha$	19.7	1.57 m	x	1 $\alpha$ , 1 $\beta$ , 2 $\beta$	1 $\alpha$ , 1 $\beta$ , 2 $\beta$
2 $\beta$		1.37 m	x	1 $\alpha$ , 1 $\beta$ , 2 $\alpha$	1 $\alpha$ , 1 $\beta$ , 2 $\alpha$
3 $\alpha$	29.4	1.29 m	2	2 $\alpha$ , 2 $\beta$ , 3 $\beta$	2 $\alpha$ , 2 $\beta$ , 3 $\beta$
3 $\beta$		1.29 m	2	2 $\alpha$ , 2 $\beta$ , 3 $\alpha$	2 $\alpha$ , 2 $\beta$ , 3 $\alpha$
4	33.8	1.84 m	2, 5, 10	14, 3 $\alpha$ , 3 $\beta$	14
5	76.4	-	-	-	-
6 $\alpha$	31.7	2.66 d, 13.9	7, 8, 10, 11	6 $\beta$	15, OCH <sub>3</sub>
6 $\beta$		2.22 dd, 1.4, 13.9	7, 11	6 $\alpha$ ,13	14, 15, OCH <sub>3</sub>
7	157.1	-	-	-	-
8	106.1	-	-	-	-
9 $\alpha$	45.2	1.82 m	5, 7, 8, 10	9 $\beta$	9 $\beta$ ,14, 15
9 $\beta$		1.82 m	8, 7, 10	9 $\alpha$	9 $\alpha$
10	38.3	-	-	-	-
11	126.4	-	-	-	-
12	171.3	-	-	-	-
13	8.2	1.76 s	7, 11, 12	6 $\beta$	OCH <sub>3</sub> ,
14	20.6	1.14 s	1, 5, 9, 10	-	4, 6 $\beta$
15	15.1	0.83 d, 6.7	3,4,5	4	OCH <sub>3</sub> ,
OCH <sub>3</sub>	49.7	3.03 s	8	-	6 $\alpha$ , 6 $\beta$ , 13, 14,
5-OH	-	3.86 s	4, 5, 6, 10		2 $\beta$ , 3 $\beta$ , 4, 6 $\beta$ , 13, 15

#### 4.4.1.1.2. E22: 5 $\beta$ ,8 $\alpha$ -dihydroxy eudesm-7(11)-en-12,8-olide (ermiasolide B)



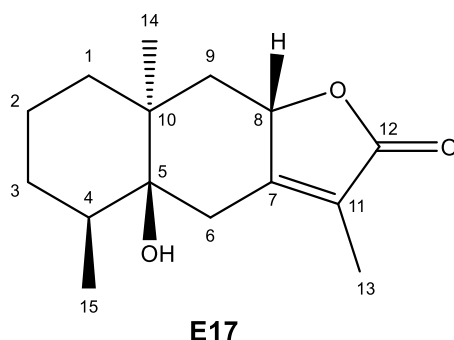
5 $\beta$ ,8 $\alpha$ -dihydroxy eudesm-7(11)-en-12,8-olide (compound **E22**) was isolated from the ethyl acetate soluble extract of the stem bark of *C. megalocarpus* as a yellowish oil. The HRMS spectrum (**Appendix 9**) of compound **E22** showed a molecular ion peak at  $m/z$  [M+H]<sup>+</sup> 267.1589 for C<sub>16</sub>H<sub>22</sub>O<sub>4</sub> (calc. C<sub>15</sub>H<sub>22</sub>O<sub>4</sub> + H,  $m/z$  267.1591). The <sup>1</sup>H NMR spectrum (**Table 4.4-4**) of this compound showed three methyl proton resonances at  $\delta_H$  1.78 (s), 1.29 (s), and

0.89 (d,  $J=6.7$ ) and missing the resonance for a methoxy group that was observed in compound **E12** (Appendix 10). The  $^{13}\text{C}$ , DEPT, and HSQCDEPT NMR spectra (Appendix 10-16) supported 15 carbon resonances, including a carbonyl resonance at  $\delta_{\text{C}}$  173.0, two double bond resonances at 158.9 and 125.3, a hemiketal methine carbon at 104.1, an oxygenated carbon resonance at 78.0, and carbon resonances for 3 methyls, 5 methylenes, and 1 methine. The  $^{13}\text{C}$  and DEPT NMR spectra were missing the methoxylated carbon resonance as in compound **E12**. The 2D spectra for compound **E22** were similar to those of compound **E12**. Compound **E22** was determined to be an undescribed derivative of compound **E12**, 5 $\beta$ ,8 $\alpha$ -dihydroxy eudesm-7(11)-en-12,8-olide, trivially named **ermiasolide B**.

Table 4.4-4: NMR data for 5 $\beta$ ,8 $\alpha$ -dihydroxy eudesm-7(11)-en-12,8-olide (ermiasolide B, E22) in  $\text{CDCl}_3$

No.	$^{13}\text{C}$ NMR	$^1\text{H}$ NMR	HMBC (H $\rightarrow$ C)	COSY	NOESY
1 $\alpha$	34.2	1.55 m	2, 10	1 $\beta$ , 2 $\alpha$ , 2 $\beta$	1 $\beta$ , 2 $\alpha$ , 2 $\beta$
1 $\beta$		1.14 m	3	1 $\alpha$ , 2 $\alpha$ , 2 $\beta$	1 $\alpha$ , 2 $\alpha$ , 2 $\beta$
2 $\alpha$	20.0	1.68 m	x	1 $\alpha$ , 1 $\beta$ , 2 $\beta$	1 $\alpha$ , 1 $\beta$ , 2 $\beta$
2 $\beta$		1.49 m	x	1 $\alpha$ , 1 $\beta$ , 2 $\alpha$	1 $\alpha$ , 1 $\beta$ , 2 $\alpha$
3 $\alpha$	30.0	1.48 m	2	2 $\alpha$ , 2 $\beta$ , 3 $\beta$	2 $\alpha$ , 2 $\beta$ , 3 $\beta$
3 $\beta$		1.27 m	2	2 $\alpha$ , 2 $\beta$ , 3 $\alpha$	2 $\alpha$ , 2 $\beta$ , 3 $\alpha$
4	34.1	1.94 m	2, 5, 10, 15	14, 3 $\alpha$ , 3 $\beta$	14
5	78.0	-	-	-	-
6 $\alpha$	31.8	2.71 d, 13.9	5, 7, 8, 10, 11	6 $\beta$	15, OCH <sub>3</sub> ,
6 $\beta$		2.43 d, 13.9	5, 7, 11	6 $\alpha$ ,13	14, 15
7	158.9	-	-	-	-
8	104.1	-	-	-	-
9 $\alpha$	47.0	1.90 m	5, 7, 8, 10, 14	9 $\beta$	9 $\beta$ ,14, 15
9 $\beta$		1.88 m	5, 7, 8, 10, 14	9 $\alpha$	9 $\alpha$
10	38.9	-	-	-	-
11	125.3	-	-	-	-
12	173.0	-	-	-	-
13	8.4	1.78 s	7, 11, 12	6 $\beta$	
14	15.2	0.89 d, 6.7	1, 5, 9, 10	-	4, 6 $\beta$
15	21.2	1.29 s	3,4,5	4	
5-OH					
8-OH					

#### 4.4.1.1.3. E17: 5 $\beta$ ,8H- $\beta$ -hydroxy eudesm-7(11)-en-12,8-olide (ermiasolide C)

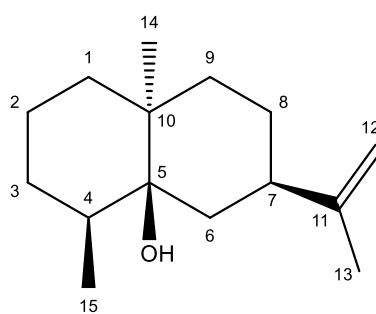


5 $\beta$ ,8H- $\beta$ -hydroxy eudesm-7(11)-en-12,8-olide (compound **E17**) was isolated from the ethyl acetate soluble extract of the stem bark of *C. megalocarpus* as a yellowish oil. Compound **E17** was determined to be an undescribed 5 $\beta$ ,8H- $\beta$ -hydroxy eudesm-7(11)-en-12,8-olide, an 8-H derivative of compounds **E22** and **E12**. The HRMS spectrum (**Appendix 17**) of compound **E17** showed a molecular ion peak at  $m/z$   $[M+H]^+$  251.1641 for  $C_{15}H_{22}O_3$  (calc.  $C_{15}H_{22}O_3 + H$ ,  $m/z$  251.1642). The  $^1H$  NMR spectrum (**Table 4.4-5**) of this compound showed three methyl proton resonances at  $\delta_H$  1.80 (s), 0.90 (d), and 0.82 (s) and missing the resonance for a methoxy group that was observed in compound **E12** (**Appendix 18**). The  $^{13}C$ , DEPT, and HSQCDEPT NMR spectra (**Appendix 19-24**) supported 15 carbon resonances, including a carbonyl resonance at  $\delta_C$  175.4, two double bond resonances at 161.4 and 121.5, an oxygenated carbon resonance at 76.5, and carbon resonances for 3 methyls, 5 methylenes, and 2 methines. The  $^{13}C$  and DEPT NMR spectra were missing the methoxylated carbon resonance, the hemiketal methine carbon at 104.1 as in compound **E12**, and only had one oxygenated carbon when compared to **E22**. The 2D spectra for compound **E17** were similar to those of compounds **E12** and **E22**. Compound **E17** was determined to be an undescribed derivative of compound **E12** and **E22**, 5 $\beta$ ,8H- $\beta$ -hydroxy eudesm-7(11)-en-12,8-olide, trivially named **ermiasolide C**.

Table 4.4-5: NMR data for 5 $\beta$ ,8H- $\beta$ -hydroxy eudesm-7(11)-en-12,8-olide (ermiasolide C, E17) in CDCl<sub>3</sub>

No.	<sup>13</sup> C NMR	<sup>1</sup> H NMR	HMBC (H→C)	COSY	NOESY
1 $\alpha$	36.9	1.50 m	10	1 $\beta$ , 2 $\alpha$ , 2 $\beta$	1 $\beta$ , 2 $\alpha$ , 2 $\beta$
1 $\beta$		1.34 m	2,3	1 $\alpha$ , 2 $\alpha$ , 2 $\beta$	1 $\alpha$ , 2 $\alpha$ , 2 $\beta$
2 $\alpha$	21.2	1.67 m	x	1 $\alpha$ , 1 $\beta$ , 2 $\beta$	1 $\alpha$ , 1 $\beta$ , 2 $\beta$
2 $\beta$		1.59 m	x	1 $\alpha$ , 1 $\beta$ , 2 $\alpha$	1 $\alpha$ , 1 $\beta$ , 2 $\alpha$
3 $\alpha$	30.2	1.50 m	2	2 $\alpha$ , 2 $\beta$ , 3 $\beta$	2 $\alpha$ , 2 $\beta$ , 3 $\beta$
3 $\beta$		1.23 m	2	2 $\alpha$ , 2 $\beta$ , 3 $\alpha$	2 $\alpha$ , 2 $\beta$ , 3 $\alpha$
4	36.2	1.81 m	2, 5, 10, 15	14, 3 $\alpha$ , 3 $\beta$	14
5	76.5	-	-	-	-
6 $\alpha$	35.4	2.55 m	5, 7, 8, 10, 11	x	15
6 $\beta$		2.55 m	5, 7, 8, 10, 11	x	14, 15
7	161.4	-	-	-	-
8	78.0	5.44 m	-	-	-
9 $\alpha$	43.2	2.24 d	1,7, 8, 14	9 $\beta$	9 $\beta$ ,14, 15
9 $\beta$		1.39 d	1,7, 8, 14	9 $\alpha$	9 $\alpha$
10	38.5	-	-	-	-
11	121.5	-	-	-	-
12	175.4	-	-	-	-
13	8.6	1.80 s	7, 11, 12	6 $\beta$	
14	14.8	0.93 d	1, 5, 9, 10	-	4, 6 $\beta$
15	23.9	0.82 s	3,4,5	4	
5-OH					

#### 4.4.1.1.4. E5: 4H- $\alpha$ ,7H- $\alpha$ ,10 $\alpha$ -eudesm-11-en-5 $\beta$ -ol



**E5**

4H- $\alpha$ ,7H- $\alpha$ ,10 $\alpha$ -eudesm-11-en-5 $\beta$ -ol (compound **E5**) was isolated from the ethyl acetate soluble extract of the stem bark of *C. megalocarpus* as a yellowish oil. Compound **E5** was determined to be the known 4H- $\alpha$ ,7H- $\alpha$ ,10 $\alpha$ -eudesm-11-en-5 $\beta$ -ol previously isolated from orange juice (Näf *et al.*, 2011). The HRMS spectrum (**Appendix 25**) of compound **E5** showed a molecular ion peak at  $m/z$   $[M+H]^+$  221.1889 for C<sub>15</sub>H<sub>24</sub>O (calc. C<sub>15</sub>H<sub>24</sub>O + H,  $m/z$  221.1900).

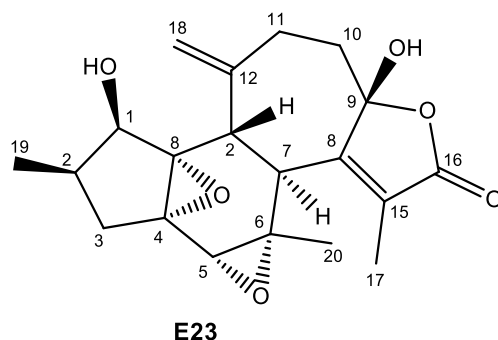
The  $^1\text{H}$  NMR spectrum (**Table 4.4-6**) of this compound showed three methyl proton resonances at 1.73 (s), 1.03 (s), and 0.79 (d,  $J=6.7$ ) (**Appendix 26**). The  $^{13}\text{C}$ , DEPT, and HSQCDEPT NMR spectra (**Appendix 27-32**) supported 15 carbon resonances, including two double bond resonances at 150.8 and 108.4, an oxygenated carbon resonance at 75.1, and carbon resonances for 3 methyls, 6 methylenes, and 2 methines. The  $^1\text{H}$  and  $^{13}\text{C}$  NMR spectra were similar to those of the known 4H- $\alpha$ ,7H- $\alpha$ ,10 $\alpha$ -eudesm-11-en-5 $\beta$ -ol previously isolated from orange juice (**Table 4.4-6**) (Näf *et al.*, 2011).

Table 4.4-6: NMR data for 4H- $\alpha$ ,7H- $\alpha$ ,10 $\alpha$ -eudesm-11-en-5 $\beta$ -ol (E5) in  $\text{CDCl}_3$

No.	$^{13}\text{C}$ NMR	$^{13}\text{C}$ NMR*	$^1\text{H}$ NMR	$^1\text{H}$ NMR*	HMBC (H $\rightarrow$ C)	COSY	NOESY
1 $\alpha$	34.8	35.0	1.58		x	1 $\beta$ , 2 $\alpha$	
1 $\beta$			1.34		x	1 $\alpha$	
2 $\alpha$	20.8	20.7	1.65 m		x	1 $\alpha$ , 1 $\beta$ , 2 $\beta$	7
2 $\beta$			1.47 m		x	2 $\alpha$	
3 $\alpha$	30.5	30.4	1.34 m		5	4	
3 $\beta$			1.42 m		5	4	15
4	34.5	34.3	1.72 m		3	3 $\alpha$ , 3 $\beta$ , 15	
5	75.1	74.8	-			-	
6 $\alpha$	26.2	26.0	1.54 m		11	7	
6 $\beta$			1.54 m		11	7	
7	40.3	40.1	2.41 m	2.41 m	x	6 $\alpha$ , 6 $\beta$ , 8 $\alpha$ 8 $\beta$	2 $\alpha$ , 8 $\alpha$
8 $\alpha$	35.8	35.70	1.57 m		11	7	7
8 $\beta$			1.34 m		11	7	
9 $\alpha$	35.2	34.6	1.57 m		x	9 $\beta$	
9 $\beta$			1.07 m		x	9 $\alpha$	
10	37.1	36.9	-		-	-	
11	150.8	150.7	-		-	-	
12A	108.6	108.4	4.72 s	4.72 s	7, 13	12B, 13	12B, 13
12B			4.69 s	4.70s	7, 13	12A, 13	12A, 13
13	20.6	20.9	1.73 s	1.74 s	7, 12, 14	12A, 12B	12A, 12B, 15
14	21.1	20.4	1.03 s	1.03 s	1, 5, 9, 10	4	3 $\beta$ , 4, 13
15	15.1	14.9	0.79 d 6.7	0.80 d 6.7	3, 4, 5	-	13
5-OH						-	

\*(Näf *et al.*, 2011)

#### 4.4.1.1.5. E23: Crotoascarin K



Compound **E23** was isolated from the ethyl acetate soluble extract of the stem bark of *C. megalocarpus* as a yellowish oil. Compound **E23** was determined to be the known crotoascarin K previously isolated from *C. cascarilloides*. The HRESIMS (**Appendix 33**) of compound **E23** showed a molecular ion peak at  $m/z$  361.1643  $[M+H]^+$  (calcd. for  $C_{20}H_{24}O_6 + H$ ,  $m/z$  361.1646). The  $^1H$ -NMR spectrum (**Table 4.4-7**) showed three methyl resonances, two oxygenated methine resonances, and exocyclic methylene protons resonated (**Appendix 34**). In contrast, the  $^{13}C$  NMR spectrum showed 20 carbon resonances, which showed a close resemblance to those of the previously reported crotoascarin K. The  $^{13}C$  NMR, DEPT, HSQCDEPT, HMBC, COSY and NOESY spectrum of **E23** is depicted in **Appendix 35-40**.

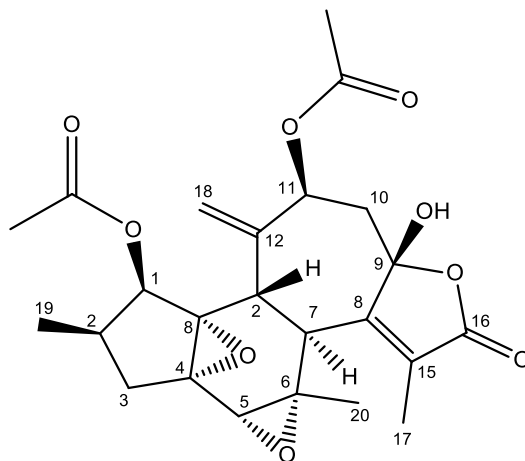
Table 4.4-7: NMR data for Crotoascarin K (E23) in  $CDCl_3$

No.	$^{13}C$ NMR	$^{13}C$ NMR*	$^1H$ NMR	$^1H$ NMR*
1	73.6	73.7	4.20 m	4.18 d 5.1
2	33.5	33.7	2.01 m	2.04 m
3 $\alpha$	36.1	36.2	2.39 m	2.39 dd 13.5, 7
3 $\beta$			1.65 m	1.68 dd 13.5, 10.2
4	60.2	60.4	-	-
5	58.0	58.2	3.17 s	3.11 s
6	56.4	56.6	-	-
7	43.9	44.1	3.01 dd 1, 12.6	2.97dd 12.6, 1.1
8	158.8	159.7	-	-
9	107.2	108.0	-	-
10 $\alpha$	41.9	41.8	2.45 m	2.53 m
10 $\beta$			1.61 m	1.56
11 $\alpha$	34.9	35.2	2.46 m	2.41 m
11 $\beta$			2.35 m	2.33 ddd 14.8, 13.4, 6.4
12	147.3	147.7	-	-
13	39.3	39.3	3.32 d 12.6	3.35 d 12.6
14	69.9	70.0	-	-
15	130.5	130.1	-	-

16	170.5	171.3	-	-
17	9.6	9.6	1.91 d 1	1.89 d 0.9
18A	114.6	114.4	5.07 br s	5.06 s
18B			5.06 br s	5.04 s
19	12.1	12.2	1.03 d 7.2	1.03 d 7.2
20	20.2	20.3	1.15 s	1.14 s

\*(Kawakami *et al.*, 2015)

#### 4.4.1.1.6. E24: 11 $\beta$ -acetoxy crotoascarin L



**E24**

Compound **E24** was isolated from the ethyl acetate soluble extract of the stem bark of *C. megalocarpus* as a yellowish oil. Compound **E24** showed a molecular ion peak at  $m/z$  445.1854  $[M+H]^+$  (calcd. for  $C_{24}H_{28}O_8 + H$ ,  $m/z$  445.1857), which gave 11 degrees of unsaturation (**Appendix 41**). The IR spectrum showed the presence of an  $\alpha,\beta$ -unsaturated lactone at  $1746\text{ cm}^{-1}$ . The  $^1\text{H}$  and  $^{13}\text{C}$  NMR spectra (**Table 4.4-8**) were similar to those of the known crotoascarin L, previously isolated from *C. cascarilloides* (Kawakami *et al.*, 2016), except for the presence of an acetoxy group due to a proton methyl resonance at 2.12 (s) and carbon resonances at  $\delta_{\text{C}}$  169.1 and 21.2 for an acetoxy group (**Appendix 42-43**). The COSY, HMBC, and NOESY spectra (**Appendix 44-48**) supported placement of the acetoxy group at the C-11 position. Notably, the exocyclic proton resonances at  $\delta_{\text{H}}$  5.32 (s) and 5.30 (s) showed a correlation in the HMBC spectrum with an oxygenated carbon resonance at 74.6, which corresponded to a proton resonance at 5.59 (t, 3.4). This proton resonance further showed a correlation with a carbonyl carbon resonance of an acetoxy group at 169.1, hence the assignment of the acetoxy group to the C-11 position.

Table 4.4-8: NMR data for 11 $\beta$ -acetoxy crotoascarin L (E24)

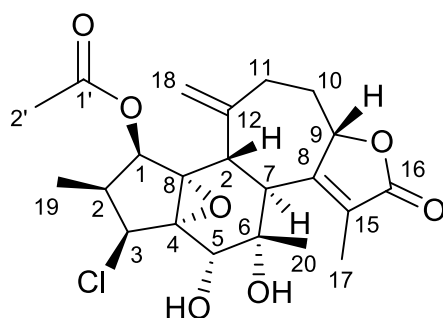
No.	<sup>13</sup> C NMR	<sup>13</sup> C NMR*	<sup>1</sup> H NMR	<sup>1</sup> H NMR*	COSY	NOESY
1	74.8	74.9	5.46 d 5.2	5.47 d 6	2	2,11
2	33.9	33.4	2.19 m	2.05 m	1,3 $\alpha$ ,3 $\beta$ ,19	1,7
3 $\alpha$	36.8	36.9	2.46 dd 6.5, 12.9	2.41 dd 14, 7	2,3 $\beta$	7
3 $\beta$				1.65 dd 14, 10	2,3 $\alpha$	13,19
4	60.8	60.5	-	-	-	-
5	57.7	57.8	3.21 s	3.16 s	20	17,20
6	56.2	56.4	-	-	-	-
7	44.2	44.1	3.17 s	2.99 dq 13, 1	13,17	2,3 $\alpha$ ,10 $\alpha$ ,13,20
8	161.1	158.9		-	-	-
9	78.2	107.8	5.03 br d 10.5	-	-	-
10 $\alpha$	42.3	42.0	2.85 dt 3.7, 14.1	2.46 o	10 $\beta$ ,11	7
10 $\beta$			1.39 m	1.59 ddd 13, 13, 5	10 $\alpha$ ,11	13
11 $\alpha$	74.6	35.0	5.59 t 3.4	2.46 o	10 $\alpha$ ,10 $\beta$ ,11	1,7
11 $\beta$				2.11 ddd 13, 13, 5	-	-
12	143.9	146.6	-	-	-	-
13	33.6	39.6	3.16 s	3.05 d 13	7	10 $\beta$ ,19
14	68.6	68.8	-	-	-	-
15	128.9	130.7	-	-	-	-
16	173.1	170.4	-	-	-	-
17	9.9	9.7	1.92 0.9	1.91 s	7	5
18A	118.9	115.1	5.32 s	5.08 s	18B	18B
18B			5.30 s	5.06 s	18A	18A
19	12.7	12.5	0.90 d 7.1	0.92 d 7	2	3 $\beta$ ,13
20	19.6	20.2	1.11 s	1.18 s	5	5,7
1-CH <sub>3</sub>	21.1	20.6	2.10 s	2.11 s	-	x
1-CO	169.3	169.5	-	-	-	-
11-CH <sub>3</sub>	21.2	x	2.12 s		-	x
11-CO	169.1	x	-	-	-	-
9-OH				3.43 br s	-	-

\*(Kawakami *et al.*, 2016)



#### 4.4.1.1.7. E37: 1 $\beta$ -Acetoxy-3 $\beta$ -chloro-5 $\alpha$ ,6 $\alpha$ -dihydroxycrotocascarin L (Ermasoid)

Compound **E37** was trivially named ermasoid, a rare example of a chlorinated crotofolane diterpenoid.



**E37**

1 $\beta$ -Acetoxy-3 $\beta$ -chloro-5 $\alpha$ ,6 $\alpha$ -dihydroxycrotocascarin L (**E37**) gave a molecular formula of C<sub>22</sub>H<sub>27</sub>ClO<sub>7</sub>, with nine degrees of unsaturation, as determined by (+)-HRESIMS analysis, which displayed an ion peak at  $m/z$  439.1514 [M+H]<sup>+</sup> (calcd for C<sub>22</sub>H<sub>27</sub>ClO<sub>8</sub> + H,  $m/z$  439.1518). The IR spectrum exhibited the presence of an  $\alpha,\beta$ -unsaturated lactone (1747 cm<sup>-1</sup>) and hydroxy groups (3436 cm<sup>-1</sup>). The <sup>1</sup>H NMR spectrum (CDCl<sub>3</sub>, **Table 4.4-9**) gave resonances for two singlet methyls ( $\delta_H$  1.62 s; 1.93 s), two doublet methyls ( $\delta_H$  1.19 d, 7.7 Hz; 1.83 d, 1.7 Hz), two olefinic protons ( $\delta_H$  5.32, s and 4.82, s), three oxygenated methine protons ( $\delta_H$  5.37 t, 5.8 Hz; 5.10 d, 8.2 Hz; 3.55 d 7.3 Hz), a halomethine proton ( $\delta_H$  3.61 s), two pairs of methylene protons ( $\delta_H$  2.32 m, and 1.61 (m); 2.31, m and 2.31, m), three methine protons ( $\delta_H$  2.81 m; 3.73 d, 11.9 Hz; 2.85 d, 11.9 Hz), and a proton of a hydroxy group ( $\delta_H$  3.96 s). The <sup>13</sup>C NMR spectrum (CDCl<sub>3</sub>, **Table 4.4-9**), together with DEPT results, showed 22 carbon resonances including two carbonyl carbon resonances at  $\delta_C$  173.7 and, 172.5, four alkene resonances at  $\delta_C$  160.2, 144.9, 129.5 and 113.9, six oxygenated carbon resonances at  $\delta_C$  80.9, 78.0, 75.6, 81.9, 82.7 and 66.3, a halogenated carbon resonance at  $\delta_C$  66.8, four methyl carbon resonances, two methylene carbon resonances, and three methine carbon resonances (**Appendix 49-57**). The use of the COSY and HMBC spectra indicated **E37** to be a derivative of crotocascarin L, previously reported from the Japanese *C. cascarilloides*, with de-hydroxylation at C-9, chlorination at the C-3 position, with the epoxy group opening to form a diol at C-5 and C-6 (Kawakami *et al.*, 2016). The two carbonyls and two double bonds, accounted for four of the nine degrees of unsaturation, and suggested that **E37** is pentacyclic. A doublet methyl group  $\delta_H$  1.19 (d, 7.7 Hz), found in the five-membered ring A, was evident in the <sup>1</sup>H and <sup>1</sup>H-<sup>1</sup>H COSY spectrum and assignable as CH<sub>3</sub>-19. This methyl group proton resonance was coupled to the

methine resonances of H-2 ( $\delta_{\text{H}}$  2.81, m) in the COSY spectrum, and in turn, H-2 was coupled to an oxygenated methine proton resonance at  $\delta_{\text{H}}$  5.10 (d, 8.2 Hz), either at the H-1 or the H-3 position. A correlation in the HMBC spectrum between this oxygenated doublet methyl with a typical C-13 methine carbon resonance at  $\delta_{\text{C}}$  44.0, allowed for its assignment as H-1 (Kawakami *et al.*, 2016). The corresponding H-13 methine proton resonance was assigned using the HSQC spectrum ( $\delta_{\text{H}}$  2.85, d,  $J = 11.9$  Hz). The H-1 resonance gave a correlation in the HMBC spectrum with a carbonyl carbon of the acetoxy group, and hence an acetate group was placed at the C-1 position. The C-12(18) exocyclic double bond, was present as in previously reported crotoascarins, as shown by two singlet H-18 proton resonances  $\delta_{\text{H}}$  5.32 and  $\delta_{\text{H}}$  4.82, which corresponded to a methylene carbon resonance at  $\delta_{\text{C}}$  113.9 in the HSQC spectrum (Kawakami *et al.*, 2016). These two resonances exhibited correlations in the HMBC spectrum with a methylene carbon resonance at  $\delta_{\text{C}}$  35.1 that was assigned to C-11. The two H-11 resonances were overlapped at  $\delta_{\text{H}}$  2.31 and coupled in the COSY spectrum with the methylene protons at  $\delta_{\text{H}}$  2.32 and  $\delta_{\text{H}}$  1.16 for H<sub>2</sub>-10, which, in turn, were coupled to a deshielded oxygenated proton resonance at  $\delta_{\text{H}}$  5.37 (t, 5.8 Hz) for H-9. The corresponding C-9 resonance occurred at  $\delta_{\text{C}}$  82.7, and gave an HMBC correlation with a methine proton resonance at  $\delta_{\text{H}}$  3.73 (d, 11.9 Hz) for H-7. H-7 and H-13 were seen to be coupled in the COSY spectrum, with a  $J$  value of 11.9 Hz, suggesting a *trans* configuration at the junction. Also, H-7 had correlations in the HMBC spectrum between the carbon resonances at  $\delta_{\text{C}}$  78.0 (C-5), 75.6 (C-6), 129.5 (C-8) and 160.2 (C-15), with the latter two typical of an  $\alpha,\beta$ -unsaturated lactone ring formed from the isopropyl group of a crotofolane derivative (Kawakami *et al.*, 2016). The CH<sub>3</sub>-17 resonance ( $\delta_{\text{H}}$  1.83, d, 1.7 Hz) displayed correlations in the HMBC spectrum between the carbon resonances at  $\delta_{\text{C}}$  173.7 (C-16), 160.2 (C-15) and 129.5 (C-8). A singlet methyl group proton resonance at  $\delta_{\text{H}}$  1.62 afforded a correlation in the HMBC spectrum with C-7, and hence was assigned as CH<sub>3</sub>-20. This resonance also gave correlations in the HMBC spectrum with a fully substituted carbon resonance at  $\delta_{\text{C}}$  75.6 (C-6) and a methine carbon resonance at 78.0 (C-5). The carbon resonances were deshielded compared to typical epoxide carbon resonances in reported crotofolanes such as crotoascarin L, (Kawakami *et al.*, 2016) consistent with hydroxy groups being present at C-5 and C-6. The resonance present at  $\delta_{\text{H}}$  3.55 (s) was assigned as H-5 using the HSQC spectrum, and it showed correlations in the HMBC spectrum between the fully substituted carbon resonances at  $\delta_{\text{C}}$  81.9 (C-4), 66.3 (C-14), and a methine carbon resonance at  $\delta_{\text{C}}$  66.8 that was determined to be attached to a Cl atom. A chlorinated carbon resonance present at C-3 in the diterpenoid, laevinoid, has been previously reported by Wang

*et al.*, (Wang *et al.*, 2013) and the chemical shift was identical to that observed for 1 $\beta$ -acetoxy-3 $\beta$ -chloro-5 $\alpha$ ,6 $\alpha$ -dihydroxycrotocascarin L. The HRMS of this compound showed a protonated molecular peak [M+H]<sup>+</sup> at *m/z* 439.1514 and a characteristic isotope at *m/z* 441.1491 [M+2] with a relative abundance of ca 32%, indicating the presence of a chlorine atom in the structure. The accurate mass value of this compound was consistent with the molecular formula, C<sub>22</sub>H<sub>27</sub>O<sub>7</sub>Cl (error = 0.68 ppm), while any non-chlorinated alternative was inconsistent with the MS (high error values) and NMR data. The NOESY spectrum (**Figure 4.4-2**) showed that H-5, H-9, H-13, 3H-19 and 3H-20 were on the same of the molecule tentatively assigned as  $\beta$ , whereas H-1, H-2, H-3 and H-7 were assigned as  $\alpha$ . This compound was determined to be an undescribed monochlorinated crotofolane trivially named *ermiasoid*.

Table 4.4-9: NMR data for 1 $\beta$ -Acetoxy-3 $\beta$ -chloro-5 $\alpha$ ,6 $\alpha$ -dihydroxycrotocascarin (*Ermiasoid*) (E37)

No.	<sup>13</sup> C NMR	<sup>1</sup> H NMR	HMBC (H→C)	COSY	NOESY
1	80.9	5.10 d 8.2	2, 14, 19	2	2, 13
2	33.5	2.81 m	3, 4, 14	1, 19	1, 7
3	66.8	3.61 s	1, 2	x	19
4	81.9	-	-	-	-
5	78.0	3.55 s	3, 4, 6, 7, 14	x	20
6	75.6	-	-	-	-
7	44.5	3.73 d 11.9	8,9, 13, 15, 16	x	20
8	129.5	-	-	-	-
9	82.7	5.37 t 5.8	x	10 $\alpha$ , 10 $\beta$ , 17	13
10 $\alpha$	34.3	2.32 m	9, 12	9, 11 $\alpha$ , 11 $\beta$	10 $\beta$ , 11 $\alpha$ , 11 $\beta$
10 $\beta$		1.61 m	9, 12	9, 11 $\alpha$ , 11 $\beta$	10 $\alpha$ , 11 $\alpha$ , 11 $\beta$
11 $\alpha$	35.1	2.31 m	x	10 $\alpha$ , 10 $\beta$ , 11 $\beta$	11 $\beta$ , 18A, 18B
11 $\beta$		2.31 m	x	10 $\alpha$ , 10 $\beta$ , 11 $\alpha$	11 $\alpha$ , 18A, 18B
12	144.9	-	-	-	-
13	44.0	2.85 d 11.9	7, 11, 12, 18	7	1, 9, 19, 20
14	66.3	-	-	-	-
15	160.2	-	-	-	-
16	173.7	-	-	-	-
17	10.5	1.83 d 1.7	8, 15, 16	9	7
18A	113.9	5.32 s	3, 11	18B	11 $\alpha$ , 11 $\beta$ , 18B
18B		4.82 s	3, 11	18A	11 $\alpha$ , 11 $\beta$ , 18A
19	10.4	1.19 d 7.7	1, 2, 3	2	3, 13, 1-CH <sub>3</sub>
20	27.5	1.62 s	5, 6, 7	-	5, 8, 13
1-CH <sub>3</sub>	20.6	1.93 s	C=O	-	19
1-CO	172.5	-	-	-	-

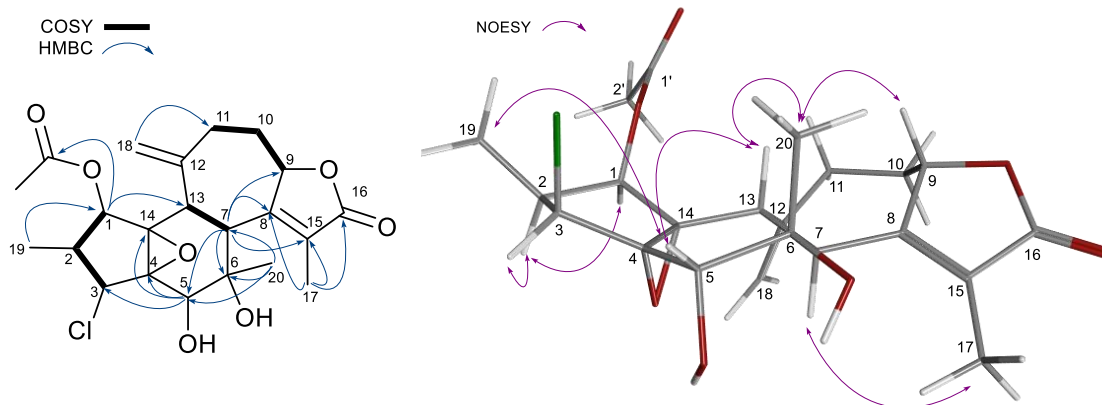
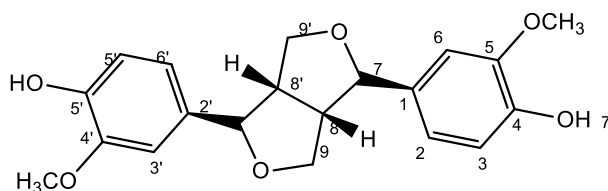


Figure 4.4-2: Key COSY, HMBC and NOESY correlations observed for 1 $\beta$ -Acetoxy-3 $\beta$ -chloro-5 $\alpha$ ,6 $\alpha$ -dihydroxycrotocascarin (Ermasoid) (E37)

#### 4.4.1.1.8. E2: Pinoresinol



**E2**

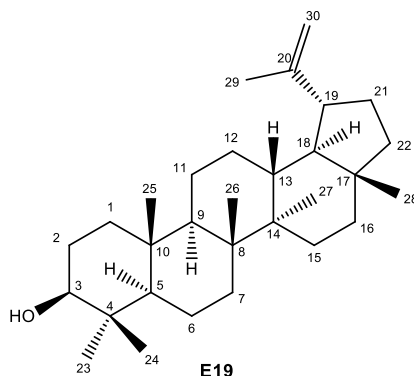
Compound **E2** was isolated from the ethyl acetate soluble extract of the stem bark of *C. megalocarpus* as a yellowish oil. The  $^1\text{H}$  NMR spectrum (**Table 4.4-10**) showed three peaks of aromatic protons at  $\delta_{\text{H}}$  6.89 (1H, s), 6.83 (1H, dd,  $J = 8.0, 2.3$  Hz) and 6.91 (1H, d,  $J = 8.0$  Hz), suggesting that the aromatic ring has three substituted positions. The oxymethine proton was evident at 4.74 (d, 4.2) ppm as a doublet, and the methylene groups bearing oxygen atoms at 4.26 and 3.88 ppm were two doublets of the doublet. A methine proton was observed at 3.10 ppm (multiplet), and a methoxy group was confirmed at 3.92 ppm (singlet). The data of compound **E2** were consistent with previously isolated pinoresinol (Trinh *et al.*, 2007). The HSQC, HMBC and COSY spectrum of **E2** is depicted in **Appendix 59-61**.

Table 4.4-10: NMR data for Pinoresinol (E2)

No.	<sup>1</sup> H NMR	<sup>1</sup> H NMR*
1/1'	-	-
2/2'	6.89 s	6.89 (2H, d, 1.5)
3/3'	-	-
4/4'	-	-
5/5'	6.91 d 8.0	6.88 (2H, d, 8.0)
6/6'	6.83 dd 2.3, 8.0	6.82 (2H, dd, 1.5, 8.0)
7/7'	4.74 d (4.2)	4.73 (2H, d, 5.0)
8/8'	3.10 m	3.10 (2H, m)
9A/9A'	4.26 dd 6.7, 10.0	4.24 (2H, dd, 7.0, 9.5)
9B/9B'	3.88 dd 4.5, 10.0	3.88 (2H, dd, 4.0, 9.5)
3-OCH <sub>3</sub> /3'-OCH <sub>3</sub>	3.92 s	3.90 (3H, s)

\*(Trinh *et al.*, 2007)

#### 4.4.1.1.9. E19: 3β-Hydroxylup-20(29)-ene (lupeol)



Compound **E19** was isolated from the ethyl acetate soluble extract of the stem bark of *C. megalocarpus* as a white solid and identified as the known lupeol, which has been isolated previously from many sources (Ahmad & Atta-ur-rahman, 1994; Burns *et al.*, 2000). The <sup>1</sup>H NMR spectrum (**Table 4.4-10**) of compound E19 showed the presence of seven methyl group proton resonances at  $\delta_{\text{H}}$  0.75, 0.78, 0.82, 0.92, 0.94, 0.94 and 1.67, which corresponded to the carbon resonances at  $\delta_{\text{C}}$  19.5, 18.2, 14.7, 16.2, 16.3, 15.6, and 28.2 in the <sup>13</sup>C NMR spectrum and HSQCDEPT spectrum (**Appendix 62-63**). The <sup>1</sup>H NMR spectrum showed a proton resonance at  $\delta_{\text{H}}$  3.18 (1H, dd,  $J=11.1$ ,  $J=4.9$  Hz), which was seen to correspond to a carbon resonance at 79.2 in the HSQCDEPT spectrum. This proton resonance and the H-5 proton resonance at 0.69 (d  $J=9.1$  Hz) were seen to correlate in the HMBC spectrum with the 3H-23 and 3H-24 methyl group resonances at 0.96 and 0.76. The HMBC spectrum (**Appendix 93-97**) showed a correlation between the downfield methyl group resonance at 1.67 and the two nonequivalent methylene proton resonances at 4.68 and 4.56, which were ascribed to H-29A

and H-29B. Compound **E19** was identified as the known 3 $\beta$ -hydroxylup-20(29)-ene, commonly known as lupeol, which has been evaluated for its anti-inflammatory and antiangiogenic activities. A literature search revealed  $^{13}\text{C}$  NMR chemical shifts similar to those of compound **E19** for lupeol.

Table 4.4-11: NMR data for lupeol (E19) in  $\text{CDCl}_3$

No.	$^{13}\text{C}$ NMR	$^{13}\text{C}$ NMR*	$^1\text{H}$ NMR	$^1\text{H}$ NMR*
1 $\alpha$	38.9	38.7	1.66 m	1.65 m
1 $\beta$			0.92 m	0.91 m
2 $\alpha$	27.6	27.4	1.59 m	1.60 m
2 $\beta$			1.66 m	1.65 m
3	79.2	79.0	3.18 dd (11.1, 4.9)	3.18 dd (11.4, 4.9)
4	39.0	38.8		-
5	55.5	55.3	0.68 d (9.2)	0.69 d (9.3)
6 $\alpha$	18.5	18.3	1.50 m	1.51 m
6 $\beta$			1.39 m	1.39 m
7 $\alpha$	34.5	34.3	1.38 m	1.38 m
7 $\beta$			1.38 m	1.38 m
8	41.0	40.8	-	-
9	50.6	50.4	1.28 m	1.27 m
10	37.4	37.2	-	-
11 $\alpha$	21.1	20.9	1.41m	1.41 m
11 $\beta$			1.20 m	1.21 m
12 $\alpha$	25.3	25.2	1.07 m	1.06 m
12 $\beta$			1.66 m	1.67 m
13	38.9	38.3	1.64 m	1.64 m
14	43.2	42.9	-	-
15 $\alpha$	28.2	27.5	1.01 m	1.00 m
15 $\beta$			1.69 m	1.67 m
16 $\alpha$	35.8	35.6	1.39 m	1.38 m
16 $\beta$			1.49nm	1.47 m
17	43.2	43.0	-	-
18	48.5	48.0	1.36 m	1.35 m
19	48.2	47.9	2.37 m	2.38 m
20	151.3	151.0	-	-
21 $\alpha$	30.0	29.9	1.33 m	1.32 m
21 $\beta$			1.92 m	1.92 m
22 $\alpha$	40.2	40.0	1.21 m	1.19 m
22 $\beta$			1.39 m	1.38 m
23	28.2	28.0	0.98 s	0.97 s
24	15.6	15.4	0.75 s	0.77 s
25	16.3	16.1	0.82 s	0.83 s
26	16.2	16.0	1.02 s	1.02 s
27	14.7	14.6	0.97 s	0.98 s
28	18.2	18.0	0.79 s	0.79 s
29A	109.5	109.3	4.56 br m	4.56 br s
29B			4.68 d (2.3)	4.68 br s
30	19.5	19.3	1.67 s	1.69 s

\*(Jamila *et al.*, 2014)

#### 4.4.1.2. Cytotoxicity and anti-HIV activity of pure compounds isolated from *C. megalocarpus*

The cytotoxic and antiviral activity findings for the pure compounds isolated from *C. megalocarpus* and the control drugs are summarized in **Table 4.4-12**. In the MTT cytotoxic assay using human T-lymphocytic MT-4 cells, the pure compounds isolated from *C. megalocarpus* showed significantly ( $p < 0.001$ ) higher  $CC_{50}$  values than the control drugs (**Figure 4.4-3**). Although the maximum cytotoxic effect ( $E_{max_c}$ ) was higher ( $>60\%$ ), the compounds (except E2 and E5) inhibited viral replication at much lower concentrations ( $IC_{50}$ ) than the maximum nontoxic concentration (MNTC), indicating the safety of the compounds (**Table 4.4-12**). Furthermore, a cytotoxicity test performed on FM-55-M1 human melanoma cells revealed the  $CC_{50}$  value of these compounds to be above  $50 \mu\text{M}$ , which indicates that these compounds could be considered safe as they need high concentrations to exert cytotoxic effects. Among the tested compounds, E12, ermasolide A, displayed the highest anti-HIV activity by inhibiting HIV-induced CPE by 93% at an  $IC_{50}$  value of  $0.002 \mu\text{g/mL}$ . Similarly, E17, E5, and E23 inhibited viral replication by 86, 83.9, and 83.3%, respectively (**Table 4.4-12**).

Table 4.4-12: Cytotoxicity and anti-HIV-1 activities of pure compounds isolated from *C. megalocarpus*

Materials	Cytotoxicity			Antiviral activity		SI
	MNTC ( $\mu\text{g/mL}$ )	$CC_{50}$ ( $\mu\text{g/mL}$ )	$E_{max_c}$ (%)	$IC_{50}$ ( $\mu\text{g/mL}$ )	$E_{max_{AV}}$ (%)	
<b>AZT</b>	$0.38 \pm 0.19$	$0.53 \pm 0.29$	$36.28 \pm 0.83$	$0.002 \pm 0.00$	$83.5 \pm 0.57$	279.4
<b>TDF</b>	$4.92 \pm 0.71$	$6.73 \pm 0.24$	$13.17 \pm 0.43$	$0.04 \pm 0.01$	$80.55 \pm 0.46$	176.5
<b>ABC</b>	$0.18 \pm 0.03$	$0.26 \pm 0.00$	$17.83 \pm 0.57$	$0.05 \pm 0.031$	$58.67 \pm 0.43$	5.0
<b>NVP</b>	$0.57 \pm 0.0$	$0.82 \pm 0.0$	$39.13 \pm 0.65$	$0.24 \pm 0.09$	$72.53 \pm 0.47$	3.5
<b>E2</b>	$1.01 \pm 0.03$	$16.14 \pm 0.41$	$65.91 \pm 0.41$	$0.02 \pm 0.01$	$63.06 \pm 0.58$	959.0
<b>E5</b>	$8.8 \pm 0.69$	$79.09 \pm 0.49$	$69.00 \pm 0.77$	$0.033 \pm 0.01$	$83.91 \pm 0.39$	2380.8
<b>E12</b>	$41.84 \pm 0.11$	$96.77 \pm 0.44$	$62.21 \pm 0.67$	$0.002 \pm 0.00$	$93.4 \pm 0.60$	39872.3
<b>E17</b>	$64.93 \pm 0.26$	$148.1 \pm 0.05$	$65.00 \pm 0.01$	$0.044 \pm 0.01$	$77.46 \pm 0.93$	3384.4
<b>E19</b>	$75.75 \pm 0.74$	$141.8 \pm 0.7$	$70.28 \pm 0.75$	$0.047 \pm 0.02$	$77.01 \pm 0.38$	3048.2
<b>E22</b>	$4.973 \pm 0.25$	$38.44 \pm 0.63$	$81.59 \pm 0.41$	$0.002 \pm 0.00$	$69.51 \pm 0.26$	25339.5
<b>E23</b>	$150.9 \pm 0.55$	$183.7 \pm 0.65$	$53.18 \pm 0.57$	$0.002 \pm 0.00$	$83.3 \pm 0.97$	89741.1
<b>E37</b>	$45.73 \pm 0.53$	$91.46 \pm 0.21$	$64.4 \pm 0.94$	$0.012 \pm 0.00$	$86.64 \pm 0.69$	7423.7

Results are shown as means  $\pm$  S.E. M (n=3)

AZT, Zidovudine; TDF, Tenofovir; ABC, Abacavir; NVP, Nevirapine; E2, Pinoresinol; E5, 4H- $\alpha$ ,7H- $\alpha$ ,10 $\alpha$ -eudesm-11-en-5 $\beta$ -ol; E12, ermasolide A; E17, ermasolide C; E19, lupeol; E22, ermasolide B; E23, Crotonoscarin K; E37, ermasolide; MNTC, Maximum nontoxic concentration;  $CC_{50}$ , 50% cytotoxic concentration;  $E_{max_c}$ , Maximum cytotoxic effect %;  $IC_{50}$ , 50% antiviral effect concentrations;  $E_{max_{AV}}$ , maximum antiviral effect %; SI, selective index.

The pure compounds (E12, E22, and E23) showed  $IC_{50}$  and  $E_{max_{AV}}$  values approximately similar to AZT's, indicating their potential antiviral efficacy (**Figure 4.4-4**). In addition, these compounds displayed higher potency than TDF, ABC, and NVP. Only E2 (pinoresinol) showed lower antiviral efficacy ( $E_{max_{AV}} = 63.06\%$ ). As depicted in **Figure 4.4-5**, the pure compounds displayed concentration-dependent inhibition of virus-induced CPE, as the % CPE inhibition increased with increasing concentrations of the pure compounds.

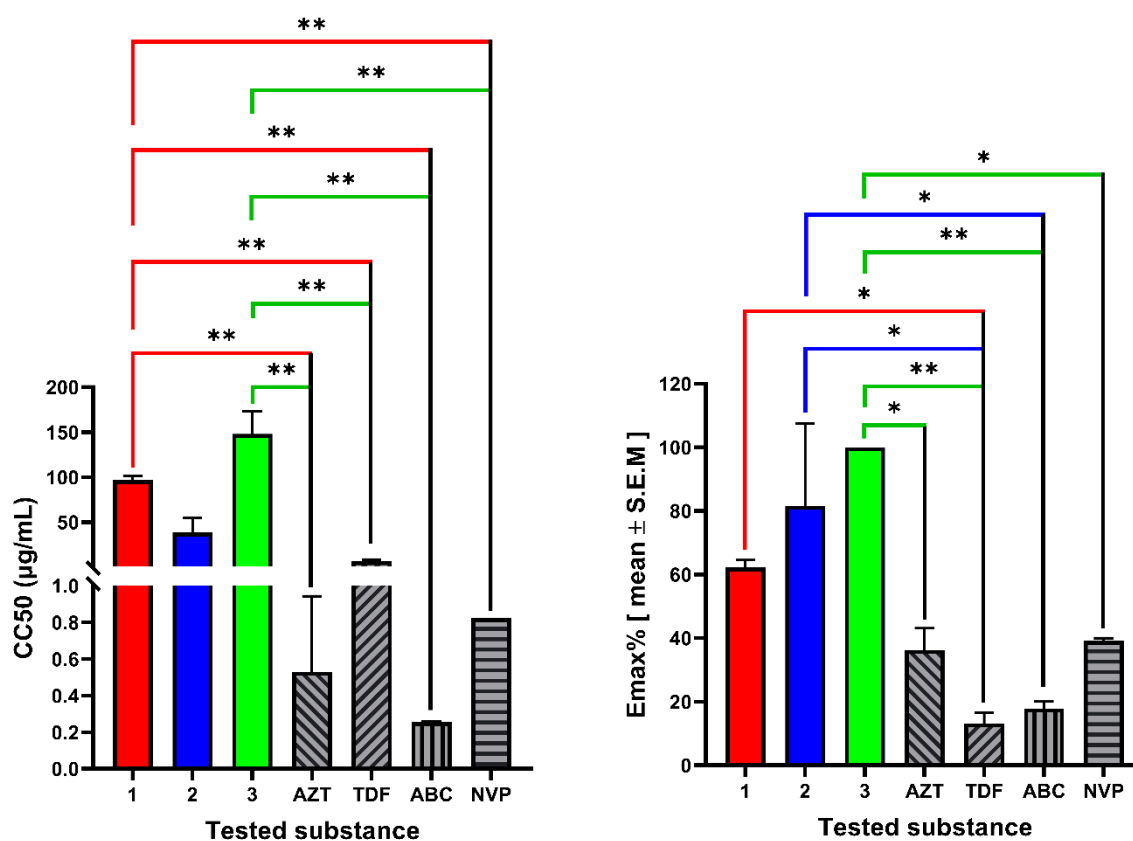


Figure 4.4-3: Cytotoxicity of ermiasolides isolated from *C. megalocarpus*

The results are expressed as the mean of three independent experiments  $\pm$  S.E.M. 1, ermiasolide A; 2, ermiasolide B; 3, ermiasolide C; AZT, zidovudine, ABC, abacavir, NVP, nevirapine; TDF, tenofovir; C, control; ns; not significant, \*Denotes p value  $< 0.05$ , \*\* Denotes p value  $< 0.01$ , \*\*\* Denotes p value  $< 0.001$ .



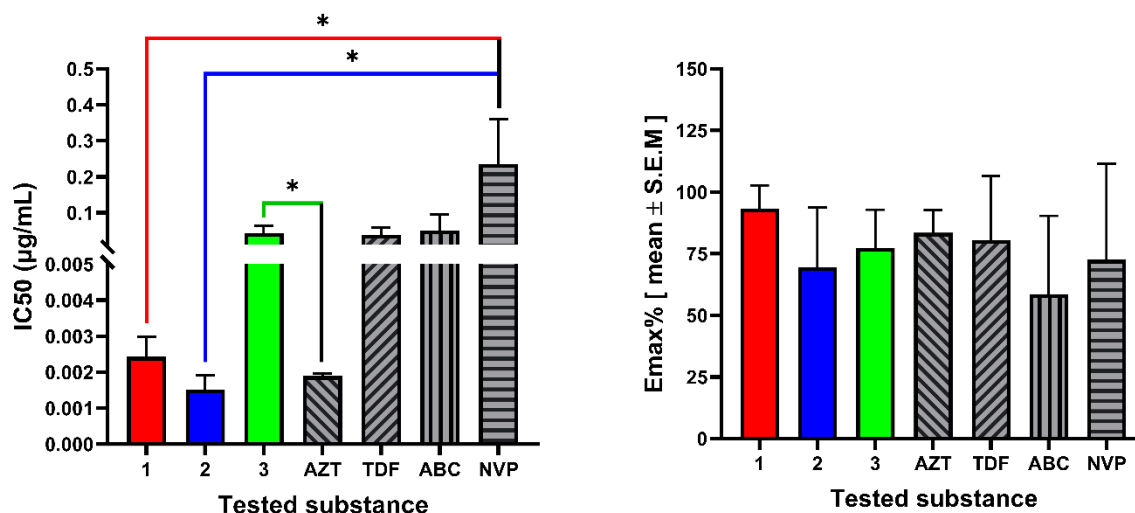


Figure 4.4-4: Anti-HIV activity of ermasolides from *C. megalocarpus*

The results are expressed as the mean of three independent experiments  $\pm$  S.E.M. AZT, Zidovudine; TDF, Tenofovir; ABC, Abacavir; NVP, Nevirapine; 1, ermasolide A; 2, ermasolide B; 3, ermasolide C. \*Denotes p value  $<0.05$

The demonstrated highest anti-HIV activity of Ermasolide A (E12) and Ermasolide B (E22) could be due to presence of hydrogen bond forming methoxy and hydroxyl groups in C-8 of the structures, respectively. These important functional groups were missing in Ermasolide C (E17) which could have contributed to its lower antiviral efficacy ( $E_{max_{AV}} = 77.46\%$ ). Furthermore, the presence of methoxy group in E12 at C-8, contributes to its highest anti-HIV activity ( $E_{max_{AV}} = 93\%$ ) as compared to E22 which has  $-OH$  group at C-8. This difference could be due to the role of the methoxy group in forming stable hydrophobic interactions at the receptor site as depicted in the *in silico* study (**Figure 4.5-5**). Previous studies have confirmed the role of hydrophobic interactions as driving force of ligand–protein interaction (Gurung *et al.*, 2021)

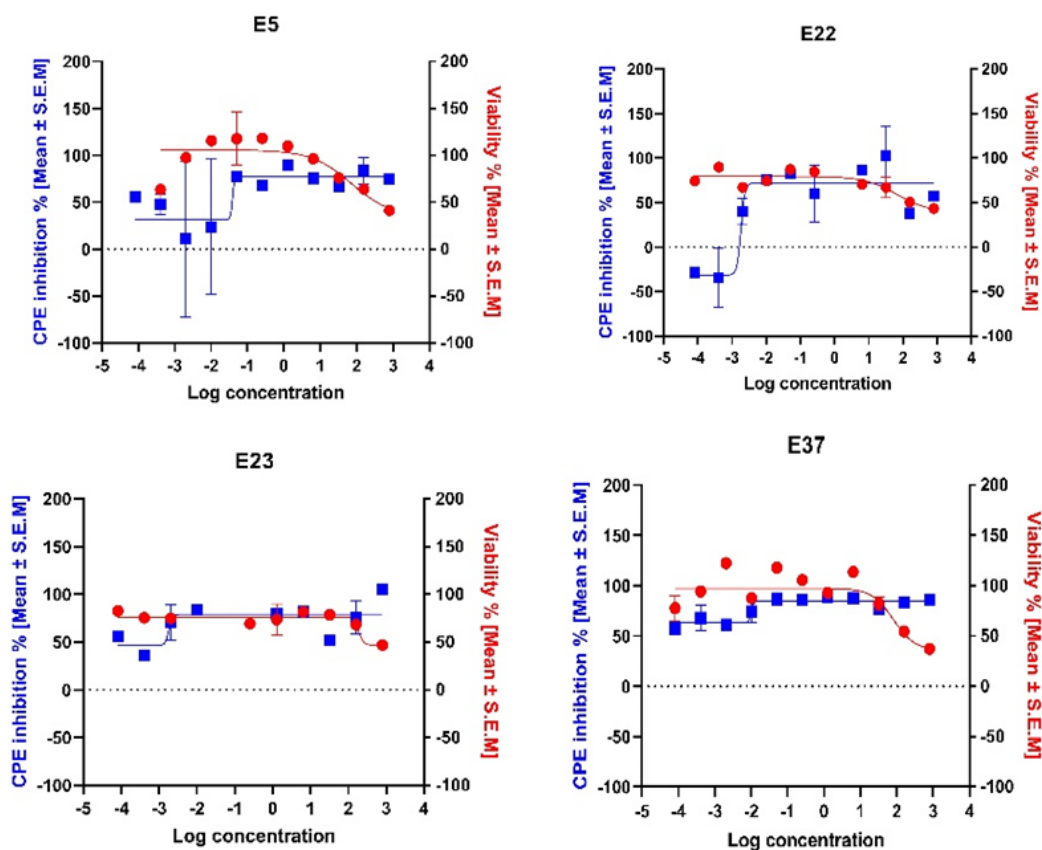


Figure 4.4-5: Concentration-response curves analysis for the anti-HIV activity of pure compounds isolated from *C. megalocarpus*.

Results presented in the curves are means  $\pm$  S.E. M of three independent experiments. Cell viability % (red line) and the inhibition % of the virus-induced cytopathic effect (blue line) associated with control drugs and the tested extracts at the concentration level ( $800 - 8.192 \times 10^5 \mu\text{g/mL}$ ). E5, 4H- $\alpha$ ,7H- $\alpha$ ,10 $\alpha$ -eudesm-11-en-5 $\beta$ -ol; E22, ermasolide B; E23, Crotoascarin K; E37, ermasoid

#### 4.4.1.3. Discussion

In this study we report the anti HIV activity of three new eudesmane type sesquiterpenes and two new crotofolane diterpenoids isolated from *C. megalocarpus*.

##### 1. Eudesmane type sesquiterpenes

Sesquiterpene lactones are a subclass of terpenoids, which is a large group of compounds found in plants. Sesquiterpene lactones play an important role in plant defense in nature, acting as antibacterials, antivirals, antifungals, and insecticides (Tuasha *et al.*, 2022). Sesquiterpene lactones have piqued the interest of researchers in recent years, primarily due to their cytotoxic and anticancer properties (Matejić *et al.*, 2014). Among isolated sesquiterpene lactones, eudesmane type sesquiterpenoids have displayed cytotoxic and potential antiviral

activity. Zhu *et al* (Zhu *et al.*, 2010) have demonstrated cytotoxic activity of three eudesmane lactones isolated from *Ajania przewalskii* Poljakov (Asteraceae).

A number of sesquiterpenes have previously been isolated from *Croton* species.  $\beta$ -caryophyllene from *C. aubrevillei*, *C. geayi*; caryophyllene oxide,  $\gamma$ -cadinene and  $\alpha$ -cadinene from *C. geayi* (Radulović *et al.*, 2006); blumenol A from *C. pedicellatus* (Langat *et al.*, 2018a); crocassins A, crocassins B (Ghosh *et al.*, 2013), cracrosone H (Qiu *et al.*, 2018), 6S-hydroxycyperenoic acid, crassifiterpenoid A (Tian *et al.*, 2019) from *C. crassifolius*, and patchoulone (Aye *et al.*, 2019) from *C. oblongifolius*. Eudesmane type sesquiterpenoids were not previously reported from *Croton* species and makes this research fundamental.

In this research, we demonstrated the anti-HIV activity of three new or previously undescribed eudesmane type sesquiterpenes, 5 $\beta$ -hydroxy-8 $\alpha$ -methoxy eudesm-7(11)-en-12,8-olide (**E12**), 5 $\beta$ ,8 $\alpha$ -dihydroxy eudesm-7(11)-en-12,8-olide (**E22**), and 5 $\beta$ ,8H- $\beta$ -hydroxy eudesm-7(11)-en-12,8-olide (**E17**) isolated from the stem bark of *C. megalocarpus* (Figure 4.4-6). As depicted in **Table 4.4-12**, E12, E22 and E17 inhibited HIV-1 replication with IC<sub>50</sub> values of 0.002  $\mu$ g/mL, 0.002  $\mu$ g/mL and 0.044  $\mu$ g/mL, respectively.

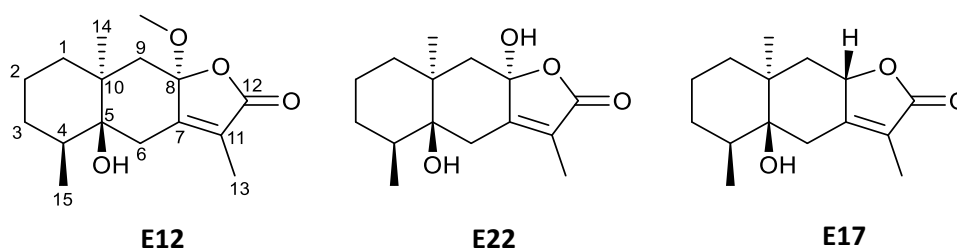


Figure 4.4-6: Eudesmane type sesquiterpenes isolated from *C. megalocarpus*

A molecular docking study **Table 4.5-2** and **4.5-3** revealed strong binding affinity of these compounds with HIV-1 protease enzyme (3EL9) compared with the HIV-1 reverse transcriptase. Docking studies indicated that the predicted free energy of binding obtained for ermasolides against HIV-1 reverse transcriptase were higher ( $\Delta G = -3.555$  kcal/mol for **E17**,  $\Delta G = -2.839$  kcal/mol for **E22**,  $\Delta G = -2.317$  kcal/mol for **E12** and  $\Delta G = -1.550$  kcal/mol for **E5**) compared to the known inhibitor nevirapine ( $\Delta G = -7.679$  kcal/mol). Lower predicted energies of binding were obtained against HIV-1 protease ( $\Delta G = -6.067$  kcal/mol for **E12**,  $\Delta G = -5.994$  kcal/mol for **E22**,  $\Delta G = -5.850$  kcal/mol for **E17** and  $\Delta G = -5.750$  kcal/mol for **E5**), although in both cases they were higher than that obtained for the positive control atazanavir ( $\Delta G = -11.49$  kcal/mol) (**Table 4.5-3**). However, the results obtained indicated that the

mechanism of action leading to the observed anti-HIV activities is through the HIV-1 protease inhibition, which agreed with the *in vitro* assay (**Table 4.5-1**).

The high anti-HIV activity of Ermiasolide A (E12) and Ermiasolide B (E22) could be due to presence of hydrogen bond forming methoxy and hydroxyl groups in C-8 of the structures, respectively. These important functional groups were missing in Ermiasolide C (E17) which could have contributed to its lower antiviral efficacy ( $E_{\text{maxAV}} = 77.46\%$ ). Furthermore, the presence of methoxy group in E12 at C-8, could contribute to its higher anti-HIV activity ( $E_{\text{maxAV}} = 93\%$ ) compared to **E22** which presents a hydroxy group at C-8 (**Figure 4.4-6**). This difference could be due to the role of the methoxy group in forming stable hydrophobic interactions at the enzyme active site as depicted in the *in silico* study (**Figure 4.5-1 and 4.5-2**). Previous studies have confirmed the role of hydrophobic interactions as driving force of ligand–protein interaction (Gurung *et al.*, 2021). The results obtained could indicate that the mechanism of action leading to the observed anti-HIV activities is through HIV-1 protease inhibition, which agrees with the data obtained in the *in vitro* assay. Figure 4.4-7 and 4.4-8 depict the interactions of the ermiasolides with HIV enzymes.

## 2. Crotofolane diterpenoids

In 1976, a crotofolane diterpenoid, crotofolin A, was reported from a Jamaican plant, *Croton corylifolius* Lam. (Euphorbiaceae) and, since then, despite several studies on the chemistry of *Croton* species, crotofolane-type diterpenoids have been reported on rarely (Burke *et al.*, 1979). Crotofolanes have fused 5-, 6- and 7-membered rings, and are biosynthesized from cembranes via casbane and lathyrane through cross annular cyclization (Kawakami *et al.*, 2015). In total, approximately 38 crotofolanes have been reported, and all are restricted to the genus *Croton*. The previous seven *Croton* species that have yielded crotofolanes are *C. argyrophyllus* (Filho *et al.*, 2013), *C. caracasanus* (Chávez *et al.*, 2013), *C. cascarilloides* (Gao *et al.*, 2018), *C. corylifolius* (Burke *et al.*, 1979), *C. dichogamus* (Aldhaher *et al.*, 2017), *C. haumanianus* (Kawakami *et al.*, 2016) and *C. insularis* (Maslovskaya *et al.*, 2014). Thus far, *C. megalocarpus* has only yielded clerodane and abietane diterpenoids (Zeng & Zhan, 2019). Chlorinated natural products have been observed only rarely, and the few that have been reported have diverse activities (Langat *et al.*, 2020). Chlorinated compounds are rare in the genus *Croton*, with only one chlorinated diterpenoid, laevinoid, reported from *Croton laevigatus* (Wang *et al.*, 2013).

In this research, we reported three crotofolane diterpenoids including previously undescribed 1 $\beta$ -acetoxy-3 $\beta$ -chloro-5 $\alpha$ ,6 $\alpha$ -dihydroxycrotocascarin L (E37) and 11 $\beta$ -

acetoxycrotocascarin L (**E24**), and known compound, crotocascarin K (**E23**) (**Figure 4.4-7**). As depicted in **Table 4.4-12** and **Figure 4.4-8**, **E37** and **E23** inhibited HIV-1 replication with  $IC_{50}$  values of 0.012  $\mu\text{g/mL}$  and 0.002  $\mu\text{g/mL}$ , respectively.

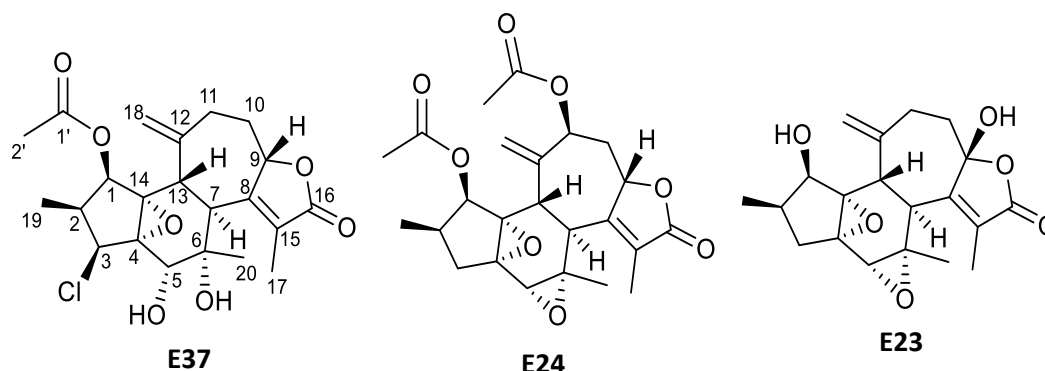


Figure 4.4-7: Crotofolane diterpenoids isolated from *C. megalocarpus*

Docking studies indicated that the predicted free energy of binding obtained for both compounds against HIV-1 reverse transcriptase were higher ( $\Delta G = -1.24$  kcal/mol for **E37**,  $\Delta G = -4.68$  kcal/mol for **E23**) compared to the known inhibitor nevirapine ( $\Delta G = -7.679$  kcal/mol). Lower predicted energies of binding were obtained against HIV-1 protease ( $\Delta G = -7.326$  kcal/mol for **E37**,  $\Delta G = -7.115$  kcal/mol for **E23**), although in both cases they were higher than that obtained for the positive control atazanavir ( $\Delta G = -11.49$  kcal/mol) (**Table 4.5-3**). However, the results obtained indicated that the mechanism of action leading to the observed anti-HIV activities is through the HIV-1 protease inhibition, which agreed with the *in vitro* assay.

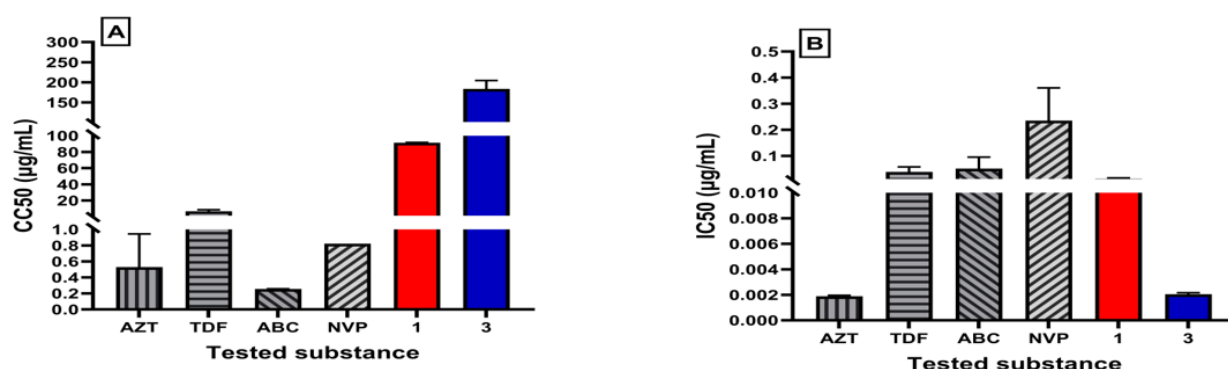


Figure 4.4-8: Cytotoxicity  $IC_{50}$  [A] and antiviral activity  $IC_{50}$  [B] values of the control drugs and the tested compounds **E37** (1) and **E23** (3). Results expressed are mean of three independent experiments  $\pm$  S.E.M.

#### 4.4.2. *Croton macrostachyus*

Based on the findings from the anti-HIV activity of the solvent fractions from *C. macrostachyus*, the hexane fraction of the leaves of *C. macrostachyus* was subjected to column chromatography to yield seven pure compounds (**Table 4.4-4**). The chemical structure of these compounds is depicted in **Figure 4.4-9**.

Table 4.4-13: Compounds isolated from the stem bark of *C. macrostachyus*

Ser. No.	Name	Code
1.	2-Methoxy benzyl benzoate	A5
2.	Betulin	A19
3.	Lupenone	A4b
4.	Lupeol acetate	A11
5.	3 $\beta$ -hydroxylup-20(29)-ene (lupeol)	A7
6.	Stigmasterol	A15
7.	Sitosterol	A16

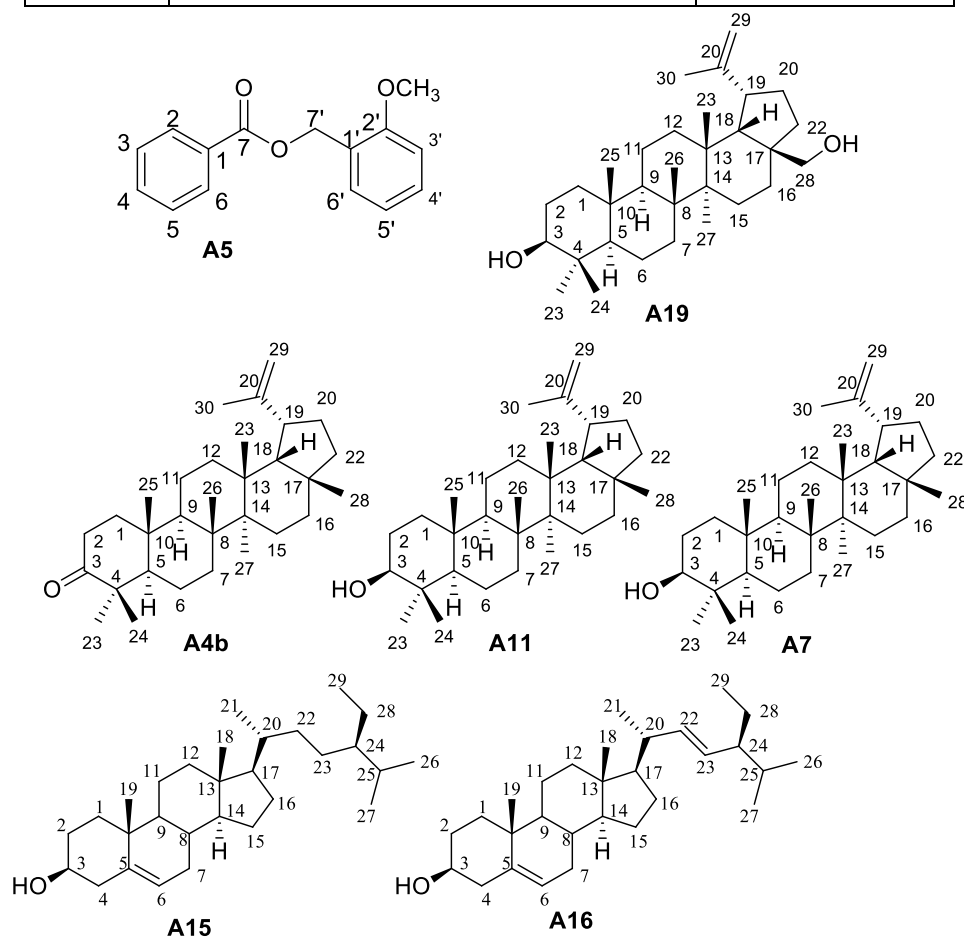
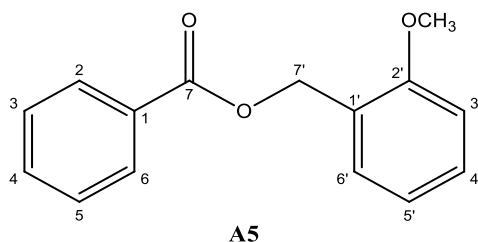


Figure 4.4-9: Pure compounds isolated from *C. macrostachyus*

#### 4.4.2.1. Chemistry of pure compounds isolated from *C. macrostachyus*

##### 4.4.2.1.1. A5: 2-Methoxy benzyl benzoate



2-Methoxy benzyl benzoate (compound **A5**) was isolated from the hexane soluble extract of the leaf of *C. macrostachyus* as a clear oil. The  $^1\text{H-NMR}$  spectrum (**Table 4.4-14**) of **A5** showed one aromatic methoxy (3.79, s), one carbinol methylene (5.45, s), and nine aromatic protons (6.89-8.02) (**Appendix 64**). The  $J$  coupling pattern of the five aromatic protons showed the presence of one monosubstituted phenyl ring. The  $^{13}\text{C}$  NMR spectrum (**Appendix 65**) indicated the presence of 15 carbons, including one carbonyl (8 166.8), one methoxy (56.7), one carbinol methylene (62.4), and two aromatic rings. These data led to identifying **A5** as a 2-methoxybenzyl benzoate, which was previously reported (Asakawa *et al.*, 1996; Nkunya, 2004; Van Kiem *et al.*, 2005a). The DEPT, HSQCDEPT, HMBC, and COSY spectrum of **A5** is depicted in **Appendix 66-69**.

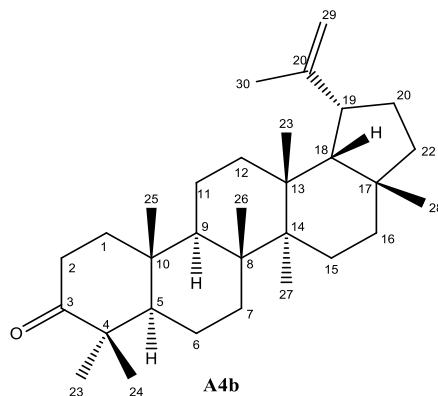
Table 4.4-14: NMR data for 2-Methoxy benzyl benzoate (A5) in  $\text{CDCl}_3$

No.	$^{13}\text{C}$ NMR	$^{13}\text{C}$ NMR*	$^1\text{H}$ NMR	$^1\text{H}$ NMR*
1	130.6	130.9	-	-
2	129.9 CH	129.8	8.02 dd 8.5, 1.7	8.13 dd 8.4, 2.1
3	129.6 CH	130.1	7.37 m	7.45 ddd 8.4, 8.0, 1.7
4	133.1 CH	133.2	7.48 ddd 8.5, 1.7, 1.4	7.58 dd 8.0, 2.1
5	129.7 CH	130.1	7.25 dd 1.8, 8.1	7.45 ddd 8.4, 8.0, 1.7
6	129.9 CH	129.8	8.02 dd 8.5, 1.7	8.13 dd 8.4, 2.1
7	166.8	167.0		-
1'	124.6	124.9	-	-
2'	157.7	158.0	-	-
3'	110.7 CH	110.9	6.89 d 8.1	6.98 dd 8.0, 1.8
4'	128.5 CH	129.8	7.37 m	7.35 dd 8.0, 7.9, 2.0
5'	120.6 CH	120.9	6.90 dd 1, 7.5	7.01 ddd 7.9, 7.5, 1.8

6'	128.5 CH	128.7	7.37 m	7.45 dd 7.5, 2.0
7'	62.4 CH <sub>2</sub>	62.6	5.36 s	5.45 s
OCH <sub>3</sub>	56.7 CH <sub>3</sub>	55.9	3.79 s	3.89 s

\*(Van Kiem *et al.*, 2005)

#### 4.4.1.1.1. A4b: Lupenone



Lupenone (compound **A4b**) was isolated from the hexane soluble extract of the leaf of *C. macrostachyus* as a white solid and identified as the widely known lupane triterpenoid lupenone. The <sup>13</sup>C NMR spectrum (**Table 4.4-15**) showed thirty carbon resonances. Two double bond carbon resonances at 109.6 and 151.6 and a carbonyl carbon resonance at  $\delta$  218.6 in conjunction with the molecular formula suggested that compound **A4b** was a pentacyclic triterpenoid. Analysis of the <sup>1</sup>H NMR, <sup>13</sup>C NMR, and DEPT spectra showed that compound **A4b** possessed seven methyl proton resonances at 1.07, 1.02, 0.93, 1.07, 1.68, 0.96, and 0.79, ten methylene groups, which included the characteristic lupane type-triterpenoid terminal double bond proton resonances at 4.69 (br s  $W_{1/2} = 5.10$  Hz) and 4.57 (br s  $W_{1/2} = 5.32$  Hz), assignable to the two H-29 protons and five methine groups (**Appendix 70-76**). The ketone carbon resonance, observed at  $\delta$  218.6, was ascribed to C-3 on biogenetic grounds (Carpenter *et al.*, 1980). A search in the literature showed that the <sup>13</sup>C NMR chemical shifts for compound **A4b** and those of the common compound lupenone (Carpenter *et al.*, 1980) isolated previously from *Poa huecu* Par., *Madhuca butyracea*, *Mangifera indica*, and many other sources were the same (Ahmad & Atta-ur-rahman, 1994). Lupenone is known to have a broad spectrum of biological activities. It is reported to be active against both gram-positive (*Bacillus subtilis*) and gram-negative (*Pseudomonas pyocyaneae*) bacteria (Kim, 2001). Lupenone has also been found to show antifungal activities against *Saccharomyces cerevisiae* and *Microsporium gypseum* (Kim, 2001; Mubiu *et al.*, 2017). Lupenone is also known to show antioxidative activity on lipid peroxidation by 6.4% (Ahmad & Atta-ur-rahman, 1994; F. Xu *et al.*, 2018).

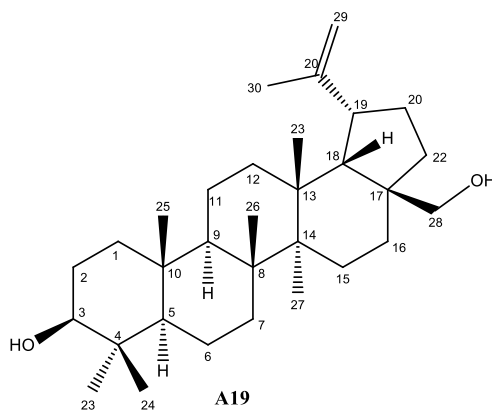


Table 4.4-15: NMR data for Lupenone (A4b) in CDCl<sub>3</sub>

No.	<sup>13</sup> C NMR	<sup>13</sup> C NMR*	<sup>1</sup> H NMR	<sup>1</sup> H NMR*
1 $\alpha$	40.0	39.6	1.92 m	1.90 m
1 $\beta$			1.42 m	1.42 m
2 $\alpha$	34.2	34.1	2.50 m-	2.48 m
2 $\beta$			2.48 m	2.42 m
3	217.8	217.9	-	-
4	47.4	47.3		-
5	54.9	54.9	1.33 m	1.34 m
6 $\alpha$	19.7	19.2	1.51 m	1.47 m
6 $\beta$			1.51 m	1.47 m
7 $\alpha$	33.6	33.5	1.45 m	1.43 m
7 $\beta$			1.45 m	1.43 m
8	40.8	40.7	-	-
9	49.8	49.7	1.39 m	1.39 m
10	36.7	36.8	-	-
11 $\alpha$	21.5	21.4	1.42 m	1.43 m
11 $\beta$			1.30 m	1.43 m
12 $\alpha$	25.2	25.1	1.70 m	1.69 m
12 $\beta$			1.12 m	1.10 m
13	38.1	38.1	1.70 m	1.68 m
14	42.8	42.8	-	-
15 $\alpha$	27.4	27.4	1.69 m	1.68 m
15 $\beta$			1.04 m	1.02 m
16 $\alpha$	35.5	35.5	1.51 m	1.50 m
16 $\beta$			1.43 m	1.41 m
17	42.9	42.9	-	-
18	48.2	48.2	1.39 m	1.39 m
19	47.9	47.9	2.40 m	2.39 m
20	150.3	150.8	-	-
21 $\alpha$	29.8	29.6	1.95 m	1.93 m
21 $\beta$			1.29 m	1.27 m
22 $\alpha$	39.6	39.4	1.43 m	1.42 m
22 $\beta$			1.23 m	1.21 m
23	26.7	26.6	1.07 s	1.07 s
24	21.1	21.0	1.02 s	1.02 s
25	16.0	15.9	1.07 s	1.07 s
26	15.8	15.7	0.93 s	0.93 s
27	14.5	14.4	0.96 s	0.96 s
28	18.0	17.9	0.79 s	0.79 s
29A	109.4	109.3	4.69 d 2.0	4.69 br s
29B			4.57 s	4.57 br s
30	19.3	19.6	1.61 s	1.68 s

\*(Carpenter *et al.*, 1980)

#### 4.4.1.1.2. A19 – Betulin



Betulin (compound **A19**) was isolated from the hexane soluble extract of the leaf of *C. macrostachyus* as a white solid and identified as the known betulin, which has been isolated previously from *C. macrostachyus* (Tala *et al.*, 2013b). The  $^1\text{H}$  NMR spectrum (**Table 4.4-16**) of compound **A19** showed the presence of seven methyl group proton resonances at 0.76, 0.81, 0.96, 0.99, 1.01 and 1.68, which corresponded to the carbon resonances at 15.3, 16.0, 27.9, 14.7, 15.9 and 19.0 in the  $^{13}\text{C}$  NMR spectrum and HSQCDEPT spectrum. The  $^1\text{H}$  NMR spectrum (**Appendix 77**) showed a proton resonance at 3.19 (1H, dd,  $J=10.8$ ,  $J=4.9$  Hz), which was seen to correspond to a carbon resonance at 79.2 in the HSQCDEPT spectrum (**Appendix 78-80**). This proton resonance and the H-5 proton resonance at 0.68 (d  $J=9.4$  Hz) were seen to correlate in the HMBC spectrum with the 3H-23 and 3H-24 methyl group resonances at 0.96 and 0.76. The HMBC spectrum (**Appendix 81-83**) showed a correlation between the downfield methyl group resonance at 1.67 and the two nonequivalent methylene proton resonances at 4.67 dd 2.1 and 4.57 (m), which were ascribed to H-29A and H-29B. In addition, two nonequivalent methylene proton resonances at 3.80 dd 1.6, 11.0 and 3.33 (d, 11.0) were ascribed to H-28A and H-28B. Compound **A19** was identified as the known betulin.

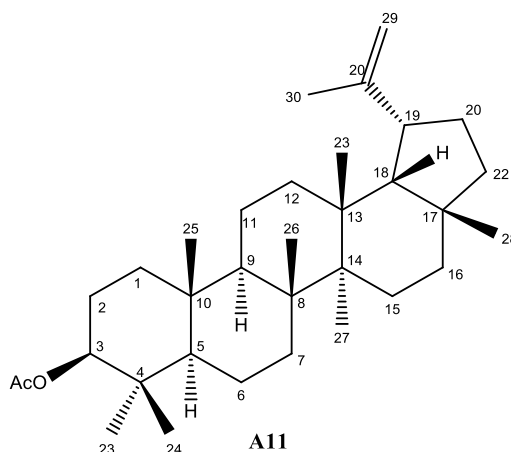
Table 4.4-16: NMR data for Betulin (A19) in  $\text{CDCl}_3$

No.	$^{13}\text{C}$ NMR	$^{13}\text{C}$ NMR*	$^1\text{H}$ NMR	$^1\text{H}$ NMR*
1 $\alpha$	38.9	38.6	1.69 m	1.65 dd 12.6, 3.6
1 $\beta$			0.88 m	0.89 dd 12.6, 3.2
2 $\alpha$	27.2	27.0	1.72 m	1.58 m
2 $\beta$			1.08 m	1.58 m
3	79.2	78.8	3.19 dd 4.9, 10.8	3.18 dd 8.0, 3.2
4	39.1	38.8	-	-
5	55.5	55.2	0.68 d 9.4	0.68 d, 18.0
6 $\alpha$	18.5	18.2	1.55 m	1.50 m
6 $\beta$			1.42 m	1.38 m

7 $\alpha$	34.4	34.2	1.41 m	1.37 m
7 $\beta$			1.41 m	1.37 m
8	41.1	40.8	-	-
9	50.9	50.3	1.32 m	1.29 m
10	37.3	37.1	-	-
11 $\alpha$	21.0	20.8	1.42 m	1.40 m
11 $\beta$			1.24 m	1.19 m
12 $\alpha$	25.4	25.1	1.64 m	1.62 m
12 $\beta$			1.06 m	1.05 m
13	37.5	37.2	1.67 m	1.63 m
14	42.9	42.6	-	-
15 $\alpha$	27.2	27.0	1.60 m	1.69 m
15 $\beta$			1.06 m	1.08 m
16 $\alpha$	29.4	29.1	1.96 m	1.89 m
16 $\beta$			1.26 m	1.28 m
17	48.0	47.7		-
18	48.9	48.7	1.57 m	1.58 m
19	48.0	47.6	2.37, m	2.36, m
20	150.7	150.3	-	-
21 $\alpha$	29.9	29.7	1.96 m	1.98 m
21 $\beta$			1.43 m	1.29 m
22 $\alpha$	34.2	33.9	1.86 m	1.85 m
22 $\beta$			1.06 m	1.04 m
23	28.2	27.9	0.96 s	0.92 s
24	15.6	15.3	0.76 s	0.74 s
25	16.3	16.0	0.81	0.79 s
26	16.2	15.9	1.01 s	0.99 s
27	15.0	14.7	0.99 s	0.94 s
28	60.7	60.8	3.80 dd 1.6, 11.0	3.75 d 9.0
			3.33 d 11.0	3.30 d 9.0
29A	109.9	109.7	4.67 d 2.1	4.65 brs
29B			4.57 m	4.55 brs
30	19.3	19.0	1.68 s	1.68 s

\*(Jamila *et al.*, 2014)

#### 4.4.1.1.3. A11: Lupeol acetate



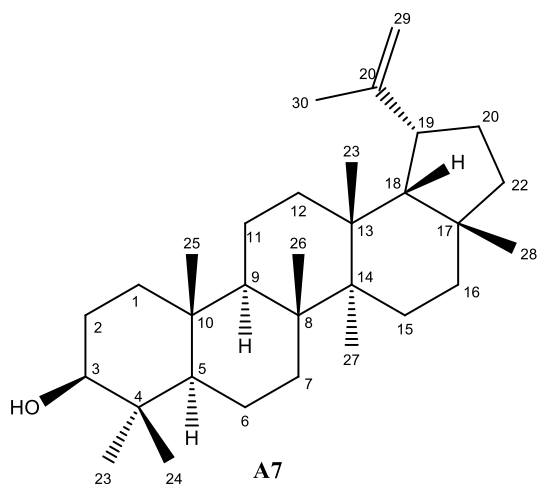
Lupeol acetate (Compound **A11**) was isolated as a white powder from the leaf of *C. macrostachyus* and identified as 3 $\beta$ -acetoxyilup-20(29)-ene, commonly called lupeol acetate. The LREIMS spectrum for compound **A11** gave a molecular ion peak at  $m/z$  468, which indicated a molecular formula of C<sub>32</sub>H<sub>52</sub>O<sub>2</sub>. The FTIR spectrum displayed an absorption band at 1732 cm<sup>-1</sup> that was attributed to a carbonyl group stretch and absorption bands at 1640, 1246, and 880 cm<sup>-1</sup> that were ascribed to terminal double bond stretches. The <sup>13</sup>C NMR spectrum (**Appendix 84-85**) showed thirty-two carbon resonances for compound **A11**. The presence of a carbonyl carbon resonance at 171.2 and two double bond carbon resonances at 109.6 and 151.2 in conjunction with the molecular formula suggested that compound **A11** was a pentacyclic acetylated triterpenoid. The <sup>1</sup>H NMR spectrum (**Table 4.4-17**) displayed seven methyl proton resonances at 1.68 (s), 0.78 (s), 0.94 (s), 0.83 (s), 0.85 (s), 1.02 (s), and 0.84 (s) and an acetate methyl group proton resonance at  $\delta$  2.04 (s) (Ahmad & Atta-ur-rahman, 1994). Furthermore, the terminal double bond proton resonances at 4.68 (br s  $W_{1/2}$  = 6.09 Hz) and  $\delta$  4.57 (br s  $W_{1/2}$  = 6.62 Hz) were characteristic of the terminal double bond of a lupane-type triterpenoid (Ahmad & Atta-ur-rahman, 1994). The two proton resonances at  $\delta$  4.68 (br s) and  $\delta$  4.57 (br s) were ascribed to the two H-29 protons. Comparing the <sup>13</sup>C NMR chemical shifts with those found in the literature confirmed that compound **A11** was the known 3 $\beta$ -acetoxyilup-20(29)-ene. 3 $\beta$ -Acetoxyilup-20(29)-ene has been previously shown to demonstrate anti-arthritis effects in complete Freund's adjuvant (CFA)-induced arthritis rats (Kweifio-Okai & Carroll, 1993). The DEPT, HSQCDEPT, HMBC, COSY and NOSEY spectra of A11 is depicted in **Appendix 86-90**.

Table 4.4-17: NMR data for Lupeol acetate (A11) in CDCl<sub>3</sub>

No.	<sup>13</sup> C NMR	<sup>13</sup> C NMR*	<sup>1</sup> H NMR	<sup>1</sup> H NMR*
1 $\alpha$	38.3	38.4	1.64 m	1.69 m
1 $\beta$			0.98 m	0.98 m
2 $\alpha$	23.6	23.7	1.58 m	1.60 m
2 $\beta$			1.58 m	1.60 m
3	80.9	81.0	4.47 dd 5.6, 10.5	4.47 dd 4.4, 12.8
4	37.9	37.8	=	-
5	55.3	55.4	0.79 m	0.76 dd 10.8, 5.8
6 $\alpha$	18.1	18.2	1.49 m	1.50 m
6 $\beta$			1.36 m	1.40 m
7 $\alpha$	34.1	33.6	1.36 m	1.38 m
7 $\beta$			1.36 m	1.38 m
8	40.7	40.9	-	-
9	50.2	50.4	1.29 m	1.30 m
10	37.0	37.1	-	-
11 $\alpha$	20.8	21.0	1.39 m	1.40 m
11 $\beta$			1.20 m	1.22 m
12 $\alpha$	25.0	25.1	1.65 m	1.68 m
12 $\beta$			1.05 m	1.07 m
13	38.0	38.1	1.65 m	1.68 m
14	42.7	42.9	-	-
15 $\alpha$	27.3	27.5	1.65 m	1.68 m
15 $\beta$			1.35 m	1.38 m
16 $\alpha$	35.5	35.6	1.46 m	1.48 m
16 $\beta$			1.35 m	1.38 m
17	42.9	43.0	-	-
18	47.9	48.0	1.37 m	1.39 m
19	48.2	48.3	2.37 dd 11.0, 5.5	2.33 dt 11.1, 5.6
20	150.9	150.9	-	-
21 $\alpha$	29.7	29.9	1.70 m	1.82 m
21 $\beta$			1.92 m	1.93 m
22 $\alpha$	39.9	40.0	1.36 m	1.38 m
22 $\beta$			1.19 m	1.20 m
23	27.8	28.0	0.85 s	0.82 s
24	16.4	16.5	0.84 s	0.82 s
25	16.1	16.2	0.83 s	0.82 s
26	15.8	16.0	1.02 s	1.00 s
27	14.4	14.5	0.95 s	0.91 s
28	17.9	18.0	0.78 s	0.81 s
29A	109.2	109.4	4.68 d 2.3	4.69 s
29B			4.56 m	4.57 s
30	19.2	19.3	1.68 s	1.68 s
1'	170.9	171.3	-	-
2'	21.2	21.7	2.04 s	2.04 s

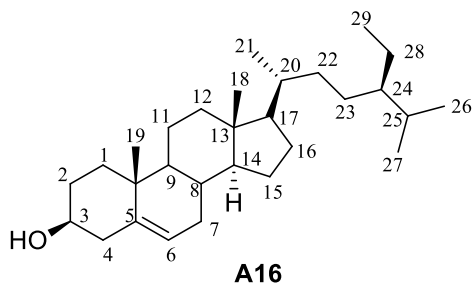
\*(Jamila *et al.*, 2014)

#### 4.4.1.1.4. A7 - 3 $\beta$ -hydroxylup-20(29)-ene (lupeol)



Lupeol (compound **A7**) was isolated from the hexane soluble extract of the leaf of *C. macrostachyus* as a white solid and was found to be the common lupeol. Furthermore, the  $^1\text{H}$  NMR and  $^{13}\text{C}$  NMR spectra for compound **A7** were the same as those of compound **E19** previously isolated from *C. megalocarpus*. Therefore, the structural elucidation description of this compound was the same as that of compound **E19**, which was also isolated from *C. megalocarpus*. The  $^1\text{H}$  NMR,  $^{13}\text{C}$  NMR, DEPT, HSQCDEPT, HMBC, COSY and NOESY spectra of A17 are depicted in **Appendix 91-97**.

#### 4.4.1.1.5. A16: Sitosterol



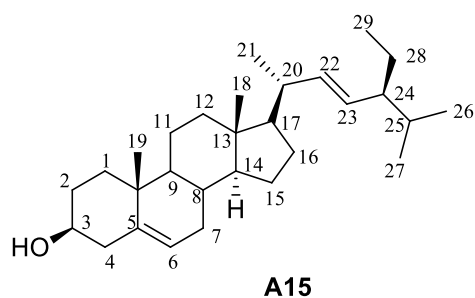
Sitosterol (compound **A16**) was isolated from the hexane soluble extract of the leaf of *C. macrostachyus* as a white solid and was identified as the known phytosterol sitosterol. The  $^1\text{H}$  NMR spectrum (**Appendix 98**) displayed proton resonances at  $\delta = 5.35$  (m), assigned to H-6. The oxymethine proton resonance at 3.52 m was assigned as H-3. The  $^{13}\text{C}$  NMR data of compound **A16** were compared to those reported by Xin Zhang *et al.*, (2006) for sitosterol and were identical. Compound **A16** was therefore identified as the widely known sitosterol (**Table 4.4-18**).

Table 4.4-18: NMR data for Sitosterol (A16) in CDCl<sub>3</sub>

No.	<sup>13</sup> C NMR	<sup>13</sup> C NMR*	<sup>1</sup> H NMR	<sup>1</sup> H NMR*
1 $\alpha$	37.3	37.5	1.85	-
1 $\beta$			1.09	-
2 $\alpha$	31.7	31.9	1.84 m	-
2 $\beta$			1.89 m	-
3	71.8	72.0	3.55 m	3.52 m
4 $\alpha$	42.3	42.5	2.25 m	-
4 $\beta$			2.29 m	-
5	140.8	140.9	-	-
6	121.8	121.9	5.37 d, <i>J</i> =5.5	5.35 d, <i>J</i> =4.9
7 $\alpha$	32.0	32.1	1.98 m	-
7 $\beta$			1.48 m	-
8	31.5	31.9	1.46 m	-
9	50.3	50.4	0.92 m	-
10	36.5	36.7	-	-
11 $\alpha$	21.1	21.3	1.48 m	-
11 $\beta$			1.38 m	-
12 $\alpha$	39.8	40.0	1.98 m	-
12 $\beta$			1.15 m	-
13	40.1	40.1	-	-
14	56.8	57.0	0.99 m	-
15 $\alpha$	24.3	24.5	1.59 m	-
15 $\beta$			1.07 m	-
16 $\alpha$	28.4	28.5	1.85 m	-
16 $\beta$	28.4	28.5	1.24 m	-
17	56.1	56.3	1.10 m	-
18	12.0	12.0	0.70 s	0.68 s
19	19.4	19.3	1.03 s	1.01 s
20	36.2	36.4	1.35 m	-
21	19.0	19.0	0.95 d, <i>J</i> =6.5	0.92 s
22 $\alpha$	33.8	34.1	1.33 m	-
22 $\beta$			1.02 m	-
23 $\alpha$	26.1	26.4	1.18 m	-
23 $\beta$			1.14 m	-
24	45.8	46.1	0.92 m	-
25	28.4	28.5	1.66 m	-
26	18.8	19.2	0.87 m	0.81 d, <i>J</i> =6.1
27	19.9	19.6	0.88 m	0.83 d, <i>J</i> =6.6
28 $\alpha$	23.4	23.3	1.27 m	-
28 $\beta$			1.22 m	-
29	11.9	12.4	0.85 t, <i>J</i> =7.1	0.84 t, <i>J</i> =7.4

\*(Xin Zhang *et al.*, 2006)

#### 4.4.1.1.6. A15: Stigmasterol



Stigmasterol (compound **A15**) was isolated from the hexane soluble extract of the leaf of *C. macrostachys* as a white solid and was identified as the known phytosterol stigmasterol. The  $^1\text{H}$  NMR spectrum (**Appendix 98**) displayed proton resonances at 5.13 (dd,  $J = 8.5, 15.2$  Hz), 4.99 (dd,  $J = 8.5, 15.2$  Hz), 5.32 (d,  $J = 5.0$  Hz) for double bond proton resonances. An oxymethine proton resonance at  $\delta$  3.49 (m) was also observed for compound **A15**. The  $^{13}\text{C}$  NMR spectrum for compound **A15** showed 29 carbon resonances, which were comparable to those reported by De-Eknamkul & Potduang, (2003) for stigmasterol (**Table 4.4-19**). Compound **A15** was therefore identified as the known stigmasterol, which is very common in the Plant Kingdom.

Table 4.4-19: NMR data for Stigmasterol (A15) in  $\text{CDCl}_3$

No	$^{13}\text{C}$ NMR	$^{13}\text{C}$ NMR*	$^1\text{H}$ NMR	$^1\text{H}$ NMR*
1 $\alpha$	37.2	37.7	1.07 dd, $J = 13.2$	-
1 $\beta$			1.85 d, $J = 13.2$	-
2 $\alpha$	31.6	32.1	1.81 m	-
2 $\beta$			1.49 m	-
3	71.8	72.0	3.51 m	-
4 $\alpha$	42.3	42.7	2.26 d, $J = 13.2$	-
4 $\beta$				-
5	140.7	140.8	-	-
6	121.7	121.8	5.34 d, $J = 5.4$	5.35 m
7 $\alpha$	31.9	32.3	1.99 m	-
7 $\beta$			1.98 m	-
8	31.6	32.2	1.48 m	-
9	50.1	50.9	0.92 m	-
10	36.5	36.9	-	-
11 $\alpha$	21.1	21.5	1.54 m	-
11 $\beta$			1.53 m	-
12 $\alpha$	40.5	40.1	1.98 m	-
12 $\beta$			1.15 m	-
13	42.2	42.6	-	-
14	56.8	57.3	0.99 m	-



15 $\alpha$	24.3	24.7	1.54 m	-
15 $\beta$			1.07 m	-
16 $\alpha$	29.3	29.4	1.71 m	-
16 $\beta$			1.24 m	-
17	56.1	56.4	1.15 m	-
18	12.2	12.2	0.69 m	0.70 s
19	19.7	19.6	1.01 m	1.01 s
20	40.5	40.9	2.07 m	-
21	21.2	21.4	1.07 d, $J=6.6$	1.02 d, $J=6.6$
22	138.3	138.8	5.17 d, $J=15.8$	5.16 dd, $J=15.4$ , 8.4
23	129.2	129.6	5.04 d, $J=15.0$	5.02 dd, $J=15.4$ , 8.8
24	51.2	51.7	1.56 m	-
25	33.9	32.3	1.48 m	-
26	19.3	19.2	0.81 m	0.85 d, $J=6.6$
27	21.1	21.3	0.83 m	0.80 d, $J=6.6$
28 $\alpha$	25.4	25.8	1.43 m	-
28 $\beta$			-	-
29	12.0	12.5	0.80 t, $J=7.2$	0.80 t, $J=7.7$

\*(Blunt & Stothers, 1977)

#### 4.4.1.2. Cytotoxicity and anti-HIV activity of pure compounds isolated from *C. macrostachyus*

The cytotoxic and antiviral activity findings for the pure compounds isolated from *C. macrostachyus* and the control drugs are summarized in **Table 4.4-20**. Among the three isolated compounds from *C. macrostachyus*, A4b (lupenone) displayed the highest CC<sub>50</sub> value of  $32.46 \pm 0.7 \mu\text{g/mL}$  (**Table 4.4-20**). Furthermore, a comparison between A4b, A11, and A19 and the control drugs showed that all three compounds had significantly ( $p < 0.001$ ) higher CC<sub>50</sub> values than AZT, ABC, and NVP, which indicates their safety and that high concentration levels are required to exert cytotoxic effects (**Figure 4.4-10**). In addition, the maximum cytotoxic effect ( $E_{\text{max}_c}$ ) of the compounds was not significantly different from the cytotoxic effect of AZT and NVP.

Betulin (E19) observed the highest anti-HIV activity, which inhibited virus-induced CPE by 76% with an IC<sub>50</sub> value of  $0.002 \pm 0.04 \mu\text{g/mL}$ , which is much lower than the maximum nontoxic concentration (MNTC), which also indicates the safety and efficacy of the compound. Furthermore, all three compounds displayed anti-HIV activity at significantly ( $p < 0.05$ ) lower IC<sub>50</sub> values than TDF and NVP (**Figure 4.4-11**), indicating their higher potency.

In addition, the three compounds displayed significantly ( $p < 0.05$ ) higher inhibition of viral-induced CPE ( $E_{\text{max}_{\text{AV}}}$ ) than ABC. The antiviral activity of the tested compounds

( $E_{max_{AV}}$ ) showed that both the control drugs (except ABC) and the tested compounds had approximately similar antiviral efficacy, as they showed non-significantly different  $E_{max_{AV}}$  values (**Figure 4.4-11**). Furthermore, the results showed that the tested compounds had a higher selectivity index, indicating their efficacy at lower cytotoxic effects. As depicted in **Figure 4.4-12**, the pure compounds (A4b, A11, and A19) displayed concentration-dependent inhibition of virus-induced CPE, as the % CPE inhibition increased with increasing concentrations of the pure compounds.

Our finding on the anti-HIV activity of these pure compounds is in agreement with previous reports. A report by Chaniad *et al.*, (2019) explained the efficacy of betulin (E19) as a potent anti-HIV compound with an  $IC_{50}$  value of  $17.7 \pm 0.6 \mu\text{M}$ . Similarly, Esposito *et al.*, (2017) reported that lupeol acetate and lupeol inhibited HIV-1 RT-associated RNase H function with  $IC_{50}$  values of 63 and  $11.6 \mu\text{M}$ , respectively.

Table 4.4-20: Cytotoxicity and anti-HIV activities of pure compounds isolated from *C. macrostachyus*

Materials	Cytotoxicity		Antiviral activity		SI	
	MNTC ( $\mu\text{g/mL}$ )	$CC_{50}$ ( $\mu\text{g/mL}$ )	$E_{max_C}$ (%)	$IC_{50}$ ( $\mu\text{g/mL}$ )		$E_{max_{AV}}$ (%)
<b>AZT</b>	$0.38 \pm 0.19$	$0.53 \pm 0.29$	$36.28 \pm 0.83$	$0.002 \pm 0.00$	$83.5 \pm 0.57$	279.4
<b>TDF</b>	$4.92 \pm 0.71$	$6.73 \pm 0.24$	$13.17 \pm 0.43$	$0.04 \pm 0.01$	$80.55 \pm 0.46$	176.5
<b>ABC</b>	$0.18 \pm 0.03$	$0.26 \pm 0.00$	$17.83 \pm 0.57$	$0.05 \pm 0.031$	$58.67 \pm 0.43$	5.0
<b>NVP</b>	$0.57 \pm 0.0$	$0.82 \pm 0.0$	$39.13 \pm 0.65$	$0.24 \pm 0.09$	$72.53 \pm 0.47$	3.5
<b>A5</b>	$0.002 \pm 0.00$	$0.001 \pm 0.00$	$39.1 \pm 2.22$	$0.25 \pm 0.02$	$53.22 \pm 3.345$	0.0073
<b>A4b</b>	$14.17 \pm 0.94$	$28.83 \pm 0.54$	$38.53 \pm 0.69$	$0.002 \pm 0.001$	$64.74 \pm 0.52$	14084.0
<b>A11</b>	$16.01 \pm 0.64$	$32.46 \pm 0.7$	$55.91 \pm 0.93$	$0.002 \pm 0.00$	$75.8 \pm 0.59$	15097.7
<b>A19</b>	$16.54 \pm 0.35$	$31.74 \pm 0.55$	$55.13 \pm 0.15$	$0.002 \pm 0.04$	$76.17 \pm 0.02$	15551.2
<b>A7</b>	$75.75 \pm 0.74$	$141.8 \pm 0.7$	$70.28 \pm 0.75$	$0.047 \pm 0.02$	$77.01 \pm 0.38$	3048.2
<b>A15</b>	$4.70 \pm 3.43$	$12.38 \pm 10.88$	$43.71 \pm 2.02$	$0.14 \pm 0.04$	$76.77 \pm 23.24$	86.5
<b>A16</b>	$4.41 \pm 0.04$	$5.83 \pm 0.20$	$42.74 \pm 0.09$	$5.58 \pm 0.231$	$84.65 \pm 0.54$	1.0

Results are shown as mean  $\pm$  S.E.M (n=3).

AZT, Zidovudine; TDF, Tenofovir; ABC, Abacavir; NVP, Nevirapine; A5, 2-methoxy benzyl benzoate; A4b, lupenone; A11, lupeol acetate; A19, betulin; A7, lupeol; A16, sitosterol; A15, stigmasterol; MNTC, Maximum nontoxic concentration;  $CC_{50}$ , 50% cytotoxic concentration;  $E_{max_C}$ , Maximum cytotoxic effect %;  $IC_{50}$ , 50% antiviral effect concentrations;  $E_{max_{AV}}$ , maximum antiviral effect %; SI, selective index.

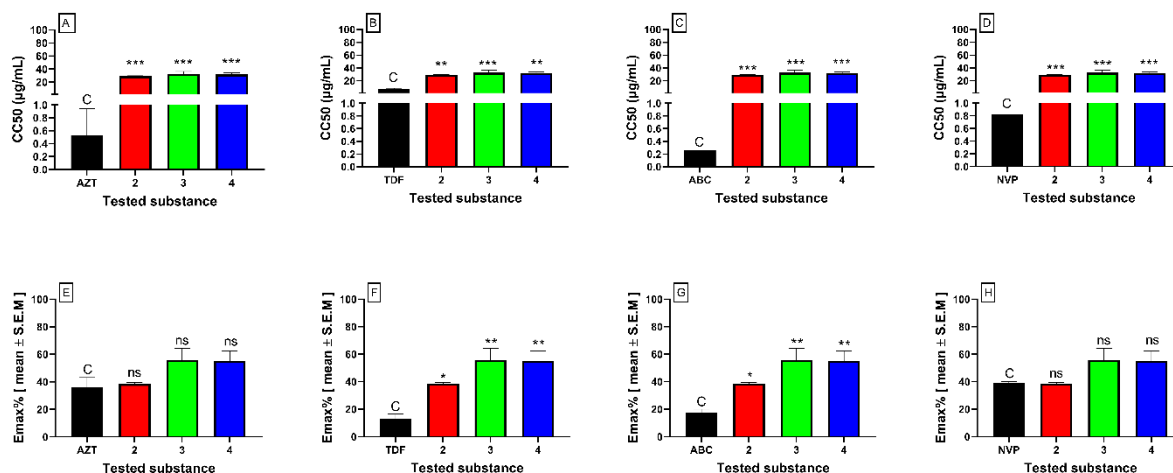


Figure 4.4-10: Cytotoxicity of pure compounds isolated from *C. macrostachyus*

The results are expressed as the mean of three independent experiments  $\pm$  S.E.M. AZT, Zidovudine; TDF, Tenofovir; ABC, Abacavir; NVP, Nevirapine; Lupenone (2); Lupeol acetate (3); Betulin (4); CC50, 50% cytotoxic concentration; Emax<sub>C</sub>, Maximum cytotoxic effect; C; control, ns, not significant, \*Denotes p value < 0.05; \*\*Denotes p value < 0.01, \*\*\*Denotes p value < 0.001.

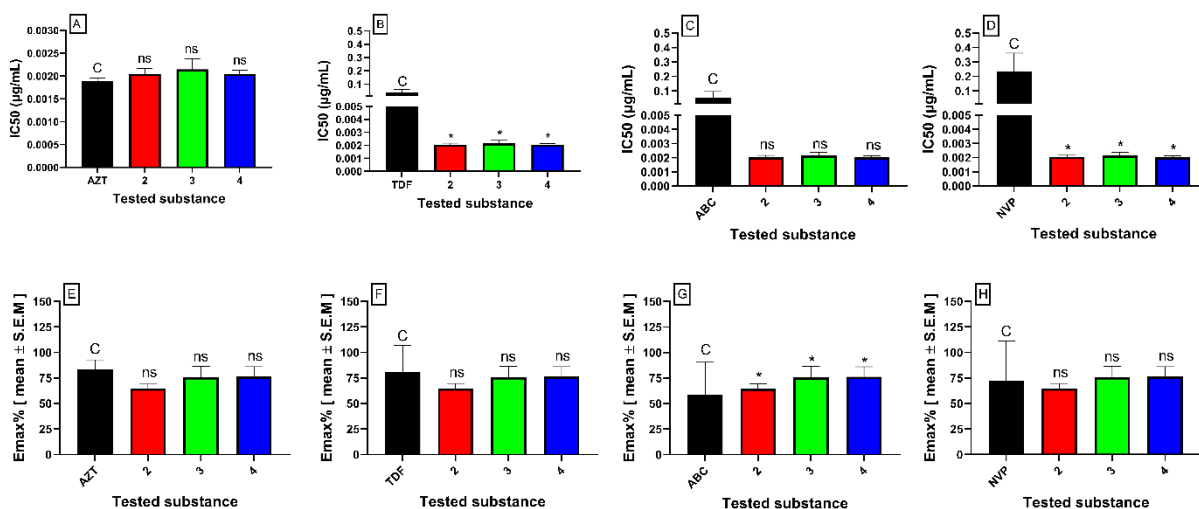


Figure 4.4-11: Anti-HIV activity of pure compounds isolated from *C. macrostachyus*

The results are expressed as the mean of three independent experiments  $\pm$  S.E.M. AZT, Zidovudine; TDF, Tenofovir; ABC, Abacavir; NVP, Nevirapine; Lupenone (2); Lupeol acetate (3); Betulin (4); CC50, 50% cytotoxic concentration; Emax<sub>C</sub>, Maximum cytotoxic effect; C; control, ns, not significant, \*Denotes p value < 0.05; \*\*Denotes p value < 0.01, \*\*\*Denotes p value < 0.001.

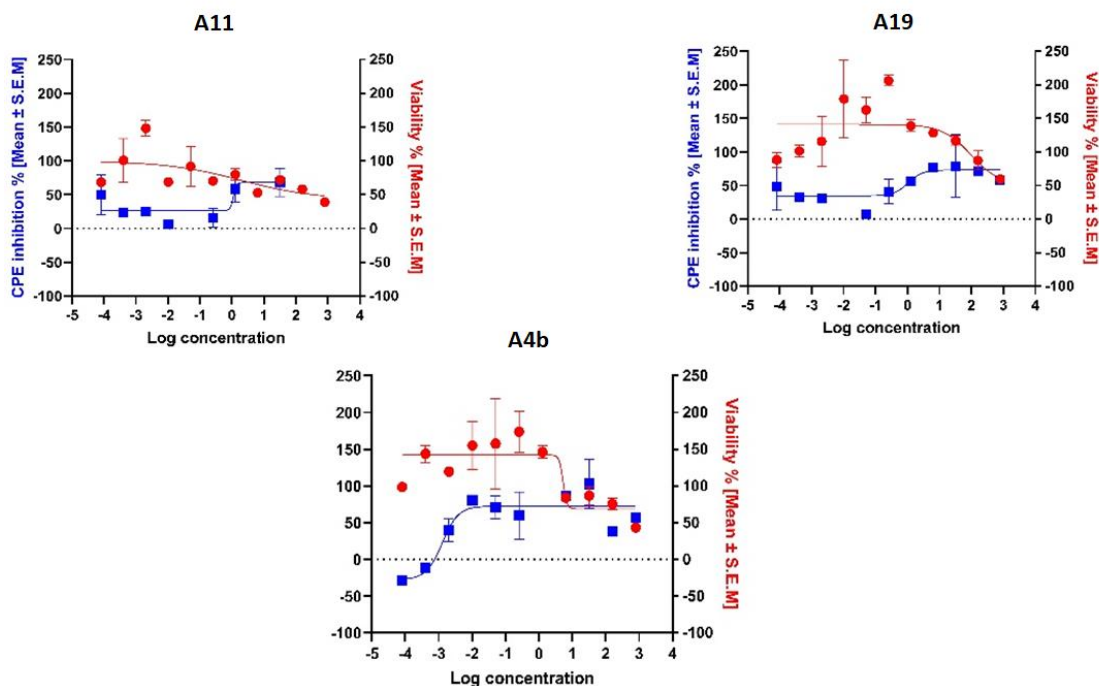


Figure 4.4-12: Concentration-response curve analysis for the anti-HIV activity of pure compounds isolated from *C. macrostachyus*

Results presented in the curves are means  $\pm$  S.E. M of three independent experiments. Cell viability % (red line) and the inhibition % of the virus-induced cytopathic effect (blue line) associated with control drugs and the tested extracts at the concentration level ( $800 - 8.192 \times 10^5$   $\mu\text{g/mL}$ ); A4b, Lupenone; A11, Lupeol acetate; A19, Betulin

#### 4.4.2. *Croton dichogamus*

Based on the findings from the anti-HIV activity of the solvent fractions from *C. dichogamus*, the methanol fraction of the twigs of *C. dichogamus* was subjected to column chromatography to yield six pure compounds (Table 4.4-21). The chemical structure of these compounds is depicted in Figure 4.4-13.

Table 4.4-21: Compounds isolated from the twigs of *C. dichogamus*

Ser. No.	Name	Code
1.	Dihydroconiferyl acetate	CD1a
2.	(4-Hydroxy-3-methoxyphenyl)-propyl benzoate	CD1b
3.	Crotocascarin $\omega$	CD12a
4.	$\beta$ -Oplopanone	CD12b
5.	3 $\beta$ -hydroxylup-20(29)-ene (lupeol)	CD4
6.	Stigmasterol	CD6a
7.	Sitosterol	CD6b

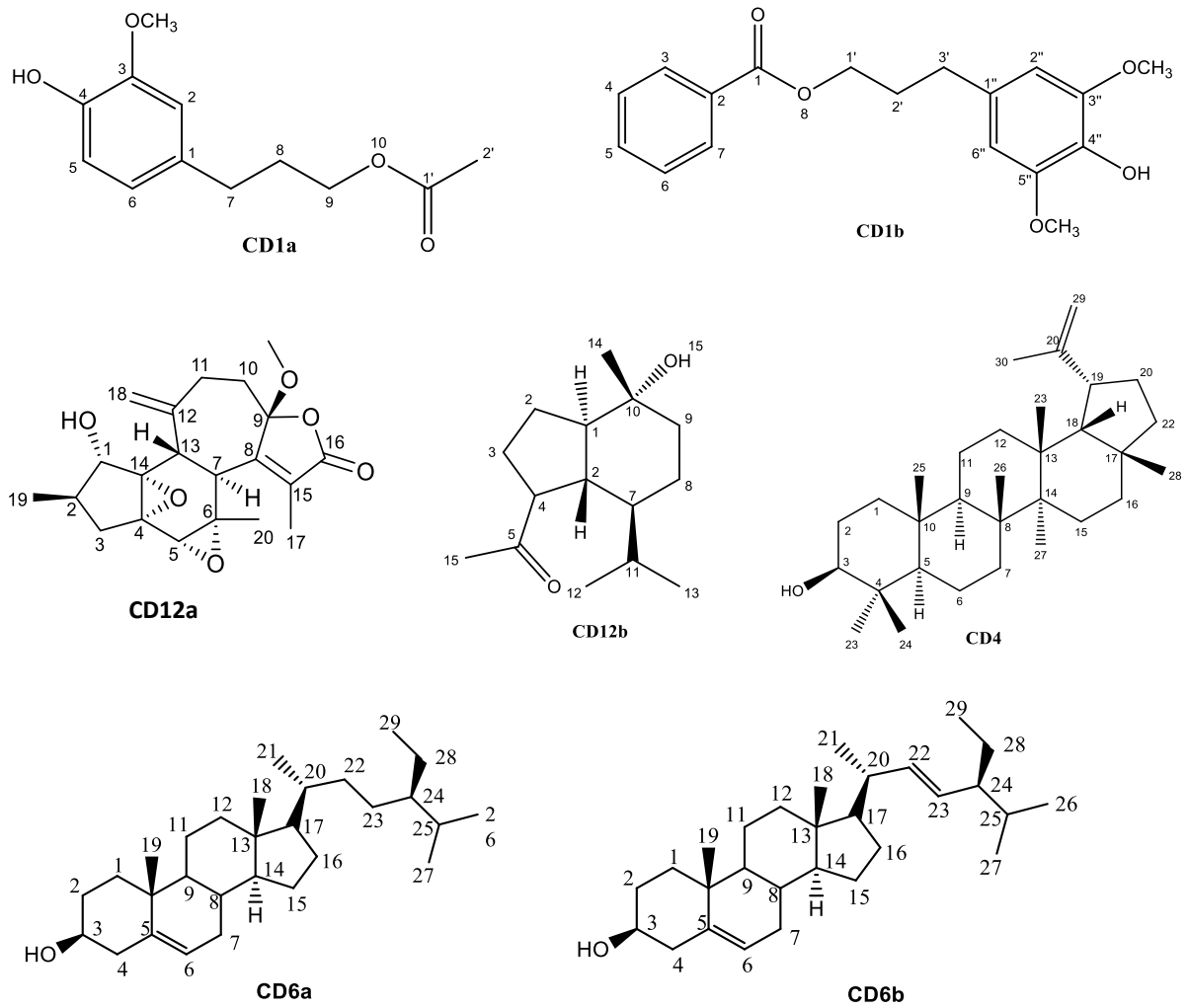
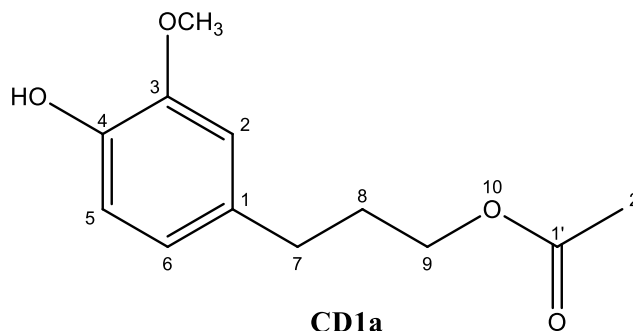


Figure 4.4-13: Pure compounds isolated from *C. dichogamus*

#### 4.4.2.1. Chemistry of compounds isolated from *C. dichogamus*

##### 4.4.2.1.1. CD1a: Dihydroconiferyl acetate



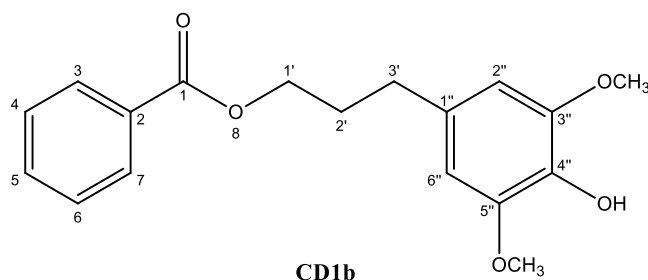
Dihydroconiferyl acetate (compound **CD1a**) was isolated from the methanol extract of the twigs of *C. dichogamus* as a white solid and identified as the known dihydroconiferyl acetate. The  $^1\text{H}$  NMR spectrum (**Table 4.4-22**) showed resonances at 2.73 (m, H-8), 2.63 (m, H-7), 4.34 (t, 6.7, H-9), 3.82 (3H, s, methyl protons of methoxy group), 6.67 (s, H-6), 6.67 (d, 8:9 Hz, H-5), and 6.76 (d, 8,9, H-2) (**Appendix 99**). The  $^{13}\text{C}$  NMR spectrum (**Appendix 100-105**) showed resonances at 31.5 (C-7), 31.5 (C-8), 56.0 (methyl carbon of methoxy group), 64.5 (C-9), 111.1 (C-2), 115.5 (C-5), 121.1 (C-6), 133.13 (C-1), 144.4 (C-4), and 146.6 (C-3). This is the first report of the isolation of dihydroconiferyl acetate from *C. dichogamus*.

Table 4.4-22: NMR data for dihydroconiferyl acetate (CD1a) in  $\text{CDCl}_3$

No.	$^{13}\text{C}$ NMR	$^{13}\text{C}$ NMR*	$^1\text{H}$ NMR	$^1\text{H}$ NMR*
1	133.3	134.1	-	-
2	111.1	113.1	6.67 s	6.75 d 1.7
3	146.6	148.9	-	-
4	144.0	145.7	-	-
5	115.5	116.1	6.76 d 8.9	6.69 d 8.0
6	121.1	121.8	6.67 d 8.9	6.60 dd 1.7, 8.0
7	32.0	32.6	2.63 m	2.59 t 7.6
8	31.5	31.7	2.73 m	1.90 ttd 6.5, 7.6, 14.9
9	64.5	65.0	4.34 t 6.7	4.04 t 6.5
1'	171.5	173.1	-	-
2'	21.2	20.8	-	2.02, s
$\text{OCH}_3$	56.0	56.3	3.82 s	3.82 s

\*(Kondo *et al.*, 2007)

#### 4.4.2.1.2. CD1b: (4-Hydroxy-3-methoxyphenyl)-propyl benzoate



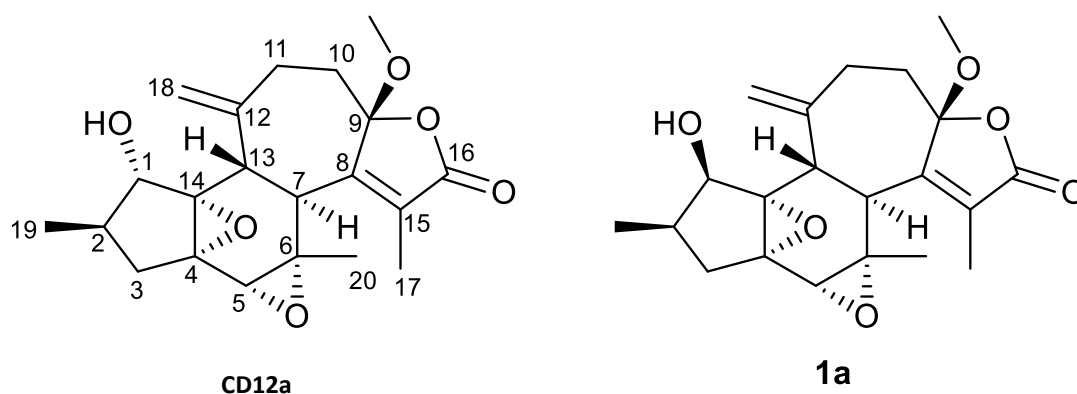
(4-Hydroxy-3-methoxyphenyl)-propyl benzoate (compound **CD1b**) was isolated from the methanol extract of the twigs of *C. dichogamus* as a white solid and identified as the known 3'-(4''-hydroxy-3'',5''-dimethoxyphenyl)-propyl benzoate. The  $^1\text{H}$  NMR spectral data (**Table 4.4-23**) showed the presence of two benzene rings. The  $^1\text{H}$  NMR spectral data (**Appendix 99**) showed three methylene groups due to resonances at 4.10, 2.71 and 2.05 bridging between benzoate and aromatic rings and two methoxyls at d 3.87 (each 3H, s) groups on the aromatic ring. The  $^{13}\text{C}$  NMR spectrum (**Appendix 100-105**) showed the signal of carbonyl ester at d 166.9. All data are consistent with the structure of 3'-(4''-hydroxy-3'',5''-dimethoxyphenyl)-propyl benzoate. This is the first report of the isolation of compound **CD1b** from *C. dichogamus*.

Table 4.4-23: NMR data for (4-Hydroxy-3-methoxyphenyl)-propyl benzoate (CD1b) in  $\text{CDCl}_3$

No.	$^{13}\text{C}$ NMR	$^{13}\text{C}$ NMR*	$^1\text{H}$ NMR	$^1\text{H}$ NMR*
1	166.9	166.8	-	-
2	130.5	130.3	-	-
3	129.6	129.5	8.04 dd 8.4, 1.4	8.04 dd 8.6, 1.1
4	128.5	128.4	7.44 t 7.3	7.45 tt 7.5, 1.6
5	133.1	132.9	7.55 t	7.57 tt 7.5, 1.1
6	128.5	128.4	7.44 t	7.45 tt 7.5, 1.6
7	129.6	129.5	8.04 dd 8.4, 1.4	8.04 dd 8.6, 1.1
1'	64.1	64.3	4.10 t 6.7	4.33 t, 6.5
2'	30.7	30.5	2.05 m	2.07 m
3'	31.5	31.3	2.71 t	2.72 br t
1''	133.1	133.2	-	-
2''	129.5	129.5	7.08 d 8.9	7.08 d 8.4
3''	114.5	115.3	6.83 d 8.9	6.77 d 8.4
4''	154.3	153.9	-	-
5''	114.5	115.3	6.83 d 8.9	6.77 d 8.4
6''	129.7	129.5	7.08 d 8.9	7.08 d 8.4
4''-OH	-	-		5.15 br s
3''-OCH <sub>3</sub>			3.87	
5''-OCH <sub>3</sub>			3.87	

\*(Athikomkulchai *et al.*, 2006)

#### 4.4.2.1.3. CD12a: Crotoascarin $\omega$



Crotoascarin  $\omega$  (compound **CD12a**) was isolated from the methanol-soluble fraction of a 1:1  $\text{CH}_2\text{Cl}_2$ : $\text{CH}_3\text{OH}$  extract of twigs of *C. dichogamus* and identified as an undescribed epimer of the known crotoascarin M (**1a**) previously isolated from *Croton cascarilloides* (Figure 1). Therefore, the compound was assigned as crotoascarin  $\omega$ . Compound (**CD12a**) has a molecular formula of  $\text{C}_{21}\text{H}_{26}\text{O}_6$ , with nine degrees of unsaturation, as determined from (+)-HRESIMS analysis, which displayed an ion peak at  $m/z$  375.1799  $[\text{M}+\text{H}]^+$  (calcd for  $\text{C}_{21}\text{H}_{26}\text{O}_6 + \text{H}$ ,  $m/z$  375.1807). The IR spectrum exhibited the presence of an  $\alpha,\beta$ -unsaturated lactone ( $1733\text{ cm}^{-1}$ ) and hydroxy groups ( $3429\text{ cm}^{-1}$ ). The  $^1\text{H}$ -NMR spectrum (Table 4.4-24) showed four methyl resonances, including a doublet resonance, downfield resonances for the methyls of a methoxy, and an acetoxy and an allylic methyl resonance, a hemiketal resonance, five oxygenated methine resonances, and exocyclic methylene proton resonances. In contrast, the  $^{13}\text{C}$  NMR spectrum showed 21 carbon resonances, including a hemiketal carbon resonance at 109.6 (Appendix 106-111). The use of HMBC and COSY showed that compound **CD12a** was an isomer of the known crotoascarin M (Kawakami *et al.* 2016) (Figure 4.4-14), with differences in the  $^{13}\text{C}$  NMR chemical shifts for C-1 (75.7 for compound **CD12a** and 73.7 for crotoascarin M), C-3 (33.3 for compound **1** and 36.3 for crotoascarin M), C-4 (62.9 for compound **CD12a** and 60.3 for crotoascarin M), C-5 (56.2.7 for compound **1** and 58.2 for crotoascarin M), C-6 (63.3 for compound **CD12a** and 56.6 for crotoascarin M), C-11 (33.1 for compound **CD12a** and 34.9 for crotoascarin M), C-12 (145.8 for compound **CD12a** and 147.7 for crotoascarin M), (45.8 for compound **CD12a** and 39.5 for crotoascarin M) and C-14 (73.3 for compound **CD12a** and 70.7 for crotoascarin M). In addition,  $^1\text{H}$  NMR showed differences for H-5, H-7, 2H-10, 2H-11, H-3, 3H-17, 2H-18, 3H-19, and 1-OH between compound **CD12a** and crotoascarin M. The NOESY spectrum showed that H-1, H-5, H-13,



9-OCH<sub>3</sub>, 3H-19, and 3H-20 were on one face, whereas 1-OH and H-7 were on the other face (**Figure 2**). The data described above supported the assignment of **CD12a** as a 1 $\alpha$ -hydroxy derivative of the known crotoascarin M (**1a**) named crotoascarin  $\omega$  (Kawakami *et al.* 2016; Kawakami *et al.* 2015).

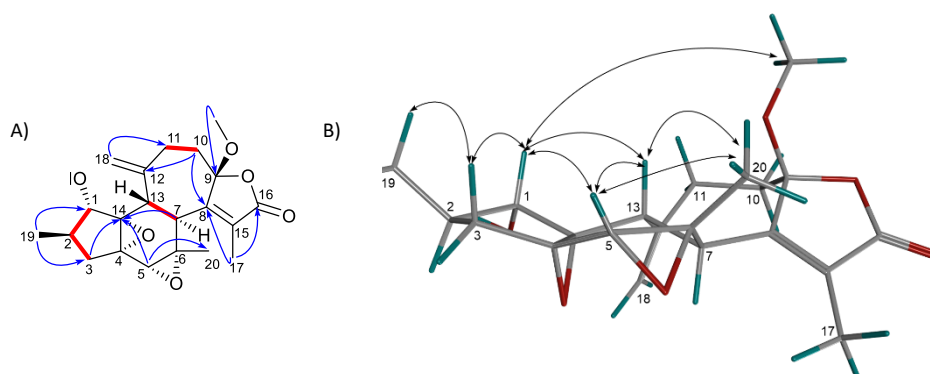


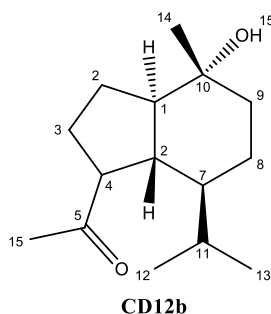
Figure 4.4-14: (A): Key COSY (red bold bonds) and HMBC (blue arrows) correlations for compound **CD12a** (B): Key NOESY (double headed arrows) correlations observed for compound **CD12a**

Table 4.4-24: NMR table for Crotoascarin  $\omega$  (CD12a)

No.	$^{13}\text{C}$ NMR	$^{13}\text{C}$ NMR*	$^1\text{H}$ NMR	$^1\text{H}$ NMR*	HMBC	COSY	NOESY
1	75.7	73.7	4.16 dd 4.6 4.6	4.19 dd 5, 5	4	2,1-OH	1-OH,9-OCH <sub>3</sub>
2	33.5	33.6	1.95 m	2.05 m	X	1,3 $\alpha$ , 3 $\beta$	19
3 $\alpha$	33.3	36.3	2.18 dd 11.5, 6.1	2.41 dd 14, 7	1,3,14	1,3 $\beta$	1,3 $\beta$
3 $\beta$			1.68 dd 11.5, 13.7	1.65 dd 14, 10	X	1,3 $\alpha$	1,3 $\alpha$
4	63.3	60.3	-	-	-	-	-
5	56.2	58.2	3.15 d 0.6	3.10 s	6, 14, 20	20	1,19
6	62.9	56.6	-	-	-	-	-
7	45.8	44.1	2.96 dd 1.4, 12.6	2.97 dq 13, 1	7,8,14	13,17	1,5,20
8	159.4	159.7	-	-	-	-	-
9	109.6	109.7	-	-	-	-	-
10 $\alpha$	35.8	35.8	2.65 m	2.81 ddd 14,7, 7	8,9	10 $\beta$ ,11 $\alpha$ ,11 $\beta$	10 $\beta$ ,11 $\alpha$ ,11 $\beta$
10 $\beta$			1.61	1.37 ddd 14, 14, 4	12	10 $\alpha$ ,11 $\alpha$ ,11 $\beta$	10 $\alpha$ , ,11 $\alpha$ ,11 $\beta$
11 $\alpha$	33.1	34.9	2.33 m	2.45 ddd 14, 4, 4	11	10 $\alpha$ ,10 $\beta$ ,11 $\beta$	10 $\alpha$ ,10 $\beta$ ,11 $\beta$
11 $\beta$			2.27 m	2.15 ddd 14, 14, 4	2	10 $\alpha$ ,10 $\beta$ ,11 $\alpha$	10 $\alpha$ ,10 $\beta$ ,11 $\alpha$
12	145.8	147.7	-	-	-	-	-
13	44.5	39.5	2.91 d 12.6	3.26 d 13	7	7	1,9-OCH <sub>3</sub>
14	73.3	70.7	-	-	-	-	-
15	129.0	129.8	-	-	-	-	-
16	171.1	170.9	-	-	-	-	-
17	10.1	9.6	1.94 d 1.3	1.89 d 1.3	8,15,16	7	x
18A	114.6	114.6	5.28 br s	5.07 s	2, 11	18B	1
B			5.16 br s	5.05 br s	2, 11	18A	11 $\alpha$ ,11 $\beta$
19	12.2	12.2	0.98 d 7.1	1.03 d 7.0	1,5	1	5,20
20	20.1	20.3	1.16 s	1.12 s	5,6,13	5	1-OH,19
9-OCH <sub>3</sub>	51.9	51.6	3.40 s	3.43 br s	9	-	1
1-OH			1.29 d 4.9	1.47 d 5	14	1	1,19

\*(Kawakami *et al.*, 2016)

#### 4.4.2.1.4. CD12b: $\beta$ -Oplopanone



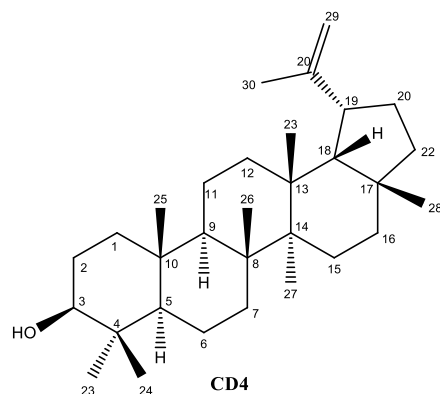
$\beta$ -Oplopanone (compound **CD12b**) was isolated from the methanol extract of the twigs of *C. dichogamus*. The  $^1\text{H}$  NMR spectrum (**Appendix 112**) of compound **CD12b** showed four methyl group resonances, including downfield resonances of 2.19 (s), 1.20 (s), 0.90 d (6.9) and 0.68 d (6.9), four methine resonances, and four methylene resonances. The  $^{13}\text{C}$  NMR spectrum (**Appendix 113**) showed 15 carbon resonances, including one ketone carbon resonance at 211.1. The  $^1\text{H}$  and  $^{13}\text{C}$  NMR data were consistent with those of the known  $\beta$ -oplopanone previously isolated from *Magnolia fargesii* (**Table 4.4-25**) (Jung *et al.*, 1997). The DEPT, HSQCDEPT, HMBC, COSY, NOESY of CD12b is depicted in **Appendix 114-118**. This is the first report of the isolation of  $\beta$ -oplopanone from *C. dichogamus*.

Table 4.4-25: NMR table for CD13:  $\beta$ -Oplopanone (CD12b)

No.	$^{13}\text{C}$ NMR	$^{13}\text{C}$ NMR	$^1\text{H}$ NMR*	$^1\text{H}$ NMR*
1	57.3	56.95	1.46 m	1.45 m
2 $\alpha$	25.5	25.27	1.80 m	1.83 m
2 $\beta$			1.41 m	1.42 m
3 $\alpha$	28.9	28.57	1.95 m	1.97 m
3 $\beta$			1.57 m	1.58 m
4	56.0	55.69	2.64 m	2.65 ddd 5.4, 5.7, 10.5
5	211.6	212.3	-	-
6	47.0	46.68	1.80 m	1.82 m
7	49.7	49.37	1.09 m	1.08 m
8 $\alpha$	23.3	22.96	1.59 m	1.60 m
8 $\beta$			1.08 m	1.10 m
9 $\alpha$	42.3	42.2	1.79 m	1.80 m
9 $\beta$			1.37 m	1.38 m
10	73.3	72.96	-	-
11	29.7	29.47	1.46 m	1.45 m
12	22.2	21.90	0.90 d 6.9	0.88 d 7.2
13	15.8	15.8	0.68 d 6.9	0.69 d 7.2
14	20.6	20.26	1.20 s	1.20 s
15	29.8	31.5	2.19 s	2.19 s

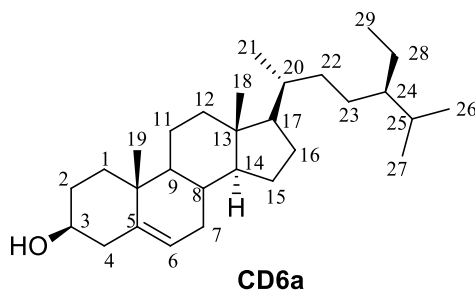
\*(Jung *et al.*, 1997)

#### 4.4.2.1.5. CD4 - Lupeol



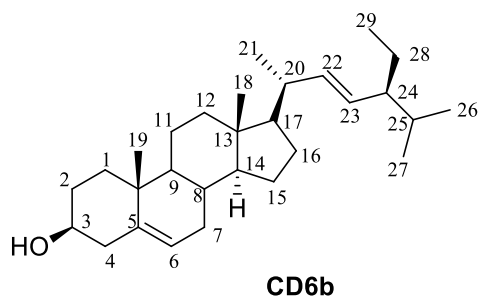
Lupeol (compound **CD4**) was isolated from the methanol soluble extract of the leaf of *C. dichogamus* as a white solid and was found to be the common lupeol. Furthermore, the  $^1\text{H}$  NMR and  $^{13}\text{C}$  NMR spectra for compound **CD4** were the same as those of compound **E19** (**Appendix 119**) and **A7**, isolated from *C. megalocarpus* and *C. macrostachyus*. Therefore, the structural elucidation description of this compound was the same as that of compound **E19** and **A7**.

#### 4.4.2.1.6. CD6a: Sitosterol



Sitosterol (compound **CD6a**) was isolated from the methanol soluble extract of the twigs of *C. dichogamus* as a white solid and was identified as the known phytosterol sitosterol. Furthermore, the  $^1\text{H}$  NMR (**Appendix 120**) and  $^{13}\text{C}$  NMR spectra for compound **CD6a** were the same as those of compound **A16** (**Appendix 98**) previously isolated from *C. macrostachyus*. Therefore, the structural elucidation description of this compound was the same as that of compound **A16**, which was also isolated from *C. macrostachyus*.

#### 4.4.2.1.7. CD6b: Stigmasterol



Stigmasterol (compound **CD6b**) was isolated from the methanol soluble extract of the twigs of *C. dichogamus* as a white solid and was identified as the known phytosterol stigmasterol. Furthermore, the  $^1\text{H}$  NMR (**Appendix 120**) and  $^{13}\text{C}$  NMR spectra for compound **CD6b** were the same as those of compound **A15** (**Appendix 98**) previously isolated from *C. macrostachyus*. Therefore, the structural elucidation description of this compound was the same as that of compound **A15**, which was also isolated from *C. macrostachyus*.

#### 4.4.2.2. Cytotoxicity and anti-HIV activity of pure compounds isolated from *C. dichogamus*

The cytotoxic and antiviral activity findings for the compounds isolated from *C. dichogamus* and the control drugs are summarized in **Table 4.4-26**. Comparison between CD12a and CD12b, and the control drugs regarding the cytotoxic effect showed that both compounds had significantly ( $p < 0.01$ ) higher maximum cytotoxic effect ( $E_{\text{max}_c}$ ) when compared with the control drugs TDF and ABC. Although the three compounds had a high maximum cytotoxic effect ( $E_{\text{max}_c}$ ), they also had a very high  $\text{CC}_{50}$ , which indicates that high concentration levels are required to exert cytotoxic effects (**Figure 4.4-15**). The antiviral activity of the tested compounds ( $E_{\text{max}_{AV}}$ ) showed that they had approximately similar antiviral efficacy as the control ones since they showed non-significantly different  $E_{\text{max}_{AV}}$  values. As depicted in **Figure 4.4-16**, the  $\text{IC}_{50}$  values of the compounds were not significantly different from those of the control drugs, indicating their comparable potency.

Table 4.4-26: Cytotoxicity and anti-HIV activities of pure compounds isolated from *C. dichogamus*

Materials	Cytotoxicity			Antiviral activity		SI
	MNTC (µg/mL)	CC <sub>50</sub> (µg/mL)	E <sub>max</sub> C (%)	IC <sub>50</sub> (µg/mL)	E <sub>max</sub> AV (%)	
AZT	0.38 ± 0.19	0.53 ± 0.29	36.28 ± 0.83	0.002 ± 0.00	83.5 ± 0.57	279.4
TDF	4.92 ± 0.71	6.73 ± 0.24	13.17 ± 0.43	0.04 ± 0.01	80.55 ± 0.46	176.5
ABC	0.18 ± 0.03	0.26 ± 0.00	17.83 ± 0.57	0.05 ± 0.031	58.67 ± 0.43	5.0
NVP	0.57 ± 0.0	0.82 ± 0.0	39.13 ± 0.65	0.24 ± 0.09	72.53 ± 0.47	3.5
CDM	15.4 ± 0.45	19.58 ± 0.79	42.2 ± 0.62	0.06 ± 0.01	90.83 ± 0.18	318.5
CD1a	46.97 ± 0.52	164.5 ± 0.25	66.54 ± 1.055	0.039 ± 0.01	80.94 ± 0.28	4205.01
CD12a	16.36±0.29	31.46±0.51	55.03±5.11	0.002±0.01	76.19±0.01	15429.1
CD12b	475.4 ± 0.3	138.7 ± 0.35	76.03 ± 0.005	0.168 ± 0.045	68.72 ± 0.05	824.1

Results are shown as means ± S.E.M (n=3)

AZT, Zidovudine; TDF, Tenofovir; ABC, Abacavir; NVP, Nevirapine; CD1a, Dihydroconiferyl acetate; CD12a, Crotonoscarin ω; CD12b, β-Oplopanone; MNTC, Maximum nontoxic concentration; CC<sub>50</sub>, 50% cytotoxic concentration; E<sub>max</sub>C, Maximum cytotoxic effect %; IC<sub>50</sub>, 50% antiviral effect concentrations; E<sub>max</sub>AV, maximum antiviral effect %; SI, selective index.

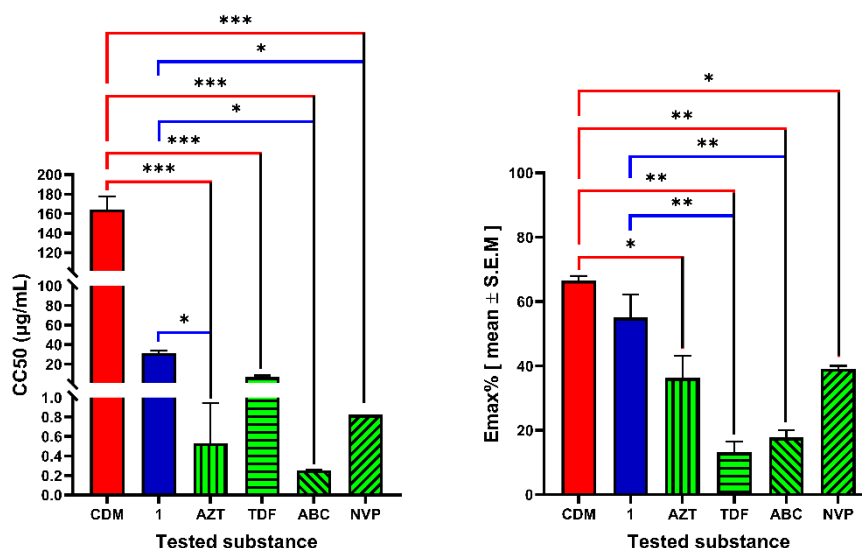


Figure 4.4-15 Cytotoxicity of Crotonoscarin ω (CD12a) (1)

Cytotoxicity of crotonoscarin ω and methanol-soluble extract (CDM) of the 1:1 CH<sub>2</sub>Cl<sub>2</sub>:CH<sub>3</sub>OH extract of the twigs of *C. dichogamus*. \*Denotes p value < 0.05; \*\*Denotes p value < 0.01, \*\*\*Denotes p value < 0.001.

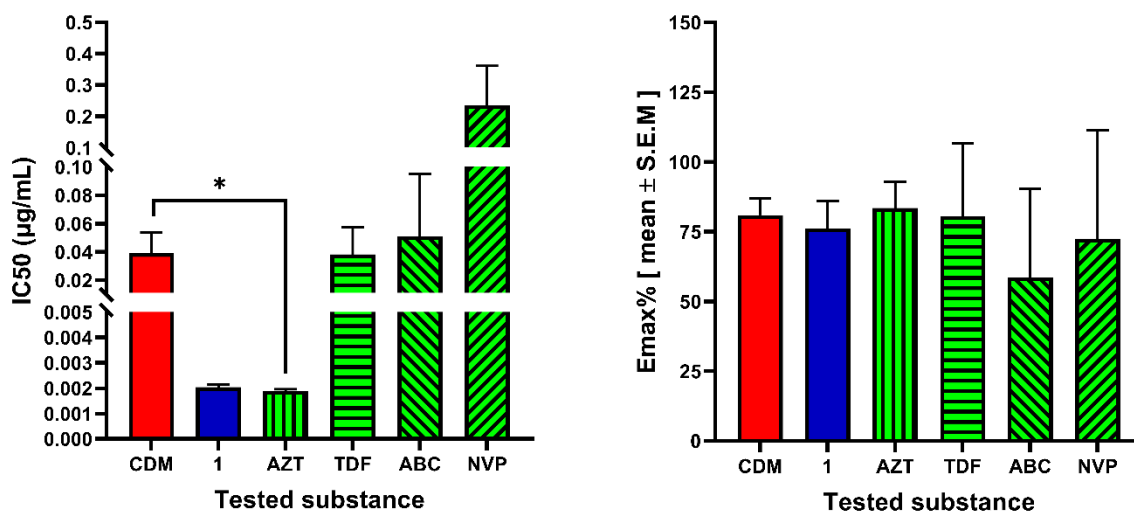


Figure 4.4-16 Anti-HIV activity effects of Crotoascarin  $\omega$  (1)

Anti HIV effect of crotoascarin  $\omega$  and methanol-soluble extract (CDM) of the 1:1 CH<sub>2</sub>Cl<sub>2</sub>:CH<sub>3</sub>OH extract of the twigs of *C. dichogamus*. \*Denotes p value < 0.05.

#### 4.4.2.3. Discussion

To propose a mode-of-action of crotoascarin  $\omega$  (CD12a), *in silico* inhibition modelling assays were carried out using HIV reverse transcriptase and HIV protease. Docking studies were performed on HIV-1 RT in complex with known inhibitor nevirapine (PDB ID 1JLB) as well as HIV-1 PR in complex with known antiviral atazanavir (PDB ID: 3EL9) using MOE2015 software. The predicted free energy of binding obtained for **CD12a** against HIV-1 RT was higher ( $\Delta G$  -1.38 kcal/mol) compared to the known inhibitor nevirapine ( $\Delta G$  -7.60 kcal/mol), due to the lack of the crucial  $\pi$ -H interaction shown by Nevirapine. The main interaction contributing to the binding was the hydrogen bond between hydroxy group at C-1 and Cys181 (**Figure 4.4-17**). For HIV-PR, the predicted free energy of binding exhibited by compound 1 was  $\Delta G$  -6.25 kcal/mol, which was also higher compared to the positive control atazanavir ( $\Delta G$  -11.49 kcal/mol). The main interaction contributing to the binding was the hydrogen bonding between one of the epoxide oxygens and the backbone N-H of Asp29(B). Asp29(B) also shows a key hydrogen bonding interaction with one of the amide carbonyls of Atazanavir (**Figure 4.4-18**). With these results it can be hypothesized that the potential anti-HIV activity of crotoascarin  $\omega$  could be caused by HIV-1 PR inhibition.

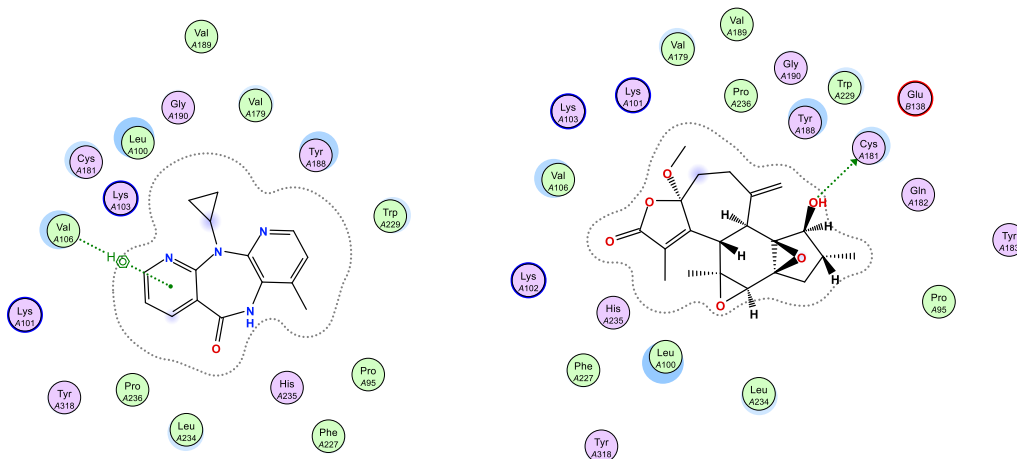


Figure 4.4-17. Ligand-protein interaction of Nevirapine and crotoascarin  $\omega$  (CD12a) with HIV-1 RT (PDB ID: 1JLB)

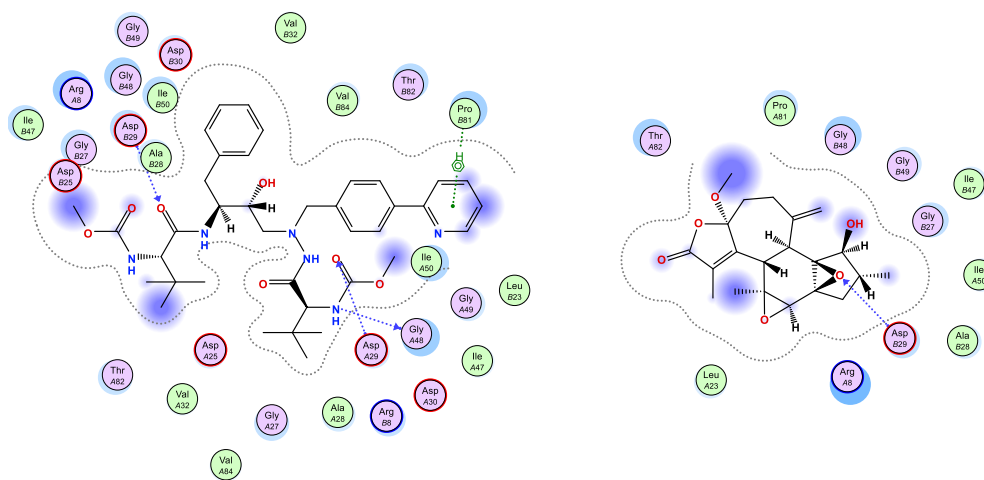


Figure 4.4-18. Ligand-protein interactions of atazanavir and crotoascarin  $\omega$  (CD12a) with HIV-1 PR (PDB ID: 3EL9)



#### 4.5. Investigation of the *in vitro* and *in silico* interaction of the isolated compounds against HIV enzymes

##### 4.5.1. *In vitro* assays on the effect of pure compounds on retroviral enzymes

To investigate the mode of action of the pure compounds, cell-free enzyme inhibition assays were carried out using HIV reverse transcriptase and HIV protease kit (*Ab211106 HIV-1 Protease Inhibitor Screening Kit (Fluorometric)*, 2020) as described previously (Rotich *et al.*, 2021). At 10  $\mu\text{g/mL}$ , none of the compounds inhibited reverse transcriptase activity; however, at the same concentration, compounds isolated from *C. megalocarpus* E22, E12 and E17 inhibited HIV-1 protease by 93.3, 87.2, and 82.4%, respectively (**Table 4.5-1**).

Table 4.5-1 HIV-1 Protease enzyme inhibition activity of compounds isolated from *C. megalocarpus*

Code	Name of compound	Concentration $\mu\text{g/mL}$	% inhibition
E37	Ermiasoid	10	63.3
E5	4H- $\alpha$ ,7H- $\alpha$ ,10 $\alpha$ -eudesm-11-en-5 $\beta$ -ol	10	94.1
E12	5 $\beta$ -hydroxy-8 $\alpha$ -methoxy eudesm-7(11)-en-12,8-olide (ermiasolide A)	10	87.2
E17	5 $\beta$ ,8H- $\beta$ -hydroxy eudesm-7(11)-en-12,8-olide (ermiasolide C)	10	82.4
E22	5 $\beta$ ,8 $\alpha$ -dihydroxy eudesm-7(11)-en-12,8-olide (ermiasolide B)	10	93.3
E24	11-acetoxy crotoascarin L	10	81.5
E23	Crotoascarin K	10	75.9
Control (Protease Inhibitor)	Pepstatin	n.d	100.0

##### 4.5.2. *In silico* anti-HIV activity of pure compounds

###### 4.5.2.1. Molecular docking study

A molecular docking study was conducted to predict the binding geometries of the compounds with HIV-1 Reverse Transcriptase and HIV-1 Protease. **Table 4.5-2** and **4.5-3** summarize the docking results for these compounds and FDA-approved antiretroviral drugs. The predicted free energy of binding obtained for the pure compounds against HIV-1 RT (PDB ID: 1JLB) was higher than the known inhibitor nevirapine ( $\Delta G$  -7.679 kcal/mol). Similarly, the compounds analyzed also gave higher predicted binding energies than the known inhibitor Atazanavir when the docking was performed on HIV-1 PR (PDB ID: 3EL9). The docked

compounds displayed strong binding affinity with HIV-1 protease enzyme (3EL9) compared with the HIV-1 reverse transcriptase. The results obtained could indicate that the mechanism of action leading to the observed anti-HIV activity is through HIV-1 protease inhibition, which agrees with the results obtained *in vitro*.

Table 4.5-2: Molecular docking analysis of against HIV-1 RT in complex with Nevirapine (PDB ID: 1JLB)

Code	Name of compounds	Free energy of binding ( $\Delta G$ ) kcal/mol
NVP	Nevirapine	-7.679
E17	5 $\beta$ ,8H- $\beta$ -hydroxy eudesm-7(11)-en-12,8-olide (ermiasolide C)	-3.555
E22	5 $\beta$ ,8 $\alpha$ -dihydroxy eudesm-7(11)-en-12,8-olide (ermiasolide B)	-2.839
E12	5 $\beta$ -hydroxy-8 $\alpha$ -methoxy eudesm-7(11)-en-12,8-olide (ermiasolide A)	-2.317
E5	4H- $\alpha$ ,7H- $\alpha$ ,10 $\alpha$ -eudesm-11-en-5 $\beta$ -ol	-1.550
CD12a	Crotocascarin $\omega$	-1.38
E23	Crotocascarin K	-1.297
E2	Pinoresinol	-1.295
E24	11-acetoxy crotocascarin L	0.611
E37	1 $\beta$ -acetoxy-3 $\beta$ -chloro-5 $\alpha$ ,6 $\alpha$ -dihydroxycrotocascarin L (Ermiasoid)	3.378

Table 4.5-3: Molecular docking analysis of against HIV-1 PR in complex with Atazanavir (3EL9)

Code	Name of Comound	Free energy of binding ( $\Delta G$ ) kcal/mol
ATV	Atazanavir	-11.49
E24	11-acetoxy crotocascarin L	-7.985
E37	1 $\beta$ -acetoxy-3 $\beta$ -chloro-5 $\alpha$ ,6 $\alpha$ -dihydroxycrotocascarin L (ermiasoid)	-7.326
E23	Crotocascarin K	-7.115
E2	Pinoresinol	-7.078
CD12a	Crotocascarin $\omega$	-6.25
E12	5 $\beta$ -hydroxy-8 $\alpha$ -methoxy eudesm-7(11)-en-12,8-olide (ermiasolide A)	-6.067
E22	5 $\beta$ ,8 $\alpha$ -dihydroxy eudesm-7(11)-en-12,8-olide (ermiasolide B)	-5.994
E17	5 $\beta$ ,8H- $\beta$ -hydroxy eudesm-7(11)-en-12,8-olide (ermiasolide C)	-5.850
E5	4H- $\alpha$ ,7H- $\alpha$ ,10 $\alpha$ -eudesm-11-en-5 $\beta$ -ol	-5.750

#### 4.5.2.2. Ligand-Protein interaction

To better understand the mode of protease enzyme inhibition of the compounds, ligand-protein interactions were visualized. The interactions of the pure compounds with the HIV-1 protease enzyme demonstrate that the ligands interact with most of the enzyme's active site residues. The residues were discussed in section 2.2.3 and are also summarized in **Table 4.5-4**. Among the intermolecular interactions, hydrophobic, hydrogen, alkyl, pi-sigma, salt bridges, and halogen bonds were involved in ligand-protein interactions (**Table 4.5-5**).

Table 4.5-4: Amino acids in the binding site of HIV-1 protease enzyme

<b>Binding site</b>	<b>Active site residues</b>
Catalytic site	Asp-25, Thr-26, Gly-27
S1 and S1' subsite	Ile-50, Ile-84, Pro-81, Thr-80, Val-82
S2 and S2' subsite	Asp-29, Asp-30, Ala-28, Ile-47, Gly-48, Ile-50
S3 and S3' subsite	Arg-8, Gly-48, Leu-23, Val-82, Thr-80, Pro-81
S4 and S4' subsite	Asp-30, Met-46, Ile-47, Gly-48, Gln-58

Table 4.5-5: Ligand-protein interaction profile for compounds docked with HIV-1 PR (3EL9)

Ser. No.	Name of compound	Hydrophobic interactions	Hydrogen bond Interactions	Pi cation interactions	Salt bridges	Halogen bond
1.	Atazanavir	<b>S1- Ile-50</b> (3.52 Å), <b>Ile-50'</b> (3.72 Å), <b>Pro-81'</b> (3.81 Å) <b>S2- Ala-28'</b> (3.59 Å), <b>Ile-47</b> (3.60 Å), <b>S3- Leu-23</b> (3.64 Å), Thr-82 (3.47 Å), Thr-82' (3.56 Å)	Catalytic site- <b>Asp-25</b> (3.07 Å), <b>Gly-27</b> (2.86 Å) <b>S1- Ile-50</b> (3.88 Å) <b>S2- Asp-29</b> (3.69 Å), <b>Gly-48</b> (3.27 Å) <b>S3- Arg-8</b> (3.72 Å), <b>Arg-8'</b> (3.26 Å),	<b>Arg-8'</b> (3.84 Å)	-	
2.	11-acetoxy crotoascarin L (E24)	<b>S1- Ile-50</b> (3.52 Å), <b>Ile 50</b> (3.78 Å) <b>S2- Asp 30</b> (3.57 Å), <b>Ile-47</b> (3.84 Å), <b>S3- Arg-8'</b> (3.99 Å), <b>Leu-23'</b> (3.77 Å),	-		Arg-8 (3.82 Å)	
3.	Ermiasoid (E37)	<b>S1- Ile-50</b> (3.34 Å), <b>Ile-50</b> (3.71 Å), <b>S3- Leu 23'</b> (3.09 Å), Thr-82' (3.84 Å)	<b>Catalytic site -Gly-27'</b> (3.23 Å), <b>S1- Ile 50</b> (3.45 Å), <b>Ile-50'</b> (3.75 Å) <b>S2- Asp-29'</b> (3.38 Å), <b>Asp-30'</b> (3.04 Å),			Asp 25 (3.23)
4.	Crotocascarin K (E23)	<b>S2- Asp-30'</b> (3.78 Å) <b>S3- Leu-23</b> (3.75 Å), Thr-82 (3.63 Å), Val-84 (3.68 Å)	<b>Catalytic site- Asp-25</b> (2.67 Å), <b>Gly-27'</b> (3.45 Å), <b>S2- Asp-29'</b> (3.16 Å)			
5.	Pinoresinol (E2)	<b>S2- Ala-28'</b> (3.57 Å)	<b>S1- Ile 50</b> (3.29 Å), <b>Ile 50'</b> (4.04 Å) <b>S2-Asp-29</b> (3.68 Å), <b>Asp-29'</b> (3.84 Å), <b>Asp-30</b> (4.01 Å),			
6.	Ermiasolide A (E12)	<b>S1- Ile-50</b> (3.70 Å), <b>Ile-50'</b> (3.66 Å), <b>S2-Ala 28</b> (3.67 Å), Thr-82' (3.81 Å)	Thr-82' (3.62 Å)			
7.	Ermiasolide B (E22)	<b>S1- Ile-50</b> (3.78 Å), <b>Ile-50'</b> (3.84 Å), <b>S2-Ala 28</b> (3.75 Å), Thr-82' (3.95 Å)	<b>Catalytic site - Asp-25</b> (2.82 Å), <b>S1- Ile 50</b> (4.04 Å), Thr-82' (3.55 Å)			
8.	Ermiasolide C (E17)	<b>S1- Ile-50</b> (3.48 Å), Val-84' (3.89 Å),	<b>Catalytic site- Asp-25'</b> (3.09 Å)			
9.	4H- $\alpha$ ,7H- $\alpha$ ,10 $\alpha$ -eudesm-11-en-5 $\beta$ -ol (E5)	<b>S1- Ile-50'</b> (3.51 Å) <b>S2-Ala-28</b> (3.93 Å), Val-32 (3.59 Å),	<b>S1- Ile 50</b> (3.95 Å), <b>Ile 50'</b> (3.68 Å)			

Residues within the active site are colored red.

## 1. Interaction of 11 $\beta$ -acetoxy crotoascarin L (E24) with Protease (PDB ID: 3EL9)

A molecular docking study showed that 11 $\beta$ -acetoxy crotoascarin L forms strong binding to the receptor with an estimated free binding energy of -7.985 kcal/mol making it superior in binding efficiency compared to all docked compounds (**Table 4.5-3**). E24 interacts with key residues in S1, S2, and S3 subsites of the HIV-PR enzyme. E24 forms hydrophobic interactions between E24 and Ile-50 (3.52 Å), Ile 50 (3.78 Å), Asp 30 (3.57 Å), Ile-47 (3.84 Å), Arg-8' (3.99 Å), and Leu-23' (3.77 Å), at the active site of the protease enzyme. Even though E24 is not binding to the catalytic domain of the enzyme, these hydrophobic interactions could interfere with the binding of the viral polypeptide to the active site of the protease by causing conformational change on the enzyme active site and later can cause inhibition of viral replication. Hydrophobic interactions are the main driving force in drug-receptor interactions (Ferreira De Freitas & Schapira, 2017a).

Furthermore, the C-11 acetoxy group forms a salt bridge with Arg-8 (3.82 Å), contributing to ligand binding (Segala *et al.*, 2016). The methyl groups at C-6 and C-15 of E24 were involved in alkyl interactions with Ile-47, Ile-50, and Val-32 (**Figure 4.5-1**). These interactions involve charge transfer and help intercalate the compound in the receptor's binding site (3EL9).

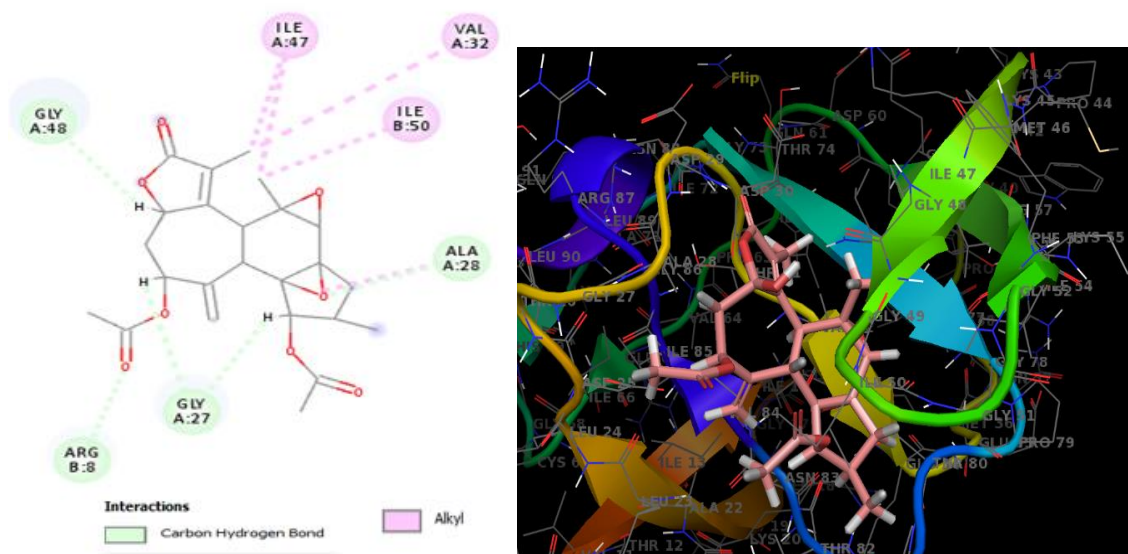


Figure 4.5-1: 2D and 3D visualization of the interaction of 11 $\beta$ -Acetoxy crotoascarin L (E24) with HIV-1 PR (3EL9)

## 2. Interaction of 1 $\beta$ -acetoxy-3 $\beta$ -chloro-5 $\alpha$ ,6 $\alpha$ -dihydroxycrotocascarin L (Ermiasoid) (E37) with protease enzyme (PDB ID: 3EL9)

Ermiasoid (E37) is a mon-chlorinated crotofolane diterpenoid isolated from the bark of *C. megalocarpus*. It has displayed promising anti-HIV activity by inhibiting more than 86 % of HIV-induced cytopathic effects in MT-4 cells at a lower concentration of 28 nM. Even though the compound was not active against the reverse transcriptase enzyme, it has displayed activity against the protease enzyme. Ermiasoid binds well with 3EL9 ligand-binding site with a free binding energy of -7.326 kcal/mol making it the second most active molecule to inhibit protease enzyme (3EL9 (**Table 4.5-3**)).

Ermiasoid (E37) forms three hydrophobic and five hydrogen bond interactions with residues in the active site of the HIV-PR enzyme. Table 4.5-5 shows that hydrophobic interactions were formed with Ile-50, Leu-23, and Thr-82 residues in S1 and S3 subsites. These interactions introduce stabilizing charges responsible for ligand binding efficiency in the receptor's binding site (3EL9). In addition, the hydroxyl groups at C-5 and C-6 contribute to the H-bonding with Gly-27 and Ile-50, respectively. This finding is exciting as compounds with dihydroxy ethylene groups are reported to have protease inhibitor activity (Coop, 2019). The epoxy group of E37 is also involved in the hydrogen bond interactions with Ile-50 and Ile-50' in S1 and S1' subsites, respectively. Similarly, the carbonyl group at C-16 forms hydrogen bonding with the Asp-29' in the S2' sub-site of the enzyme. Ermiasoid forms a halogen bond with Asp-25, key catalytic residue for HIV-PR (**Figure 4.5-2**). Halogen bonds play a key role in membrane permeability, affinity with proteins, metabolic stability of compounds (Ferreira De Freitas & Schapira, 2017b) and also can form specific molecular interactions that contribute to the recognition of ligands by proteins (Scholfield *et al.*, 2013). These interactions interfere binding of the viral polypeptide with the protease enzyme and reduce or inhibit the HIV-PR enzyme's catalytic function, hence contributing to the anti-HIV activity of ermiasoid.

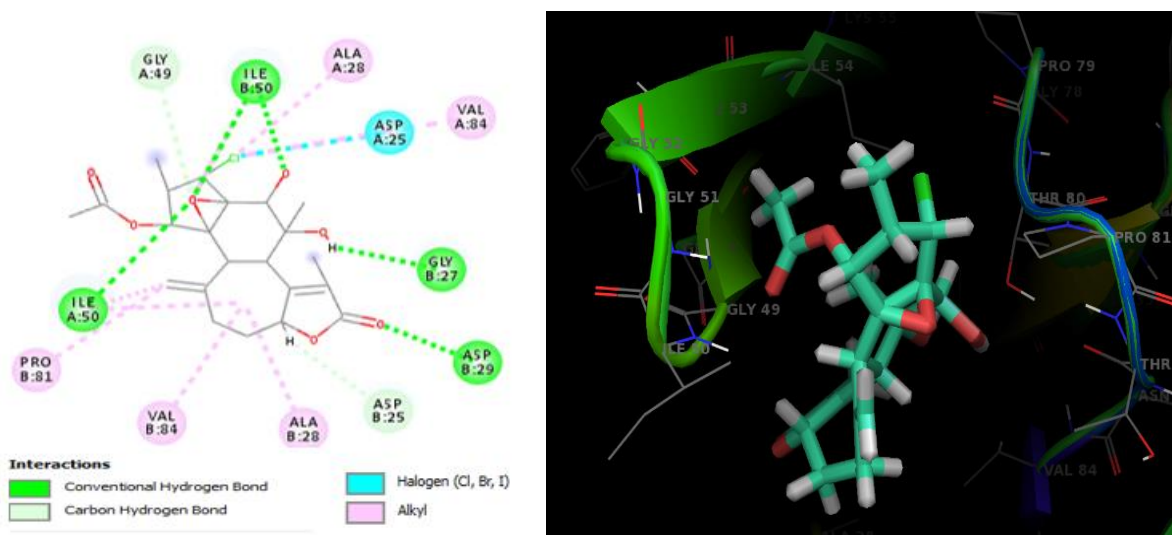


Figure 4.5-2: 2D and 3D visualization of the interaction of Ermasoid (E37) with HIV-1 PR (3EL9)

### 3. Interaction of crotoascarin K (E23) with Protease enzyme (PDB ID: 3EL9)

Crotoascarin K is a crotofolane diterpenoid isolated from the ethyl acetate fraction of *C. megalocarpus*. The *in vitro* assay has displayed strong anti-HIV activity by inhibiting viral replication by 83.3 % with an IC<sub>50</sub> value of 0.002 µg/mL. In addition, it has shown protease inhibitor activity by inhibiting 76 % of the HIV-1 PR enzyme *in vitro* activity. As depicted in **Table 4.5-3**, the binding energy of the interaction of crotoascarin K with 3EL9 was -7.115 kcal/mol making it the 3<sup>rd</sup> most active compound with the ability to inhibit the protease enzyme.

Crotoascarin K's high affinity for the enzyme could be attributed due to its ability to form two hydrophobic and three hydrogen bond interactions with residues in the active site of the HIV-PR enzyme. The hydrophobic interactions were formed with Asp-30' and Leu-23 at S2' and S3 subsites of the protease enzyme (**Table 4.5-5**). The methyl group at C-15, and the cyclopentane ring form an alkyl interaction with Ile-47', Ala -28', Ile-50 and Ile-50' (**Figure 4.5-3**). These interactions help in stabilizing the compound in the binding site of the receptor (3EL9).

The β-hydroxyl group at C-9 of E23 forms hydrogen bond interactions with Asp-25. Similarly, the β-hydroxyl group at C-1 forms a hydrogen bond with Gly-27' and Asp-29' at S2' subsite of the enzyme. The formation of hydrogen bonds with the residues at the catalytic region (Asp-25 and Gly-27) will impair the enzyme's activity. In biological complexes, hydrogen bonds are the most common directed intermolecular interactions, and they contribute significantly to the specificity of molecular recognition

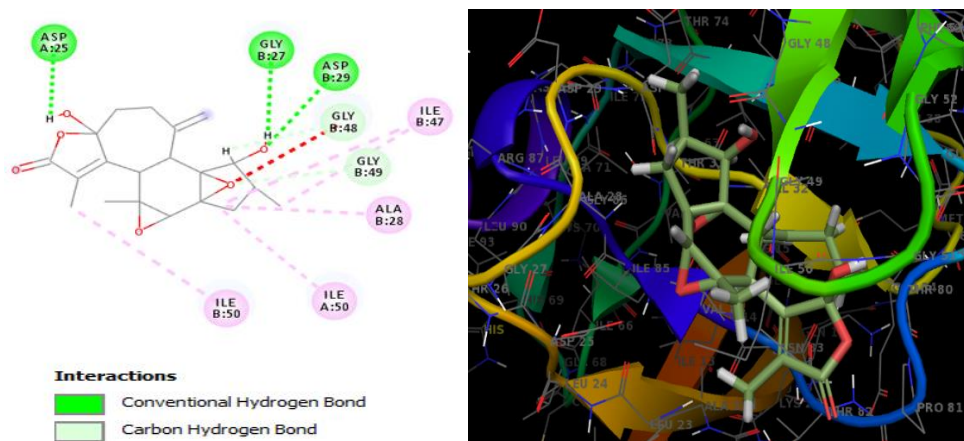


Figure 4.5-3: 2D and 3D visualization of interactions of crotoascarin K (E23) with HIV-1 PR (3EL9)

#### 4. Interaction of Pinoresinol (E2) with Protease enzyme (PDB ID: 3EL9)

Pinoresinol binds to the protein satisfactorily with an estimated free binding energy of -7.078 kcal/mol making it the fourth most active drug with the ability to inhibit protease enzyme (3EL9). Table 4.5-4 shows that Pinoresinol (E2) forms five hydrogen bond interactions with HIV-PR (3EL9). The methoxy group at C-4' contributes to the hydrogen bond interaction with Asp-29, while the -OCH<sub>3</sub> group at C-5 plays a role in van der Waals interactions with Asp-30 in the S2 subsite of the enzyme. The two aromatic rings of pinoresinol form hydrophobic interaction with Ala-28 in the S2 subsite of the HIV-1 PR enzyme (**Figure 4.5-4**). This interaction stabilizes the compound in the enzyme's binding site and renders the substrate's binding to the enzyme. In addition, the oxygen in the tetrahydrofuran moiety is involved in hydrogen bonding with Ile-50 in both S1 and S1' sub-sites of the enzyme.

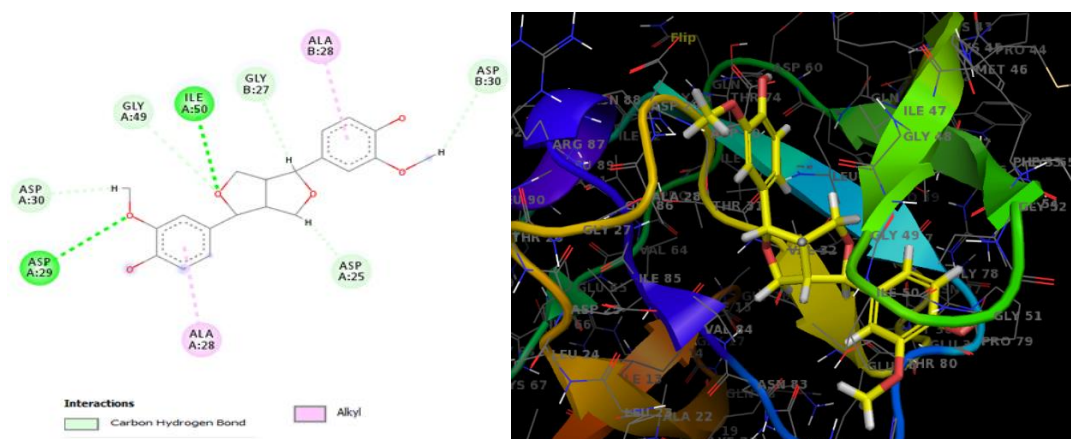


Figure 4.5-4: 2D and 3D visualization of the interaction of pinoresinol (E2) with HIV-1 PR (3EL9)



## 5. Interaction of 5 $\beta$ -hydroxy-8 $\alpha$ -methoxy eudesm-7(11)-en-12, 8-olide (ermiasolide A) with HIV-1 Protease enzyme (PDB ID: 3EL9)

Ermiasolide A binds to the protease enzyme with an estimated free binding energy of -6.067kcal/mol making it the fifth most active drug. Ermiasolide A (**E12**) forms 3 hydrophobic interactions in the S1 and S2 subsites of the protease enzyme (**Table 4.5-5**). The methyl group at C-4 and the two cyclohexane rings are involved in hydrophobic interactions with Ala-28, Ile-50, and Val-84 (**Figure 4.5-5**). Furthermore, the methoxy group at C-8 contributes in hydrophobic interaction and in stabilizing the compound within the binding pocket. In addition, E12 forms hydrogen bonding with Thr-80 and Thr-82. The binding of E12 with Thr-82 is similar to that seen in Atazanavir and E37, suggesting this amino acid is embedded within the hydrophobic pocket of the receptor and plays a role in molecular recognition.

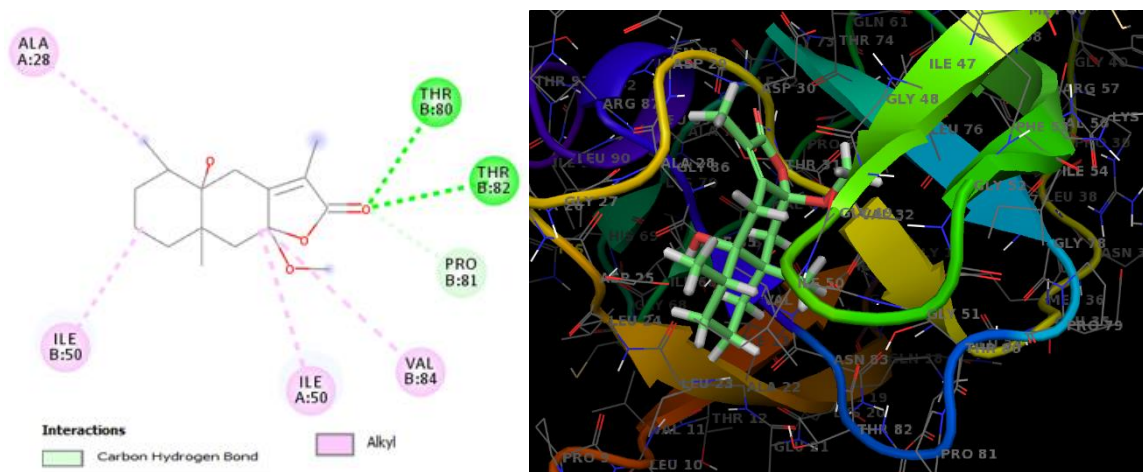


Figure 4.5-5: 2D and 3D visualization of the interactions of ermiasolide A (E12) with HIV-1 PR (3EL9)

## CHAPTER FIVE

### CONCLUSION AND RECOMMENDATIONS

This research reports the chemistry, anti-HIV activity, and mode of action of five new previously undescribed compounds isolated from three Kenyan *Croton* species.

1. The crude (1:1 v/v dichloromethane: methanol) extracts of *C. macrostachyus*, *C. megalocarpus* and *C. dichogamus* showed varying degrees of anti-HIV activity. The crude extract of *C. dichogamus* displayed the highest anti-HIV activity ( $E_{\text{maxAV}} = 73.7$  percent).
2. Among the four solvent fractions (hexane, dichloromethane, ethyl acetate, and methanol) tested, the methanol fraction of the twigs of *C. dichogamus* displayed the highest anti-HIV activity ( $E_{\text{maxAV}} = 90.8$  %), followed by the ethyl acetate fraction of the bark of *C. megalocarpus* ( $E_{\text{maxAV}} = 88.0$  %) and the hexane fraction of the leaves of *C. macrostachyus* ( $E_{\text{maxAV}} = 83$  %).
3. Using bioassay-guided fractionation, 19 known and 6 new previously undescribed compounds were isolated and characterized from the three *Croton* species. Four new compounds with anti-HIV activity were isolated from *C. megalocarpus*, while two new compounds were from *C. dichogamus*. Twenty-one of the isolated compounds have displayed anti-HIV activity by inhibiting more than 75 % of HIV-induced cytopathic effects on the Human T-lymphocytic cell line.
4. Among the isolated compounds, four eudesmane type sesquiterpenes, Ermiasolide A, B, C, 4H- $\alpha$ ,7H- $\alpha$ ,10 $\alpha$ -eudesm-11-en-5 $\beta$ -ol, and three crotofolane diterpenoids, ermiasoid, crotoascarin K and crotoascarin  $\omega$  displayed the highest protease inhibitor efficacy. In addition, these compounds displayed the lowest predicted binding energy (strong affinity) against HIV-1 PR ( $\Delta G < -5.0$  kcal/mol) in an *in silico* study. Mechanistic studies showed that the isolated pure compounds form hydrophobic interactions with several residues in the binding pocket and hydrogen bonding with the key residues in the catalytic domain of the HIV-1 protease, including ASP 25 and GLY 27, GLY 48.

## Recommendations

- I. *In silico* quantitative structure-activity relationship (QSAR) studies should be conducted to analyze the responsible functional groups for the observed anti-HIV activity.
- II. Since most of the compounds isolated in this study had a higher cytotoxicity effect, investigation of these compounds for their anticancer effect should be carried out.
- III. Anti-HIV activity of the pure compounds should also be determined in an *in vivo* animal model.
- IV. Studies involving the synthesis of the bioactive compounds should be conducted to perform additional *in vitro* and *in vivo* studies.

## REFERENCES

- ab211106 HIV-1 Protease Inhibitor Screening Kit (Fluorometric). (2020).
- Abdon, A. P. V., Leal-Cardoso, J. H., Coelho-de-Souza, A. N., Morais, S. M., & Santos, C. F. (2002). Antinociceptive effects of the essential oil of *Croton nepetaefolius* on mice. *Brazilian Journal of Medical and Biological Research*. <https://doi.org/10.1590/S0100-879X2002001000015>
- Abo, K. A., Ogunleye, V. O., & Ashidi, J. S. (1999). Antimicrobial potential of *Spondias mombin*, *Croton zambesicus* and *Zygotritonia crocea*. *Phytotherapy Research*. [https://doi.org/10.1002/\(SICI\)1099-1573\(199909\)13:6<494::AID-PTR490>3.0.CO;2-9](https://doi.org/10.1002/(SICI)1099-1573(199909)13:6<494::AID-PTR490>3.0.CO;2-9)
- Abosi, A. O., & Majinda, R. R. T. (2015). Anti-plasmodial and Radical Scavenging Activities of *Croton megalobotrys*. *Journal of Pharmacognosy and Phytochemistry*.
- ACTG Laboratory Technologist Committee. (2004). TCID50 (50% Tissue Culture Infectious Dose) Determination Quantitation of Viable HIV-1 Virions in Culture Supernatants. 50(May), 1–10.
- Adamson, C. S., & Freed, E. O. (2007). Human Immunodeficiency Virus Type 1 Assembly, Release, and Maturation. In *Advances in Pharmacology*. [https://doi.org/10.1016/S1054-3589\(07\)55010-6](https://doi.org/10.1016/S1054-3589(07)55010-6)
- Adasme, M. F., Linnemann, K. L., Bolz, S. N., Kaiser, F., Salentin, S., Haupt, V. J., & Schroeder, M. (2021). PLIP 2021: expanding the scope of the protein–ligand interaction profiler to DNA and RNA. *Nucleic Acids Research*, 49(W1), W530–W534. <https://doi.org/10.1093/NAR/GKAB294>
- Addae-Mensah, Muriuki, Karanja, W., & Waibel, and A. (1992). Constituents of the stem bark and twigs of *Croton macrostachyus* (p. 81). *Fitoterapia*, vol. 63, no. 1,.
- Addae-Mensah, I., Waibel, R., Achenbach, H., Muriuki, G., Pearce, C., & Sanders, J. K. M. (1989). A clerodane diterpene and other constituents of *Croton megalocarpus*. *Phytochemistry*. [https://doi.org/10.1016/S0031-9422\(00\)98083-X](https://doi.org/10.1016/S0031-9422(00)98083-X)
- Agisho, H., Osie, M., & Lambore, T. (2014). Traditional Medicinal Plants Utilization, Management and Threats in Hadiya Zone, Ethiopia. *Journal of Medicinal Plants Studies*. [https://doi.org/10.1016/s0160-7383\(73\)80011-8](https://doi.org/10.1016/s0160-7383(73)80011-8)
- Aguilar-Guadarrama, A. B., & Rios, M. Y. (2004). Three new sesquiterpenes from *Croton arboreous*. *Journal of Natural Products*, 67(5), 914–917. <https://doi.org/10.1021/np030485f>

- Ahmad, V., & Atta-ur-rahman. (1994). Handbook of natural products data. Volume 2: pentacyclic triterpenoids.
- Ahmed, B., Alam, T., Varshney, M., & Khan, S. A. (2002). Hepatoprotective activity of two plants belonging to the Apiaceae and the Euphorbiaceae family. *Journal of Ethnopharmacology*. [https://doi.org/10.1016/S0378-8741\(01\)00392-0](https://doi.org/10.1016/S0378-8741(01)00392-0)
- Ahmed, M., Laing, M. D., & Nsahlai, I. V. (2013). *In vitro* anthelmintic activity of crude extracts of selected medicinal plants against *Haemonchus contortus* from sheep. *Journal of Helminthology*. <https://doi.org/10.1017/S0022149X1200020X>
- Ahn, M. J., Yoon, K. D., Min, S. Y., Lee, J. S., Kim, J. H., Kim, T. G., Kim, S. H., Kim, N. G., Huh, H., & Kim, J. (2004). Inhibition of HIV-1 reverse transcriptase and protease by phlorotannins from the brown alga *Ecklonia cava*. *Biol Pharm Bull*. <https://doi.org/10.1248/bpb.27.544>
- AIDSinfo.nih.gov. (2018). AIDSinfo Glossary of HIV/AIDS-Related Terms. @AIDSinfo.Nih.Gov, 9, 1–204.
- Al-Asmari, A. K., Albalawi, S. M., Athar, M. T., Khan, A. Q., Al-Shahrani, H., & Islam, M. (2015). *Moringa oleifera* as an anti-cancer agent against breast and colorectal cancer cell lines. *PLoS ONE*. <https://doi.org/10.1371/journal.pone.0135814>
- Aldhafer, A., Langat, M., Ndunda, B., Chirchir, D., Midiwo, J. O., Njue, A., Schwikkard, S., Carew, M., & Mulholland, D. (2017a). Diterpenoids from the roots of *Croton dichogamus* Pax. *Phytochemistry*, 144, 1–8. <https://doi.org/10.1016/j.phytochem.2017.08.014>
- Alhakmani, F., Kumar, S., & Khan, S. A. (2013). Estimation of total phenolic content, in-vitro antioxidant and anti-inflammatory activity of flowers of *Moringa oleifera*. *Asian Pacific Journal of Tropical Biomedicine*. [https://doi.org/10.1016/S2221-1691\(13\)60126-4](https://doi.org/10.1016/S2221-1691(13)60126-4)
- Ali, H., König, G. M., Khalid, S. A., Wright, A. D., & Kaminsky, R. (2002). Evaluation of selected Sudanese medicinal plants for their in vitro activity against hemoflagellates, selected bacteria, HIV-1-RT and tyrosine kinase inhibitory, and for cytotoxicity. *Journal of Ethnopharmacology*, 83(3), 219–228. [https://doi.org/10.1016/S0378-8741\(02\)00245-3](https://doi.org/10.1016/S0378-8741(02)00245-3)
- Aloia, R. C., Tian, H., & Jensen, F. C. (1993). Lipid composition and fluidity of the human immunodeficiency virus envelope and host cell plasma membranes. *Proceedings of the National Academy of Sciences*. <https://doi.org/10.1073/pnas.90.11.5181>
- Alonso-Castro, A. J., Ortiz-Sánchez, E., Domínguez, F., López-Toledo, G., Chávez, M., Ortiz-

- Tello, A. D. J., & García-Carrancá, A. (2012). Antitumor effect of *Croton lechleri* Mull. Arg. (Euphorbiaceae). *Journal of Ethnopharmacology*. <https://doi.org/10.1016/j.jep.2012.01.009>
- Alqahtani, A. (2015). Phytochemical investigation of members of the Asparagaceae and Euphorbiaceae families. *University of Surey, PhD Disertation, I*(Volume 1).
- Altmann, A. A. (2010). Bioinformatical Approaches to Ranking of anti-HIV Combination Therapies and Planning of Treatment Schedules. Dissertation.
- Alviano, W. S., Mendonça-Filho, R. R., Alviano, D. S., Bizzo, H. R., Souto-Padrón, T., Rodrigues, M. L., Bolognese, A. M., Alviano, C. S., & Souza, M. M. G. (2005). Antimicrobial activity of *Croton cajucara* Benth linalool-rich essential oil on artificial biofilms and planktonic microorganisms. *Oral Microbiology and Immunology*. <https://doi.org/10.1111/j.1399-302X.2004.00201.x>
- Amuamuta, A., Mekonnen, Z., & Gebeyehu, E. (2015). Traditional therapeutic uses and phytochemical screening of some selected indigenous medicinal plants from Northwest Ethiopia. *African Journal of Pharmacology and Therapeutics*, 4(3), 80–85. <http://journals.uonbi.ac.ke/ajpt/article/view/1359>
- An, P., & Winkler, C. A. (2010). Host genes associated with HIV/AIDS: advances in gene discovery. In *Trends in Genetics*. <https://doi.org/10.1016/j.tig.2010.01.002>
- Anazetti, Maristella C., Melo, P. S., Durán, N., & Haun, M. (2004). Dehydrocrotonin and its derivative, dimethylamide-crotonin induce apoptosis with lipid peroxidation and activation of caspases-2, -6 and -9 in human leukemic cells HL60. *Toxicology*. <https://doi.org/10.1016/j.tox.2004.06.003>
- Anazetti, Maristella Conte, Melo, P. S., Durán, N., & Haun, M. (2003). Comparative cytotoxicity of dimethylamide-crotonin in the promyelocytic leukemia cell line (HL60) and human peripheral blood mononuclear cells. *Toxicology*. [https://doi.org/10.1016/S0300-483X\(03\)00089-1](https://doi.org/10.1016/S0300-483X(03)00089-1)
- Andersson, H. O., Fridborg, K., Löwgren, S., Alterman, M., Mühlman, A., Björsne, M., Garg, N., Kvarnström, I., Schaal, W., & Classon, B. (2003). Optimization of P1–P3 groups in symmetric and asymmetric HIV-1 protease inhibitors. *European Journal of Biochemistry*, 270(8), 1746–1758.
- Andrade, T. C. B., Lima, S. G. D., Freitas, R. M., Rocha, M. S., Islam, T., Silva, T. G. D., & Militão, G. C. G. (2015). Isolation, characterization and evaluation of antimicrobial and

cytotoxic activity of estragole, obtained from the essential oil of *Croton zehntneri* (Euphorbiaceae). *Anais Da Academia Brasileira de Ciencias*. <https://doi.org/10.1590/0001-3765201520140111>

Araújo, M. G., Maia, I. C. C., De Sousa, B. D., De Moraes, S. M., & Freitas, S. M. (2006). Effect of stalk and leaf extracts from Euphorbiaceae species on *Aedes aegypti* (Diptera, Culicidae) larvae. *Revista Do Instituto de Medicina Tropical de Sao Paulo*. <https://doi.org/10.1590/S0036-46652006000400007>

Arika, W.M., Abdirahman, Y.A., Mawia, M.A., Wambua, K.F., Nyamai, D.M., Ogola, P.E., Kiboi, N.G., Nyandoro, H.O., Agyirifo, D.S., Ngugi, M.P., Njagi, E. N. M. (2015). In vivo antidiabetic activity of the aqueous leaf extract of *Croton macrostachyus* in alloxan induced diabetic mice. *Pharm Anal Acta*, 6(November 2015). <https://doi.org/10.4172/21532435.1000447>

Arts, E. J., & Hazuda, D. J. (2012). HIV-1 antiretroviral drug therapy. *Cold Spring Harbor Perspectives in Medicine*. <https://doi.org/10.1101/cshperspect.a007161>

Asakawa, Y., Toyota, M., Nakaishi, E., & Tada, Y. (1996). Distribution of terpenoids and aromatic compounds in New Zealand liverworts. *Journal of the Hattori Botanical Laboratory*, 80(80), 271–295. [https://doi.org/10.18968/jhbl.80.0\\_271](https://doi.org/10.18968/jhbl.80.0_271)

Ashby, J., Goldmeier, D., & Sadeghi-Nejad, H. (2014). Hypogonadism in human immunodeficiency virus-positive men. In *Korean Journal of Urology*. <https://doi.org/10.4111/kju.2014.55.1.9>

Asres, K., Bucar, F., Kartnig, T., Witvrouw, M., Pannecouque, C., & De Clercq, E. (2001). Antiviral activity against human immunodeficiency virus type 1 (HIV-1) and type 2 (HIV-2) of ethnobotanically selected Ethiopian medicinal plants. *Phytotherapy Research*, 15(1), 62–69. [https://doi.org/10.1002/1099-1573\(200102\)15:1<62::AID-PTR956>3.0.CO;2-X](https://doi.org/10.1002/1099-1573(200102)15:1<62::AID-PTR956>3.0.CO;2-X)

Asres, Kaleab, & Bucar, F. (2005). Anti-HIV activity against immunodeficiency virus type 1 (HIV-I) and type II (HIV-II) of compounds isolated from the stem bark of *Combretum molle*. *Ethiopian Medical Journal*, 43(1), 15–20. <http://www.ncbi.nlm.nih.gov/pubmed/16370525>

Assis, L. C., Hort, M. A., De Souza, G. V., Martini, A. C., Forner, S., Martins, D. F., Silva, J. C., Horst, H., Dos Santos, A. R. S., Pizzolatti, M. G., Rae, G. A., Koepp, J., De Bem, A. F., & Do Valle, R. M. R. (2014). Neuroprotective effect of the proanthocyanidin-rich fraction in experimental model of spinal cord injury. *Journal of Pharmacy and Pharmacology*.

<https://doi.org/10.1111/jphp.12177>

- Athikomkulchai, S., Prawat, H., Thasana, N., Ruangrunsi, N., & Ruchirawat, S. (2006). COX-1, COX-2 inhibitors and antifungal agents from *Croton hutchinsonianus*. *Chemical and Pharmaceutical Bulletin*, *54*(2), 262–264. <https://doi.org/10.1248/cpb.54.262>
- Ayatollahi, A. M., Zarei, S. M., Memarnejadian, A., Ghanadian, M., Moghadam, M. H., & Kobarfard, F. (2016). Triterpene Constituents of *Euphorbia erythradenia* Bioss. and their Anti-HIV Activity. *Iranian Journal of Pharmaceutical Research*, *15*(Suppl), 19–27. <https://doi.org/10.22037/ijpr.2016.1858>
- Babine, R. E., & Bender, S. L. (1997). Molecular recognition of protein-ligand complexes: Applications to drug design. *Chemical Reviews*, *97*(5), 1359–1472. <https://doi.org/10.1021/cr960370z>
- Bachelor, L. T., Anton, E. D., Kudish, P., Baker, D., Bunville, J., Krakowski, K., Bolling, L., Aujay, M., Wang, X. V., Ellis, D., Becker, M. F., Lasut, A. L., George, H. J., Spalding, D. R., Hollis, G., & Abremski, K. (2000). Human immunodeficiency virus type 1 mutations selected in patients failing efavirenz combination therapy. *Antimicrobial Agents and Chemotherapy*. <https://doi.org/10.1128/AAC.44.9.2475-2484.2000>
- Bahuguna, A., Khan, I., Bajpai, V. K., & Kang, S. C. (2017). MTT assay to evaluate the cytotoxic potential of a drug. *Bangladesh Journal of Pharmacology*, *12*(2), 115–118. <https://doi.org/10.3329/bjp.v12i2.30892>
- Bantie, L., Assefa, S., Teklehaimanot, T., & Engidawork, E. (2014). In vivo antimalarial activity of the crude leaf extract and solvent fractions of *Croton macrostachyus* Hocsht. (Euphorbiaceae) against *Plasmodium berghei* in mice. *BMC Complementary and Alternative Medicine*. <https://doi.org/10.1186/1472-6882-14-79>
- Barbaro, G. (2005). HIV-associated cardiomyopathy: Etiopathogenesis and clinical aspects. *Herz*. <https://doi.org/10.1007/s00059-005-2728-z>
- Barbosa, P. R., Fascio, M., Martins, D., Silva Guedes, M. L., & Roque, N. F. (2003). Triterpenes of *Croton betulaster* (Euphorbiaceae). *Biochemical Systematics and Ecology*. [https://doi.org/10.1016/S0305-1978\(02\)00145-X](https://doi.org/10.1016/S0305-1978(02)00145-X)
- Barnard, D. L., Smee, D. F., Huffman, J. H., Meyerson, L. R., & Sidwell, R. W. (1993). Antiherpesvirus activity and mode of action of SP 303, a novel plant flavonoid. *Chemotherapy*. <https://doi.org/10.1159/000239127>



- Barré-Sinoussi, F., Chermann, J. C., Rey, F., Nugeyre, M. T., Chamaret, S., Gruest, J., Dauguet, C., Axler-Blin, C., Vézinet-Brun, F., Rouzioux, C., Rozenbaum, W., & Montagnier, L. (1983). Isolation of a T-lymphotropic retrovirus from a patient at risk for acquired immune deficiency syndrome (AIDS). *Revista de Investigacion Clinica*.  
<https://doi.org/10.1126/science.6189183>
- Barreto, M. B., Gomes, C. L., De Freitas, J. V. B., Das Chagas L. Pinto, F., Silveira, E. R., Gramosa, N. V., & Torres, D. S. C. (2013). Flavonoides e terpenoides de *Croton muscicarpa* (Euphorbiaceae). *Quimica Nova*. <https://doi.org/10.1590/S0100-40422013000500011>
- Behbahani, M. (2014). Evaluation of anti-HIV-1 activity of a new iridoid glycoside isolated from *Avicenna marina*, *in vitro*. *International Immunopharmacology*, 23(1), 262–266.  
<https://doi.org/10.1016/j.intimp.2014.09.003>
- Bekele, G., & Reddy, P. R. (2015). Ethnobotanical Study of Medicinal Plants Used to Treat Human Ailments by Guji Oromo Tribes in Abaya District ., *Universal Journal of Plant Science*, 3(1), 1–8. <https://doi.org/10.13189/ujps.2015.030101>
- Bernardi, M. M., De Souza-Spinosa, H., Batatinha, M. J. M., & Giorgi, R. (1991). *Croton zehntneri*: possible central nervous system effects in rodents. *Journal of Ethnopharmacology*.  
[https://doi.org/10.1016/0378-8741\(91\)90090-Z](https://doi.org/10.1016/0378-8741(91)90090-Z)
- Berridge, M. V., Herst, P. M., & Tan, A. S. (2005). Tetrazolium dyes as tools in cell biology: New insights into their cellular reduction. In *Biotechnology Annual Review*.  
[https://doi.org/10.1016/S1387-2656\(05\)11004-7](https://doi.org/10.1016/S1387-2656(05)11004-7)
- Berry, P. E., Hipp, A. L., Wurdack, K. J., Van Ee, B., & Riina, R. (2005). Molecular phylogenetics of the giant genus *Croton* and tribe Crotonaeae (Euphorbiaceae sensu stricto) using ITS and trnL-trnF DNA sequence data. *American Journal of Botany*.  
<https://doi.org/10.3732/ajb.92.9.1520>
- Bessong, P. O., & Obi, C. L. (2006). Ethnopharmacology of human immunodeficiency virus in South Africa - A minireview. In *African Journal of Biotechnology* (Vol. 5, Issue 19, pp. 1693–1699). <https://doi.org/10.4314/ajb.v5i19.55828>
- Betancur-Galvis, L. A., Morales, G. E., Forero, J. E., & Roldan, J. (2002). Cytotoxic and antiviral activities of Colombian medicinal plant extracts of the *Euphorbia* genus. *Memorias Do Instituto Oswaldo Cruz*, 97(4), 541–546.  
<https://doi.org/10.1590/S0074-02762002000400017>

- Bhatarai, B., & Garg, R. (2008). Comparative QSAR as a Cheminformatics Tool in the Design of Dihydro Pyranone Based HIV-1 Protease Inhibitors. *Current Computer Aided-Drug Design*, 4(4), 283–310. <https://doi.org/10.2174/157340908786786029>
- Bighetti, E. J., Hiruma-Lima, C. A., Gracioso, J. S., & Brito, a R. (1999). Anti-inflammatory and antinociceptive effects in rodents of the essential oil of *Croton cajucara* Benth. *The Journal of Pharmacy and Pharmacology*. <https://doi.org/10.1211/0022357991777100>
- Bighetti, E. J., Souza-Brito, A. R., de Faria, E. C., & Oliveira, H. C. (2004). Chronic treatment with bark infusion from *Croton cajucara* lowers plasma triglyceride levels in genetic hyperlipidemic mice. *Can J Physiol Pharmacol*. <https://doi.org/10.1139/y04-040> [pii]
- BIOVIA, D. S. (2017). Discovery Studio Modeling Environment,. *San Diego: Dassault Systèmes*. [www.3ds.com](http://www.3ds.com).
- Biscaro, F., Parisotto, E. B., Zanette, V. C., Günther, T. M. F., Ferreira, E. A., Gris, E. F., Correia, J. F. G., Pich, C. T., Mattivi, F., Filho, D. W., & Pedrosa, R. C. (2013). Anticancer activity of flavonol and flavan-3-ol rich extracts from *Croton celtidifolius* latex. *Pharmaceutical Biology*. <https://doi.org/10.3109/13880209.2013.764331>
- Block, S., Stévigny, C., De Pauw-Gillet, M. C., De Hoffmann, E., Llabrès, G., Adjakidjé, V., & Quetin-Leclercq, J. (2002). ent-trachyloban-3 $\beta$ -ol, a new cytotoxic diterpene from *Croton zambesicus*. *Planta Medica*. <https://doi.org/10.1055/s-2002-32903>
- Blunt, J. W., & Stothers, J. B. (1977). <sup>13</sup>C NMR. spectra of steroids —a survey and commentary. *Organic Magnetic Resonance*, 9(8), 439–464. <https://doi.org/10.1002/MRC.1270090802>
- Boesecke, C., & Cooper, D. A. (2008). Toxicity of HIV protease inhibitors: Clinical considerations. In *Current Opinion in HIV and AIDS*. <https://doi.org/10.1097/COH.0b013e328312c392>
- Bowen, L. N., Smith, B., Reich, D., Quezado, M., & Nath, A. (2016). HIV-associated opportunistic CNS infections: Pathophysiology, diagnosis and treatment. In *Nature Reviews Neurology*. <https://doi.org/10.1038/nrneurol.2016.149>
- Brenchley, J. M., Schacker, T. W., Ruff, L. E., Price, D. A., Taylor, J. H., Beilman, G. J., Nguyen, P. L., Khoruts, A., Larson, M., Haase, A. T., & Douek, D. C. (2004). CD4<sup>+</sup> T Cell Depletion during all Stages of HIV Disease Occurs Predominantly in the Gastrointestinal Tract. *The Journal of Experimental Medicine*. <https://doi.org/10.1084/jem.20040874>

- Brito, A. R., Rodriguez, J. A., Hiruma-Lima, C. A., Haun, M., & Nunes, D. S. (1998). Antiulcerogenic activity of trans-dehydrocrotonin from *Croton cajucara*. *Planta Medica*. <https://doi.org/10.1016/j.protcy.2012.09.021>
- Brunton, L. L., Hilal-Dandan, R., & Knollmann, B. C. (2017). *Goodman & Gilman's The Pharmacological Basis of Therapeutics*. <https://doi.org/10.1111/j.1600-0528.2011.00618.x>
- Buchsacher, G. L. (2003). *Lentiviral vector systems for gene transfer* (Issue April). <https://www.springer.com/gb/book/9780306477027>
- Burack, J. H., Cohen, M. R., Hahn, J. A., & Abrams, D. I. (1996). Pilot randomized controlled trial of Chinese herbal treatment for HIV- associated symptoms. *Journal of Acquired Immune Deficiency Syndromes and Human Retrovirology*, 12(4), 386–393. <https://doi.org/10.1097/00042560-199608010-00009>
- Burgos, A., Barua, J., Flores-Giubi, M. E., Bazan, D., Ferro, E., & Alvarenga, N. L. (2015). Antibacterial activity of the alkaloid extract and isolated compounds from *Croton bonplandianum* Baill. (Euphorbiaceae). *Revista Brasileira de Plantas Mediciniais*. [https://doi.org/10.1590/1983-084X/14\\_097](https://doi.org/10.1590/1983-084X/14_097)
- Burns, D., Reynolds, W. F., Buchanan, G., Reese, P. B., & Enriquez, R. G. (2000). Assignment of <sup>1</sup>H and <sup>13</sup>C spectra and investigation of hindered side-chain rotation in lupeol derivatives. *Magnetic Resonance in Chemistry*, 38(7), 488–493. [https://doi.org/10.1002/1097-458x\(200007\)38:7<488::aid-mrc704>3.0.co;2-g](https://doi.org/10.1002/1097-458x(200007)38:7<488::aid-mrc704>3.0.co;2-g)
- Bussmann, R. W. (2006). Ethnobotany of the Samburu of Mt. Nyiru, South Turkana, Kenya. *Journal of Ethnobiology and Ethnomedicine*. <https://doi.org/10.1186/1746-4269-2-35>
- Busti, A. J., Hall, R. G., & Margolis, D. M. (2004). Atazanavir for the treatment of human immunodeficiency virus infection. In *Pharmacotherapy*. <https://doi.org/10.1592/phco.24.17.1732.52347>
- Cai, Y., Chen, Z. P., & Phillipson, J. D. (1993). Clerodane diterpenoids from *Croton lechleri*. *Phytochemistry*. [https://doi.org/10.1016/S0031-9422\(00\)90816-1](https://doi.org/10.1016/S0031-9422(00)90816-1)
- Cai, Y., Evans, F. J., Roberts, M. F., Phillipson, J. D., Zenk, M. H., & Gleba, Y. Y. (1991). Polyphenolic compounds from *Croton lechleri*. *Phytochemistry*. [https://doi.org/10.1016/0031-9422\(91\)85063-6](https://doi.org/10.1016/0031-9422(91)85063-6)
- Campos, A. R., Albuquerque, F. A. A., Rao, V. S. N., Maciel, M. A. M., & Pinto, A. C. (2002). Investigations on the antinociceptive activity of crude extracts from *Croton cajucara* leaves

- in mice. *Fitoterapia*, 73(2), 116–120. [https://doi.org/10.1016/S0367-326X\(02\)00004-7](https://doi.org/10.1016/S0367-326X(02)00004-7)
- Camurça-Vasconcelos, A. L. F., Bevilaqua, C. M. L., Morais, S. M., Maciel, M. V., Costa, C. T. C., Macedo, I. T. F., Oliveira, L. M. B., Braga, R. R., Silva, R. A., & Vieira, L. S. (2007). Anthelmintic activity of *Croton zehntneri* and *Lippia sidoides* essential oils. *Veterinary Parasitology*. <https://doi.org/10.1016/j.vetpar.2007.06.012>
- Capriotti, T. (2018). HIV/AIDS. *Home Healthcare Now*. <https://doi.org/10.1097/NHH.0000000000000706>
- Carneiro, V. A., Dos Santos, H. S., Arruda, F. V. S., Bandeira, P. N., Albuquerque, M. R. J. R., Pereira, M. O., Henriques, M., Cavada, B. S., & Teixeira, E. H. (2011). Casbane diterpene as a promising natural antimicrobial agent against biofilm-associated infections. *Molecules*. <https://doi.org/10.3390/molecules16010190>
- Carpenter, R. C., Sotheeswaran, S., Sultanbawa, M. U. S., & Ternai, B. (1980). <sup>13</sup>C NMR studies of some lupane and taraxerane triterpenes. *Organic Magnetic Resonance*, 14(6), 462–465. <https://doi.org/10.1002/MRC.1270140608>
- Caruzo, M. B. R., van Ee, B. W., Cordeiro, I., Berry, P. E., & Riina, R. (2011). Molecular phylogenetics and character evolution of the “sacaca” clade: Novel relationships of *Croton* section *Cleodora* (Euphorbiaceae). *Molecular Phylogenetics and Evolution*. <https://doi.org/10.1016/j.ympev.2011.04.013>
- Carvalho, J. C. T., Silva, M. F. C., Maciel, M. A. M., Da Cunha Pinto, A., Nunes, D. S., Lima, R. M., Bastos, J. K., & Sarti, S. J. (1996). Investigation of anti-inflammatory and antinociceptive activities of trans-dehydrocrotonin, a 19-nor-clerodane diterpene from *Croton cajucara*. Part 1. *Planta Medica*. <https://doi.org/10.1055/s-2006-957925>
- Cavalcanti, J. M., Leal-Cardoso, J. H., Diniz, L. R. L., Portella, V. G., Costa, C. O., Linard, C. F. B., Alves, K., Rocha, M. V. A. P., Lima, C. C., Cecatto, V. M., & Coelho-de-Souza, A. N. (2012). The essential oil of *Croton zehntneri* and trans-anethole improves cutaneous wound healing. *Journal of Ethnopharmacology*. <https://doi.org/10.1016/j.jep.2012.08.030>
- CDC. (2009). US Department of Health and Human Services-Biosafety in Microbiological and Biomedical Laboratories. *Public Health Service, 5th Editio* (Revised December), 438. <https://doi.org/citeulike-article-id:3658941>
- Centers for Disease, C., & Prevention. (2006). The Global HIV/AIDS pandemic, 2006. *MMWR Morb Mortal Wkly Rep*. <https://doi.org/mm5531a1> [pii]

- Chan, D. C., Fass, D., Berger, J. M., & Kim, P. S. (1997). Core structure of gp41 from the HIV envelope glycoprotein. *Cell*. [https://doi.org/10.1016/S0092-8674\(00\)80205-6](https://doi.org/10.1016/S0092-8674(00)80205-6)
- Chaniad, P., Sudsai, T., Septama, A. W., Chukaew, A., & Tewtrakul, S. (2019). Evaluation of Anti-HIV-1 integrase and anti-inflammatory activities of compounds from *Betula alnoides* buch-ham. *Advances in Pharmacological Sciences*, 2019. <https://doi.org/10.1155/2019/2573965>
- Chapman, T. M., McGavin, J. K., & Noble, S. (2003). Tenofovir disoproxil fumarate. In *Drugs*. <https://doi.org/10.2165/00003495-200363150-00006>
- Checkley, M. A., Lutge, B. G., & Freed, E. O. (2011). HIV-1 envelope glycoprotein biosynthesis, trafficking, and incorporation. In *Journal of Molecular Biology*. <https://doi.org/10.1016/j.jmb.2011.04.042>
- Chen, Z. P., Cai, Y., & Phillipson, J. D. (1994). Studies on the anti-tumour, anti-bacterial, and wound-healing properties of Dragon's blood. *Planta Medica*. <https://doi.org/10.1055/s-2006-959567>
- Chien, Kuo, Y. L., Lee, W. J., Yap, H. Y., & Wang, S. H. (2016). Antidermatophytic Activity of Ethanolic Extract from *Croton tiglium*. *BioMed Research International*. <https://doi.org/10.1155/2016/3237586>
- Chingwaru, W., Vidmar, J., & Kapewangolo, P. T. (2015). The potential of sub-saharan african plants in the management of human immunodeficiency virus infections: A review. In *Phytotherapy Research* (Vol. 29, Issue 10, pp. 1452–1487). John Wiley and Sons Ltd. <https://doi.org/10.1002/ptr.5433>
- Christenhusz, M. J. M., & Byng, J. W. (2016). Phytotaxa. *Phytotaxa*, 261(3), 201–217. <https://doi.org/10.11646/phytotaxa.261.3.1>
- Cihlar, T., & Ray, A. S. (2010). Nucleoside and nucleotide HIV reverse transcriptase inhibitors: 25 years after zidovudine. In *Antiviral Research*. <https://doi.org/10.1016/j.antiviral.2009.09.014>
- Cimarelli, A., & Darlix, J. L. (2014). HIV-1 reverse transcription. *Methods in Molecular Biology*. [https://doi.org/10.1007/978-1-62703-670-2\\_6](https://doi.org/10.1007/978-1-62703-670-2_6)
- Clark, A. M., & Labute, P. (2007). 2D depiction of protein-ligand complexes. *Journal of Chemical Information and Modeling*, 47(5), 1933–1944. <https://doi.org/10.1021/ci7001473>
- Clavel, F., & Hance, A. J. (2004). HIV Drug Resistance. *The New England Journal of Medicine*.

<https://doi.org/10.1056/NEJMra025195>

- Coelho-de-Souza, A. N., Lahlou, S., Barreto, J. E. F., Yum, M. E. M., Oliveira, A. C., Oliveira, H. D., Celedônio, N. R., Feitosa, R. G. F., Duarte, G. P., Santos, C. F., De Albuquerque, A. A. C., & Leal-Cardoso, J. H. (2013). Essential oil of *Croton zehntneri* and its major constituent anethole display gastroprotective effect by increasing the surface mucous layer. *Fundamental and Clinical Pharmacology*. <https://doi.org/10.1111/j.1472-8206.2011.01021.x>
- Colorado, B. E. J., Duarte, E., Muñoz, K., & Stashenko, E. (2010). Volatile chemical composition of essential oil from Colombian *Croton malambo* H. Karst. And determination of its antioxidant activity. *Revista Cubana de Plantas Medicinales*.
- Coop, A. (2019). Introduction to medicinal chemistry. *Foye's Principles of Medicinal Chemistry*, 3–6. [https://doi.org/10.1016/0307-4412\(76\)90096-0](https://doi.org/10.1016/0307-4412(76)90096-0)
- Cordeiro, K. W., Felipe, J. L., Malange, K. F., Do Prado, P. R., De Oliveira Figueiredo, P., Garcez, F. R., De Cássia Freitas, K., Garcez, W. S., & Toffoli-Kadri, M. C. (2016). Anti-inflammatory and antinociceptive activities of *Croton urucurana* Baillon bark. *Journal of Ethnopharmacology*. <https://doi.org/10.1016/j.jep.2016.02.051>
- Cos, P., Hermans, N., De Bruyne, T., Apers, S., Sindambiwe, J. B., Witvrouw, M., De Clercq, E., Vanden Berghe, D., Pieters, L., & Vlietinck, A. J. (2002). Antiviral activity of Rwandan medicinal plants against human immunodeficiency virus type-1 (HIV-1). *Phytomedicine*, 9(1), 62–68. <https://doi.org/10.1078/0944-7113-00083>
- Cos, P., Maes, L., Berghe, D. Vanden, Hermans, N., Apers, S., & Vlietinck, A. J. (2009). Plants and plant substances against aids and other viral diseases. *Ethanopharmacology*, II, 1–35.
- Coutinho, H. D. M., Matias, E. F. F., Santos, K. K. A., Tintino, S. R., Souza, C. E. S., Guedes, G. M. M., Santos, F. A. D., Costa, J. G. M., Falcão-Silva, V. S., & Siqueira-Júnior, J. P. (2010). Enhancement of the Norfloxacin Antibiotic Activity by Gaseous Contact with the Essential Oil of *Croton zehntneri*. *Journal of Young Pharmacists*. <https://doi.org/10.4103/0975-1483.71625>
- Cox, P. A. (1993). Saving the ethnopharmacological heritage of Samoa. *Journal of Ethnopharmacology*, 38(2–3), 177–180. [https://doi.org/10.1016/0378-8741\(93\)90014-V](https://doi.org/10.1016/0378-8741(93)90014-V)
- Cyrus, W. G., Daniel, G. W., Nanyingi, M. O., Njonge, F. K., & Mbaria, J. M. (2008). Antibacterial and cytotoxic activity of Kenyan medicinal plants. *Memorias Do Instituto Oswaldo Cruz*. <https://doi.org/10.1590/S0074-02762008000700004>

- Daar, E. S., Pilcher, C. D., & Hecht, F. M. (2008). Clinical presentation and diagnosis of primary HIV-1 infection. In *Current Opinion in HIV and AIDS*.  
<https://doi.org/10.1097/COH.0b013e3282f2e295>
- DalBó, S., Jürgensen, S., Horst, H., Ruzza, Â. A., Soethe, D. N., Santos, A. R. S., Pizzolatti, M. G., & Ribeiro-do-Valle, R. M. (2005). Antinociceptive effect of proanthocyanidins from *Croton celtidifolius* bark. *Journal of Pharmacy and Pharmacology*.  
<https://doi.org/10.1211/0022357056091>
- DalBó, S., Jürgensen, S., Horst, H., Soethe, D. N., Santos, A. R. S., Pizzolatti, M. G., & Ribeiro-do-Valle, R. M. (2006). Analysis of the antinociceptive effect of the proanthocyanidin-rich fraction obtained from *Croton celtidifolius* barks: Evidence for a role of the dopaminergic system. *Pharmacology Biochemistry and Behavior*.  
<https://doi.org/10.1016/j.pbb.2006.08.014>
- Dam, E., Quercia, R., Glass, B., Descamps, D., Launay, O., Duval, X., Kräusslich, H. G., Hance, A. J., & Clavel, F. (2009). Gag mutations strongly contribute to HIV-1 resistance to protease inhibitors in highly drug-experienced patients besides compensating for fitness loss. *PLoS Pathogens*. <https://doi.org/10.1371/journal.ppat.1000345>
- Dassault Systèmes BIOVIA. (2018). *Discovery Studio Visualization*. Version 19, San Diego: Dassault Systèmes,. <https://www.3dsbiovia.com/products/collaborative-science/biovia-discovery-studio/visualization-download.php>
- De-Eknamkul, W., & Potduang, B. (2003). Biosynthesis of  $\beta$ -sitosterol and stigmasterol in *Croton sublyratus* proceeds via a mixed origin of isoprene units. *Phytochemistry*, 62(3), 389–398.  
[https://doi.org/10.1016/S0031-9422\(02\)00555-1](https://doi.org/10.1016/S0031-9422(02)00555-1)
- de Béthune, M. P. (2010). Non-nucleoside reverse transcriptase inhibitors (NNRTIs), their discovery, development, and use in the treatment of HIV-1 infection: A review of the last 20 years (1989-2009). In *Antiviral Research*. <https://doi.org/10.1016/j.antiviral.2009.09.008>
- De Clercq, E. (2004). Antiviral drugs in current clinical use. In *Journal of Clinical Virology*.  
<https://doi.org/10.1016/j.jcv.2004.02.009>
- De Lima, F. O., Alves, V., Filho, J. M. B., Da Silva Almeida, J. R. G., Rodrigues, L. C., Soares, M. B. P., & Villarreal, C. F. (2013). Antinociceptive effect of lupeol: Evidence for a role of cytokines inhibition. *Phytotherapy Research*, 27(10), 1557–1563.  
<https://doi.org/10.1002/ptr.4902>

- De Paula, A. C. B., Gracioso, J. S., Toma, W., Hiruma-Lima, C. A., Carneiro, E. M., & Souza Brito, A. R. M. (2008). The antiulcer effect of *Croton cajucara* Benth in normoproteic and malnourished rats. *Phytomedicine*. <https://doi.org/10.1016/j.phymed.2008.02.024>
- Degu, A., Engidawork, E., & Shibeshi, W. (2016). Evaluation of the anti-diarrheal activity of the leaf extract of *Croton macrostachyus* Hocst. ex Del. (Euphorbiaceae) in mice model. *BMC Complementary and Alternative Medicine*. <https://doi.org/10.1186/s12906-016-1357-9>
- Desta, B. (1993). Ethiopian traditional herbal drugs. Part II: Antimicrobial activity of 63 medicinal plants. *Journal of Ethnopharmacology*. [https://doi.org/10.1016/0378-8741\(93\)90028-4](https://doi.org/10.1016/0378-8741(93)90028-4)
- di Marzo Veronese, F., Copeland, T. D., DeVico, A. L., Rahman, R., Oroszlan, S., Gallo, R. C., & Sarngadharan, M. G. (1986). Characterization of highly immunogenic p66/p51 as the reverse transcriptase of HTLV-III/LAV. *Science*, *231*(4743), 1289–1291.
- Ding, J., Das, K., Moereels, H., Koymans, L., Andries, K., Janssen, P. A. J., Hughes, S. H., & Arnold, E. (1995). Structure of HIV-1 RT/TIBO R 86183 complex reveals similarity in the binding of diverse nonnucleoside inhibitors. *Nature Structural Biology*, *2*(5), 407–415. <https://doi.org/10.1038/nsb0595-407>
- Divya, S., Krishna, K. N., Ramachandran, S., & Dhanaraju, M. D. (2011). Wound Healing and In Vitro Antioxidant Activities of *Croton bonplandianum* Leaf Extract in Rats. *Global Journal of Pharmacology*.
- Donati, M., Mondin, A., Chen, Z., Miranda, F. M., Do Nascimento, B. B., Schirato, G., Pastore, P., & Frolidi, G. (2015). Radical scavenging and antimicrobial activities of *Croton zehntneri*, *Pterodon emarginatus* and *Schinopsis brasiliensis* essential oils and their major constituents: Estragole, trans -anethole,  $\beta$ -caryophyllene and myrcene. *Natural Product Research*. <https://doi.org/10.1080/14786419.2014.964709>
- Douek, D. C., Brenchley, J. M., Betts, M. R., Ambrozak, D. R., Hill, B. J., Okamoto, Y., Casazza, J. P., Kuruppu, J., Kunstman, K., Wolinsky, S., Grossman, Z., Dybul, M., Oxenius, A., Price, D. A., Connors, M., & Koup, R. A. (2002). HIV preferentially infects HIV-specific CD4+ T cells. *Nature*. <https://doi.org/10.1038/417095a>
- Dragic, T., Trkola, A., Thompson, D. A. D., Cormier, E. G., Kajumo, F. A., Maxwell, E., Lin, S. W., Ying, W., Smith, S. O., Sakmar, T. P., & Moore, J. P. (2000). A binding pocket for a small molecule inhibitor of HIV-1 entry within the transmembrane helices of CCR5. *Proceedings of the National Academy of Sciences*. <https://doi.org/10.1073/pnas.090576697>



- Duan, H., Takaishi, Y., Imakura, Y., Jia, Y., Li, D., Cosentino, L. M., & Lee, K. H. (2000). Sesquiterpene alkaloids from *Tripterygium hypoglaucum* and *Tripterygium wilfordii*: A new class of potent anti-HIV agents. *Journal of Natural Products*, 63(3), 357–361. <https://doi.org/10.1021/np990281s>
- Dubale, A. A., Chandravanshi, B. S., & Gebremariam, K. F. (2015). Levels of major and trace metals in the leaves and infusions of *Croton macrostachyus*. *Bulletin of the Chemical Society of Ethiopia*. <https://doi.org/10.4314/bcse.v29i1.2>
- Duric, K., Kovac-Besovic, E., Niksic, H., & Sofic, E. (2013). Antibacterial Activity of Methanolic Extracts, Decoction and Isolated Triterpene Products from Different Parts of Birch, *Betula pendula*, Roth. *Journal of Plant Studies*. <https://doi.org/10.5539/jps.v2n2p61>
- E., L., E., K., T., B., & H., Y. (2008). An ethnobotanical study of medicinal plants in Mana Angetu district, southeastern Ethiopia. *Journal of Ethnobiology and Ethnomedicine*.
- Ebeling, S., Naumann, K., Pollok, S., Wardecki, T., Vidal-y-Sy, S., Nascimento, J. M., Boerries, M., Schmidt, G., Brandner, J. M., & Merfort, I. (2014). From a traditional medicinal plant to a rational drug: Understanding the clinically proven wound healing efficacy of birch bark extract. *PLoS ONE*. <https://doi.org/10.1371/journal.pone.0086147>
- Echevarria, K. L., Hardin, T. C., & Smith, J. A. (1999). Hyperlipidemia associated with protease inhibitor therapy. *Annals of Pharmacotherapy*. <https://doi.org/10.1345/aph.18174>
- Edwards S, Tadesse M., and H. I. (1995). *Flora of Ethiopia and Eritrea: Canellaceae to Euphorbiaceae: Vol. 2.2.*
- Egualé, T., Tilahun, G., Debella, A., Feleke, A., & Makonnen, E. (2007). *In vitro* and *in vivo* anthelmintic activity of crude extracts of *Coriandrum sativum* against *Haemonchus contortus*. *Journal of Ethnopharmacology*. <https://doi.org/10.1016/j.jep.2006.10.003>
- El-Mekkawy, S., Meselhy, M. R., Nakamura, N., Hattori, M., Kawahata, T., & Otake, T. (2000). Anti-HIV-1 phorbol esters from the seeds of *Croton tiglium*. *Phytochemistry*. [https://doi.org/10.1016/S0031-9422\(99\)00556-7](https://doi.org/10.1016/S0031-9422(99)00556-7)
- El-Mekkawy, S., Meselhy, M. R., Nakamura, N., Tezuka, Y., Hattori, M., Kakiuchi, N., Shimotohno, K., Kawahata, T., & Otake, T. (1998). Anti-HIV-1 and anti-HIV-1-protease substances from *Ganoderma lucidum*. *Phytochemistry*. [https://doi.org/10.1016/S0031-9422\(98\)00254-4](https://doi.org/10.1016/S0031-9422(98)00254-4)
- Engelman, A., Bushman, F. D., & Craigie, R. (1993). Identification of discrete functional domains

- of HIV-1 integrase and their organization within an active multimeric complex. *The EMBO Journal*, 12(8), 3269–3275.
- Engelman, A., & Cherepanov, P. (2012). The structural biology of HIV-1: Mechanistic and therapeutic insights. In *Nature Reviews Microbiology*. <https://doi.org/10.1038/nrmicro2747>
- Erik. (2010). Antiretroviral drugs. In *Current Opinion in Pharmacology*. <https://doi.org/10.1016/j.coph.2010.04.011>
- Esposito, F., Mandrone, M., Del Vecchio, C., Carli, I., Distinto, S., Corona, A., Lianza, M., Piano, D., Tacchini, M., Maccioni, E., Cottiglia, F., Saccon, E., Poli, F., Parolin, C., & Tramontano, E. (2017). Multi-target activity of *Hemidesmus indicus* decoction against innovative HIV-1 drug targets and characterization of Lupeol mode of action. *Pathogens and Disease*, 75(6). <https://doi.org/10.1093/femspd/ftx065>
- Esposito, F., Sanna, C., Del Vecchio, C., Cannas, V., Venditti, A., Corona, A., Bianco, A., Serrilli, A. M., Guarcini, L., Parolin, C., Ballero, M., & Tramontano, E. (2013). *Hypericum hircinum* L. Components as new single-molecule inhibitors of both HIV-1 reverse transcriptase-associated DNA polymerase and ribonuclease H activities. *Pathogens and Disease*, 68(3), 116–124. <https://doi.org/10.1111/2049-632X.12051>
- Esté, J. A., & Telenti, A. (2007). HIV entry inhibitors. In *Lancet*. [https://doi.org/10.1016/S0140-6736\(07\)61052-6](https://doi.org/10.1016/S0140-6736(07)61052-6)
- Evans, S. R., Ellis, R. J., Chen, H., Yeh, T. M., Lee, A. J., Schifitto, G., Wu, K., Bosch, R. J., McArthur, J. C., Simpson, D. M., & Clifford, D. B. (2011). Peripheral neuropathy in HIV: Prevalence and risk factors. *AIDS*. <https://doi.org/10.1097/QAD.0b013e328345889d>
- Fassati, A., & Goff, S. P. (2001). Characterization of Intracellular Reverse Transcription Complexes of Human Immunodeficiency Virus Type 1. *Journal of Virology*. <https://doi.org/10.1128/JVI.75.8.3626-3635.2001>
- Ferreira De Freitas, R., & Schapira, M. (2017a). A systematic analysis of atomic protein-ligand interactions in the PDB. *MedChemComm*, 8(10), 1970–1981. <https://doi.org/10.1039/c7md00381a>
- Ferreira De Freitas, R., & Schapira, M. (2017b). A systematic analysis of atomic protein–ligand interactions in the PDB. *MedChemComm*, 8(10), 1970–1981. <https://doi.org/10.1039/C7MD00381A>
- Fettig, J., Swaminathan, M., Murrill, C. S., & Kaplan, J. E. (2014). Global epidemiology of HIV.

- In *Infectious Disease Clinics of North America*. <https://doi.org/10.1016/j.idc.2014.05.001>
- Focho, D. A., Newu, M. C., Anjah, M. G., Nwana, F. A., & Ambo, F. B. (2009). Ethnobotanical survey of trees in Fundong, Northwest Region, Cameroon. *Journal of Ethnobiology and Ethnomedicine*. <https://doi.org/10.1186/1746-4269-5-17>
- Fontenelle, R. O. S., Morais, S. M., Brito, E. H. S., Brilhante, R. S. N., Cordeiro, R. A., Nascimento, N. R. F., Kerntopf, M. R., Sidrim, J. J. C., & Rocha, M. F. G. (2008). Antifungal activity of essential oils of Croton species from the Brazilian Caatinga biome. *Journal of Applied Microbiology*. <https://doi.org/10.1111/j.1365-2672.2007.03707.x>
- Foster, C., & Lyall, H. (2008). HIV and mitochondrial toxicity in children. *Journal of Antimicrobial Chemotherapy*. <https://doi.org/10.1093/jac/dkm411>
- Fox, J., & Fidler, S. (2010). Sexual transmission of HIV-1. In *Antiviral Research*. <https://doi.org/10.1016/j.antiviral.2009.10.012>
- Frankel, A. D., & Young, J. A. T. (1998). HIV-1: Fifteen Proteins and an RNA. *Annual Review of Biochemistry*. <https://doi.org/10.1146/annurev.biochem.67.1.1>
- Fransen, S., Gupta, S., Danovich, R., Hazuda, D., Miller, M., Witmer, M., Petropoulos, C. J., & Huang, W. (2009). Loss of Raltegravir Susceptibility by Human Immunodeficiency Virus Type 1 Is Conferred via Multiple Nonoverlapping Genetic Pathways. *Journal of Virology*. <https://doi.org/10.1128/JVI.01168-09>
- Fratkin, E. (1996). Traditional medicine and concepts of healing among Samburu pastoralists of Kenya. *Journal of Ethnobiology*.
- Freed, E. O. (1998). HIV-1 Gag proteins: Diverse functions in the virus life cycle. In *Virology*. <https://doi.org/10.1006/viro.1998.9398>
- Freed, E. O. (2001). HIV-1 replication. In *Somatic Cell and Molecular Genetics*. <https://doi.org/10.1023/A:1021070512287>
- Freires, I. A., Denny, C., Benso, B., De Alencar, S. M., & Rosalen, P. L. (2015). Antibacterial activity of essential oils and their isolated constituents against cariogenic bacteria: A systematic review. In *Molecules*. <https://doi.org/10.3390/molecules20047329>
- Froldi, G., Zagotto, G., Filippini, R., Montopoli, M., Dorigo, P., & Caparrotta, L. (2009). Activity of sap from *Croton lechleri* on rat vascular and gastric smooth muscles. *Phytomedicine*. <https://doi.org/10.1016/j.phymed.2009.02.003>
- Fuller, R. W., Blunt, J. W., Boswell, J. L., Cardellina, J. H., & Boyd, M. R. (1999). Guttiferone F,

- the first prenylated benzophenone from *Allanblackia stuhlmannii*. *Journal of Natural Products*, 62(1), 130–132. <https://doi.org/10.1021/np9801514>
- Gakuubi, M. M., & Wanzala, W. (2012). A survey of plants and plant products traditionally used in livestock health management in Buuri district, Meru County, Kenya. *Journal of Ethnobiology and Ethnomedicine*. <https://doi.org/10.1186/1746-4269-8-39>
- Galinis, D. L., Fuller, R. W., McKee, T. C., Cardellina, J. H., Gulakowski, R. J., McMahon, J. B., & Boyd, M. R. (1996). Structure-activity modifications of the HIV-1 inhibitors (+)-calanolide A and (-)-calanolide B. *Journal of Medicinal Chemistry*, 39(22), 4507–4510. <https://doi.org/10.1021/jm9602827>
- Gallant, J. E. (2006). The M184V mutation: What it does, how to prevent it, and what to do with it when it's there. In *AIDS Reader*.
- Gallo, R. C., Sarin, P. S., Gelmann, E. P., Robert-Guroff, M., Richardson, E., Kalyanaraman, V. S., Mann, D., Sidhu, G. D., Stahl, R. E., Zolla-Pazner, S., Leibowitch, J., & Popovic, M. (1983). Isolation of human T-cell leukemia virus in acquired immune deficiency syndrome (AIDS). *Science*. <https://doi.org/10.1126/science.6601823>
- Gao, H.-Q., Boyer, P. L., Arnold, E., & Hughes, S. H. (1998). Effects of mutations in the polymerase domain on the polymerase, RNase H and strand transfer activities of human immunodeficiency virus type 1 reverse transcriptase. *Journal of Molecular Biology*, 277(3), 559–572.
- Gao, Y., Nankya, I., Abraha, A., Troyer, R. M., Nelson, K. N., Rubio, A., & Arts, E. J. (2009). Calculating HIV-1 infectious titre using a virtual TCID<sub>50</sub> method. *Methods in Molecular Biology*. [https://doi.org/10.1007/978-1-59745-170-3\\_3](https://doi.org/10.1007/978-1-59745-170-3_3)
- Geetha, T., & Varalakshmi, P. (1998). Anti-inflammatory activity of lupeol and lupeol linoleate in adjuvant- induced arthritis. *Fitoterapia*.
- Gelmon, L., Kenya, P., Oguya, F., Cheluget, B., Haile, G., & Kenya Ministry of Health. (2009). Kenya: HIV prevention response and modes of transmission analysis. *Kenya National AIDS Control Council*. <https://doi.org/10.1021/ja01139a010>
- Gemechu, A., Giday, M., Worku, A., & Ameni, G. (2013). In vitro Anti-mycobacterial activity of selected medicinal plants against *Mycobacterium tuberculosis* and *Mycobacterium bovis* Strains. *BMC Complementary and Alternative Medicine*. <https://doi.org/10.1186/1472-6882-13-291>

- Gerencsér, M., Turecek, P. L., Kistner, O., Mitterer, A., Savidis-Dacho, H., & Barrett, N. P. (2006). In vitro and in vivo anti-retroviral activity of the substance purified from the aqueous extract of *Chelidonium majus* L. *Antiviral Research*, 72(2), 153–156.  
<https://doi.org/10.1016/j.antiviral.2006.03.008>
- Gerton, J. L., Ohgi, S., Olsen, M., DeRisi, J., & Brown, P. O. (1998). Effects of mutations in residues near the active site of human immunodeficiency virus type 1 integrase on specific enzyme-substrate interactions. *Journal of Virology*, 72(6), 5046–5055.
- Ghose, A. K., Viswanadhan, V. N., & Wendoloski, J. J. (1999). A knowledge-based approach in designing combinatorial or medicinal chemistry libraries for drug discovery. 1. A qualitative and quantitative characterization of known drug databases. *Journal of Combinatorial Chemistry*, 1(1), 55–68. <https://doi.org/10.1021/cc9800071>
- Ghosh, M., Jacques, P. S., Rodgers, D. W., Ottman, M., Darlix, J.-L., & Le Grice, S. F. J. (1996). Alterations to the primer grip of p66 HIV-1 reverse transcriptase and their consequences for template-primer utilization. *Biochemistry*, 35(26), 8553–8562.
- Giang, P. M., Jin, H. Z., Son, P. T., Lee, J. H., Hong, Y. S., & Lee, J. J. (2003). ent-Kaurane diterpenoids from *Croton tonkinensis* inhibit LPS-induced NF-kappaB activation and NO production. *Journal of Natural Products*. <https://doi.org/10.1021/np030139y>
- Giang, P. M., Son, P. T., Matsunami, K., & Otsuka, H. (2006). Anti-staphylococcal activity of ent-kaurane-type diterpenoids from *Croton tonkinensis*. *Journal of Natural Medicines*. <https://doi.org/10.1007/s11418-005-0011-5>
- Gichui, W. G. (2016). Antinociceptive activities of extracts of *Croton megalocarpus* Hutch. (Euphorbiaceae) using animal models. M.Sc. Thesis, University of Nairobi, Nairobi.
- Giorgi, R., Batatinha, M. J. M., Bernardi, M. M., DeSouza-Spinosa, H., Spinosa, F. R. N., & Palermo-Neto, J. (1991). Effects of *Croton zehntneri* aqueous extracts on some cholinergic- and dopaminergic-related behaviours of laboratory rodents. *Journal of Ethnopharmacology*. [https://doi.org/10.1016/0378-8741\(91\)90036-D](https://doi.org/10.1016/0378-8741(91)90036-D)
- Gomes, G. P., De Souza, T. M., De Paula Freire, G., Farias, D. F., Cunha, A. P., Ricardo, N. M. P. S., De Moraes, S. M., & Carvalho, A. F. U. (2013). Further insecticidal activities of essential oils from *Lippia sidoides* and *Croton* species against *Aedes aegypti* L. *Parasitology Research*. <https://doi.org/10.1007/s00436-013-3351-1>
- Götte, M., Li, X., & Wainberg, M. A. (1999). HIV-1 reverse transcription: A brief overview

- focused on structure- function relationships among molecules involved in initiation of the reaction. *Archives of Biochemistry and Biophysics*, 365(2), 199–210.  
<https://doi.org/10.1006/abbi.1999.1209>
- Gottlieb, M. S., Schroff, R., Schanker, H. M., Weisman, J. D., Fan, P. T., Wolf, R. A., & Saxon, A. (1981). Pneumocystis carinii Pneumonia and Mucosal Candidiasis in Previously Healthy Homosexual Men: Evidence of a New Acquired Cellular Immunodeficiency. *N Engl J Med*.  
<https://doi.org/10.1056/NEJM198112103052401>
- Govaerts, R., Frodin, D. G., & Radcliffe-Smith, A. (2000). World Checklist and Bibliography of Euphorbiaceae (with Pandaceae): *Croton excoecariopsis*. In *World Checklists and Bibliographies*. <https://doi.org/10.2307/2666560>
- Graham, J. G., Quinn, M. L., Fabricant, D. S., & Farnsworth, N. R. (2000). Plants used against cancer - An extension of the work of Jonathan Hartwell. In *Journal of Ethnopharmacology*.  
[https://doi.org/10.1016/S0378-8741\(00\)00341-X](https://doi.org/10.1016/S0378-8741(00)00341-X)
- Graikou, K., Aligiannis, N., Chinou, I., Skaltsounis, A.-L., Tillequin, F., & Litaudon, M. (2005). Chemical Constituents from *Croton insularis*. *Helvetica Chimica Acta*, 88(10), 2654–2660.  
<https://doi.org/10.1002/hlca.200590206>
- Granchi, C., Capecchi, A., Frate, G. Del, Martinelli, A., Macchia, M., Minutolo, F., & Tuccinardi, T. (2015). Development and Validation of a Docking-Based Virtual Screening Platform for the Identification of New Lactate Dehydrogenase Inhibitors. *Molecules*, 20(5), 8772.  
<https://doi.org/10.3390/MOLECULES20058772>
- Gray, J. M., & Cohn, D. L. (2013). Tuberculosis and HIV coinfection. *Seminars in Respiratory and Critical Care Medicine*. <https://doi.org/10.1055/s-0032-1333469>
- Grossman, Z., Meier-Schellersheim, M., Sousa, A. E., Victorino, R. M. M., & Paul, W. E. (2002). CD4+T-cell depletion in HIV infection: Are we closer to understanding the cause? *Nature Medicine*. <https://doi.org/10.1038/nm0402-319>
- Guerrero, M. F., Carrón, R., Martín, M. L., San Román, L., & Reguero, M. T. (2001a). Antihypertensive and vasorelaxant effects of aqueous extract from *Croton schiedeanus* Schlecht in rats. *Journal of Ethnopharmacology*, 75(1), 33–36.  
[https://doi.org/10.1016/S0378-8741\(00\)00391-3](https://doi.org/10.1016/S0378-8741(00)00391-3)
- Guerrero, M. F., Carrón, R., Martín, M. L., San Román, L., & Reguero, M. T. (2001b). Antihypertensive and vasorelaxant effects of aqueous extract from *Croton schiedeanus*

- Schlecht in rats. *Journal of Ethnopharmacology*. [https://doi.org/10.1016/S0378-8741\(00\)00391-3](https://doi.org/10.1016/S0378-8741(00)00391-3)
- Guerrero, M. F., Puebla, P., Carrón, R., Martín, M. L., Arteaga, L., & Román, L. S. (2002). Assessment of the antihypertensive and vasodilator effects of ethanolic extracts of some Colombian medicinal plants. *Journal of Ethnopharmacology*. [https://doi.org/10.1016/S0378-8741\(01\)00420-2](https://doi.org/10.1016/S0378-8741(01)00420-2)
- Guerrero, M. F., Puebla, P., Carrón, R., Martín, M. L., & San Román, L. (2004). Vasorelaxant effect of new neo-clerodane diterpenoids isolated from *Croton schiedeanus*. *Journal of Ethnopharmacology*. <https://doi.org/10.1016/j.jep.2004.05.018>
- Gupta, M., Mazumder, U. K., Vamsi, M. L. M., Sivakumar, T., & Kandar, C. C. (2004). Anti-steroidogenic activity of the two Indian medicinal plants in mice. *Journal of Ethnopharmacology*. <https://doi.org/10.1016/j.jep.2003.09.002>
- Gupta, M. P., Monge, A., Karikas, G. A., DeCeraín, A. L., Solis, P. N., DeLeon, E., Trujillo, M., Suarez, O., Wilson, F., Montenegro, G., Noriega, Y., Santana, A. I., Correa, M., & Sanchez, C. (1996). Screening of Panamanian medicinal plants for brine shrimp toxicity, crown gall tumor inhibition, cytotoxicity and DNA intercalation. *International Journal of Pharmacognosy*. <https://doi.org/10.1076/phbi.34.1.19.13180>
- Gupta, R. K., Jordan, M. R., Sultan, B. J., Hill, A., Davis, D. H. J., Gregson, J., Sawyer, A. W., Hamers, R. L., Ndembi, N., Pillay, D., & Bertagnolio, S. (2012). Global trends in antiretroviral resistance in treatment-naïve individuals with HIV after rollout of antiretroviral treatment in resource-limited settings: A global collaborative study and meta-regression analysis. *The Lancet*. [https://doi.org/10.1016/S0140-6736\(12\)61038-1](https://doi.org/10.1016/S0140-6736(12)61038-1)
- Gurgel, L. A., Sidrim, J. J. C., Martins, D. T., Filho, V. C., & Rao, V. S. (2005). In vitro antifungal activity of dragon's blood from *Croton urucurana* against dermatophytes. *Journal of Ethnopharmacology*. <https://doi.org/10.1016/j.jep.2004.11.033>
- Gurung, A. B., Ali, M. A., Lee, J., Farah, M. A., & Al-Anazi, K. M. (2021). An Updated Review of Computer-Aided Drug Design and Its Application to COVID-19. *BioMed Research International, 2021*. <https://doi.org/10.1155/2021/8853056>
- Gustafson, K. R., McKee, T. C., & Bokesch, H. R. (2004). Anti-HIV cyclotides. *Current Protein & Peptide Science*. <https://doi.org/10.2174/1389203043379468>
- Gutiérrez-Nicolás, F., Gordillo-Román, B., Oberti, J. C., Estévez-Braun, A., Ravelo, Á. G., &

- Joseph-Nathan, P. (2012). Synthesis and anti-HIV activity of lupane and olean-18-ene derivatives. Absolute configuration of 19,20-epoxylupanes by VCD. *Journal of Natural Products*, 75(4), 669–676. <https://doi.org/10.1021/np200910u>
- Hajimahdi, Z., & Zarghi, A. (2016). Progress in HIV-1 integrase inhibitors: A review of their chemical structure diversity. *Iranian Journal of Pharmaceutical Research*, 15(4), 595–628. <https://doi.org/10.22037/ijpr.2016.1935>
- Harada, S., Koyanagi, Y., & Yamamoto, N. (1985). Infection of HTLV-III/LAV in HTLV-I-carrying cells MT-2 and MT-4 and application in a plaque assay. *Science*. <https://doi.org/10.1126/science.2992081>
- Harada, S., & Yamamoto, N. (1985). Quantitative Analysis of Aids-Related Virus-Carrying Cells by Plaque-Forming Assay Using an Htlv-I-Positive Mt-4 Cell Line. *Japanese Journal of Cancer Research GANN*. <https://doi.org/10.1016/j.joms.2006.09.031>
- Hare, S., Vos, A. M., Clayton, R. F., Thuring, J. W., Cummings, M. D., & Cherepanov, P. (2010). Molecular mechanisms of retroviral integrase inhibition and the evolution of viral resistance. *Proceedings of the National Academy of Sciences*. <https://doi.org/10.1073/pnas.1010246107>
- Harinantenaina, L., & Asakawa, Y. (2007). Malagasy Liverworts, Source of New and Biologically Active Compounds. *Natural Product Communications*, 2(6), 1934578X0700200. <https://doi.org/10.1177/1934578X0700200616>
- Harinantenaina, L., Takahara, Y., Nishizawa, T., Kohchi, C., Soma, G. I., & Asakawa, Y. (2006). Chemical constituents of malagasy liverworts, part V: Prenyl bibenzyls and clerodane diterpenoids with nitric oxide inhibitory activity from *Radula appressa* and *Thysananthus spathulistipus*. *Chemical and Pharmaceutical Bulletin*. <https://doi.org/10.1248/cpb.54.1046>
- Hasegawa, H., Matsumiya, S., Uchiyama, M., Kurokawa, T., Inouye, Y., Kasai, R., Ishibashi, S., & Yamasaki, K. (1994). Inhibitory effect of some triterpenoid saponins on glucose transport in tumor cells and its application to in vitro cytotoxic and antiviral activities. *Planta Medica*, 60(3), 240–243. <https://doi.org/10.1055/s-2006-959467>
- Hayashi, K., Kamiya, M., & Hayashi, T. (1995). Virucidal effects of the steam distillate from *Houttuynia cordata* and its components on HSV-1, influenza virus, and HIV. *Planta Medica*, 61(3), 237–241. <https://doi.org/10.1055/s-2006-958063>
- Hazenbergh, M. D., Otto, S. A., Hamann, D., Roos, M. T. L., Schuitemaker, H., De Boer, R. J., & Miedema, F. (2003). Depletion of naive CD4 T cells by CXCR4-using HIV-1 variants occurs



- mainly through increased T-cell death and activation. *AIDS*.  
<https://doi.org/10.1097/00002030-200307040-00001>
- Hazuda, D. J., Felock, P., Witmer, M., Wolfe, A., Stillmock, K., Grobler, J. A., Espeseth, A., Gabryelski, L., Schleif, W., Blau, C., & Miller, M. D. (2000). Inhibitors of strand transfer that prevent integration and inhibit HIV-1 replication in cells. *Science*.  
<https://doi.org/10.1126/science.287.5453.646>
- Hedberg, I., Hedberg, O., Madat, P. J., Mshigeni, K. E., Mshiu, E. N., & Samuelsson, G. (1983). Inventory of plants used in traditional medicine in Tanzania. II. Plants of the families dilleniaceae—Opiliaceae. *Journal of Ethnopharmacology*, 9(1).  
[https://doi.org/10.1016/0378-8741\(83\)90030-2](https://doi.org/10.1016/0378-8741(83)90030-2)
- Heeney, J. L., Dalglish, A. G., & Weiss, R. A. (2006). Origins of HIV and the evolution of resistance to AIDS. In *Science*. <https://doi.org/10.1126/science.1123016>
- Herbert, S., Chung, E., & Waters, L. (2014). HIV Treatment. *Current Treatment Options in Infectious Diseases*. <https://doi.org/10.1007/s40506-014-0023-3>
- Herman, J. S., & Easterbrook, P. J. (2001). The metabolic toxicities of antiretroviral therapy. In *International Journal of STD and AIDS*. <https://doi.org/10.1258/0956462011923714>
- Hornak, V., Okur, A., Rizzo, R. C., & Simmerling, C. (2006). HIV-1 protease flaps spontaneously open and reclose in molecular dynamics simulations. *Proceedings of the National Academy of Sciences*, 103(4), 915–920.
- Hort, M. A., Straliootto, M. R., Duz, M. S., Netto, P. M., Souza, C. B., Schulz, T., Horst, H., Pizzolatti, M. G., de Bem, A. F., & Ribeiro-do-Valle, R. M. (2012). Cardioprotective effects of a proanthocyanidin-rich fraction from *Croton celtidifolius* Baill: Focus on atherosclerosis. *Food and Chemical Toxicology*. <https://doi.org/10.1016/j.fct.2012.07.050>
- Hsieh, P. W., Chang, F. R., Lee, K. H., Hwang, T. L., Chang, S. M., & Wu, Y. C. (2004). A new anti-HIV alkaloid, drymaritin, and a new C-glycoside flavonoid, diandraflavone, from *Drymaria diandra*. *Journal of Natural Products*, 67(7), 1175–1177.  
<https://doi.org/10.1021/np0400196>
- Hsiou, Y., Ding, J., Das, K., Clark, A. D., Hughes, S. H., & Arnold, E. (1996). Structure of unliganded HIV-1 reverse transcriptase at 2.7 Å resolution: Implications of conformational changes for polymerization and inhibition mechanisms. *Structure*, 4(7), 853–860.  
[https://doi.org/10.1016/S0969-2126\(96\)00091-3](https://doi.org/10.1016/S0969-2126(96)00091-3)

- Hughes, W.-S. H. and S. H. (2014). HIV-1 reverse transcription. *Methods in Molecular Biology*, 1087, 55–70. [https://doi.org/10.1007/978-1-62703-670-2\\_6](https://doi.org/10.1007/978-1-62703-670-2_6)
- Hull, M. W., & Montaner, J. S. G. (2011). Ritonavir-boosted protease inhibitors in HIV therapy. *Annals of Medicine*. <https://doi.org/10.3109/07853890.2011.572905>
- Hussein, G., Miyashiro, H., Nakamura, N., Hattori, M., Kawahata, T., Otake, T., Kakiuchi, N., & Shimotohno, K. (1999). Inhibitory effects of Sudanese plant extracts on HIV-1 replication and HIV-1 protease. *Phytotherapy Research*, 13(1), 31–36. [https://doi.org/10.1002/\(SICI\)1099-1573\(199902\)13:1<31::AID-PTR381>3.0.CO;2-C](https://doi.org/10.1002/(SICI)1099-1573(199902)13:1<31::AID-PTR381>3.0.CO;2-C)
- Hyde, M.A., B.T. Wursten, P. B. and S. D. (2012). *Flora of mozambique: species information: Urera trinervis*. [http://www.mozambiqueflora.com/speciesdata/species.php?species\\_id=120490](http://www.mozambiqueflora.com/speciesdata/species.php?species_id=120490).
- Hyde, M.A., B. T. W. and P. B. (2013). *Flora of Zimbabwe: Species information: Kirkia acuminata*. [http://www.zimbabweflora.co.zw/speciesdata/species.php?species\\_id=133250](http://www.zimbabweflora.co.zw/speciesdata/species.php?species_id=133250).
- Ibrahim, F., & Ibrahim, B. (1998). The Maasai herbalists in Arusha town, Tanzania. *GeoJournal*. <https://doi.org/10.1023/A:1006963632571>
- Ichikawa, M. (1987). A preliminary report on the ethnobotany of the Suei Dorobo in Northern Kenya. *African Study Monographs, Suppl.* <https://doi.org/DOI 10.1016/j.seizure.2009.06.009>
- Inzaule, S. C., Weidle, P. J., Yang, C., Ndiege, K., Hamers, R. L., de Wit, T. F. R., Thomas, T., & Zeh, C. (2016). Prevalence and dynamics of the K65R drug resistance mutation in HIV-1-infected infants exposed to maternal therapy with lamivudine, zidovudine and either nevirapine or nelfinavir in breast milk. *Journal of Antimicrobial Chemotherapy*. <https://doi.org/10.1093/jac/dkw039>
- Ishima, R., Ghirlando, R., Tözsér, J., Gronenborn, A. M., Torchia, D. A., & Louis, J. M. (2001). Folded monomer of HIV-1 protease. *Journal of Biological Chemistry*, 276(52), 49110–49116.
- Ismail, T., & Lee, C. (2011). HIV associated opportunistic pneumonias. *Medical Journal of Malaysia*. <https://doi.org/10.1111/j.1440-1843.2009.01534.x>
- Jacobo-Molina, A., Ding, J., Nanni, R. G., Clark, A. D., Lu, X., Tantillo, C., Williams, R. L., Kamer, G., Ferris, A. L., & Clark, P. (1993). Crystal structure of human immunodeficiency virus type 1 reverse transcriptase complexed with double-stranded DNA at 3.0 Å resolution shows bent DNA. *Proceedings of the National Academy of Sciences*, 90(13), 6320–6324.

- James H. Strauss, & Strauss, E. G. (2008). Viruses and Human diseases. In *感染症誌* (Vol. 91). British Library.
- Jamila, N., Khairuddean, M., Khan, S. N., Khan, N., & Osman, H. (2014). Phytochemicals from the Bark of *Garcinia hombroniana* and their biological activities. *Nat. Prod*, 8, 312–316.
- Jang, W. S., Jyoti, M. A., Kim, S., Nam, K. W., Ha, T. K. Q., Oh, W. K., & Song, H. Y. (2016). In vitro antituberculosis activity of diterpenoids from the Vietnamese medicinal plant *Croton tonkinensis*. *Journal of Natural Medicines*. <https://doi.org/10.1007/s11418-015-0937-1>
- Jeeshna, M. V., Paulsamy, S., & Mallikadevi, T. (2011). Phytochemical Constituents and Antimicrobial Studies of the Exotic Plant Species, *Croton bonplandianum* Baill. *Journal of Life Sciences*. <https://doi.org/10.1080/09751270.2011.11885165>
- Jeruto, P., Lukhoba, C., Ouma, G., Otieno, D., & Mutai, C. (2008). An ethnobotanical study of medicinal plants used by the Nandi people in Kenya. *Journal of Ethnopharmacology*. <https://doi.org/10.1016/j.jep.2007.11.041>
- Jiratchariyakul, W., Wiwat, C., Vongsakul, M., Somanabandhu, A., Leelamanit, W., Fujii, I., Suwannaroj, N., & Ebizuka, Y. (2001). HIV inhibitor from Thai bitter gourd. *Planta Medica*, 67(4), 350–353. <https://doi.org/10.1055/s-2001-14323>
- Jogia, M. K., Andersen, R. J., Párkányi, L., Clardy, J., Dublin, H. T., & Sinclair, A. R. E. (1989). Crotofolane Diterpenoids from the African Shrub *Croton dichogamus* Pax. *Journal of Organic Chemistry*, 54(7), 1654–1657. <https://doi.org/10.1021/jo00268a029>
- Johns, T, Mahunnah, R. L. ., Sanaya, P., Chapman, L., & Ticktin, T. (1999). Saponins and phenolic content in plant dietary additives of a traditional subsistence community, the Batemi of Ngorongoro District, Tanzania. *Journal of Ethnopharmacology*, 66(1). [https://doi.org/10.1016/S0378-8741\(98\)00179-2](https://doi.org/10.1016/S0378-8741(98)00179-2)
- Johns, Timothy, Mhoro, E. B., Sanaya, P., & Kimanani, E. K. (1994). Herbal remedies of the Batemi of Ngorongoro District, Tanzania: a quantitative appraisal. *Economic Botany*. <https://doi.org/10.1007/BF02901389>
- Jones, K. (2003). Review of *Sangre de Drago* ( *Croton lechleri* ) - A South American Tree Sap in the Treatment of Diarrhea, Inflammation, Insect Bites, Viral Infections, and Wounds: Traditional Uses to Clinical Research. *The Journal of Alternative and Complementary Medicine*, 9(6), 877–896. <https://doi.org/10.1089/107555303771952235>
- Jung, K. Y., Kim, D. S., Oh, S. R., Lee, I. S., Lee, J. J., Lee, H. K., Shin, D. H., Kim, E. H., &

- Cheong, C. J. (1997). Sesquiterpene components from the flower buds of *Magnolia fargesii*. In *Archives of Pharmacal Research* (Vol. 20, Issue 4, pp. 363–367).  
<https://doi.org/10.1007/BF02976201>
- Kagan, R. M., Johnson, E. P., Siaw, M., Biswas, P., Chapman, D. S., Su, Z., Platt, J. L., & Pesano, R. L. (2012). A Genotypic Test for HIV-1 Tropism Combining Sanger Sequencing with Ultradeep Sequencing Predicts Virologic Response in Treatment-Experienced Patients. *PLoS ONE*. <https://doi.org/10.1371/journal.pone.0046334>
- Kakuda, T. N. (2000). Pharmacology of nucleoside and nucleotide reverse transcriptase inhibitor-induced mitochondrial toxicity. In *Clinical Therapeutics*. [https://doi.org/10.1016/S0149-2918\(00\)90004-3](https://doi.org/10.1016/S0149-2918(00)90004-3)
- Kalayou, S., Haileselassie, M., Gebre-egziabher, G., Tiku'e, T., Sahle, S., Taddele, H., & Ghezu, M. (2012). In-vitro antimicrobial activity screening of some ethnoveterinary medicinal plants traditionally used against mastitis, wound and gastrointestinal tract complication in Tigray Region, Ethiopia. *Asian Pacific Journal of Tropical Biomedicine*.  
[https://doi.org/10.1016/S2221-1691\(12\)60088-4](https://doi.org/10.1016/S2221-1691(12)60088-4)
- Kamanyi, A., Mbiantcha, M., Nguelefack, T. B., Ateufack, G., Watcho, P., Ndontsa, B. L., & Tane, P. (2009). Anti-nociceptive and anti-inflammatory activities of extracts from the stem bark of *Croton macrostachyus* (Euphorbiaceae) in mice and rats. *Journal of Complementary and Integrative Medicine*. <https://doi.org/10.2202/1553-3840.1255>
- Kamau, L. N., Mbaabu, P. M., Mbaria, J. M., Gathumbi, P. K., & Kiama, S. G. (2016). Ethnobotanical survey and threats to medicinal plants traditionally used for the management of human diseases in Nyeri County, Kenya. *Humanitas Medicine*, 6(3), 1–15.
- Kapingu, M. C., Guillaume, D., Mbwambo, Z. H., Moshi, M. J., Uliso, F. C., & Mahunnah, R. L. A. (2000). Diterpenoids from the roots of *Croton macrostachys*. *Phytochemistry*.  
[https://doi.org/10.1016/S0031-9422\(00\)00166-7](https://doi.org/10.1016/S0031-9422(00)00166-7)
- Kareru, P. G., Kenji, G. M., Gachanja, A. N., Keriko, J. M., & Mungai, G. (2007). Traditional medicines among the Embu and Mbeere peoples of Kenya. *African Journal of Traditional, Complementary and Alternative Medicines*. <https://doi.org/10.4314/ajtcam.v4i1.31193>
- Kariuki, D. K., Miaron, J. O., Mugweru, J., & Kerubo, L. O. (2014). Antibacterial Activity of Five Medicinal Plant Extracts Used By the Maasai People of Kenya. *International Journal of Humanities, Arts, Medicine and Sciences*.

- Karn, J., & Stoltzfus, C. M. (2012). Transcriptional and posttranscriptional regulation of HIV-1 gene expression. *Cold Spring Harbor Perspectives in Medicine*.  
<https://doi.org/10.1101/cshperspect.a006916>
- Karunamoorthi, K., & Ilango, K. (2010). Larvicidal activity of *Cymbopogon citratus* (DC) Stapf. and *Croton macrostachyus* Del. against *Anopheles arabiensis* Patton, a potent malaria vector. *European Review for Medical and Pharmacological Sciences*.
- Kawai, K., Tsuno, N. H., Kitayama, J., Okaji, Y., Yazawa, K., Asakage, M., Yamashita, H., Watanabe, T., Takahashi, K., & Nagawa, H. (2005). Anti-angiogenic properties of plaunotol. *Anti-Cancer Drugs*. <https://doi.org/10.1097/00001813-200504000-00006>
- Kawakami, S., Inagaki, M., Matsunami, K., Otsuka, H., Kawahata, M., & Yamaguchi, K. (2016). Crotofolane-Type Diterpenoids, Crotoascarins L–Q, and a Rearranged Crotofolane-Type Diterpenoid, Neocrotoascarin, from the Stems of *Croton cascarilloides*. *Chemical and Pharmaceutical Bulletin*, 64(10), 1492–1498. <https://doi.org/10.1248/CPB.C16-00500>
- Kawakami, S., Matsunami, K., Otsuka, H., Inagaki, M., Takeda, Y., Kawahata, M., & Yamaguchi, K. (2015). Crotoascarins I–K: Crotofolane-Type Diterpenoids, Crotoascarin  $\gamma$ , Isocrotofolane Glucoside and Phenolic Glycoside from the Leaves of *Croton cascarilloides*. *Chemical and Pharmaceutical Bulletin*, 63(12), 1047–1054.  
<https://doi.org/10.1248/CPB.C15-00635>
- Ke, C., Shi, Q., Fujioka, T., Zhang, D. C., Hu, C. Q., Jin, J. Q., Kilkuskie, R. E., & Lee, K. H. (1992). Anti-aids agents, 4. Tripterifordin, a novel anti-HIV principle from *Tripterigium wilfordii*: Isolation and structural elucidation. *Journal of Natural Products*, 55(1), 88–92.  
<https://doi.org/10.1021/np50079a013>
- Keerthana, G., Kalaivani, M. K., & Sumathy, A. (2013). In-vitro alpha amylase inhibitory and anti-oxidant activities of ethanolic leaf extract of *Croton bonplandianum*. *Asian Journal of Pharmaceutical and Clinical Research*. <https://doi.org/10.1159/000292358>
- Keter, L. K., & Mutiso, P. C. (2012). Ethnobotanical studies of medicinal plants used by Traditional Health Practitioners in the management of diabetes in Lower Eastern Province, Kenya. *Journal of Ethnopharmacology*. <https://doi.org/10.1016/j.jep.2011.10.014>
- Khanra, K., Panja, S., Choudhuri, I., Chakraborty, A., & Bhattacharyya, N. (2016). Antimicrobial and cytotoxicity effect of silver nanoparticle synthesized by *Croton bonplandianum* Baill. leaves. *Nanomed. Journal*. <https://doi.org/10.7508/nmj.2016.01.002>

- Kilby, J. M., Hopkins, S., Venetta, T. M., Dimassimo, B., Cloud, G. A., Lee, J. Y., Alldredge, L., Hunter, E., Lambert, D., Bolognesi, D., Matthews, T., Johnson, M. R., Nowak, M. A., Shaw, G. M., & Saag, M. S. (1998). Potent suppression of HIV-1 replication in humans by T-20, a peptide inhibitor of gp41-mediated virus entry. *Nature Medicine*.  
<https://doi.org/10.3952/physics.v58i1.3649>
- Kim, E. M. H. R. T. J. (2001). Purification, Structure Determination and Biological Activities of 20(29)-lupen-3-one from *Daedaleopsis tricolor* (Bull.ex Fr.) Bond.et Sing. *Bulletin of the Korean Chemical Society*, 22(1), 59–62.
- Kipkore, W., Wanjohi, B., Rono, H., & Kigen, G. (2014). A study of the medicinal plants used by the Marakwet Community in Kenya. *Journal of Ethnobiology and Ethnomedicine*.  
<https://doi.org/10.1186/1746-4269-10-24>
- Kiringe, J. (2006). A Survey of Traditional Health Remedies Used by the Maasai of Southern Kaijiado District, Kenya. *Ethnobotany Research and Applications*.
- Kitazawa, E., Ogiso, A., Takahashi, S., Aiya, S., Kurabayashi, M., Kuwano, H., Hata, T., & Tamura, C. (1979). Plaunol A and B, new anti-ulcer diterpenelactones from *Croton sublyratus*. *Tetrahedron Letters*. [https://doi.org/10.1016/S0040-4039\(01\)86079-2](https://doi.org/10.1016/S0040-4039(01)86079-2)
- Kitchen, D. B., Decornez, H., Furr, J. R., & Bajorath, J. (2004). Docking and scoring in virtual screening for drug discovery: Methods and applications. In *Nature Reviews Drug Discovery*.  
<https://doi.org/10.1038/nrd1549>
- Kivevele, T. T., Mbarawa, M. M., Bereczky, A., Laza, T., & Madarasz, J. (2011). Impact of antioxidant additives on the oxidation stability of biodiesel produced from *Croton Megalocarpus* oil. *Fuel Processing Technology*.  
<https://doi.org/10.1016/j.fuproc.2011.02.009>
- Klos, M., van de Venter, M., Milne, P. J., Traore, H. N., Meyer, D., & Oosthuizen, V. (2009). In vitro anti-HIV activity of five selected South African medicinal plant extracts. *Journal of Ethnopharmacology*, 124(2), 182–188. <https://doi.org/10.1016/j.jep.2009.04.043>
- Kohl, N. E., Emini, E. A., Schleif, W. A., Davis, L. J., Heimbach, J. C., Dixon, R. A., Scolnick, E. M., & Sigal, I. S. (1988). Active human immunodeficiency virus protease is required for viral infectivity. *Proceedings of the National Academy of Sciences*.  
<https://doi.org/10.1073/pnas.85.13.4686>
- Kokwaro, J. O. (1976). *Medicinal plants of East Africa*. East African Literature Bureau.

<https://agris.fao.org/agris-search/search.do?recordID=KE2005100575>

- Kondo, M., Oyama-Okubo, N., Sagae, M., Ando, T., Marchesi, E., & Nakayama, M. (2007). Metabolic regulation of floral scent in *Petunia axillaris* lines: Biosynthetic relationship between dihydroconiferyl acetate and iso-eugenol. *Bioscience, Biotechnology and Biochemistry*, *71*(2), 458–463. <https://doi.org/10.1271/bbb.60507>
- Kulkosky, J., Jones, K. S., Katz, R. A., Mack, J. P., & Skalka, A. M. (1992). Residues critical for retroviral integrative recombination in a region that is highly conserved among retroviral/retrotransposon integrases and bacterial insertion sequence transposases. *Molecular and Cellular Biology*, *12*(5), 2331–2338.
- Kumar, K. M., Anbarasu, A., & Ramaiah, S. (2014). Molecular docking and molecular dynamics studies on  $\beta$ -lactamases and penicillin binding proteins. *Molecular BioSystems*, *10*(4), 891–900. <https://doi.org/10.1039/c3mb70537d>
- Kuo, P. C., Yang, M. L., Hwang, T. L., Lai, Y. Y., Li, Y. C., Thang, T. D., & Wu, T. S. (2013). Anti-inflammatory diterpenoids from *croton tonkinensis*. *Journal of Natural Products*. <https://doi.org/10.1021/np300699f>
- Kuo, Y. H., & Kuo, L. M. Y. (1997). Antitumour and anti-AIDS triterpenes from *Celastrus hindsii*. *Phytochemistry*, *44*(7), 1275–1281. [https://doi.org/10.1016/S0031-9422\(96\)00719-4](https://doi.org/10.1016/S0031-9422(96)00719-4)
- Kupchan, S., Uchida, I., Branfman, A., Dailey, R., & Fei, B. (1976). Antileukemic principles isolated from euphorbiaceae plants. *Science*. <https://doi.org/10.1126/science.1251193>
- Kweifio-Okai, G., & Carroll, A. R. (1993). Antiarthritic effect of lupeol acetate. *Phytotherapy Research*, *7*(2), 213–215. <https://doi.org/10.1002/PTR.2650070227>
- Lahlou, S., Leal-Cardoso, J. H., & Magalhães, P. J. C. (2000). Essential oil of *Croton nepetaefolius* decreases blood pressure through an action upon vascular smooth muscle: Studies in DOCA-salt hypertensive rats. *Planta Medica*, *66*(2), 138–143. <https://doi.org/10.1055/s-2000-11133>
- Lahlou, S., Leal-Cardoso, J. H., Magalhães, P. J. C., Coelho-de-Souza, A. N., & Duarte, G. P. (1999). Cardiovascular effects of the essential oil of *Croton nepetaefolius* in rats: Role of the autonomic nervous system. *Planta Medica*. <https://doi.org/10.1055/s-1999-14025>
- Lalezari, J. P., Henry, K., O'Hearn, M., Montaner, J. S. G., Piliero, P. J., Trottier, B., Walmsley, S., Cohen, C., Kuritzkes, D. R., Eron, J. J., Chung, J., DeMasi, R., Donatucci, L., Drobnes, C., Delehanty, J., & Salgo, M. (2003). Enfuvirtide, an HIV-1 Fusion Inhibitor, for Drug-Resistant HIV Infection in North and South America. *New England Journal of Medicine*.

<https://doi.org/10.1056/NEJMoa035026>

- Lall, N., Weiganand, O., Hussein, A. A., & Meyer, J. J. M. (2006). Antifungal activity of naphthoquinones and triterpenes isolated from the root bark of *Euclea natalensis*. *South African Journal of Botany*. <https://doi.org/10.1016/j.sajb.2006.03.005>
- Langat, M. K., Crouch, N. R., Pohjala, L., Tammela, P., Smith, P. J., & Mulholland, D. A. (2012). Ent-kauren-19-oic acid derivatives from the stem bark of *Croton pseudopulchellus* Pax. *Phytochemistry Letters*. <https://doi.org/10.1016/j.phytol.2012.03.002>
- Larder, B. A., Darby, G., & Richman, D. D. (1989). HIV with reduced sensitivity to zidovudine (AZT) isolated during prolonged therapy. *Science*, 243(4899), 1731–1734. <https://doi.org/10.1126/science.2467383>
- Laskowski, R. A., & Swindells, M. B. (2011). LigPlot+: multiple ligand-protein interaction diagrams for drug discovery. *Journal of Chemical Information and Modeling*, 51(10), 2778–2786. <https://doi.org/10.1021/CI200227U>
- Lazarini, C. A., Uema, A. H., Brandão, G. M. S., Guimarães, A. P. C., & Bernardi, M. M. (2000). *Croton zehntneri* essential oil: Effects on behavioral models related to depression and anxiety. *Phytomedicine*. [https://doi.org/10.1016/S0944-7113\(00\)80033-1](https://doi.org/10.1016/S0944-7113(00)80033-1)
- Lee-Huang, S., Huang, P. L., Bourinbaiar, A. S., Chen, H. C., & Kung, H. F. (1995). Inhibition of the integrase of human immunodeficiency virus (HIV) type 1 by anti-HIV plant proteins MAP30 and GAP31. *Proceedings of the National Academy of Sciences*. <https://doi.org/10.1073/pnas.92.19.8818>
- Lee, H., Hanes, J., & Johnson, K. A. (2003). Toxicity of nucleoside analogues used to treat AIDS and the selectivity of the mitochondrial DNA polymerase. In *Biochemistry*. <https://doi.org/10.1021/bi035596s>
- Lepik, K. J., Yip, B., Ulloa, A. C., Wang, L., Toy, J., Akagi, L., Lima, V. D., Guillemi, S., Montaner, J. S. G., & Barrios, R. (2018). Adverse drug reactions to integrase strand transfer inhibitors. *AIDS*. <https://doi.org/10.1097/QAD.0000000000001781>
- Leth, F., Phanuphak, P., Ruxrungtham, K., Baraldi, E., Miller, S., Gazzard, B., Cahn, P., Lalloo, U. G., Van Der Westhuizen, I. P., Malan, D. R., Johnson, M. A., Santos, B. R., Mulcahy, F., Wood, R., Levi, G. C., Reboredo, G., Squires, K., Cassetti, I., Petit, D., Lange, J. M. A. (2004). Comparison of first-line antiretroviral therapy with regimens including nevirapine, efavirenz, or both drugs, plus stavudine and lamivudine: A randomised open-label trial, the



- 2NN Study. *Lancet*. [https://doi.org/10.1016/S0140-6736\(04\)15997-7](https://doi.org/10.1016/S0140-6736(04)15997-7)
- Leung, D., Abbenante, G., & Fairlie, D. P. (2000). Protease inhibitors: Current status and future prospects. In *Journal of Medicinal Chemistry*. <https://doi.org/10.1021/jm990412m>
- Lewinska, A., Zebrowski, J., Duda, M., Gorka, A., & Wnuk, M. (2015). Fatty acid profile and biological activities of linseed and rapeseed oils. *Molecules*. <https://doi.org/10.3390/molecules201219887>
- Li, N., Wang, Y., Pothukuchy, A., Syrett, A., Husain, N., Gopalakrishna, S., Kosaraju, P., & Ellington, A. D. (2008). Aptamers that recognize drug-resistant HIV-1 reverse transcriptase. *Nucleic Acids Research*. <https://doi.org/10.1093/nar/gkn775>
- Li, Y., Carbone, M., Vitale, R. M., Amodeo, P., Castelluccio, F., Sicilia, G., Mollo, E., Nappo, M., Cimino, G., Guo, Y. W., & Gavagnin, M. (2010). Rare casbane diterpenoids from the hainan soft coral *Sinularia depressa*. *Journal of Natural Products*, 73(2), 133–138. <https://doi.org/10.1021/np900484k>
- Lightfoote, M. M., Coligan, J. E., Folks, T. M., Fauci, A. S., Martin, M. A., & Venkatesan, S. (1986). Structural characterization of reverse transcriptase and endonuclease polypeptides of the acquired immunodeficiency syndrome retrovirus. *Journal of Virology*, 60(2), 771–775. <https://doi.org/10.1128/jvi.60.2.771-775.1986>
- Lima, D.F., S., J.M., F., R.C.P., L. J., A.R., T., J.H.L., C., & M.G.R., Q. (2008). *Croton zehntneri* essential oil prevents acetaminophen-induced acute hepatotoxicity in mice. *Records of Natural Products*.
- Lima, G. S., Castro-Pinto, D. B., MacHado, G. C., Maciel, M. A. M., & Echevarria, A. (2015). Antileishmanial activity and trypanothione reductase effects of terpenes from the Amazonian species *Croton cajucara* Benth (Euphorbiaceae). *Phytomedicine*. <https://doi.org/10.1016/j.phymed.2015.08.012>
- Lin, Y. C., Cheng, H. Y., Huang, T. H., Huang, H. W., Lee, Y. H., & Peng, W. H. (2009). Analgesic and anti-inflammatory activities of *Torenia concolor* Lindley var. *formosana* Yamazaki and betulin in mice. *Am J Chin Med*. <https://doi.org/10.1142/S0192415X09006606>
- Lipinski, C. A., Lombardo, F., Dominy, B. W., & Feeney, P. J. (2001). Experimental and computational approaches to estimate solubility and permeability in drug discovery and development settings. *Advanced Drug Delivery Reviews*, 46(1–3), 3–26. [https://doi.org/10.1016/S0169-409X\(00\)00129-0](https://doi.org/10.1016/S0169-409X(00)00129-0)

- Liu, C. P., Xu, J. B., Zhao, J. X., Xu, C. H., Dong, L., Ding, J., & Yue, J. M. (2014). Diterpenoids from *Croton laui* and their cytotoxic and antimicrobial activities. *Journal of Natural Products*, 77(4), 1013–1020. <https://doi.org/10.1021/np500042c>
- Lobritz, M. A., Ratcliff, A. N., & Arts, E. J. (2010). HIV-1 entry, inhibitors, and resistance. In *Viruses*. <https://doi.org/10.3390/v2051069>
- Lopes, M. I. L. E., Saffi, J., Echeverrigaray, S., Henriques, J. A. P., & Salvador, M. (2004). Mutagenic and antioxidant activities of *Croton lechleri* sap in biological systems. *Journal of Ethnopharmacology*. <https://doi.org/10.1016/j.jep.2004.08.025>
- Lulekal, E., Asfaw, Z., Kelbessa, E., & Van Damme, P. (2013). Ethnomedicinal study of plants used for human ailments in Ankober District, North Shewa Zone, Amhara Region, Ethiopia. *Journal of Ethnobiology and Ethnomedicine*. <https://doi.org/10.1186/1746-4269-9-63>
- Lulekal, E., Kelbessa, E., Bekele, T., & Yineger, H. (2008). An ethnobotanical study of medicinal plants in Mana Angetu District, southeastern Ethiopia. *Journal of Ethnobiology and Ethnomedicine*. <https://doi.org/10.1186/1746-4269-4-10>
- Lv, Z., Chu, Y., & Wang, Y. (2015a). HIV protease inhibitors: A review of molecular selectivity and toxicity. *HIV/AIDS - Research and Palliative Care*, 7, 95–104. <https://doi.org/10.2147/HIV.S79956>
- Lv, Z., Chu, Y., & Wang, Y. (2015b). HIV protease inhibitors: a review of molecular selectivity and toxicity. *HIV/AIDS (Auckland, N.Z.)*, 7, 95. <https://doi.org/10.2147/HIV.S79956>
- Maartens, G., Celum, C., & Lewin, S. R. (2014). HIV infection: Epidemiology, pathogenesis, treatment, and prevention. *The Lancet*. [https://doi.org/10.1016/S0140-6736\(14\)60164-1](https://doi.org/10.1016/S0140-6736(14)60164-1)
- Mabberley, D. J. (2008). The Plant-Book: A portable dictionary of the vascular plants. *Feddes Repertorium*. <https://doi.org/10.1016/j.margeo.2009.07.012>
- Maciel, M. A. M., Pinto, A. C., Arruda, A. C., Pamplona, S. G. S. R., Vanderlinde, F. A., Lapa, A. J., Echevarria, A., Grynberg, N. F., Cólus, I. M. S., Farias, R. A. F., Luna Costa, A. M., & Rao, V. S. N. (2000). Ethnopharmacology, phytochemistry and pharmacology: A successful combination in the study of *Croton cajucara*. *Journal of Ethnopharmacology*. [https://doi.org/10.1016/S0378-8741\(99\)00159-2](https://doi.org/10.1016/S0378-8741(99)00159-2)
- Magadula, J. (2012). Anti-Mycobacterial and Toxicity Activities of Some Priority Medicinal Plants from Lake Victoria Basin, Tanzania. *European Journal of Medicinal Plants*, 2(2). <https://doi.org/10.9734/EJMP/2012/739>

- Magalhães, P. J C, Criddle, D. N., Tavares, R. A., Melo, E. M., Mota, T. L., & Leal-Cardoso, J. H. (1998). Intestinal myorelaxant and antispasmodic effects of the essential oil of *Croton nepetaefolius* and its constituents cineole, methyl-eugenol and terpineol. *Phytotherapy Research*.  
[https://doi.org/10.1002/\(SICI\)1099-1573\(199805\)12:3<172::AID-PTR212>3.0.CO;2-E](https://doi.org/10.1002/(SICI)1099-1573(199805)12:3<172::AID-PTR212>3.0.CO;2-E)
- Magalhães, Pedro Jorge Caldas, Lahlou, S., & Leal-Cardoso, J. H. (2004). Antispasmodic effects of the essential oil of *Croton nepetaefolius* on guinea-pig ileum: A myogenic activity. *Fundamental and Clinical Pharmacology*. <https://doi.org/10.1111/j.1472-8206.2004.00276.x>
- Mahbubur Rahman, A., & Iffat Ara Gulshana, M. (2014). Taxonomy and Medicinal Uses on Amaranthaceae Family of Rajshahi, Bangladesh. *Applied Ecology and Environmental Sciences*. <https://doi.org/10.12691/aees-2-2-3>
- Mahmood, N., Pizza, C., Aquino, R., De Tommasi, N., Piacente, S., Colman, S., Burke, A., & Hay, A. J. (1993). Inhibition of HIV infection by flavanoids. *Antiviral Research*, 22(2–3), 189–199. [https://doi.org/10.1016/0166-3542\(93\)90095-Z](https://doi.org/10.1016/0166-3542(93)90095-Z)
- Mahomoodally, M. F. (2013). Traditional medicines in Africa: An appraisal of ten potent African medicinal plants. In *Evidence-based Complementary and Alternative Medicine* (Vol. 2013). <https://doi.org/10.1155/2013/617459>
- Malveira Cavalcanti, J., Henrique Leal-Cardoso, J., Leite Diniz, L. R., Gomes Portella, V., Oliveira Costa, C., Barreto Medeiros Linard, C. F., Alves, K., De Paula Rocha, M. V. A., Calado Lima, C., Marilande Cecatto, V., & Coelho-De-Souza, A. N. (2012). The essential oil of *Croton zehntneri* and trans-anethole improves cutaneous wound healing. *Journal of Ethnopharmacology*. <https://doi.org/10.1016/j.jep.2012.08.030>
- Marcelin, A. G., Delaugerre, C., Wiriden, M., Viegas, P., Simon, A., Katlama, C., & Calvez, V. (2004). Thymidine Analogue Reverse Transcriptase Inhibitors Resistance Mutations Profiles and Association to Other Nucleoside Reverse Transcriptase Inhibitors Resistance Mutations Observed in the Context of Virological Failure. *Journal of Medical Virology*. <https://doi.org/10.1002/jmv.10550>
- Markó, I. E., Wiaux, M., Warriner, S. M., Giles, P. R., Eustace, P., Dean, D., & Bailey, M. (1999). Towards the total synthesis of clerocidin. Efficient assembly of the decalin subunit. *Tetrahedron Letters*. [https://doi.org/10.1016/S0040-4039\(99\)01048-5](https://doi.org/10.1016/S0040-4039(99)01048-5)
- Maroyi, A. (2014). Alternative Medicines for HIV/AIDS in Resource-Poor Settings: Insight from

- Traditional Medicines Use in Sub-Saharan Africa. *Tropical Journal of Pharmaceutical Research*, 13(9), 1527–1536. <https://doi.org/10.4314/tjpr.v13i9.21>
- Maroyi, A. (2017a). *Croton megalocarpus* Hutch. in Tropical Africa: Phytochemistry, Pharmacology and Medicinal Potential. *Research Journal of Medicinal Plants*, 11(4), 124–133. <https://doi.org/10.3923/rjmp.2017.124.133>
- Maroyi, A. (2017b). Ethnomedicinal uses and pharmacological activities of *Croton megalobotrys* Müll Arg: A systematic review. *Tropical Journal of Pharmaceutical Research*, 16(10), 2535–2543. <https://doi.org/10.4314/tjpr.v16i10.30>
- Maroyi, A. (2017c). Ethnopharmacological Uses, Phytochemistry, and Pharmacological Properties of *Croton macrostachyus* Hochst. Ex Delile: A Comprehensive Review. *Evidence-Based Complementary and Alternative Medicine*. <https://doi.org/10.1155/2017/1694671>
- Maroyi, A. (2017d). Pharmacological Properties of *Croton macrostachyus* Hochst. *Ex Delile : A Comprehensive Review*. 2017.
- Maroyi, A. (2017e). Traditional usage, phytochemistry and pharmacology of *Croton sylvaticus* Hochst. ex C. Krauss. In *Asian Pacific Journal of Tropical Medicine*. <https://doi.org/10.1016/j.apjtm.2017.05.002>
- Masuda, T., & Harada, S. (1993). Modulation of host cell nuclear proteins that bind to hiv-1 trans-activation-responsive element rna by phorbol ester. *Virology*. <https://doi.org/10.1006/viro.1993.1091>
- Matsuse, I. T., Lim, Y. A., Hattori, M., Correa, M., & Gupta, M. P. (1998). A search for anti-viral properties in Panamanian medicinal plants. The effects on HIV and its essential enzymes. *Journal of Ethnopharmacology*, 64(1), 15–22. [https://doi.org/10.1016/S0378-8741\(98\)00099-3](https://doi.org/10.1016/S0378-8741(98)00099-3)
- Matu, E. N., & Van Staden, J. (2003). Antibacterial and anti-inflammatory activities of some plants used for medicinal purposes in Kenya. *Journal of Ethnopharmacology*. [https://doi.org/10.1016/S0378-8741\(03\)00107-7](https://doi.org/10.1016/S0378-8741(03)00107-7)
- Mazzanti, Bolle, P., Martinoli, L., Piccinelli, D., Grgurina, I., Animati, F., & Mugnè, Y. (1987). *Croton macrostachys*, a plant used in traditional medicine: purgative and inflammatory activity. *Journal of Ethnopharmacology*. [https://doi.org/10.1016/0378-8741\(87\)90043-2](https://doi.org/10.1016/0378-8741(87)90043-2)
- McCull, D. J., & Chen, X. (2010). Strand transfer inhibitors of HIV-1 integrase: Bringing IN a new era of antiretroviral therapy. In *Antiviral Research*.

<https://doi.org/10.1016/j.antiviral.2009.11.004>

- McCrindle, R., Nakamura, E., & Anderson, A. B. (1976). Constituents of *Solidago* species. Part VII. Constitution and stereochemistry of the cis-clerodanes from *Solidago arguta* ait. and of related siterpenoids. *Journal of the Chemical Society, Perkin Transactions 1*, 15, 1590–1597. <https://doi.org/10.1039/p19760001590>
- Mcgilvray, M., & Willis, N. (2004). All About Antiretrovirals A Nurse Training Programme *Trainer's Manual*. [www.busconnex.co.za](http://www.busconnex.co.za)
- McLeod, G. X., & Hammer, S. M. (1992). Zidovudine: Five years later. In *Annals of Internal Medicine*. <https://doi.org/10.7326/0003-4819-117-6-487>
- Melhuish, A., & Lewthwaite, P. (2018). Natural history of HIV and AIDS. In *Medicine (United Kingdom)*. <https://doi.org/10.1016/j.mpmed.2018.03.010>
- Melo, P. S., Justo, G. Z., Durán, N., & Haun, M. (2004). Natural killer cell activity and anti-tumour effects of dehydrocrotonin and its synthetic derivatives. *European Journal of Pharmacology*. <https://doi.org/10.1016/j.ejphar.2004.01.027>
- Menéndez-Arias, L. (2009). Mutation rates and intrinsic fidelity of retroviral reverse transcriptases. In *Viruses*. <https://doi.org/10.3390/v1031137>
- Mesfin, F., Demissew, S., & Teklehaymanot, T. (2009). An ethnobotanical study of medicinal plants in Wonago Woreda, SNNPR, Ethiopia. *Journal of Ethnobiology and Ethnomedicine*. <https://doi.org/10.1186/1746-4269-5-28>
- Miceli, M. H., Díaz, J. A., & Lee, S. A. (2011). Emerging opportunistic yeast infections. In *The Lancet Infectious Diseases*. [https://doi.org/10.1016/S1473-3099\(10\)70218-8](https://doi.org/10.1016/S1473-3099(10)70218-8)
- Miguel, M. G., Nunes, S., Dandlen, S. A., Cavaco, A. M., & Antunes, M. D. (2014). Phenols, flavonoids and antioxidant activity of aqueous and methanolic extracts of propolis (*Apis mellifera* L.) from Algarve, South Portugal. *Food Science and Technology*, 34(1), 16–23. <https://doi.org/10.1590/S0101-20612014000100002>
- Miller, M. D. (2004). K65R, TAMs and tenofovir. In *AIDS Reviews*.
- Miller, M. D., Farnet, C. M., & Bushman, F. D. (1997). Human immunodeficiency virus type 1 preintegration complexes: studies of organization and composition . Human Immunodeficiency Virus Type 1 Preintegration Complexes: Studies of Organization and Composition. *Journal of Virology*. <https://doi.org/10.1128/jvi.75.8.3626-3635.2001>
- Miller, M. J. S., Bobrowski, P., Shukla, M., Gupta, K., & Haqqi, T. M. (2007). Chondroprotective

- effects of a proanthocyanidin rich Amazonian genonutrient reflects direct inhibition of matrix metalloproteinases and upregulation of IGF-1 production by human chondrocytes. *Journal of Inflammation*. <https://doi.org/10.1186/1476-9255-4-16>
- Miller, M. J. S., Macnaughton, W. K., Zhang, X., Jane, H., Charbonnet, R. M., Bobrowski, P., Lao, J., Marie, A., Sandoval, M., Naughton, W. K. M. A. C., Thompson, J. H., Trentacosti, A. N. N. M., Mark, J. S., Zhang, J., & Trentacosti, A. M. (2012). Treatment of gastric ulcers and diarrhea with the Amazonian herbal medicine, *sangre de grado* 192–200.
- Miller, M. J. S., Vergnolle, N., McKnight, W., Musah, R. A., Davison, C. A., Trentacosti, A. M., Thompson, J. H., Sandoval, M., & Wallace, J. L. (2001). Inhibition of neurogenic inflammation by the Amazonian herbal medicine *sangre de grado*. *Journal of Investigative Dermatology*. <https://doi.org/10.1046/j.0022-202X.2001.01446.x>
- Miller, V. (2001). Resistance to Protease Inhibitors. *Journal of Acquired Immune Deficiency Syndromes*. <https://doi.org/10.1097/00042560-200103011-00005>
- Minja M. M. J. (1994). Medicinal plants used in the promotion of animal health in Tanzania. *Revue Scientifique et Technique de l'OIE*. <https://doi.org/10.20506/rst.13.3.800>
- Minuto, J. J., & Haubrich, R. (2008). Etravirine: A second-generation NNRTI for treatment-experienced adults with resistant HIV-1 infection. *Future HIV Therapy*. <https://doi.org/10.2217/17469600.2.6.525>
- Miyauchi, K., Kim, Y., Latinovic, O., Morozov, V., & Melikyan, G. B. (2009). HIV Enters Cells via Endocytosis and Dynamin-Dependent Fusion with Endosomes. *Cell*. <https://doi.org/10.1016/j.cell.2009.02.046>
- Miyoshi, I., Yoshimoto, S., Fujishita, M., Taguchi, H., Kubonishi, I., Niiya, K., & Minezawa, M. (1982). Natural adult T-cell leukaemia virus infection in Japanese monkeys. In *The Lancet*. [https://doi.org/10.1016/S0140-6736\(82\)92757-X](https://doi.org/10.1016/S0140-6736(82)92757-X)
- Mohammed, M. M. D., Ibrahim, N. A., Awad, N. E., Matloub, A. A., Mohamed-Ali, A. G., Barakat, E. E., Mohamed, A. E., & Colla, P. L. (2012). Anti-HIV-1 and cytotoxicity of the alkaloids of *Erythrina abyssinica* Lam. growing in Sudan. *Natural Product Research*, 26(17), 1565–1575. <https://doi.org/10.1080/14786419.2011.573791>
- Montessori, V., Press, N., Harris, M., Akagi, L., & Montaner, J. S. G. (2004). Adverse effects of antiretroviral therapy for HIV infection. In *CMAJ*. [https://doi.org/10.1016/S0140-6736\(00\)02854-3](https://doi.org/10.1016/S0140-6736(00)02854-3)

- Montopoli, M., Bertin, R., Chen, Z., Bolcato, J., Caparrotta, L., & Froidi, G. (2012). *Croton lechleri* sap and isolated alkaloid taspine exhibit inhibition against human melanoma SK23 and colon cancer HT29 cell lines. *Journal of Ethnopharmacology*.  
<https://doi.org/10.1016/j.jep.2012.10.032>
- Morais, Selene Maia de, Júnior, F. E. A. C., Silva, A. R. A. da, Stone, J. M. N., & Rondina, D. (2006). Antioxidant activity of essential oils from northeastern Brazilian croton species. *Quimica Nova*.
- Morais, Selene M, Cavalcanti, E. S. B., Bertini, L. M., Oliveira, C. L. L., Rodrigues, J. R. B., & Cardoso, J. H. L. (2006). Larvicidal activity of essential oils from Brazilian Croton species against *Aedes aegypti* L. *J Am Mosq Control Assoc*. [https://doi.org/10.2987/8756-971X\(2006\)22\[161:LAOEOF\]2.0.CO;2](https://doi.org/10.2987/8756-971X(2006)22[161:LAOEOF]2.0.CO;2)
- Moreira, E. L. G., Rial, D., Duarte, F. S., De Carvalho, C. R., Horst, H., Pizzolatti, M. G., Prediger, R. D. S., & Ribeiro-Do-Valle, R. M. (2010). Central nervous system activity of the proanthocyanidin-rich fraction obtained from *Croton celtidifolius* in rats. *Journal of Pharmacy and Pharmacology*. <https://doi.org/10.1111/j.2042-7158.2010.01124.x>
- Morris Kupchan, S., Hemingway, R. J., & Smith, R. M. (1969). Tumor Inhibitors. XLV. Crotepoxide, a Novel Cyclohexane Diepoxide Tumor Inhibitor from *Croton macrostachys*. *Journal of Organic Chemistry*. <https://doi.org/10.1021/jo01264a033>
- Mosmann, T. (1983). Rapid colorimetric assay for cellular growth and survival: Application to proliferation and cytotoxicity assays. *Journal of Immunological Methods*.  
[https://doi.org/10.1016/0022-1759\(83\)90303-4](https://doi.org/10.1016/0022-1759(83)90303-4)
- Mota, A. S., De Lima, A. B., Albuquerque, T. L. F., Silveira, T. S., Do Nascimento, J. L. M., Da Silva, J. K. R., Ribeiro, A. F., Maia, J. G. S., & Bastos, G. N. T. (2015). Antinociceptive activity and toxicity evaluation of the fatty oil from *Plukenetia polyadenia* mull. arg. (euphorbiaceae). *Molecules*. <https://doi.org/10.3390/molecules20057925>
- Mota, M. L., Lobo, L. T. C., Galberto Da Costa, J. M., Costa, L. S., Rocha, H. A. O., Rocha E Silva, L. F., Pohlit, A. M., & De Andrade Neto, V. F. (2012). *In vitro* and *in vivo* antimalarial activity of essential oils and chemical components from three medicinal plants found in Northeastern Brazil. *Planta Medica*. <https://doi.org/10.1055/s-0031-1298333>
- Moyle, G. (2000). Clinical manifestations and management of antiretroviral nucleoside analog-related mitochondrial toxicity. *Clinical Therapeutics*. <https://doi.org/10.1016/S0149->

2918(00)80064-8

- Mubiu, J. K., Ndwigah, S. N., Abuga, K. O., & Ongarora, D. S. B. (2017). Antimicrobial activity of extracts and phytosterols from the root bark of *Lonchocarpus eriocalyx*. *The East and Central African Journal of Pharmaceutical Sciences*, 20((1-3)), 13–16.  
<http://uonjournals.uonbi.ac.ke/ojs/index.php/ecajps/article/view/217>
- Murillo, R. M., Jakupovic, J., Rivera, J., & Castro, V. H. (2001). Diterpenes and other constituents from *Croton draco* (Euphorbiaceae). *Revista de Biología Tropical*.  
[https://doi.org/10.1016/0031-9422\(92\)80479-X](https://doi.org/10.1016/0031-9422(92)80479-X)
- Muthee, J. K., Gakuya, D. W., Mbaria, J. M., Kareru, P. G., Mulei, C. M., & Njonge, F. K. (2011). Ethnobotanical study of anthelmintic and other medicinal plants traditionally used in Loitokitok district of Kenya. *Journal of Ethnopharmacology*.  
<https://doi.org/10.1016/j.jep.2011.02.005>
- Näf, R., Velluz, A., & Meyer, A. P. (2011). Volatile Constituents of Blood and Blond Orange Juices: A Comparison. *Http://Dx.Doi.Org/10.1080/10412905.1996.9701025*, 8(6), 587–595.  
<https://doi.org/10.1080/10412905.1996.9701025>
- Nakamura, N. (2004). [Inhibitory effects of some traditional medicines on proliferation of HIV-1 and its protease]. *Yakugaku Zasshi: Journal of the Pharmaceutical Society of Japan*.  
<https://doi.org/10.1248/yakushi.124.519>
- Nanyingi, M. O., Mbaria, J. M., Lanyasunya, A. L., Wagate, C. G., Koros, K. B., Kaburia, H. F., Munenge, R. W., & Ogara, W. O. (2008). Ethnopharmacological survey of Samburu district, Kenya. *Journal of Ethnobiology and Ethnomedicine*. <https://doi.org/10.1186/1746-4269-4-14>
- Narayan, L. C., Rai, V. R., & Tewtrakul, S. (2013). Emerging need to use phytopharmaceuticals in the treatment of HIV. *Journal of Pharmacy Research*, 6(1), 218–223.  
<https://doi.org/10.1016/j.jopr.2012.11.002>
- Nardi, G. M., Felippi, R., DalBó, S., Siqueira-Junior, J. M., Arruda, D. C., Delle Monache, F., Timbola, A. K., Pizzolatti, M. G., Ckless, K., & Ribeiro-do-Valle, R. M. (2003). Anti-inflammatory and antioxidant effects of *Croton celtidifolius* bark. *Phytomedicine*.  
<https://doi.org/10.1078/094471103321659906>
- Nardi, G. M., Siqueira Junior, J. M., Delle Monache, F., Pizzolatti, M. G., Ckless, K., & Ribeiro-do-Valle, R. M. (2007). Antioxidant and anti-inflammatory effects of products from *Croton celtidifolius* Bailon on carrageenan-induced pleurisy in rats. *Phytomedicine*.



<https://doi.org/10.1016/j.phymed.2006.03.002>

- Nardi, Geisson Marcos, DalBó, S., Monache, F. D., Pizzolatti, M. G., & Ribeiro-do-Valle, R. M. (2006). Antinociceptive effect of *Croton celtidifolius* Baill (Euphorbiaceae). *Journal of Ethnopharmacology*. <https://doi.org/10.1016/j.jep.2006.02.012>
- Naturgucker., N. de. (2018). *naturgucker.de. naturgucker. Occurrence dataset* <https://doi.org/10.15468/uc1apo> accessed via GBIF.org on 2018-12-24. <https://www.gbif.org/occurrence/1338462599>.
- Ndubani, P., & Höjer, B. (1999). Traditional healers and the treatment of sexually transmitted illnesses in rural Zambia. *Journal of Ethnopharmacology*. [https://doi.org/10.1016/S0378-8741\(99\)00075-6](https://doi.org/10.1016/S0378-8741(99)00075-6)
- Ndunda B. (2014). Phytochemistry and bioactivity investigations of three Kenyan Croton species (p. 307). PhD Thesis, University of Nairobi, Nairobi.
- Ndunda, B., Langat, M. K., Wanjohi, J. M., Midiwo, J. O., & Kerubo, L. O. (2013). Alienusolin, a new 4  $\alpha$ -deoxyphorbol ester derivative, and crotonimide C, a new glutarimide alkaloid from the Kenyan *Croton alienus*. *Planta Medica*, 79(18), 1762–1766. <https://doi.org/10.1055/s-0033-1351044>
- Neiva, T. de J. C., Moraes, A. C. R. de, Buchele, C., Pizzolatti, M. G., D'Amico, E. A., Fries, D. M., & Rocha, T. R. F. da. (2008). Antiplatelet activity of *Croton celtidifolius*. *Revista Brasileira de Ciências Farmacêuticas*. <https://doi.org/10.1590/S1516-93322008000100014>
- Nemecek, P. M., Polsky, B., & Gottlieb, M. S. (2000). Treatment guidelines for HIV-associated wasting. *Mayo Clinic Proceedings*. <https://doi.org/10.4065/75.4.386>
- Ng, T. B., Au, T. K., Lam, T. L., Ye, X. Y., & Wan, D. C. C. (2002). Inhibitory effects of antifungal proteins on human immunodeficiency virus type 1 reverse transcriptase, protease and integrase. *Life Sciences*. [https://doi.org/10.1016/S0024-3205\(01\)01458-8](https://doi.org/10.1016/S0024-3205(01)01458-8)
- Ng, T. B., Lam, T. L., Au, T. K., Ye, X. Y., & Wan, C. C. (2001). Inhibition of human immunodeficiency virus type 1 reverse transcriptase, protease and integrase by bovine milk proteins. *Life Sciences*. [https://doi.org/10.1016/S0024-3205\(01\)01311-X](https://doi.org/10.1016/S0024-3205(01)01311-X)
- Ngadjui, B. T., Abegaz, B. M., Keumedjio, F., Folefoc, G. N., & Kapche, G. W. F. (2002). Diterpenoids from the stem bark of *Croton zambesicus*. *Phytochemistry*. [https://doi.org/10.1016/S0031-9422\(02\)00034-1](https://doi.org/10.1016/S0031-9422(02)00034-1)
- Ngamrojnvanich, N., Tonsiengsom, S., Lertpratchya, P., Roengsumran, S., Puthong, S., &

- Petsom, A. (2003). Diterpenoids from the stem barks of *Croton robustus*. *Archives of Pharmacal Research*. <https://doi.org/10.1007/BF02980196>
- Ngo Bum, E., Ngah, E., Ngo Mune, R. M., Ze Minkoulou, D. M., Talla, E., Moto, F. C., Ngoupaye, G. T., Taiwe, G. S., Rakotonirina, A., & Rakotonirina, S. V. (2012). Decoctions of *Bridelia micrantha* and *Croton macrostachyus* may have anticonvulsant and sedative effects. *Epilepsy & Behavior: E&B*. <https://doi.org/10.1016/j.yebeh.2012.03.028>
- Nguelefack, T. B., Dutra, R. C., Paszcuk, A. F., de Andrade, E. L., & Calixto, J. B. (2015). TRPV1 channel inhibition contributes to the antinociceptive effects of *Croton macrostachyus* extract in mice. *BMC Complementary and Alternative Medicine*. <https://doi.org/10.1186/s12906-015-0816-z>
- Nirmal, S. A., Pal Subodh, C., Subhash, C. M., & Anuja, N. P. (2012). Analgesic and anti-inflammatory activity of b-sitosterol isolated from *Nyctanthes arbortristis* leaves. *Inflammopharmacology*. <https://doi.org/10.1007/s10787-011-0110-8>
- Nisar, M., Ali, S., Qaisar, M., Gilani, S. N., Shah, M. R., Khan, I., & Ali, G. (2013). Antifungal activity of bioactive constituents and bark extracts of *Rhododendron arboreum*. *Bangladesh Journal of Pharmacology*. <https://doi.org/10.3329/bjp.v8i2.14054>
- Njoroge, G. N., Kaibui, I. M., Njenga, P. K., & Odhiambo, P. O. (2010). Utilisation of priority traditional medicinal plants and local people's knowledge on their conservation status in arid lands of Kenya (Mwingi District). *Journal of Ethnobiology and Ethnomedicine*. <https://doi.org/10.1186/1746-4269-6-22>
- Njoroge, & N., G. (2012). Traditional medicinal plants in two urban areas in Kenya (Thika and Nairobi): Diversity of traded species and conservation concerns. *Ethnobotany Research and Applications*. <https://doi.org/10.17348/era.10.0.329-338>
- Njoroge N., G., & Bussmann, R. W. (2006). Traditional management of ear, nose and throat (ENT) diseases in Central Kenya. *Journal of Ethnobiology and Ethnomedicine*, 2. <https://doi.org/10.1186/1746-4269-2-54>
- Nkunya, M. H. H. (2004). 7-Methyljuglone, Diuvaretin, and Benzyl Benzoates from the Root Bark of *Uvaria kirkii*. *Journal of Natural Products*, 48(6), 999–1000. <https://doi.org/10.1021/NP50042A028>
- Nutan, Modi, M., Goelb, T., Das, T., Malik, S., Suri, S., Singh Rawat, A. K., Srivastava, S. K., Tuli, R., Malhotra, S., & Gupta, S. K. (2013). Ellagic acid & gallic acid from *Lagerstroemia*

- speciosa* L. inhibit HIV-1 infection through inhibition of HIV-1 protease & reverse transcriptase activity. *Indian Journal of Medical Research*.  
[https://doi.org/IndianJMedRes\\_2013\\_137\\_3\\_540\\_111020](https://doi.org/IndianJMedRes_2013_137_3_540_111020) [pii]
- Obey, J. K., von Wright, A., Orjala, J., Kauhanen, J., & Tikkanen-Kaukanen, C. (2016a). Antimicrobial Activity of *Croton macrostachyus* Stem Bark Extracts against Several Human Pathogenic Bacteria. *Journal of Pathogens*. <https://doi.org/10.1155/2016/1453428>
- Obey, J. K., von Wright, A., Orjala, J., Kauhanen, J., & Tikkanen-Kaukanen, C. (2016b). Antimicrobial Activity of *Croton macrostachyus* Stem Bark Extracts against Several Human Pathogenic Bacteria. *Journal of Pathogens*. <https://doi.org/10.1155/2016/1453428>
- Okello, S. V., Nyunja, R. O., Netondo, G. W., & Onyango, J. C. (2010a). Ethnobotanical study of medicinal plants used by sabaots of mt. Elgon kenya. *African Journal of Traditional, Complementary and Alternative Medicines*. <https://doi.org/10.4314/ajtcam.v7i1.57223>
- Okello, S. V., Nyunja, R. O., Netondo, G. W., & Onyango, J. C. (2010b). Ethnobotanical study of medicinal plants used by sabaots of mt. Elgon kenya. *African Journal of Traditional, Complementary and Alternative Medicines*, 7(1), 1–10.  
<https://doi.org/10.4314/ajtcam.v7i1.57223>
- Okokon, J. E., & Nwafor, P. A. (2009a). Antiplasmodial activity of root extract and fractions of *Croton zambesicus*. *Journal of Ethnopharmacology*.  
<https://doi.org/10.1016/j.jep.2008.09.034>
- Okokon, J. E., & Nwafor, P. A. (2009b). Antiulcer and anticonvulsant activity of *Croton zambesicus*. *Pakistan Journal of Pharmaceutical Sciences*.  
<https://doi.org/10.1177/1043659614526253>
- Okokon, J. E., & Nwafor, P. A. (2010a). Antiinflammatory, analgesic and antipyretic activities of ethanolic root extract of *Croton zambesicus*. *Pakistan Journal of Pharmaceutical Sciences*.  
<https://doi.org/10.1016/j.jep.2008.09.034>
- Okokon, J. E., & Nwafor, P. A. (2010b). Antimicrobial activity of root extract and crude fractions of *Croton zambesicus*. *Pakistan Journal of Pharmaceutical Sciences*.  
<https://doi.org/10.1016/j.jep.2008.09.034>
- Okokon, J. E., Nwafor, P. A., & Noah, K. (2011). Nephroprotective effect of *Croton zambesicus* root extract against gentimicin-induced kidney injury. *Asian Pacific Journal of Tropical Medicine*. [https://doi.org/10.1016/S1995-7645\(11\)60228-9](https://doi.org/10.1016/S1995-7645(11)60228-9)

- Oliveira, A. C., Leal-Cardoso, J. H., Santos, C. F., Morais, S. M., & Coelho-de-Souza, A. N. (2001). Antinociceptive effects of the essential oil of *Croton zehntneri* in mice. *Brazilian Journal of Medical and Biological Research*. <https://doi.org/10.1590/S0100-879X2001001100016>
- Oliveira, I. S., Lima, J. C. S., Silva, R. M., & Martins, D. T. O. (2008). Triagem da atividade antibacteriana in vitro do látex e extratos de *Croton urucurana* Baillon. *Brazilian Journal of Pharmacognosy*. <https://doi.org/10.1590/S0102-695X2008000400016>
- Omara, T. (2020). Antimalarial Plants Used across Kenyan Communities. *Evidence-Based Complementary and Alternative Medicine, 2020*. <https://doi.org/10.1155/2020/4538602>
- Orlandi-Mattos PE , R Geremias, CAS Cordova, TB Creczynski-Pasa, JM Rebello, D Wilhelm, DTO Martins, S Llesuy, R. P. (2002). Protective properties of *Croton urucurana* latex against lipid peroxidation and action as free radical scavenger (pp. S242–S242). Pergamon-elsevier science ltd.
- Orozco-Topete, R., Sierra-Madero, J., Cano-Dominguez, C., Kershenovich, J., Ortiz-Pedroza, G., Vazquez-Valls, E., Garcia-Cosio, C., Soria-Cordoba, A., Armendariz, A. M., Teran-Toledo, X., Romo-Garcia, J., Fernandez, H., & Rozhon, E. J. (1997). Safety and efficacy of Virend® for topical treatment of genital and anal herpes simplex lesions in patients with AIDS. *Antiviral Research*. [https://doi.org/10.1016/S0166-3542\(97\)00015-6](https://doi.org/10.1016/S0166-3542(97)00015-6)
- Othumpangat, S., & Noti, J. D. (2018). Antiviral Drugs. In *Side Effects of Drugs Annual*. <https://doi.org/10.1016/bs.seda.2018.08.005>
- Ouattara, B., Simard, R. E., Holley, R. A., Piette, G. J. P., & Bégin, A. (1997). Antibacterial activity of selected fatty acids and essential oils against six meat spoilage organisms. *International Journal of Food Microbiology*. [https://doi.org/10.1016/S0168-1605\(97\)00070-6](https://doi.org/10.1016/S0168-1605(97)00070-6)
- Overbaugh, J., & Morris, L. (2012). The antibody response against HIV-1. *Cold Spring Harbor Perspectives in Medicine*. <https://doi.org/10.1101/cshperspect.a007039>
- Owuor, B. O., Ochanda, J. O., Kokwaro, J. O., Cheruiyot, A. C., Yeda, R. A., Okudo, C. A., & Akala, H. M. (2012). *In vitro* antiplasmodial activity of selected Luo and Kuria medicinal plants. *Journal of Ethnopharmacology*. <https://doi.org/10.1016/j.jep.2012.09.045>
- Palgrave, K. (2002). *Trees of Southern Africa* (pp. 415–420). Struick, Cape Town, South Africa.
- Panda, Dutta, & Bastia, A. K. (2010). Antibacterial activity of *Croton roxburghii* Balak. against

- the enteric pathogens. *Journal of Advanced Pharmaceutical Technology & Research*.  
<https://doi.org/10.4103/0110-5558.76442>
- Panda, S. K., Bastia, A. K., & Dutta, S. K. (2010). Anticandidal activity of croton roxburghii balak. *International Journal of Current Pharmaceutical Research*.
- Pascaline, J., & Charles, M. (2011). An inventory of medicinal plants that the people of Nandi use to treat malaria. *Journal of Animal & Plant ...*, 9(3), 1192–1200.  
<http://www.m.elewa.org/JAPS/2011/9.3/4.pdf>
- Pascaline, J., Charles, M., George, O., Lukhoba, C., Ruth, L., & D, M. S. (2010). Ethnobotanical survey and propagation of some endangered medicinal plants from south Nandi district of Kenya. *Journal of Animal & Plant Sciences*.
- Pauwels, R., Balzarini, J., Baba, M., Snoeck, R., Schols, D., Herdewijn, P., Desmyter, J., & De Clercq, E. (1988). Rapid and automated tetrazolium-based calorimetric assay for the detection of anti-HIV compounds. *Journal of Virological Methods*, 20, 309–321.
- Pauwels, R., De Clercq, E., Desmyter, J., Balzarini, J., Goubau, P., Herdewijn, P., Vanderhaeghe, H., & Vandeputte, M. (1987). Sensitive and rapid assay on MT-4 cells for detection of antiviral compounds against the AIDS virus. *Journal of Virological Methods*, 16(3), 171–185. [https://doi.org/10.1016/0166-0934\(87\)90002-4](https://doi.org/10.1016/0166-0934(87)90002-4)
- Pavlova, N. I., Savinova, O. V., Nikolaeva, S. N., Boreko, E. I., & Flekhter, O. B. (2003). Antiviral activity of betulin, betulinic and betulonic acids against some enveloped and non-enveloped viruses. *Fitoterapia*, 74(5), 489–492. [https://doi.org/10.1016/S0367-326X\(03\)00123-0](https://doi.org/10.1016/S0367-326X(03)00123-0)
- Penzak, S. R., & Chuck, S. K. (2000). Hyperlipidemia associated with HIV protease inhibitor use: pathophysiology, prevalence, risk factors and treatment. *Scand J Infect Dis*.  
<https://doi.org/10.1080/003655400750045196>
- Perdue, G. P., Blomster, R. N., Blake, D. A., & Farnsworth, N. R. (1979). South american plants II: Taspine isolation and anti-inflammatory activity. In *Journal of Pharmaceutical Sciences*.  
<https://doi.org/10.1002/jps.2600680145>
- Pereira, A. S., Amaral, A. C. F., Barnes, R. A., Cardoso, J. N., & Aquino Neto, F. R. (1999). Identification of isoquinoline alkaloids in crude extracts by high temperature gas chromatography-mass spectrometry. *Phytochemical Analysis*.  
[https://doi.org/10.1002/\(SICI\)1099-1565\(199909/10\)10:5<254::AID-PCA462>3.0.CO;2-Q](https://doi.org/10.1002/(SICI)1099-1565(199909/10)10:5<254::AID-PCA462>3.0.CO;2-Q)
- Peres, M. T. L. P., Delle Monache, F., Cruz, A. B., Pizzolatti, M. G., & Yunes, R. A. (1997).

- Chemical composition and antimicrobial activity of *Croton urucurana* Baillon (Euphorbiaceae). *Journal of Ethnopharmacology*, 56(3), 223–226.  
[https://doi.org/10.1016/S0378-8741\(97\)00039-1](https://doi.org/10.1016/S0378-8741(97)00039-1)
- Piacente, S., Dos Santos, L. C., Mahmood, N., & Pizza, C. (2006). Triterpenes from *Maytenus macrocarpa* and evaluation of their anti-hiv activity. *Natural Product Communications*, 1(12), 1073–1078. <https://doi.org/10.1177/1934578x0600101201>
- Piacente, S., Pizza, C., De Tommasi, N., & Mahmood, N. (1996). Constituents of *Ardisia japonica* and their in vitro anti-HIV activity. *Journal of Natural Products*, 59(6), 565–569. <https://doi.org/10.1021/np960074h>
- Pieters, L., de Bruyne, T., Claeys, M., Vlietinck, A., Calomme, M., & vanden Berghe, D. (1993). Isolation of a dihydrobenzofuran lignan from south american dragon's blood (*Croton* spp.) as an inhibitor of cell proliferation. *Journal of Natural Products*.  
<https://doi.org/10.1021/np50096a013>
- Pommier, Y., & Neamati, N. (1999). Inhibitors of Human Immunodeficiency Virus Integrase. *Advances in Virus Research*. [https://doi.org/10.1016/S0065-3527\(08\)60310-3](https://doi.org/10.1016/S0065-3527(08)60310-3)
- Popovic, M., Sarngadharan, M. G., Read, E., & Gallo, R. C. (1984a). Detection, isolation, and continuous production of cytopathic retroviruses (HTLV-III) from patients with AIDS and pre-AIDS. *Science*. <https://doi.org/10.1126/science.6200935>
- Popovic, M., Sarngadharan, M. G., Read, E., & Gallo, R. C. (1984b). Detection, isolation, and continuous production of cytopathic retroviruses (HTLV-III) from patients with AIDS and pre-AIDS. *Science*, 224(4648), 497–500. <https://doi.org/10.1126/science.6200935>
- Porrás-Reyes, B. H., Lewis, W. H., Roman, J., Simchowitz, L., & Mustoe, T. A. (1993). Enhancement of wound healing by the alkaloid taspine defining mechanism of action. *Proceedings of the Society for Experimental Biology & Medicine*.  
<https://doi.org/10.3181/00379727-203-43567>
- Powell, M. D., Ghosh, M., Jacques, P. S., Howard, K. J., Le Grice, S. J., & Levin, J. (1997). Alanine-scanning Mutations in the; Primer Grip; of p66 HIV-1 Reverse Transcriptase Result in Selective Loss of RNA Priming Activity. *Journal of Biological Chemistry*, 272(20), 13262–13269.
- Prieto-Martínez, F. D., López-López, E., Eurídice Juárez-Mercado, K., & Medina-Franco, J. L. (2019). Computational Drug Design Methods—Current and Future Perspectives. *In Silico*

- Drug Design*, 19–44. <https://doi.org/10.1016/B978-0-12-816125-8.00002-X>
- Prinsloo, G., Meyer, J. J. M., Hussein, A. A., Munoz, E., & Sanchez, R. (2010). A cardiac glucoside with invitro anti-HIV activity isolated from *Elaeodendron croceum*. *Natural Product Research*, 24(18), 1743–1746. <https://doi.org/10.1080/14786410903211912>
- Pudhom, K., & Sommit, D. (2011). Clerodane diterpenoids and a trisubstituted furan from *Croton oblongifolius*. *Phytochemistry Letters*, 4(2), 147–150. <https://doi.org/10.1016/j.phytol.2011.02.004>
- Qaisar, M. N., Chaudhary, B. A., Sajid, M. U., & Hussain, N. (2014). Evaluation of  $\alpha$ -glucosidase inhibitory activity of dichloromethane and methanol extracts of *Croton bonplandianum* baill. *Tropical Journal of Pharmaceutical Research*. <https://doi.org/10.4314/tjpr.v13i11.9>
- Quashie, P. K., Sloan, R. D., & Wainberg, M. A. (2012). Novel therapeutic strategies targeting HIV integrase. *BMC Medicine*, 10, 1–11. <https://doi.org/10.1186/1741-7015-10-34>
- Radcliffe-Smith. (2001). *Genera Euphorbiacearum* (p. 464p.). Royal Botanic Gardens, , Kew.
- Rainer Seitz. (2016). Human Immunodeficiency Virus (HIV). *Transfus Med Hemother*. 2016 May; 43(3): 203–222., 43(3), 203–222. <https://doi.org/10.1159/000445852>
- Ramakrishnan, M. A. (2016). Determination of 50% endpoint titer using a simple formula. *World Journal of Virology*, 5(2), 85. <https://doi.org/10.5501/WJV.V5.I2.85>
- Rangsin, R., Chiu, J., Khamboonruang, C., Sirisopana, N., Eiumtrakul, S., Brown, A. E., Robb, M., Beyrer, C., Ruangyuttikarn, C., Markowitz, L. E., & Nelson, K. E. (2004). The Natural History of HIV-1 Infection in Young Thai Men after Seroconversion. *Journal of Acquired Immune Deficiency Syndromes*. <https://doi.org/10.1097/00126334-200405010-00011>
- Rashid, M., Gustafson, K., Kashmani, Y., Cardellina, J., McMahon, J., & Boyd, M. (1995). Anti-Hiv alkaloids from *Toddalia asiatica*. *Natural Product Letters*, 6(2), 153–156. <https://doi.org/10.1080/10575639508044104>
- Rath, S., Patra, J. K., Mohapatra, N., Mohanty, G., Dutta, S., & Thatoi, H. (2011). In Vitro Antibacterial and Antioxidant Studies of *Croton roxburghii* L., from Similipal Biosphere Reserve. *Indian Journal of Microbiology*. <https://doi.org/10.1007/s12088-011-0133-2>
- Ravanelli, N., Santos, K. P., Motta, L. B., Lago, J. H. G., & Furlan, C. M. (2016). Alkaloids from *Croton echinocarpus* Baill.: Anti-HIV potential. *South African Journal of Botany*, 102, 153–156. <https://doi.org/10.1016/j.sajb.2015.06.011>
- Reed, L. J., & Muench, H. (1938). A simple method of estimating fifty per cent endpoints.

- American Journal of Epidemiology*, 27(3), 493–497.  
<https://doi.org/10.1093/oxfordjournals.aje.a118408>
- Rege, A. A., Ambaye, R. Y., & Deshmukh, R. A. (2010). In-vitro testing of anti-HIV activity of some medicinal plants. *Indian Journal of Natural Products and Resources*, 1(2), 193–199.
- Reust, C. E. (2011). Common adverse effects of antiretroviral therapy for HIV disease. *American Family Physician*. <https://doi.org/d8785> [pii]
- Risco, E., Ghia, F., Vila, R., Iglesias, J., Álvarez, E., & Cañigüeral, S. (2003). Immunomodulatory Activity and Chemical Characterisation of Sangre de Drago (Dragon's Blood) from *Croton lechleri*. *Planta Medica*. <https://doi.org/10.1055/s-2003-43208>
- Robert, S., Baccelli, C., Devel, P., Dogné, J. M., & Quetin-Leclercq, J. (2010). Effects of leaf extracts from *Croton zambesicus* Müell. Arg. on hemostasis. *Journal of Ethnopharmacology*. <https://doi.org/10.1016/j.jep.2010.02.007>
- Rochira, V., & Guaraldi, G. (2014). Hypogonadism in the HIV-Infected Man. In *Endocrinology and Metabolism Clinics of North America*. <https://doi.org/10.1016/j.ecl.2014.06.005>
- Rodrigues, G. R., Di Naso, F. C., Porawski, M., Marcolin, É., Kretzmann, N. A., Ferraz, A. D. B. F., Richter, M. F., Marroni, C. A., & Marroni, N. P. (2012). Treatment with aqueous extract from *Croton cajucara* Benth reduces hepatic oxidative stress in Streptozotocin-diabetic rats. *Journal of Biomedicine and Biotechnology*. <https://doi.org/10.1155/2012/902351>
- Roengsumran, S., Musikul, K., Petsom, A., Vilaivan, T., Sangvanich, P., Pornpakakul, S., Puthong, S., Chaichantipyuth, C., Jaiboon, N., & Chaichit, N. (2002). Croblongifolin, a new anticancer clerodane from *Croton oblongifolius*. *Planta Medica*. <https://doi.org/10.1055/s-2002-23138>
- Roengsumran, S., Petsom, A., Kuptiyanuwat, N., Vilaivan, T., Ngamrojnavanich, N., Chaichantipyuth, C., & Phuthong, S. (2001a). Cytotoxic labdane diterpenoids from *Croton oblongifolius*. *Phytochemistry*. [https://doi.org/10.1016/S0031-9422\(00\)00358-7](https://doi.org/10.1016/S0031-9422(00)00358-7)
- Roengsumran, S., Petsom, A., Kuptiyanuwat, N., Vilaivan, T., Ngamrojnavanich, N., Chaichantipyuth, C., & Phuthong, S. (2001b). Cytotoxic labdane diterpenoids from *Croton oblongifolius*. *Phytochemistry*, 56(1), 103–107. [https://doi.org/10.1016/S0031-9422\(00\)00358-7](https://doi.org/10.1016/S0031-9422(00)00358-7)
- Roengsumran, S., Pornpakakul, S., Muangsin, N., Sangvanich, P., Nhujak, T., Singtothong, P., Chaichit, N., Puthong, S., & Petsom, A. (2004a). New Halimane Diterpenoids from *Croton*



- oblongifolius*. *Planta Medica*. <https://doi.org/10.1055/s-2004-815466>
- Roengsumran, S., Pornpakakul, S., Muangsin, N., Sangvanich, P., Nhujak, T., Singtothong, P., Chaichit, N., Puthong, S., & Petsom, A. (2004b). New Halimane Diterpenoids from *Croton oblongifolius*. *Planta Medica*, 70(1), 87–89. <https://doi.org/10.1055/s-2004-815466>
- Rosa, M. do S. S., Mendonça-Filho, R. R., Bizzo, H. R., Rodrigues, I. de A., Soares, R. M. A., Souto-Padrón, T., Alviano, C. S., & Lopes, A. H. C. S. (2003). Antileishmanial activity of a linalool-rich essential oil from *Croton cajucara*. *Antimicrobial Agents and Chemotherapy*. <https://doi.org/10.1128/AAC.47.6.1895-1901.2003>
- Rossi, D., Bruni, R., Bianchi, N., Chiarabelli, C., Gambari, R., Medici, A., Lista, A., & Paganetto, G. (2003). Evaluation of the mutagenic, antimutagenic and antiproliferative potential of *Croton lechleri* (Muell. Arg.) latex. *Phytomedicine*. <https://doi.org/10.1078/094471103321659843>
- Rotich, W., Sadgrove, N. J., Mas-Claret, E., Padilla-González, G. F., Guantai, A., & Langat, M. K. (2021). HIV-1 Reverse Transcriptase Inhibition by Major Compounds in a Kenyan Multi-Herbal Composition (CareVid™): *In Vitro* and *In Silico* Contrast. *Pharmaceuticals 2021*, Vol. 14, Page 1009, 14(10), 1009. <https://doi.org/10.3390/PH14101009>
- Russell B., Wang, L., & Williams, P. L. (2008). Toxicities Associated with Dual Nucleoside Reverse-Transcriptase Inhibitor Regimens in HIV-Infected Children. *The Journal of Infectious Diseases*. <https://doi.org/10.1086/593022>
- Sá, N. C., Cavalcante, T. T. A., Araújo, A. X., Santos, H. S. Dos, Albuquerque, M. R. J. R., Bandeira, P. N., Cunha, R. M. S. Da, Cavada, B. S., & Teixeira, E. H. (2012). Antimicrobial and antibiofilm action of Casbane Diterpene from *Croton nepetaefolius* against oral bacteria. *Archives of Oral Biology*. <https://doi.org/10.1016/j.archoralbio.2011.10.016>
- Sabin, C. A., & Lundgren, J. D. (2013). The natural history of HIV infection. In *Current Opinion in HIV and AIDS*. <https://doi.org/10.1097/COH.0b013e328361fa66>
- Saikia, L. R., & Upadhyaya, S. (2011). Antioxidant activity, phenol and flavonoid content of some less known medicinal plants of Assam. *International Journal of Pharma and Bio Sciences*.
- Salatino, A., Salatino, M. L. F., & Negri, G. (2007). Traditional uses, chemistry and pharmacology of *Croton* species (Euphorbiaceae). *Journal of the Brazilian Chemical Society*, 18(1), 11–33. <https://doi.org/10.1590/S0103-50532007000100002>
- Sandoval, M., Okuhama, N. N., Clark, M., Angeles, F. M., Lao, J., Bustamante, S., & Miller, M.

- J. S. (2002). Sangre de grado *Croton palanostigma* induces apoptosis in human gastrointestinal cancer cells. *Journal of Ethnopharmacology*. [https://doi.org/10.1016/S0378-8741\(02\)00013-2](https://doi.org/10.1016/S0378-8741(02)00013-2)
- Santos, F. A., Jeferson, F. A., Santos, C. C., Silveira, E. R., & Rao, V. S. N. (2005). Antinociceptive effect of leaf essential oil from *Croton sonderianus* in mice. *Life Sciences*. <https://doi.org/10.1016/j.lfs.2005.05.032>
- Sarafianos, S. G., Das, K., Tantillo, C., Clark, A. D., Ding, J., Whitcomb, J. M., Boyer, P. L., Hughes, S. H., & Arnold, E. (2001). Crystal structure of HIV-1 reverse transcriptase in complex with a polypurine tract RNA: DNA. *The EMBO Journal*, 20(6), 1449–1461.
- Saslis-Lagoudakis, C. H., Savolainen, V., Williamson, E. M., Forest, F., Wagstaff, S. J., Baral, S. R., Watson, M. F., Pendry, C. A., & Hawkins, J. A. (2012). Phylogenies reveal predictive power of traditional medicine in bioprospecting. *Proceedings of the National Academy of Sciences*, 109(39), 15835–15840. <https://doi.org/10.1073/PNAS.1202242109>
- Scheller, C., & Jassoy, C. (2001). Syncytium formation amplifies apoptotic signals: A new view on apoptosis in HIV infection in vitro. *Virology*. <https://doi.org/10.1006/viro.2000.0811>
- Schinazi, R. F., Kohler, J. J., & Kim, B. (2013). Reverse Transcription. In *Brenner's Encyclopedia of Genetics: Second Edition*. <https://doi.org/10.1016/B978-0-12-374984-0.01327-9>
- Scholfield, M. R., Vander Zanden, C. M., Carter, M., & Ho, P. S. (2013). Halogen bonding (X-bonding): a biological perspective. *Protein Science: A Publication of the Protein Society*, 22(2), 139–152. <https://doi.org/10.1002/PRO.2201>
- Schröder, H. C., Merz, H., Steffen, R., Müller, W. E. G., Sarin, P. S., Trumm, S., Schulz, J., & Eich, E. (1990). Differential in vitro Anti-HIV activity of natural lignans. *Zeitschrift Fur Naturforschung Section C Journal of Biosciences*, 45(11–12), 1215–1221. <https://doi.org/10.1515/znc-1990-11-1222>
- Schuitmaker, H., Koot, M., Kootstra, N. A., Dercksen, M. W., de Goede, R. E., van Steenwijk, R. P., Lange, J. M., Schattenkerk, J. K., Miedema, F., & Tersmette, M. (1992). Biological phenotype of human immunodeficiency virus type 1 clones at different stages of infection: progression of disease is associated with a shift from monocytotropic to T-cell-tropic virus population. *Journal of Virology*. <https://doi.org/10.1016/j.tetlet.2009.06.089>
- Seal, A., Aykkal, R., & Ghosh, M. G. (2011). Docking study of HIV-1 reverse transcriptase with phytochemicals. *Bioinformation*, 5(10), 430–439. <https://doi.org/10.6026/97320630005430>

- Segala, E., Guo, D., Cheng, R. K. Y., Bortolato, A., Deflorian, F., Doré, A. S., Errey, J. C., Heitman, L. H., Ijzerman, A. P., Marshall, F. H., & Cooke, R. M. (2016). Controlling the Dissociation of Ligands from the Adenosine A2A Receptor through Modulation of Salt Bridge Strength. *Journal of Medicinal Chemistry*, 59(13), 6470–6479.  
<https://doi.org/10.1021/ACS.JMEDCHEM.6B00653>
- Selowa, S. C., Shai, L. J., Masoko, P., Mokgotho, M. P., & Magano, S. R. (2010). Antibacterial activity of extracts of three Croton species collected in Mpumalanga region in South Africa. *African Journal of Traditional, Complementary and Alternative Medicines*.  
<https://doi.org/10.4314/ajtcam.v7i2.50861>
- Semba, R. D., & Tang, A. M. (1999). Micronutrients and the pathogenesis of human immunodeficiency virus infection. In *British Journal of Nutrition*.  
<https://doi.org/10.1017/S0007114599000379>
- Semenya, S. S., & Maroyi, A. (2013). Medicinal plants used for the treatment of tuberculosis by Bapedi traditional healers in three districts of the Limpopo Province, South Africa. *African Journal of Traditional, Complementary, and Alternative Medicines : AJTCAM / African Networks on Ethnomedicines*, 10(2), 316–323. <https://doi.org/10.4314/ajtcam.v10i2.17>
- Seniya, C., Yadav, A., Khan, G. J., & Sah, N. K. (2015). *In-silico* Studies Show Potent Inhibition of HIV-1 Reverse Transcriptase Activity by a Herbal Drug. *IEEE/ACM Transactions on Computational Biology and Bioinformatics*, 12(6), 1355–1364.  
<https://doi.org/10.1109/TCBB.2015.2415771>
- Sethi, M.L. (1977). *Inhibition of RNA-directed DNA polymerase activity of RNA tumor viruses by taspine*. (pp. 12,7–9.). Canadian Journal of Pharmaceutical Sciences.
- Shang, S. Z., Kong, L. M., Yang, L. P., Jiang, J., Huang, J., Zhang, H. B., Shi, Y. M., Zhao, W., Li, H. L., Luo, H. R., Li, Y., Xiao, W. L., & Sun, H. D. (2013). Bioactive phenolics and terpenoids from *Manglietia insignis*. *Fitoterapia*, 84(1), 58–63.  
<https://doi.org/10.1016/j.fitote.2012.10.010>
- Sharp, P. M., & Hahn, B. H. (2011). Origins of HIV and the AIDS pandemic. *Cold Spring Harbor Perspectives in Medicine*. <https://doi.org/10.1101/cshperspect.a006841>
- Simionatto, E., Bonani, V. F. L., Morel, A. F., Ré Poppi, N., Raposo, J. L., Stuker, C. Z., Peruzzo, G. M., Peres, M. T. L. P., & Hessa, S. C. (2007). Chemical composition and evaluation of antibacterial and antioxidant activities of the essential oil of *Croton urucurana* baillon

- (Euphorbiaceae) stem bark. *Journal of the Brazilian Chemical Society*.  
<https://doi.org/10.1590/S0103-50532007000500002>
- Singh, A. (2018). Ethnomedicinal , Pharmacological and Antimicrobial Aspects of *Moringa oleifera* Lam .: A review. *The Journal of Phytopharmacology*, 7(1), 45–50.
- Singh, M., Pal, M., & Sharma, R. P. (1999). Biological Activity of the Labdane Diterpenes\*. *Planta Medica*. <https://doi.org/10.1055/s-1999-13952>
- Sluis-Cremer, N., Arion, D., Abram, M. E., & Parniak, M. A. (2004). Proteolytic processing of an HIV-1 pol polyprotein precursor: insights into the mechanism of reverse transcriptase p66/p51 heterodimer formation. *The International Journal of Biochemistry & Cell Biology*, 36(9), 1836–1847.
- Sluis-Cremer, N., & Tachedjian, G. (2008). Mechanisms of inhibition of HIV replication by non-nucleoside reverse transcriptase inhibitors. *Virus Research*.  
<https://doi.org/10.1016/j.virusres.2008.01.002>
- Sluis-Cremer, N., & Tachedjian, G. (2002). Modulation of the oligomeric structures of HIV-1 retroviral enzymes by synthetic peptides and small molecules. *European Journal of Biochemistry*, 269(21), 5103–5111.
- Sommit, D., Petsom, A., Ishikawa, T., & Roengsumran, S. (2003). Cytotoxic activity of natural labdanes and their semi-synthetic modified derivatives from *Croton oblongifolius*. *Planta Medica*. <https://doi.org/10.1055/s-2003-37708>
- Somteds, A., Tantapakul, C., Kanokmedhakul, K., Laphookhieo, S., Phukhatmuen, P., & Kanokmedhakul, S. (2019). Inhibition of nitric oxide production by clerodane diterpenoids from leaves and stems of *Croton poomae* Esser. *Natural Product Research*.  
<https://doi.org/10.1080/14786419.2019.1667350>
- Sperling, R. (1998a). Zidovudine. *Infectious Diseases in Obstetrics and Gynecology*.  
[https://doi.org/10.1002/\(SICI\)1098-0997\(1998\)6:5<197::AID-IDOG2>3.0.CO;2-1](https://doi.org/10.1002/(SICI)1098-0997(1998)6:5<197::AID-IDOG2>3.0.CO;2-1)
- Strebel, K. (2013). HIV accessory proteins versus host restriction factors. *In Current Opinion in Virology*. <https://doi.org/10.1016/j.coviro.2013.08.004>
- Strober, W. (2015). Trypan Blue Exclusion Test of Cell Viability. *Current Protocols in Immunology*. <https://doi.org/10.1002/0471142735.ima03bs111>
- Suárez, A. I., Compagnone, R. S., Salazar-Bookaman, M. M., Tillett, S., Delle Monache, F., Di Giulio, C., & Bruges, G. (2003). Antinociceptive and anti-inflammatory effects of *Croton*

- malambo* bark aqueous extract. *Journal of Ethnopharmacology*, 88(1), 11–14.  
[https://doi.org/10.1016/S0378-8741\(03\)00179-X](https://doi.org/10.1016/S0378-8741(03)00179-X)
- Suárez, A. I., Vásquez, L. J., Taddei, A., Arvelo, F., & Compagnone, R. S. (2008). Antibacterial and cytotoxic activity of leaf essential oil of *Croton malambo*. *Journal of Essential Oil-Bearing Plants*. <https://doi.org/10.1080/0972060X.2008.10643622>
- Sundquist, W. I., & Kräusslich, H. G. (2012). HIV-1 assembly, budding, and maturation. In *Cold Spring Harbor Perspectives in Medicine*. <https://doi.org/10.1101/cshperspect.a006924>
- Świderek, K., Martí, S., & Moliner, V. (2012). Theoretical studies of HIV-1 reverse transcriptase inhibition. *Physical Chemistry Chemical Physics*. <https://doi.org/10.1039/c2cp40953d>
- Szucs, G., Melnick, J. L., & Hollinger, F. B. (1988). A simple assay based on HIV infection preventing the reclustering of MT-4 cells. *Bulletin of the World Health Organization*.
- Tala, M. F., Tan, N. H., Ndontsa, B. L., & Tane, P. (2013a). Triterpenoids and phenolic compounds from *Croton macrostachyus*. *Biochemical Systematics and Ecology*.  
<https://doi.org/10.1016/j.bse.2013.08.001>
- Tala, M. F., Tan, N. H., Ndontsa, B. L., & Tane, P. (2013b). Triterpenoids and phenolic compounds from *Croton macrostachyus*. *Biochemical Systematics and Ecology*, 51, 138–141.  
<https://doi.org/10.1016/J.BSE.2013.08.001>
- Tamariz Ortiz, J. H., Capcha Mendoza, R., Palomino Cadenas, E. J., & Aguilar Olano, J. (2013). Actividad antibacteriana de la Sangre de Grado (*Croton lechleri*) frente al *Helicobacter pylori*. *Med Hered*.
- Tan, I. L., Smith, B. R., von Geldern, G., Mateen, F. J., & McArthur, J. C. (2012). HIV-associated opportunistic infections of the CNS. In *The Lancet Neurology*.  
[https://doi.org/10.1016/S1474-4422\(12\)70098-4](https://doi.org/10.1016/S1474-4422(12)70098-4)
- Tane, P., Tatsimo, S., & Connolly, J. D. (2004). Crotomacrine, a new clerodane diterpene from the fruits of *Croton macrostachyus*. *Tetrahedron Letters*.  
<https://doi.org/10.1016/j.tetlet.2004.08.001>
- Taniguchi, M., & Kubo, I. (1993). Ethnobotanical drug discovery based on medicine men's trials in the African savanna: Screening of East African plants for antimicrobial activity II. *Journal of Natural Products*. <https://doi.org/10.1021/np50099a012>
- Tansakul, P., & De-Eknamkul, W. (1998). Geranylgeraniol-18-hydroxylase: The last enzyme on the plaunotol biosynthetic pathway in *Croton sublyratus*. *Phytochemistry*.

[https://doi.org/10.1016/S0031-9422\(97\)00743-7](https://doi.org/10.1016/S0031-9422(97)00743-7)

- Taye, B., Giday, M., Animut, A., & Seid, J. (2011a). Antibacterial activities of selected medicinal plants in traditional treatment of human wounds in Ethiopia. *Asian Pacific Journal of Tropical Biomedicine*. [https://doi.org/10.1016/S2221-1691\(11\)60082-8](https://doi.org/10.1016/S2221-1691(11)60082-8)
- Taye, B., Giday, M., Animut, A., & Seid, J. (2011b). Antibacterial activities of selected medicinal plants in traditional treatment of human wounds in Ethiopia. *Asian Pacific Journal of Tropical Biomedicine*, 1(5), 370–375. [https://doi.org/10.1016/S2221-1691\(11\)60082-8](https://doi.org/10.1016/S2221-1691(11)60082-8)
- Taylor, D. L., Nash, R., Fellows, L. E., Kang, M. S., & Tyms, A. S. (2016). Naturally Occurring Pyrrolizidines: Inhibition of  $\alpha$ -Glucosidase 1 and Anti-HIV Activity of One Stereoisomer: <Http://Dx.Doi.Org/10.1177/095632029200300504>, 3(5), 273–277. <https://doi.org/10.1177/095632029200300504>
- Tchissambou, L., Chiaroni, A., Riche, C., & Khuong-Huu, F. (1990). Crotoeryliferan and crotohaumanoxide, new diterpenes from *Croton haumanianus* J. Leonard. *Tetrahedron*, 46(15), 5199–5202. [https://doi.org/10.1016/S0040-4020\(01\)87826-1](https://doi.org/10.1016/S0040-4020(01)87826-1)
- Tefera, M., Geyid, A., & Debella, A. (2012). In vitro anti-Neisseria gonorrhoeae activity of *Albizia gummifera* and *Croton macrostachyus*. *Pharmacologyonline*.
- Teklay, A., Abera, B., & Giday, M. (2013). An ethnobotanical study of medicinal plants used in Kilte Awulaelo district, Tigray region of Ethiopia. *Journal of Ethnobiology and Ethnomedicine*. <https://doi.org/10.1186/1746-4269-9-65>
- Teklehaymanot, T. (2009). Ethnobotanical study of knowledge and medicinal plants use by the people in Dek Island in Ethiopia. *Journal of Ethnopharmacology*. <https://doi.org/10.1016/j.jep.2009.04.005>
- Teklehaymanot, T., Giday, M., Medhin, G., & Mekonnen, Y. (2007). Knowledge and use of medicinal plants by people around Debre Libanos monastery in Ethiopia. *Journal of Ethnopharmacology*. <https://doi.org/10.1016/j.jep.2006.11.019>
- Tene, M., Ndontsa, B. L., Tane, P., Tamokou, J. D. D., & Kuate, J. (2009). Antimicrobial diterpenoids and triterpenoids from the stem bark of *Croton macrostachys*. *International Journal of Biological and Chemical Sciences*.
- Teugwa Mofor C., Sonfack Dontsa C. R., Fokom R., P. B. V. and A. Z. P. H. (2013). Antifungal and antioxidant activity of crude extracts of three medicinal plants from Cameroon pharmacopea. *Journal of Medicinal Plants Research*, 7(21), 1537–1542.

<https://doi.org/10.5897/JMPR13.2581>

- Thijssen, R. (1996). *Croton megalocarpus*, The Poultry-Feed Tree: How Local Knowledge Could Help to Feed The World. In: Domestication and Commercialization of Non-Timber Forest Products in Agroforestry Systems (pp. 226–234). FAO., Rome, Italy.
- Thompson, L. U. (1993). Potential health benefits and problems associated with antinutrients in foods. *Food Research International*, 26(2). [https://doi.org/10.1016/0963-9969\(93\)90069-U](https://doi.org/10.1016/0963-9969(93)90069-U)
- Thongtan, J., Kittakoop, P., Ruangrunsi, N., Saenboonrueng, J., & Thebtaranonth, Y. (2003). New Antimycobacterial and Antimalarial 8,9-Secokaurane Diterpenes from *Croton kongensis*. *Journal of Natural Products*. <https://doi.org/10.1021/np030067a>
- Tietjen, I., Gatonye, T., Ngwenya, B. N., Namushe, A., Simonambanga, S., Muzila, M., Mwimanzi, P., Xiao, J., Fedida, D., Brumme, Z. L., Brockman, M. A., & Andrae-Marobela, K. (2016a). *Croton megalobotrys* Müll Arg. and *Vitex doniana* (Sweet): Traditional medicinal plants in a three-step treatment regimen that inhibit in vitro replication of HIV-1. *Journal of Ethnopharmacology*, 191, 331–340. <https://doi.org/10.1016/j.jep.2016.06.040>
- Tilton, J. C., & Doms, R. W. (2010). Entry inhibitors in the treatment of HIV-1 infection. In *Antiviral Research*. <https://doi.org/10.1016/j.antiviral.2009.07.022>
- Torti, C., Pozniak, A., Nelson, M., Hertogs, K., & Gazzard, B. G. (2001). Distribution of K103N and/or Y181C HIV-1 Mutations by Exposure to Zidovudine and Non-nucleoside Reverse Transcriptase Inhibitors. *The Journal of Antimicrobial Chemotherapy*.
- Tradtrantip, L., Namkung, W., & Verkman, A. S. (2010). Crofelemer, an Antisecretory Antidiarrheal Proanthocyanidin Oligomer Extracted from *Croton lechleri*, Targets Two Distinct Intestinal Chloride Channels. *Molecular Pharmacology*. <https://doi.org/10.1124/mol.109.061051>
- Trinh, T. D., Phan, V. K., Nguyen, T. D., Nguyen, H. T., Bui, T. B., Chau, V. M., & Braca, A. (2007). Pinoresinol and 3,4',5,7-Tetrahydroxy-3'- Methoxyflavanone From the Fruits of *Silybum marianum* (L.) Gaertn. *Journal of Chemistry*, 45(2), 219–222.
- Tsai, J. C., Tsai, S., & Chang, W. C. (2004). Effect of ethanol extracts of three Chinese medicinal plants with laxative properties on ion transport of the rat intestinal epithelia. *Biol Pharm Bull*. <https://doi.org/10.1248/bpb.27.162>
- Ubillas, R., Jolad, S. D., Bruening, R. C., Kernan, M. R., King, S. R., Sesin, D. F., Barrett, M., Stoddart, C. A., Flaster, T., Kuo, J., Ayala, F., Meza, E., Castañel, M., Mcmeekin, D.,

- Rozhon, E., Tempesta, M. S., Barnard, D., Huffman, J., Smee, D., Nakanishi, K. (1994). SP-303, an antiviral oligomeric proanthocyanidin from the latex of *Croton lechleri* (Sangre de Drago). *Phytomedicine*. [https://doi.org/10.1016/S0944-7113\(11\)80026-7](https://doi.org/10.1016/S0944-7113(11)80026-7)
- Uğur, D., Güneş, H., Gülneş, F., & Mammadov, R. (2017). Cytotoxic Activities of Certain Medicinal Plants on Different Cancer Cell Lines. *Turkish Journal of Pharmaceutical Sciences*, *14*(3), 222–230. <https://doi.org/10.4274/TJPS.80299>
- Umberto Quattrocchi. (2012). CRC World Dictionary of Medicinal and Poisonous Plants: Common Names Umberto Quattrocchi- *Google Books*. CRC Press. <https://doi.org/10.1201/b16504>
- UNAIDS. (2016). The AIDS Epidemic Can Be Ended by 2030 With Your Help (15pps). [http://www.nytimes.com/2013/08/21/opinion/global/the-aids-epidemic-can-be-ended.html?smid=fb-share&\\_r=1&&pagewanted=print](http://www.nytimes.com/2013/08/21/opinion/global/the-aids-epidemic-can-be-ended.html?smid=fb-share&_r=1&&pagewanted=print)
- UNAIDS. (2020). Global HIV & AIDS statistics — 2020 fact sheet | UNAIDS. <https://www.unaids.org/en/resources/fact-sheet>
- Van Heuverswyn, F., Li, Y., Neel, C., Bailes, E., Keele, B. F., Liu, W., Loul, S., Butel, C., Liegeois, F., Bienvenue, Y., Ngolle, E. M., Sharp, P. M., Shaw, G. M., Delaporte, E., Hahn, B. H., & Peeters, M. (2006). Human immunodeficiency viruses: SIV infection in wild gorillas. *Nature*. <https://doi.org/10.1038/444164a>
- Van Kiem, P., Van Minh, C., Huong, H. T., Lee, J. J., Lee, I. S., & Kim, Y. H. (2005). Phenolic constituents with inhibitory activity against NFAT transcription from *Desmos chinensis*. *Archives of Pharmacal Research* *28*:12, 28(12), 1345–1349. <https://doi.org/10.1007/BF02977900>
- Van Lint, C., Bouchat, S., & Marcello, A. (2013). HIV-1 transcription and latency: An update. In *Retrovirology*. <https://doi.org/10.1186/1742-4690-10-67>
- Veber, D. F., Johnson, S. R., Cheng, H. Y., Smith, B. R., Ward, K. W., & Kopple, K. D. (2002). Molecular properties that influence the oral bioavailability of drug candidates. *Journal of Medicinal Chemistry*, *45*(12), 2615–2623. <https://doi.org/10.1021/jm020017n>
- Vigor, C., Fabre, N., Fourasté, I., & Moulis, C. (2001). Three clerodane diterpenoids from *Croton eluteria* Bennett. *Phytochemistry*, *57*(8), 1209–1212. [https://doi.org/10.1016/S0031-9422\(01\)00183-2](https://doi.org/10.1016/S0031-9422(01)00183-2)
- Voigt, E., Wickesberg, A., Wasmuth, J. C., Gute, P., Locher, L., Salzberger, B., Wöhrmann, A.,



- Adam, A., Weitner, L., & Rockstroh, J. K. (2002). First-line ritonavir/indinavir 100/800 mg twice daily plus nucleoside reverse transcriptase inhibitors in a German multicentre study: 48-week results. *HIV Medicine*. <https://doi.org/10.1046/j.1468-1293.2002.00123.x>
- Vongchareonsathit, A., & De-Eknamkul, W. (1998). Rapid TLC-densitometric analysis of plaunotol from *Croton sublyratus* leaves. *Planta Medica*. <https://doi.org/10.1055/s-2006-957428>
- Voukeng, I. K., Beng, V. P., & Kuete, V. (2016). Antibacterial activity of six medicinal Cameroonian plants against Gram-positive and Gram-negative multidrug resistant phenotypes. *BMC Complementary and Alternative Medicine*. <https://doi.org/10.1186/s12906-016-1371-y>
- Walker, B. D., & Burton, D. R. (2008). *Towards an AIDS Vaccine*. 760(2008). <https://doi.org/10.1126/science.1152622>
- Wambugu, F. K., & Waweru. (2016). Evaluation of wound healing activity of ethanolic extract of leaves of *Croton megalocarpus* using excision wound model on Wistar albino rats. (pp. 4: 182-194.). *Int. J. Sci. Res. Methodol.*
- Wang, G. C., Zhang, H., Liu, H. B., & Yue, J. M. (2013). Laevinoids A and B: Two diterpenoids with an unprecedented backbone from *Croton laevigatus*. *Organic Letters*, 15(18), 4880–4883. <https://doi.org/10.1021/ol402318m>
- Wang, G. P., Ciuffi, A., Leipzig, J., Berry, C. C., & Bushman, F. D. (2007). HIV integration site selection: Analysis by massively parallel pyrosequencing reveals association with epigenetic modifications. *Genome Research*. <https://doi.org/10.1101/gr.6286907>
- Wang, X., Zhang, F. M., Liu, Z. X., Feng, H. Z., Yu, Z. Bin, Lu, Y. Y., Zhai, H. H., Bai, F. H., Shi, Y. Q., Lan, M., Jin, J. P., & Fan, D. M. (2008). Effects of essential oil from *Croton tiglium* L. on intestinal transit in mice. *Journal of Ethnopharmacology*. <https://doi.org/10.1016/j.jep.2008.01.023>
- Waters, L., John, L., & Nelson, M. (2007). Non-nucleoside reverse transcriptase inhibitors: A review. In *International Journal of Clinical Practice*. <https://doi.org/10.1111/j.1742-1241.2006.01146.x>
- Wei, X., Decker, J. M., Liu, H., Zhang, Z., Arani, R. B., Kilby, J. M., Saag, M. S., Wu, X., Shaw, G. M., & Kappes, J. C. (2002). Emergence of resistant human immunodeficiency virus type 1 in patients receiving fusion inhibitor (T-20) monotherapy. *Antimicrobial Agents and*

- Chemotherapy*. <https://doi.org/10.1128/AAC.46.6.1896-1905.2002>
- Weislow, O. S., Kiser, R., Fine, D. L., Bader, J., Shoemaker, R. H., & Boyd, M. R. (1989). New soluble-formazan assay for HIV-1 cytopathic effects: Application to high-flux screening of synthetic and natural products for AIDS-antiviral activity. *Journal of the National Cancer Institute*. <https://doi.org/10.1093/jnci/81.8.577>
- Wensing, A. M. J., van Maarseveen, N. M., & Nijhuis, M. (2010). Fifteen years of HIV Protease Inhibitors: raising the barrier to resistance. In *Antiviral Research*. <https://doi.org/10.1016/j.antiviral.2009.10.003>
- Williams, L., Coscaró, M. C., Dellapé, P. M., & Roane, T. M. (2005). The shield-backed bug, *Pachycoris stallii*: Description of immature stages, effect of maternal care on nymphs, and notes on life history. *Journal of Insect Science*. <https://doi.org/10.1093/jis/5.1.29>
- Williams, L., Evans, P. E., & Bowers, W. S. (2001). Defensive chemistry of an aposematic bug, *Pachycoris stallii* uhler and volatile compounds of its host plant *Croton californicus* Muell.-Arg. *Journal of Chemical Ecology*. <https://doi.org/10.1023/A:1005692502595>
- Winslow, C. Y., & Kerdel, F. A. (2015). Human immunodeficiency virus. In *Dermatological Manifestations of Kidney Disease*. [https://doi.org/10.1007/978-1-4939-2395-3\\_4](https://doi.org/10.1007/978-1-4939-2395-3_4)
- Wlodawer, A., & Vondrasek, J. (1998). Inhibitors of HIV-1 protease: A Major Success of Structure-Assisted Drug Design. *Annual Review of Biophysics and Biomolecular Structure*. <https://doi.org/10.1146/annurev.biophys.27.1.249>
- Wolff Cordeiro, K., Aparecida Pinto, L., Nazari Formagio, A. S., Faloni De Andrade, S., Leite Kassuya, C. A., & De Cássia Freitas, K. (2012). Antiulcerogenic effect of *Croton urucurana* Baillon bark. *Journal of Ethnopharmacology*. <https://doi.org/10.1016/j.jep.2012.06.044>
- World Health Organization. (2013). Phasing out stavudine : progress and *challenges*. 69–85.
- World Health Organization. (2016). Progress Report 2016, prevent HIV, test and treat all. In *WHO/HIV/2016.24*.
- Wu, P. L., Su, G. C., & Wu, T. S. (2003). Constituents from the stems of *Aristolochia manshuriensis*. *Journal of Natural Products*, 66(7), 996–998. <https://doi.org/10.1021/np0301238>
- Wu, Y. C., Hung, Y. C., Chang, F. R., Cosentino, M., Wang, H. K., & Lee, K. H. (1996). Identification of ent-16 $\beta$ ,17-dihydroxykauran-19-oic acid as an anti- HIV principle and isolation of the new diterpenoids annosquamosins A and B from *Annona squamosa*. *Journal*

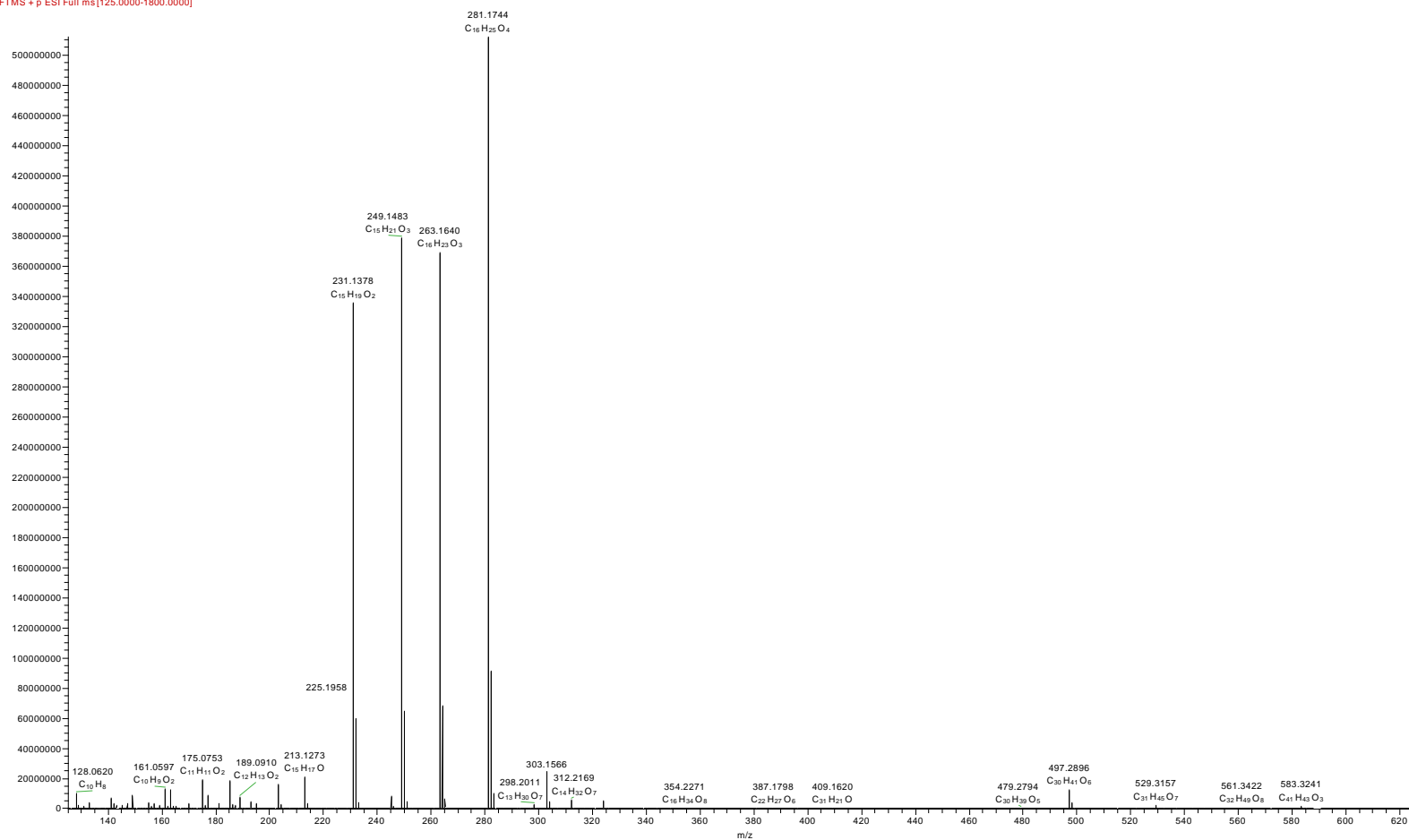
- of Natural Products*, 59(6), 635–637. <https://doi.org/10.1021/np960416j>
- Wurdack, K. J., & Davis, C. C. (2009). Malpighiales phylogenetics: Gaining ground on one of the most recalcitrant clades in the angiosperm tree of life. *American Journal of Botany*. <https://doi.org/10.3732/ajb.0800207>
- Wyatt, C. M., & Klotman, P. E. (2009). HIV-associated Nephropathy. In *Genetic Diseases of the Kidney*. <https://doi.org/10.1016/B978-0-12-449851-8.00047-4>
- Wyde, P. R., Ambrose, M. W., Meyerson, L. R., & Gilbert, B. E. (1993). The antiviral activity of SP-303, a natural polyphenolic polymer, against respiratory syncytial and parainfluenza type 3 viruses in cotton rats. *Antiviral Research*. [https://doi.org/10.1016/0166-3542\(93\)90004-3](https://doi.org/10.1016/0166-3542(93)90004-3)
- Xin Zhang, Amandine Cambrai, Michel Miesch, Stamatiki Roussi, Francis Raul, Dalal Aoude-Werner, and Eric Marchioni (2006). Separation of  $\Delta 5$ - and  $\Delta 7$ -Phytosterols by Adsorption Chromatography and Semipreparative Reversed Phase High-Performance Liquid Chromatography for Quantitative Analysis of Phytosterols in Foods. *Journal of Agricultural and Food Chemistry*, 54(4), 1196–1202. <https://doi.org/10.1021/JF052761X>
- Xu, F., Huang, X., Wu, H., & Wang, X. (2018). Beneficial health effects of lupenone triterpene: A review. *Biomedicine and Pharmacotherapy*, 103(April), 198–203. <https://doi.org/10.1016/j.biopha.2018.04.019>
- Xu, H.-X., Wan, M., Loh, B.-N., Kon, O.-L., Chow, P.-W., & Sim, K.-Y. (1996). Screening of Traditional Medicines for their Inhibitory Activity Against HIV-1 Protease. *Phytotherapy Research*, 10(3), 207–210. [https://doi.org/10.1002/\(SICI\)1099-1573\(199605\)10:3<207::AID-PTR812>3.0.CO;2-U](https://doi.org/10.1002/(SICI)1099-1573(199605)10:3<207::AID-PTR812>3.0.CO;2-U)
- Yagi, S., Babiker, R., Tzanova, T., & Schohn, H. (2016). Chemical composition, antiproliferative, antioxidant and antibacterial activities of essential oils from aromatic plants growing in Sudan. *Asian Pacific Journal of Tropical Medicine*. <https://doi.org/10.1016/j.apjtm.2016.06.009>
- Yannick Stephane, F. F., Dawe, A., Angelbert Fusi, A., Jean Jules, B. K., Ulrich, K. K. D., Lateef, M., Bruno, L. N., Ali, M. S., & Ngouela, S. A. (2019). Crotoliganfuran, a new clerodane-type furano-diterpenoid from *Croton oligandrus* Pierre ex Hutch. *Natural Product Research*, 0(0), 1–9. <https://doi.org/10.1080/14786419.2019.1613399>
- Yoshitatsu Ichihara, Koichi Takeya, Yukio Hitotsuyanagi, Hiroshi Morita, Satomi Okuyama, Masami Suganuma, Hirota Fujiki, Mario Motidome, H. I. (1992). Cajucarinolide and

- Isocajucarinolide: Anti-Inflammatory Diterpenes from *Croton cajucara*. *Planta Med*, 58(6)(August 1988), 549–551. <https://doi.org/10.1055/s-2006-961547>
- Yust, M. D. M., Pedroche, J., Megías, C., Girón-Calle, J., Alaiz, M., Millán, F., & Vioque, J. (2004). Rapeseed protein hydrolysates: A source of HIV protease peptide inhibitors. *Food Chemistry*. <https://doi.org/10.1016/j.foodchem.2003.11.020>
- Zhang, H., Lu, Z., Tan, G. T., Qiu, S., Farnsworth, N. R., Pezzuto, J. M., & Fong, H. H. S. (2002). Polyacetyleneginsenoside-Ro, a novel triterpene saponin from *Panax ginseng*. *Tetrahedron Letters*, 43(6), 973–977. [https://doi.org/10.1016/S0040-4039\(01\)02310-3](https://doi.org/10.1016/S0040-4039(01)02310-3)
- Zhang, L., Luo, R. H., Wang, F., Jiang, M. Y., Dong, Z. J., Yang, L. M., Zheng, Y. T., & Liu, J. K. (2010). Highly functionalized daphnane diterpenoids from *Trigonostemon thyrsoideum*. *Organic Letters*, 12(1), 152–155. <https://doi.org/10.1021/ol9025638>
- Zhao, G., Etherton, T. D., Martin, K. R., Vanden Heuvel, J. P., Gillies, P. J., West, S. G., & Kris-Etherton, P. M. (2005). Anti-inflammatory effects of polyunsaturated fatty acids in THP-1 cells. *Biochemical and Biophysical Research Communications*. <https://doi.org/10.1016/j.bbrc.2005.08.204>
- Zhao, J. X., Liu, C. P., Qi, W. Y., Han, M. L., Han, Y. S., Wainberg, M. A., & Yue, J. M. (2014). Eurifoloids A-R, structurally diverse diterpenoids from *Euphorbia neriifolia*. *Journal of Natural Products*, 77(10), 2224–2233. <https://doi.org/10.1021/np5004752>
- Zheng, R., Jenkins, T. M., & Craigie, R. (1996). Zinc folds the N-terminal domain of HIV-1 integrase, promotes multimerization, and enhances catalytic activity. *Proceedings of the National Academy of Sciences*, 93(24), 13659–13664.

# APPENDICES

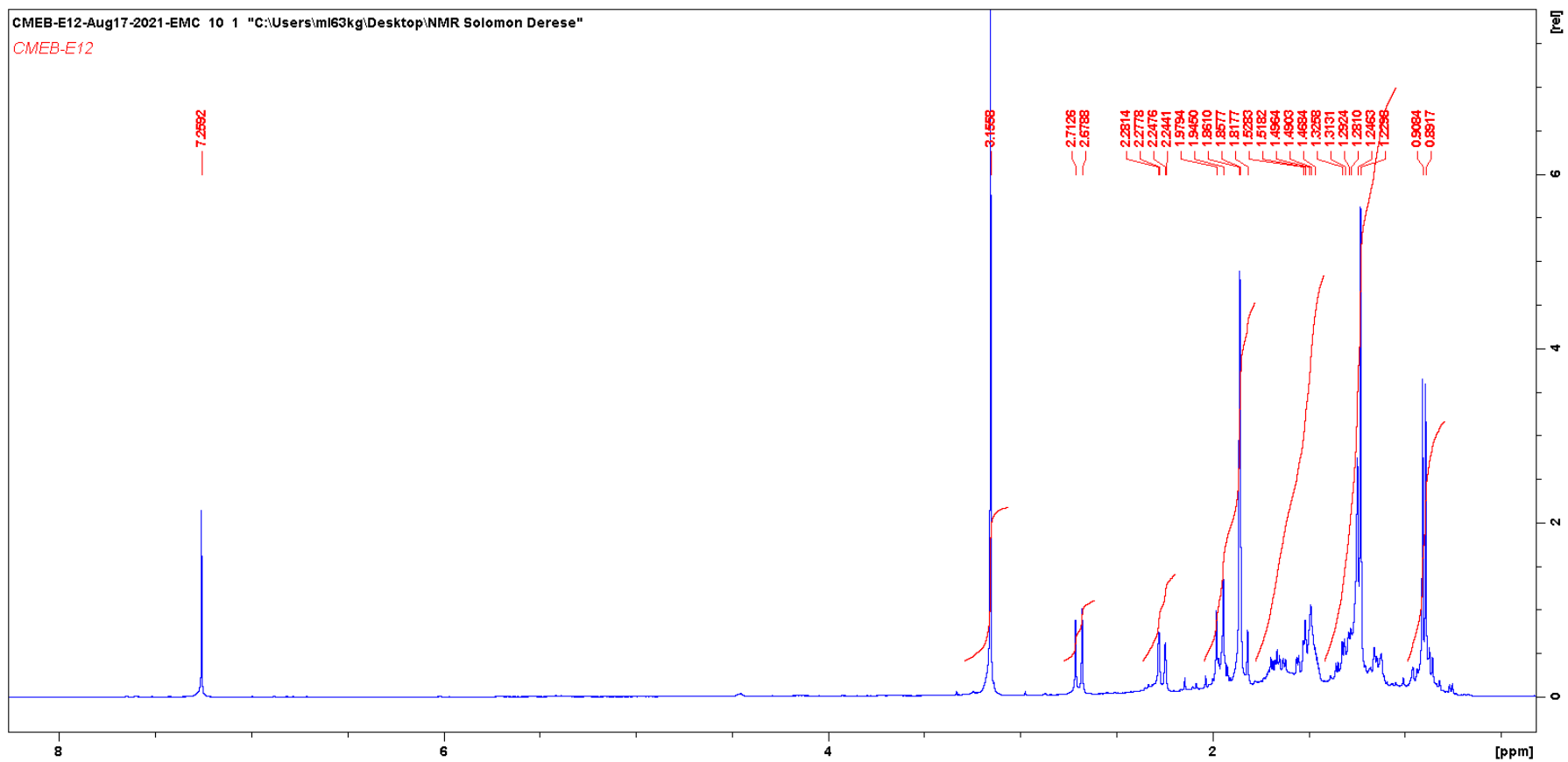
## Appendix 1 Mass Spectrum of 5 $\beta$ -hydroxy-8 $\alpha$ -methoxy eudesm-7(11)-en-12, 8-olide (ermiasolide A) (E12)

CMEB-E12 #5584 RT: 19.14 AV: 1 NL: 5.12E8  
F: FTMS + p ESI Full ms [125.0000-1800.0000]

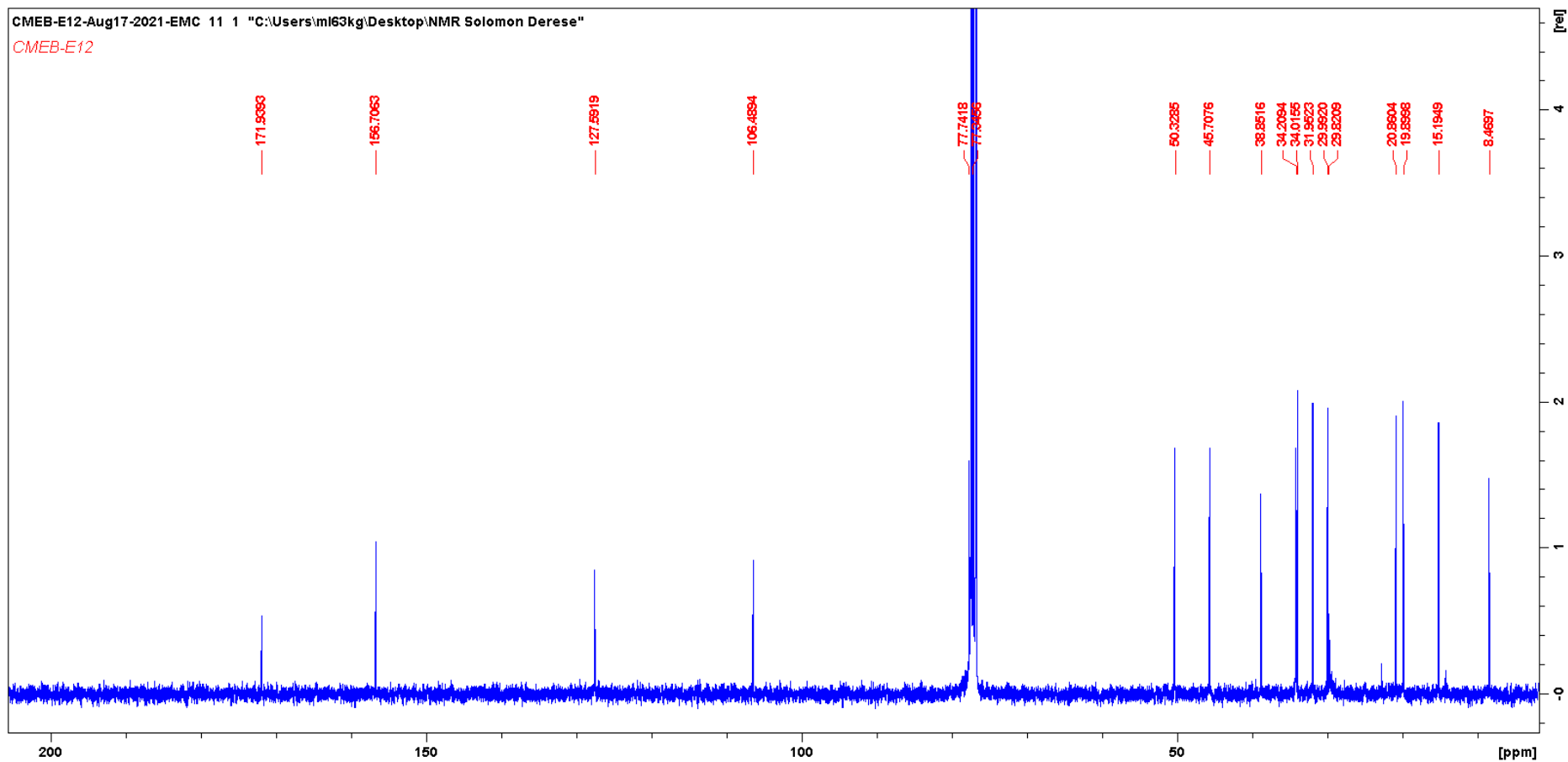


HRESIMS  $m/z$  281.1744 [M+H]<sup>+</sup> (calcd. for C<sub>16</sub>H<sub>24</sub>O<sub>4</sub> + H,  $m/z$  281.1747)

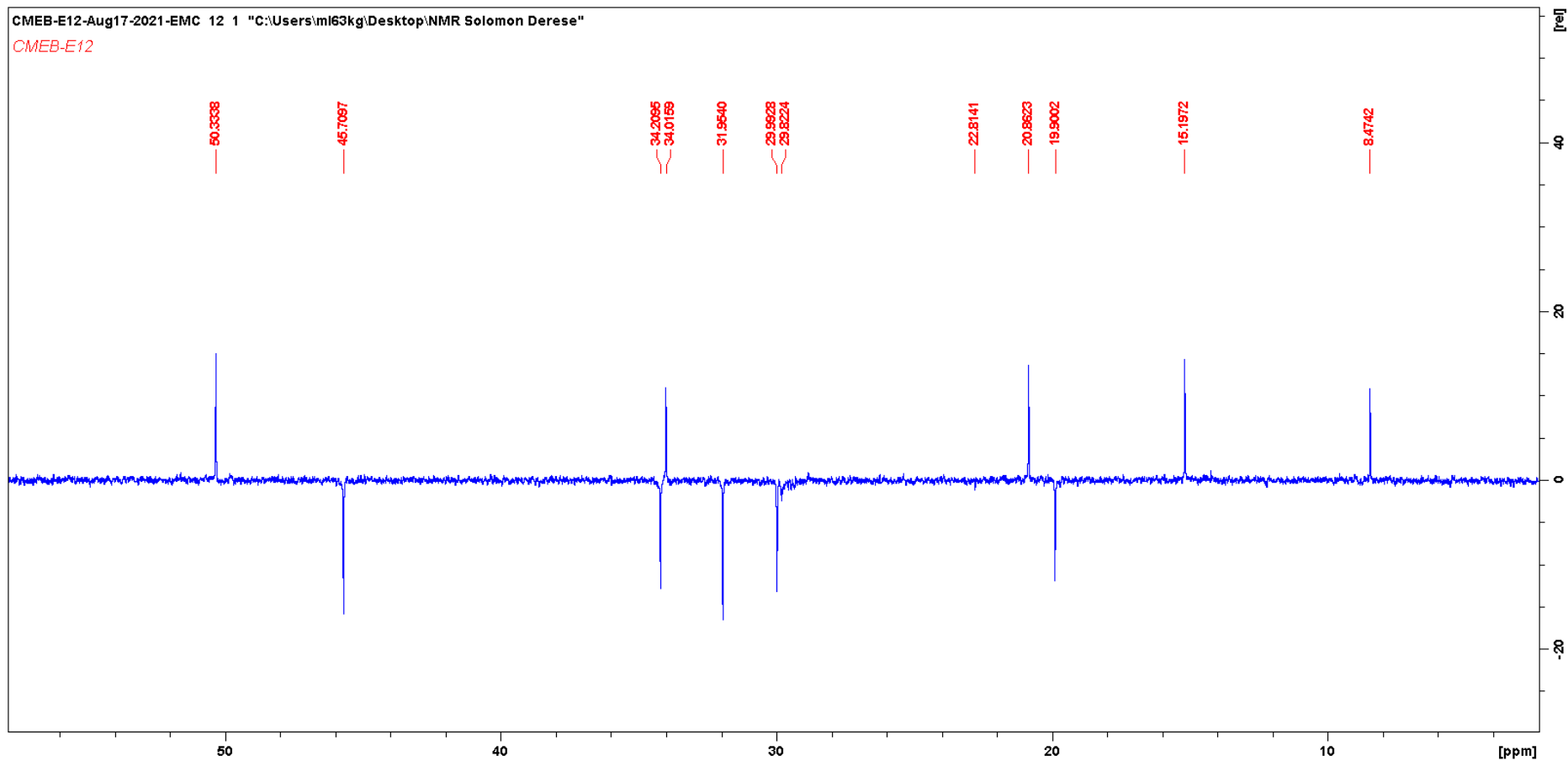
Appendix 2  $^1\text{H}$  NMR Spectra for  $5\beta$ -hydroxy- $8\alpha$ -methoxy eudesm-7(11)-en-12,8-olide (ermiasolide A) (E12)



Appendix 3  $^{13}\text{C}$  NMR Spectra for  $5\beta$ -hydroxy- $8\alpha$ -methoxy eudesm-7(11)-en-12, 8-olide (ermiasolide A) (E12)

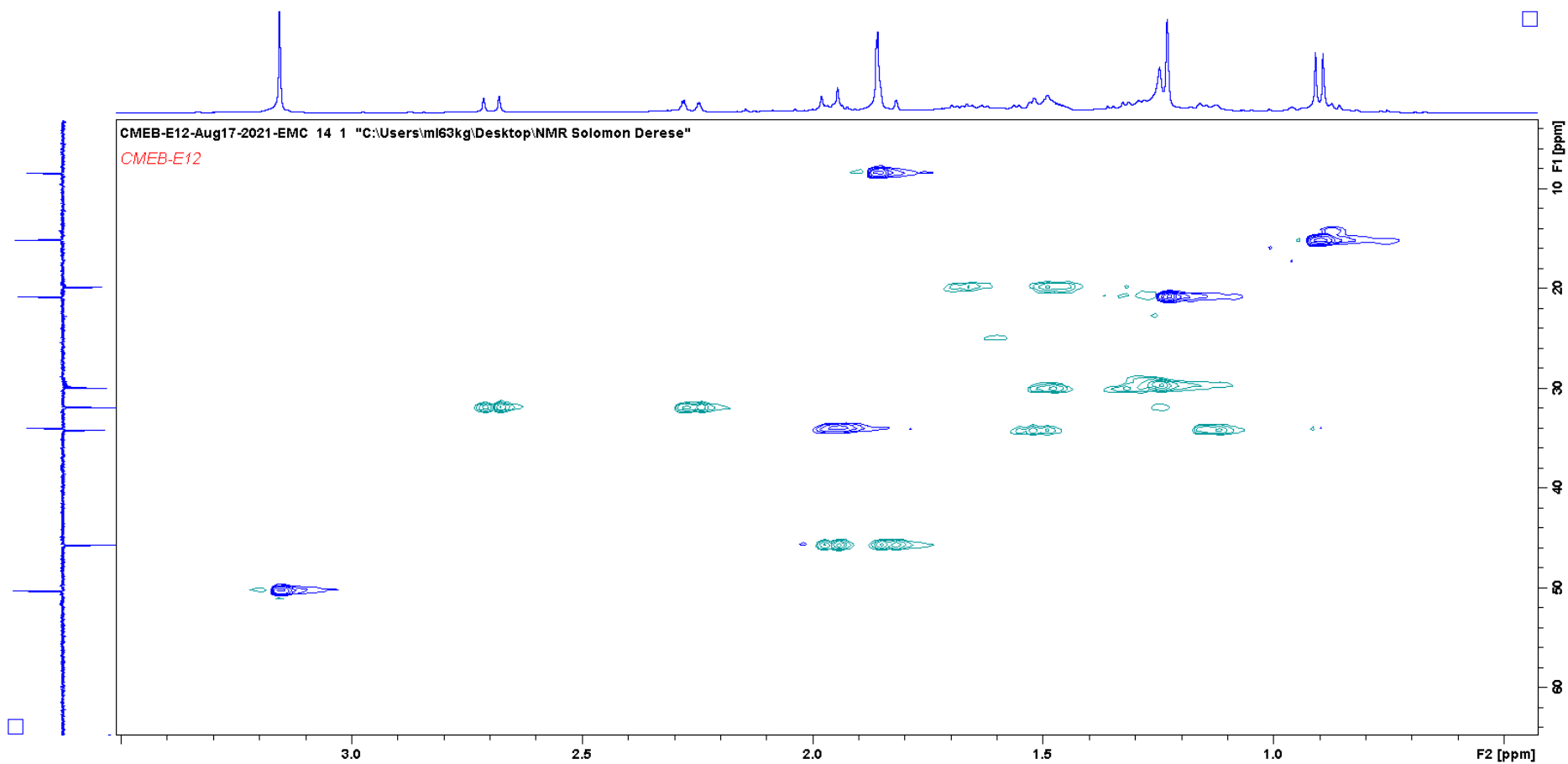


Appendix 4 DEPT Spectrum for 5 $\beta$ -hydroxy-8 $\alpha$ -methoxy eudesm-7(11)-en-12, 8-olide (ermiasolide A) (E12)

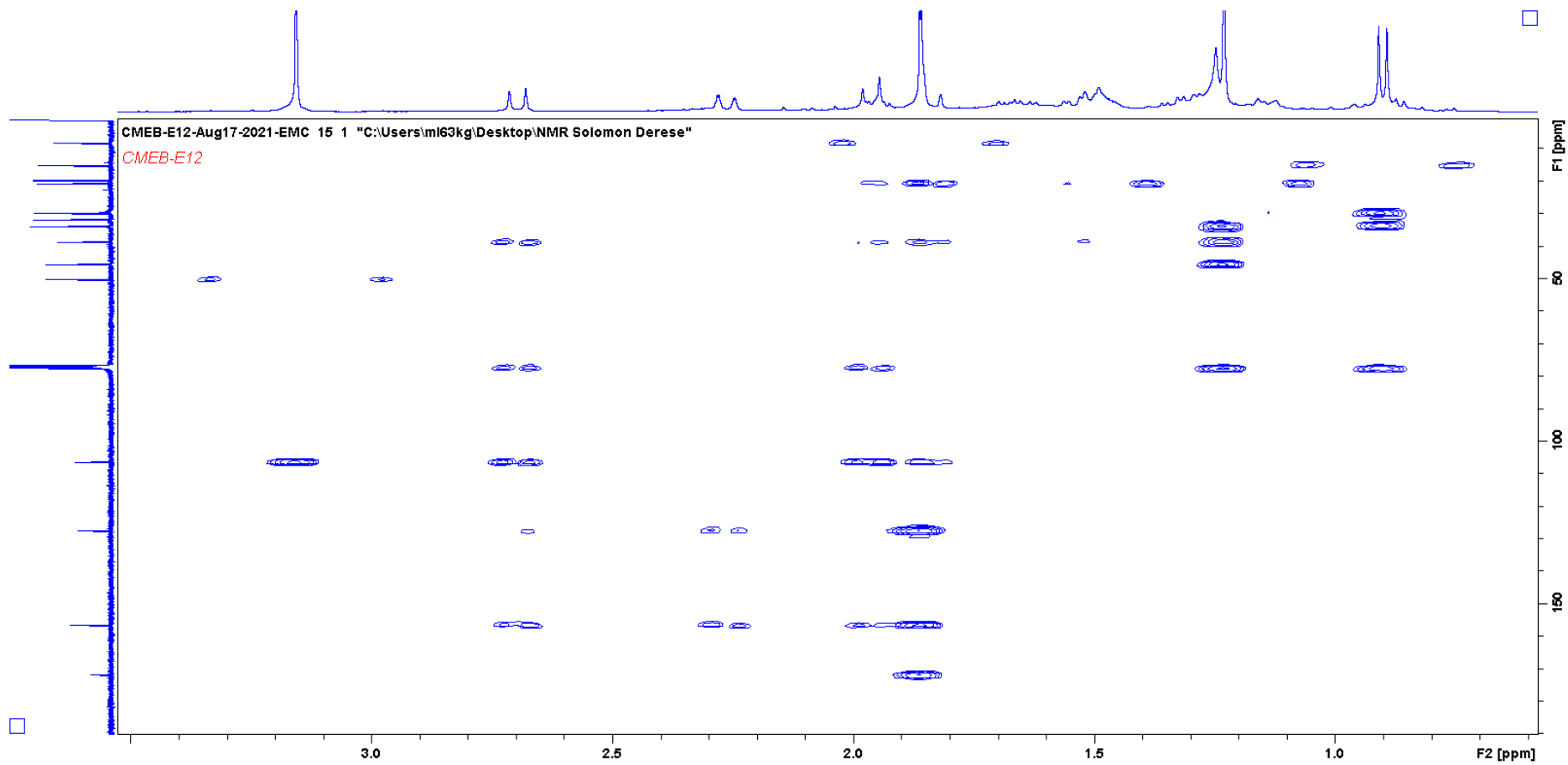




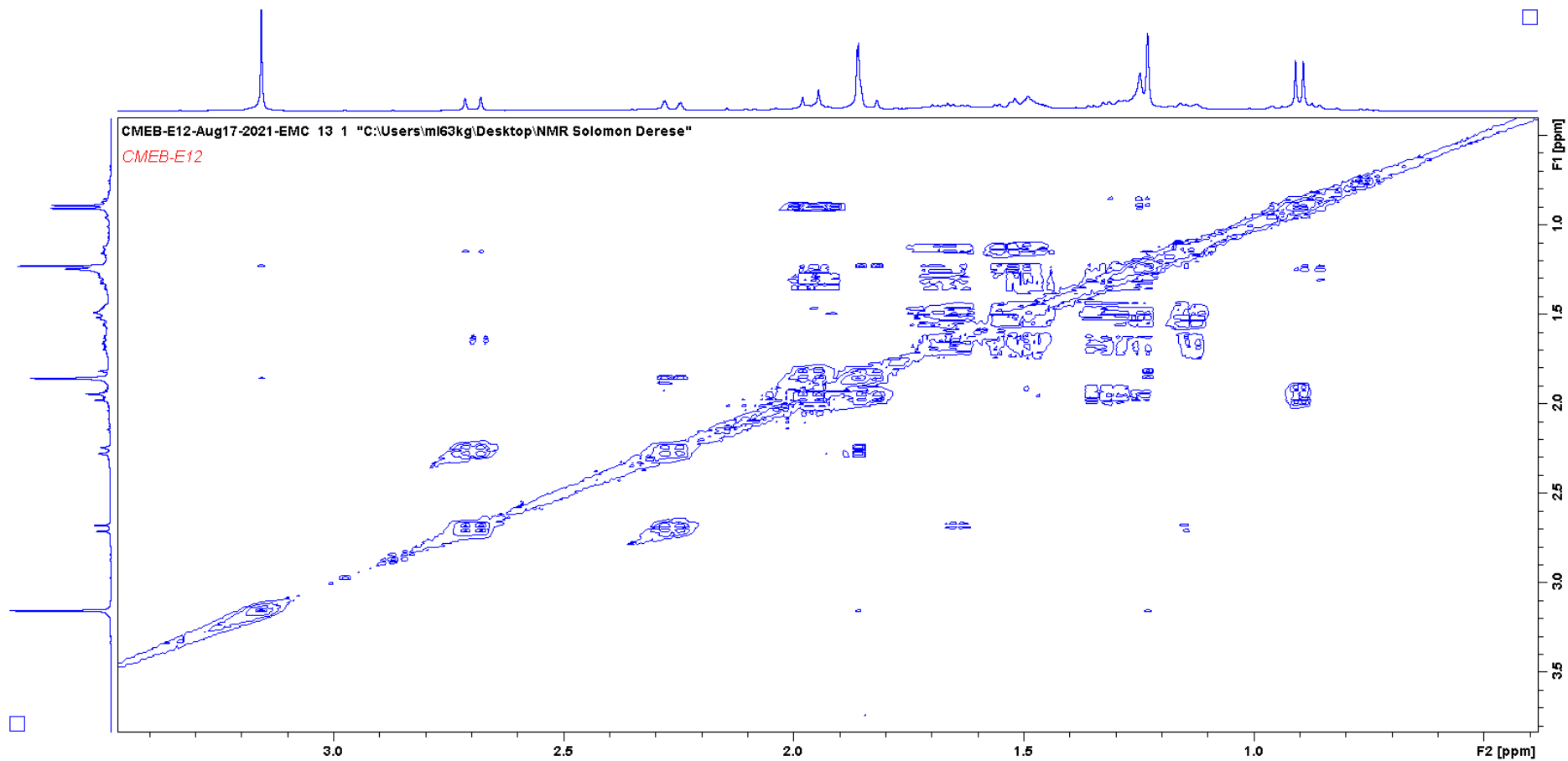
Appendix 5 HSQCDEPT Spectra for 5 $\beta$ -hydroxy-8 $\alpha$ -methoxy eudesm-7(11)-en-12,8-olide (ermiasolide A) (E12)



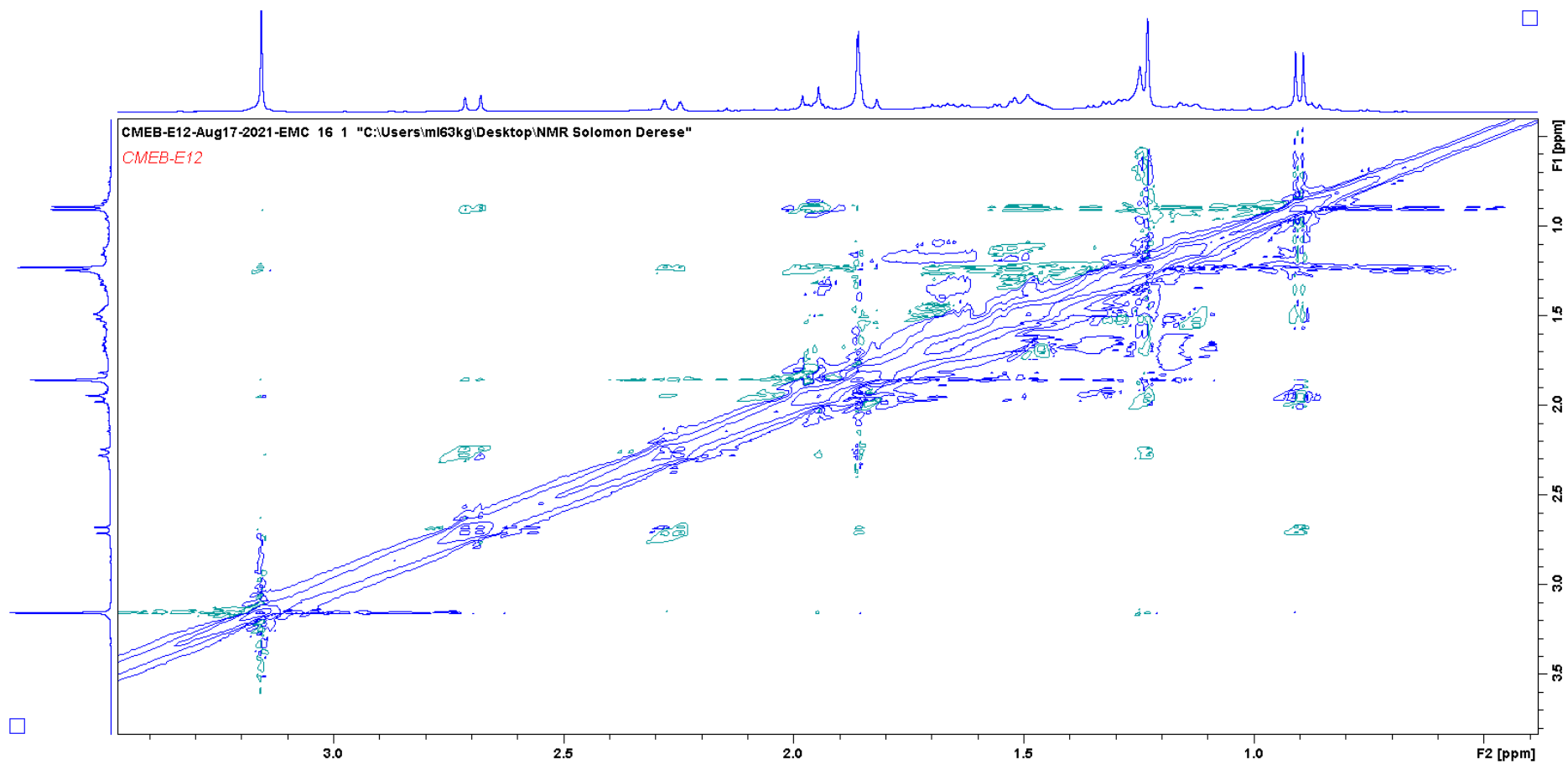
Appendix 6 HMBC Spectrum for 5 $\beta$ -hydroxy-8 $\alpha$ -methoxy eudesm-7(11)-en-12, 8-olide (ermiasolide A) (E12)



Appendix 7 COSY Spectrum for 5 $\beta$ -hydroxy-8 $\alpha$ -methoxy eudesm-7(11)-en-12,8-olide (ermiasolide A) (E12)



Appendix 8 NOSEY Spectrum for 5 $\beta$ -hydroxy-8 $\alpha$ -methoxy eudesm-7(11)-en-12,8-olide (ermiasolide A) (E12)



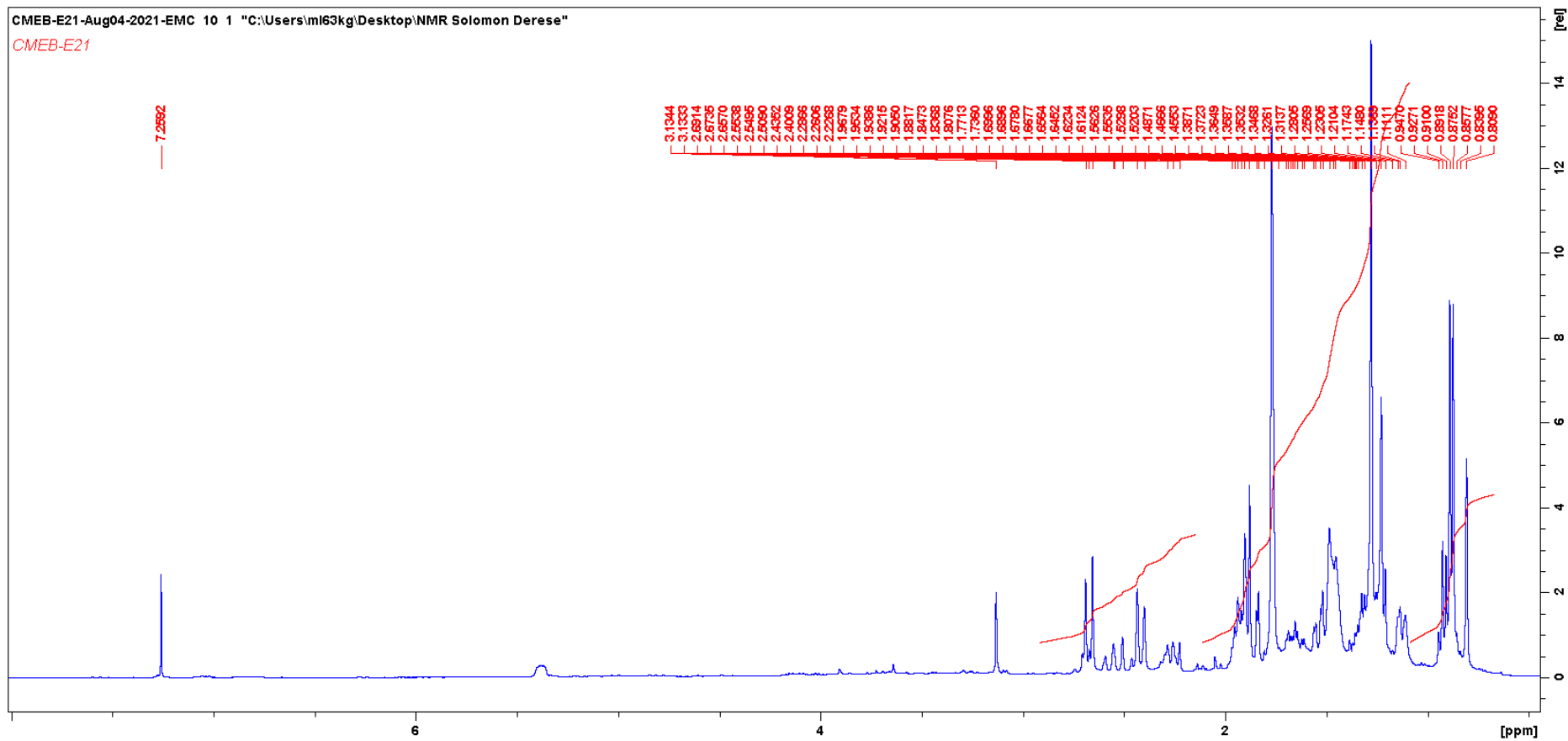
# Appendix 9 Mass Spectrum of 5 $\beta$ ,8 $\alpha$ -dihydroxy eudesm-7(11)-en-12,8-olide (ermiasolide B) (E22)

CMEB-E22 #6748 RT: 16.21 AV: 1 NL: 4.53E8  
F: FTMS + p ESI Full ms[125.0000-1800.0000]

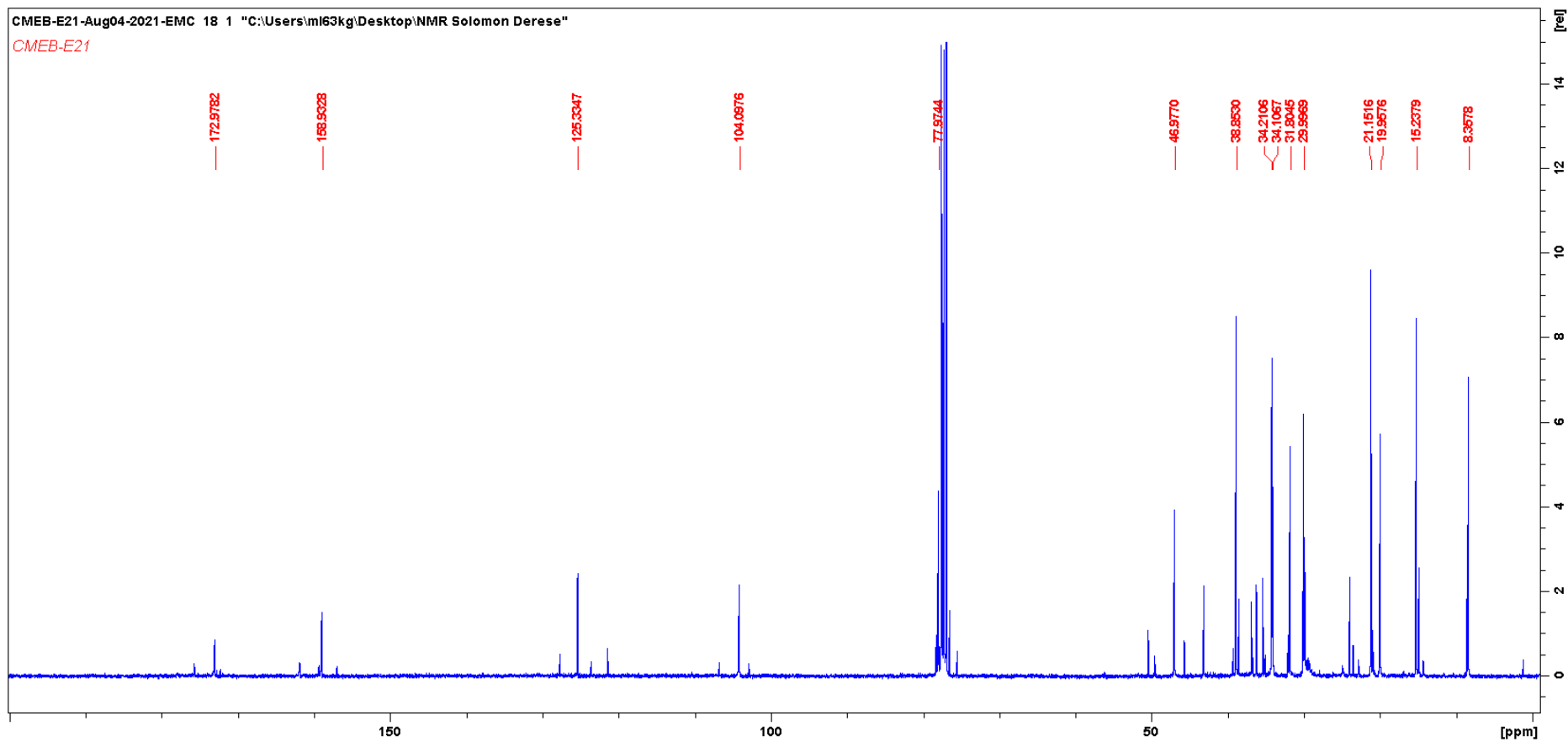


HRESIMS  $m/z$  267.1589 [M+H]<sup>+</sup> (calcd. for C<sub>15</sub>H<sub>22</sub>O<sub>4</sub> + H,  $m/z$  267.1591)

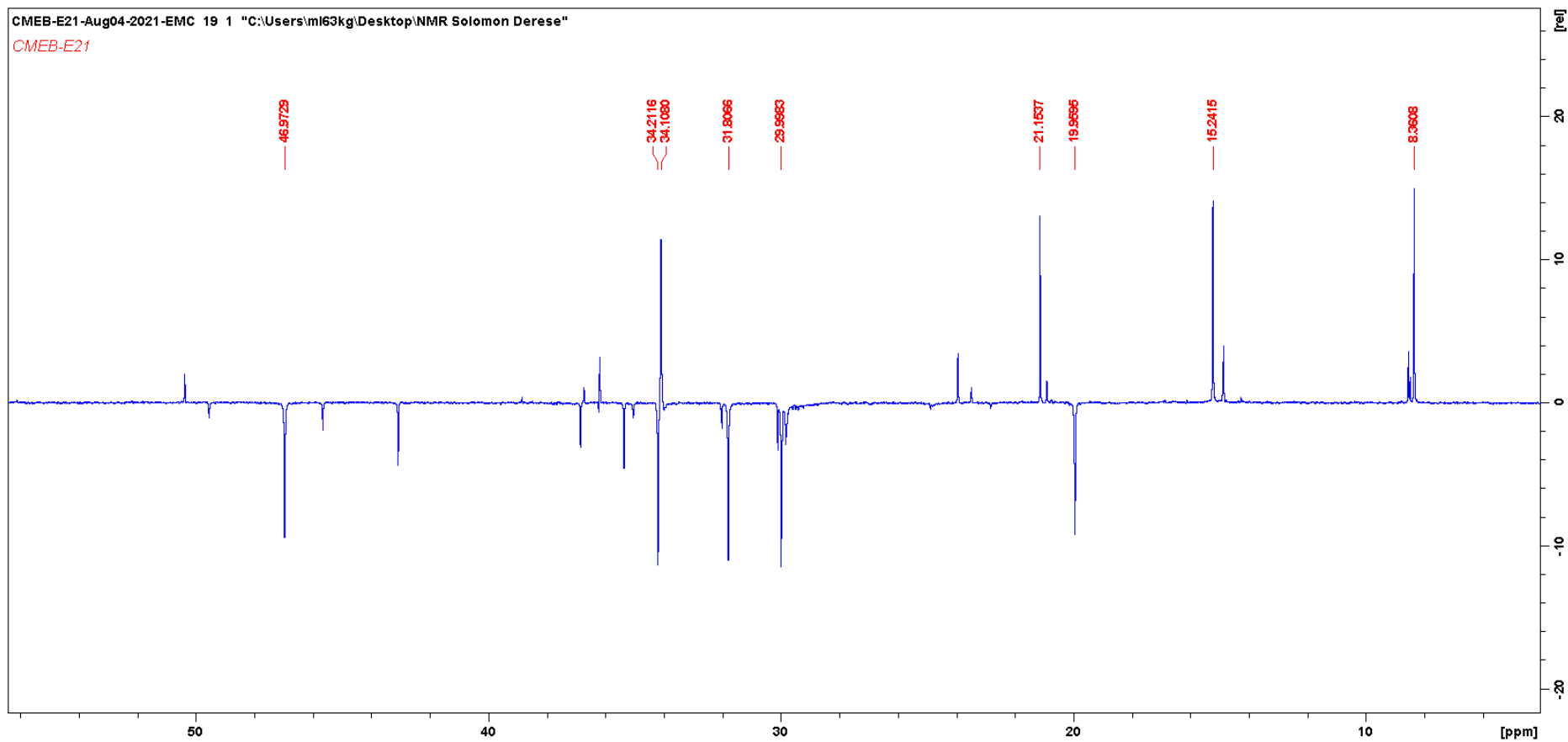
Appendix 10  $^1\text{H}$  NMR spectra of  $5\beta,8\alpha$ -dihydroxy eudesm-7(11)-en-12,8-olide (ermiasolide B) (E22)



Appendix 11  $^{13}\text{C}$  NMR spectra of  $5\beta,8\alpha$ -dihydroxy eudesm-7(11)-en-12,8-olide (ermiasolide B) (E22)

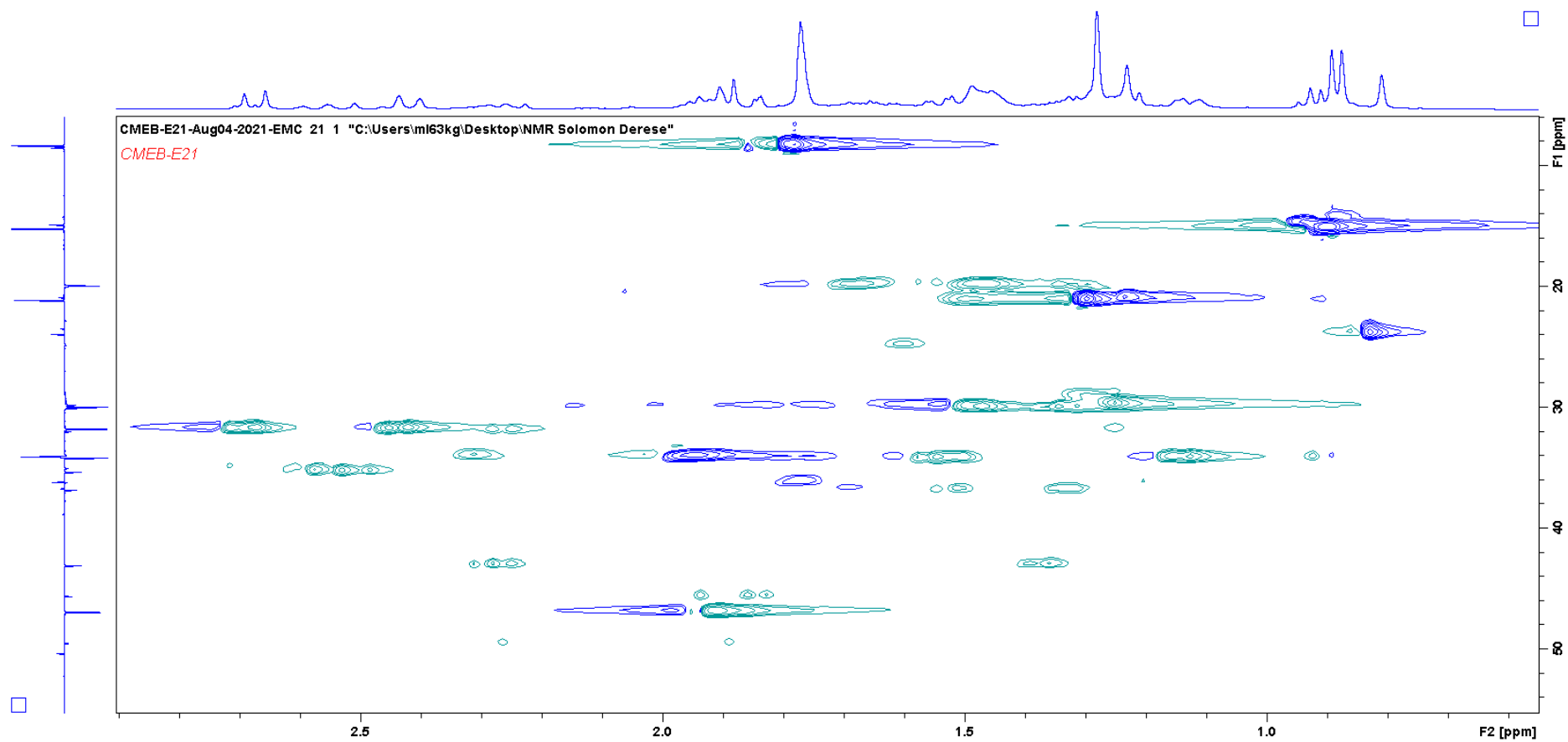


Appendix 12 DEPT spectrum of 5 $\beta$ ,8 $\alpha$ -dihydroxy eudesm-7(11)-en-12,8-olide (ermiasolide B) (E22)

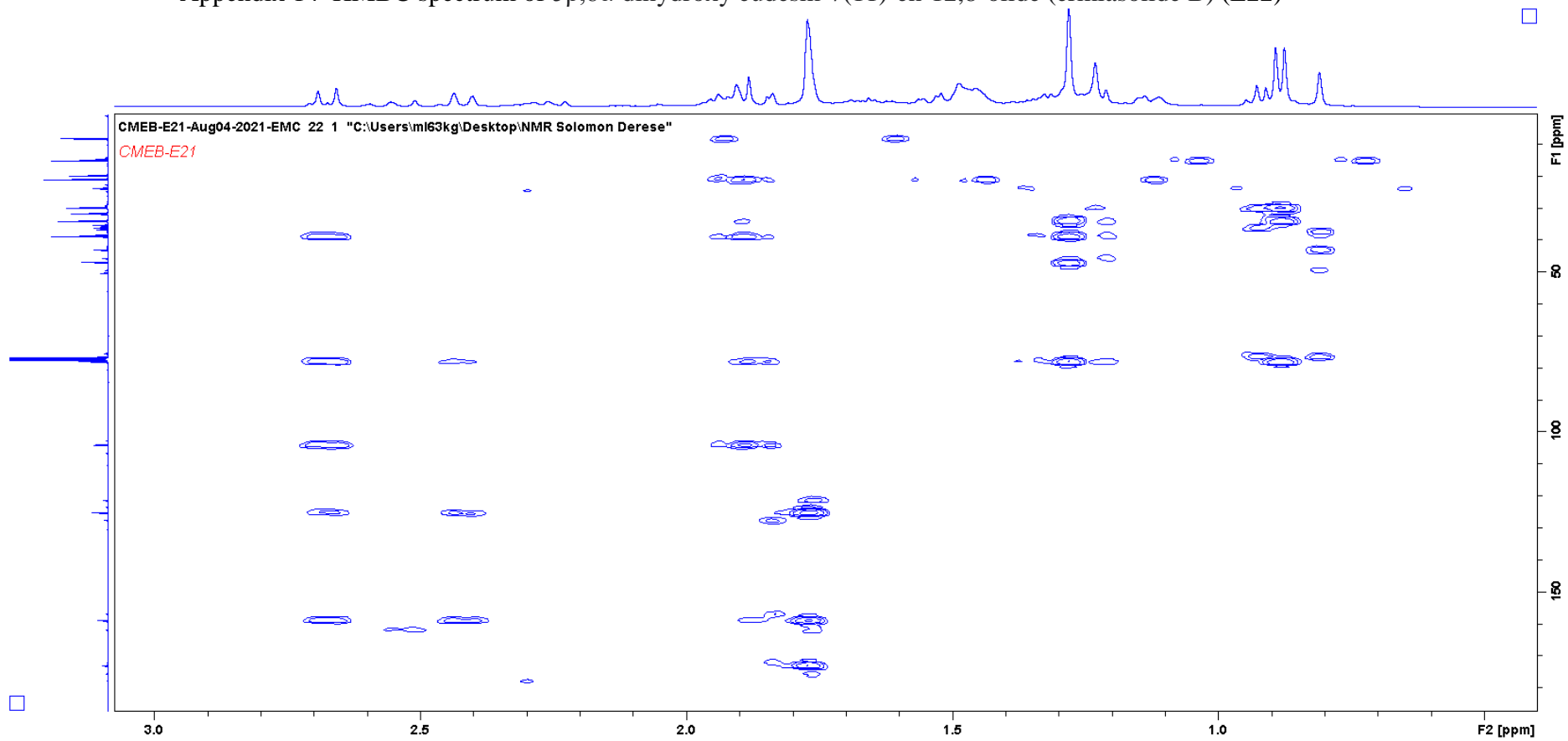




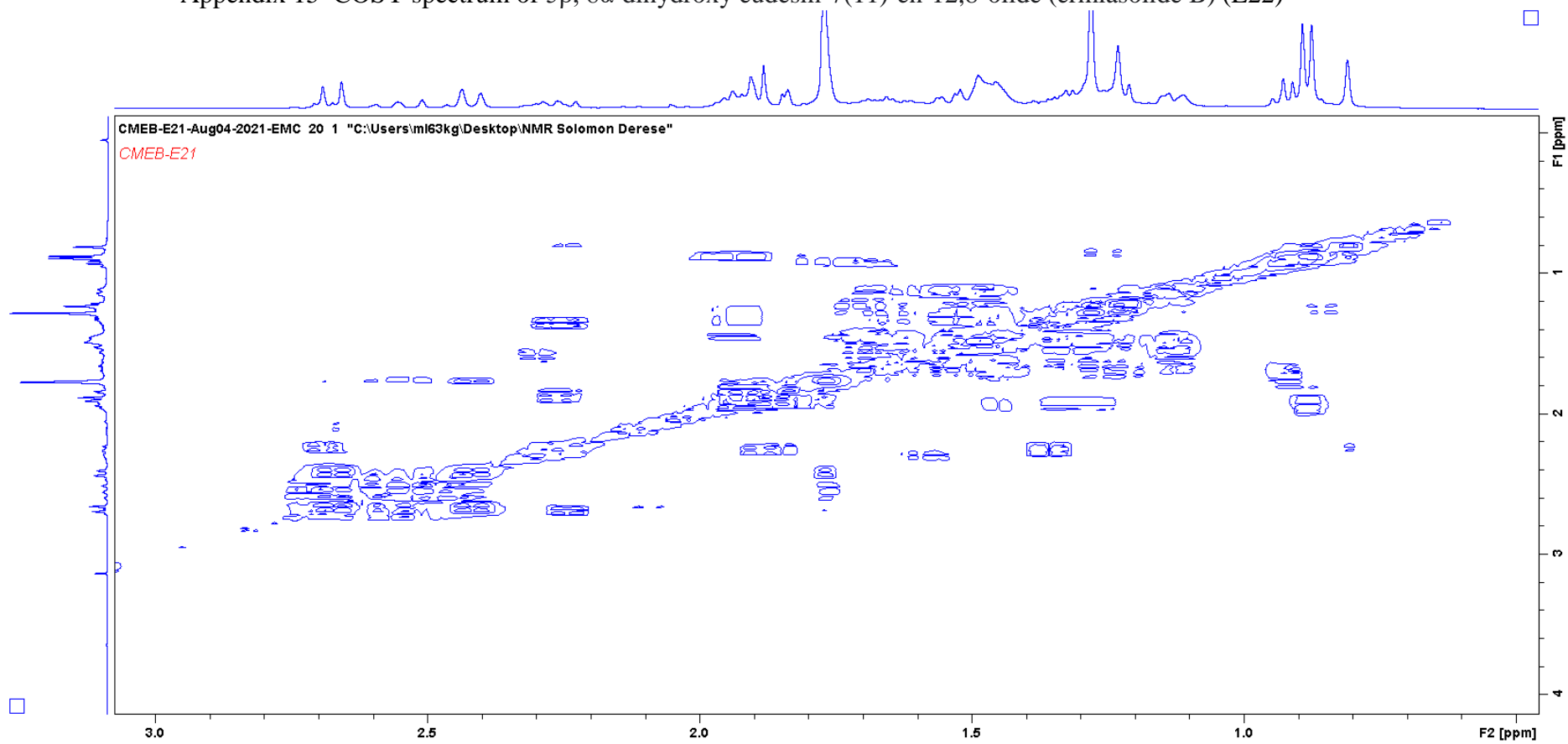
Appendix 13 HSQCDEPT spectrum of  $5\beta$ ,  $8\alpha$ -dihydroxy eudesm-7(11)-en-12,8-olide (ermiasolide B) (E22)



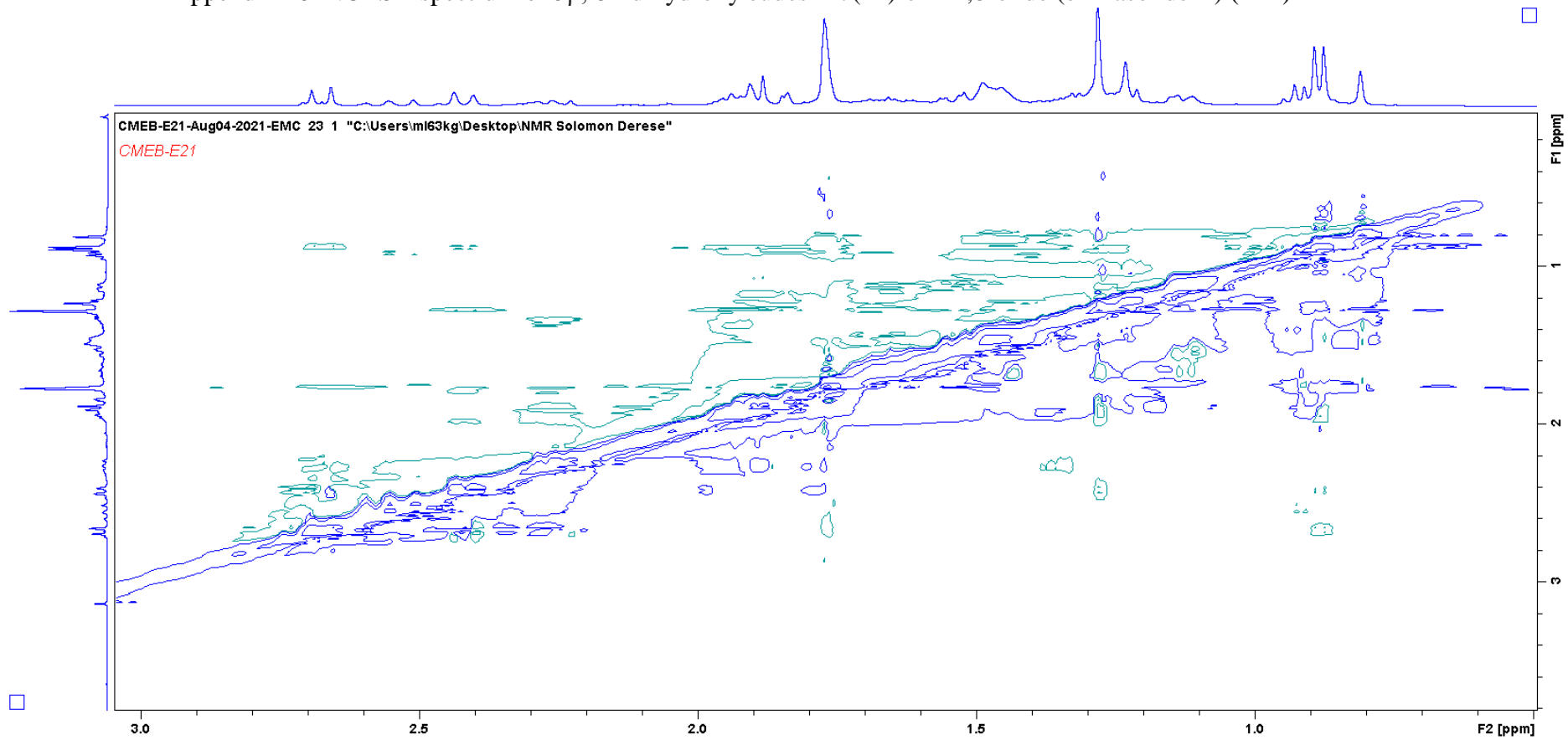
Appendix 14 HMBC spectrum of 5 $\beta$ ,8 $\alpha$ -dihydroxy eudesm-7(11)-en-12,8-olide (ermiasolide B) (E22)



Appendix 15 COSY spectrum of 5 $\beta$ , 8 $\alpha$ -dihydroxy eudesm-7(11)-en-12,8-olide (ermiasolide B) (E22)

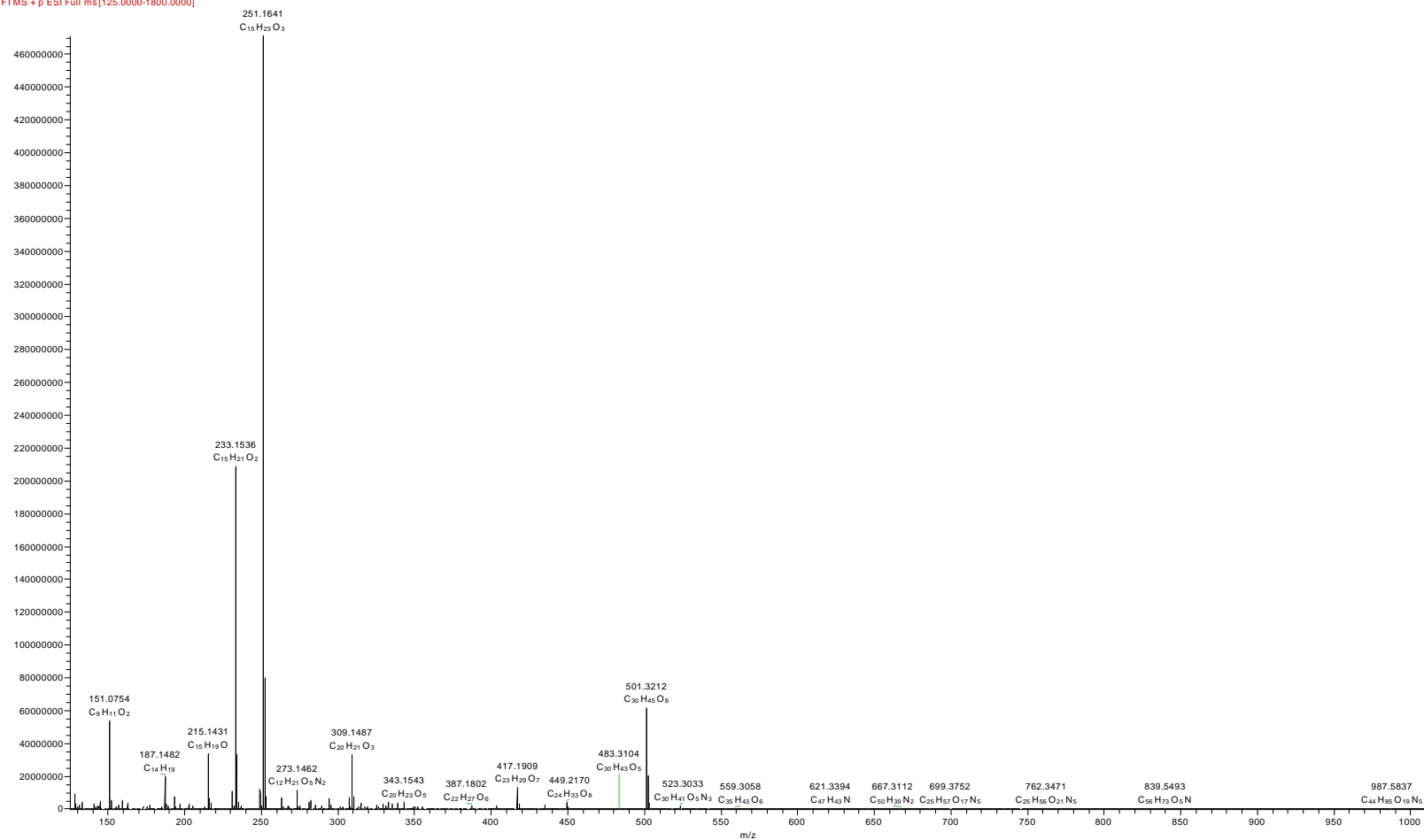


Appendix 16 NOESY spectrum of  $5\beta$ ,  $8\alpha$ -dihydroxy eudesm-7(11)-en-12,8-olide (ermiasolide B) (E22)



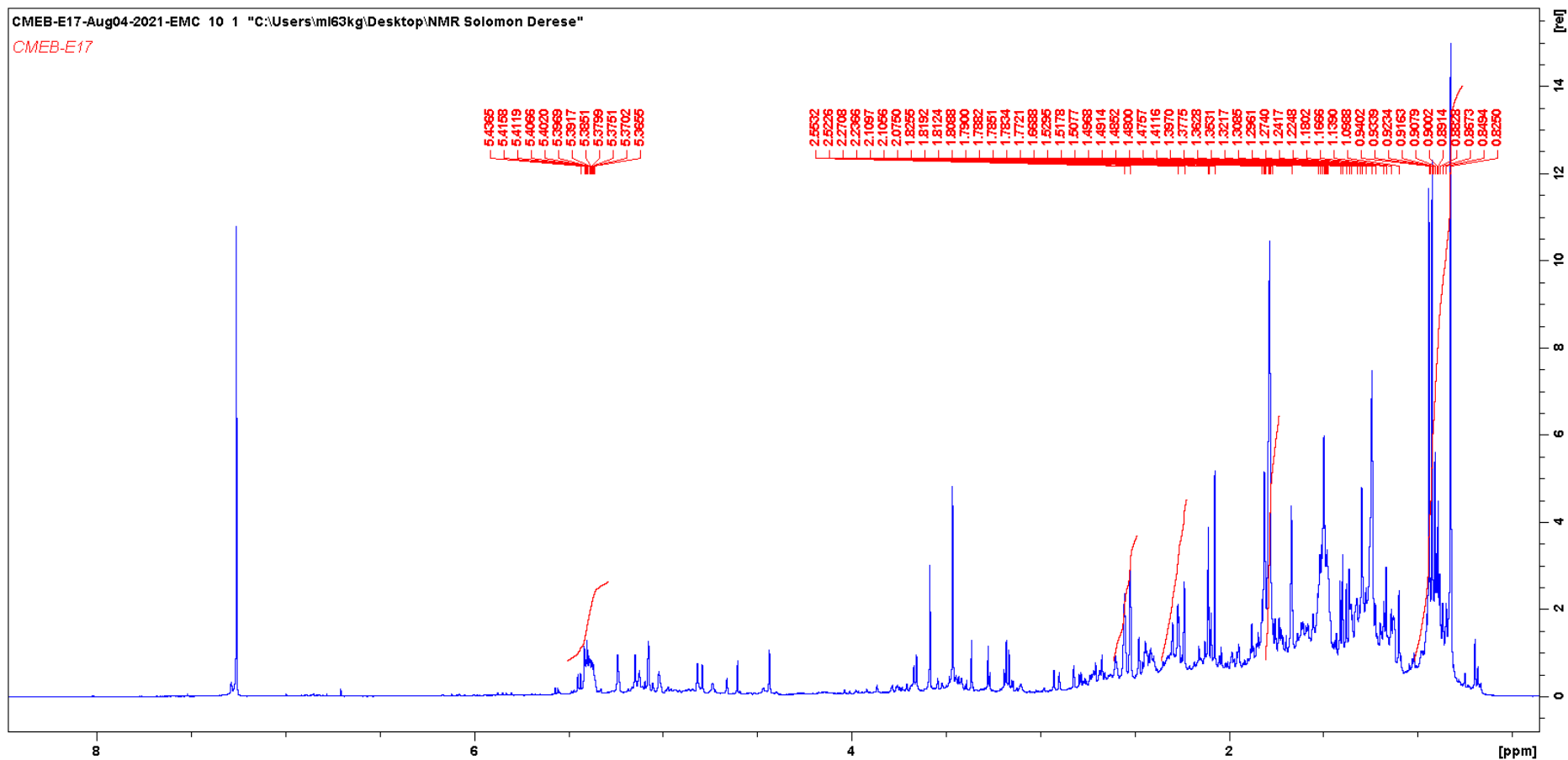
# Appendix 17 Mass spectrum of 5 $\beta$ ,8H- $\beta$ -hydroxy eudesm-7(11)-en-12, 8-olide (ermiasolide C) (E17)

CMEB-E17 #7230 RT: 18.18 AV: 1 NL: 4.71E8  
F: FTMS + p ESI Full ms [125.0000-1800.0000]

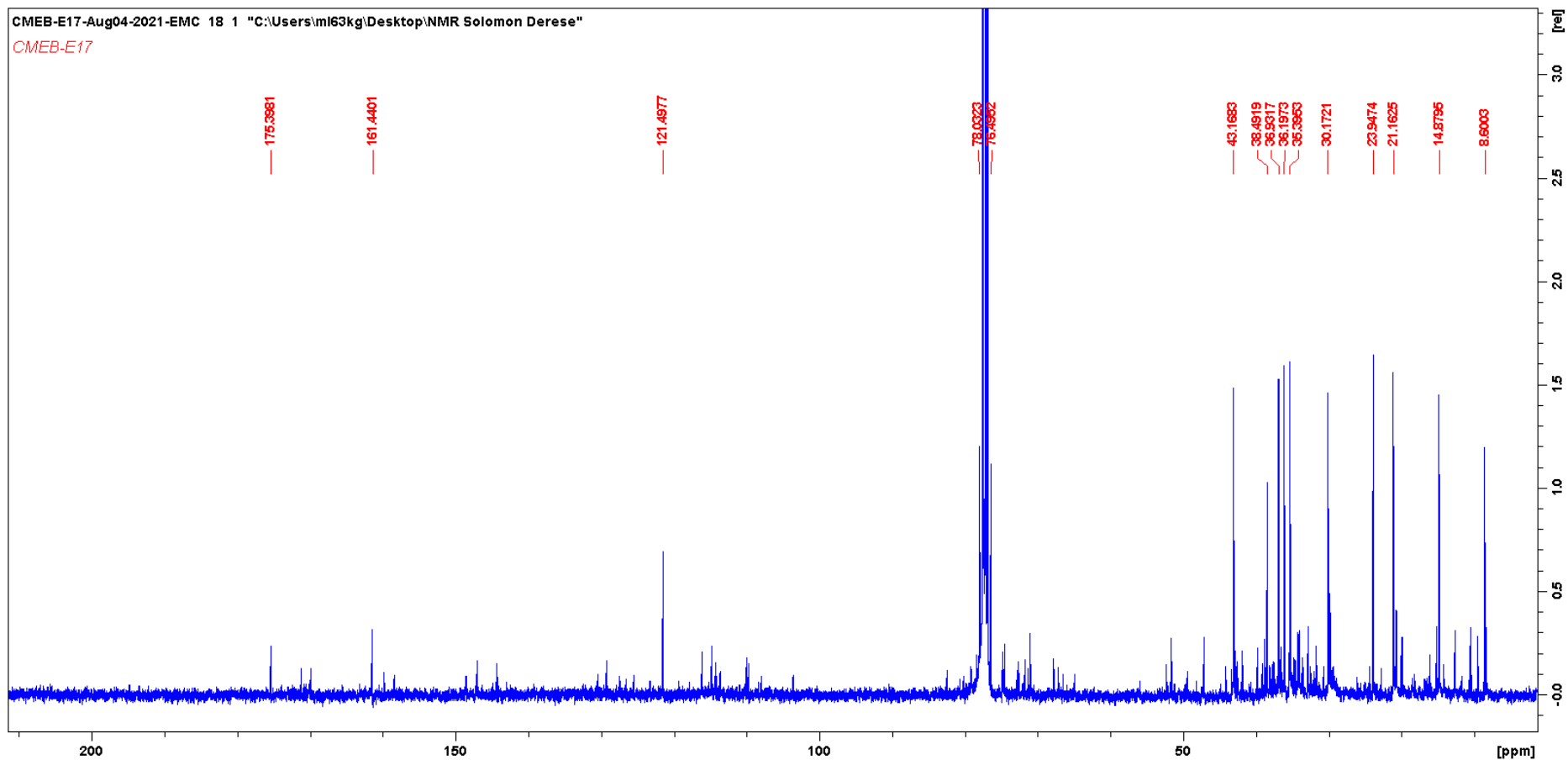


HRESIMS  $m/z$ , 251.1641 [M+H]<sup>+</sup> (calcd. for C<sub>15</sub>H<sub>22</sub>O<sub>3</sub> + H,  $m/z$ , 251.1642)

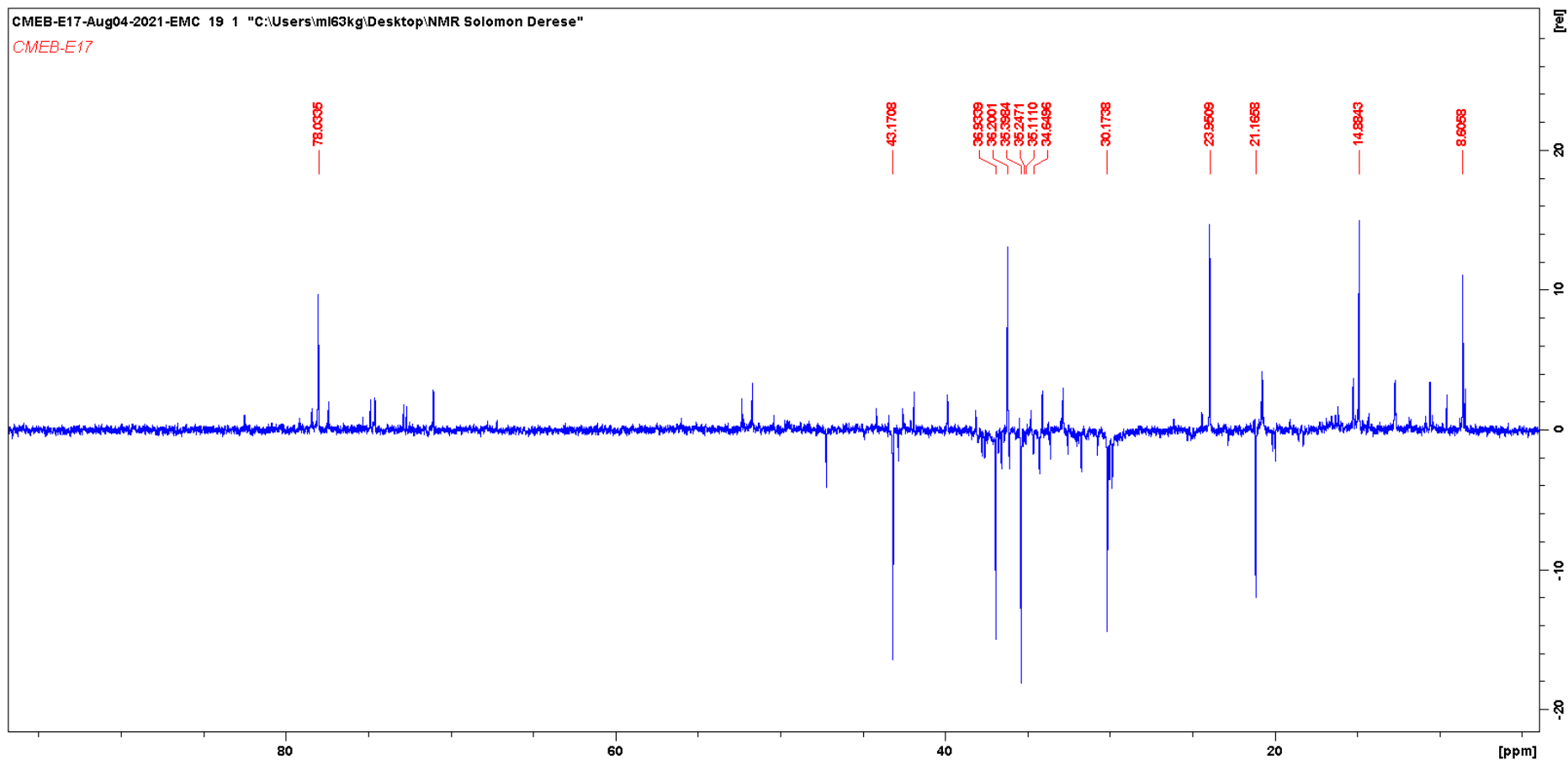
Appendix 18  $^1\text{H}$  NMR spectra of  $5\beta,8\text{H-}\beta\text{-hydroxy eudesm-7(11)\text{-en-12, 8-olide (ermiasolide C) (E17)}$



Appendix 19  $^{13}\text{C}$  NMR spectra of 5 $\beta$ ,8H- $\beta$ -hydroxy eudesm-7(11)-en-12, 8-olide (ermiasolide C) (E17)

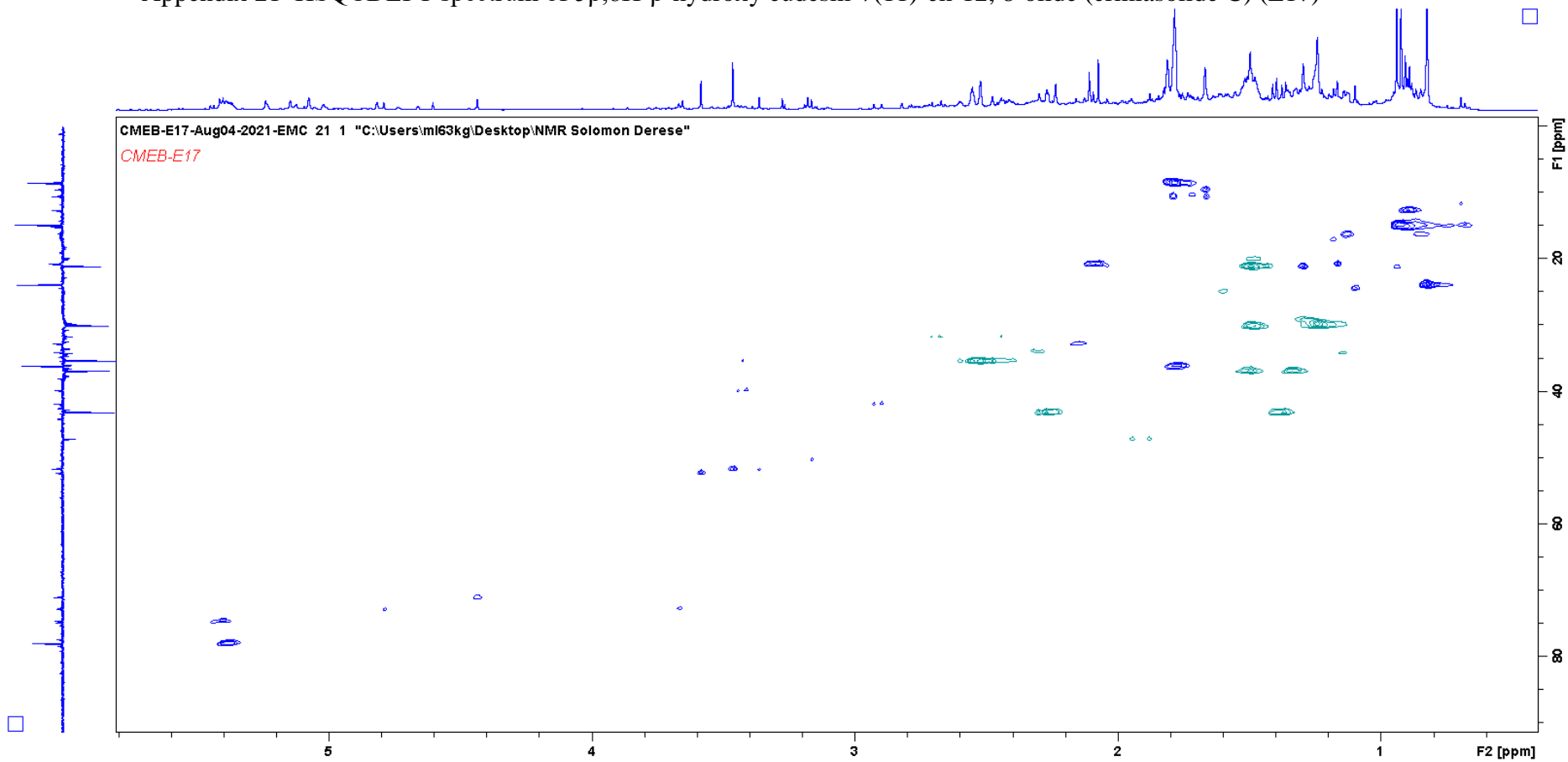


Appendix 20 DEPT spectrum of 5 $\beta$ ,8H- $\beta$ -hydroxy eudesm-7(11)-en-12, 8-olide (ermiasolide C) (E17)

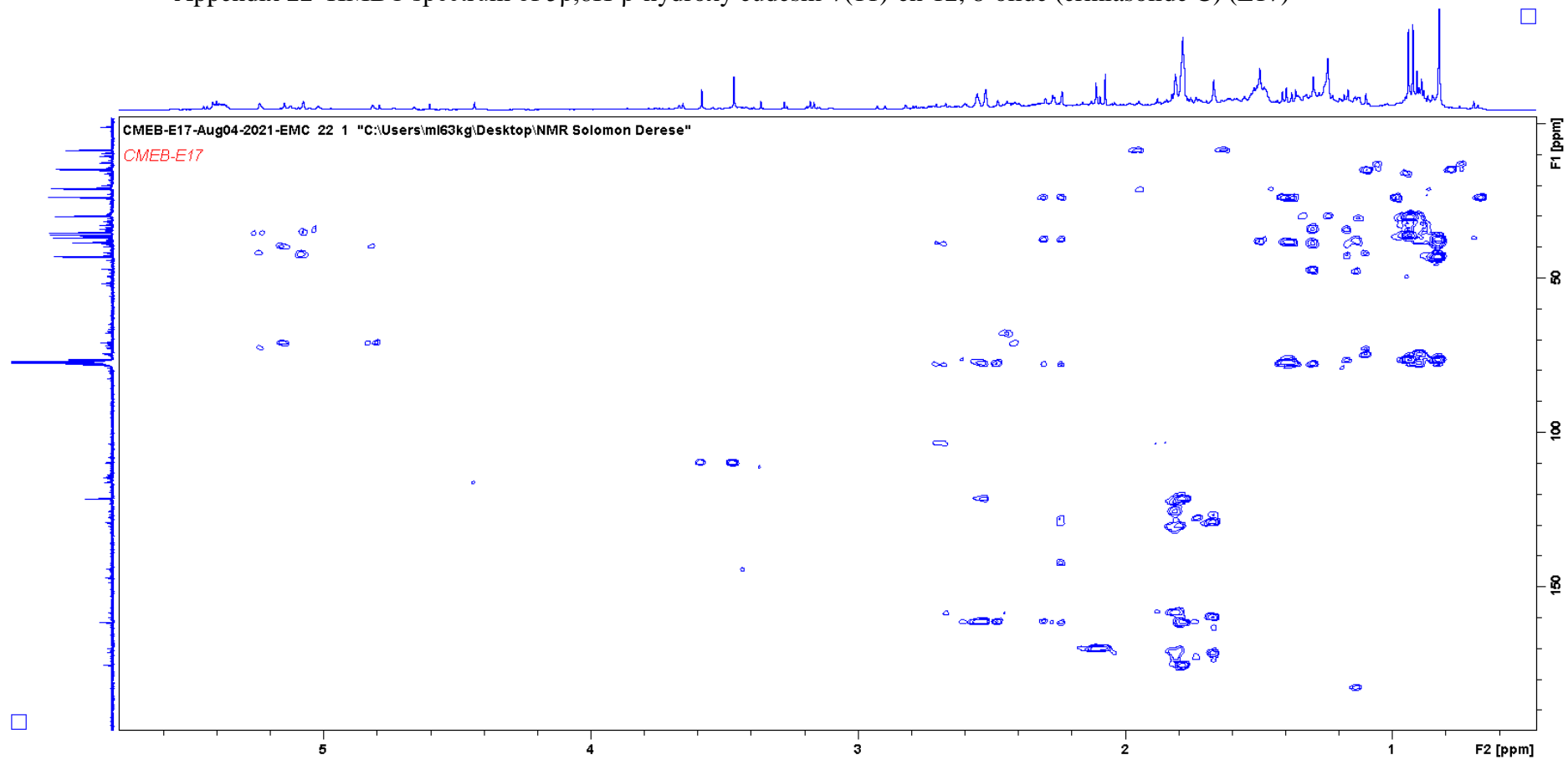




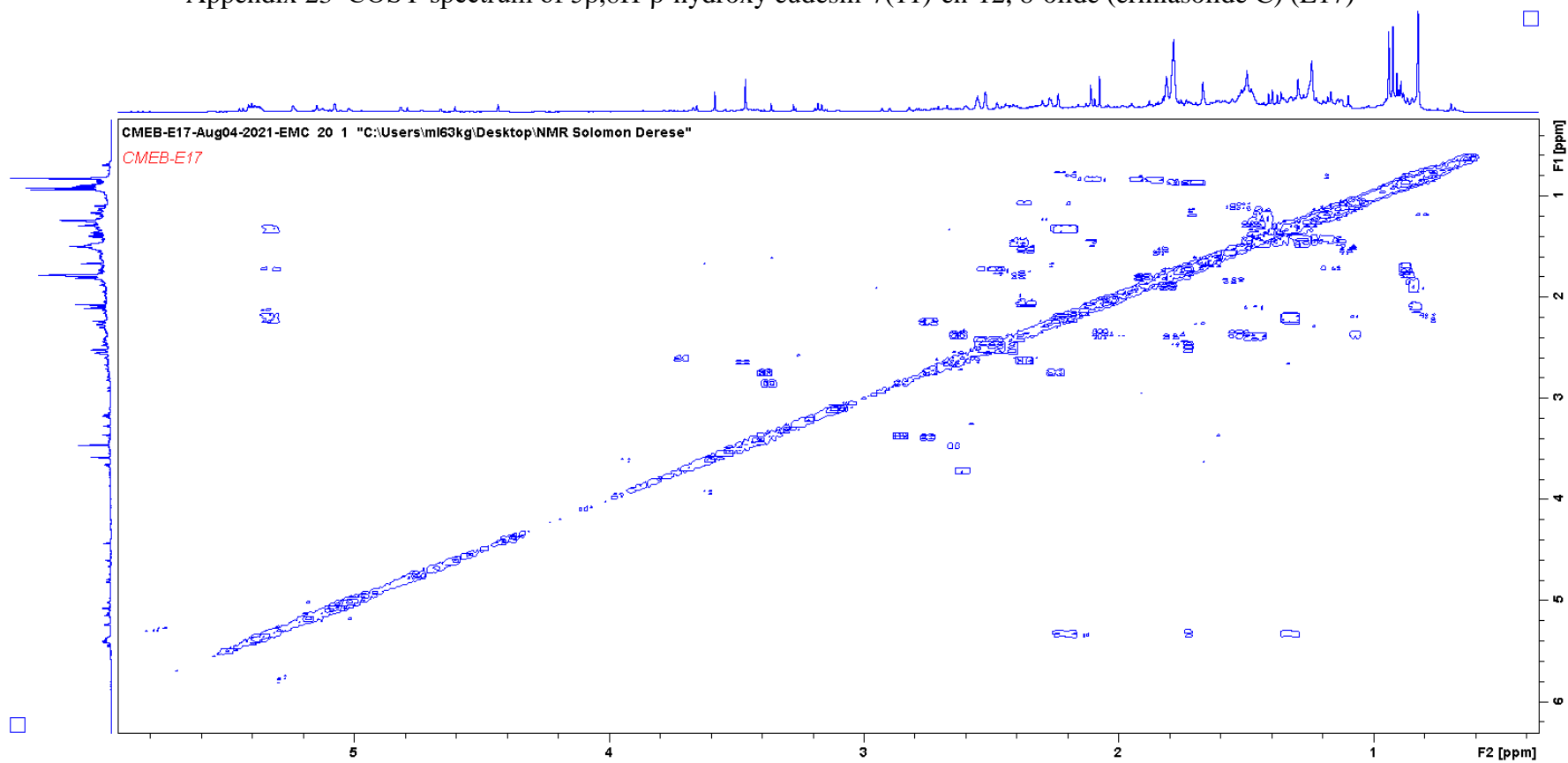
Appendix 21 HSQCDEPT spectrum of 5 $\beta$ ,8H- $\beta$ -hydroxy eudesm-7(11)-en-12, 8-olide (ermiasolide C) (E17)



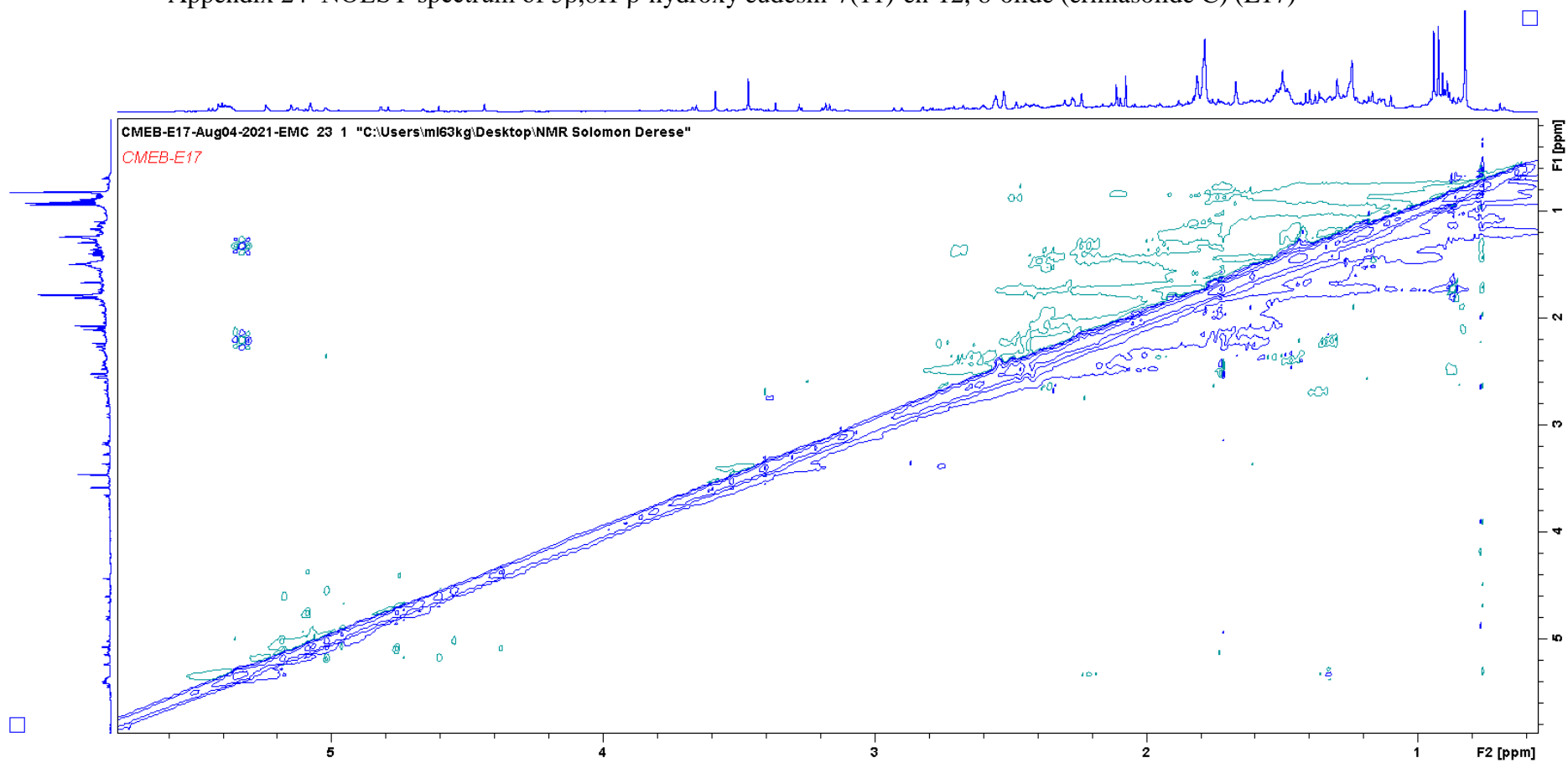
Appendix 22 HMBC spectrum of 5 $\beta$ ,8H- $\beta$ -hydroxy eudesm-7(11)-en-12, 8-olide (ermiasolide C) (E17)



Appendix 23 COSY spectrum of 5 $\beta$ ,8H- $\beta$ -hydroxy eudesm-7(11)-en-12, 8-olide (ermiasolide C) (E17)

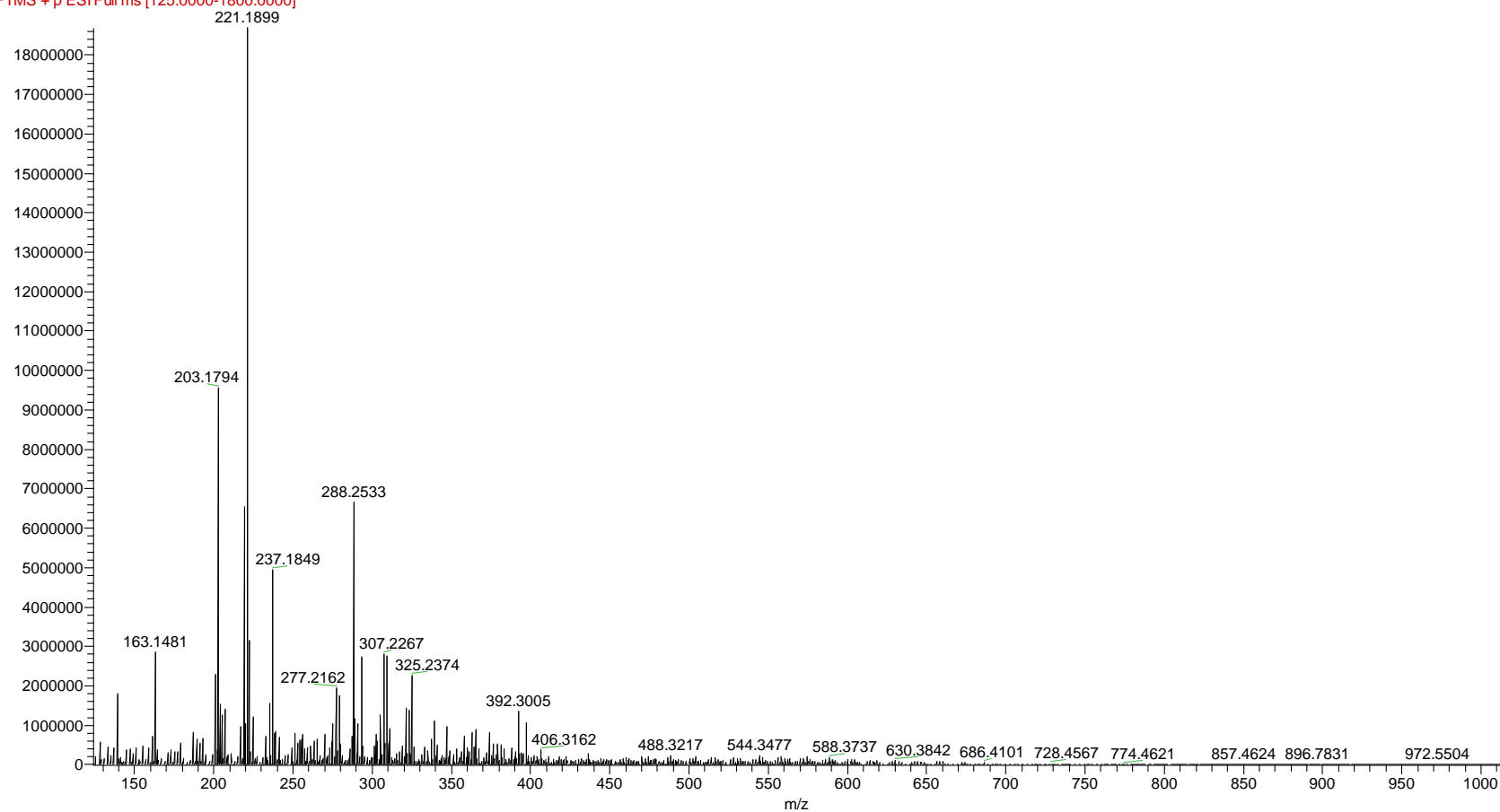


Appendix 24 NOESY spectrum of  $5\beta,8H$ - $\beta$ -hydroxy eudesm-7(11)-en-12, 8-olide (ermiasolide C) (E17)



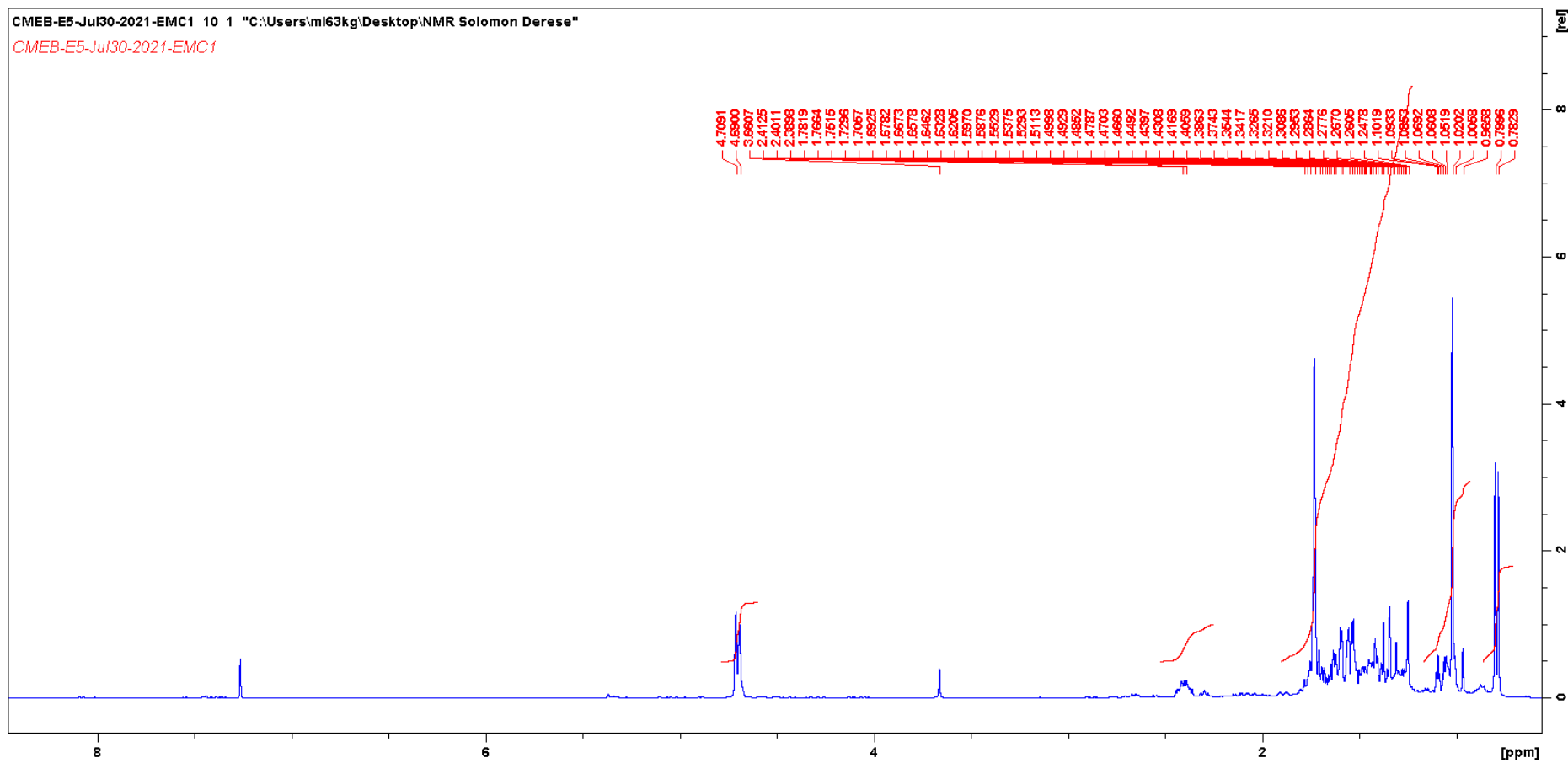
## Appendix 25 Mass spectrum of 4H- $\alpha$ ,7H- $\alpha$ ,10 $\alpha$ -eudesm-11-en-5 $\beta$ -ol (E5)

CMEB-E5 #5435-6071 RT: 19.49-20.90 AV: 33 NL: 1.87E7  
F: FTMS + p ESI Full ms [125.0000-1800.0000]

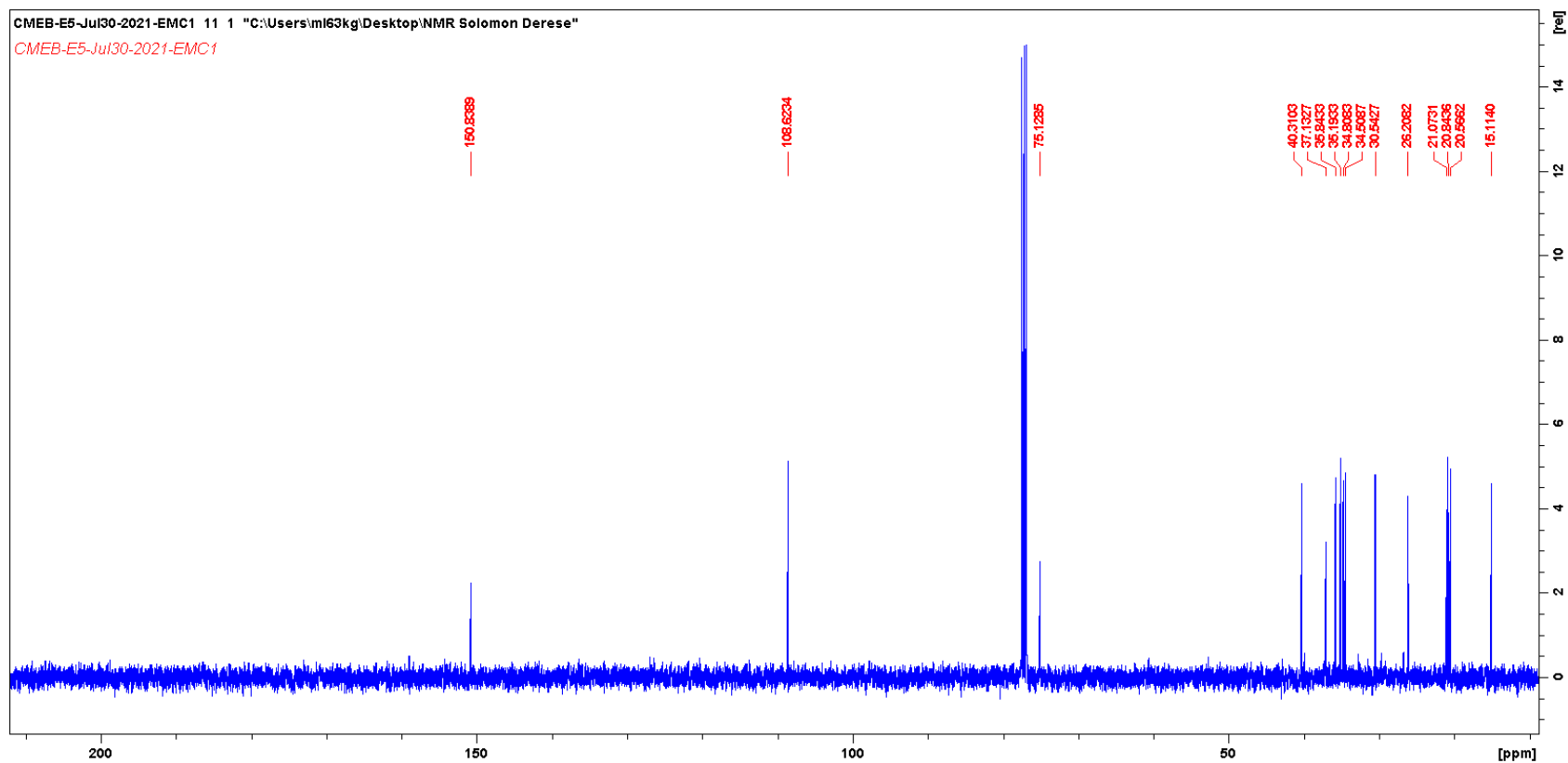


HRESIMS  $m/z$  221.1899  $[M+H]^+$  (calcd. for  $C_{15}H_{24}O + H$ ,  $m/z$  221.1900)

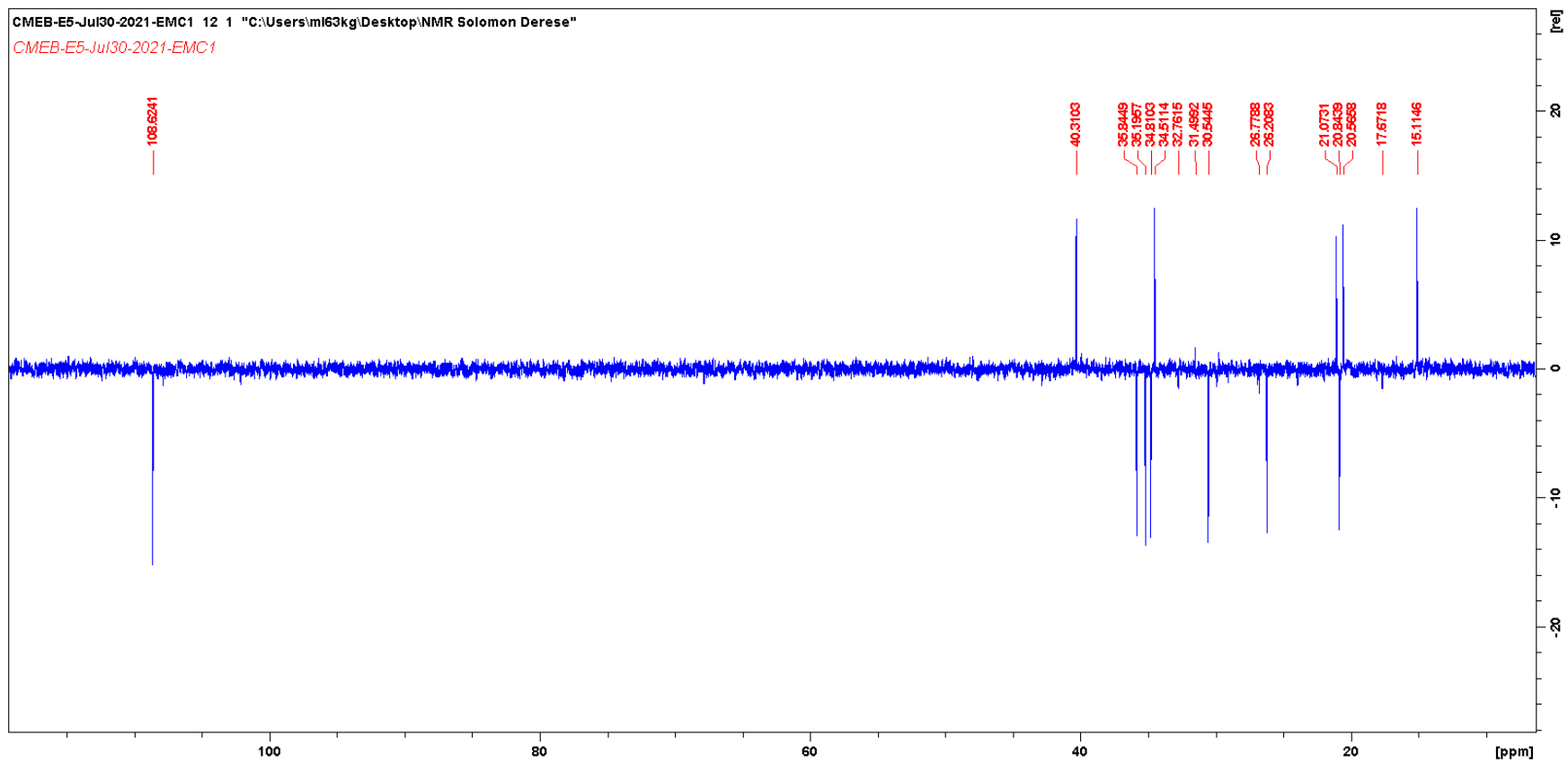
Appendix 26  $^1\text{H}$  NMR spectrum of 4H- $\alpha$ ,7H- $\alpha$ ,10 $\alpha$ -eudesm-11-en-5 $\beta$ -ol (E5)



Appendix 27  $^{13}\text{C}$  NMR spectrum of 4H- $\alpha$ ,7H- $\alpha$ ,10 $\alpha$ -eudesm-11-en-5 $\beta$ -ol (E5)

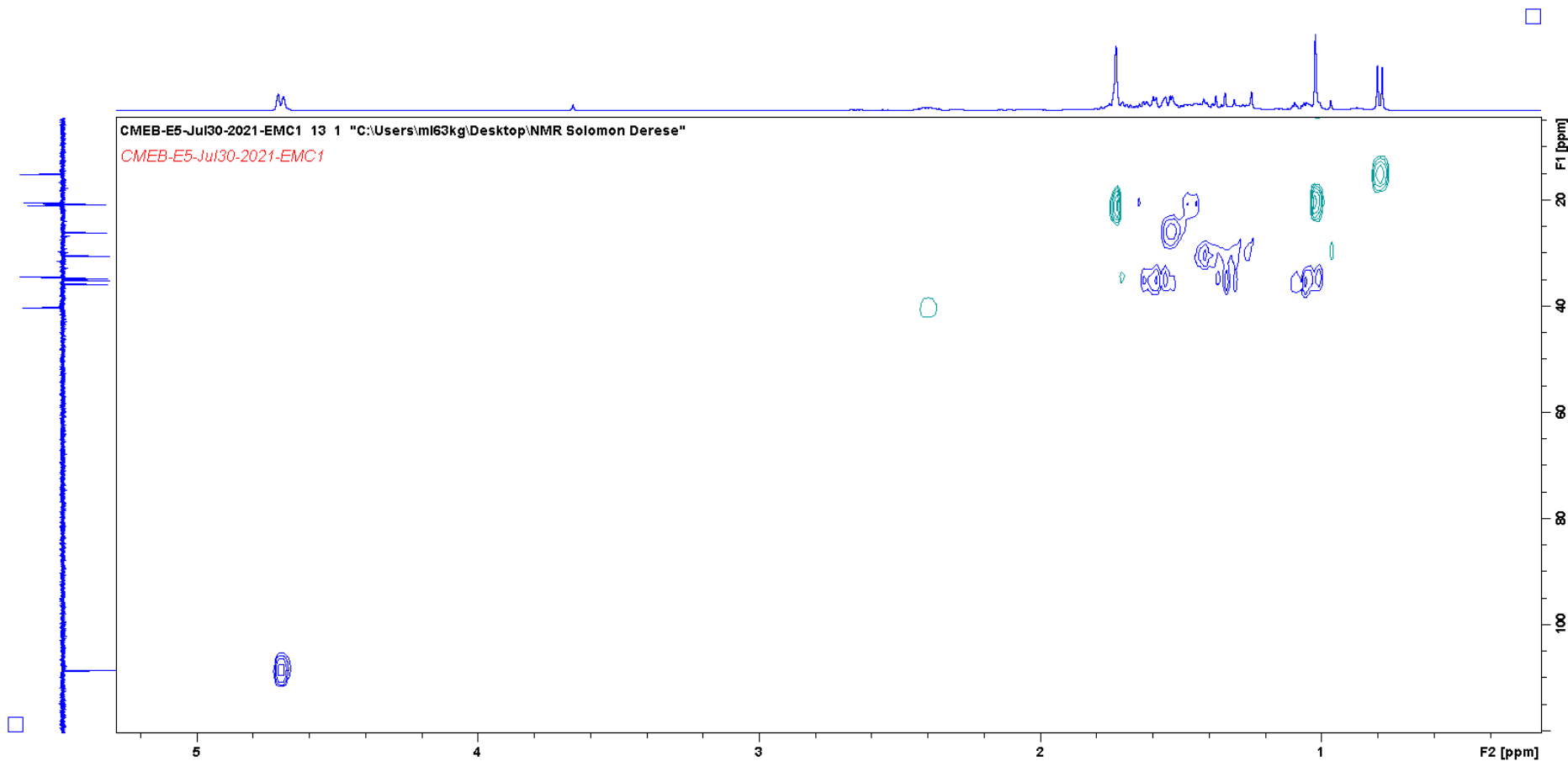


Appendix 28 DEPT spectrum of 4H- $\alpha$ ,7H- $\alpha$ ,10 $\alpha$ -eudesm-11-en-5 $\beta$ -ol (E5)

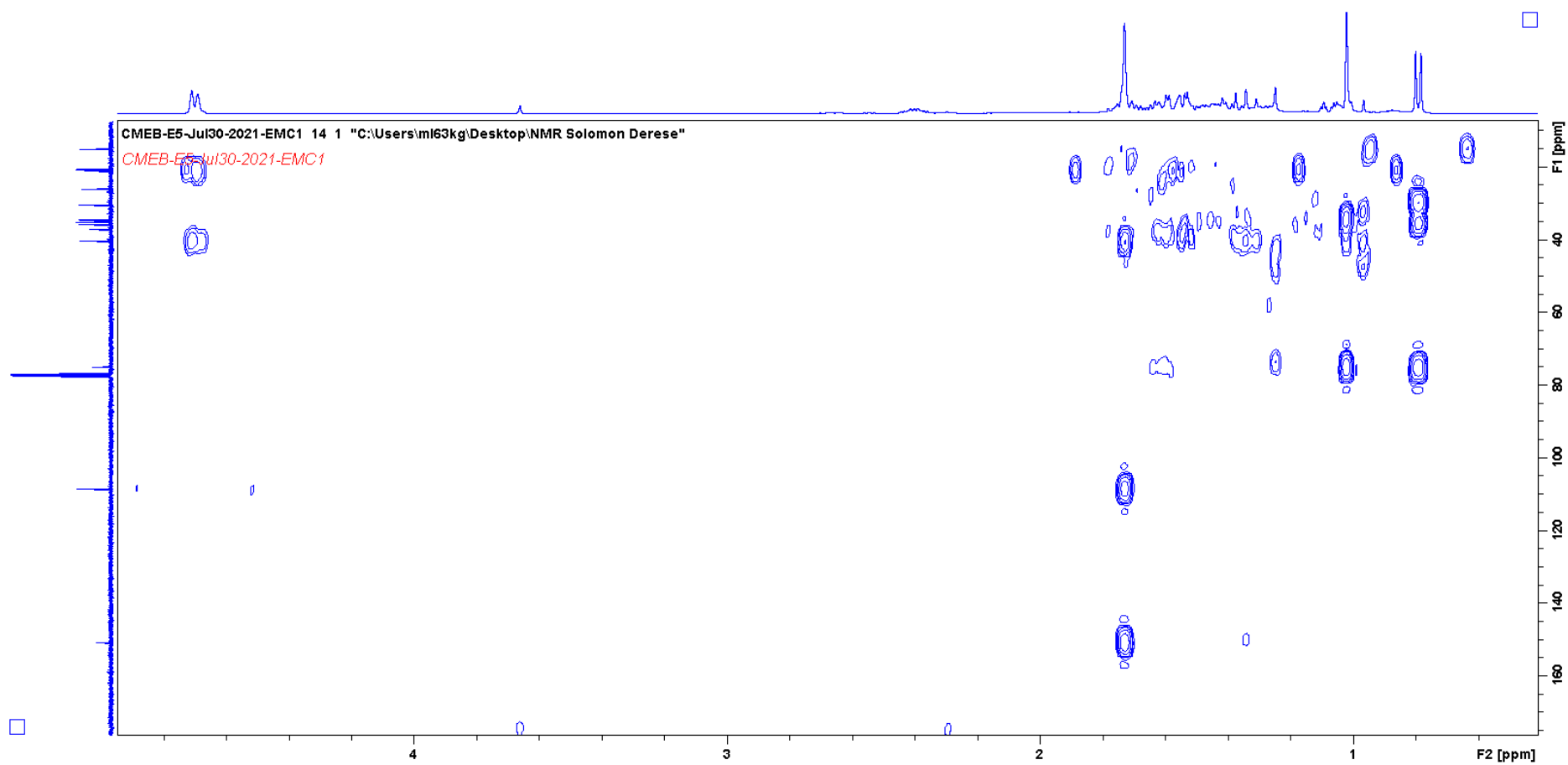




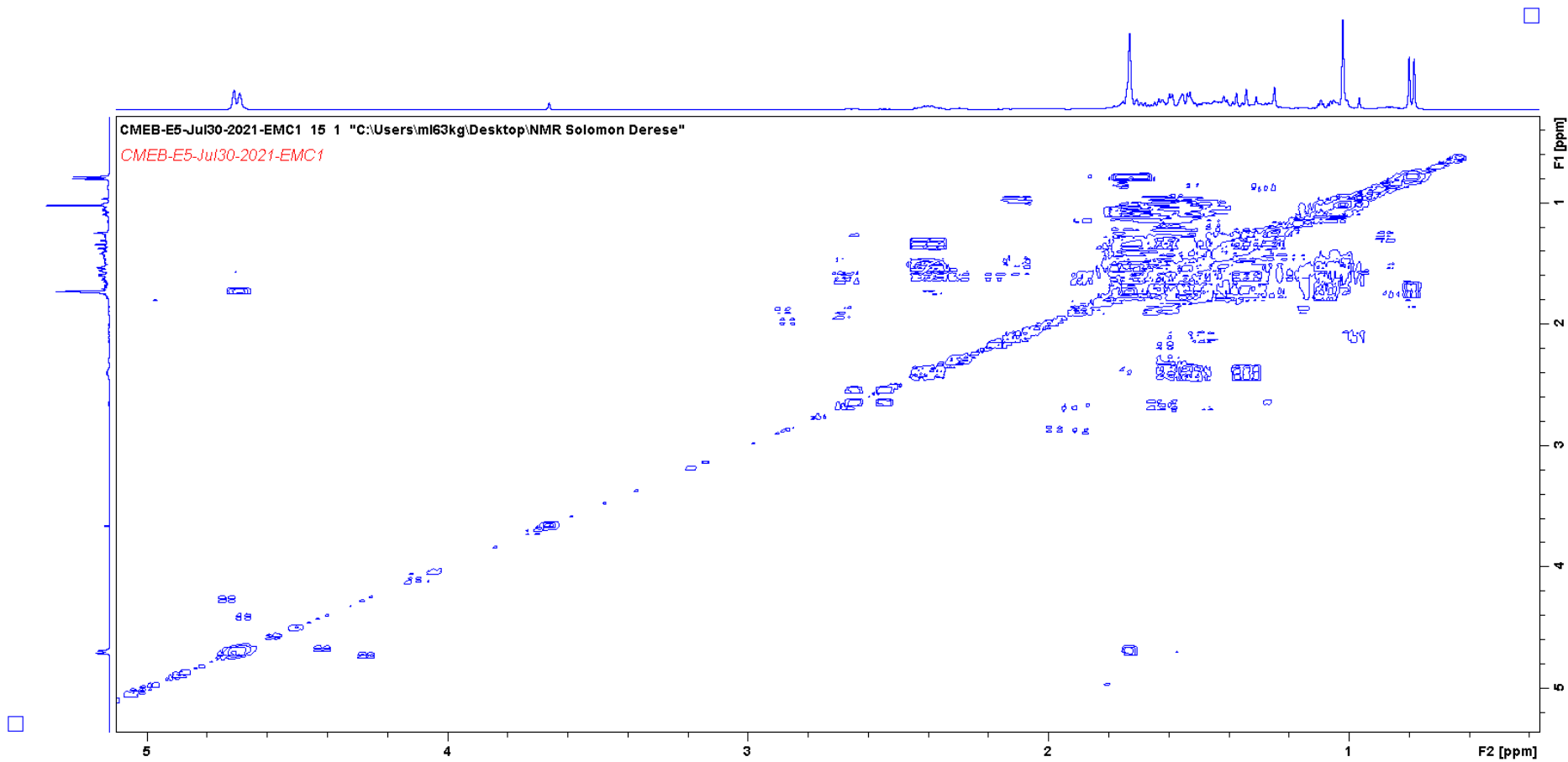
Appendix 29 HSQCDEPT spectrum of 4H- $\alpha$ ,7H- $\alpha$ ,10 $\alpha$ -eudesm-11-en-5 $\beta$ -ol (E5)



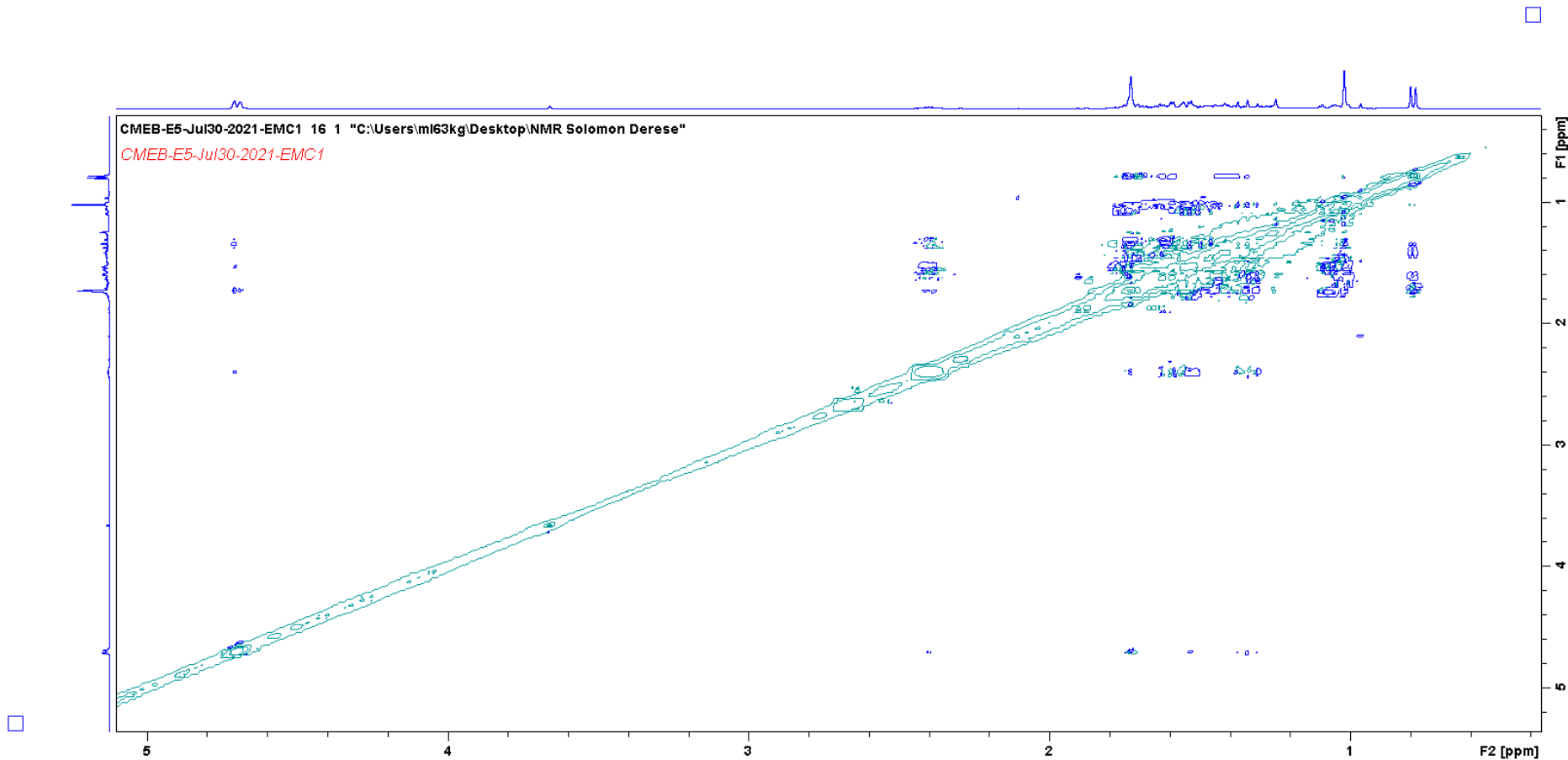
Appendix 30 HMBC spectrum of 4H- $\alpha$ ,7H- $\alpha$ ,10 $\alpha$ -eudesm-11-en-5 $\beta$ -ol (E5)



Appendix 31 COSY spectrum of 4H- $\alpha$ ,7H- $\alpha$ ,10 $\alpha$ -eudesm-11-en-5 $\beta$ -ol (E5)

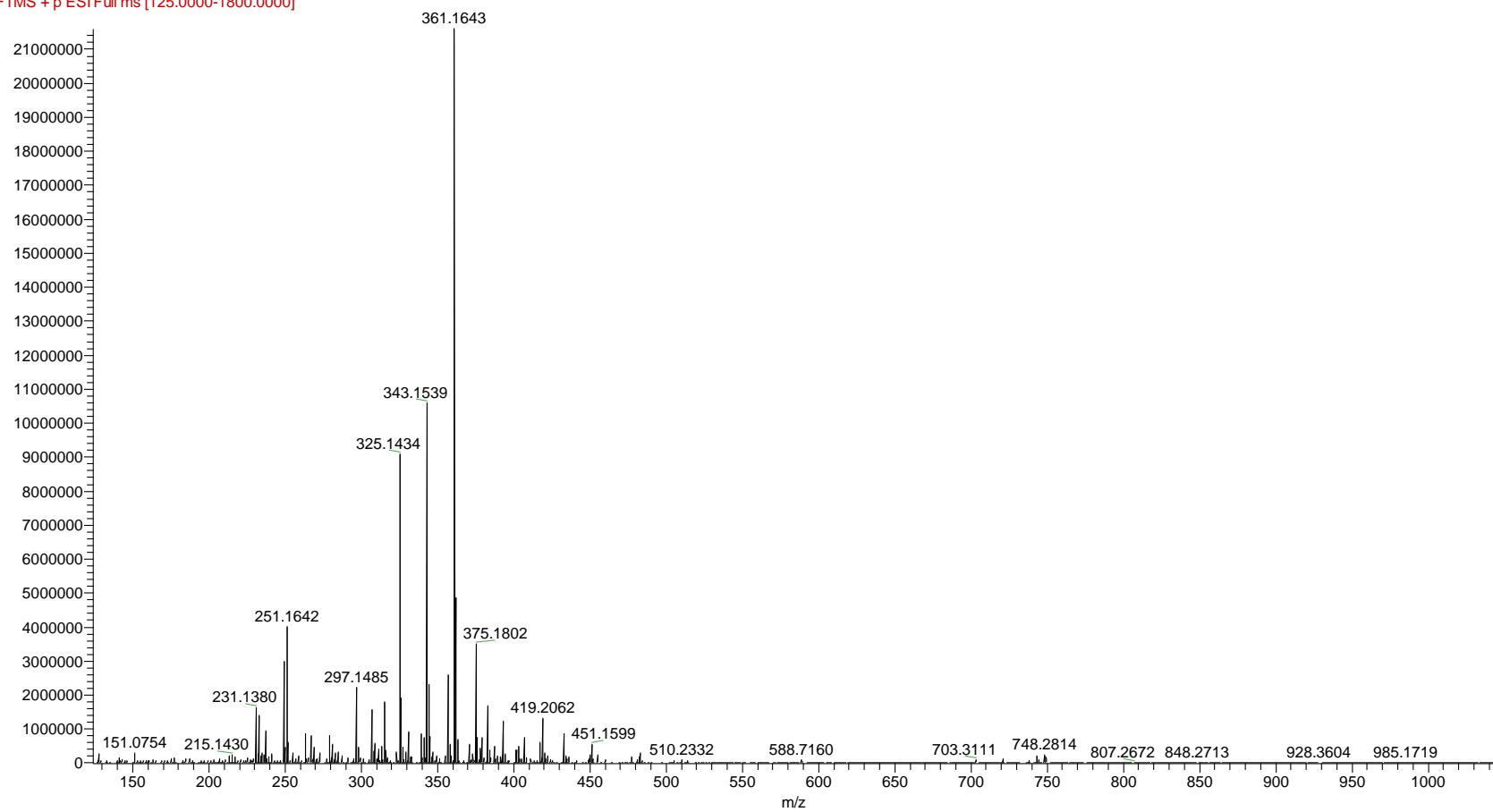


Appendix 32 NOSEY spectrum of 4H- $\alpha$ ,7H- $\alpha$ ,10 $\alpha$ -eudesm-11-en-5 $\beta$ -ol (E5)



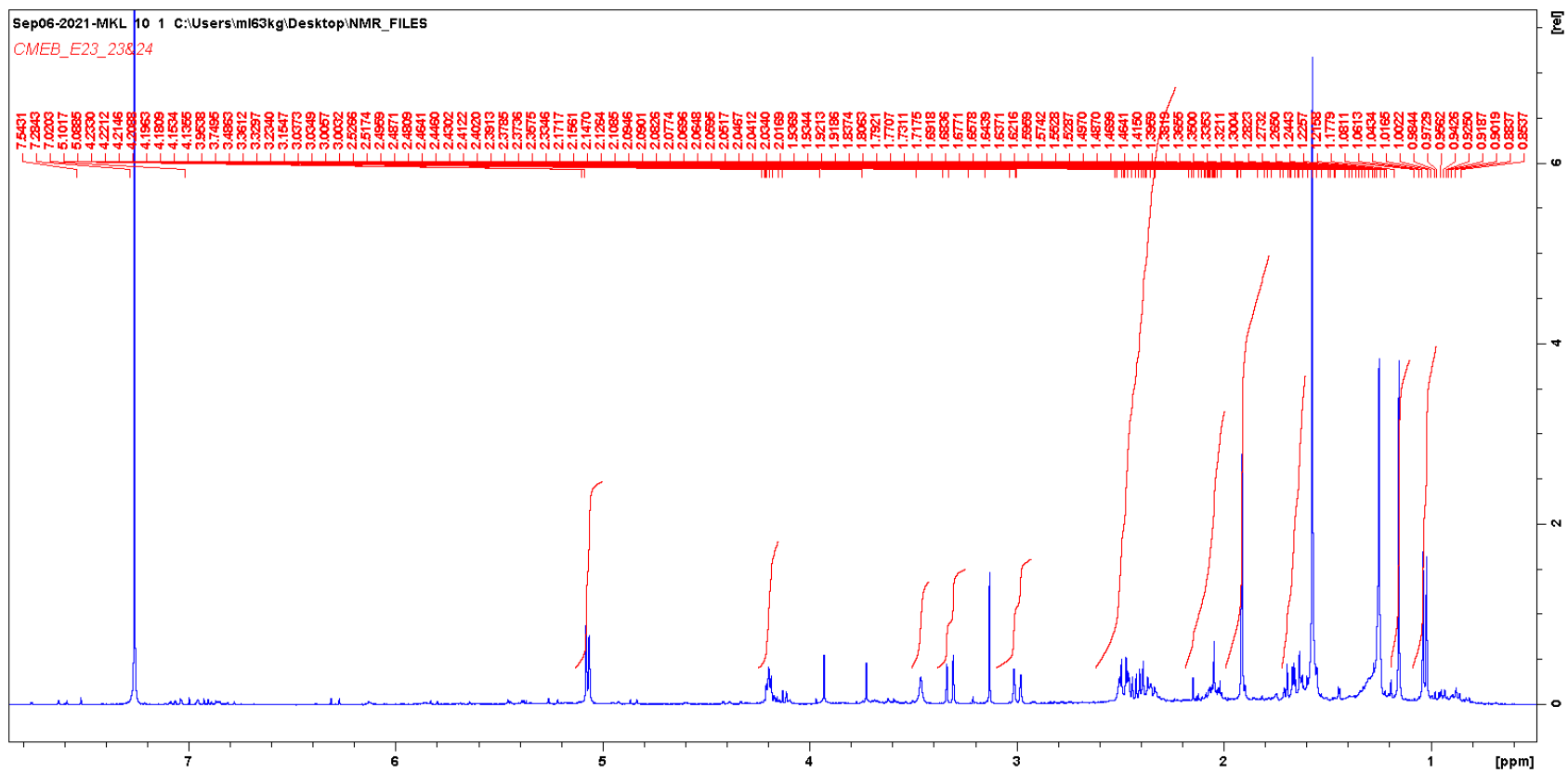
### Appendix 33 Mass spectrum of Crotoascarin K (E23)

CMEB-E23 #5110-5270 RT: 15.22-15.51 AV: 7 NL: 2.16E7  
F: FTMS +p ESI Full ms [125.0000-1800.0000]

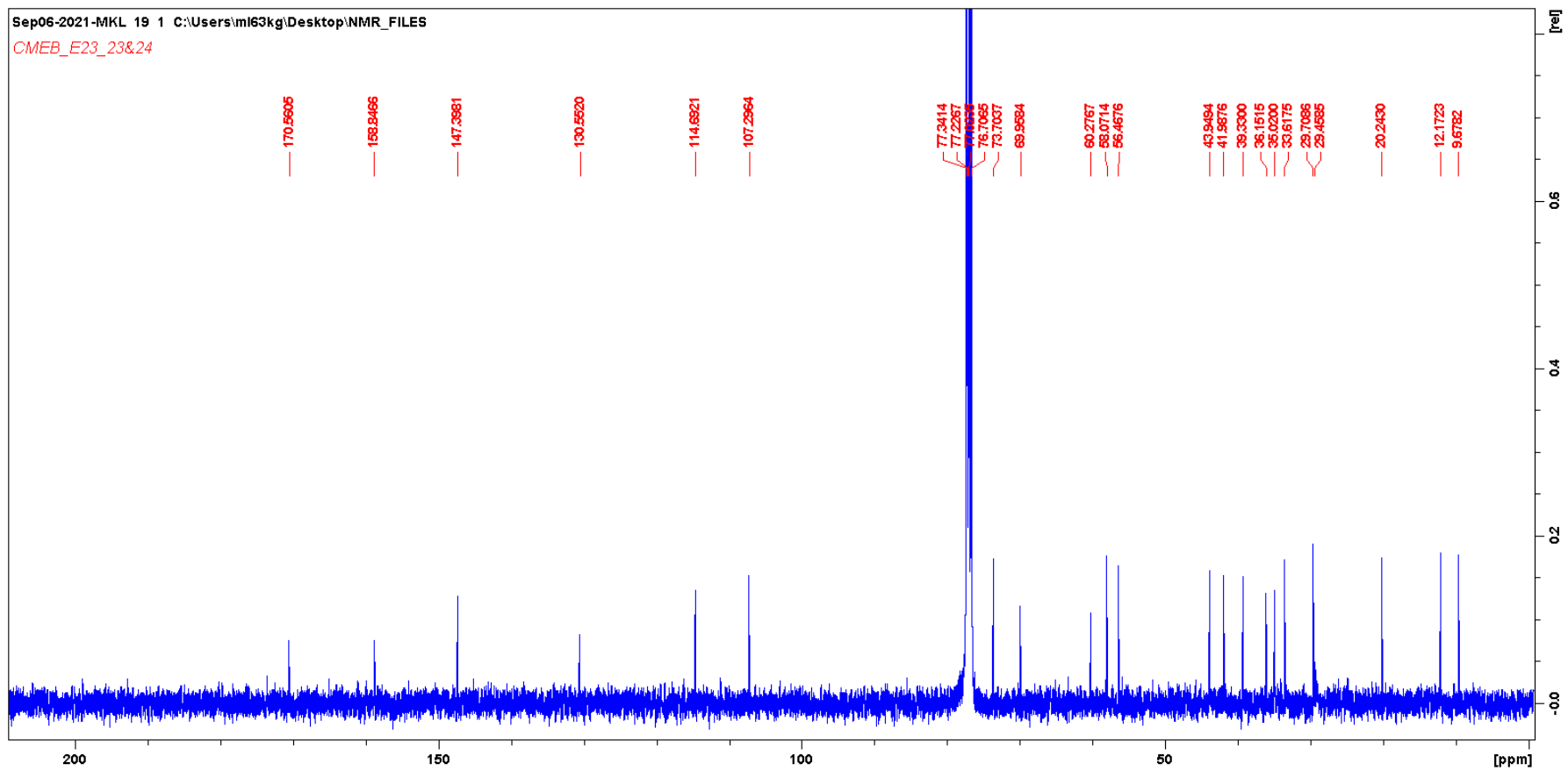


HRESIMS  $m/z$  361.1643  $[M+H]^+$  (calcd. for  $C_{20}H_{24}O_6 + H$ ,  $m/z$  361.1646)

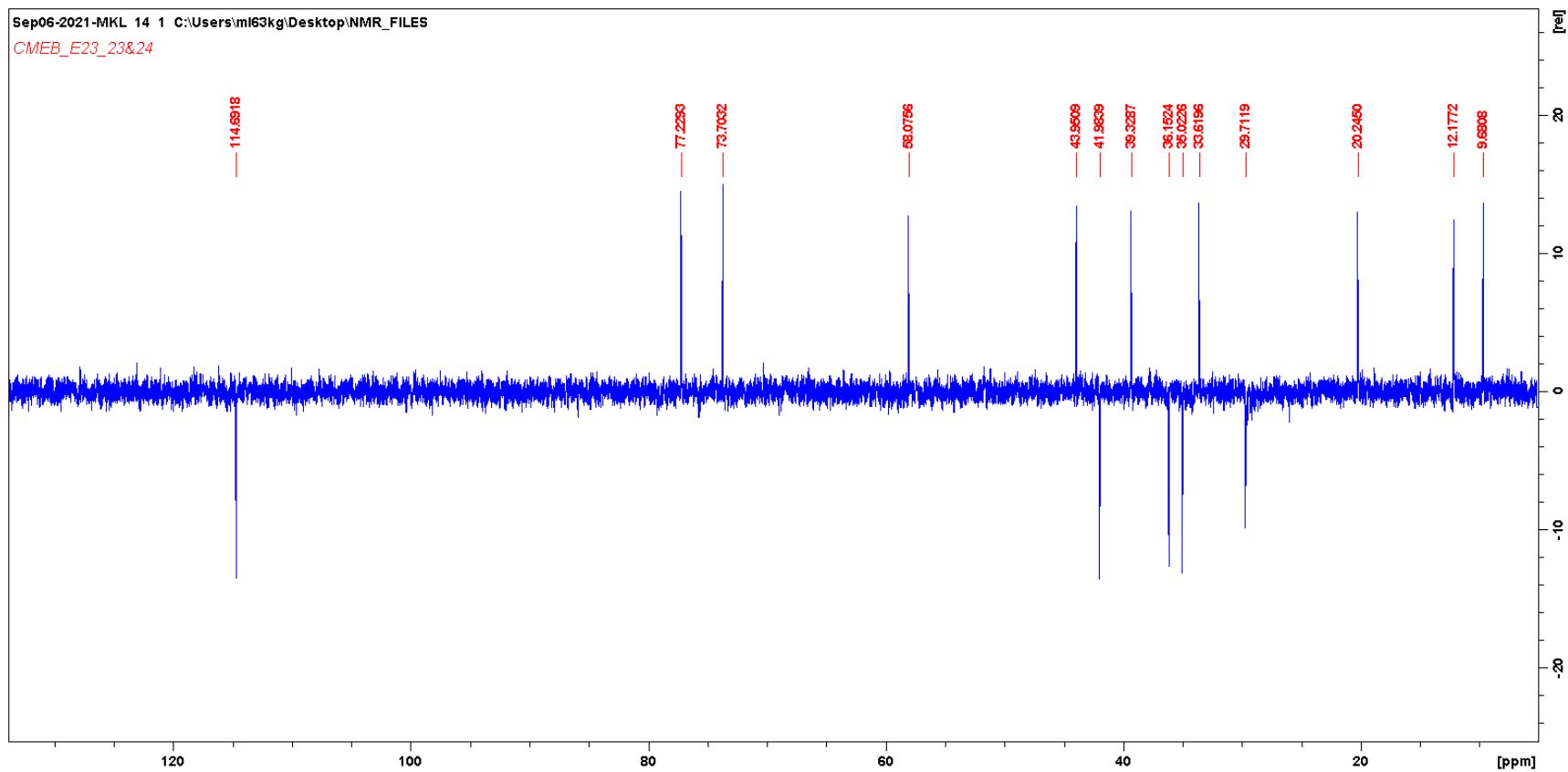
Appendix 34  $^1\text{H}$  NMR spectrum of Crotoascarin K (E23)



Appendix 35  $^{13}\text{C}$  NMR spectrum of Crotoascarin K (E23)

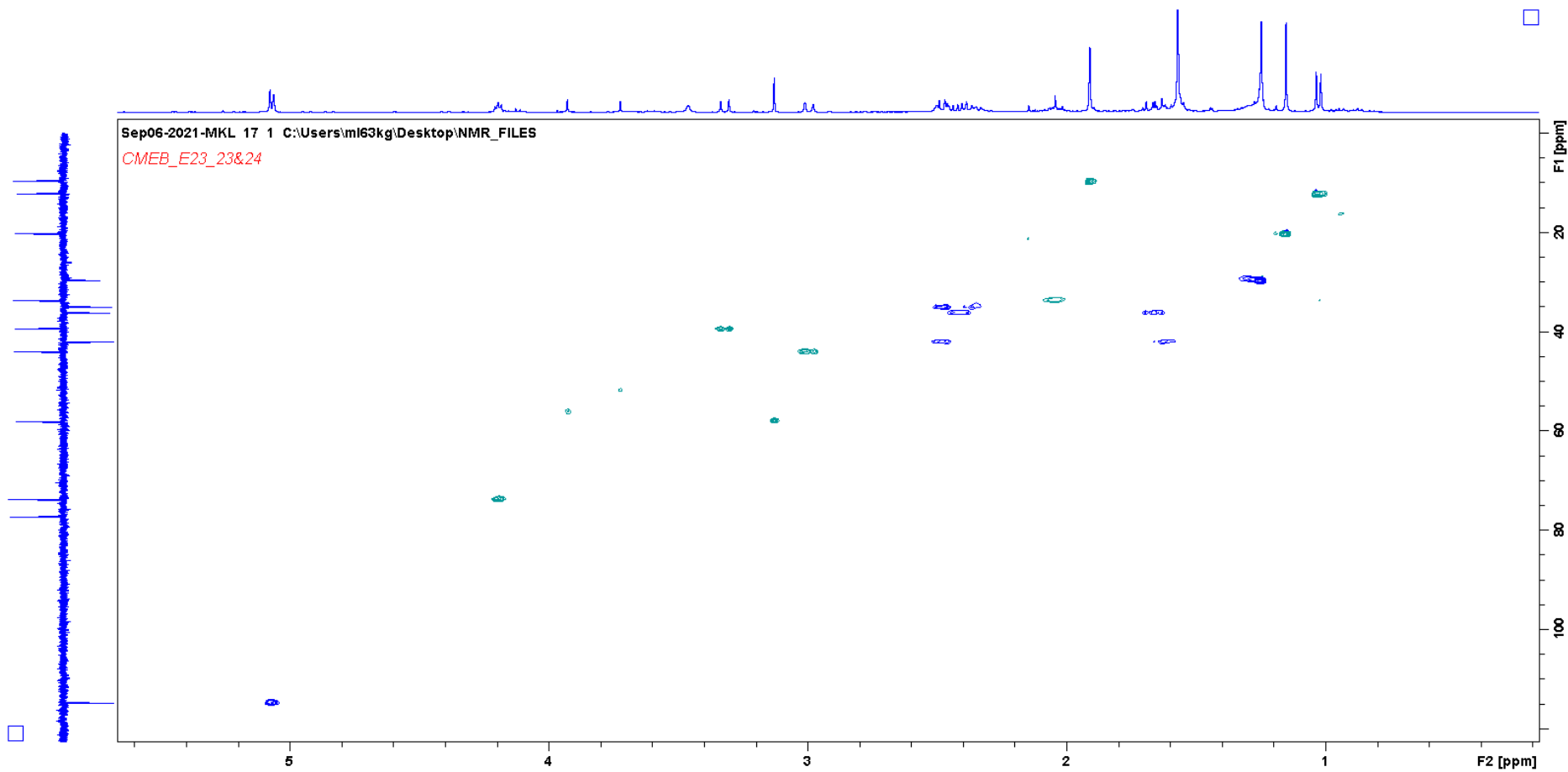


# Appendix 36 DEPT spectrum of Crotoascarin K (E23)

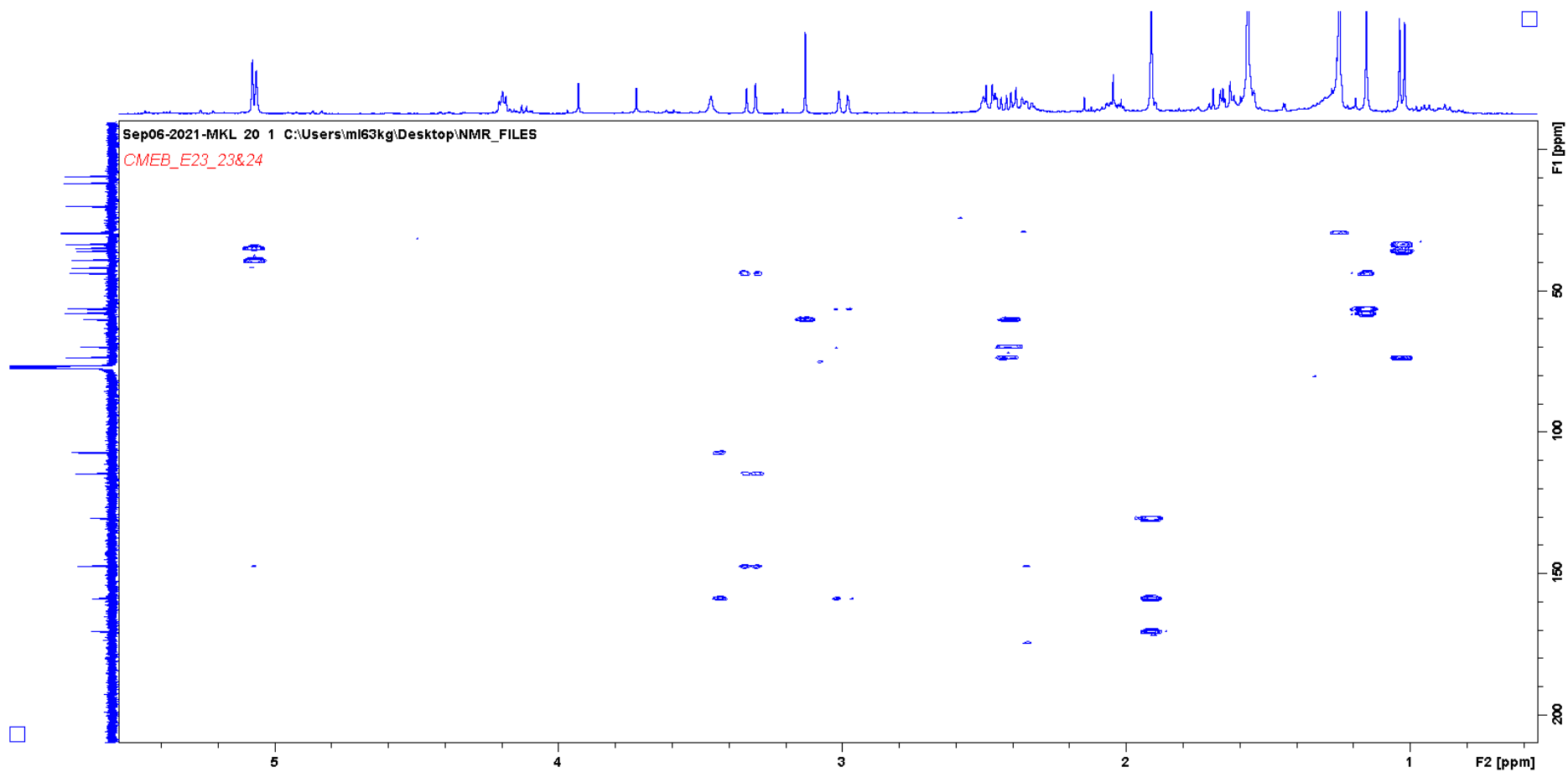




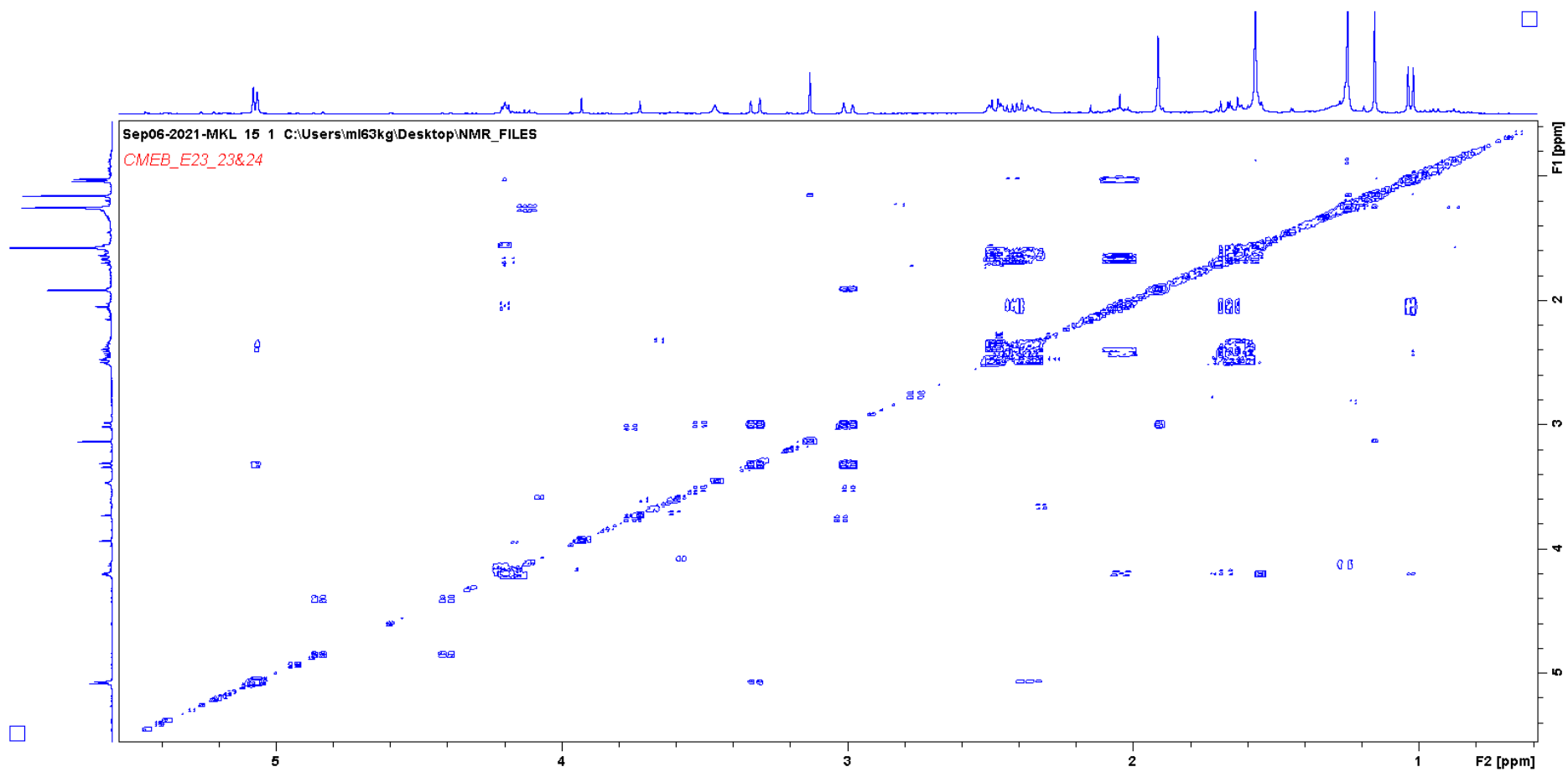
Appendix 37 HSQCDEPT spectrum of Crotoascarin K (E23)



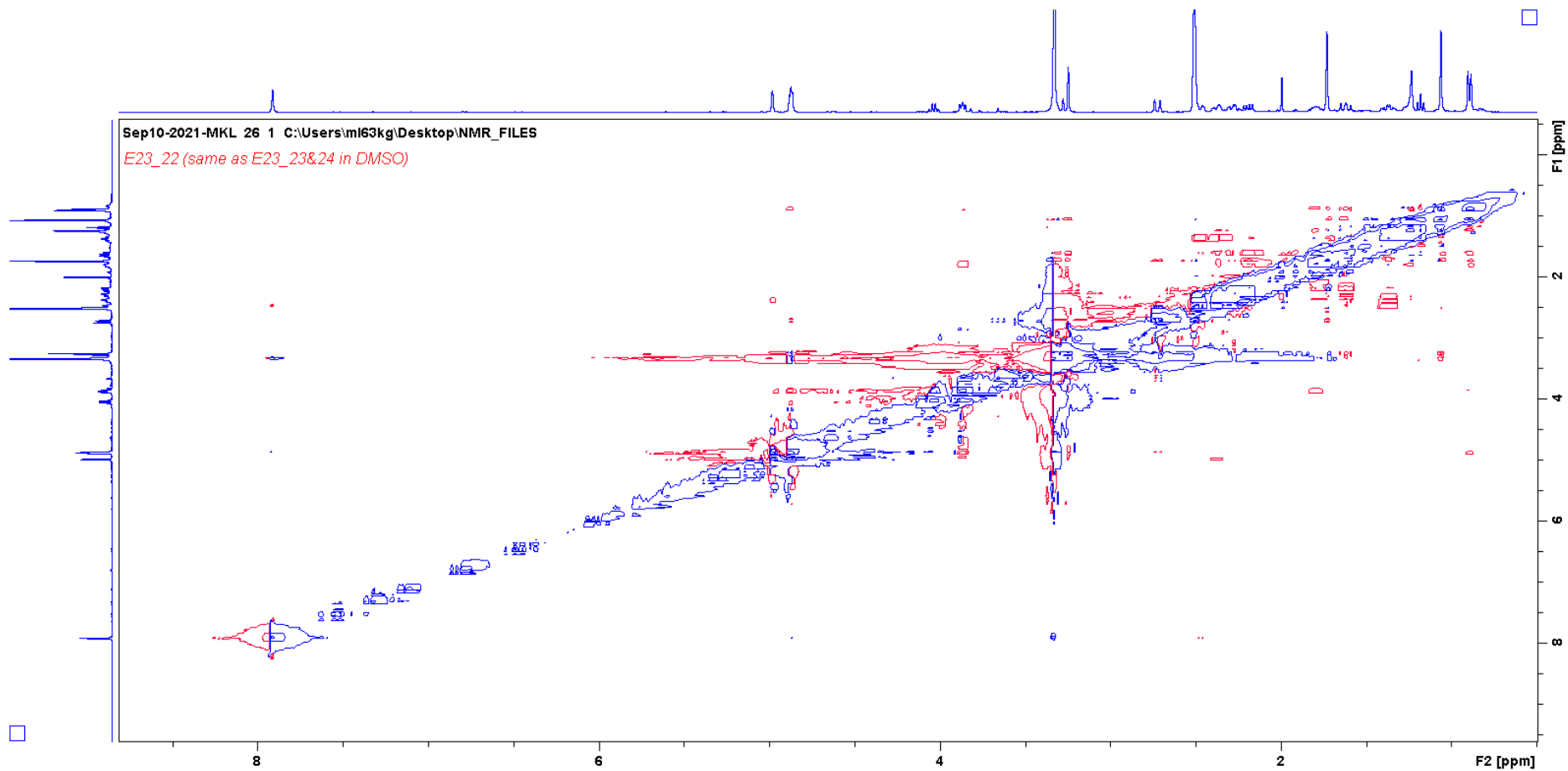
Appendix 38 HMBC spectrum of Crotoascarin K (E23)



Appendix 39 COSY spectrum of Crotoascarin K (E23)

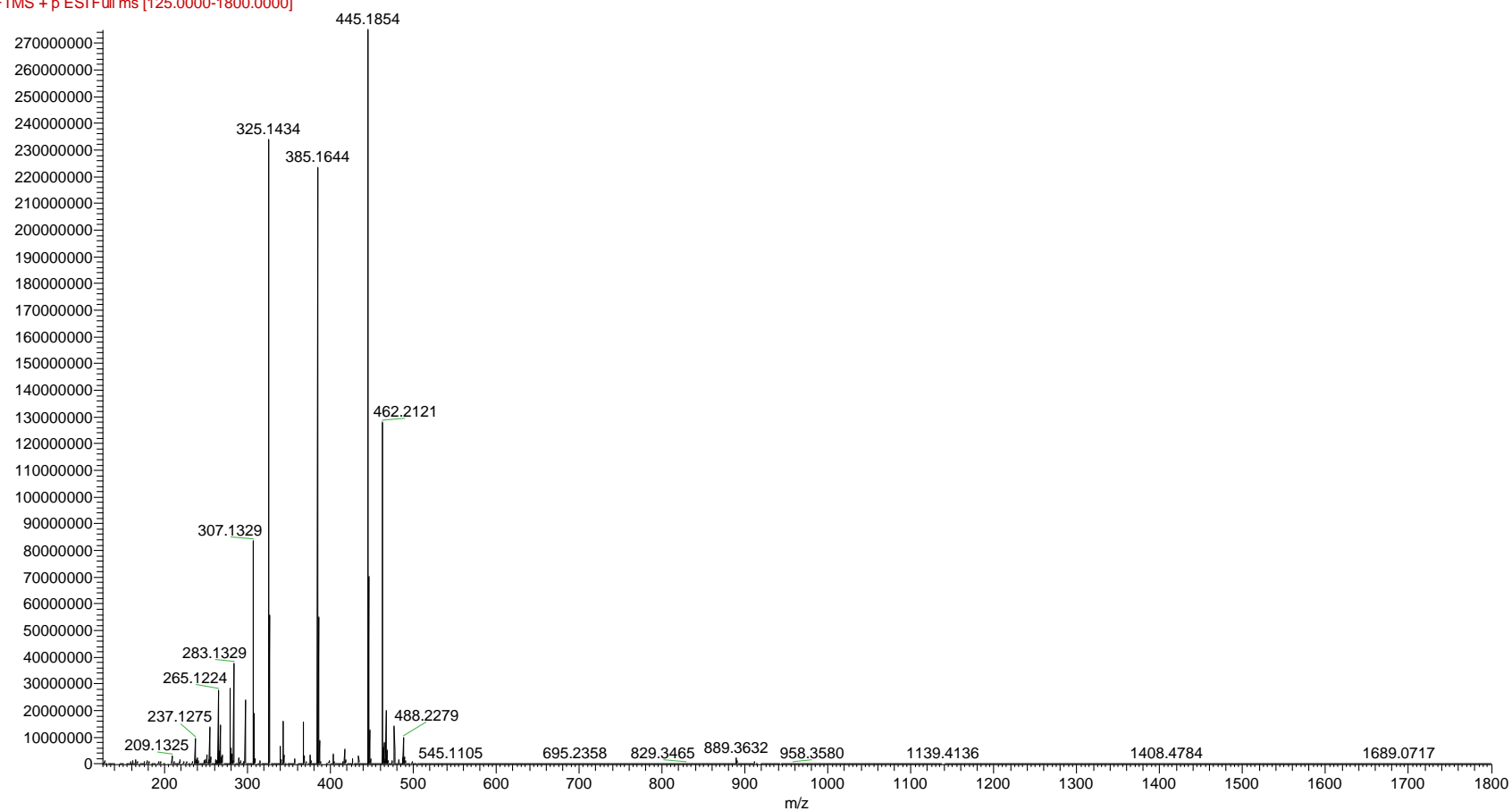


Appendix 40 NOESY spectrum of Crotoascarin K (E23)



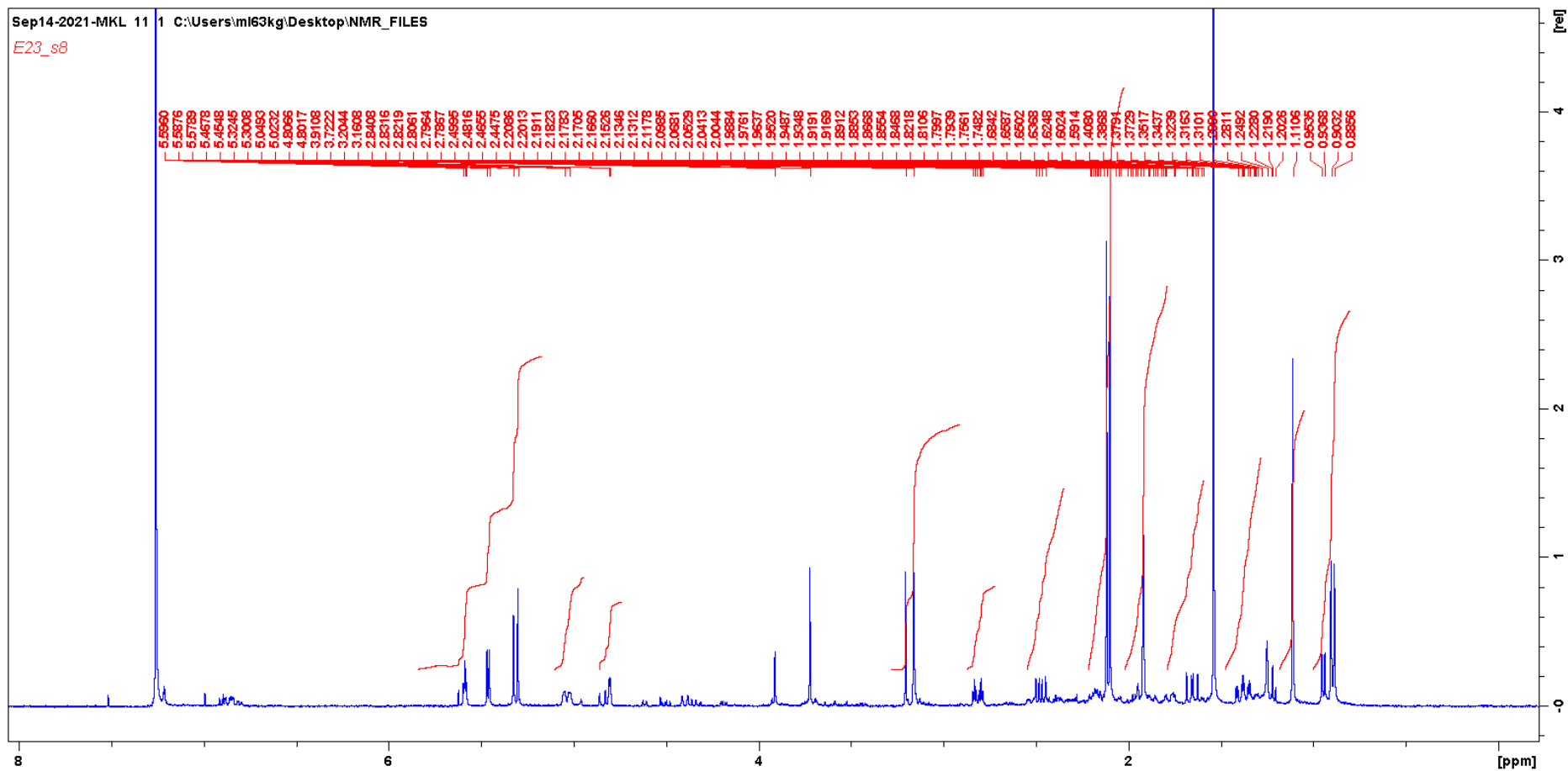
# Appendix 41 Mass spectrum of 11-acetoxy crotoascarin L (E24)

CMEB-E23-s7-8 #5422 RT: 16.60 AV: 1 NL: 2.75E8  
F: FTMS + p ESI Full ms [125.0000-1800.0000]

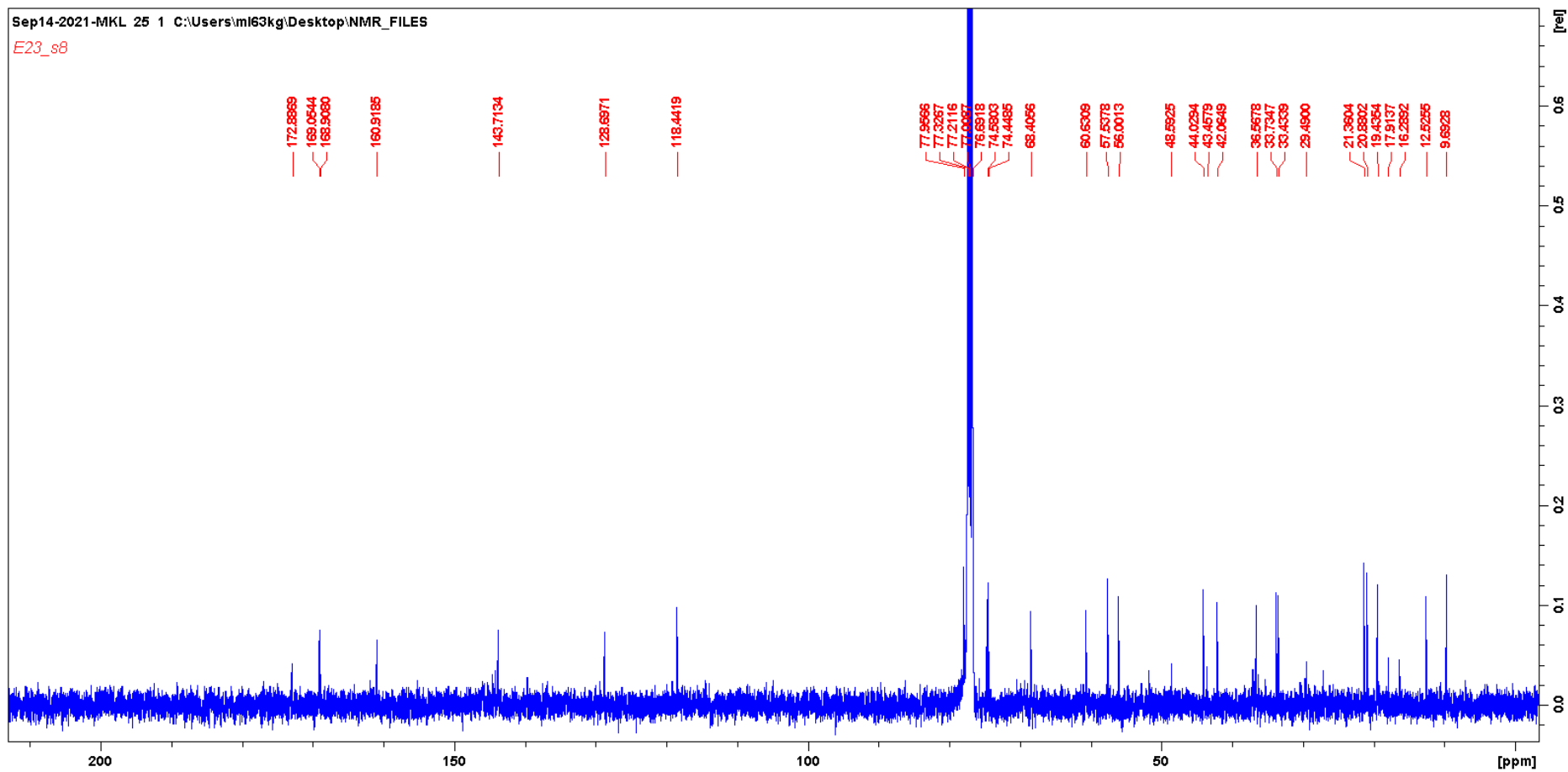


HRESIMS  $m/z$  445.1854  $[M+H]^+$  (calcd. for  $C_{24}H_{28}O_8 + H$ ,  $m/z$  445.1857)

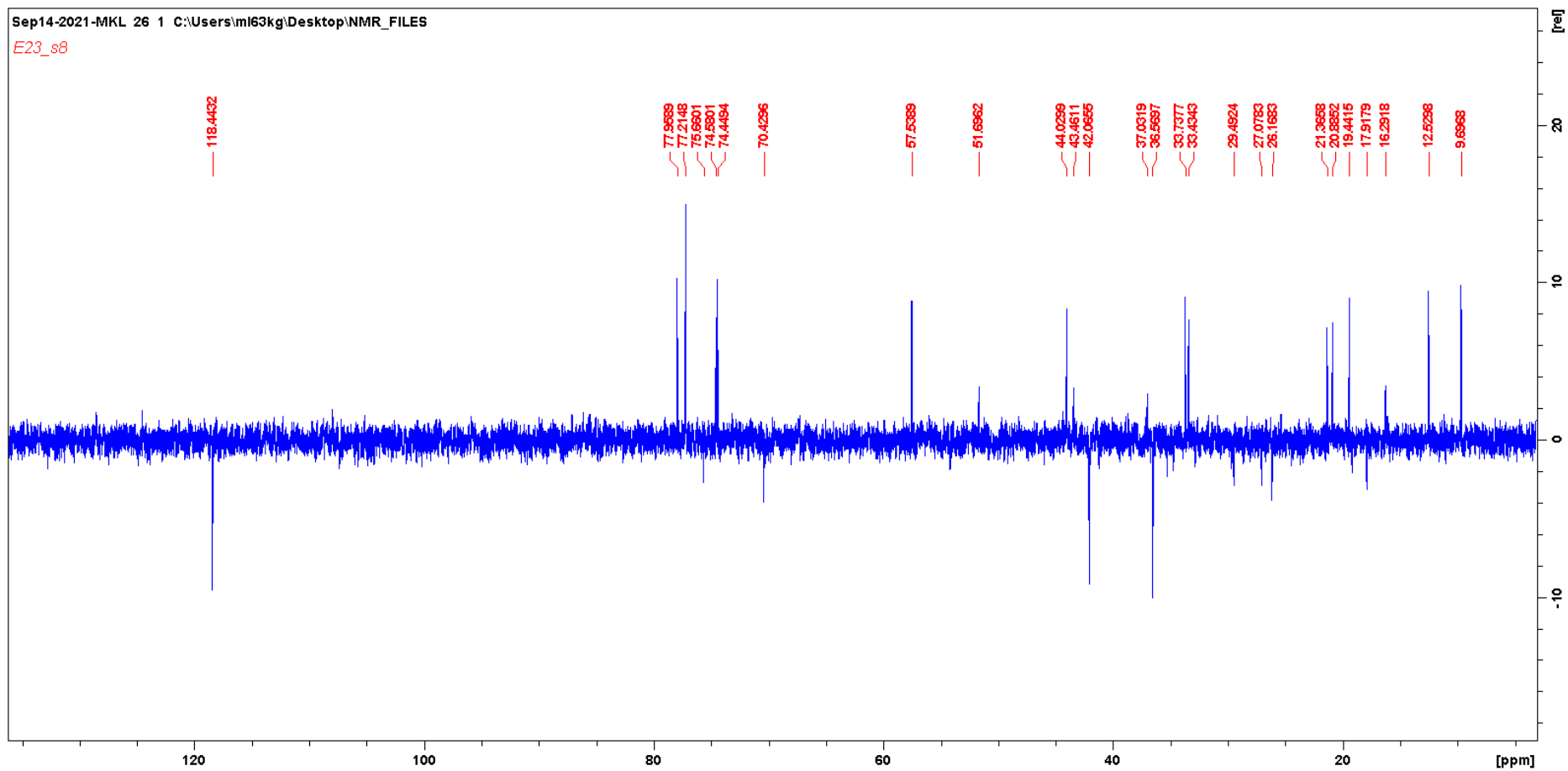
Appendix 42 <sup>1</sup>H NMR spectrum of 11-acetoxy crotoascarin L (E24)



Appendix 43  $^{13}\text{C}$  NMR spectrum of 11-acetoxy crotoascarin L (E24)

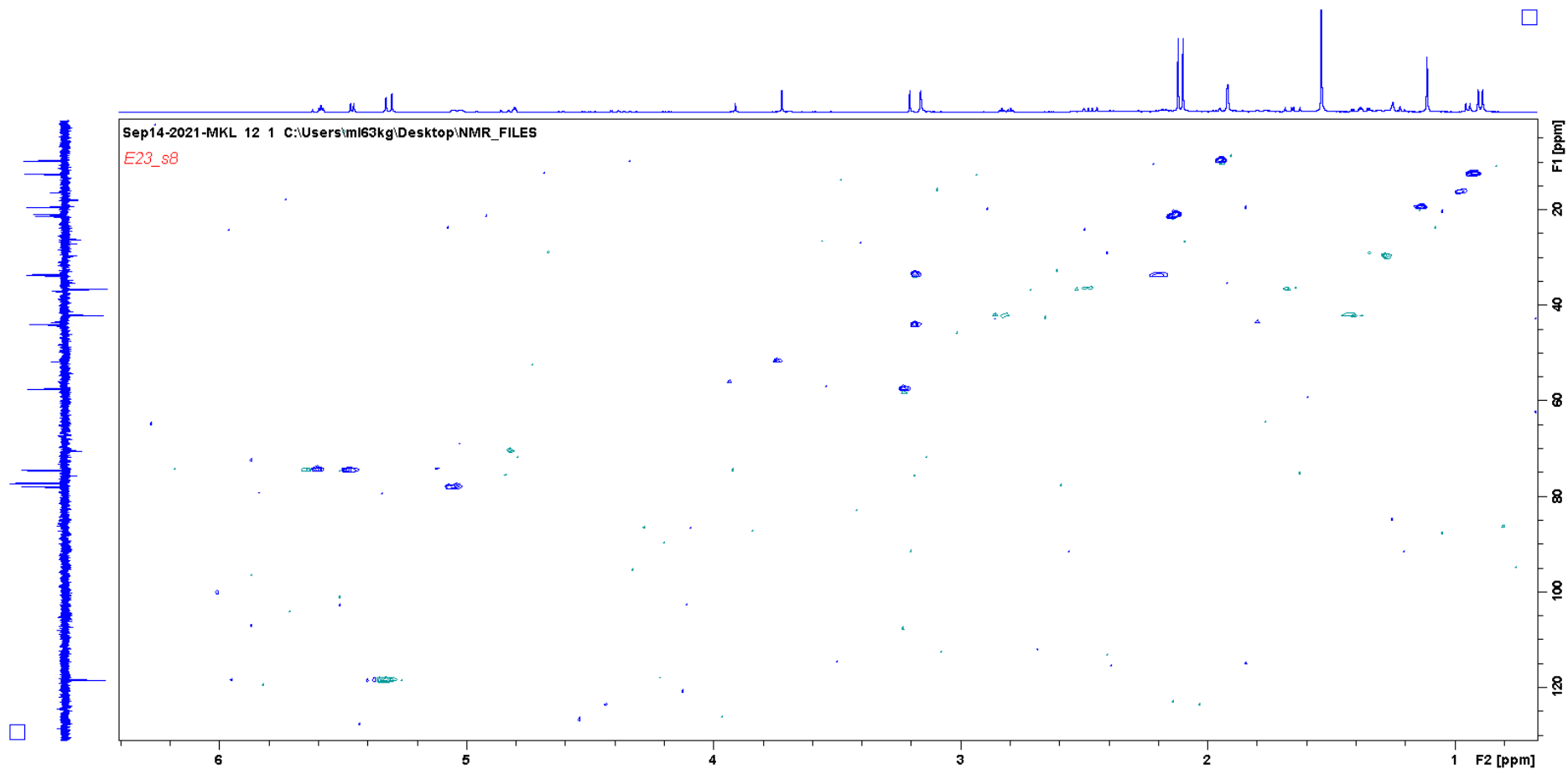


Appendix 44 DEPT spectrum of 11-acetoxy crotoascarin L (E24)

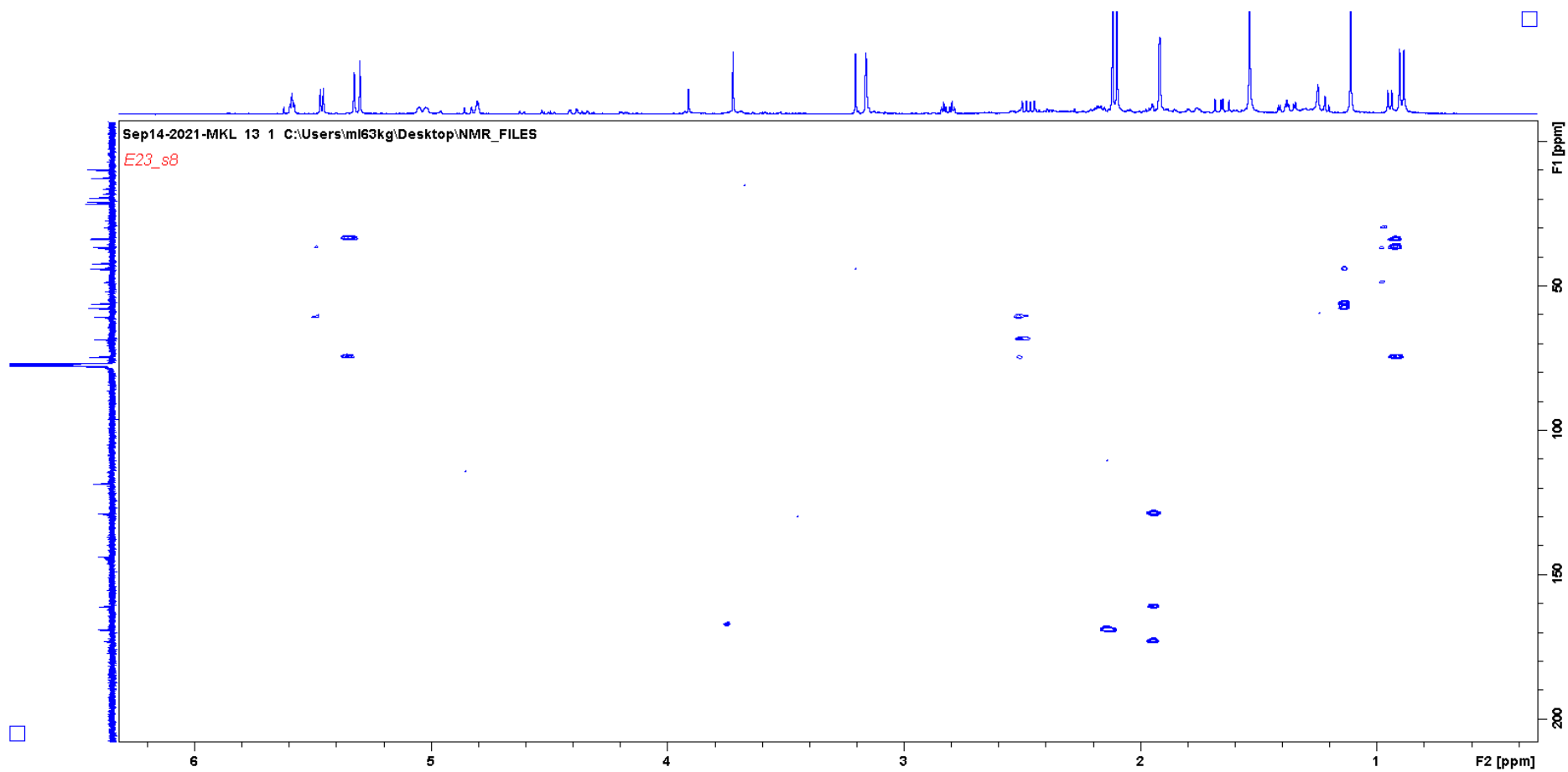




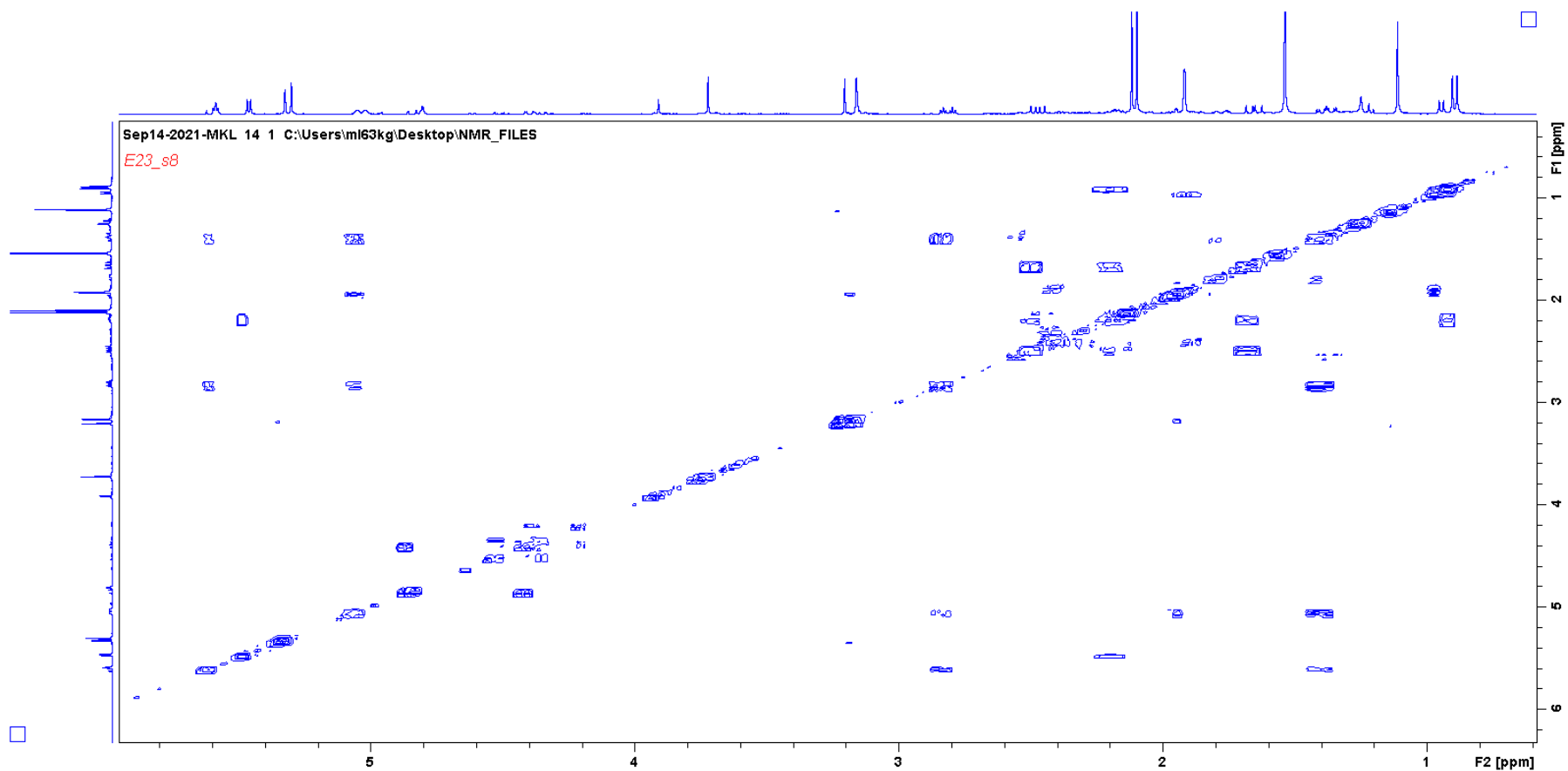
Appendix 45 HSQCDEPT spectrum of 11-acetoxy crotoascarin L (E24)



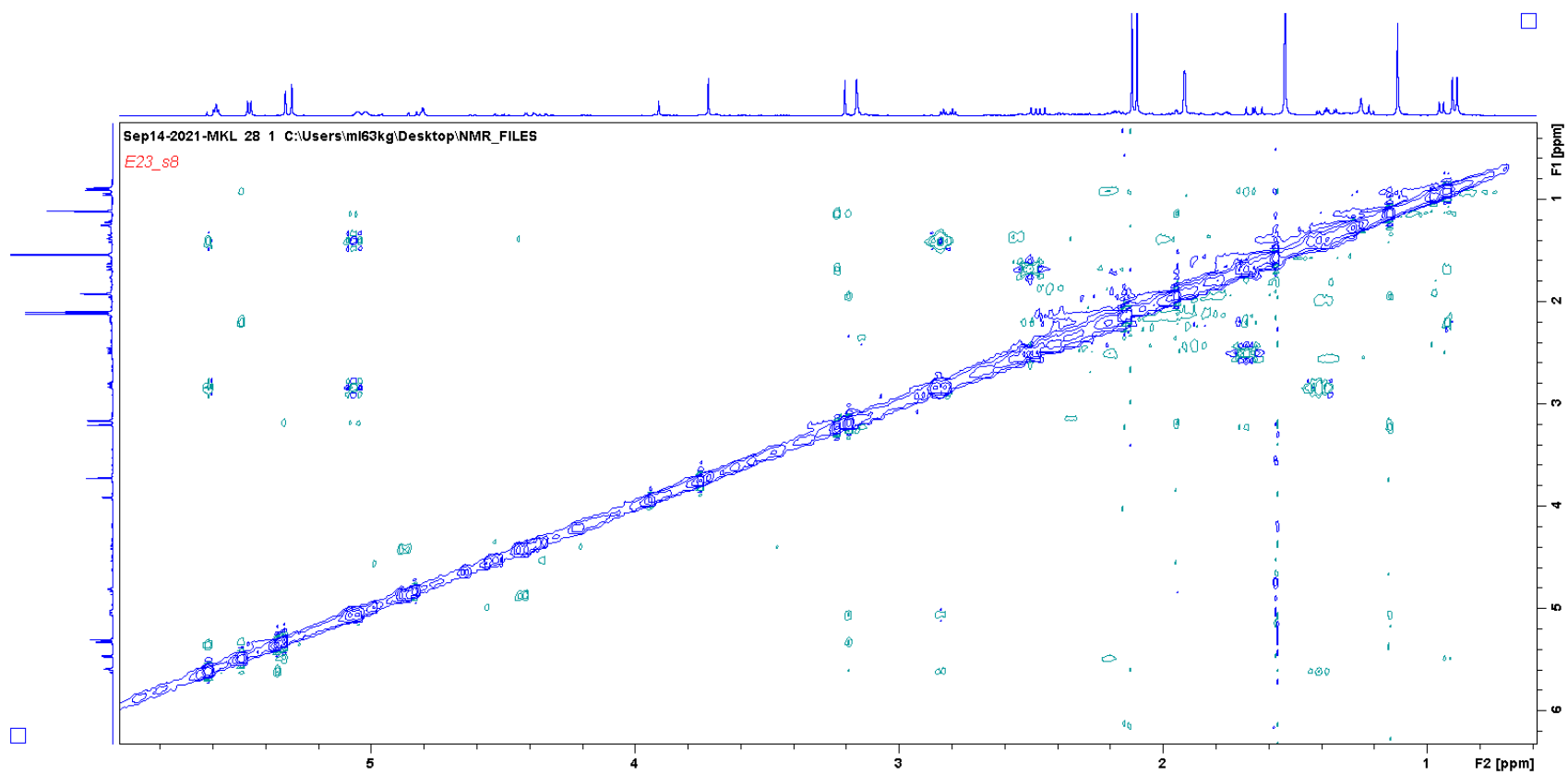
Appendix 46 HMBC spectrum of 11-acetoxy crotoascarin L (E24)



Appendix 47 COSY spectrum of 11-acetoxy crotoascarin L (E24)

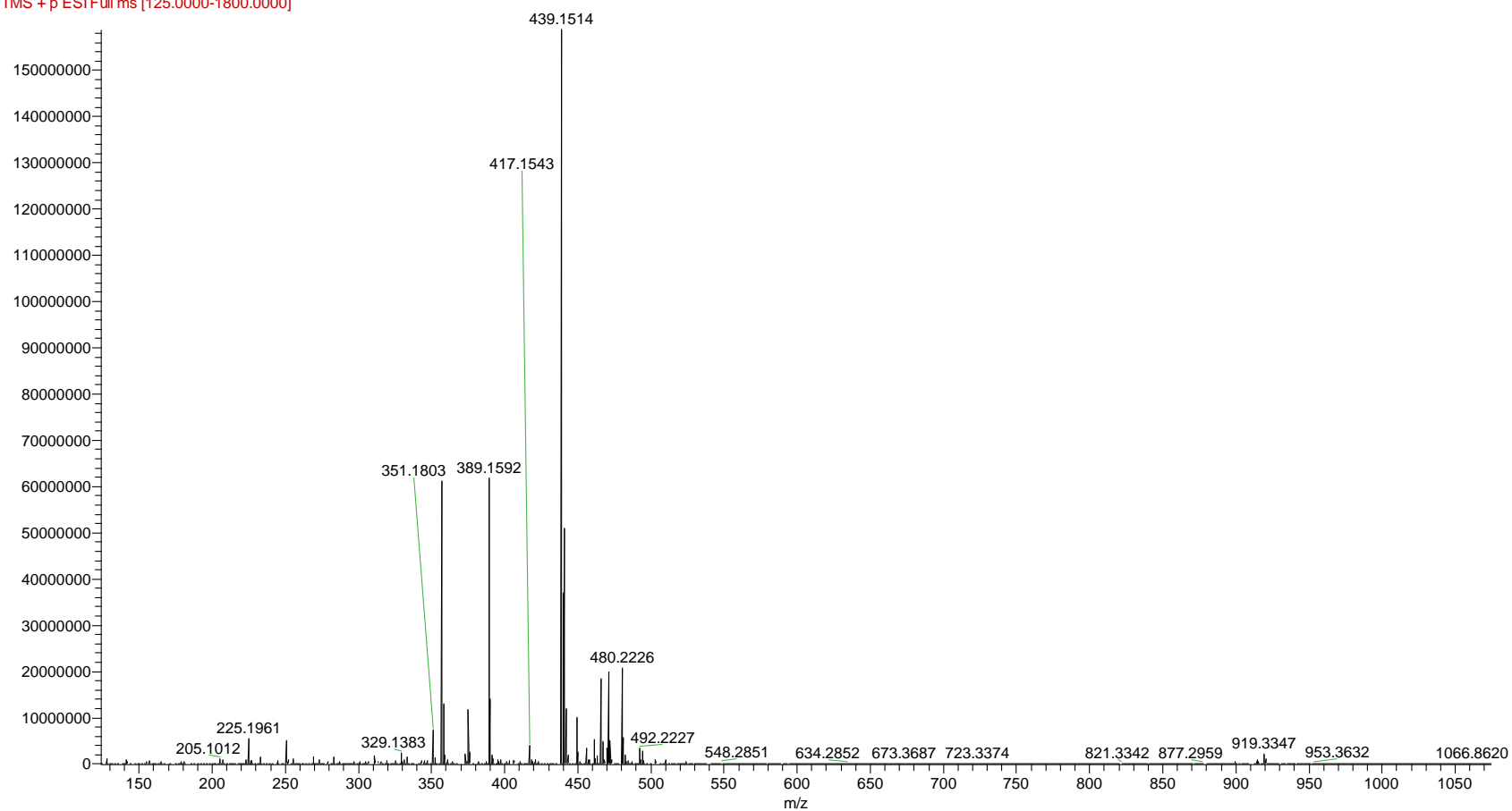


Appendix 48 NOESY spectrum of 11-acetoxy crotonoscarin L (E24)



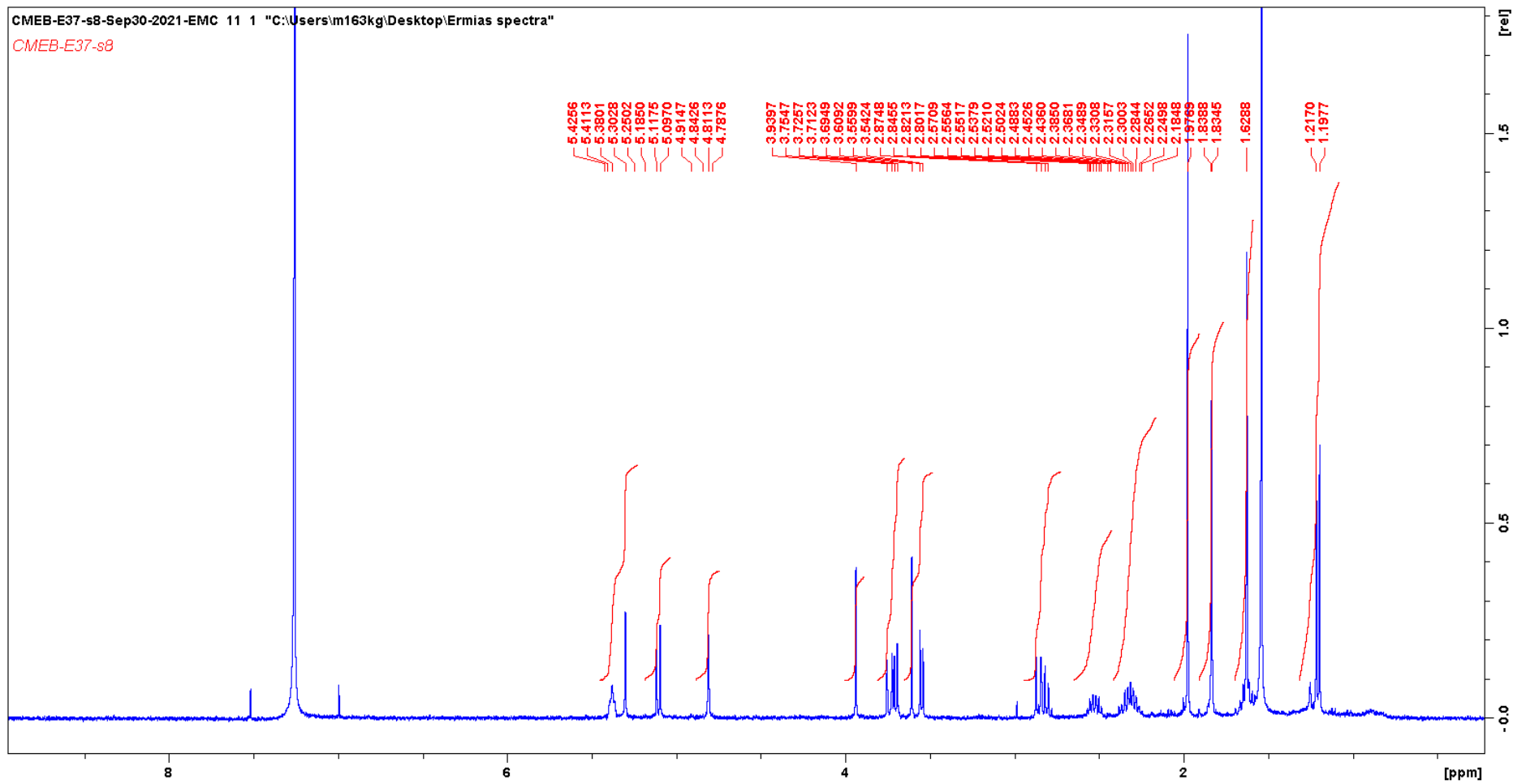
Appendix 49 Mass spectrum of 1 $\beta$ -acetoxy-3 $\beta$ -chloro-5 $\alpha$ ,6 $\alpha$ -dihydroxycrotocascarin L (Ermiasoid) (E37)

E37 #6086-6179 RT: 16.89-17.03 AV: 4 NL: 1.59E8  
F: FTMS +p ESI Full ms [125.0000-1800.0000]

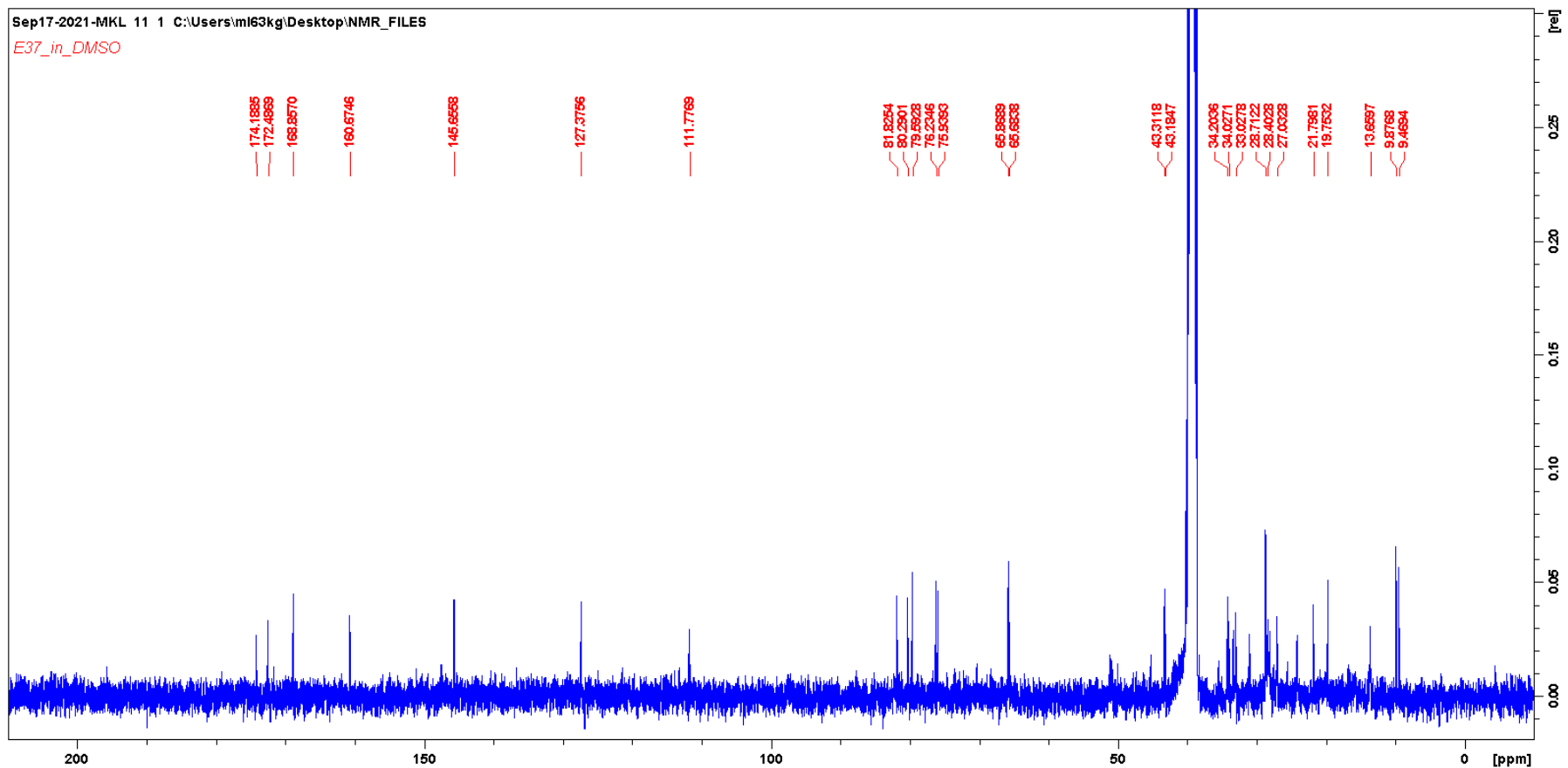


HRESIMS  $m/z$  439.1514 [M+H]<sup>+</sup> (calcd. for C<sub>22</sub>H<sub>27</sub>ClO<sub>8</sub> + H,  $m/z$  439.1518)

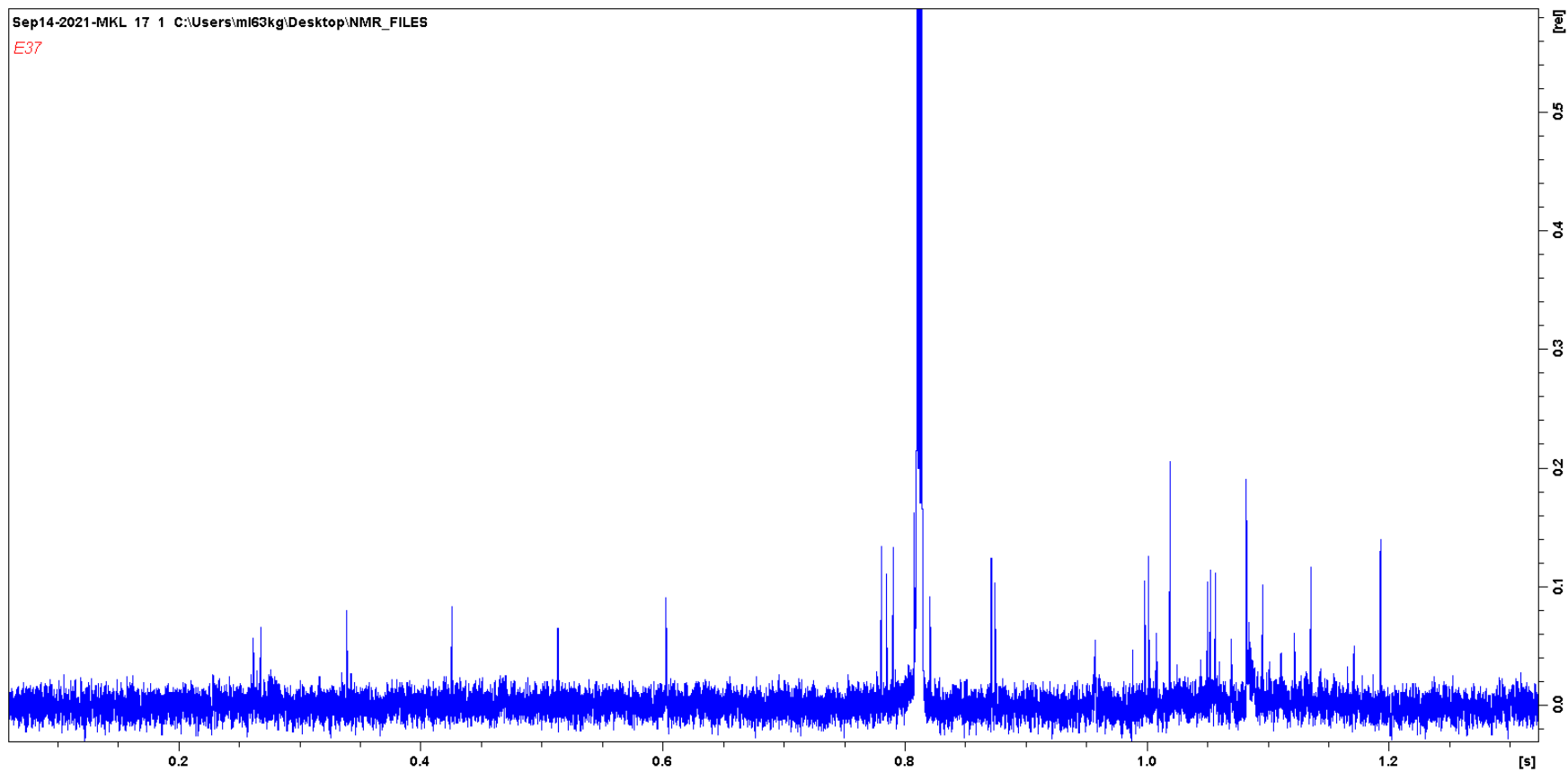
Appendix 50  $^1\text{H}$  NMR spectrum of  $1\beta$ -acetoxy- $3\beta$ -chloro- $5\alpha,6\alpha$ -dihydroxycrotocascarin L (Ermasoid) (E37)



Appendix 51  $^{13}\text{C}$  NMR spectrum in DMSO of 1 $\beta$ -acetoxy-3 $\beta$ -chloro-5 $\alpha$ ,6 $\alpha$ -dihydroxycrotocascarin L (Ermasoid) (E37)

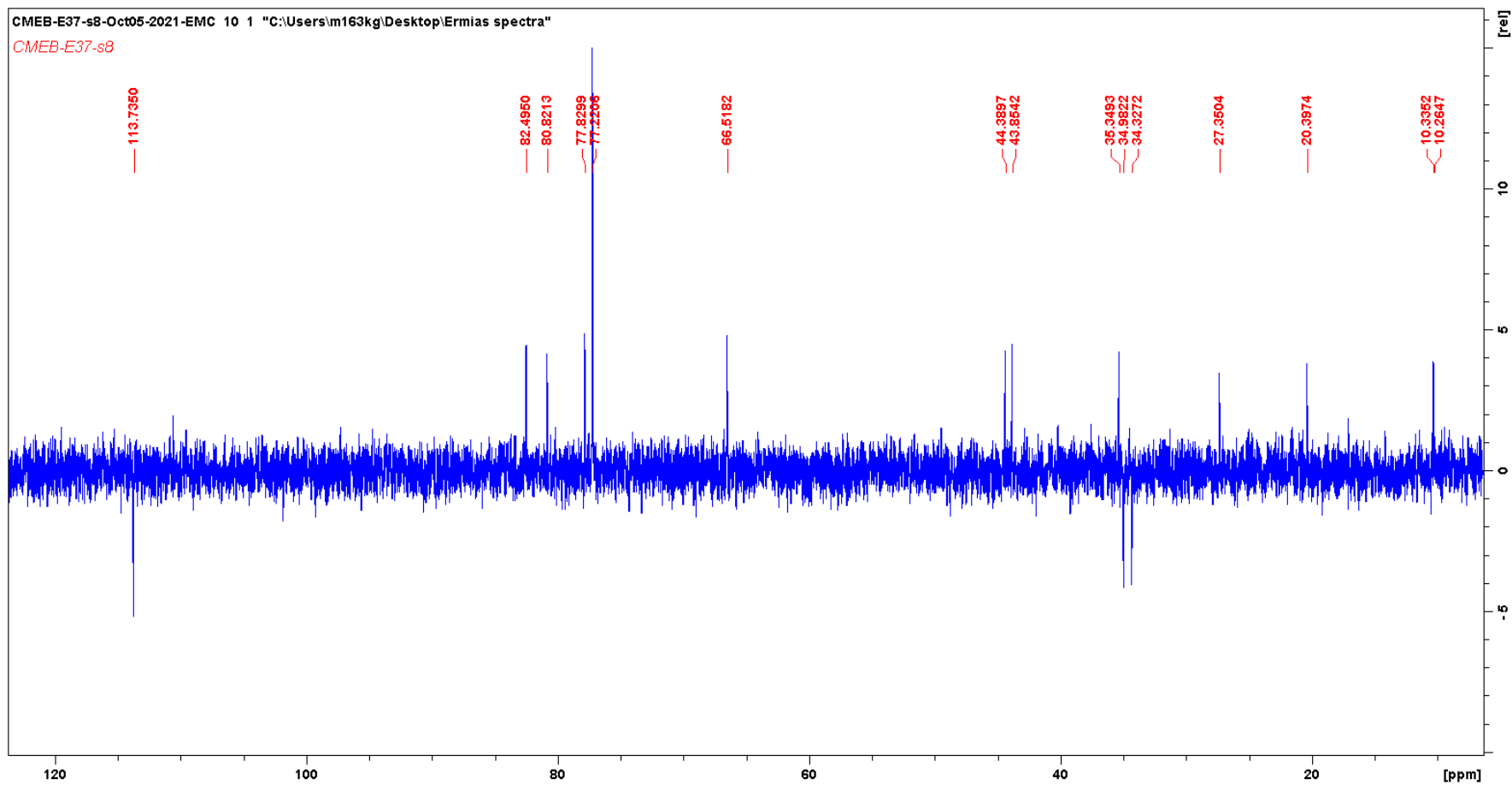


Appendix 52  $^{13}\text{C}$  NMR spectrum of 1 $\beta$ -acetoxy-3 $\beta$ -chloro-5 $\alpha$ ,6 $\alpha$ -dihydroxycrotocascarin L (Ermiasoid) (E37)

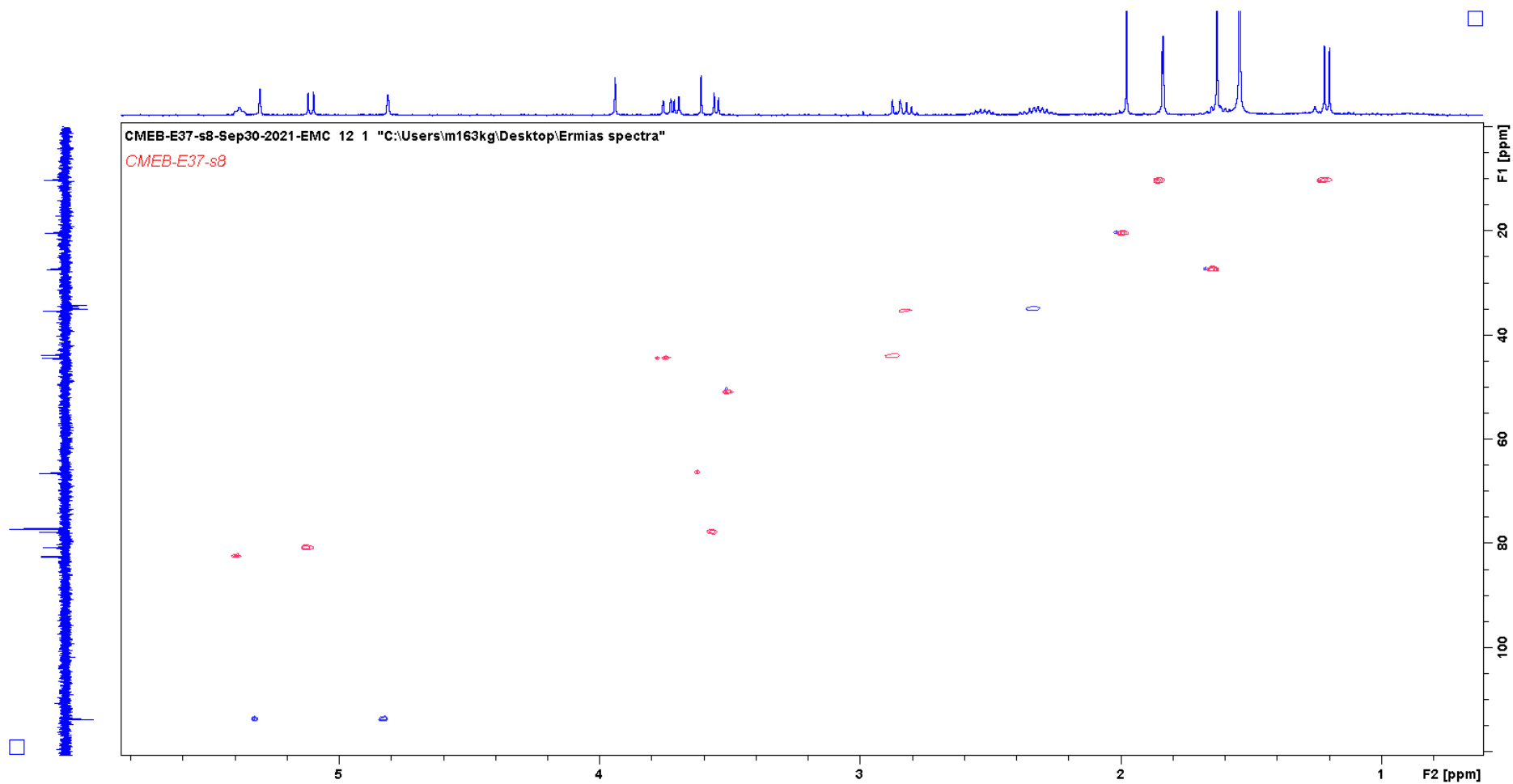




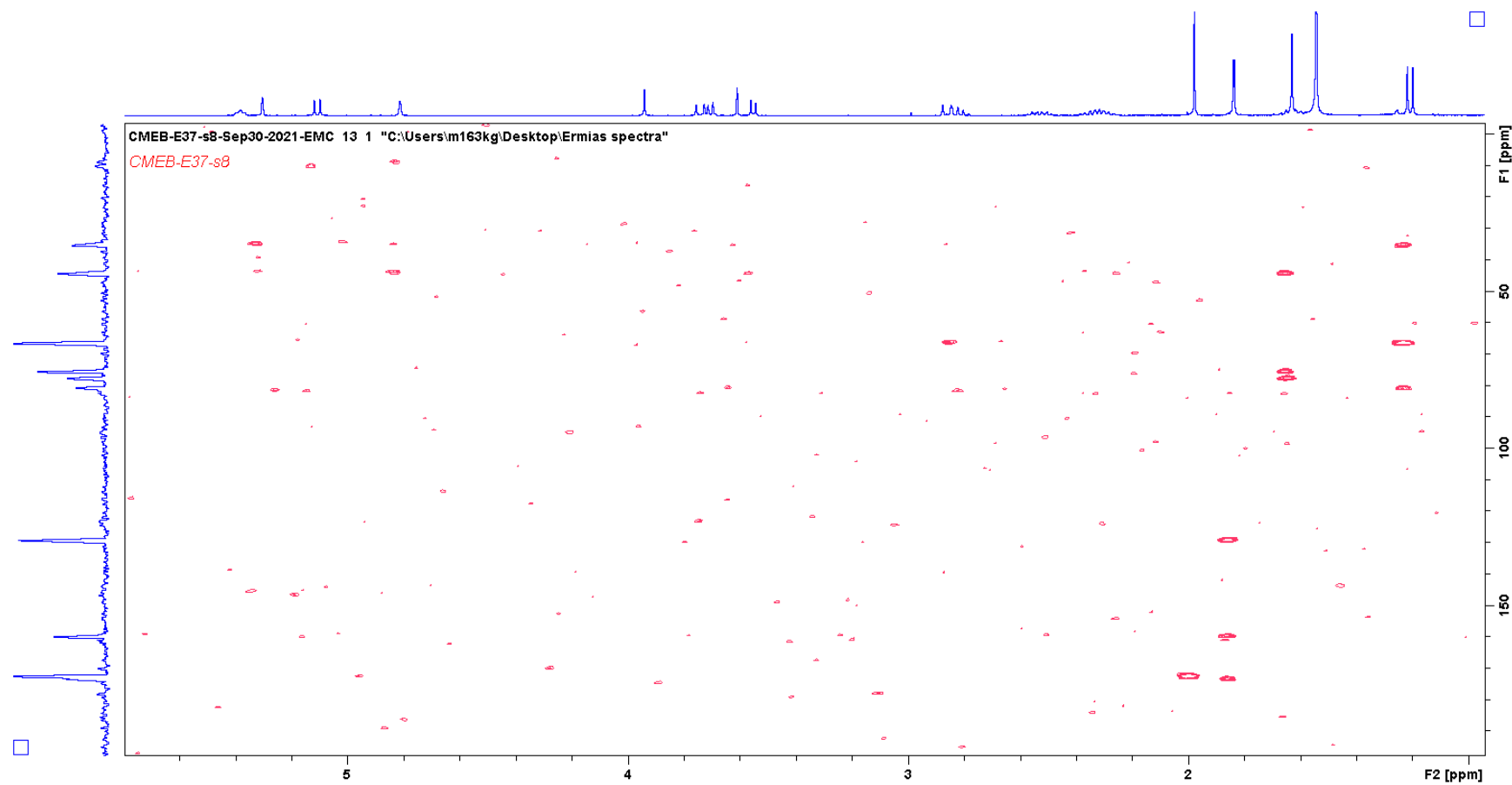
Appendix 53 DEPT spectrum of 1 $\beta$ -acetoxy-3 $\beta$ -chloro-5 $\alpha$ ,6 $\alpha$ -dihydroxycrotocascarin L (Ermiasoid) (E37)



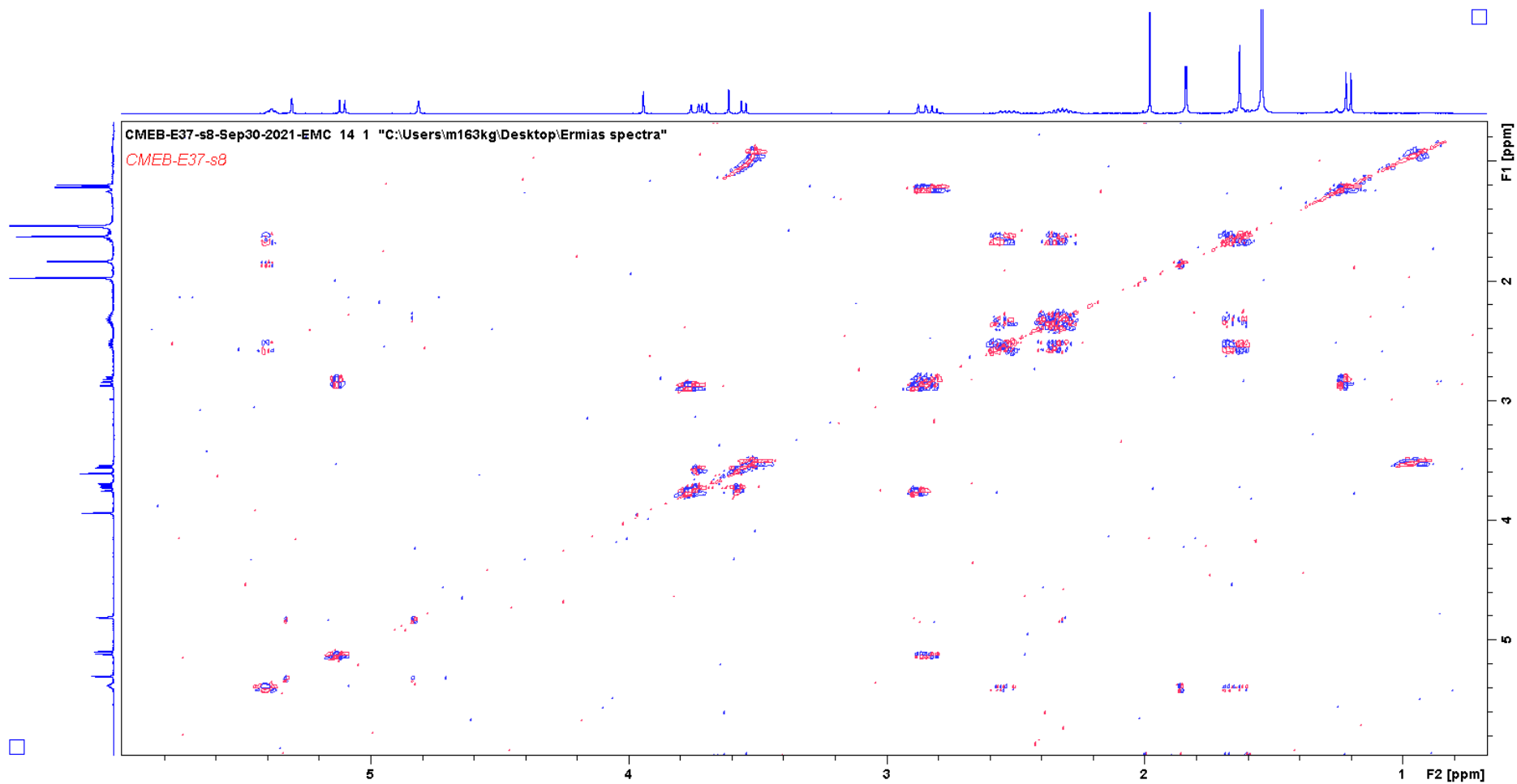
Appendix 54 HSQCDEPT spectrum of 1 $\beta$ -acetoxy-3 $\beta$ -chloro-5 $\alpha$ ,6 $\alpha$ -dihydroxycrotocascarin L (Ermiasoid) (E37)



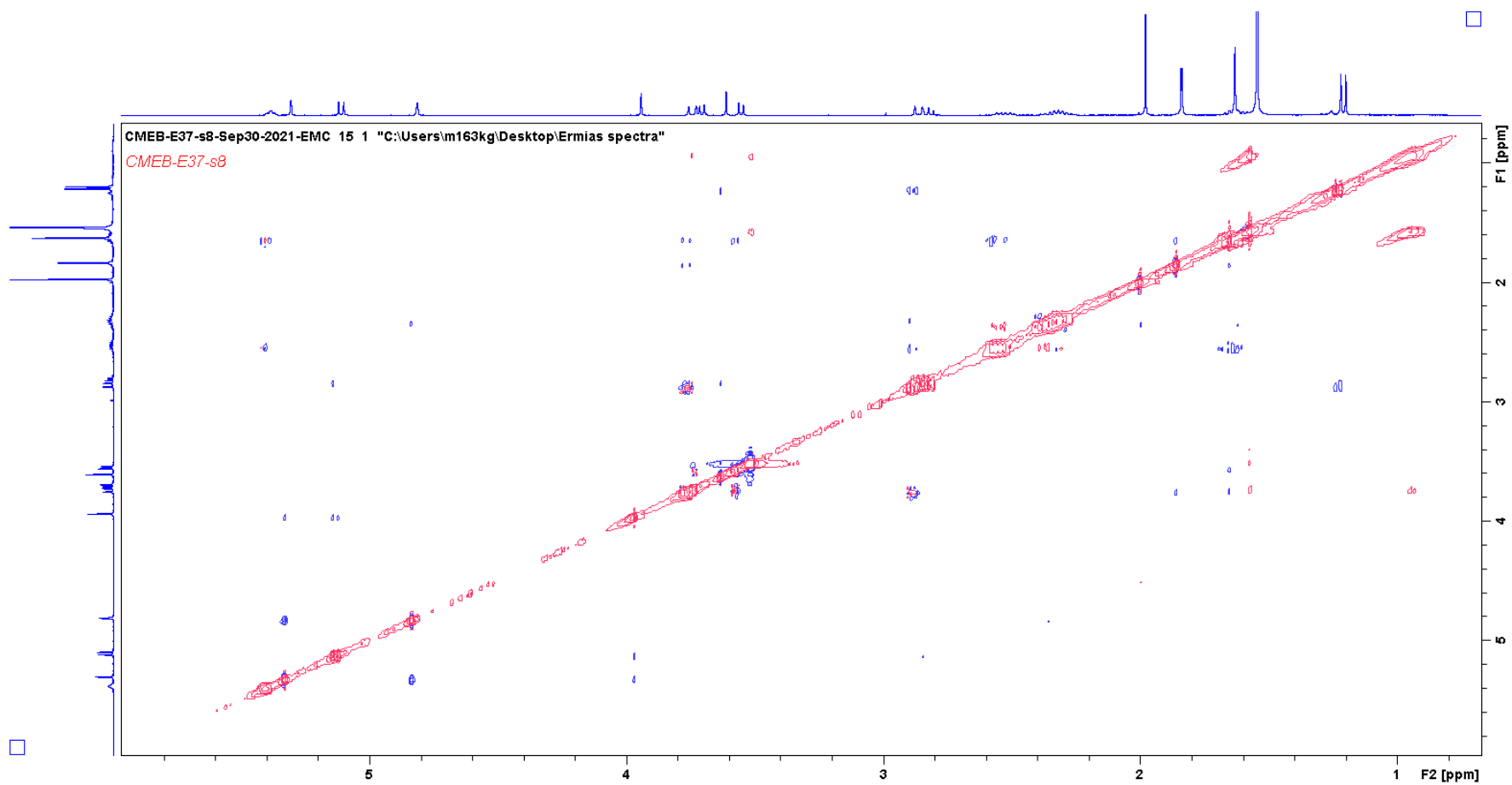
Appendix 55 HMBC spectrum of 1 $\beta$ -acetoxy-3 $\beta$ -chloro-5 $\alpha$ ,6 $\alpha$ -dihydroxycrotocascarin L (Ermiasoid) (E37)



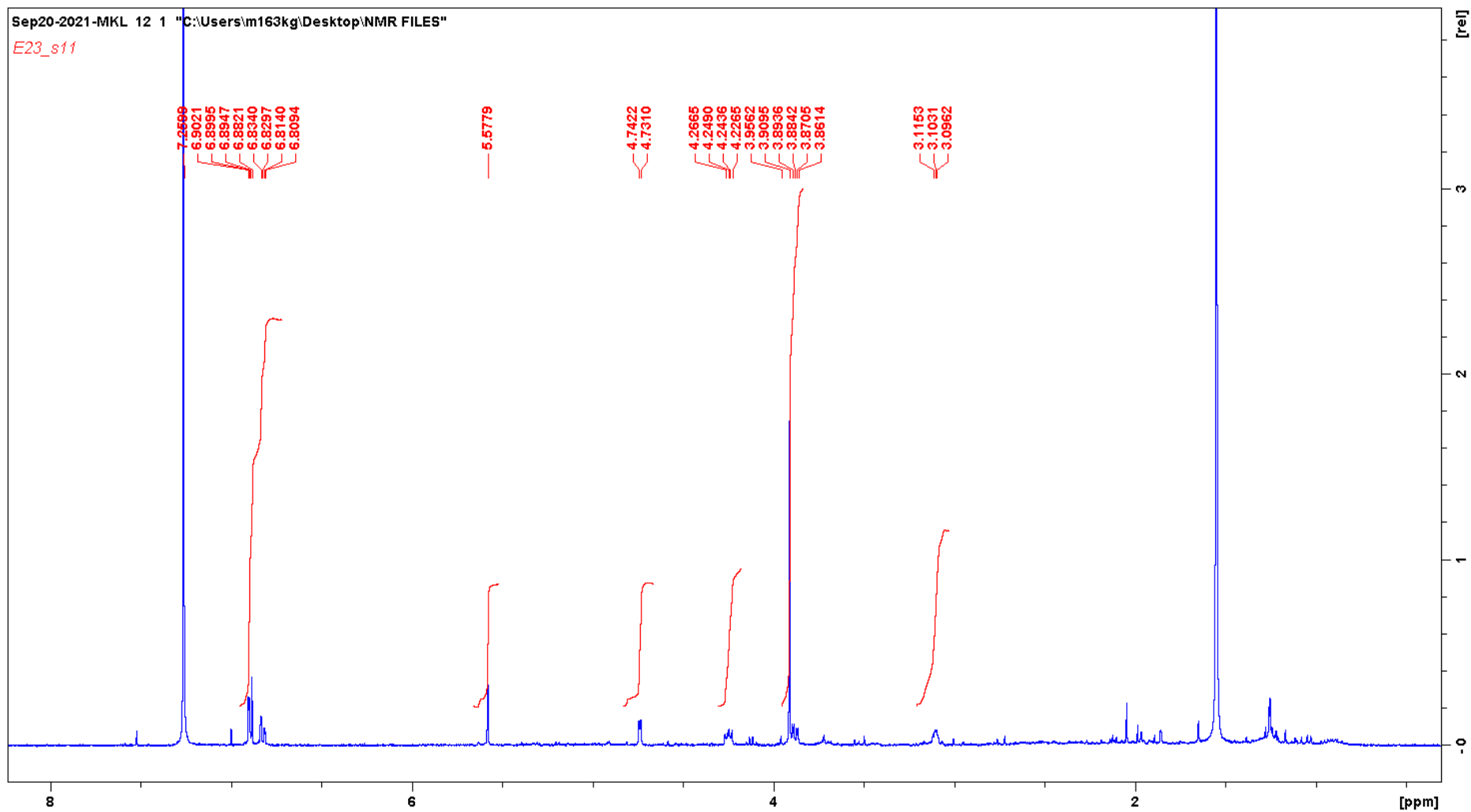
Appendix 56 COSY spectrum of 1 $\beta$ -acetoxy-3 $\beta$ -chloro-5 $\alpha$ ,6 $\alpha$ -dihydroxycrotocascarin L (Ermiasoid) (E37)



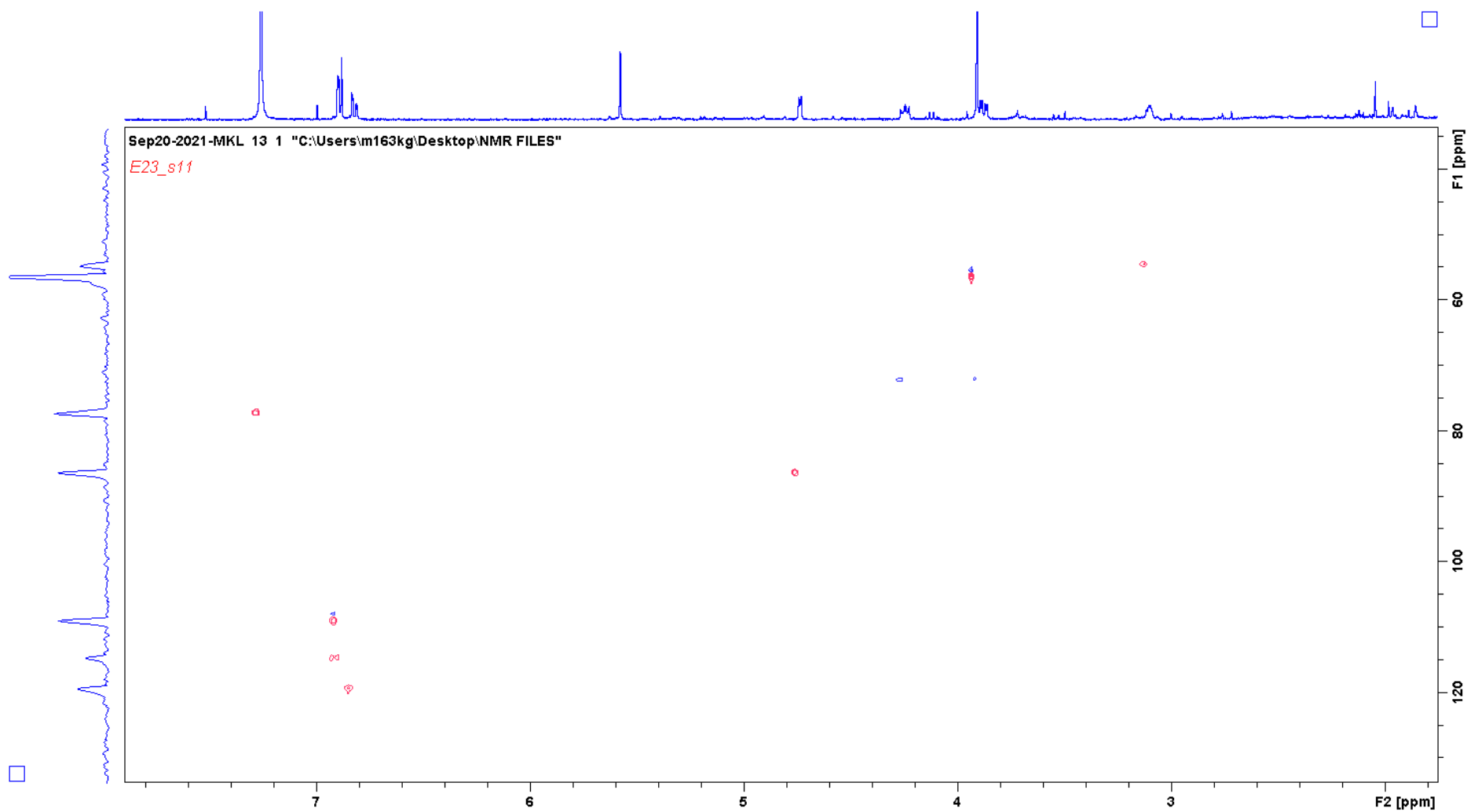
Appendix 57 NOESY spectrum of 1 $\beta$ -acetoxy-3 $\beta$ -chloro-5 $\alpha$ ,6 $\alpha$ -dihydroxycrotocascarin L (Ermiasoid) (E37)



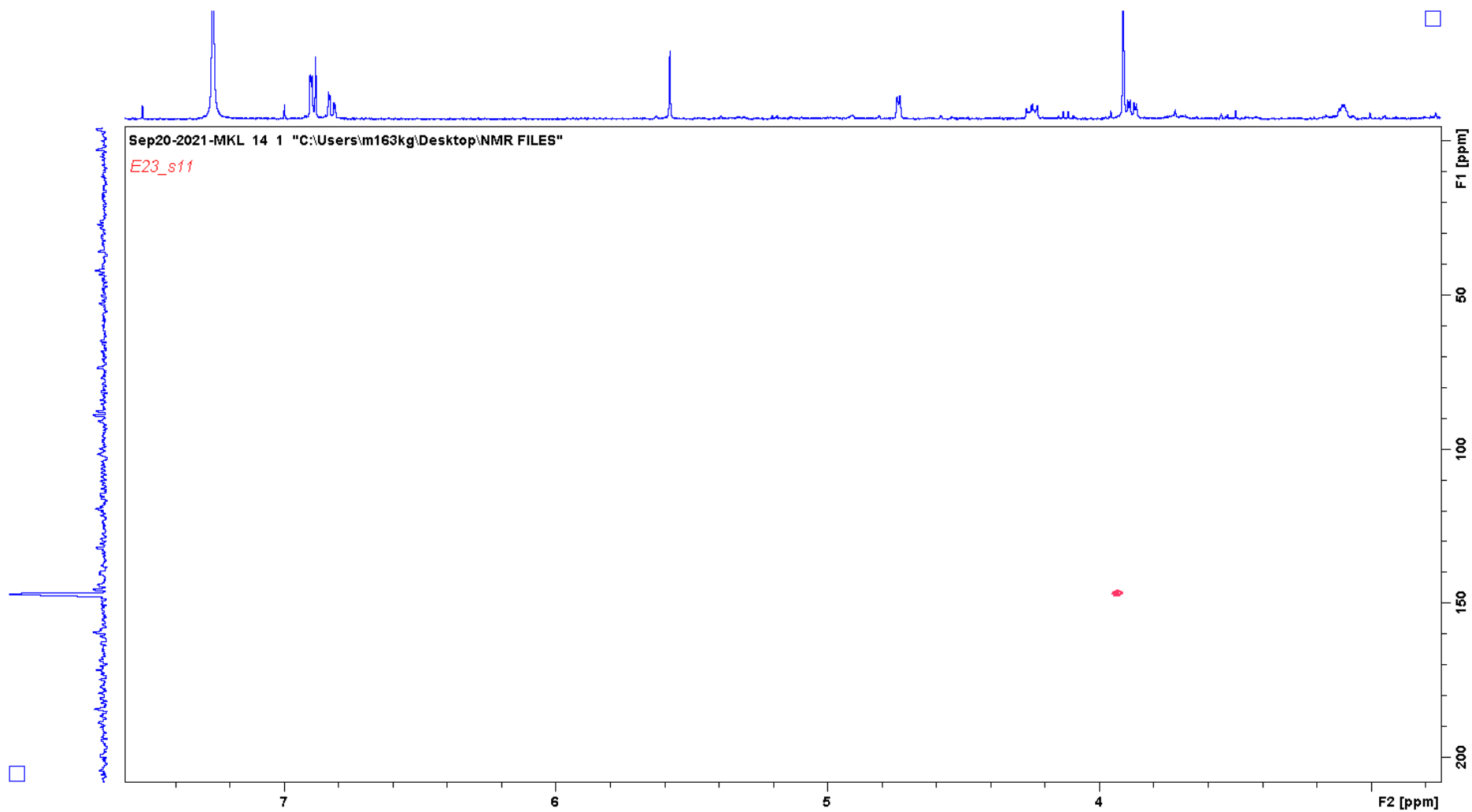
Appendix 58  $^1\text{H}$  NMR spectra of Pinoresinol (E2)



Appendix 59 HSQC spectrum of Pinoresinol (E2)

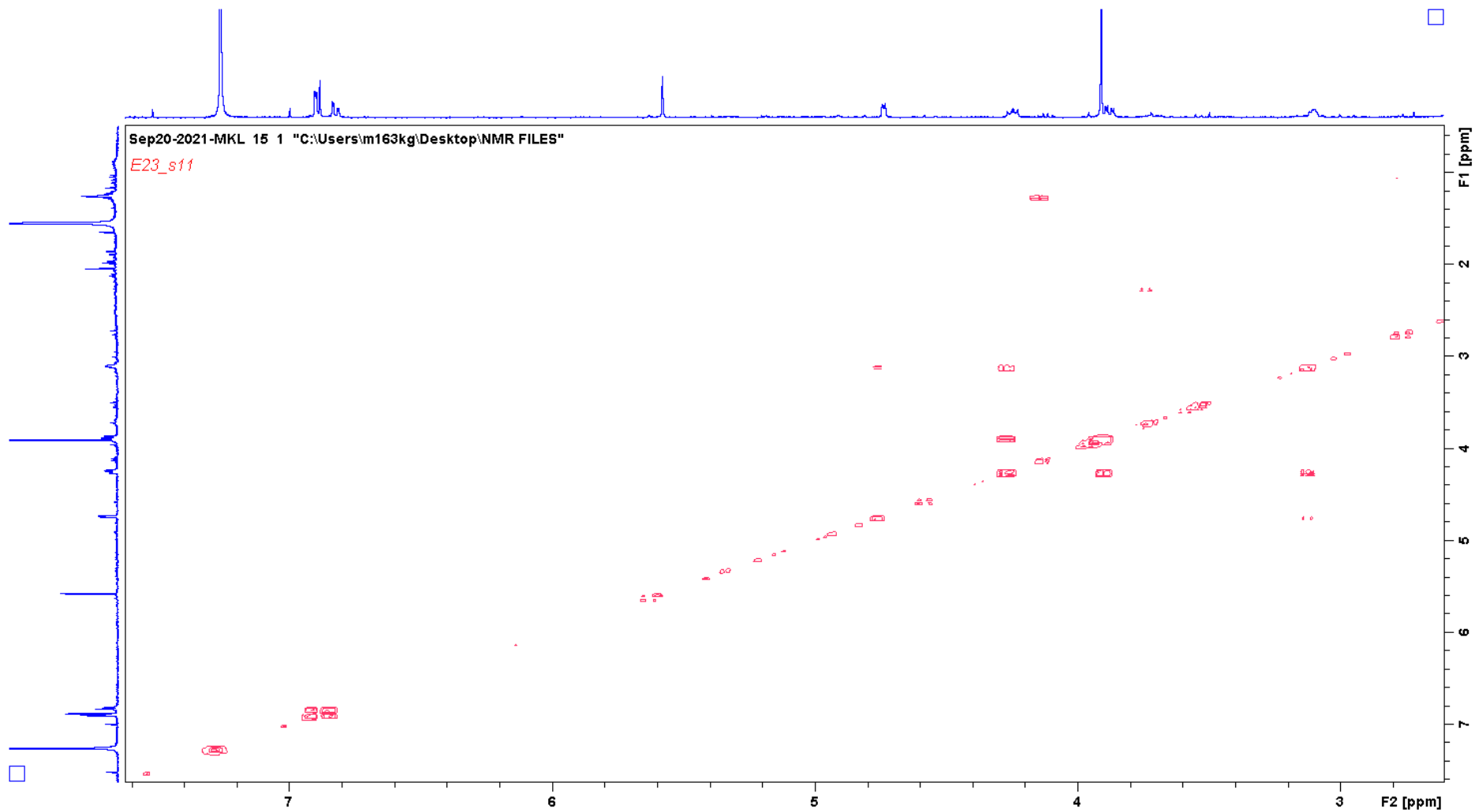


Appendix 60 HMBC spectrum of Pinoresinol (E2)

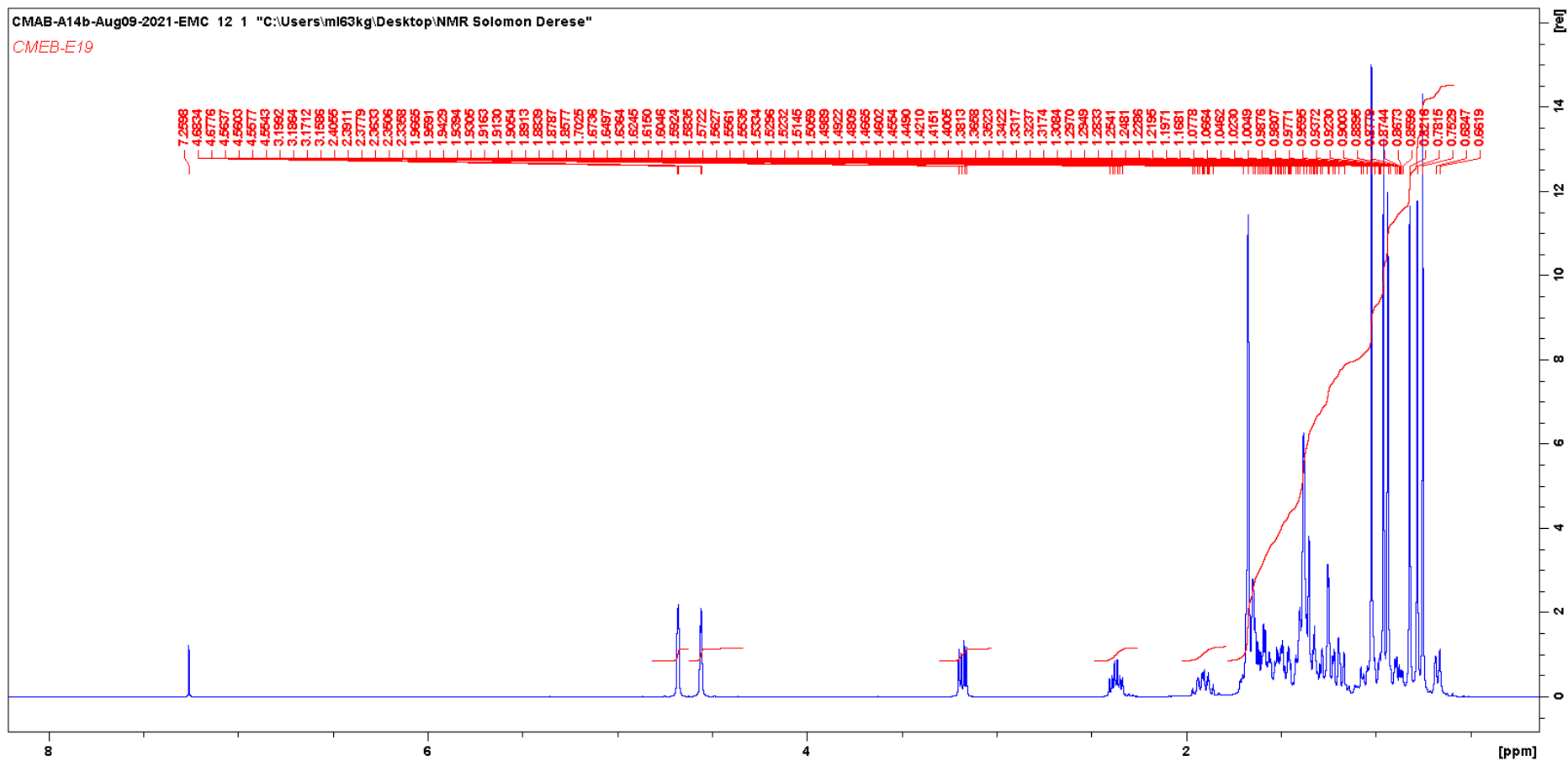




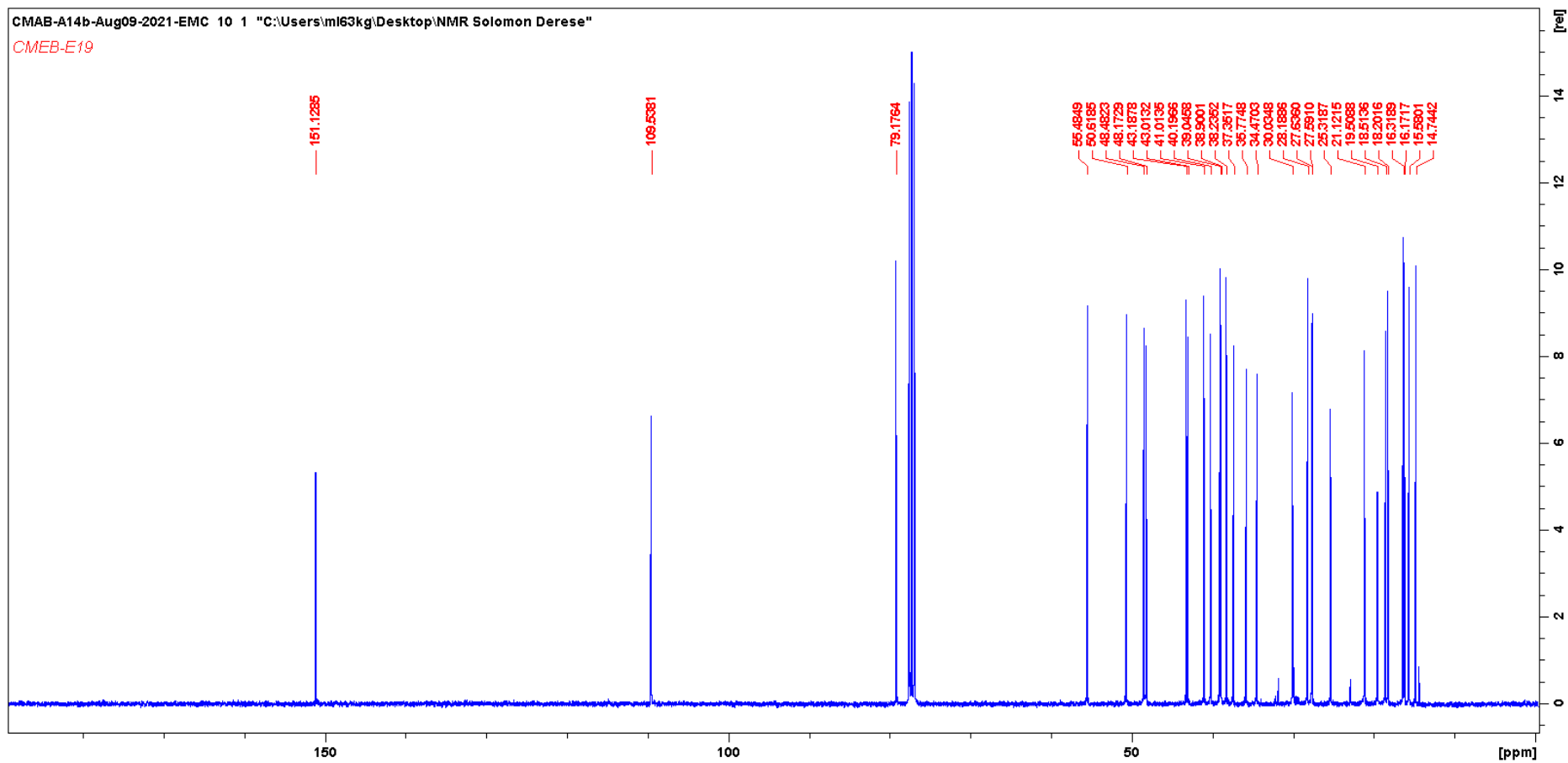
Appendix 61 COSY spectrum of Pinoresinol (E2)



Appendix 62 <sup>1</sup>H NMR spectra of 3β-Hydroxylup-20(29)-ene (lupeol) (E19)

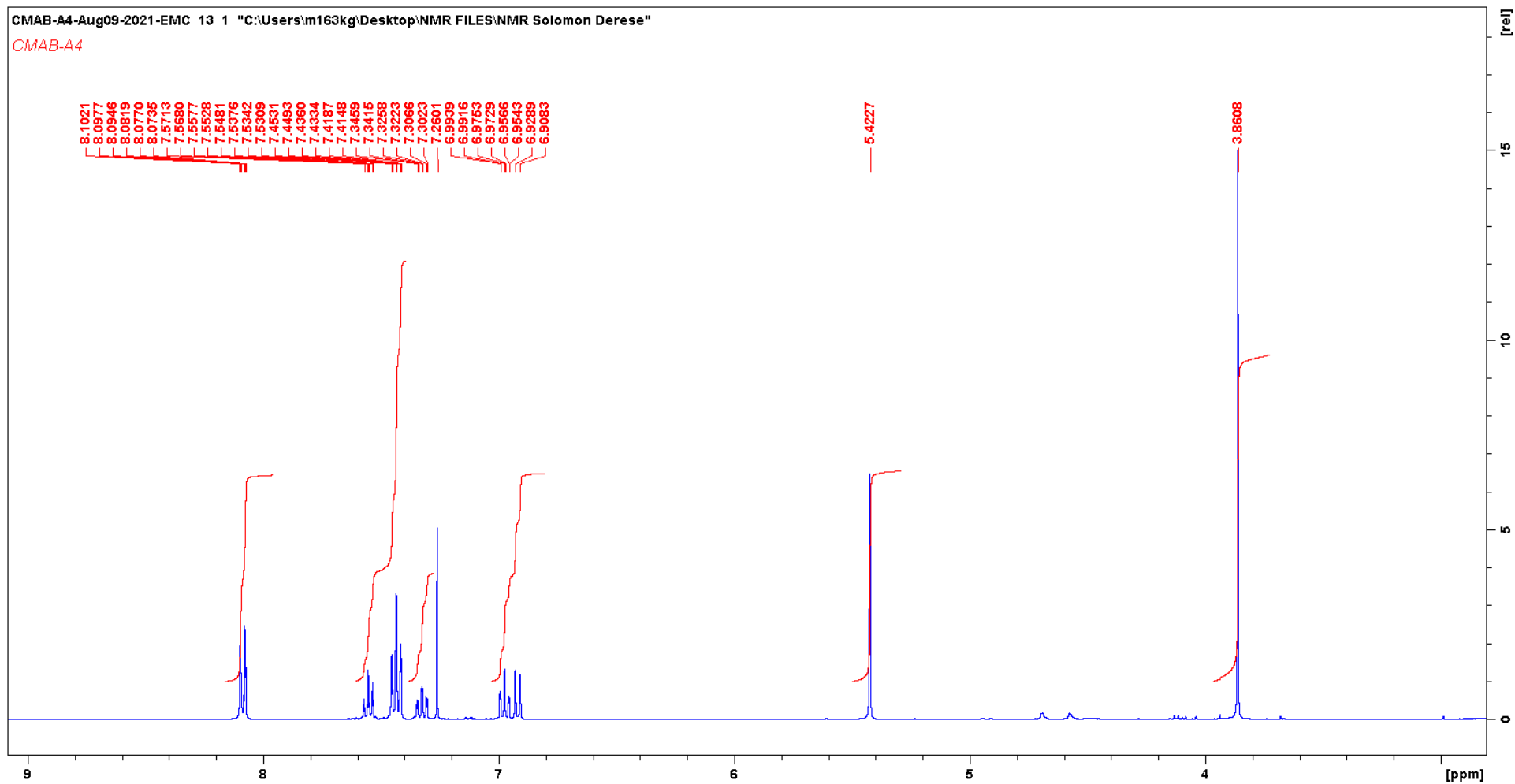


Appendix 63  $^{13}\text{C}$  NMR spectra of  $3\beta$ -Hydroxylup-20(29)-ene (lupeol) (E19)

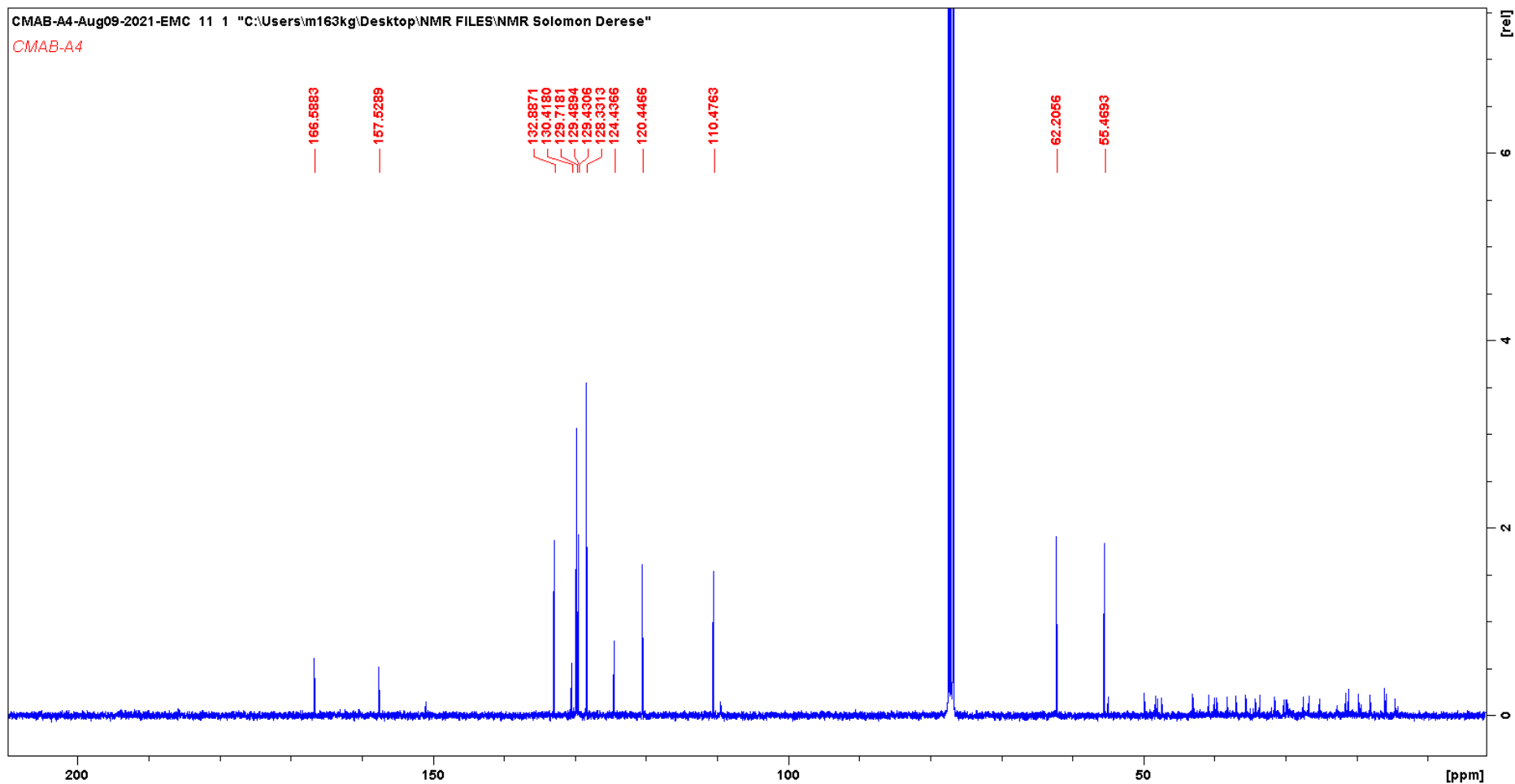


\*For DEPT, HSQCDEPT, COSY, HMBC, NOESY of lupeol see appendix 93-97

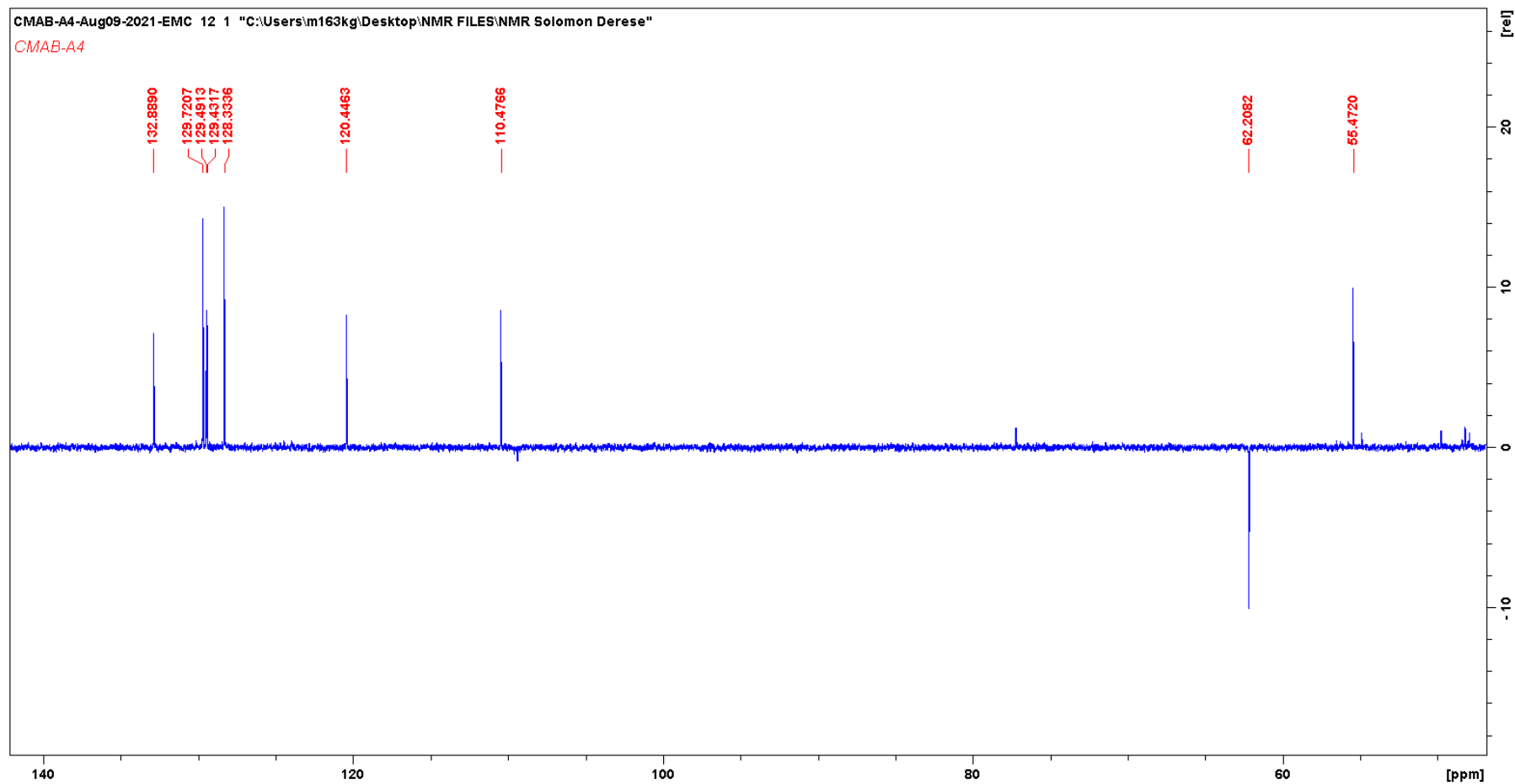
Appendix 64 <sup>1</sup>H NMR spectra of 2-Methoxy benzyl benzoate (A5)



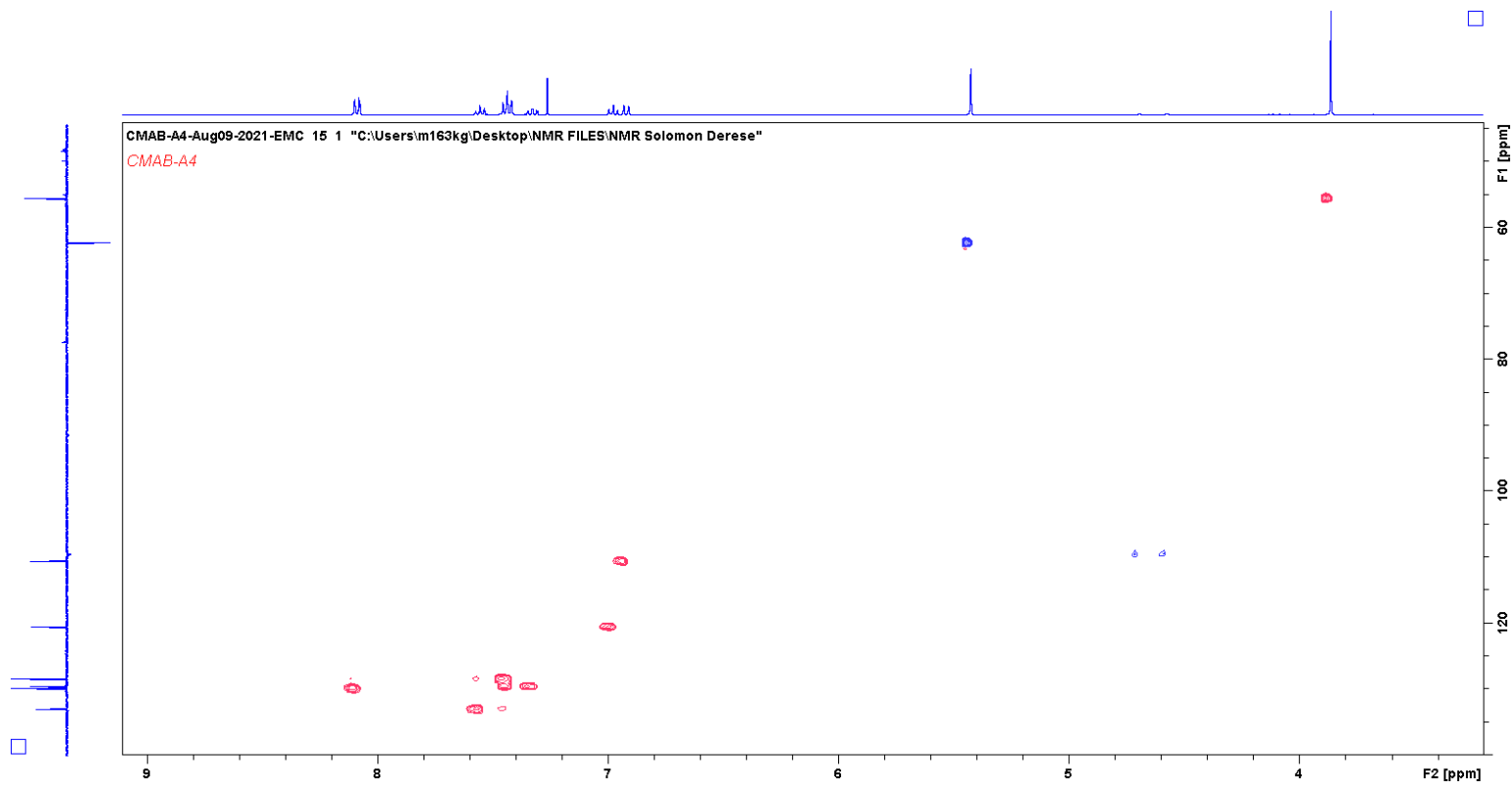
Appendix 65  $^{13}\text{C}$  NMR spectra of 2-Methoxy benzyl benzoate (A5)



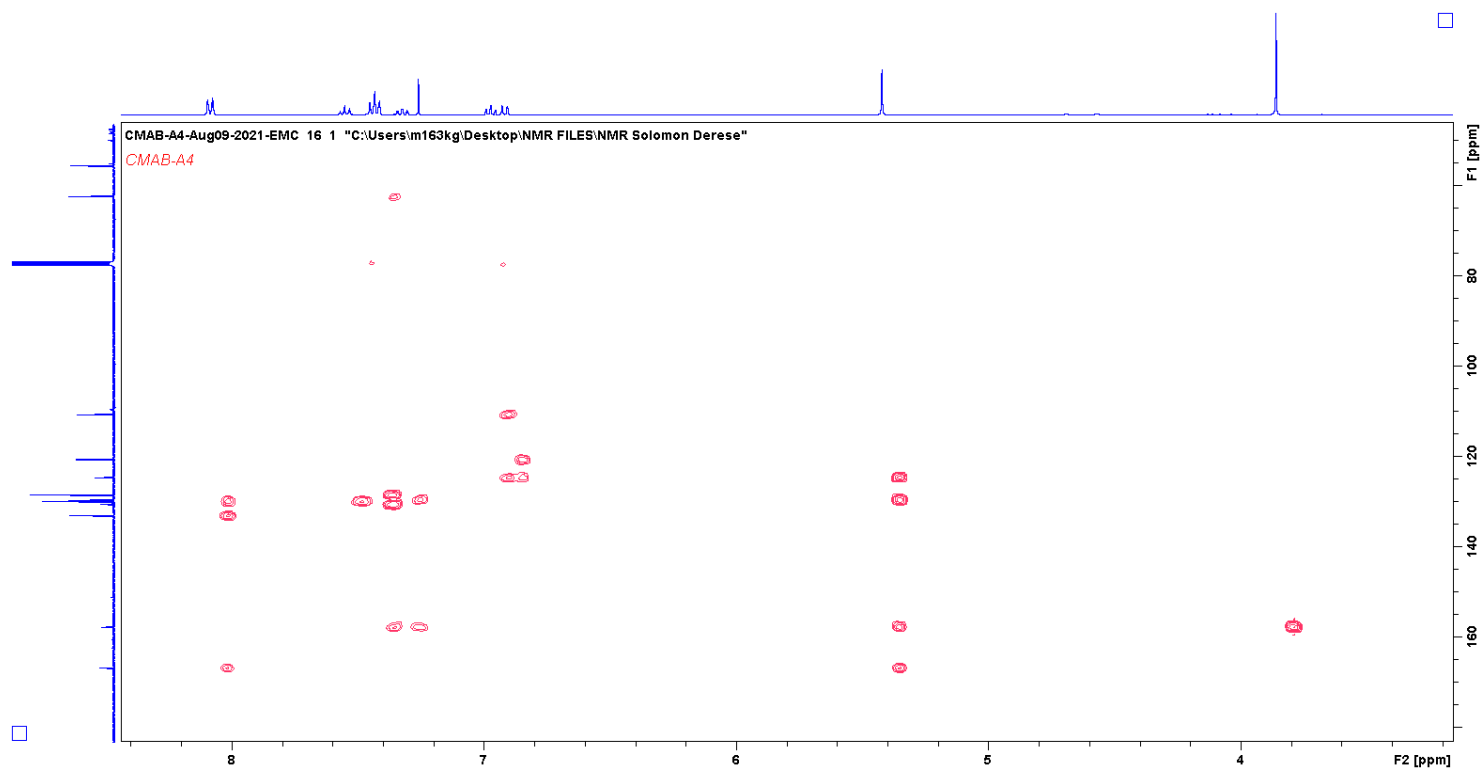
Appendix 66 DEPT spectrum of 2-Methoxy benzyl benzoate (A5)



Appendix 67 HSQCDEPT spectrum of 2-Methoxy benzyl benzoate (A5)

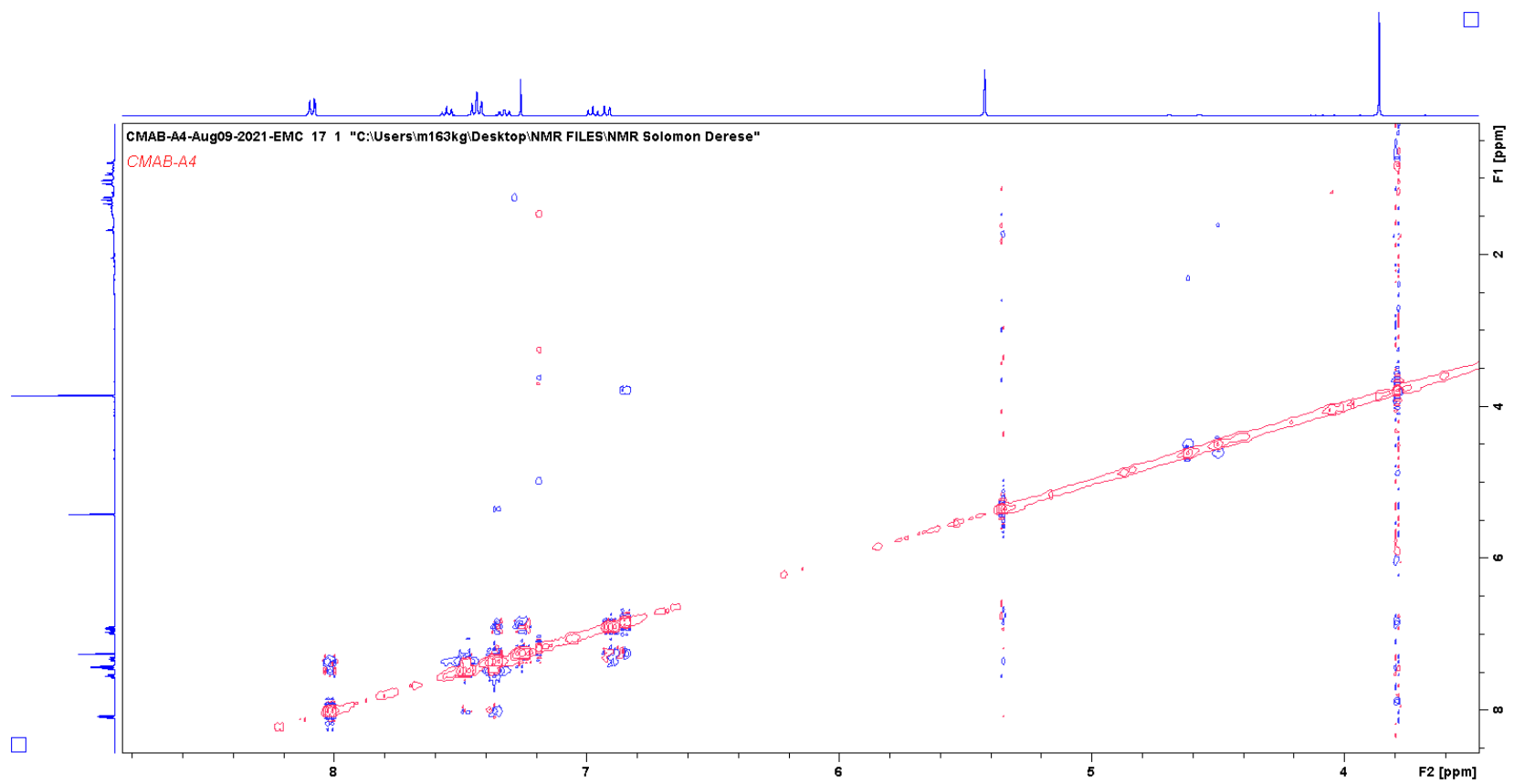


Appendix 68 HMBC spectrum of 2-Methoxy benzyl benzoate (A5)

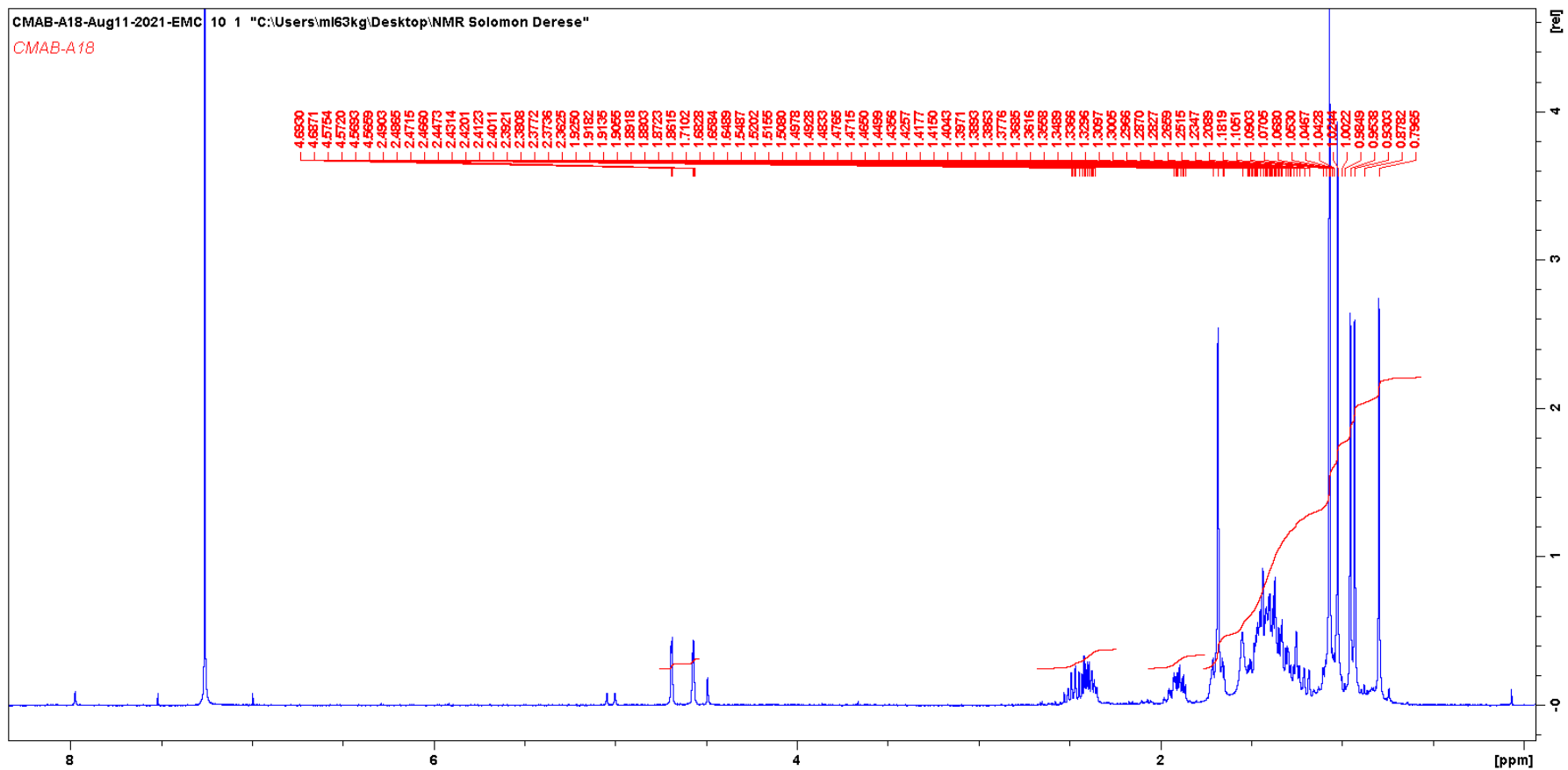




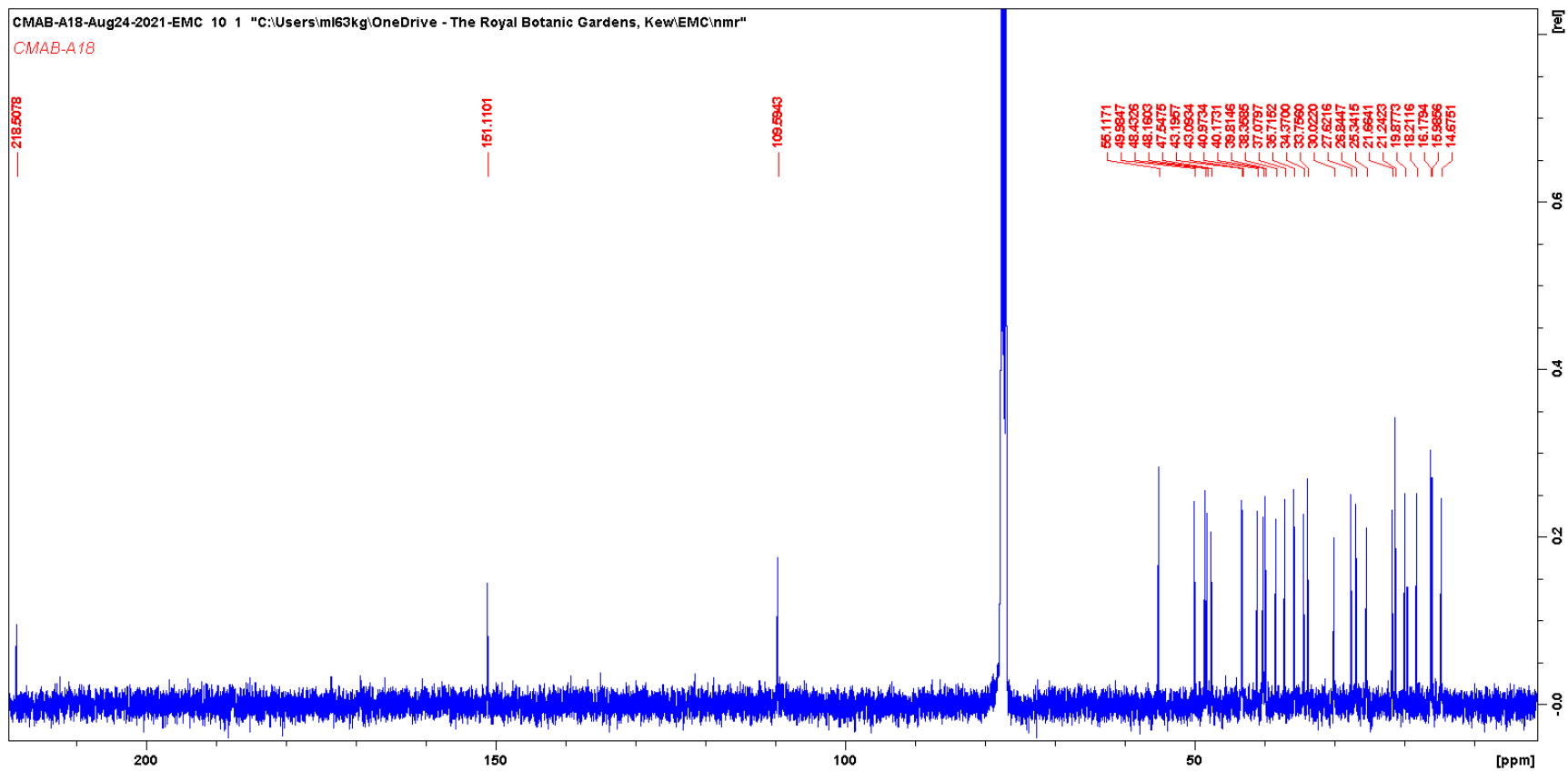
Appendix 69 COSY spectrum of 2-Methoxy benzyl benzoate (A5)



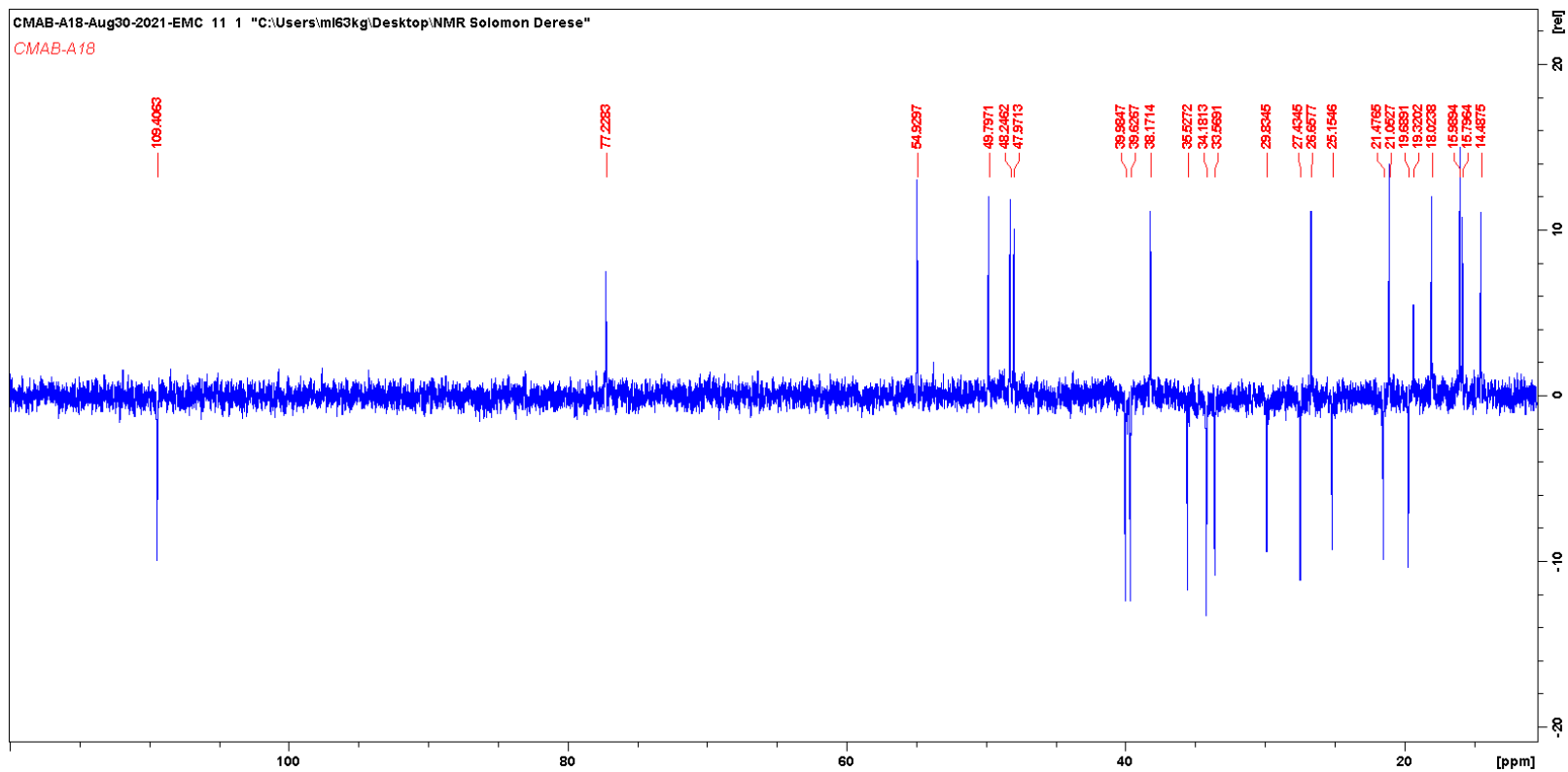
Appendix 70  $^1\text{H}$  NMR spectrum of Lupenone (A4b)



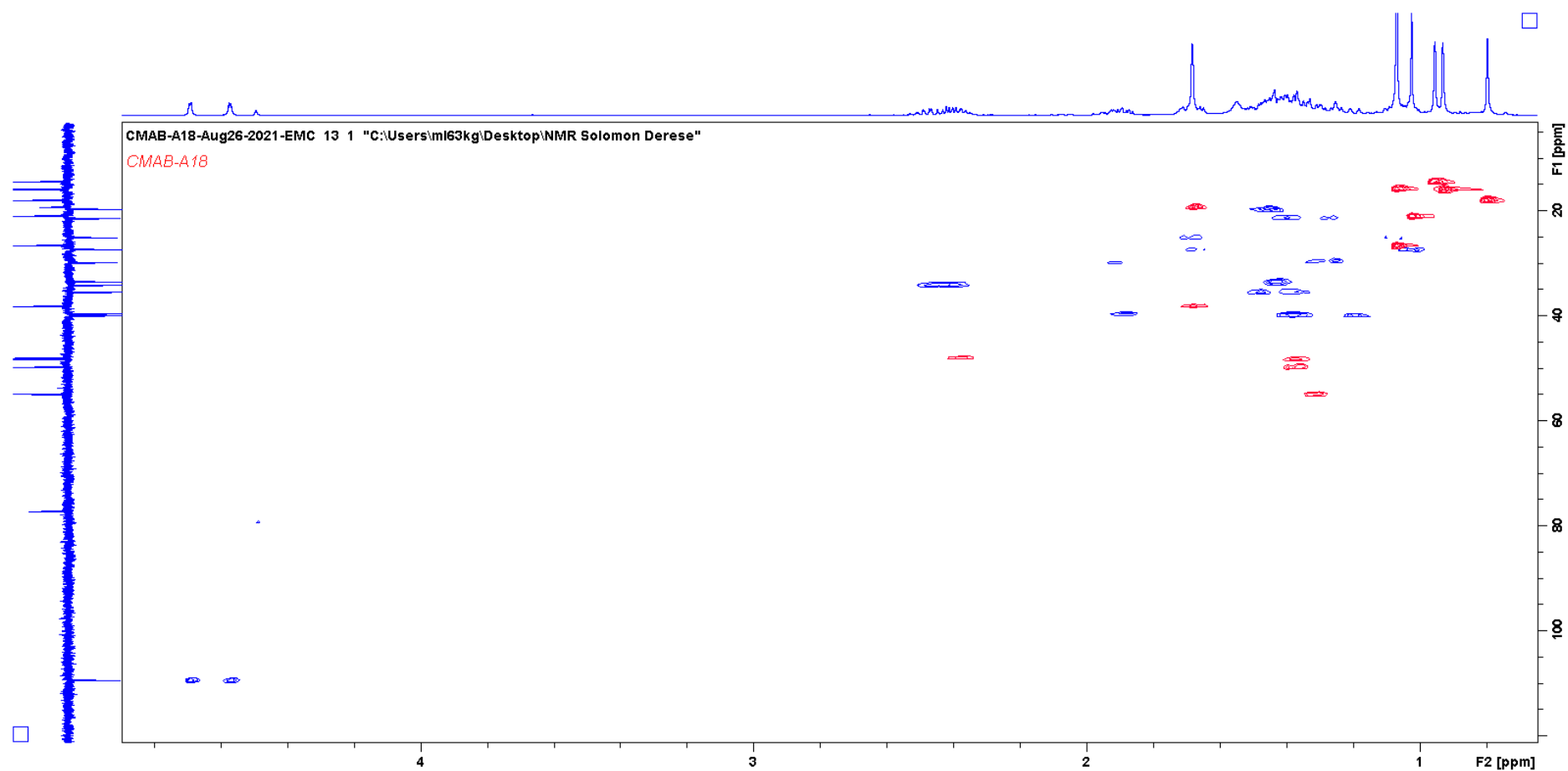
Appendix 71  $^{13}\text{C}$  NMR spectrum of Lupenone (A4b)



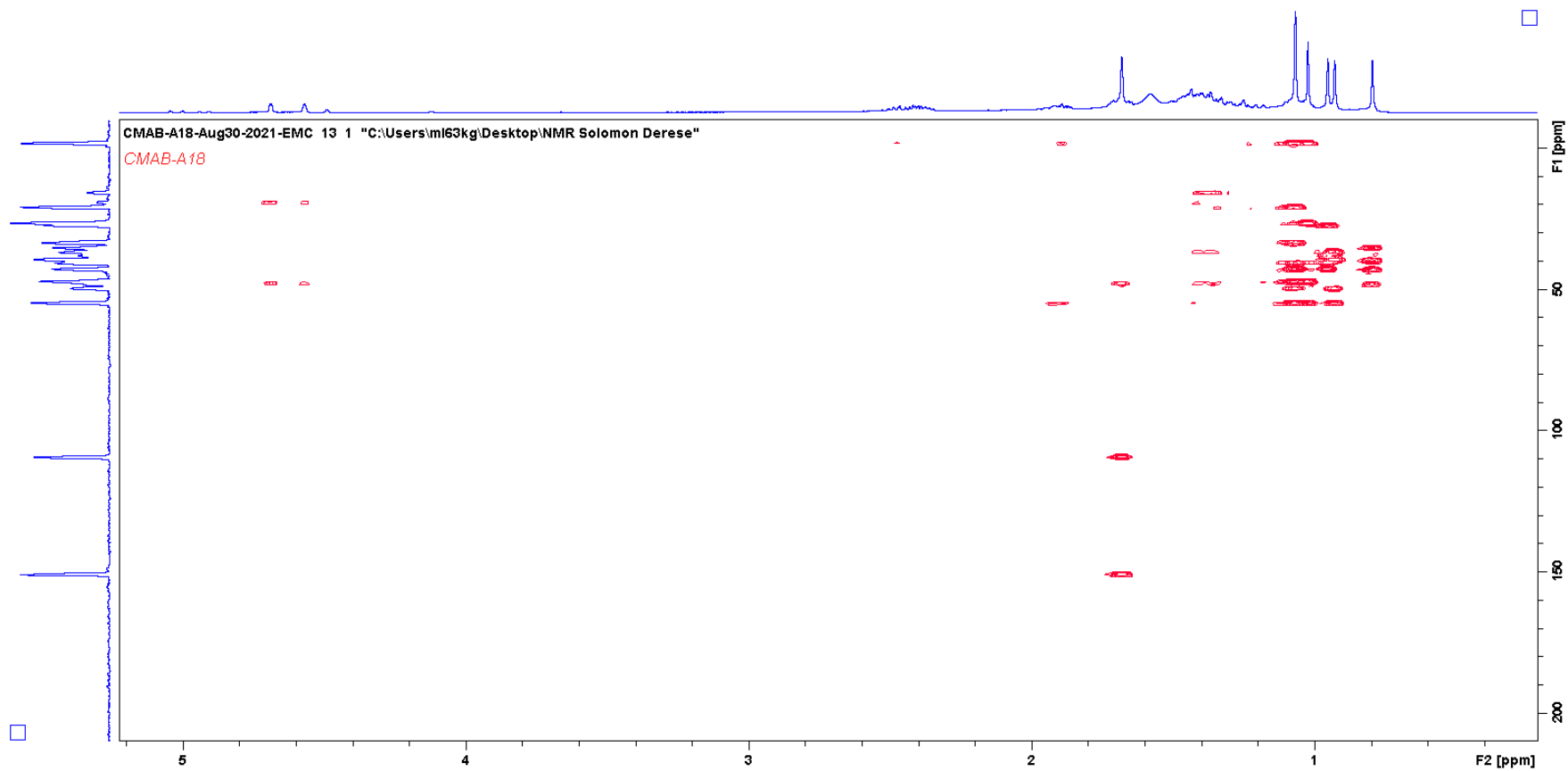
# Appendix 72 DEPT spectrum of Lupenone (A4b)



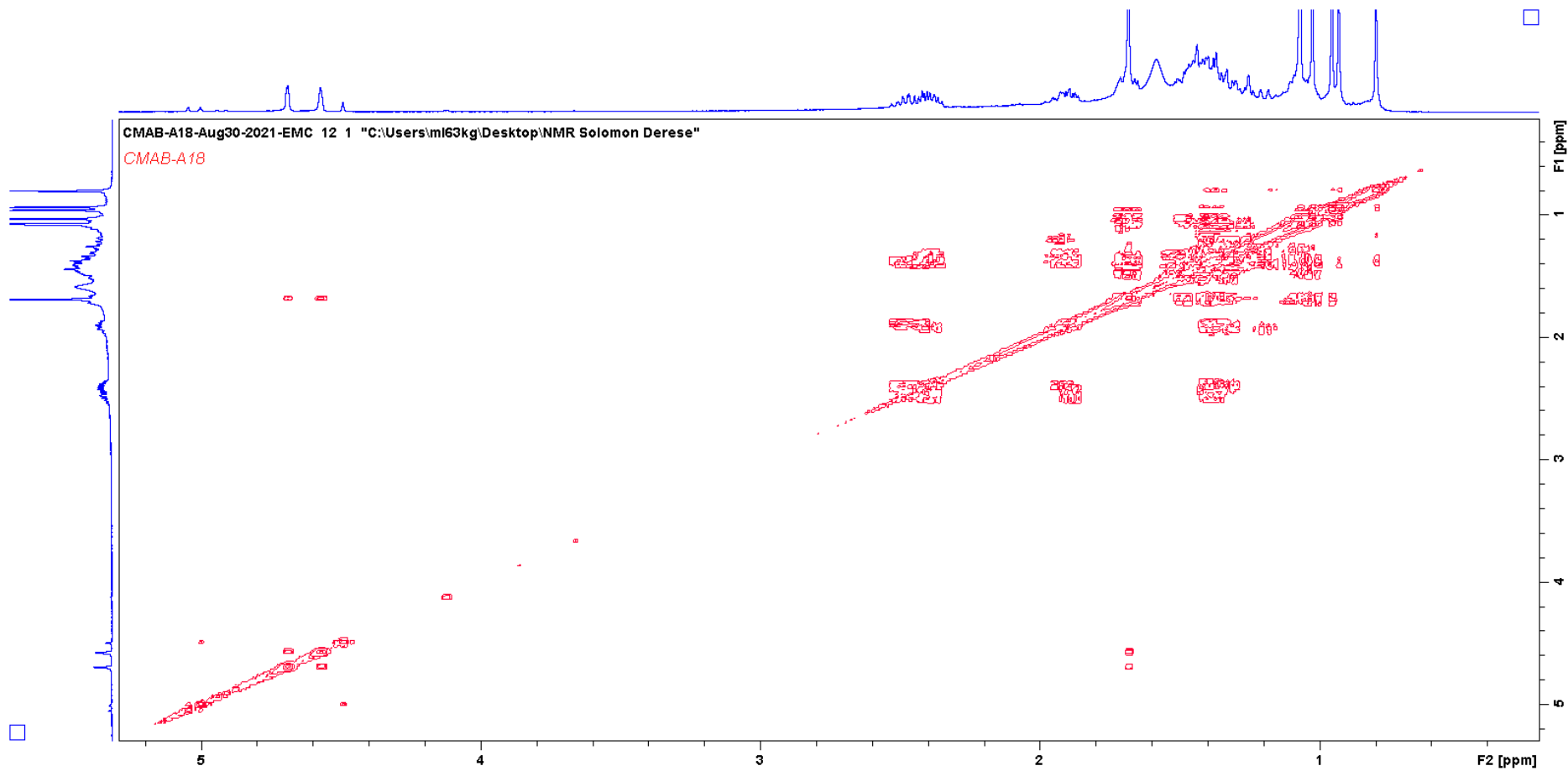
Appendix 73 HSQCDEPT spectrum of Lupenone (A4b)



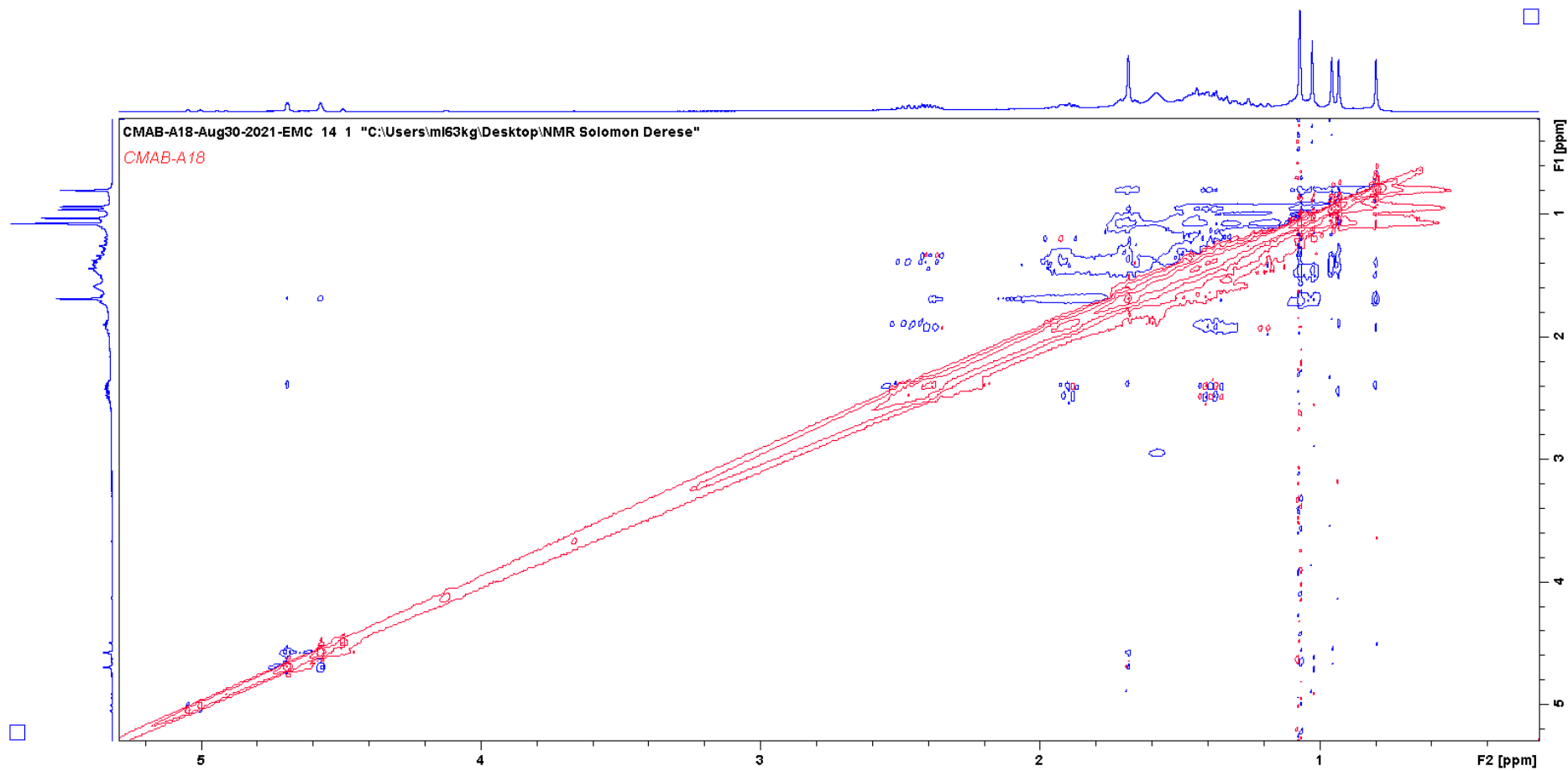
Appendix 74 HMBC spectrum of Lupenone (A4b)



Appendix 75 COSY spectrum of Lupenone (A4b)

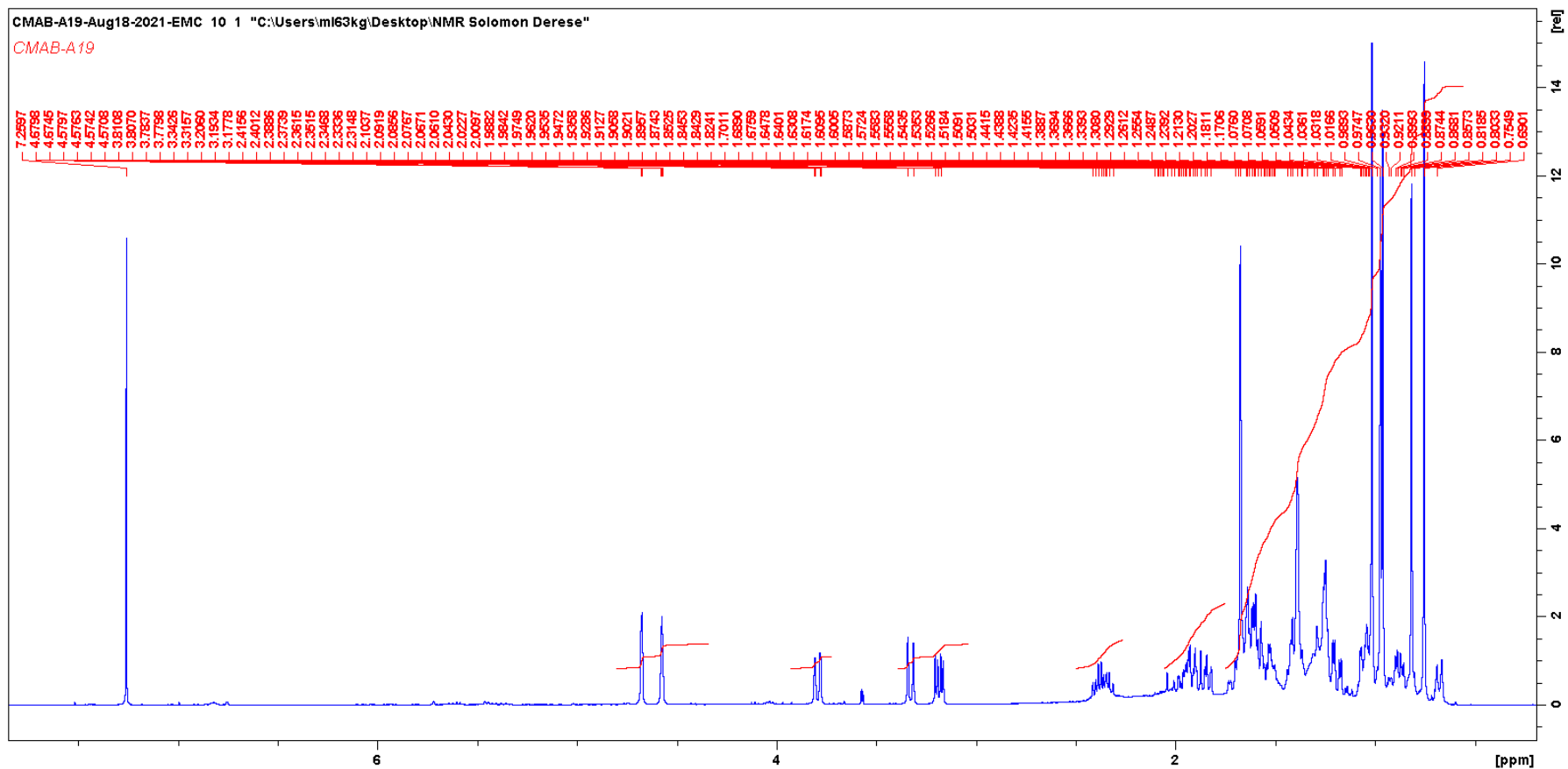


Appendix 76 NOESY spectrum of Lupenone (A4b)

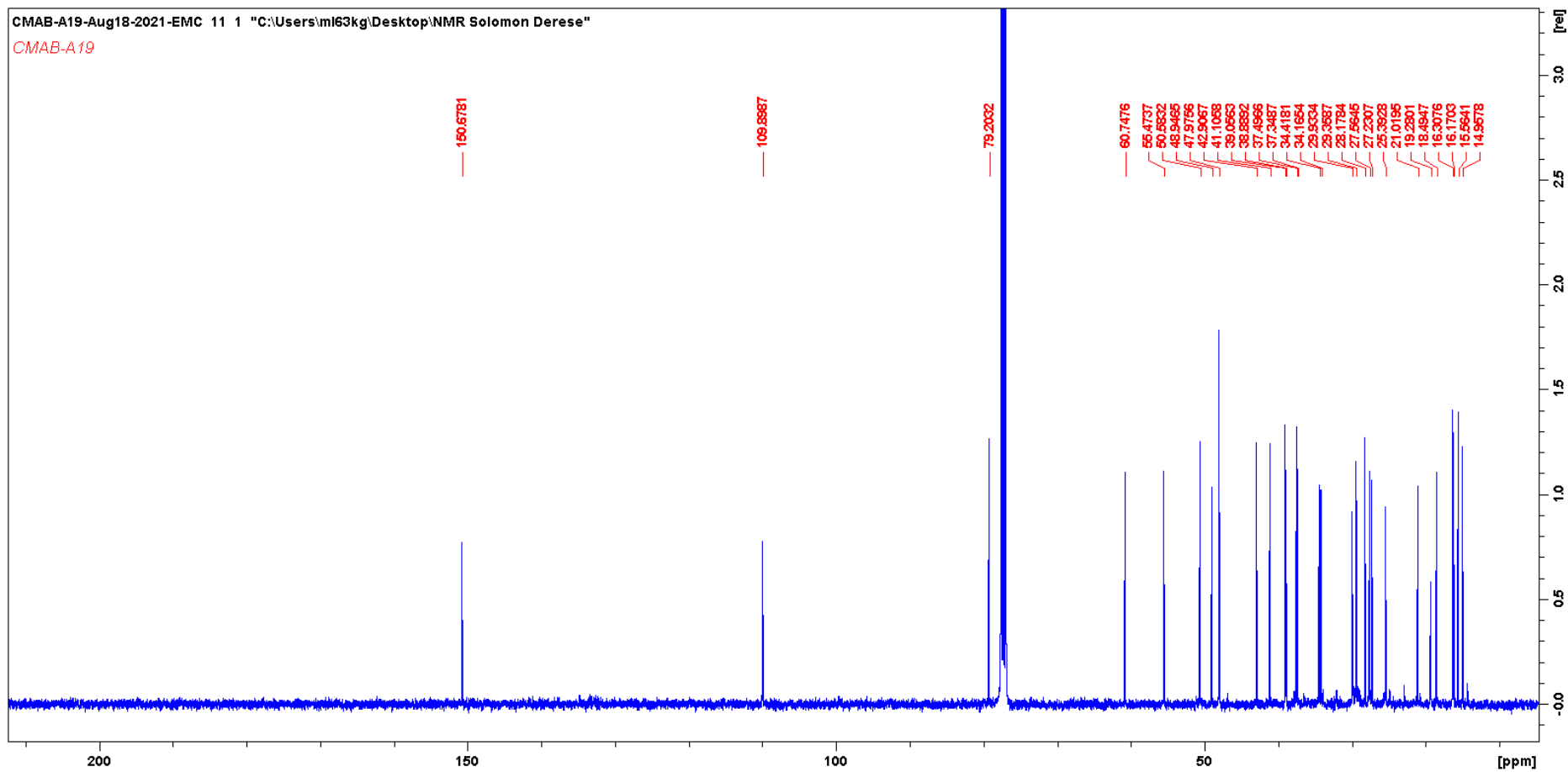




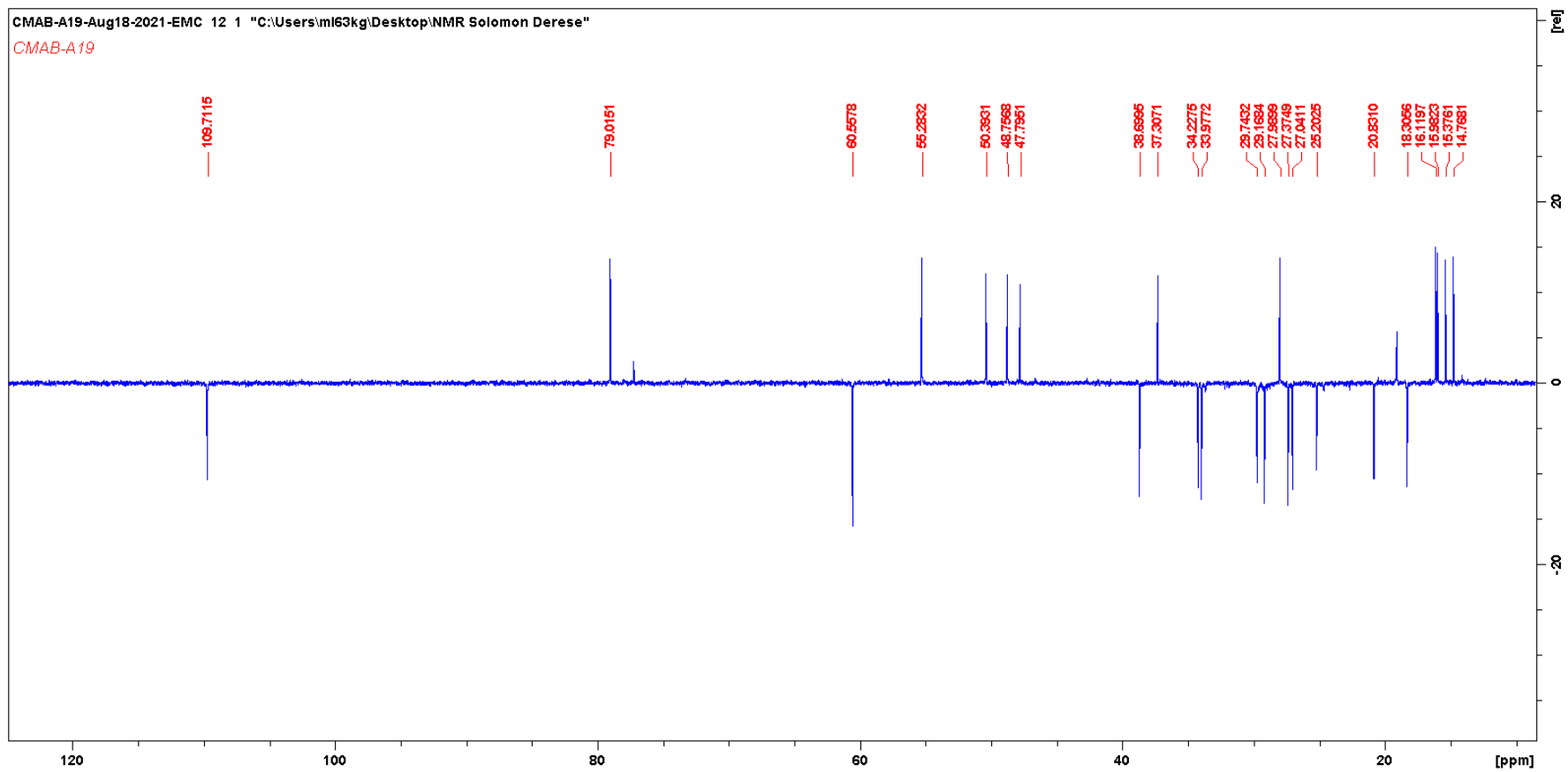
Appendix 77  $^1\text{H}$  NMR spectrum of Betulin (A19)



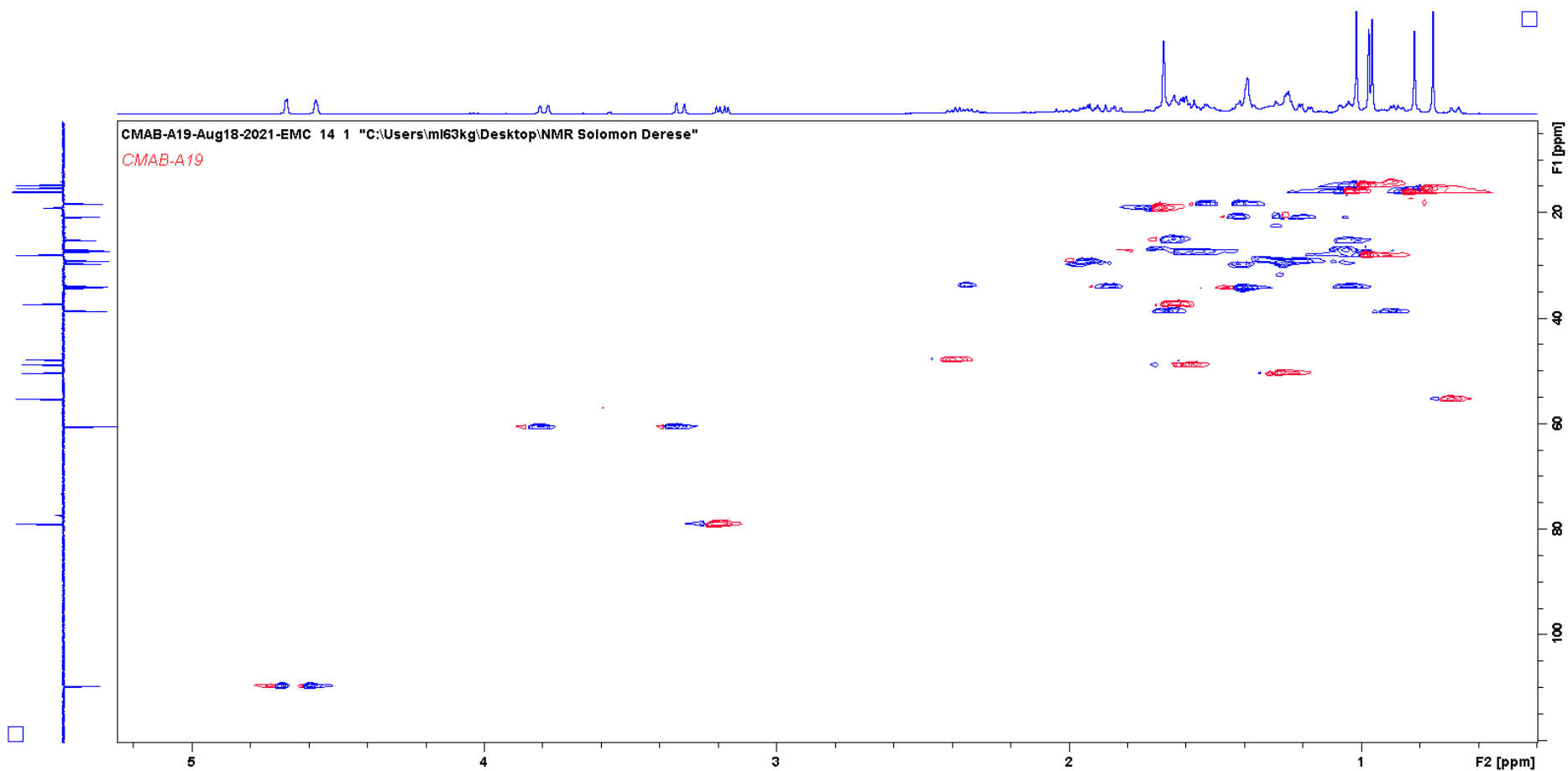
Appendix 78  $^{13}\text{C}$  NMR spectrum of Betulin (A19)



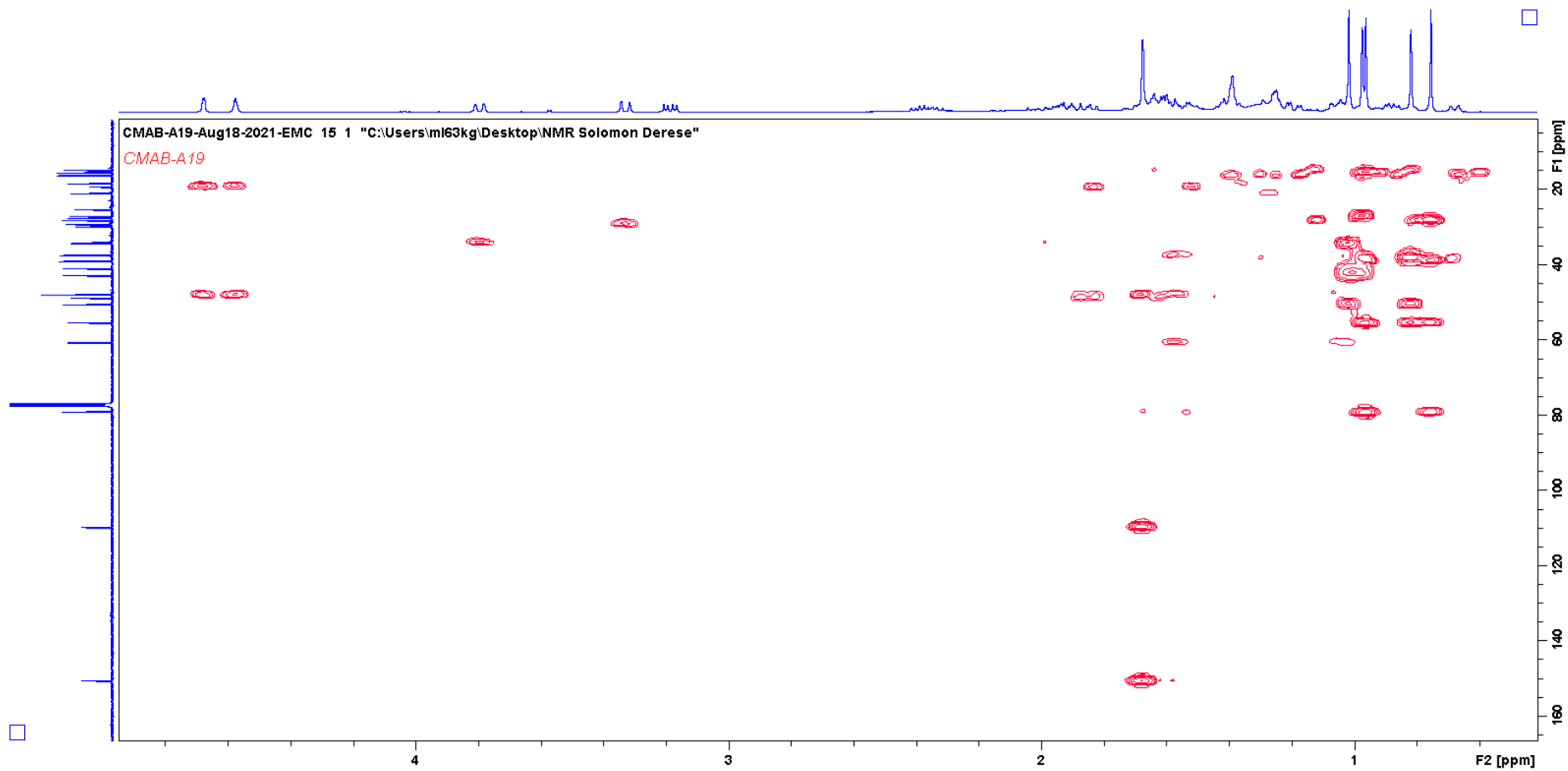
# Appendix 79 DEPT spectrum of Betulin (A19)



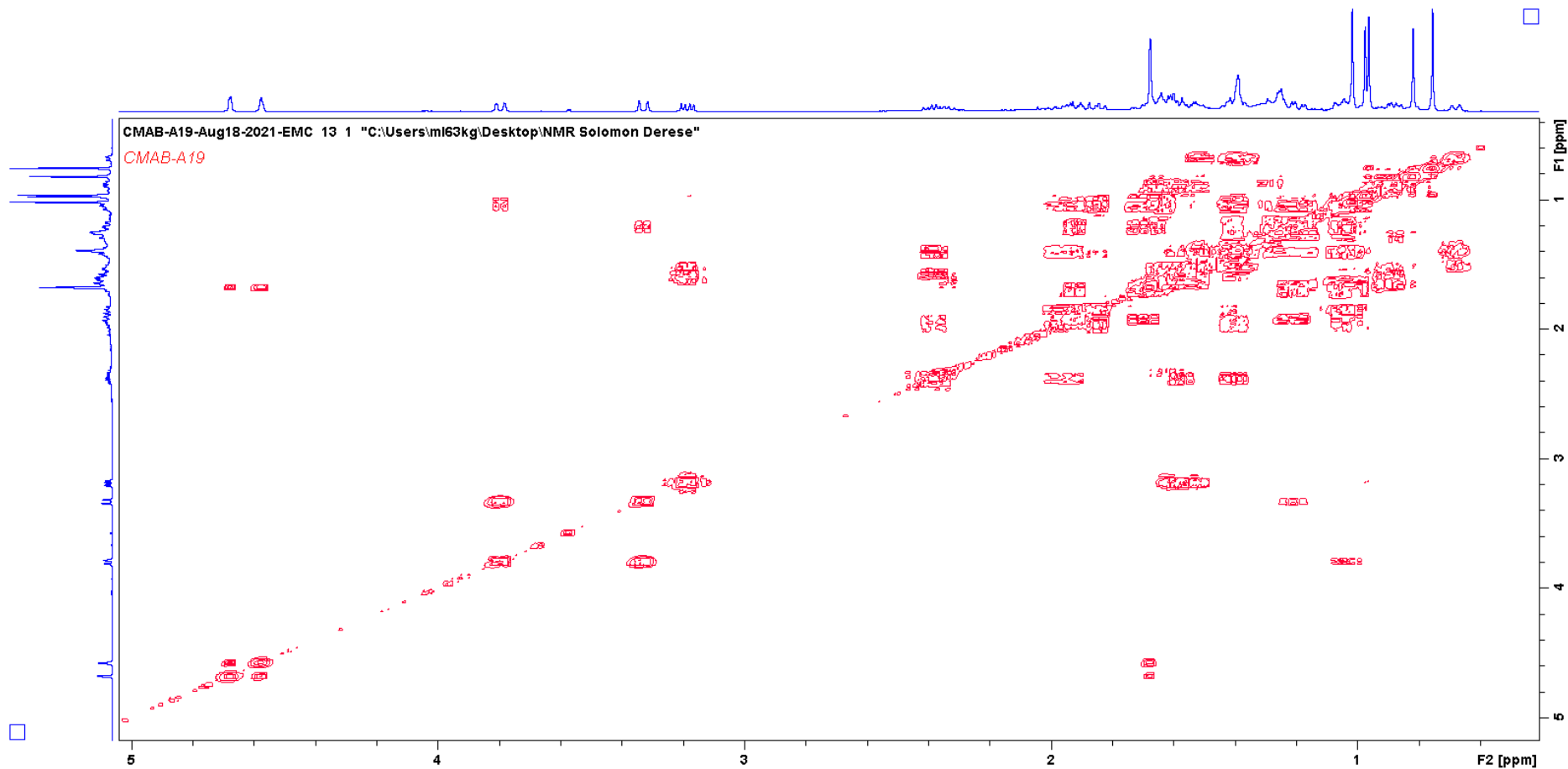
Appendix 80 HSQCDEPT spectrum of Betulin (A19)



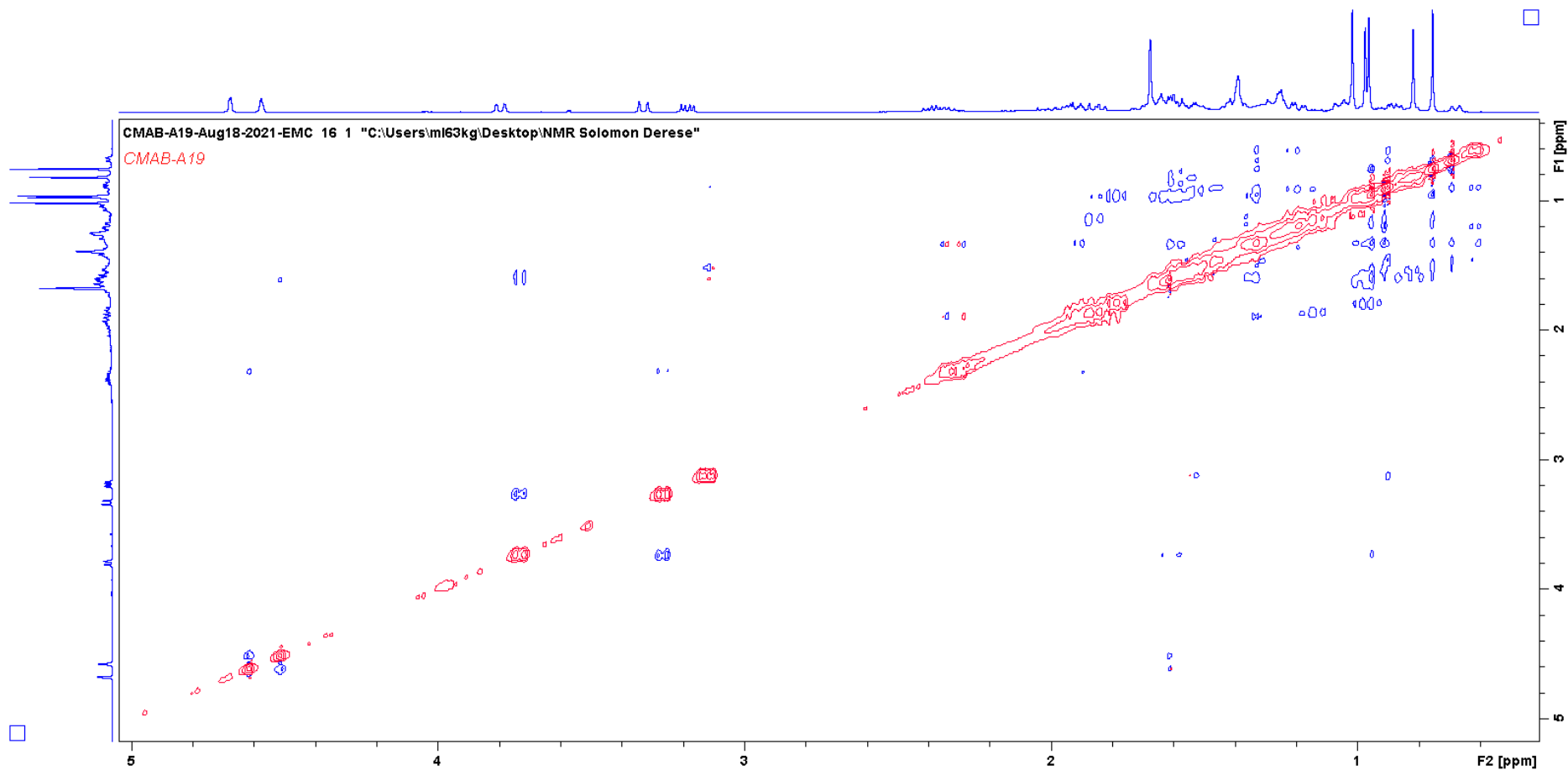
Appendix 81 HMBC spectrum of Betulin (A19)



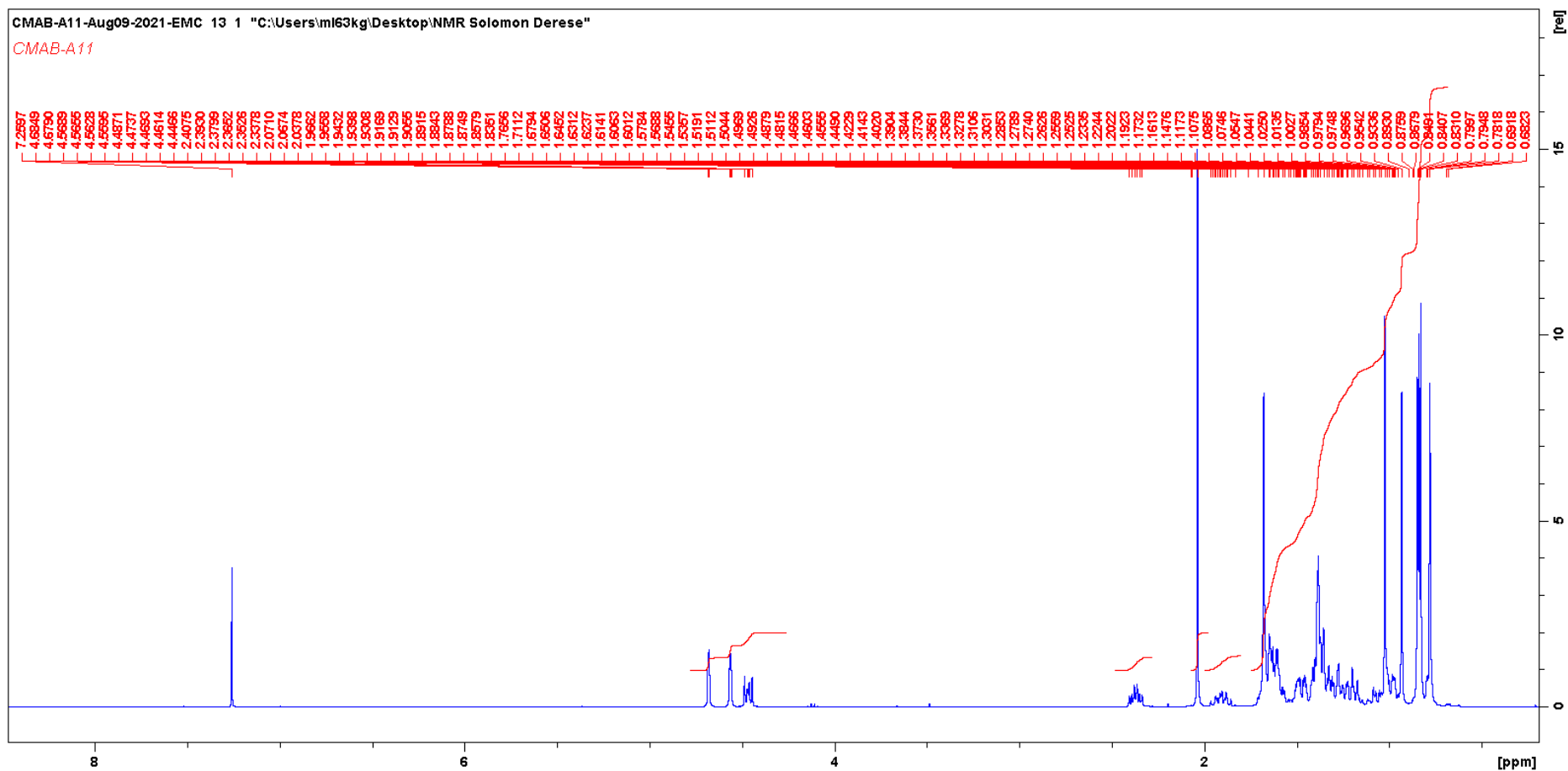
Appendix 82 COSY spectrum of Betulin (A19)



Appendix 83 NOSEY spectrum of Betulin (A19)

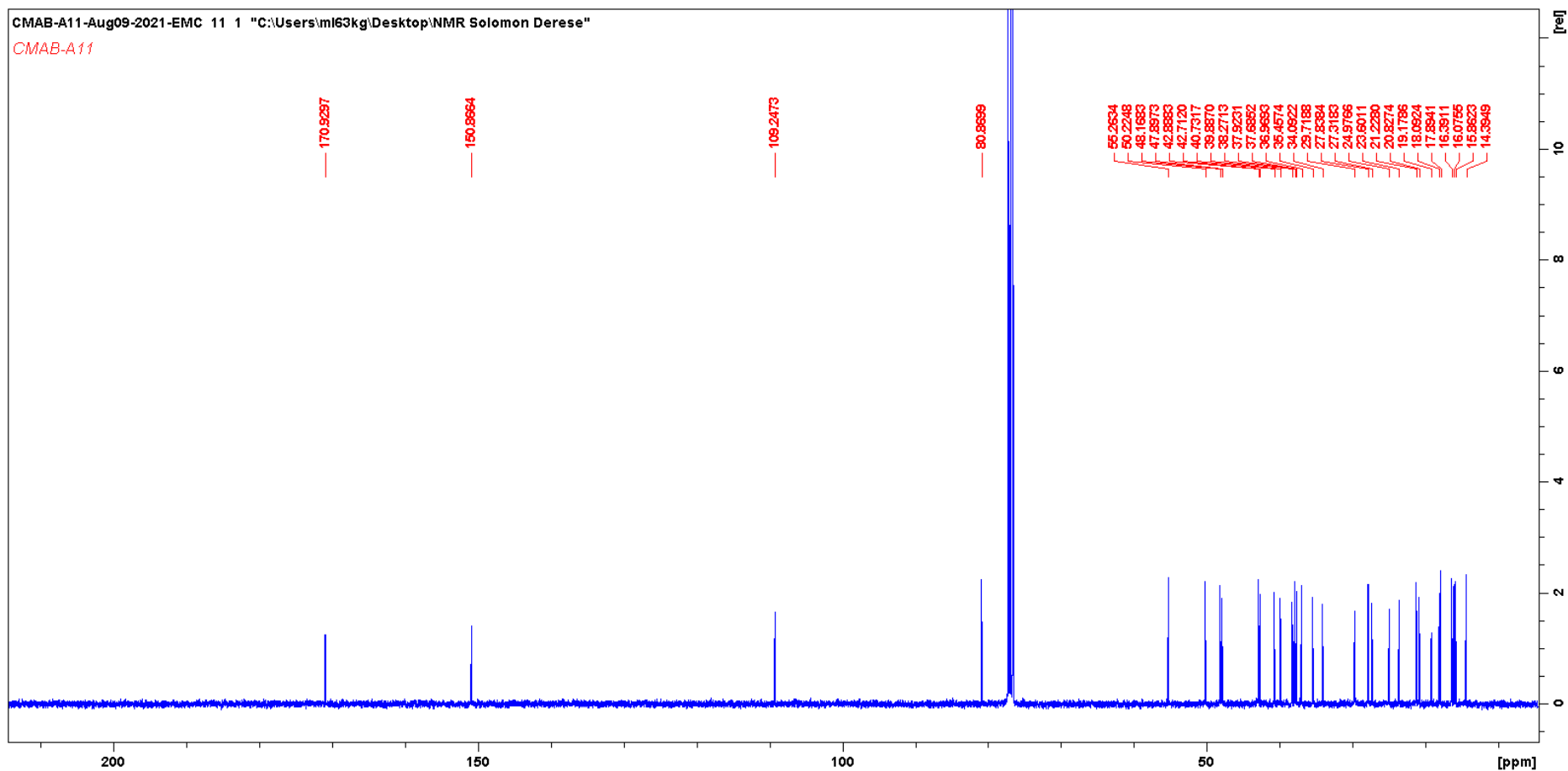


Appendix 84 <sup>1</sup>H NMR spectrum of Lupeol acetate (A11)

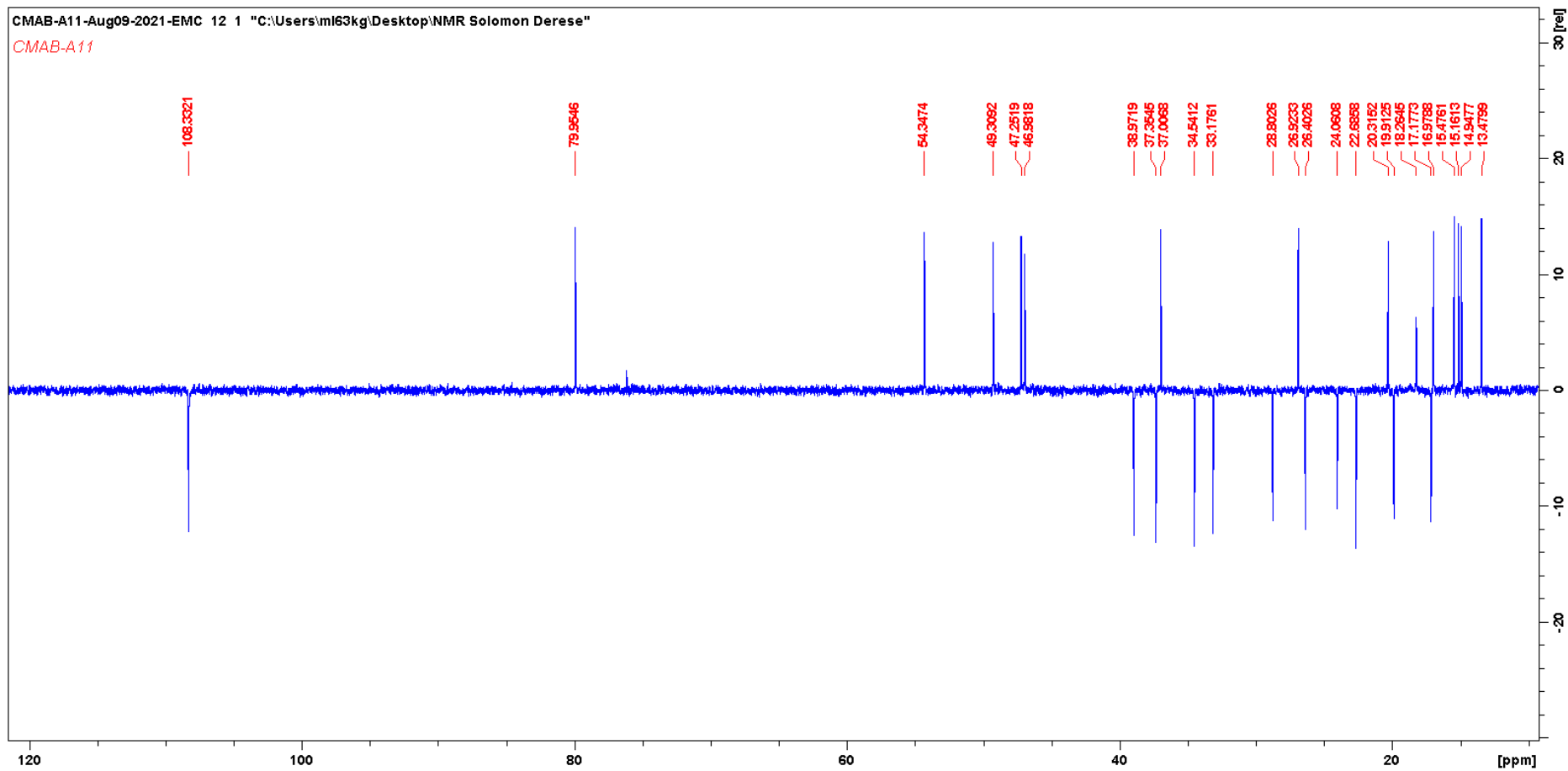




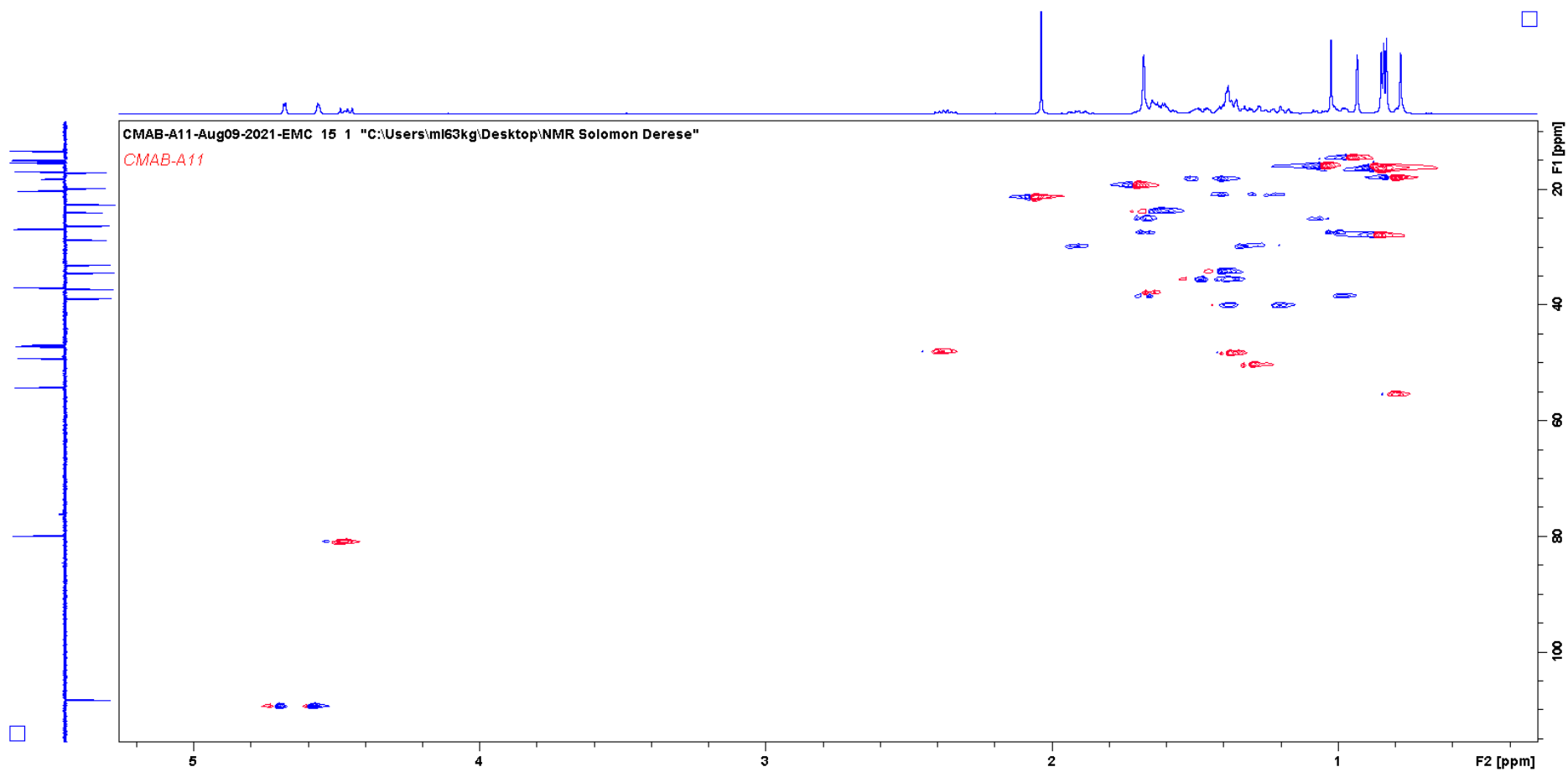
Appendix 85  $^{13}\text{C}$  NMR spectrum of Lupeol acetate (A11)



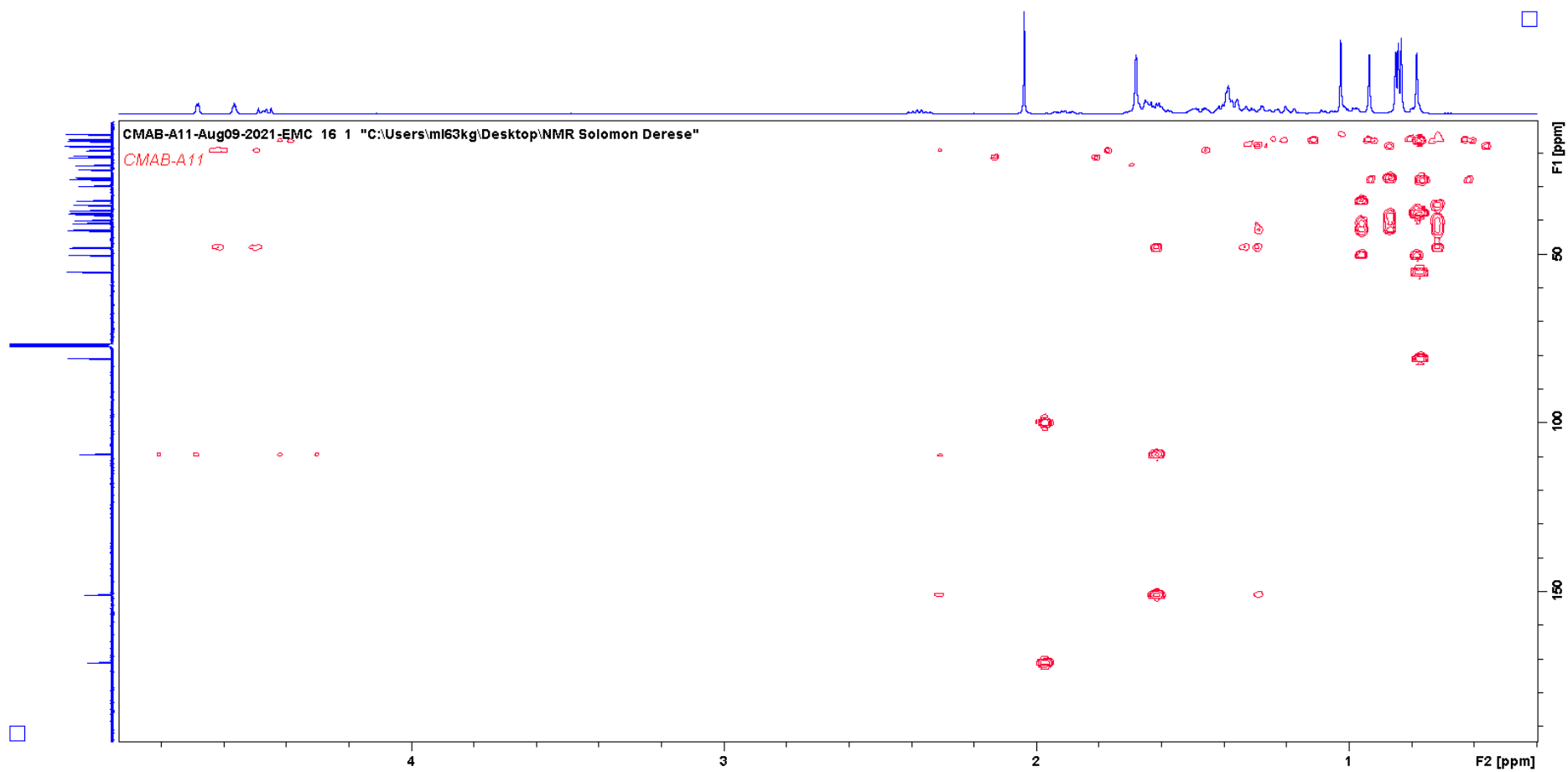
Appendix 86 DEPT spectrum of Lupeol acetate (A11)



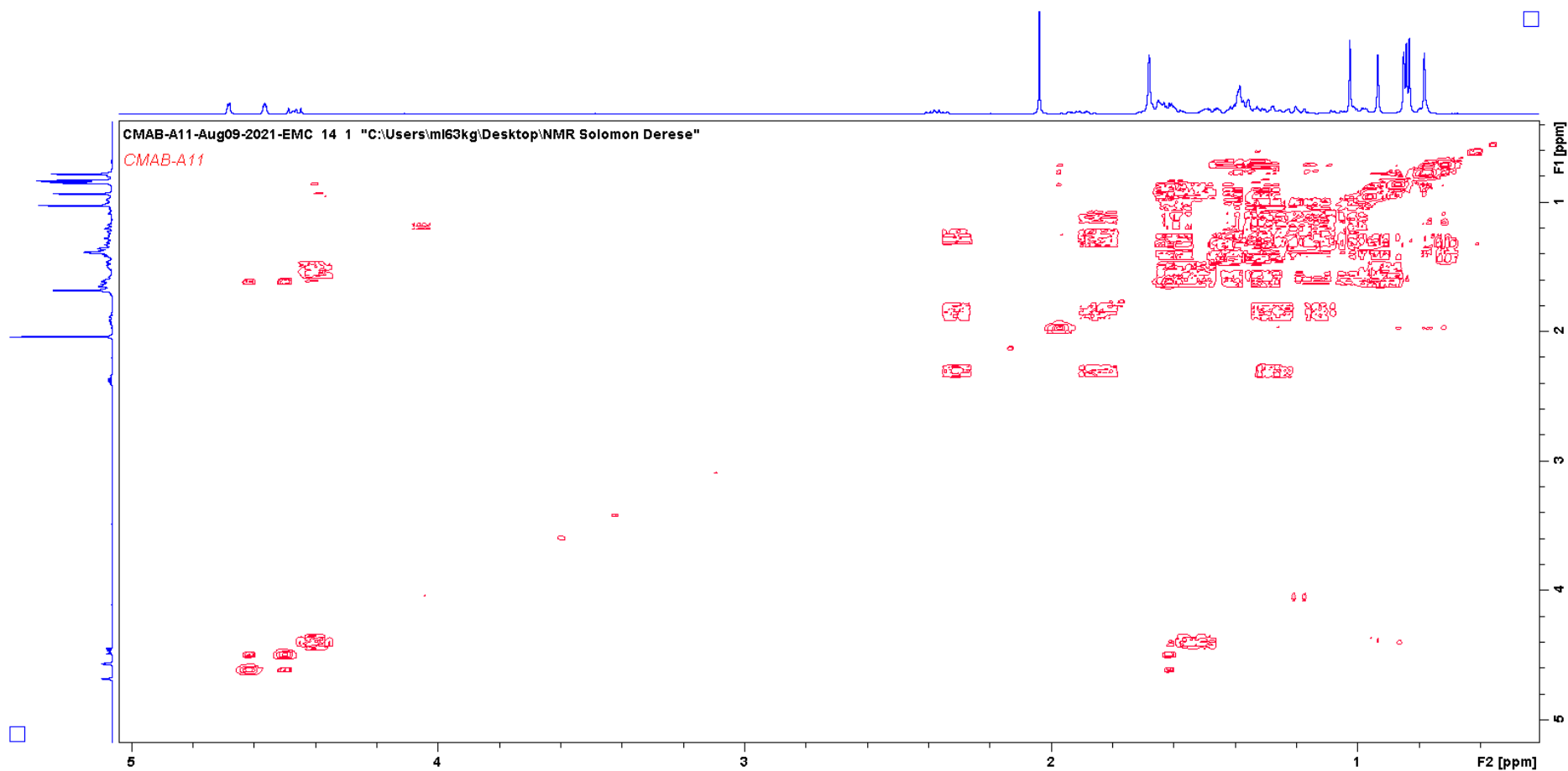
Appendix 87 HSQCDEPT spectrum of Lupeol acetate (A11)



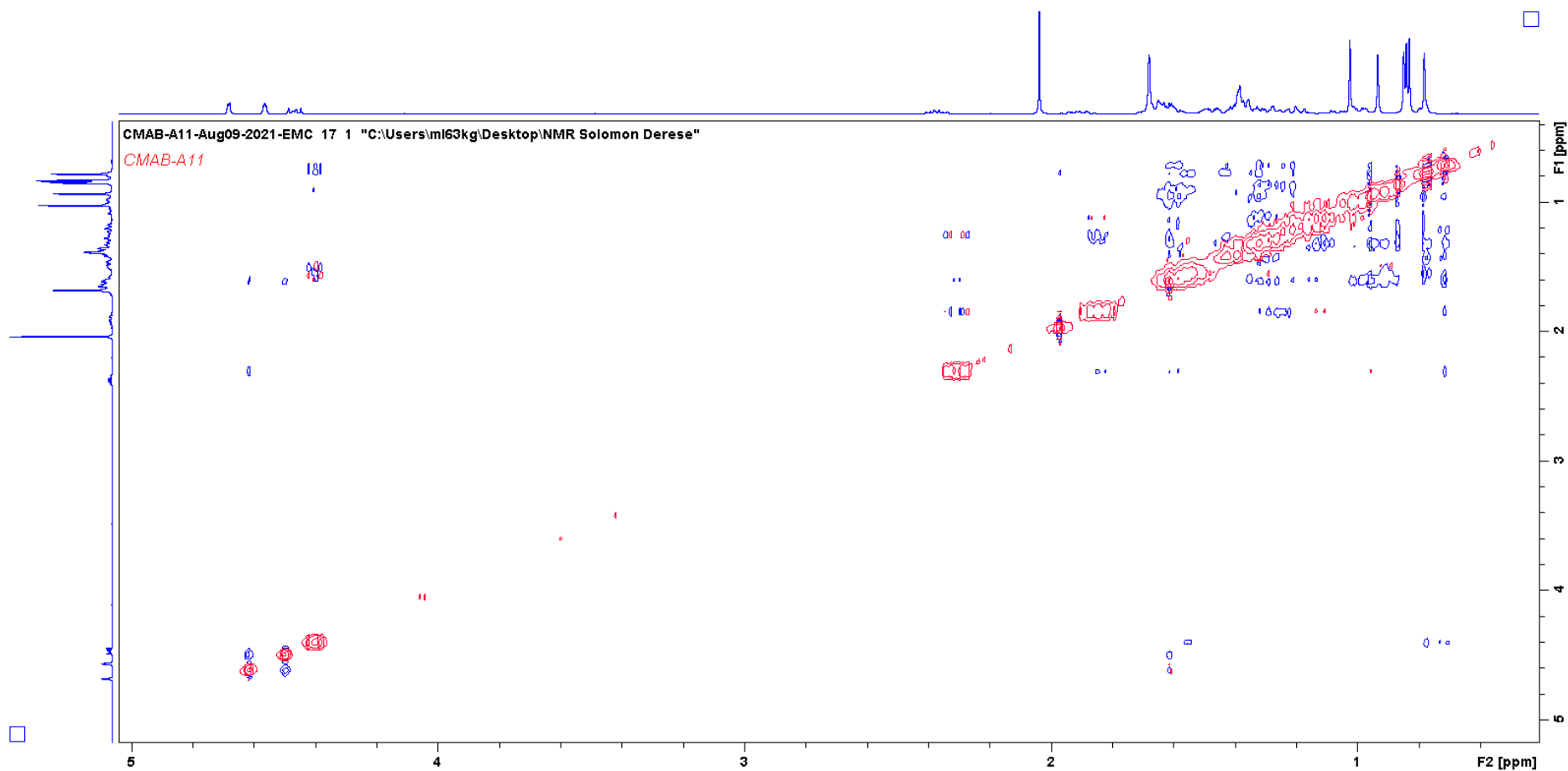
Appendix 88 HMBC spectrum of Lupeol acetate (A11)



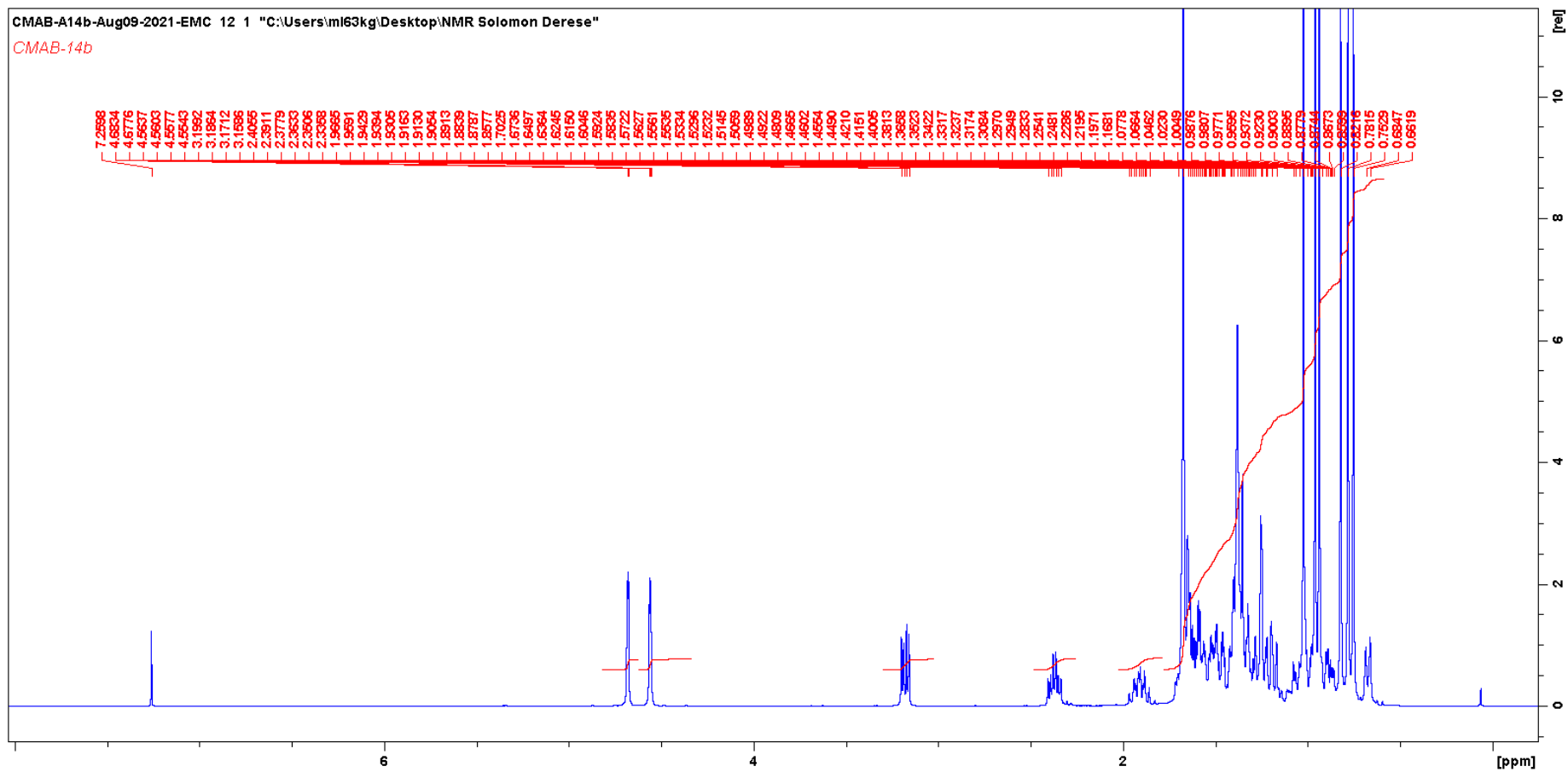
Appendix 89 COSY spectrum of Lupeol acetate (A11)



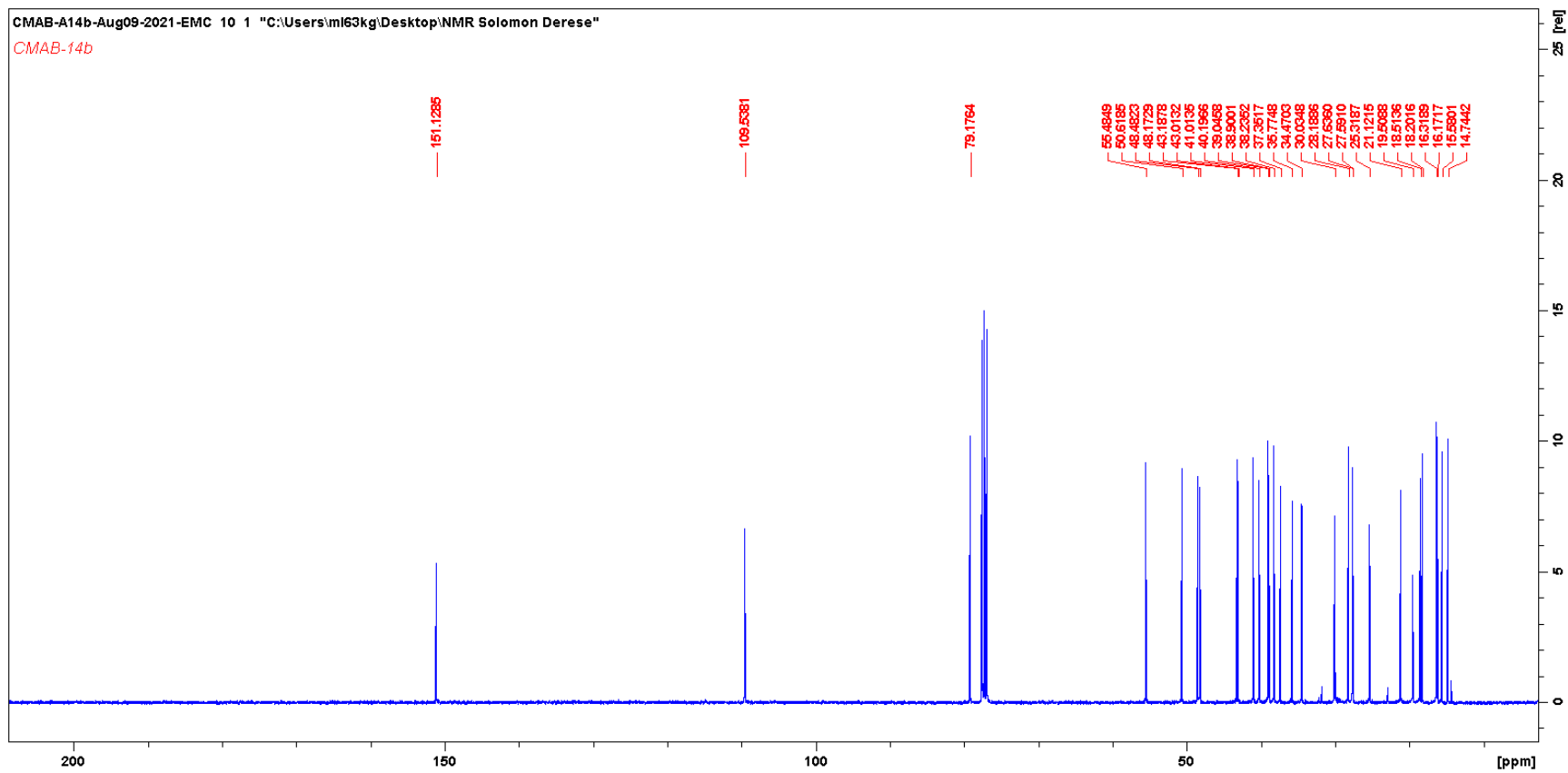
Appendix 90 NOSEY spectrum of Lupeol acetate (A11)



Appendix 91 <sup>1</sup>H NMR spectrum of Lupeol (A7)

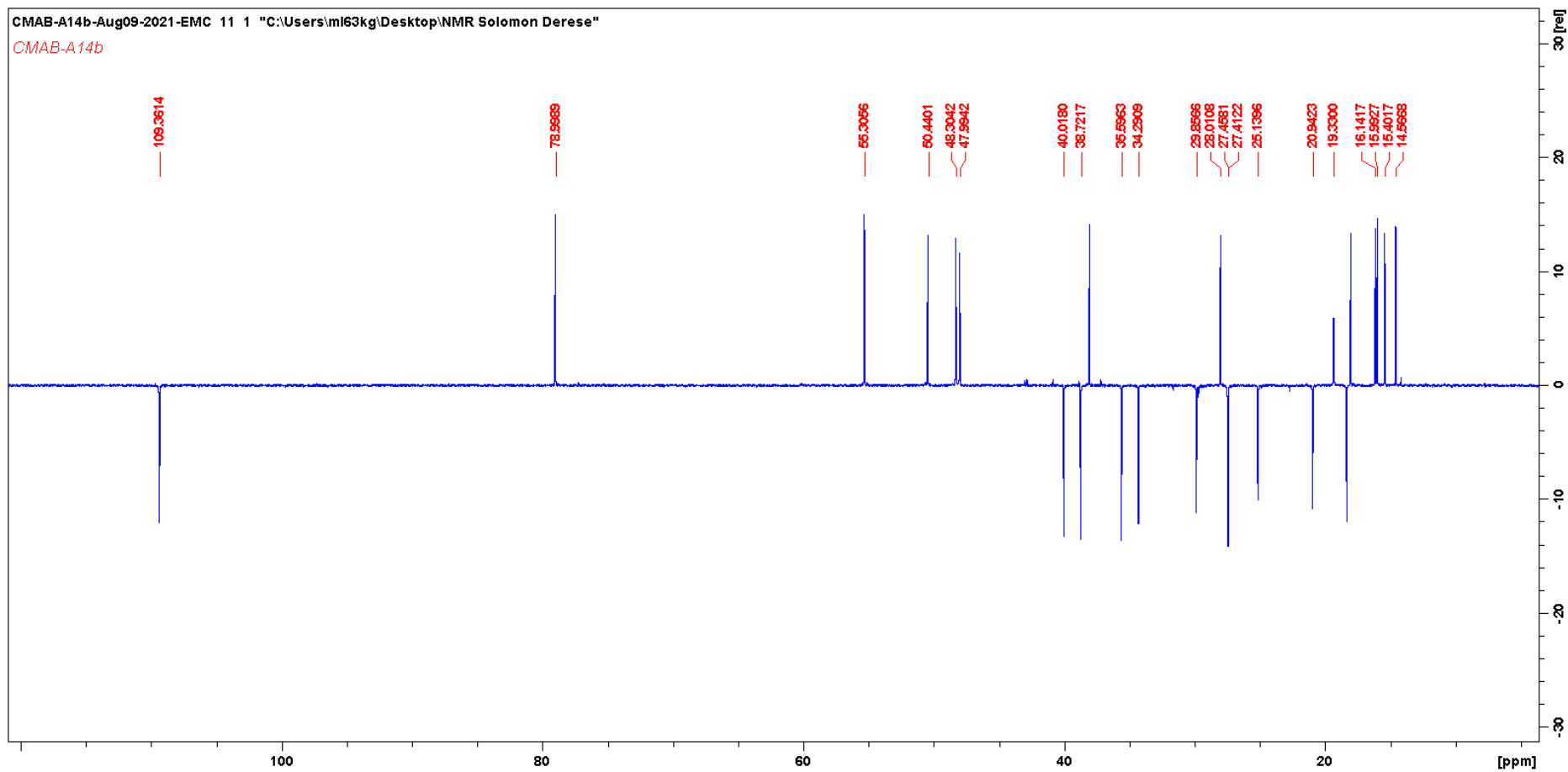


Appendix 92  $^{13}\text{C}$  NMR spectrum of Lupeol (A7)

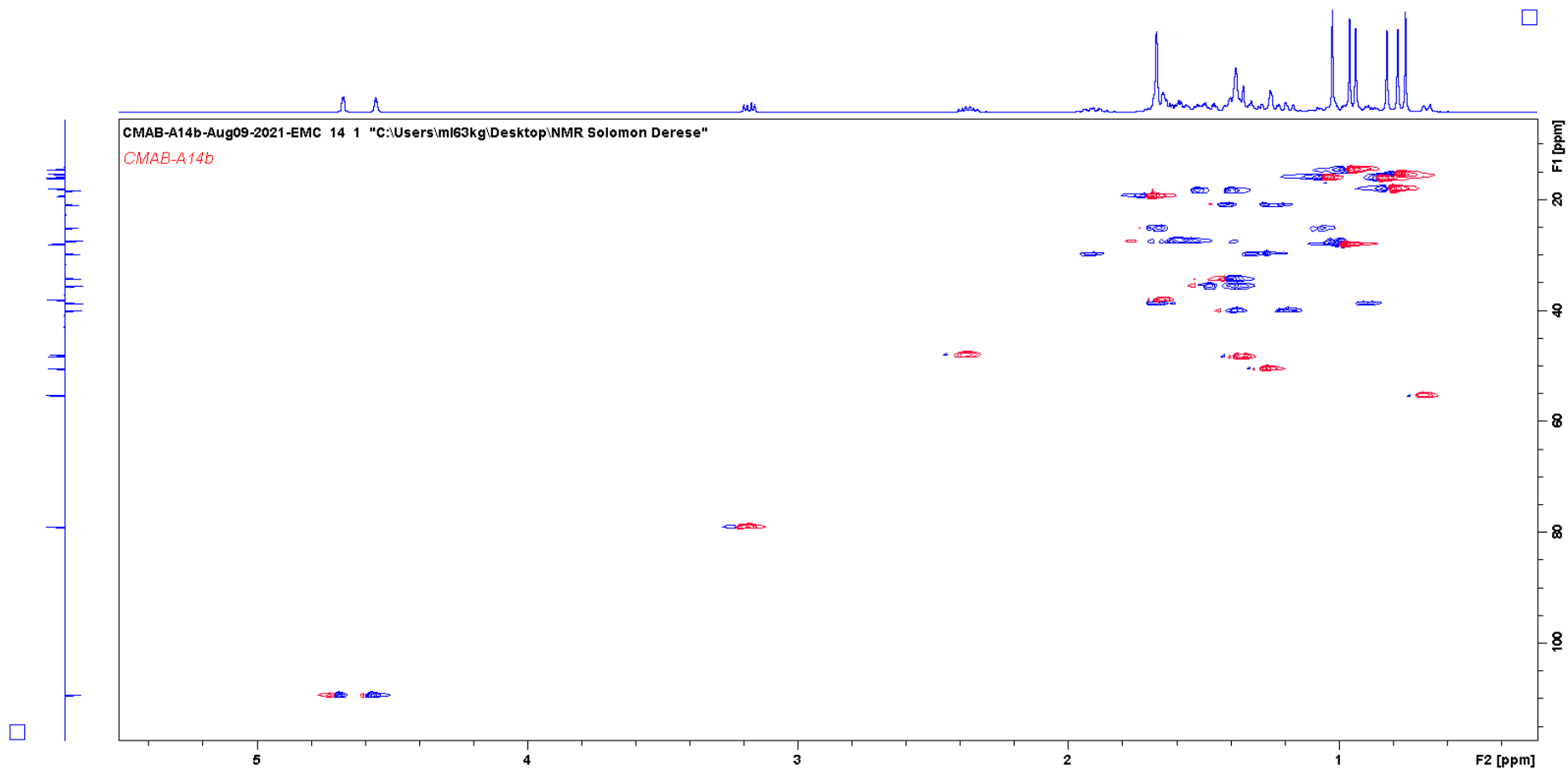




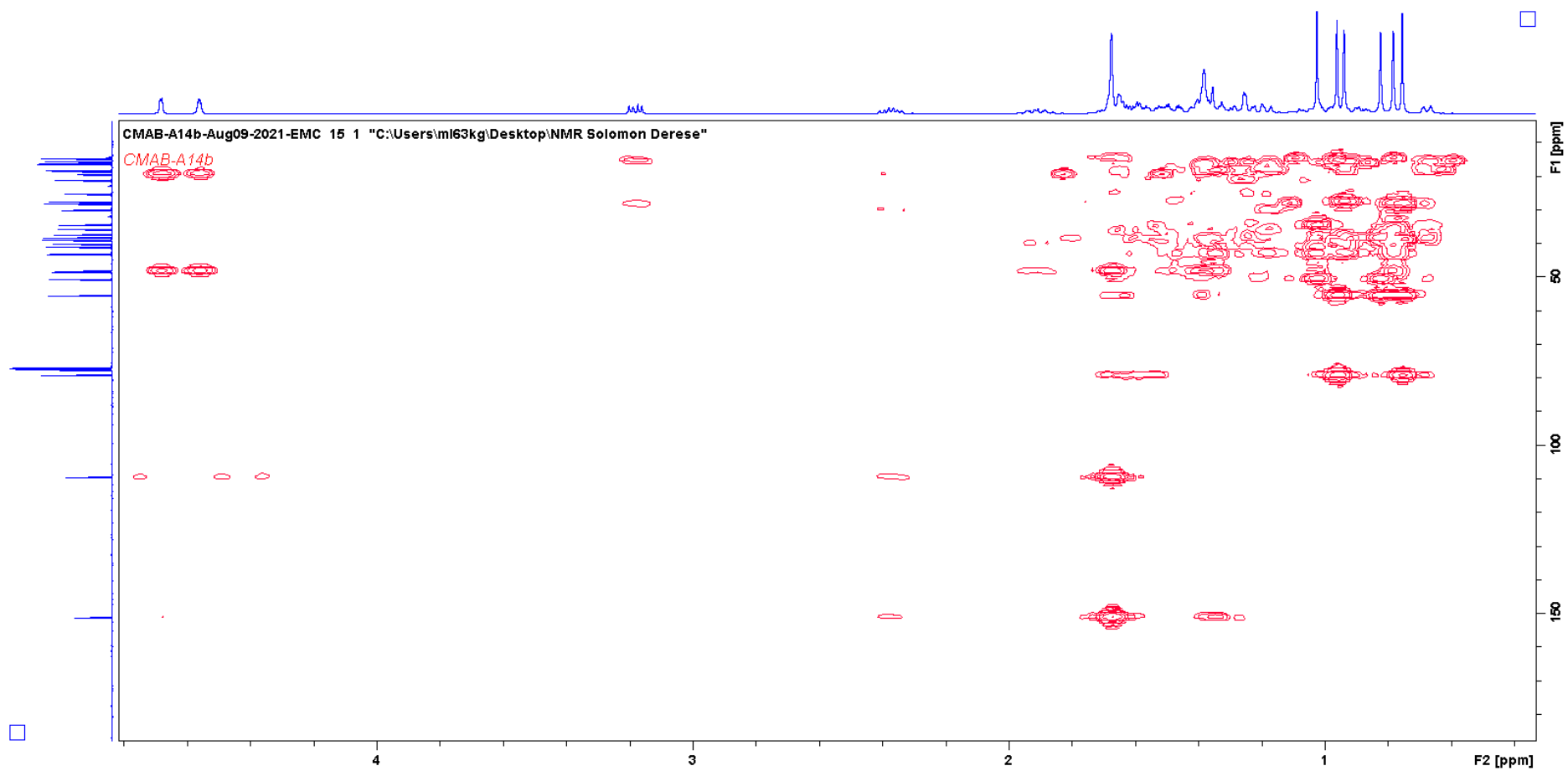
Appendix 93 DEPT spectrum of Lupeol (A7)



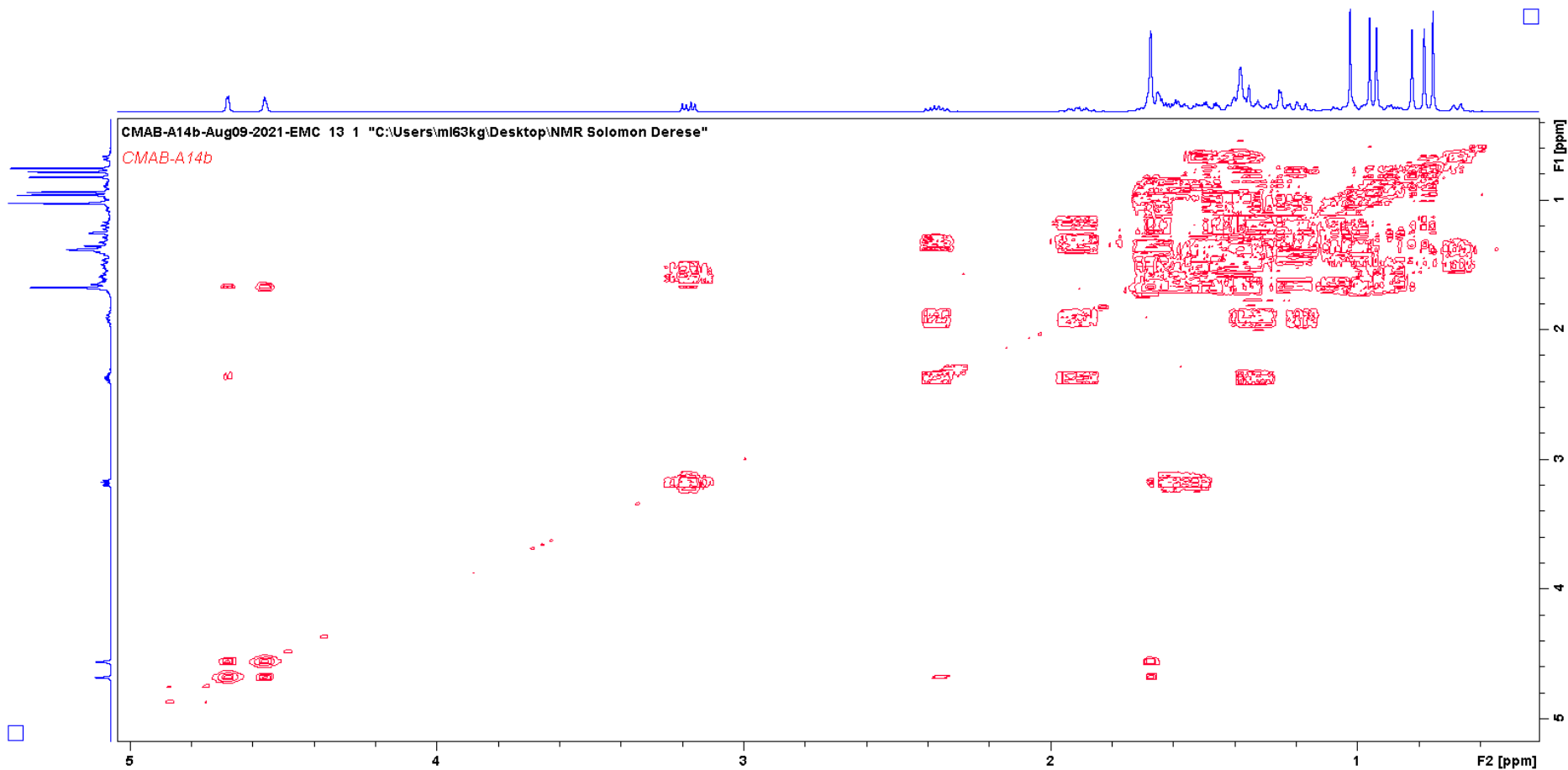
Appendix 94 HSQCDEPT spectrum of Lupeol (A7)



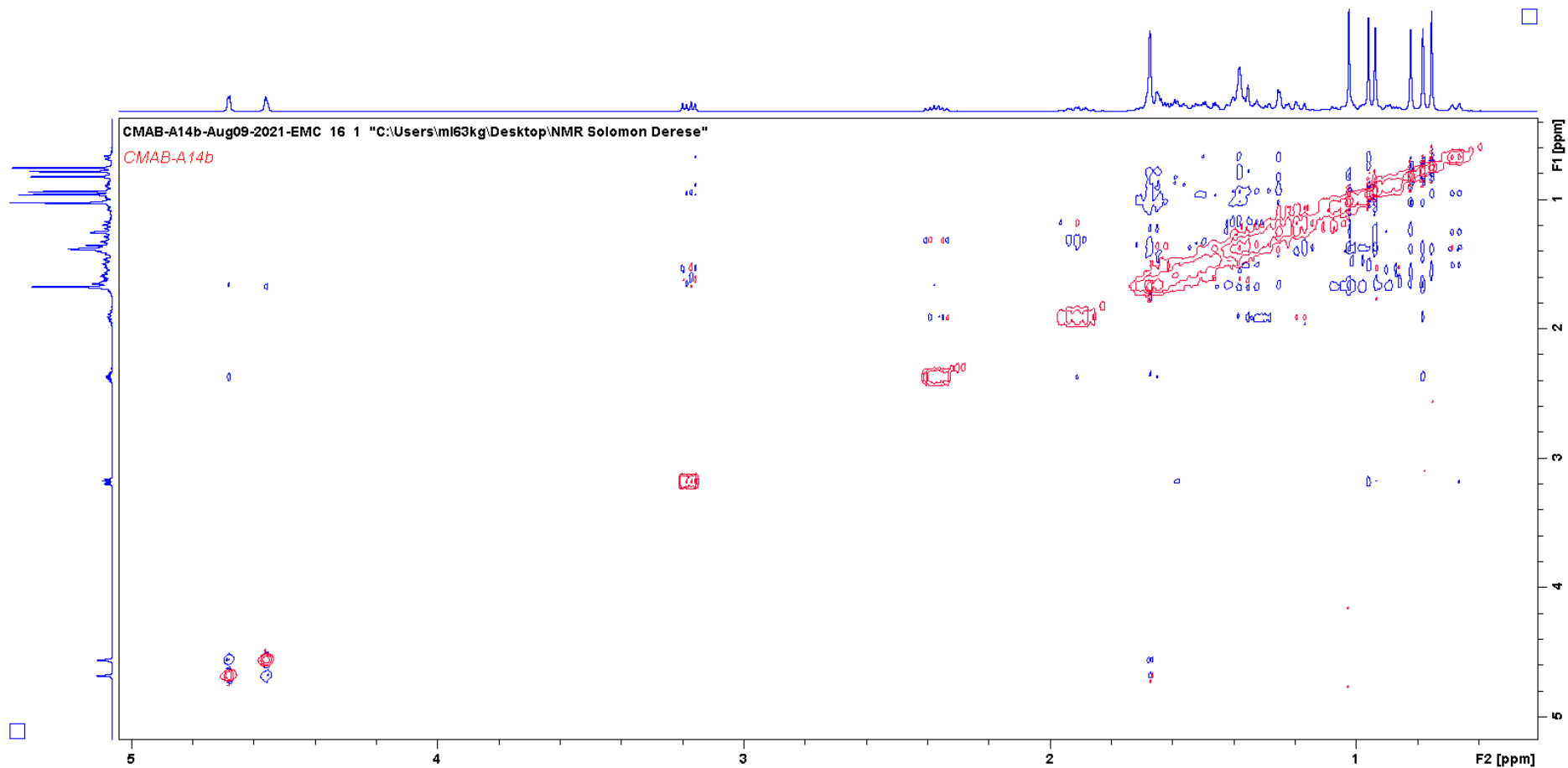
Appendix 95 HMBC spectrum of Lupeol (A7)



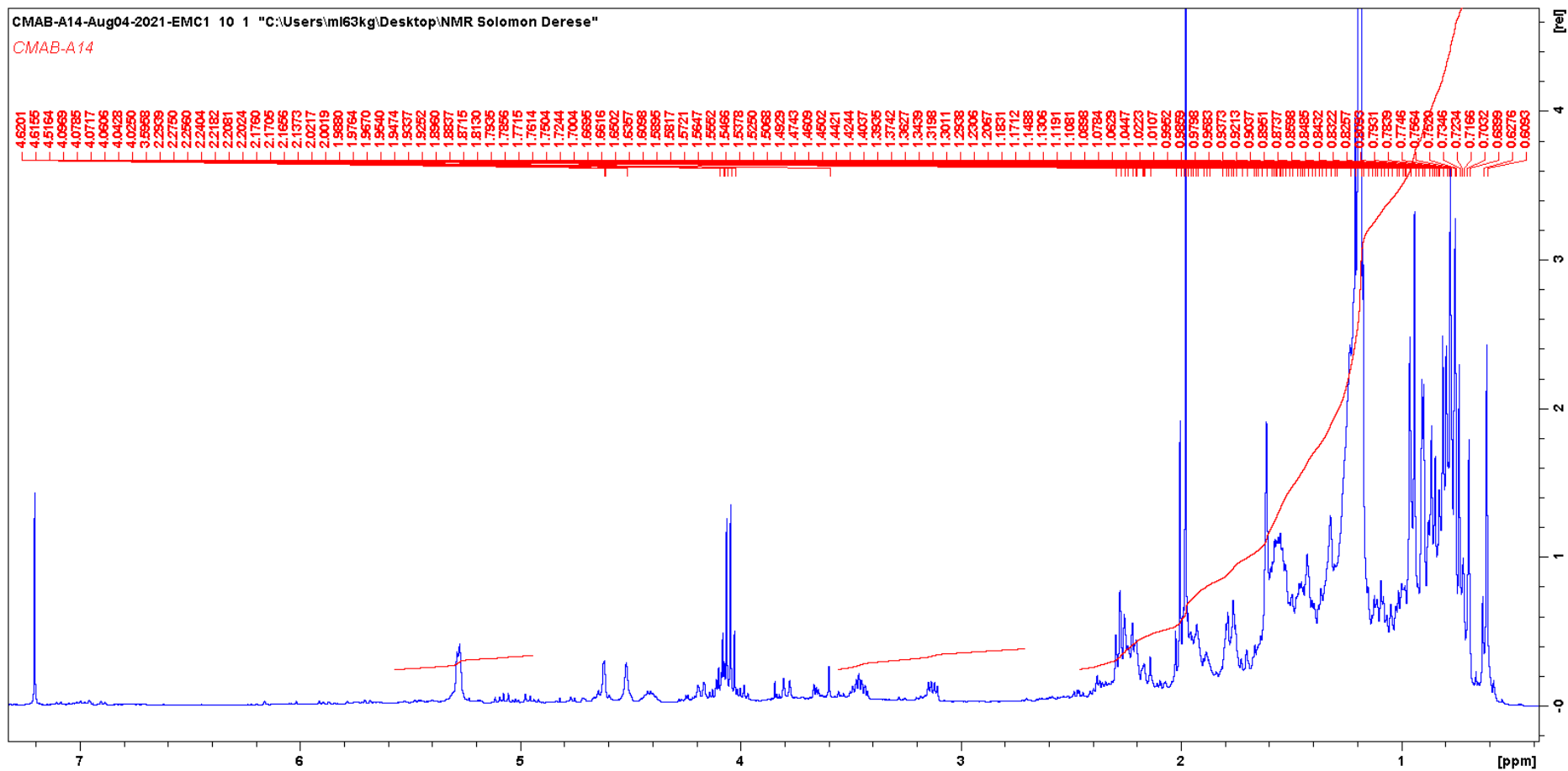
Appendix 96 COSY spectrum of Lupeol (A7)



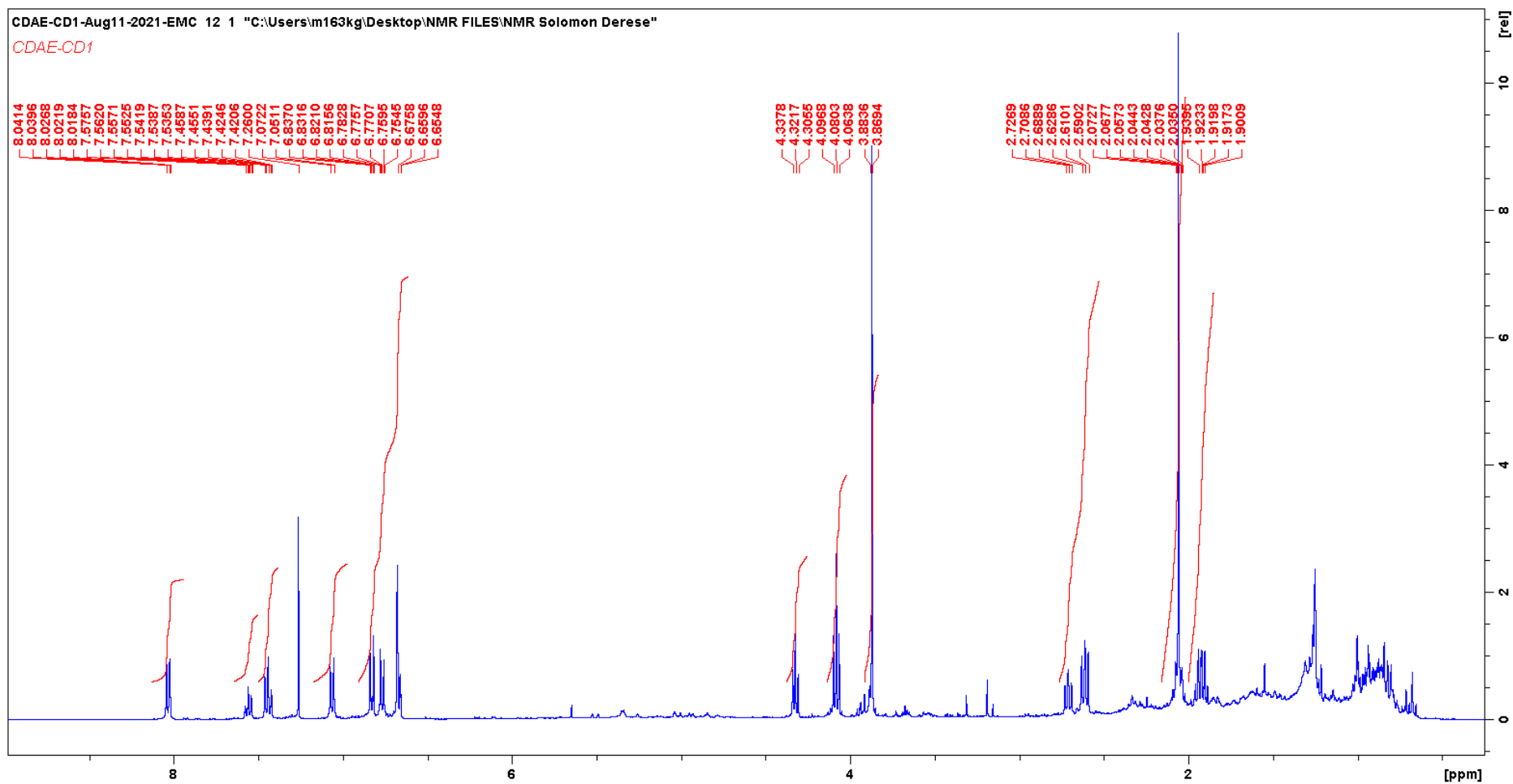
Appendix 97 NOESY spectrum of Lupeol (A7)



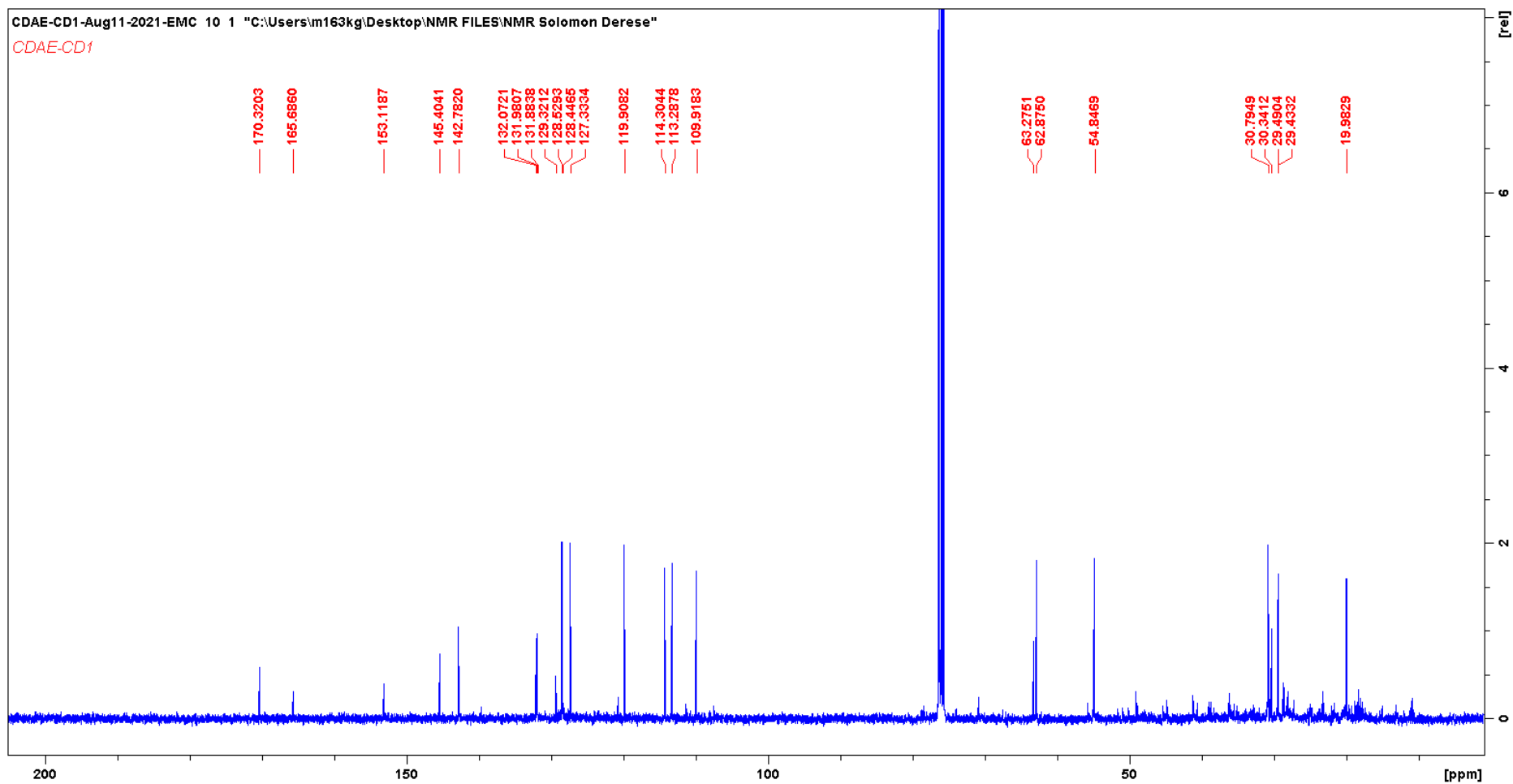
Appendix 98 <sup>1</sup>H NMR Spectra for Sitosterol (A15) and Stigmasterol (A16)



Appendix 99 <sup>1</sup>H NMR Spectra for CD1 (mixture of Dihydroconiferyl acetate (CD1a) and (4-Hydroxy-3-methoxyphenyl)-propyl benzoate (CD1b))

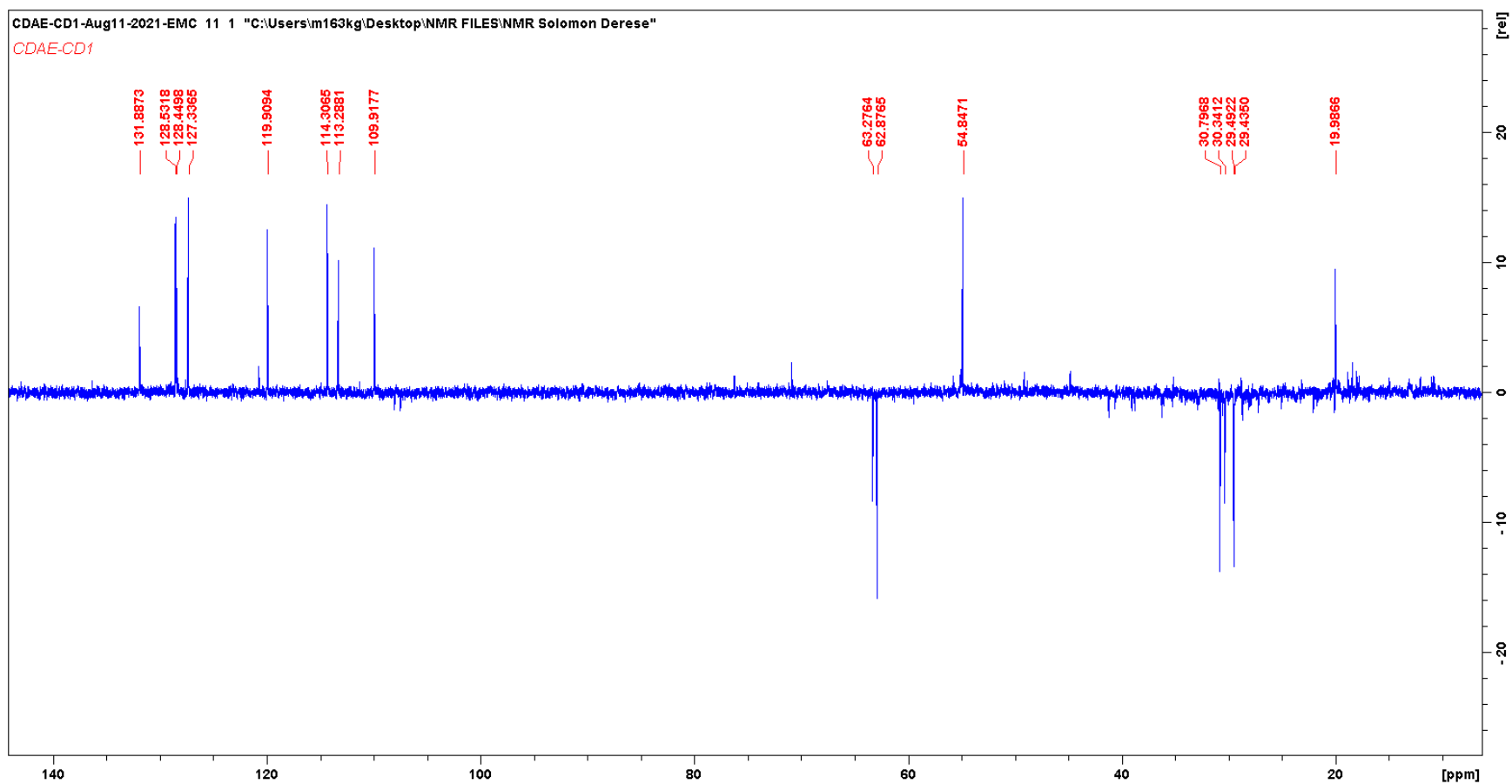


Appendix 100  $^{13}\text{C}$  NMR Spectra for CD1 (mixture of Dihydroconiferyl acetate (CD1a) and (4-Hydroxy-3-methoxyphenyl)-propyl benzoate (CD1b))

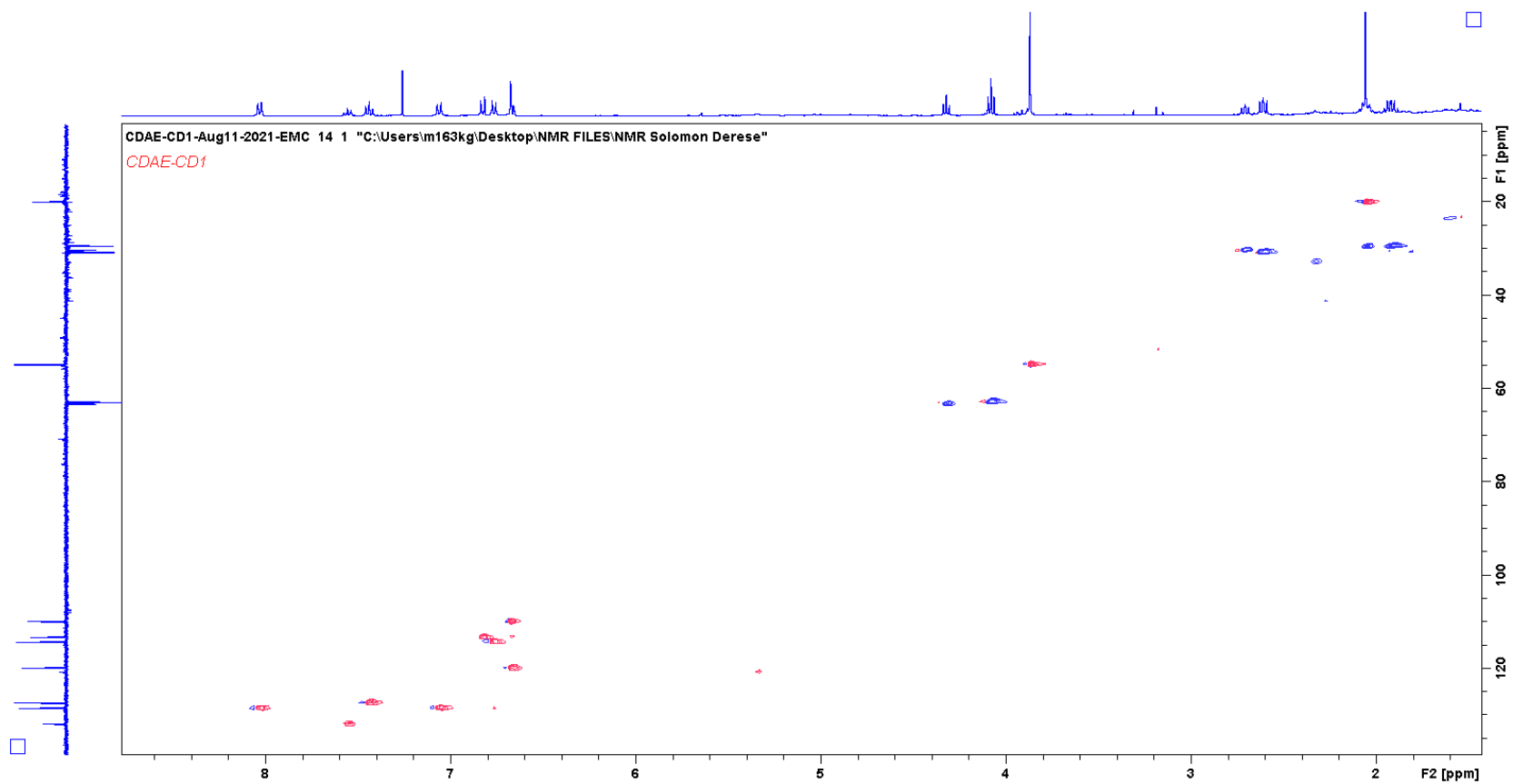




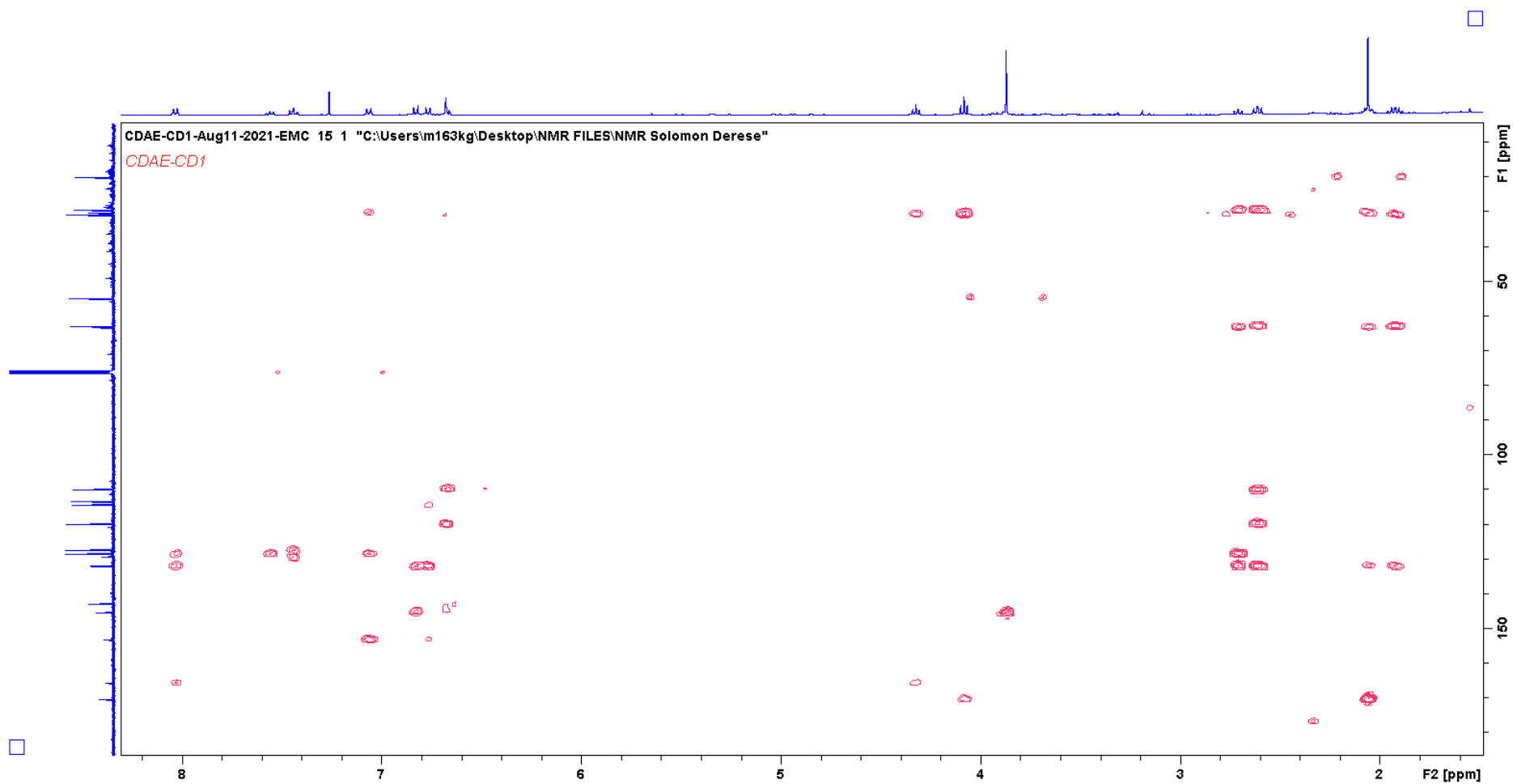
Appendix 101 DEPT Spectra for CD1 (mixture of Dihydroconiferyl acetate (CD1a) and (4-Hydroxy-3-methoxyphenyl)-propyl benzoate (CD1b))



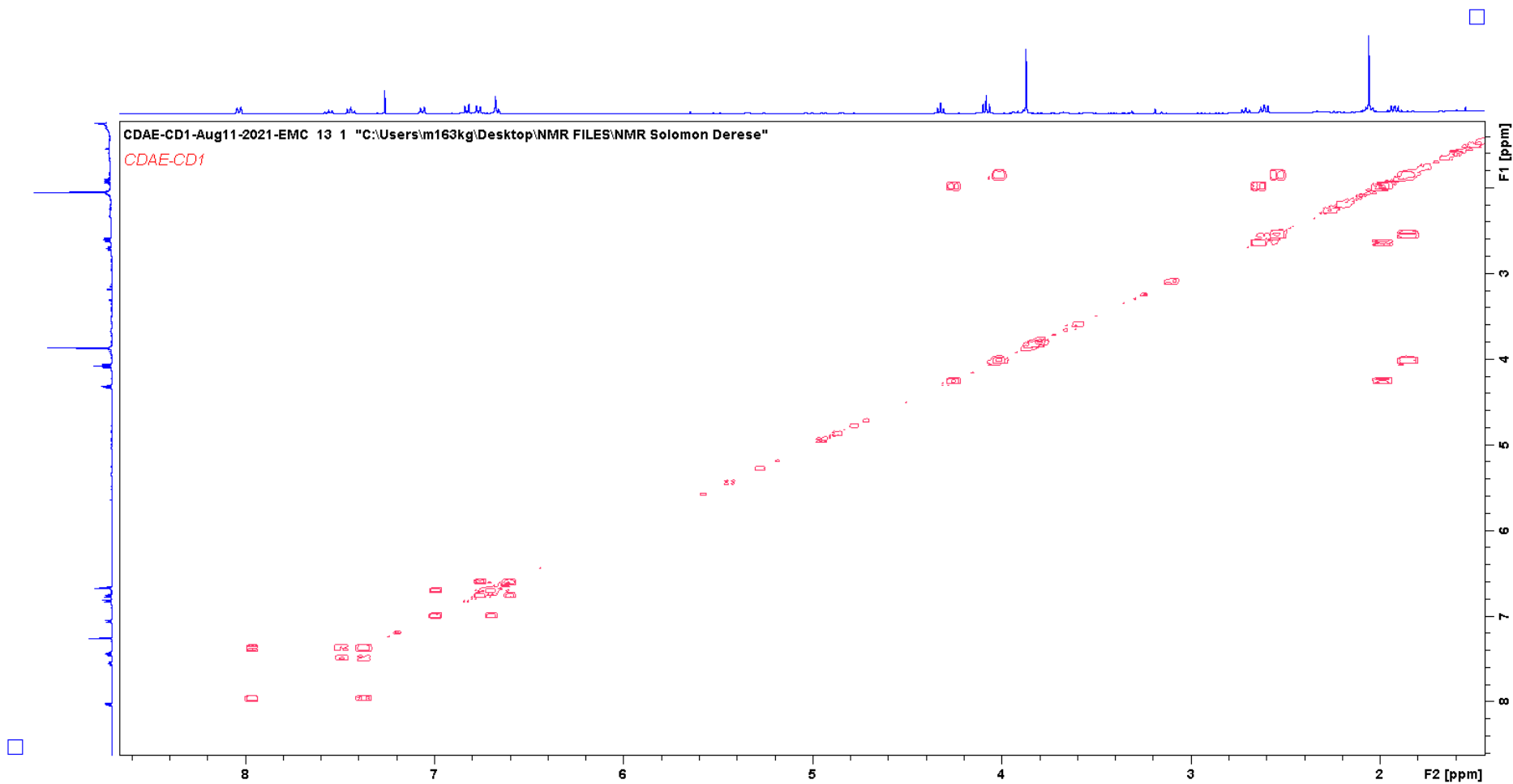
Appendix 102 HSQCDEPT Spectra for CD1 (mixture of Dihydroconiferyl acetate (CD1a) and (4-Hydroxy-3-methoxyphenyl)-propyl benzoate (CD1b)



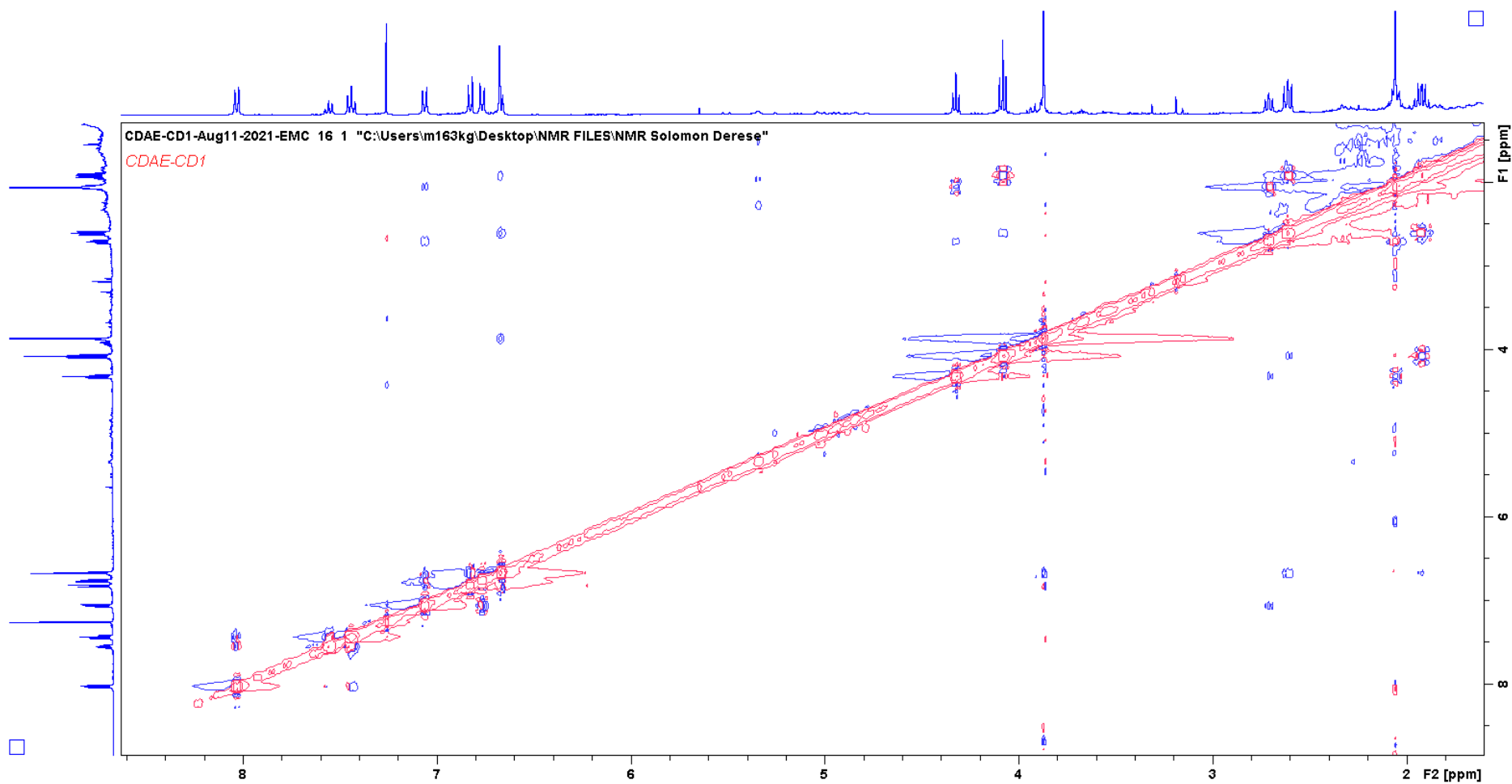
Appendix 103 HMBC Spectra for CD1 (mixture of Dihydroconiferyl acetate (CD1a) and (4-Hydroxy-3-methoxyphenyl)-propyl benzoate (CD1b))



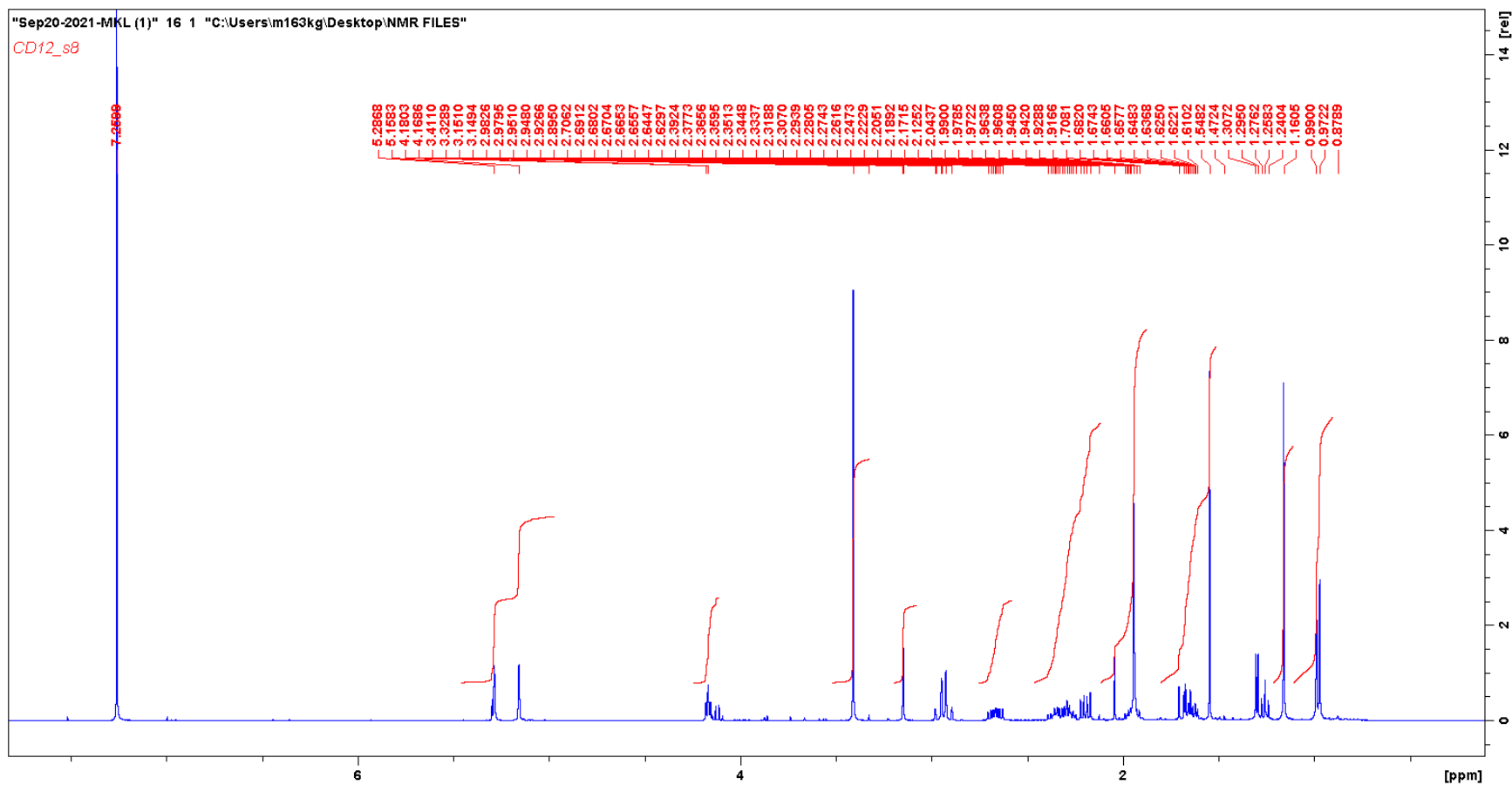
Appendix 104 COSY Spectra for CD1 (mixture of Dihydroconiferyl acetate (CD1a) and (4-Hydroxy-3-methoxyphenyl)-propyl benzoate (CD1b))



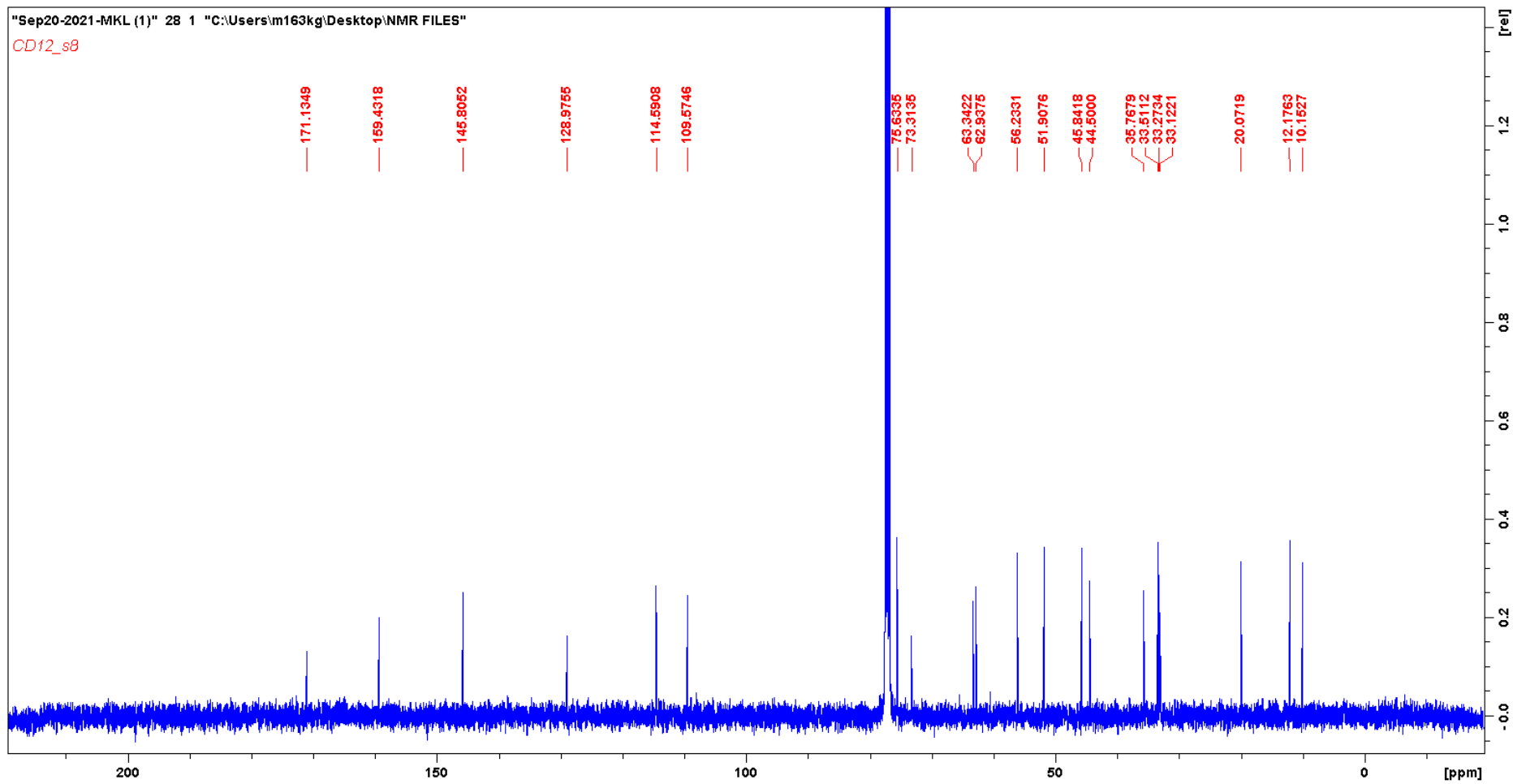
Appendix 105 NOESY Spectra for CD1 (mixture of Dihydroconiferyl acetate (CD1a) and (4-Hydroxy-3-methoxyphenyl)-propyl benzoate (CD1b))



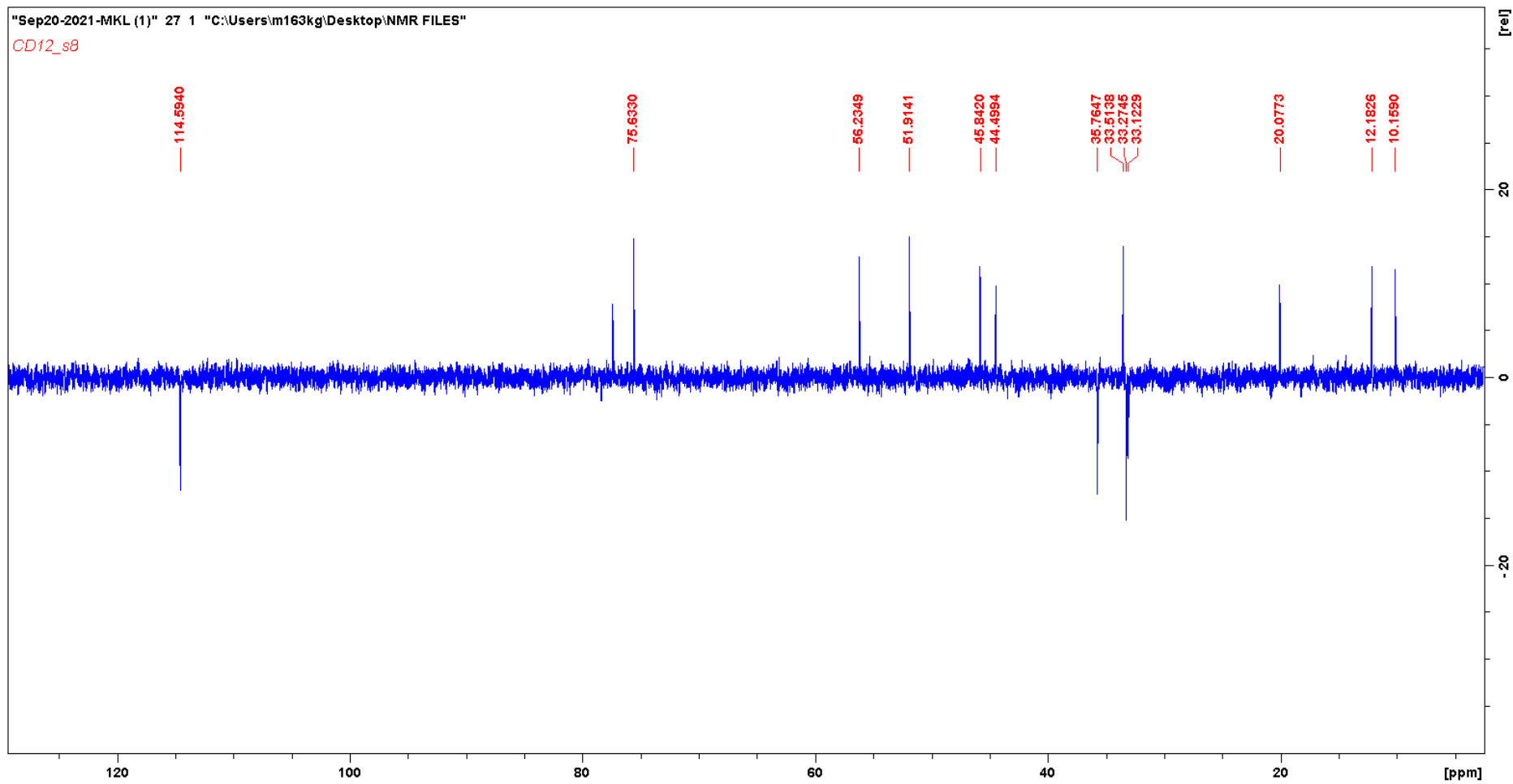
Appendix 106  $^1\text{H}$  NMR Spectra for crotoascararin  $\omega$  (CD12a)



Appendix 107  $^{13}\text{C}$  NMR Spectra for crotoascarin  $\omega$  (CD12a)

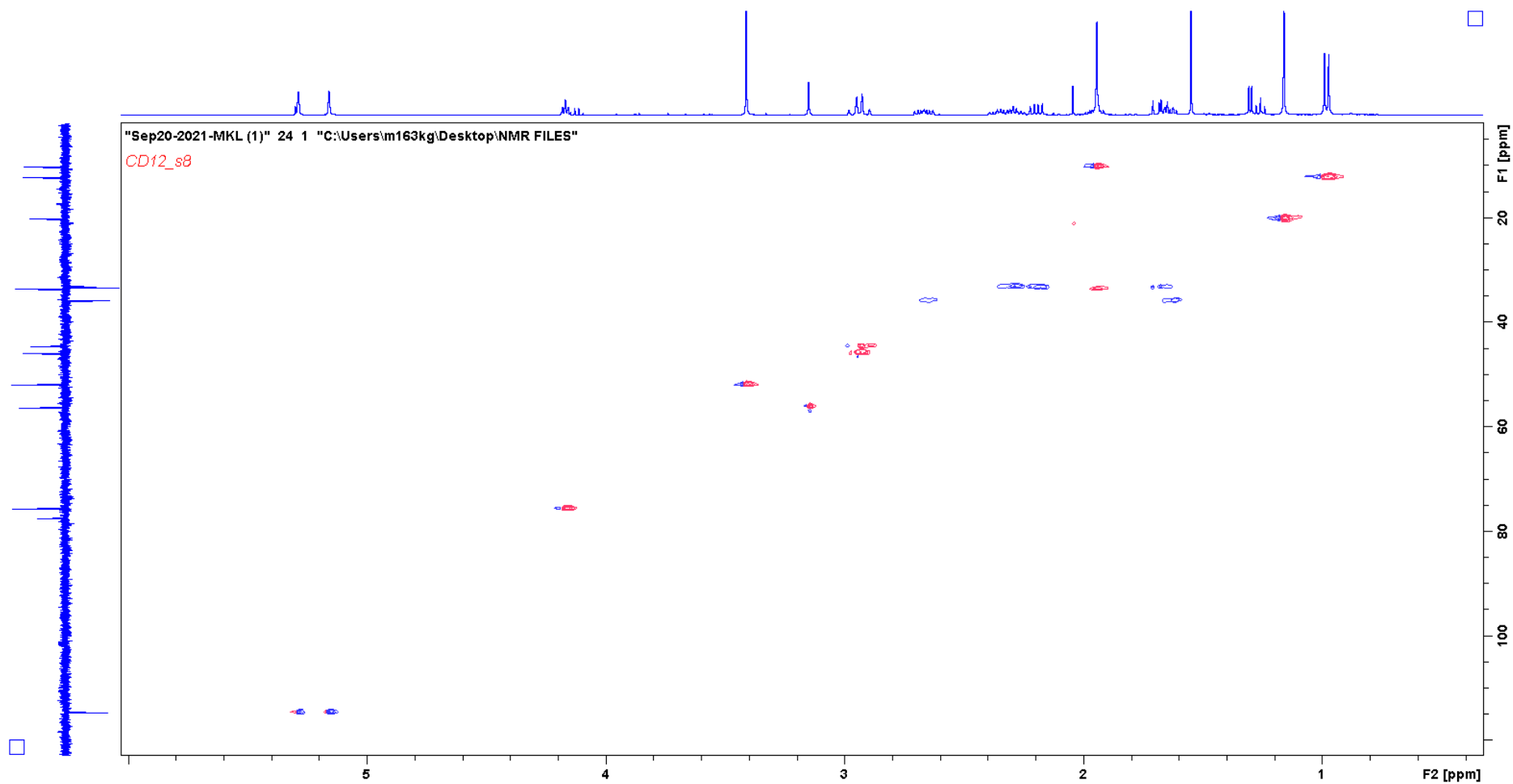


Appendix 108 DEPT Spectra for crotoascarin  $\omega$  (CD12a)

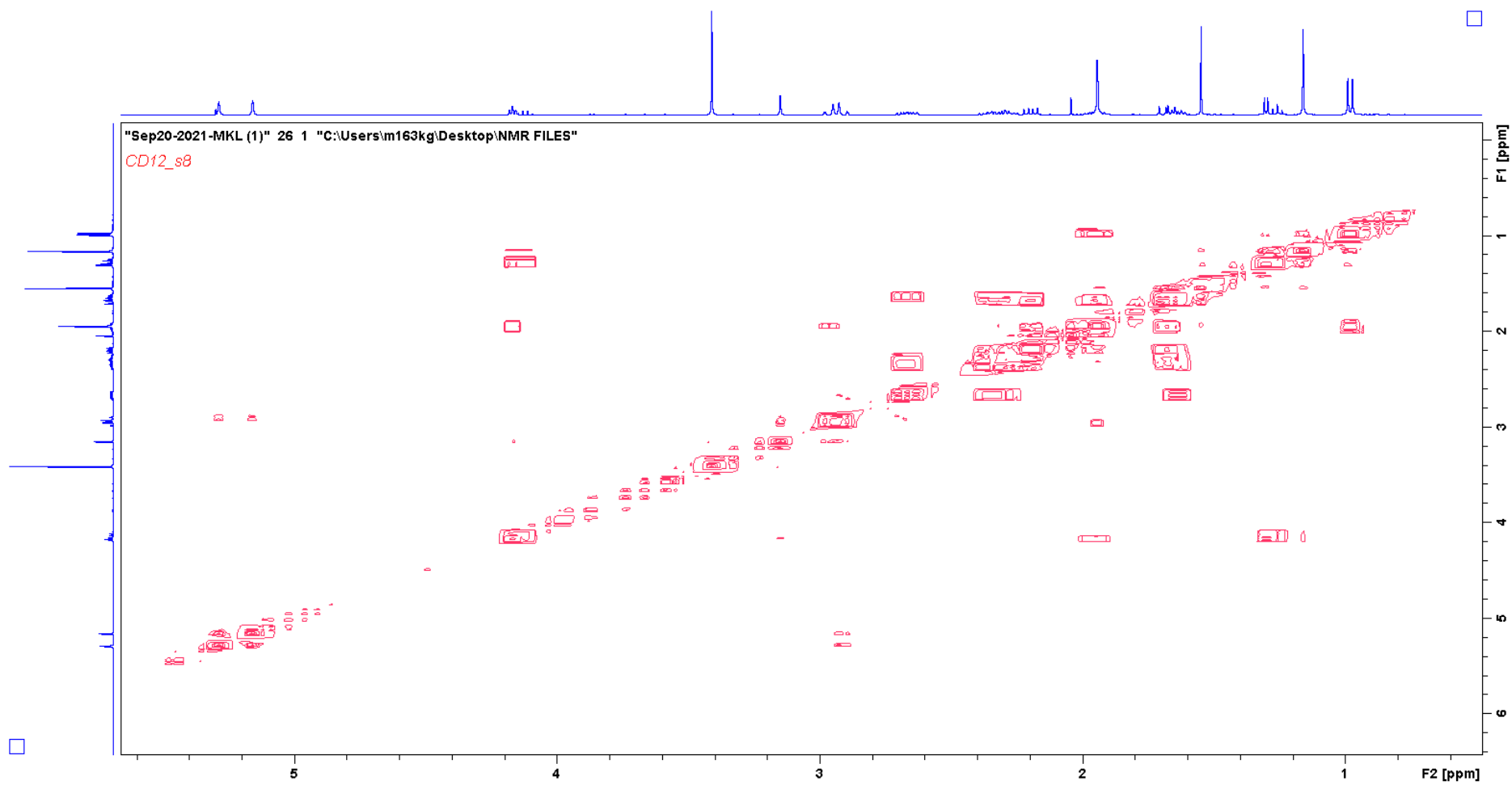




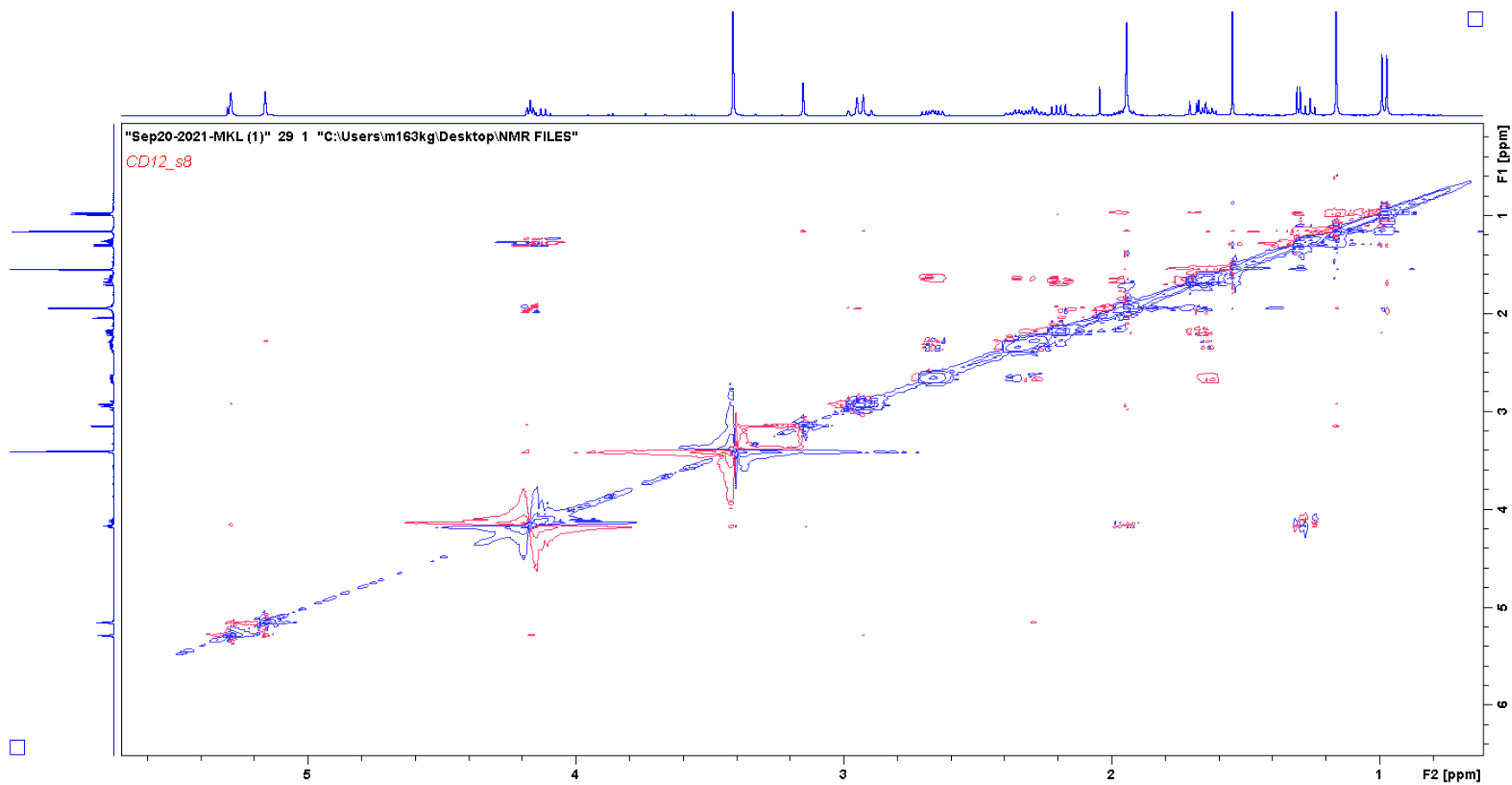
Appendix 109 HSQCDEPT Spectra for crotoascarin  $\omega$  (CD12a)



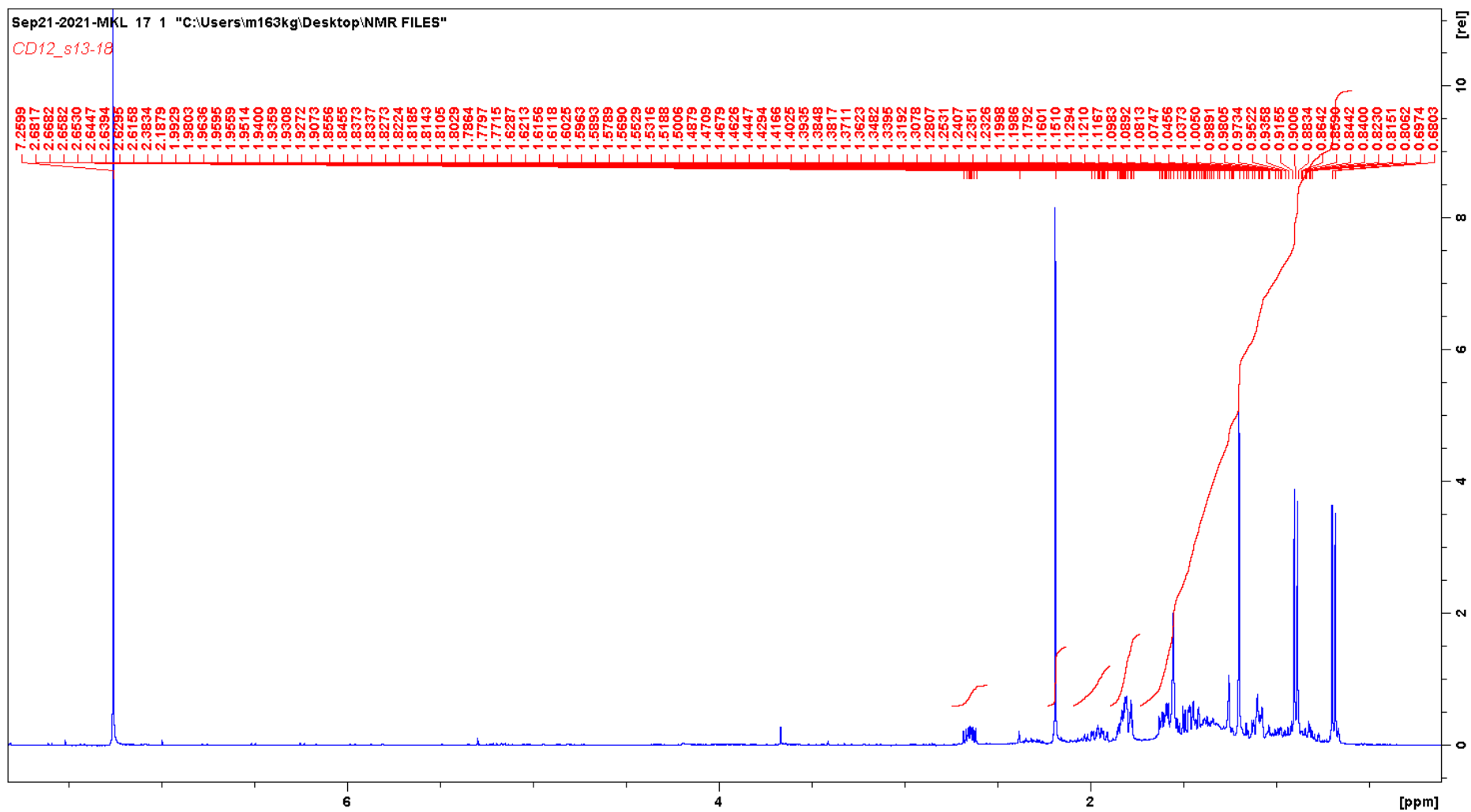
Appendix 110 COSY Spectra for crotoascarin  $\omega$  (CD12a)



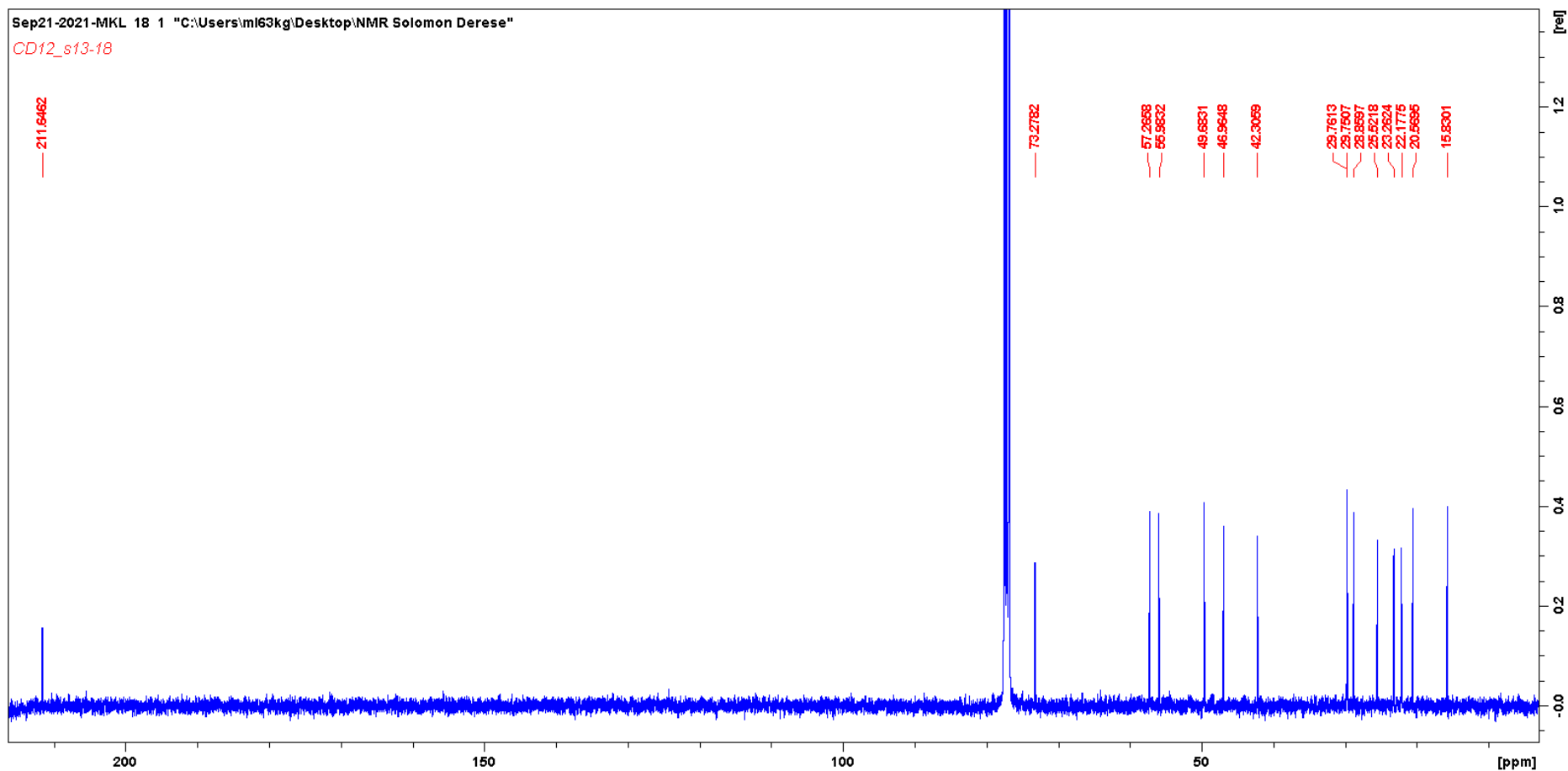
Appendix 111 NOESY Spectra for crotoascarin  $\omega$  (CD12a)



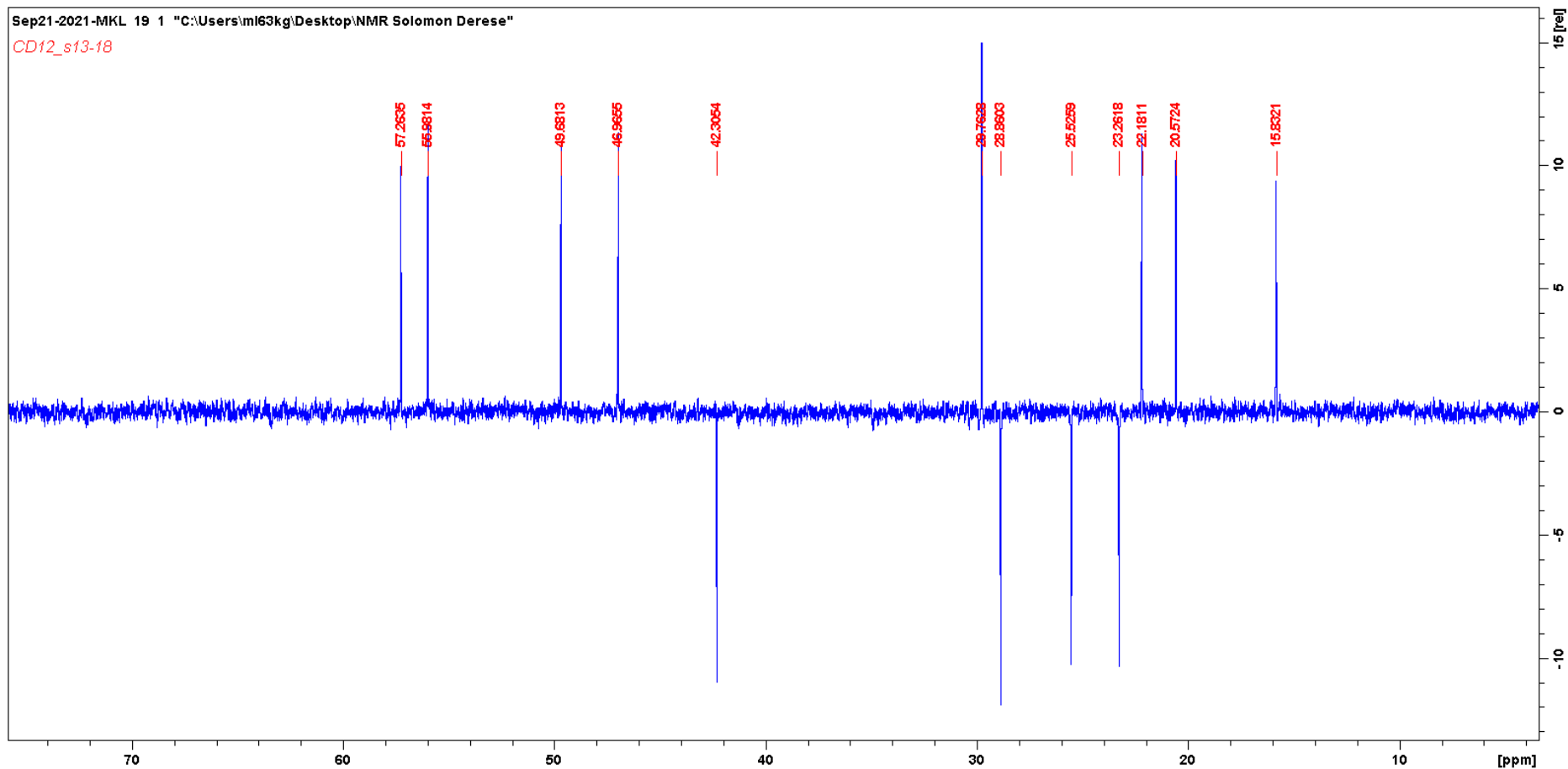
Appendix 112 <sup>1</sup>H NMR Spectra for β-Oplonanone (CD12b)



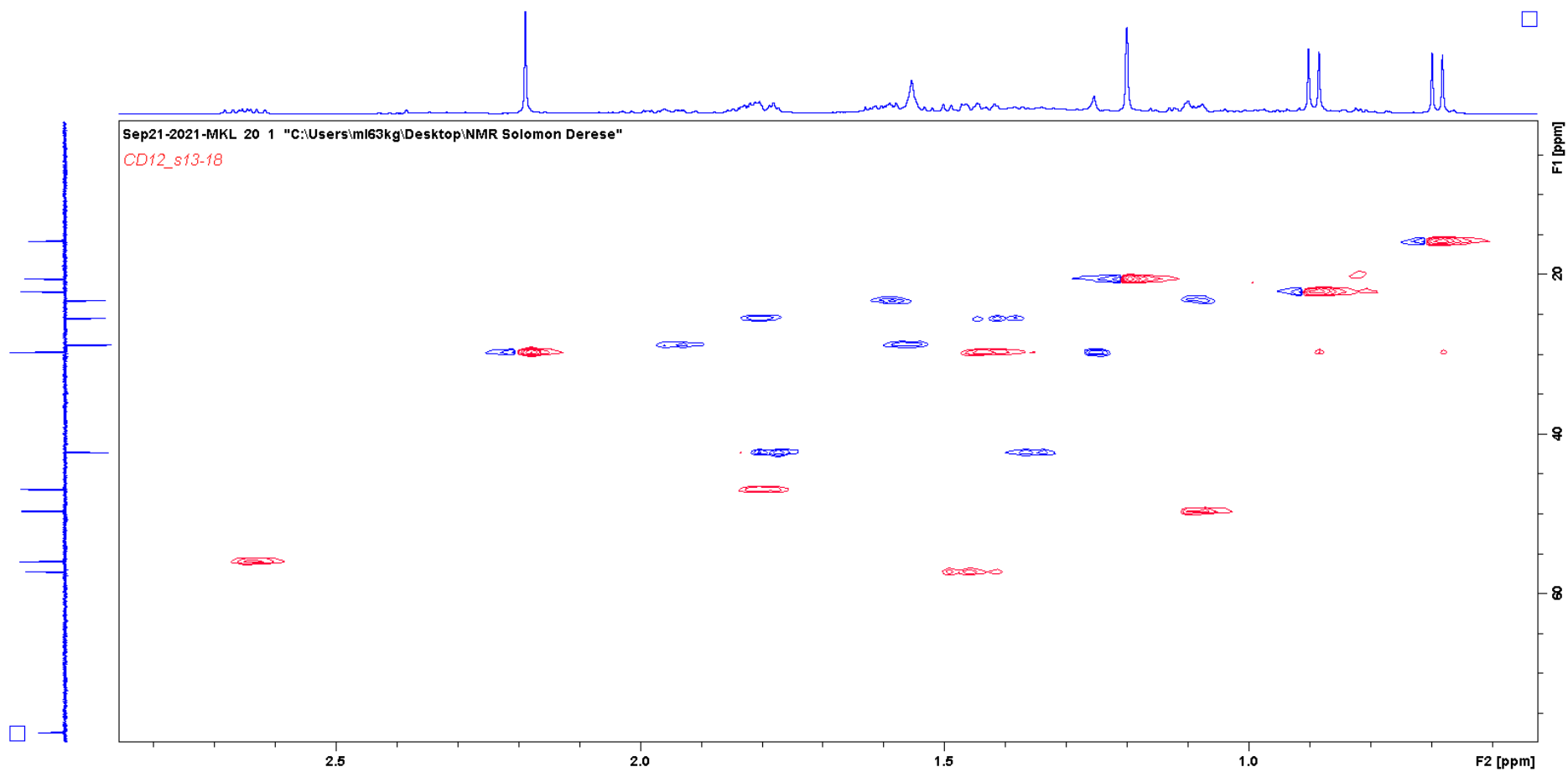
Appendix 113  $^{13}\text{C}$  NMR Spectra for  $\beta$ -Oplopanone (CD12b)



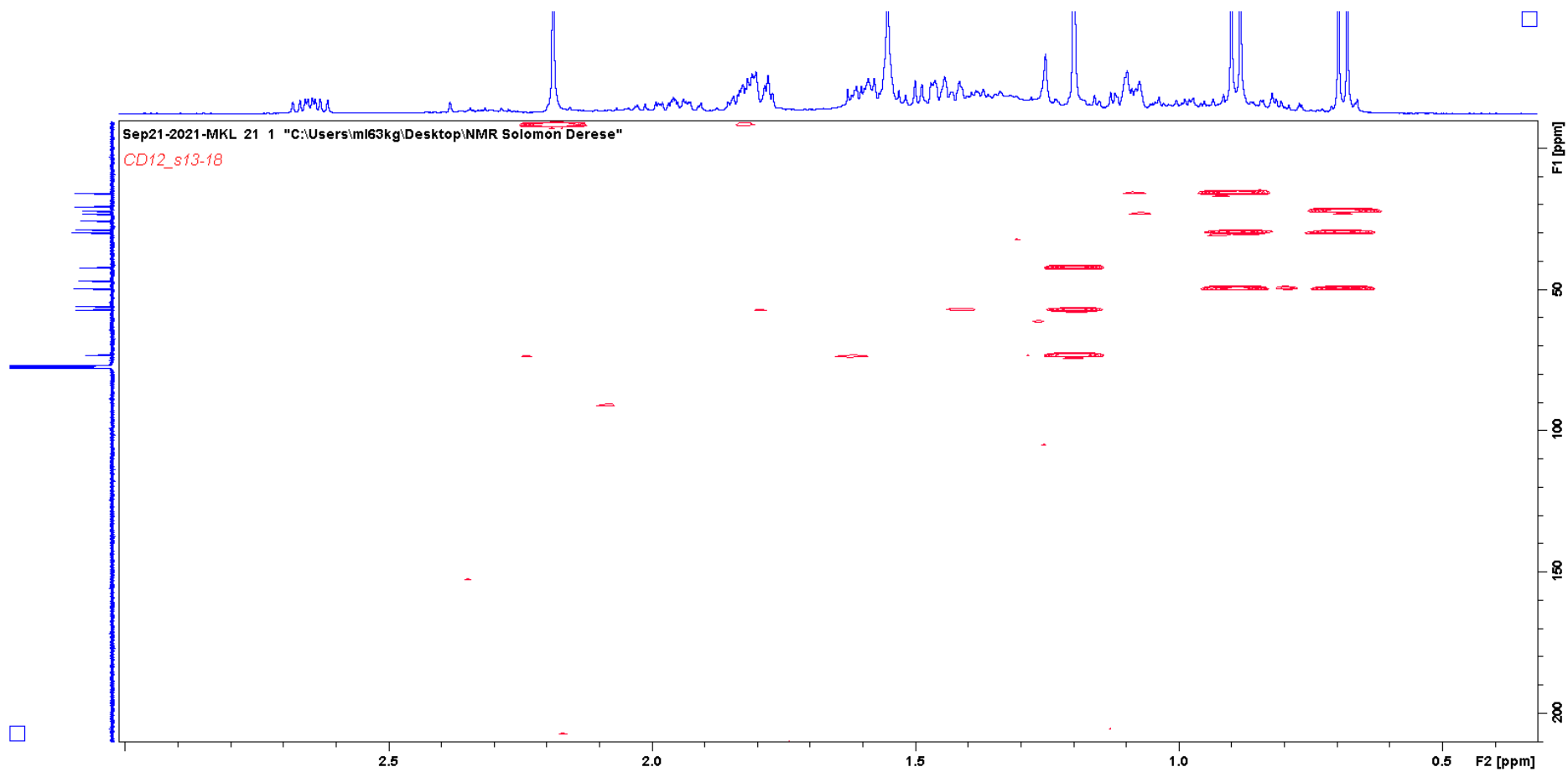
Appendix 114 DEPT Spectra for  $\beta$ -Oplopanone (CD12b)



Appendix 115 HSQCDEPT Spectra for  $\beta$ -Oplopanone (CD12b)

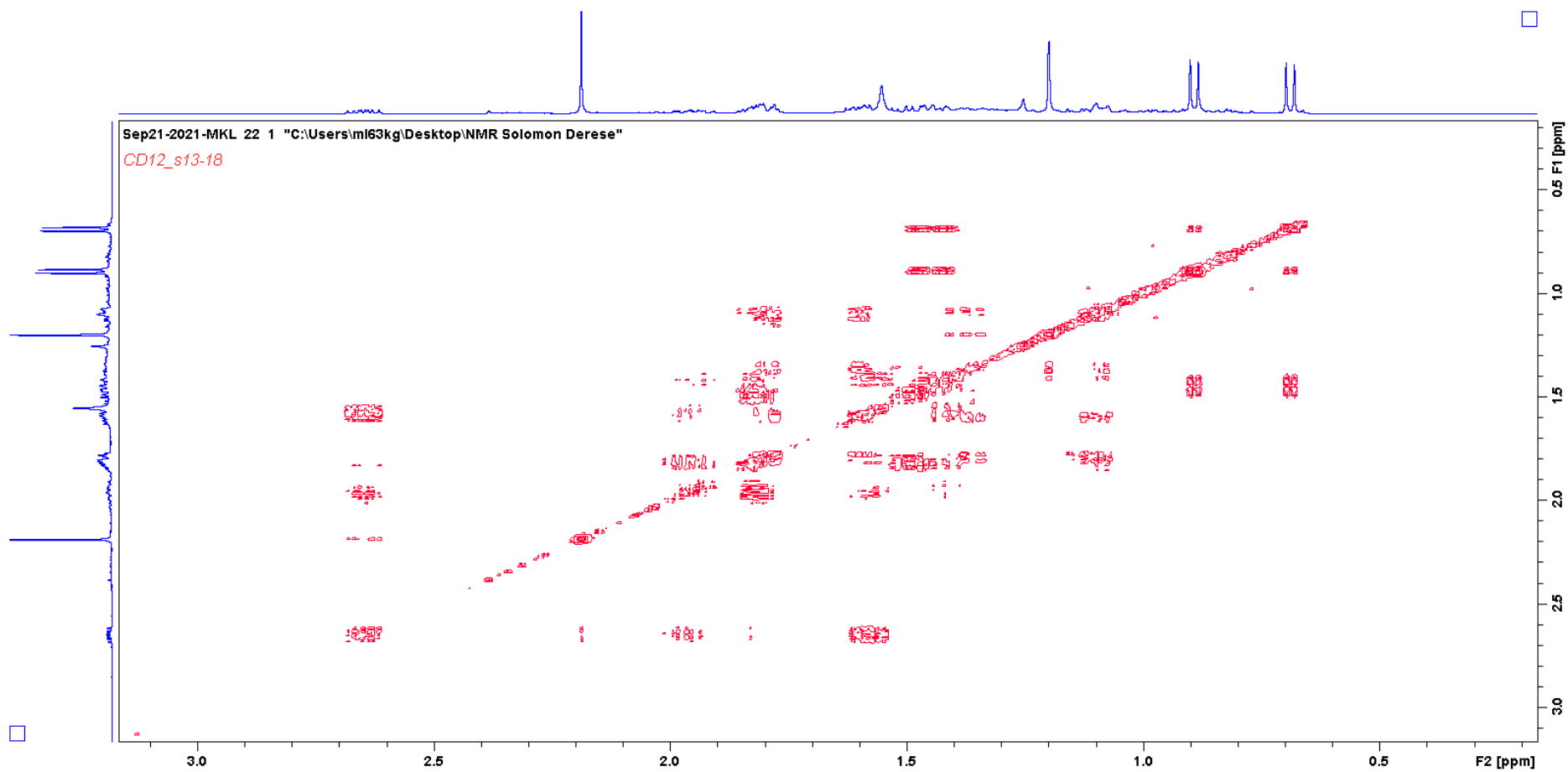


Appendix 116 HMBC Spectra for  $\beta$ -Oplopanone (CD12b)





Appendix 117 COSY Spectra for  $\beta$ -Oplopanone (CD12b)





Appendix 119 <sup>1</sup>H NMR CD6a and CD6b (Sitosterol and stigmasterol)

